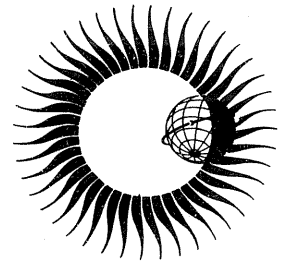


WORLD DATA CENTER A
for
Solar-Terrestrial Physics



COLLECTED DATA REPORTS
ON
AUGUST 1972 SOLAR - TERRESTRIAL EVENTS



JULY 1973

WORLD DATA CENTER A

National Academy of Sciences

2101 Constitution Avenue, N. W. Washington, D. C. U.S.A., 20418

World Data Center A consists of the Coordination Office

and eight subcenters:

World Data Center A
Coordination Office
National Academy of Sciences
2101 Constitution Avenue, N.W.
Washington, D. C., U.S.A. 20418
Telephone (202) 961-1478

Solar and Interplanetary Phenomena,
Ionospheric Phenomena, Flare-Associated
Events, Geomagnetic Variations, Magnetospheric
and Interplanetary Magnetic Phenomena,
Aurora, Cosmic Rays, Airglow:

World Data Center A
for Solar-Terrestrial Physics
National Oceanic and Atmospheric
Administration
Boulder, Colorado, U.S.A. 80302
Telephone (303) 499-1000 Ext. 6467

Geomagnetism, Seismology, Gravity (and
Upper Mantle Project Archives):

World Data Center A:
Geomagnetism, Seismology and Gravity
Environmental Data Service, NOAA
Boulder, Colorado, U.S.A. 80302
Telephone (303) 499-1000 Ext. 6311

Glaciology:

World Data Center A:
Glaciology
U. S. Geological Survey
1305 Tacoma Avenue South
Tacoma, Washington, U.S.A. 98402
Telephone (206) 383-2861 Ext. 318

Longitude and Latitude:

World Data Center A:
Longitude and Latitude
U. S. Naval Observatory
Washington, D. C., U.S.A. 20390
Telephone (202) 698-8422

Meteorology (and Nuclear Radiation):

World Data Center A:
Meteorology
National Climatic Center
Federal Building
Asheville, North Carolina, U.S.A. 28801
Telephone (704) 254-0961

Oceanography:

World Data Center A:
Oceanography
National Oceanic and
Atmospheric Administration
Rockville, Maryland, U.S.A. 20852
Telephone (202) 426-9052

Rockets and Satellites:

World Data Center A:
Rockets and Satellites
Goddard Space Flight Center
Code 601
Greenbelt, Maryland, U.S.A. 20771
Telephone (301) 982-6695

Tsunami:

World Data Center A:
Tsunami
National Oceanic and Atmospheric
Administration
P.O. Box 3887
Honolulu, Hawaii, U.S.A. 96812
Telephone (808) 546-5698

Notes:

- (1) World Data Centers conduct international exchange of geophysical observations in accordance with the principles set forth by the International Council of Scientific Unions. WDC-A is established in the United States under the auspices of the National Academy of Sciences.
- (2) Communications regarding data interchange matters in general and World Data Center A as a whole should be addressed to: World Data Center A, Coordination Office (see address above).
- (3) Inquiries and communications concerning data in specific disciplines should be addressed to the appropriate subcenter listed above.

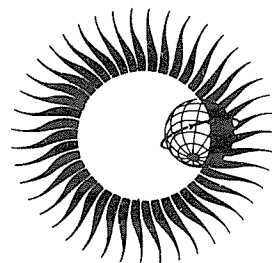
WORLD DATA CENTER A for Solar-Terrestrial Physics



REPORT UAG - 28 PART I

COLLECTED DATA REPORTS ON AUGUST 1972 SOLAR - TERRESTRIAL EVENTS

Helen E. Coffey, Editor
WDC-A for Solar - Terrestrial Physics
Boulder, Colorado U.S.A.



Prepared by World Data Center A for
Solar-Terrestrial Physics, NOAA, Boulder, Colorado
and published by

U.S. DEPARTMENT OF COMMERCE
NATIONAL OCEANIC AND ATMOSPHERIC ADMINISTRATION

ENVIRONMENTAL DATA SERVICE
Asheville, North Carolina, USA 28801

July 1973

SUBSCRIPTION PRICE: \$9.00 a year; \$2.50 additional for foreign mailing; single copy price varies.* Checks and money orders should be made payable to the Department of Commerce, NOAA. Remittance and correspondence regarding subscriptions should be sent to the National Climatic Center, Federal Building, Asheville, NC 28801, Attn: Publications.

* PRICE THIS ISSUE \$1.50

BOULDER

Np

H α

07

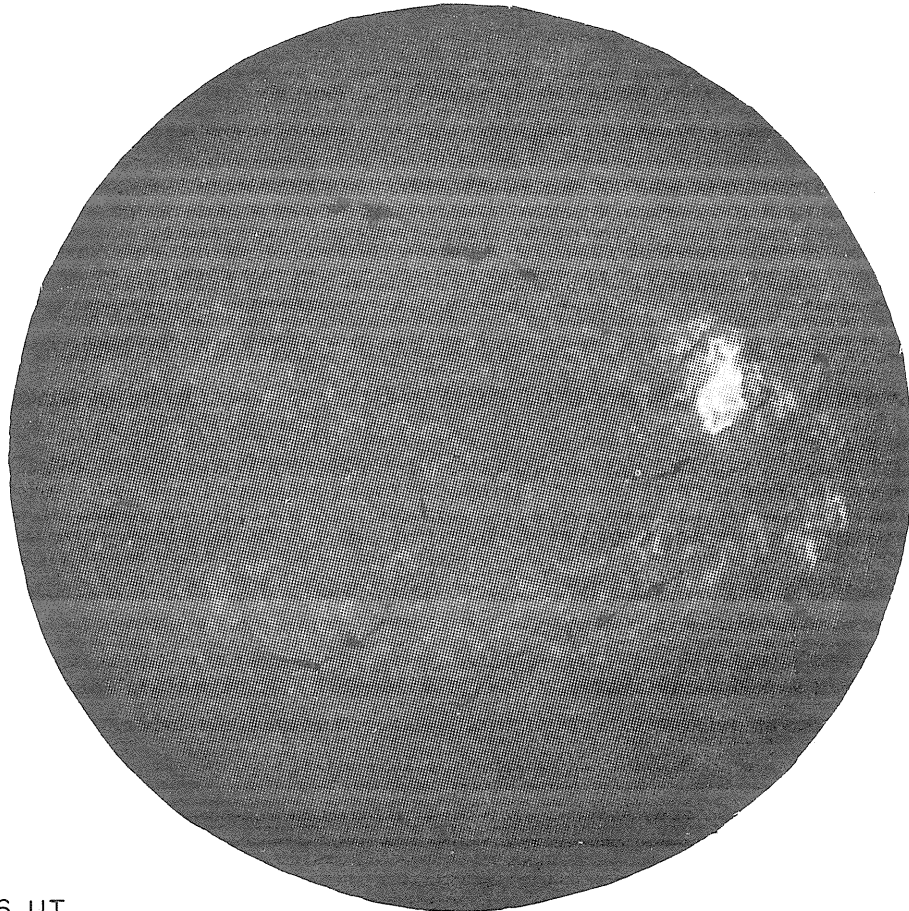
E

W

1526 UT

Sp

FLARE OF 07 AUGUST 1972



FOREWORD

The assembling of a volume of detailed data reports on the August 1972 solar-terrestrial events has come about because of recommendations by the ICSU Special Committee on Solar-Terrestrial Physics (SCOSTP), the International Union of Radio Science and numerous leaders in the international complex of scientific organizations. A circular letter from World Data Center A to the largest available list of observers resulted in the about 150 contributions collected in this special WDC-A data report.

The August 1972 events were a self-declared retrospective interval (confirmed by the SCOSTP) for intensive research and study, and the subject of a number of national and international symposia in the succeeding year. While a number of prompt data reports (see below) have appeared, the present volume is a channel for detailed data reports and brief discussion by individual observers. These data reports should facilitate multi-station or interdisciplinary interpretation of the complex phenomena and make more efficient the future scientific symposia on their physical explanation, notably the 1973 IAGA symposium at Kyoto.

The data reports in this volume have been given a minimum of editing, and where there has been editing there has not been time to check back with the authors and still have the volume distributed in a timely fashion. It is hoped that not too many substantive errors have thus crept in, but the compilers had no alternative.

The data reports are grouped under seven major headings, but many reports cover several of the major disciplines of solar-terrestrial physics. The index may help identify where data in one discipline are reported in a data report primarily concerned with another discipline.

Brief summaries of each major discipline appear at the front of the volume. These were written on short notice by members of the MONSEE Steering Committee of the ICSU Special Committee on Solar-Terrestrial Physics, each for his specialty. The time schedule was such that not all reports were available at the time the summaries were written, although most titles were available. The writers were asked to provide summaries or "overviews" and specifically not to attempt critical review articles. The summary articles may, however, serve as a guide to the detailed data reports; they attempt to meet a justified criticism of earlier detailed data reports on cosmic events compiled by WDC-A.

At the very beginning is a summary of the discipline summaries. While Dr. J. Roederer agreed to prepare this section, not enough material was available before he had to be absent on pressing matters and the overall summary was completed by the undersigned who should therefore take all responsibility.

Attention should be called to other data compilations on the August 1972 events. Many basic data and indices appear in UAG-21 issued by WDC-A in November 1972. That report includes the systematic data tables* and solar maps which appear in "Solar-Geophysical Data" and other data periodicals; these data are not repeated in this volume, but in Appendix I is reprinted the table of contents and the introduction for UAG-21. Appendix I also includes selected additional data (primary and analyzed) which have been received at WDC-A, as well as lists of detailed and special data held at WDC-A and elsewhere. Much data obtained in Japan in all solar-terrestrial disciplines appear in "Report of Ionospheric and Space Research in Japan", 26, 1972. In addition, much data and discussions have already appeared in standard journals or have been presented at scientific meetings and symposia. Appendix II lists many of these and should identify the many additional scientists who are actively interested in understanding the August 1972 phenomena and events.

The huge job of preparing these data reports for publication has been mainly borne by Helen E. Coffey, but with editing and checking assistance from most of the staff of the U.S. National Geophysical and Solar-Terrestrial Data Center, notably J. V. Lincoln, N. Smith, J. H. Allen, J. N. Barfield, K. Kawasaki, S. M. Ostrow, and D. B. Bucknam. The contribution of many typists and draftsmen can easily be appreciated and that of the printing operation of the U.S. National Climatic Center. The whole undertaking has been done in less than three months.

A. H. Shapley
Chairman, MONSEE Steering Committee
ICSU Special Committee on Solar-Terrestrial Physics

Director, National Geophysical and Solar-Terrestrial Data Center
Environmental Data Service
U.S. National Oceanic and Atmospheric Administration

*There is an erratum in the table of Geomagnetic Activity Indices on page 118 of UAG-21: for August 1 the Kp sum should be 17 rather than 70

SUMMARY TABLE OF CONTENTS

PART I

FOREWORD

1. SUMMARIES OF AUGUST 1972 EVENTS
2. SOLAR OPTICAL DATA
3. SOLAR RADIO DATA

PART II

4. SPACE OBSERVATIONS
5. COSMIC RAYS
6. IONOSPHERE

PART III

6. IONOSPHERE (continued)
7. GEOMAGNETISM
8. AERONOMY AND MISCELLANEOUS

APPENDIX I: Miscellaneous Data and Information from WDC-A

APPENDIX II: Other References

APPENDIX III: Explanation of Solar Radio Chart and Table

ALPHABETICAL INDEX

AUTHOR INDEX

TABLE OF CONTENTS FOR PART I

	<u>Page</u>
FOREWORD	i
PART I	
1. SUMMARIES OF AUGUST 1972 EVENTS	1
"Overall Summary of August 1972 Phenomena and Data" (J. Roederer and A. H. Shapley)	1
"Optical Solar Observations Around the August 1972 Events" (F. W. Jäger)	3
"Solar Radio Observations in August 1972" (H. Tanaka)	4
"Summary of Space Observations" (James I. Vette)	4
"Cosmic-Ray Data for the August 1972 Solar Events" (M. A. Shea)	8
"Ionospheric Observations of August 1972 Events" (A. H. Shapley)	8
"Geomagnetism and the August 1972 Solar Events" (D. van Sabben)	10
2. SOLAR OPTICAL DATA	11
"The IUWDS Forecast of the August Events" (P. Simon)	12
"Evaluation of the August 1972 Region as a Solar Center of (McMath Plage 11976)" (Helen W. Dodson and E. Ruth Hedeman)	16
"Evolution of Solar Active Region MM 11976 (H α and K faculae and spots)" (G. Godoli, V. Sciuto and R. A. Zappala)	23
"The Great Sunspot Group of August, 1972" (Patrick S. McIntosh)	30
"Proper Motion in the Large Sunspot from July 30 to August 10, 1972" (H. J. Pfister)	35
"Some Results of Spectrophotometric Studies of Prominences during July and August 1972" (A. I. Kiryukhina)	40
"Contribution of Meudon to the Observations of the August Solar Events" (M. J. Martres)	46
"A Photographic Record of Solar Activity from 5 to 13 August 1972 at Manila Observatory" (Francis J. Heyden, S.J.)	56
"Flares and Active Prominences Observed at Catania from July 26 to August 14, 1972 in the MM 11976 Region" (G. Godoli, V. Sciuto and R. A. Zappala)	68
"Coronal Magnetic Field Maps, before, during, after the Period 26 July to 14 August 1972. (Current-free approximation)." (M. D. Altschuler and D. E. Trotter)	74
"Occurrence of the August 1972 Proton-Flare Region in the Frame of the Large-Scale Magnetic Field Regularities" (V. Bumba)	77
"Magnetic Field Development of the August 1972 Proton-Flare Region" (V. Bumba)	80
"Observations of the Magnetic Fields of the August 1972 Sunspot Group" (G. A. Chapman)	85
"Photospheric and Chromospheric Magnetograms Related to the 3B Flare of 4 August 1972" (W. C. Livingston)	95
"Observation of the Flares of August 1, 2, and 4, 1972" (G. F. Sitnik, A. I. Kiryukhina, O. N. Mitropolskaja, I. F. Nikulin, G. A. Porfirjeva, V. S. Prokudina, E. M. Roschina, A. I. Khlistov, T. P. Khromova, and G. V. Jakunina)	103
"A Flare of August 2, 1972" (J. Kubota, H. Kurokawa and T. Kureizumi)	118
"The Flares of August 1972" (Harold Zirin and Katsuo Tanaka)	121

TABLE OF CONTENTS FOR PART I (continued)

	<u>Page</u>
"The Flare of August 4, 1972" (K. Maeda, N. Oda, K. Nakayama and M. Shimizu)	134
"On the Dynamics of the Proton Flare of August 4, 1972, at IZMIRAN" (E. I. Mogilevsky)	139
"Observations of the August 4, 1972 Chromosphere Flare at Abastumani" (M. Sh. Gigolashvili and E. I. Tetrushvili)	145
"The D ₃ (5875 Å) Line in the Solar Flare of August 7, 1972" (Juan M. Fontenla and Jorge R. Seibold)	150
"Changes in the Photosphere around the Locations of the Knots of the August 7, 1972 White-Light Flare" (V. Bumba and J. Suda)	155
"The Limb Flare of August 11, 1972" (M. Waldmeier)	160
"The Great Limb Phenomenon of August 11, 1972" (Claes Bernes and Ulf Kusoffsky)	161
 3. SOLAR RADIO DATA	 167
"Total Flux and High Resolution Fan Beam Observations of the 2800 MHz Solar Activity in August 1972" (A. E. Covington and M. B. Bell)	168
"Highlights of Radio Activity during Disk Passage of McMath Plage No. 11976" (John P. Castelli, William R. Barron and Victor L. Badillo)	183
"A Synoptic View of the Slowly Varying Component of the Solar Radio Emission During 1972. With Special Emphasis on the Period 26 July Through 14 August" (W. J. Decker and F. L. Wefer)	202
"Solar Radio Events at 9.4 to 71 GHz in the Period 26 July - 14 August 1972" (D. L. Croom and L. D. J. Harris)	210
"Solar Radio Emission for July 28 to August 13" (H. Tanaka and S. Enomé)	215
"Culgoora Observations of Radio Burst Activity from 1972 July 26 to August 14" (T. W. Cole)	222
"Metric Radio Continuum Activity Associate with the Active Region McMath No. 11976 in August 1972" (Kunitomo Sakurai)	229
"Pulses in Radio Bursts of August 1972 Proton Events" (V. L. Badillo)	231
"Preliminary Report on the Solar Radio Events of August 1972 Observed at Ahmedabad (India)" (R. V. Bhonsle, S. S. Degaonkar and H. S. Sawant)	234
"Solar Radio Emission on 100, 200 and 500 MHz Observed at Hiraiso" (F. Yamashita)	239
"Interferometric Radio Spectra of the Solar Corona 1-11 August 1972" (James C. Dodge)	242
"Dynamic Spectra of Four Solar Radio Bursts During the Period 1972 August 2-7" (Alan Maxwell)	255
"On the Type IV Bursts of August 2, 4 and 7, 1972" (A. Böhme and A. Krüger)	260
"The Type IV Bursts of August 4 and 7, 1972 Associated with p-Flares" (H. Urbarz)	269
"About Two Type IV Events on August 4 and 7, 1972 Polarimetric Measurements at 237 MHz" (Paolo Santin and Paolo Zlobec)	279
"Swept Frequency Interferometer Data Analysis for the Type IV Event of 1972, August 12" (Anthony C. Riddle)	283

1. SUMMARIES OF AUGUST 1972 EVENTS

Overall Summary of August 1972 Phenomena and Data

by

J. Roederer* and A. H. Shapley**
Special Committee on Solar-Terrestrial Physics, ICSU

The solar-terrestrial events of August 1972 have aroused great interest for many reasons. The solar activity was exceptional for the declining stage of the solar cycle; the principal solar region was in the highest activity class on an absolute scale; two flares reached outstanding level of importance (3B), one of which was definitely a proton flare; two other flares were classed as importance 2B, seven as importance 1 and some 50 as subflares; the proton flux in the interplanetary medium was the highest on record; ground-based neutron monitors recorded two major flare-associated increases and a major Forbush decrease; the geomagnetic storm of August 4-6 was a great one and that of August 9 was the third largest of the year; the accompanying ionospheric and auroral phenomena were correspondingly severe and complex, with at least two "polar cap absorption" events. The disruptions to telecommunications and the effects on other systems by solar-terrestrial disturbances were the most severe in a decade.

Further, the phenomena were quite thoroughly observed by ground and spacecraft sensors. These were the largest events since many of the newer instruments were in operation and, thus, the first opportunity to apply powerful new techniques to the study of large magnitude events.

Optical Solar Observations. The principal region, McMath 11976, was outstanding in solar cycle 20 because of the complexity of its magnetic field and its high flare productivity for the declining phase of the cycle. The region was unusually well observed and much quantitative data are available on the evolution of the photospheric and chromospheric structure, the magnetic field and limb features. The magnetic field data showed large gradients after the August 4 flare. Spectral data are available in many lines on individual features. The forecasts of the X-ray events on August 2 and the proton flare of August 4 were successful but not that of the proton flare of August 7.

Solar Radio Observations. The solar radio data are very complete for the August 1972 period and provide relevant data both on the evolution of the active region and the time histories of the four principal flares throughout the radio wave-length range. In particular there were observations of a peculiar feature of polarization distribution across the active region favorable to the occurrence of a proton flare. The absence of Type II bursts in the meter wave range, except for the August 7 burst, was a feature of the flares and bursts of the period.

Space Observations. The August 1972 events have been observed quite extensively by spacecraft, balloons, lunar-based instruments, and rockets. Detailed information on X-ray, γ -ray and energetic charged particle emissions is available in this document. Unfortunately many in situ solar wind and interplanetary magnetic field observations are not included here; however, from radio scintillation studies and data from Pioneer 9, it is clear that several interplanetary shocks were present, and that extremely large values of solar wind speed occurred on several occasions. A good data coverage is available on X-ray fluxes in the energy region of 0.6-300 keV, thus allowing the observation of both the thermal emission from hot solar plasma and the bremsstrahlung from non-thermal electrons. There were 12 events in which X-ray energy fluxes exceeded 10^{-1} erg/cm² sec in the 0.6-1.5 keV range. γ -ray line emission observations allow for the first time to establish that positrons, deuterium, and excited states of C¹² and O¹⁶ are produced by nuclear reactions between solar-flare-accelerated baryons and the solar atmosphere. Finally, a good data coverage is also available on energetic solar protons detected in space. All observations display a rather complex structure, related to multiple injections by various flares. There is also information on bow-shock- and interplanetary-shock-accelerated particles.

Cosmic Rays. The unusual features of the August 1972 solar-terrestrial conditions are confirmed in the cosmic ray observations, indicative of solar particle activity and of conditions in the interplanetary medium. Two ground-level increases measure the former and three Forbush decreases indicate the latter. These are all in suitable time association with the major solar flares, but the phenomena overlap in time, making interpretation of single-station data difficult, especially during August 3-5. The ground-level event on August 7 and the Forbush decrease beginning on August 9 are almost classical, though unusual for this stage of the solar cycle.

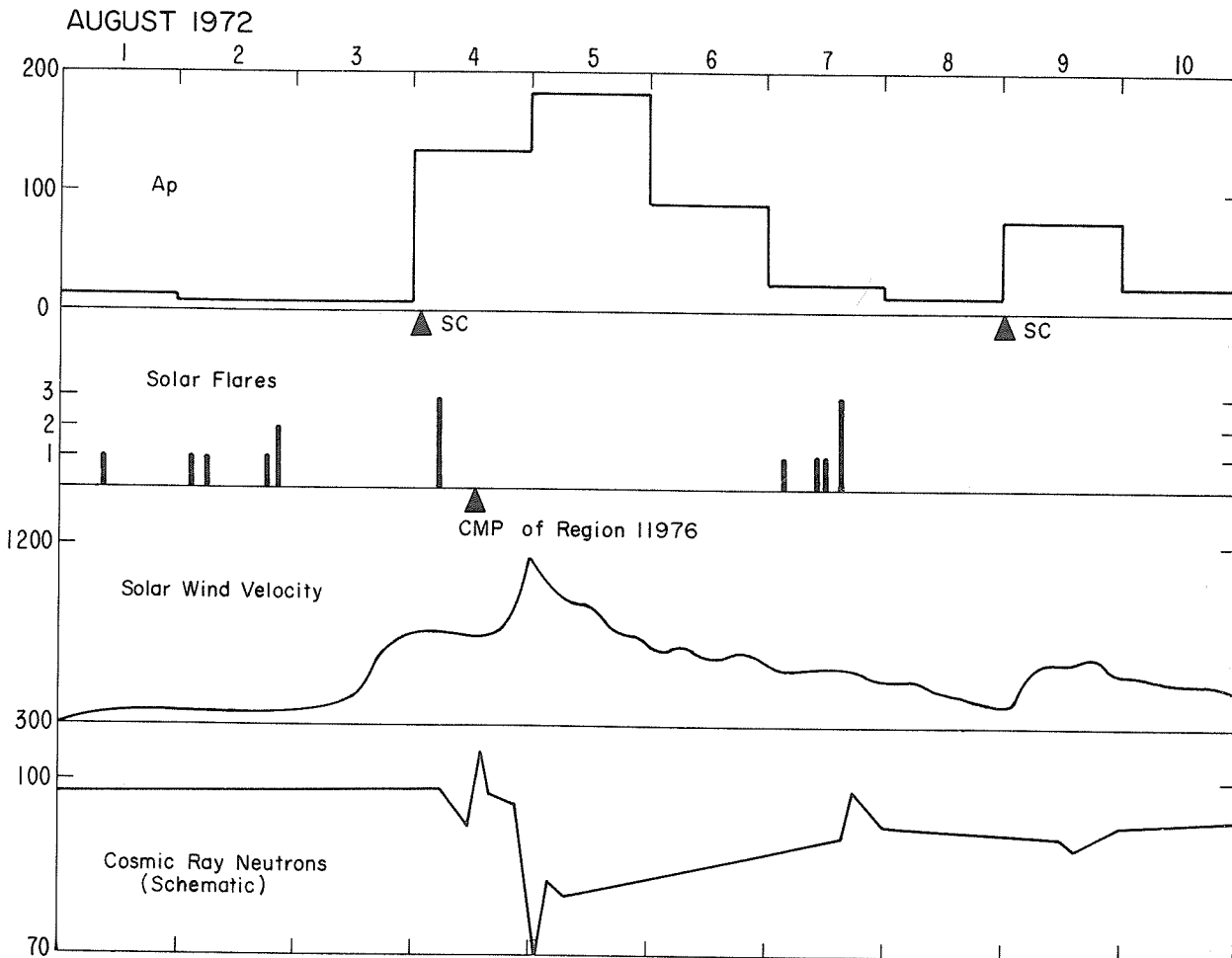
* University of Denver, Denver, Colorado U.S.A.

** Environmental Data Service, NOAA, Boulder, Colorado U.S.A.

Ionospheric Observations. During the August 1972 solar-terrestrial events, a number of identifiable effects upon the ionization of the entire ionosphere have been detected. There appeared to be two periods of storminess, separated by a short, partial recovery period. The ionization in the F-region showed the typical depressed foF2 during and after the storm periods; the D-region ionization responded to the SID events by producing numerous SWF's, SPA's, and also a continued background of enhanced wave absorption for MF and HF waves. The total electron content of the ionosphere did not change dramatically at mid-latitudes, but showed peaks at certain times at high geomagnetic latitude. Absorption measurements by the A3 method clearly showed the SWF's as well as the persistent night-time absorption indicating continued enhanced D-region ionization. HF Doppler observations indicate storm effects on upper atmosphere and ionosphere motions. VLF observations are available, indicating disturbances generally distributed throughout the whole period; whistlers were observed at unexpected times during the day beginning on August 4 and persisted over most of the disturbed period.

Geomagnetic Observations. A considerable volume of geomagnetic data is available, including magnetograms from selected stations, Kp, Ap, Cp, AE and Dst indices, lists of sudden commencements and solar flare effects. From these data it appears that there have been two main storms, starting on August 4 and 9, respectively; each storm began with two successive sudden commencements. Detailed analyses of these storms, the prestorm perturbations and their correlation with the interplanetary field, the relation between substorms and "mother" storms, etc., are presented in this document. A number of papers concentrate on magnetic pulsations of various types.

Aeronomy and Miscellaneous. Visual aurora was reported from many low latitude places during the August 4-6 geomagnetic storm. The data are certainly not complete, but the lowest geomagnetic latitudes reported are in Colorado in the Western Hemisphere and Ondrejov in the Eastern. Radar observations are reported from both hemispheres as well as scattered airglow data. Satellite drag measurements show major increases in atmospheric density at 300 to 900 km altitude for both the August 4-6 and the August 9-10 geomagnetically disturbed periods. A significant jump in the length of the day is linked to the August 2 flare. Electric field and other terrestrial phenomena are also reported.



Optical Solar Observations Around the August 1972 Events

by

F. W. Jäger
Heinrich-Herz Institut
Potsdam, GDR

General activity of the August 1972 region:

The duration of the whole perturbation in the principal region was seven rotations. The August events were outstanding in solar cycle 20 because of the complexity of its magnetic fields and the frequency of occurrence of great flares; the region, comparable to two other regions in the earlier years of this cycle, is located in a position on the sun that was relatively quiet until late in cycle 20.

Forecast of the August 1972 events:

A retrospective discussion of the IUWDS forecast shows: the X-ray events on August 2 and the proton flare on August 4 were correctly forecasted by several stations; however, the proton flare on August 7 was not forecasted at all.

Photospheric structure:

August 7: Changes in structure around the location of the August 7 white light flare have been derived from several hundred photographs; especially remarkable are the formation of light bridges and the disintegration of sunspot umbrae. Proper motions of the individual umbrae within the large penumbra, observed by different workers from August 5-10 and from July 30 to August 10, were severely distorted by the flare and show characteristic relationships to the shape of penumbrae filaments.

Chromospheric structure:

August 2: $H\alpha$ -filtergrams, some in different parts of the line, show a large two-ribbon flare appearing on both sides of a stable filament, one ribbon crossing an umbra.

August 4: High resolution $H\alpha$ -filtergrams taken repeatedly in discrete positions of the pass-band enable the studying of short-time changes and Doppler velocities of fine structure elements within the large proton flare. In the emission phase quasiperiodical fluctuations of the Doppler velocity up to 25 km/sec can be seen; in the eruption phase Doppler shifts to the red corresponding to more than 200 km/sec were observed in connection with arch filaments. From other $H\alpha$ -filtergrams the velocity of the expansion of the flare ribbons was estimated to be about 25 km/sec.

August 4, 7, 11: Comparison between the three main flares indicates that the flares can be regarded as homologous.

August 5-13: The overall development of the active region can be seen from daily filtergrams in $H\alpha$ and K.

Chromospheric lines:

August 2: Line spectra taken in five spectral ranges between 3850 and 6640 Å on August 1, 2, 4 show a remarkable line doubling in $H\alpha$ and K lines above sunspots, dark ejections with redshifts corresponding up to 200 km/sec, and in some places emissions also in He and $H\delta$ lines. Non-thermal motions of the matter in the flare were studied by time sequence spectra of lines of Fe II, Mg I and Na I.

August 4: Investigations are reported of line contours of $H\alpha$, $H\beta$, $H\epsilon$; H, K; D_1 , D_2 , D_3 . One of the main results is that near the centers of $H\alpha$ and $H\beta$, discrete emissions occur having Doppler velocities of +40 km/sec. Also the Doppler velocities of dark matter in these lines and in the He D_3 amount to 100 km/sec and 40 km/sec respectively.

August 7: For the He D_3 line of the umbra and the penumbra of the main spot the optical depth, Doppler width, kinetic temperature, source function, population of levels, and electron density have been derived.

Limb features:

August 11: From $H\alpha$ records of a limb flare, an ejection of matter with a vertical speed increasing from 165 to 745 km/sec was calculated; in the post flare loops, which also were a source of intensive X-ray emission, an unusually high intensity of the yellow corona line (λ 5694 Å) was observed.

July 26 - August 14: Spectra of 19 prominences containing numerous lines in the region 3000-4400 Å were used to study the limb passage of all active regions, including the principal one responsible for the August events.

Magnetic fields:

August 3 - 9: Magnetic spectroheliograms in the line Fe I λ 6103 Å show the longitudinal field structure with a typical resolution of 3 arc-seconds; the large sunspot group seems to be an isolated system having no remarkable interaction with the surrounding network.

August 4: From isogauss maps in the lines Fe I λ 5233 Å, Mg I λ 5173 Å, and H, it could be concluded that the flare produced no alteration of the magnetic field structure. Photographic magnetic field measurements indicate after the break of the central umbra of N polarity very large magnetic gradients of 0.4-1.0 gauss/km.

Long-time and large-scale magnetic field pattern: As was derived from the daily Mt. Wilson magnetic maps, the complex active region in question came into being by the merging of two regions which were still separated two rotations before the event; it suffered a fast disintegration just after the rotation in which the proton flare occurred. Calculations of the coronal magnetic fields were performed on the basis of longitudinal photospheric field measurements.

Solar Radio Observations in August 1972

by

H. Tanaka
Nagoya University
Toyokawa, Japan

In the late declining phase of the 20th solar cycle, an active region, McMath 11976, displayed prominent activity from July 28 to August 13, 1972. From the radio-astronomical viewpoint, this active region was associated with strong S-component during the course of its passage across the solar disk and produced four major radio bursts on August 2, 2, 4, and 7.

General overview of the activity is conveniently summarized in the Solar Activity Chart and its attached Table prepared at WDC-C2, Toyokawa; the format is that being considered by IAU Subcommittee 10a and is explained in Appendix III of this data report. Evolution of the S-component is described and illustrated in the data reports from Ottawa and Toyokawa, in which is shown a peculiar feature of polarization distribution across the active region favorable for the occurrence of a proton flare. Time histories of four major bursts are displayed and explained in the data reports from Manila, Berlin, Ottawa and Toyokawa for microwaves, and Weissenau, Hiraiso and Berlin for meter waves. For radio bursts on August 11 and 12, interesting results of meter-wave spectral and interferometric observations are obtained at Weissenau and Boulder.

A preliminary interdisciplinary analysis has already been undertaken at AFCRL for the August 7 burst in which the association of the white light flare with the hardness of the spectrum has been noted. In the report from Berlin, it has been noticed that except for the August 7 burst all other events were not associated with Type II burst in the meter wave range, while the first major event of August 2 was reportedly accompanied by a strong interplanetary shock front observed by Pioneer X.

Finally, it has to be noted that there are some discrepancies among the reported maximum fluxes at microwave frequencies, particularly for the event on August 4. It is hoped that this problem will be solved by a future study of establishing better calibration of burst intensity.

Summary of Space Observations

by

James I. Vette
U.S. National Space Science Data Center, NASA
Greenbelt, Maryland U.S.A.

The spectacular events which were produced from the flares generated in McMath region 11976 during early August have been observed quite extensively by spacecraft, balloons, lunar-based instruments, and rockets. The series of papers which follow here for Space Observations describe in detail the X-ray and γ -ray emissions generated near the solar surface and the energetic electrons, protons, and alpha particles accelerated there and propagated to the vicinity of the earth.

SOLAR ACTIVITY TABLE
(for detailed explanations see Appendix III)

Date 1972 Aug.	Start UT	End UT	Max UT	Dur. min.	10 cm Peak	Flux Integr	Flux at fp Peak	Integr	Intensity dm	Burst m	Shape Spectrum	Stations	SGD Group No.	QBSA No.	Lat.	Long.	McMath Region	Imp.	
2	0303	0310	0308	7	15						P.R. C	P4	TYKW, MANI, CRON, IRKU	45482	0203	N13	E35	11976	1B
	0310	0510	0405	120	2600	6600					P.I. C			45482	0204	N14	E34	11976	2N
	0510	0800	0510	1700	55	510													
	0300	0825							2	2	IS, CONT	CULG, WEIS							
	0312	0315							1	1	V	CULG							
	0326	0722							2	2	IIIS, U	CULG							
	0326	0450							1	1	UNCLF	CULG							
2	1045	1047	1045	2	30	2	65	6			S	P9	GORK, OTTA, SGMR, BERL, SLOU	45487	0205	S12	W42	11970	1N
2	1838	1849	1840	11	610	190	960				S	P5U15/37	SLOU, OTTA, SGMR, CANR, HUAN	45491	0206	N14	E26	11976	1B
	1839	1843							2		IV	HARV							
2	1959	2320	2148	201	9700	38000	9300	32000			C	P4	OTTA, TYKW, SGMR, BOUL	45492	0207	N13	E27	11976	2B
	2320	0300	2320	220	97	880					P.I. C	2.5\35	SGMR, TYKW, HUAN						
	1959	2003							2	2	IIIG	HARV							
	2021	2100							1	3	IIIS	HARV, CULG							
	2021	0728							3	3	IVorCONT	HARV, SGMR, BOUL, CULG							
	2243	2339							1	2	IIIG	HARV, CULG							
3	1502	1507	1504	5	66	12	185	63			S	P9	SGMR, OTTA, CANR, PENN, BERL	45503	0301	S12	W57	11970	1N
	1503	1505							2		IIIG	HARV							
3	2203	2253	2214	50	20	25	48	63			C	1.5/9	TYKW, OTTA, PENN, HUAN	No Flare Patrol					
	2241	2243							3	2	2	IIIG	HARV						
4	0525	0537	0529	12	62	34					C	1.5/4	TYKW, MANI, GORK, CRON, CRIM	45508	0401	N15	E09	11976	-N
	0537	0607			30	57					P.I. C								
4	0607	0619			12	30					P.R. C								
	0619	0715	0636	56	7600	11000	25000				P.R. C	P20	SLOU, TYKW, MANI, CRON, GORK	45509	0402	N14	E08	11976	2B
	0715	0920			65	380					P.I. C		IRKU						
	0706	0713	0707	7	110	32	145	59			S	2\9.5	TYKW						
	0717	0739	0719	22	1800	290					C	P4	TYKW, GORK						
	0743	0803	0753	20	105	90					C	3\9.5	TYKW, GORK						
	0805	0826	0810	21	95	63	580	230			C	1\9.5	TYKW						
	0834	0847	0840	13	50	26	220	200			S	1\9.5	TYKW						
	0605	0606									1	3	IIIG	CULG					
	0610	0714							1	3	IIIG	CULG, WEIS							
	0621	1245							3	3	IVorCONT	WEIS, CULG							
	0622	1156							3	3	IIIG	WEIS, CULG							
4	1307	1348	1318	41	9	16	32				S	1\U3/5	PENN, SGMR, BORD, CANR	45512	0403	N13	W01	11976	-N
	1313	1330							3	2	IIIG, DP	WEIS, HARV							
	1315	1338							3	3	IVP	HARV							
4	1513	1518	1514	5	35	6	36	11			C	P4	SGMR, OTTA, BOUL, BERL, PENN	45513		N13	W01	11976	--N
	1514	1518							3	3	3	IIIG, DP	WEIS, HARV						
	1514	1518							3	3	3	IIIG, DP	WEIS, HARV						
5	0231	0243	0233	12	26	7	35	5			C	1\9.5	TYKW, CRON, MANI, IRKU	*TEHR		N14	E19	11976	-F
	0226	0243							3	2	1	IIIG	CULG						
6	1613	1615	1614	2	25	2					C	Narrow B.	OTTA, BOUL, SGMR, CANR, PENN	45564		N17	W19	11976	--F
7	0251	0253	0252	2	66	4	430D	54			C	3/10	TYKW, MANI, CRON, IRKU	45569	0701	N15	W30	11976	-N
7	0346	0516	0355	90	49	180	195	400			C	1.5/10	TYKW, MANI, GORK, IRKU, CRON	45570	0702	N15	W30	11976	1B
7	1055	1102	1057	7	67	24	90				C	P9	BERL, OTTA, SGMR, GORK, SLOU	45577	0704	N14	W34	11976	1N
	1430	1505			17						P.R. C		CANR, CRIM						
	1505	1610	1528	65	4500	7100	15000	12000			P.R. C	3/9.5	HUAN, OTTA, SGMR, CANR, BOUL	45580	0707	N14	W36	11976	3B
	1610	1940			50	360	27000	45000			P.I. C	P9	SGMR, SLOU						
	1647	1656	1651	9	26	10	38	18			S	1\3	PENN, OTTA, CANR						
	1511	1530							3	2	IIIG, V	WEIS, HARV, SGMR							
	1519	1614							3	3	II	HARV, WEIS, BOUL							
	1508	1807							3	3	3	IV, CONT	HARV, BOUL, SGMR						
	1756	1802							2	2	IIIG	HARV							
11	1210	1212	1210	2	23	1	58	3			S	P7	SGMR, OTTA, CANR, GORK, HUAN	No Report					
11	1217	1221	1218	4	99	17					C	1.5/3	OTTA, SGMR, BERL, PENN, GORK	45643	1105	N12	W90	11976	1B
11	1231	1248	1236	17	70	36					C	0.6-9	OTTA, SGMR, GORK, BORD, PENN	45643	1105	N12	W90	11976	1B
	1239	1243					123	31			P9	SGMR, OTTA, GORK, PENN, SLOU							
	1239	1251							2	2	IIIG	BOUL, WEIS							
	1248	1254							1	1	II	BOUL, WEIS							
	1247	1355							3	2	II	BOUL, SGMR							
	1313	1340	1320	27	84	76			2	2	IV	BOUL, SGMR							
11	1315	1318							2	2	S	P3	OTTA, SGMR, BOUL, PENN, SLOU	No Report					
	1247	1355							2	2	II	BOUL							
	1247	1355	(Common to the above event)						2	2	IV	BOUL, SGMR							
	1345	1350							3		UNCLF	HARV							

Unfortunately, many in situ solar wind and field observations are not given here and one has to rely on the two papers concerning the ground-based method of radio scintillation to obtain the general picture of the solar wind conditions and the interplanetary shocks. However, the Pioneer 9 plasma wave observations (Scarf*) and the long path electron density (Croft) measurements do show convincingly the presence of several shocks at 0.77AU during early August. There is only one paper (Ondoh) concerning effects seen inside the magnetosphere. These indicate disturbed conditions (particle precipitation, whistler duct formation, plasmopause motion) during magnetic storms, but the exposition of many interesting details will have to await later publications.

In the X-ray region the energies covered (0.6-300 keV) allow the observation of both the thermal emission from a hot solar plasma and the bremsstrahlung from non-thermal electrons. The major events occurred at 0200 UT and 1830, August 2; at 0620, August 4; and 1500, August 7. Peterson's report provides a good description of the character of X-ray events, catalogs 23 events observed between July 28 and August 9, and presents details of the 1830 UT, August 2 event. The most extensive data coverage is given by Dere where energy fluxes based on black body spectra are presented for the period July 26 - August 14 for photon energies between 0.8 and 25 keV. There were 12 events in which energy fluxes exceeded 10^{-1} ergs/cm²-sec in the 0.6 to 1.5 keV energy range. The paper by Van Beek provides flux and spectral measurements of some of these events.

Some of the most extraordinary observations are reported by Chupp for the γ -ray energy range 0.3-8 MeV. For the major events on August 4 and 7, line emission at .511, 2.23, 4.43, and 6.13 MeV has been seen for the first time and establishes that positrons, deuterium, and excited states of C¹² and O¹⁶ are produced by nuclear reactions between accelerated charged baryons and the solar atmosphere.

The largest solar charged particle events of the 20th solar cycle occurred during the flares between August 2 and 7. Peak proton fluxes at the earth during August 4-5 displayed rather complex structure and it is highly likely that flares 1B E26, 2B E28, and 3B E09 all contributed particles. A second peak occurring during August 8-9 most likely resulted from the 3B flare at W37. There are five papers (Kohl, Lin, Lanzerotti, Domingo, Yates) which present extensive spacecraft results covering the whole time period emphasized in this retrospective interval. Experiments on Explorers 41 and 43, HEOS-2, and OV5-6 collectively provided electron energy coverage starting at 40 keV and extending to 3.5 MeV in several channels, proton energies from 0.2 - 100 MeV in numerous channels and alpha particles covering the range 2 - 25 MeV/nucleon in several channels. Comparison of the various results provides reasonable confidence in the flux values and detailed spectra are available so that further study and interpretation can be done. Balloon measurements of protons, the production of higher Z particles and even the activation of Apollo 17 samples collected some 4 months after the events are reported in other papers in this collection.

Unfortunately, the Apollo ALSEP instruments which measure electrons and ions in the solar wind energy ranges (.01 - 20 keV) were not pointing near the solar direction during the time interval of these events. However, the energetic particles just discussed penetrate the instruments and are detected. In addition, these instruments did detect low energy particles during special time periods. The paper by Moore reports on electron observations during August 4 which show two periods of heating. As the author points out, these particles are most likely energized at the earth's bow shock and propagate back upstream to the moon. Medrano presents some special ion events with sharply peaked spectra around 2.5 keV commencing on August 3 which are probably ejected from the bow shock. On August 4 streams of ions with broad energy spectra were observed which are suggestive of particles associated with an interplanetary shock wave generated by the flare at 2200 UT, August 2.

It is clear from the radio scintillation measurements reported by Armstrong and also Houminer that extremely large values of the solar wind speed occurred as a result of the flares of 0200 UT and 2200, August 2; 0600, August 4; and 1500, August 7 and that interplanetary shock waves were likely present. A solar wind speed in excess of 2000 km/sec at 1 AU may have resulted from the August 4 flare. In situ plasma and field measurements made during August should provide important results for understanding the extreme conditions present in the interplanetary medium.

In conclusion, the papers presented here give the reader detailed information on the X-, γ -ray, and energetic charged particle emissions from the sun at earth during the July 26 - August 14 interval. The conditions of the solar wind, the character of the interplanetary shocks, the nature of magnetic and electric fields, and the response of the magnetosphere to the highly disturbed conditions are exposed enough to draw interest to further study of one of the most interesting periods of solar emission ever observed. The detailed studies and correlations which this document hopefully will stimulate should lead to a much greater understanding of solar-terrestrial phenomena.

* In this summary, only the first author is given in the references to detailed data reports in this compilation.

Cosmic-Ray Data for the August 1972 Solar Events

by

M. A. Shea
Air Force Cambridge Research Laboratories
Bedford, Massachusetts U.S.A.

The information on the cosmic-ray events during August 1972 submitted by various scientists to this data compilation indicates most strikingly that this is an extremely complex period. The occurrence of many types of phenomena including two ground-level cosmic-ray increases and three Forbush decreases have been identified between 4 and 9 August 1972. In addition, the solar disturbances and corresponding changes in the interplanetary medium modulated the galactic cosmic rays up to very high energies. This is indicated by the cosmic-ray data from the underground muon detectors where these modulations may be observed to at least 60 M.W.E. (meters water equivalent) with indication of the general features of the high energy cosmic-ray modulation detectable at 80 M.W.E. While it is not the intention of this overview to be a critical analysis, it is perhaps appropriate to point out that the underground muon detectors located in Japan are viewing in almost opposite direction of those in the American hemisphere, and a comparison of the data indicates the presence of a galactic cosmic-ray anisotropy during this time period. Furthermore, complex modulations are occurring at about the same time as the ground-level cosmic-ray increases, and care must be taken to identify correctly the responsible phenomena.

The major features of interest detectable by ground-level cosmic-ray sensors throughout this period can be summarized as follows. An enhanced modulation of the neutron monitor intensity was observed at many stations on 3 August. Early on 4 August, at ~ 0130 UT occurred the first distinct Forbush decrease, a sudden sharp decrease in galactic cosmic-ray intensity. This Forbush decrease was complicated by a positive modulation of the high energy cosmic-rays upon which is superimposed a most unusual ground-level cosmic-ray increase detectable by very high latitude neutron monitors (vertical cutoff rigidity ~ 1.2 GV). An extremely intense Forbush decrease was detectable at all observable cosmic-ray energies with an onset time between 21 and 22 hours UT on 4 August. This event is very unusual in that the decrease is very rapid, the maximum depression is extremely deep for a very short time period (1-2 hours), and there is a very rapid recovery observed at neutron monitor energies (a few GeV). A correspondingly slower recovery is observed at higher energies detected by the underground muon telescopes. In addition, there is an intriguing coincidence between the rapid recovery of this Forbush decrease as detected by neutron monitors, and the shocks observed by satellite detectors in the interplanetary medium. After these phenomena early on 5 August there was a relatively normal recovery from the Forbush decreases as observed by neutron monitor until a second ground-level event occurred at ~ 1530 UT on 7 August. This ground-level event differs from the one on 4 August in that a very prompt arrival of particles was observed by neutron monitors with favorable asymptotic viewing directions. In addition, higher rigidity particles of at least 2 GV were detected in this second event. After the ground-level event on 7 August, there is a third smaller Forbush decrease on 9 August which is almost classical in its behavior with a rapid decrease in intensity followed by a slowly rising intensity to pre-decrease level.

As mentioned previously this is a very complex period and extreme care must be utilized in unraveling the ground-level and satellite observations to gain an understanding of the various phenomena that occurred in interplanetary space. The papers in this section contain valuable data that will be utilized not only by cosmic-ray scientists but also by scientists in related disciplines of solar-terrestrial physics in the analyses of their data for this most unusual period of the solar events of August 1972.

Ionospheric Observations of August 1972 Events

by

A. H. Shapley*
Environmental Data Service, NOAA
Boulder, Colorado U.S.A.

There are a large number of diverse contributions concerning the ionosphere to these data reports on the August 1972 solar-terrestrial phenomena. They contain a wealth of information but, as with any group of contributed reports, are not comprehensive or necessarily balanced. In addition to the group of detailed data reports, attention is called to Appendix 1 in which is reprinted from other sources a convenient set of hourly f-plots for eight ionosonde stations and hourly values of foF2 for August 1-11 for 64 ionosonde stations.

* Based on contributions by W. R. Piggott, Radio and Space Research Station, Slough, U.K., and N. Smith, Environmental Data Service, NOAA, Boulder, Colorado U.S.A.

The ionosphere showed no especially unusual features in the period under review until the Importance 2B flare on August 2 beginning at 1958 UT. The accompanying Sudden Ionospheric Disturbance (SID) was seen essentially everywhere in the daylight hemisphere by all relevant techniques. The Polar Cap Absorption event (PCA) began by about 0400 UT on August 3 as shown by riometer data and by about 0700 as shown by ionogram blackout (Godhavn, in Appendix I). Further study is needed of the data in this volume, including Appendix I, and indeed probably of the concert of ionograms and riometer recordings to ascertain the first arrival of ionizing solar protons and the morphology of the PCA as a function of geomagnetic latitude.

The PCA blended into the ionospheric storm introduced by the geomagnetic sc at 0119 UT August 4. At first glance, at least the D-, E-, and F-region characteristics of the storm were not atypical. There was strong D-region absorption (blackout or high f-min on ionosondes) almost continuously through August 8 in the higher latitudes, above about $\phi=70$, and during daylight hours in the latitude zone $\phi=55-70$. Riometer data give a more quantitative measure of changes in D-region ionization below 75 km, while the ionosonde data are a crude measure of unusual ionization in the upper D-region. When the F-layer could be seen through the absorption, the usual storm time behaviour was generally observed. Of especial note are the incoherent scatter measurements at Chatanika, Alaska, on August 5 when ionosondes were blacked out; these indicate that foF2 in the auroral zone is relatively low during an intense storm as it is during moderate disturbances when ionosondes are not blacked out. Temperate latitude phenomena seem to have followed the usual storm-time trends, but multi-station studies from these data sources will be needed before this conclusion is confirmed.

The "Sporadic E" (Es) types and "night E" which are typical of high latitudes were seen at lower latitudes than normal during the intense disturbance. At still lower latitudes, Es phenomena were complex; there are reports of both decreases and increases in the amount of Es present. This is not unusual: zones which show much sequential Es in quiet conditions usually show less Es in magnetically disturbed periods whereas high latitude types of Es are increasingly present during disturbed conditions. On the other hand, at stations where the typical dense summer types of Es are common, its prevalence is so variable from day to day that little can be deduced from data for single stations on particular days. Data from the winter hemisphere were not available when this summary was written.

One should note the apparent large increase in neutral atmosphere density just above F-region heights on August 4, as measured by satellite drag (Jacchia et al.). This contrasts with the behaviour of the electron density.

By the time the 3B flare of August 7 began at 1455 UT, the geomagnetic field had quieted down, and the low and middle latitude F-region was generally normal. However, on the polar cap, absorption was still very high, whether a continuation of the PCA of August 3 or the aftermath of the ionospheric storm which began August 4. One can only barely recognize a new PCA beginning following the flare from the ionosonde data (0600 at Narssarsuaq), but riometer data indicate one did begin by 0500 UT. There would seem to be a definite difference in the proton energy spectrum of the August 3 and August 8 PCA events, which detailed study of these data could specify.

The ionospheric storm starting from the geomagnetic sudden commencement on August 8 at 2354 UT seems fairly ordinary and much shorter-lived. In fact, the PCA in the polar zone seems to have lasted as long as the magnetic storm effects.

There are many special observations of special interest. The incoherent scatter data at Millstone Hill before, during, and after the August 7 flare should be studied carefully, and the same kind of observations in Alaska throughout the period are probably the first of their kind in the auroral zone in a period of great disturbance. It is clearly useful to gather together the many VLF and LF data both for the flares and for the storm periods. Total electron content measurements include a flare-associated perturbation on August 7. This has not yet been confirmed by observations at other stations, for example by f-plots of foF2 on a 5- or 10-minute time scale for suitable ionosonde stations. The same technique could be used for searching for perturbations of foF2 associated with large geomagnetic sudden commencements, especially as Doppler movements of the height of the layer have been reported.

Geomagnetism and the August 1972 Solar Events

by

D. van Sabben
Royal Netherlands Meteorological Institute
De Bilt, Netherlands

The series of papers on geomagnetic effects begins with the presentation of some of the basic indices: the auroral electrojet index AE and the equatorial Dst-index; already published in the companion data volume, Report UAG-21, are the planetary indices Kp, Ap, and Cp, the usual lists of data from observatories on "principal magnetic storms", sudden commencements and solar flare effects and a number of magnetograms from selected stations.

From these data it appears already that there have been two main storms during the interval, roughly from August 4 to 6 and on August 9. Both storms began with two successive sudden commencements (ssc) namely at August 4, 0119 and 0220 UT and at August 8, 2354 and August 9, 0037 UT, respectively.

Many of the subsequent papers begin with general description of the storms and of the related solar activity. For those papers which were available at the moment of writing of this survey, some main points are indicated here. Loomer and Jansen Van Beek concentrate on the magnetic perturbations preceding the storms. They present the equivalent current systems for these perturbations and indicate a relation between the type of the current vortices in the polar cap and the direction of the interplanetary magnetic field. Riometer data on polar cap absorption from Loparskaya and the occurrence of bays and pulsations in relation to the storm phases are discussed by Brunelli et al. They report large pc-5 between 0900 and 1200 UT on August 5, with periods ranging from 4 to 6 minutes and amplitudes about 500γ.

An analysis of substorms based on the records of two mid-latitude and two equatorial stations is made by Selzer and Roquet. They discuss the double ssc-structure and the relation between the substorms and the "mother storm." A description of the effects at three low-latitude stations, including two equatorial electrojet stations, is given by Bhargava. He reports extremely heavy disturbance after the si-event of August 4, 2238 UT.

There are also papers concentrating on pulsations. Bolshakova et al. give a survey of pulsations of the types pi 1, 2 and pc 1-5 which occurred at Borok (58° N, 39° E) between August 4 and August 10. They noted the absence of pulsations of the type IPDP during the interval 2-8 August. A description of the records of the geomagnetic X-component at Manila is given by Salcedo, with emphasis on the pulsations with periods ranging from 1-5 minutes and amplitudes up to 200γ which occurred during daytime between August 4, 2238 UT and August 5, 0740 UT.

Micropulsations activity at an unmanned observatory in Antarctica (near McMurdo) is reported by Willard, Helms, and Liemohn. The data which were transmitted via satellite in digitized form are presented in daily diagrams of micropulsation power, as recorded in 21 separate frequency bands, for the period August 2-6.

Heacock, Hessler, Kivinen, Reid and Olesen describe micropulsations as recorded in four auroral zone stations and one polar cap station (Thule). They especially discuss the pc 1-2 pulsations associated with ssc's and the periodically structured pc 1 during the storm recovery phases.

2. SOLAR OPTICAL DATA

Summary on page 3

Charts of Flare Observations in Appendix I

The IUWDS Forecast of the August Events

by

P. Simon, Chairman of the IUWDS
Observatoire de Meudon, France

After the occurrence of such a series of outstanding solar events, one is tempted to scrutinize the relevant forecasts and to evaluate the utility of a service devoted to prompt distribution of the data and the issuance of daily forecasts.

Of course no service preparing forecasts could pretend to succeed all the time and the study of a long series of forecasts would give a better basis for evaluation of its efficiency. Such a work has already been published [P. Simon et al., 1972]. However, we can review the forecasts issued between 29 July and 11 August 1972. In addition this could help users become familiar with these kinds of information.

Forecasts of Solar Activity.

Forecasts are issued in a double wording format:

1. A forecast of the activity of each spot group according to the following four categories:

- (a) Quiet: No more than one small flare a day is expected.
- (b) Eruptive: Several flares or subflares a day, but only a few radio or X-ray bursts are expected.
- (c) Active: Large centimeter or X-ray bursts accompanying flares are expected but they will not be followed by a prompt arrival of protons at the Earth.
- (d) Proton: A prompt proton arrival at the Earth is expected following a large solar event accompanied by centimeter and X-ray bursts.

For the last two categories one cannot specify the date of the event: this kind of forecast is repeated daily for as long as the event is expected to occur.

2. An Alert:

- (a) Solalert: The solar activity will increase.
- (b) Protonalert: A solar event followed by a prompt proton arrival is expected somewhere on the sun.

Several Warning Centers cannot use these categories of forecast and use either the wording "flare expected" for a large flare (importance 2) expected or only an alert: Solalert or Protonalert.

Evaluation of the Forecasts.

According to Table 1, the three events on 2 August with large X-ray bursts were correctly forecasted by PA, SY and KO. The proton event on 4 August was forecasted by SY, GE and PA. The proton event on 7 August was not forecasted at all.

Forecasts of Geomagnetic Activity.

Usually one uses the Alert system along with an evaluation of the time of occurrence of the event: MAGALERT 30/04 means that a magnetic storm is expected to start on either 3 or 4 August. Several Warning Centers transmit "expect a magnetic storm" instead.

Evaluation of the Forecasts.

According to Table 2, SY was the only Warning Center to forecast the geomagnetic storm of 5 August as a severe one. Obviously some disturbance was expected to follow the flare of 4 August, though we cannot say whether a new storm was superimposed on the declining geomagnetic activity. The magnetic storm of 9 August was correctly forecasted, but we can suspect that several Warning Centers expected a longer storm than the one which actually occurred.

Comment on the Forecast of the Proton Events.

The term "proton event" is applied to a large variety of solar situations which are far from being understood. Solar forecasters have to base their warning upon well-established criteria, even though many proton arrivals do not fit in with them. During this period two well-established criteria were fulfilled and one datum was difficult to evaluate.

1. The centimetric spectra of the center:

During the whole of its disk crossing, the flux ratio 3 cm to 8 cm of this center of activity was equal to or above 1.00 and the 3 cm flux was above 25 fu (Table 3).

2. A high magnetic field gradient:

On 31 July the observers at Meudon noticed an unusual value of the magnetic field gradient. In their program of observation of sunspot magnetic fields, the observatories in USSR supplied useful information on the magnetic structures of the group, and obviously the observers at Kislovodsk were aware of the unusual value of this gradient on 3 August at 0500 UT.

Table 1

Forecasts Issued by the Warning Centers and the World Warning Agency (Geoalert) and Solar Events Occurring during This Period

Eruptive	Active	Proton	Flare Exp. or Alert	Events
PA291400	PA311500(1)		SY010100(SO)	
GE010400	PA011300		SY020115(SO)	020309 TenFlare1900fu
DA011200			KO020135	021838 TenFlare 600fu
BO020200	PA021330(SO)		SY030110(PN)	021958 TenFlare9700fu
GE020400	BO030200(SO)	GE030400(PN)	KO030216	
DA021200		PA031330(PN)	SY040130(PN)	040621 TenFlare5600fu
DA031329(PN)			KO040120	Proton Event
GE040400	GE050400	PA041330(PN)	NE041200	
DA041300			SY050120(PN)	
	PA051400(SO)		KO050135	
	GE060400(SO)		BO050200(SO)	
			KO060130	
	GE070400(SO)		SY060135(SO)	
DA071201	PA071330(SO)		BO060300(SO)	
			SY070105(SO)	
			KO070130	
			BO070200(SO)	
			NE071200	071505 TenFlare4500fu
			SY080100(PN)	GLE Proton Event
			KO09 ^o 125	
DA081200(PN)	GE080400(PN)	PA081330(PN)	BO080200(PN)	
			SY090120(SO)	
			KO090125	
	GE090400(PN)	PA091530(PN)	BO090200(SO)	
DA090930			NE091200	
			SY100130(SO)	
			KO100135	
DA101320	GE100400(SO)	PA101330(PN)	BO100200(SO)	
			SY110120(SO)	
			KO110125	
		GE110400(PN)	BO110200(PN)	
DA112156		PA111330(PN)		111217LimbFlare
(1)Complex Magnetic Field Structure				
PA=Meudon	DA=Darmstadt	KO=Tokyo	BO=Boulder	(SO) = Solalert
NE=Nera	MO=Moscou	SY=Sydney	GE=Geoalert	(PN) = Protonalert

Table 2

Forecasts of the Geomagnetic Activity and Reported Events

Forecasts	Events reported
PA021330 MAGALERT 03/04	
MO021600 MAGALERT	
SY030110 MAGALERT PIANO LITTLE DATA RECEIVED ON LATER EVENTS	
K0030216 MAGSTORM EXPECTED	
B0030200 MAGALERT	
GE030400 MAGALERT 03/05	
PA031330 MAGALERT 03/05	
DA031329 MAGALERT 03/05	
MO031600 MAGALERT	
SY040130 SEVERE MAGSTORM EXPECTED 5th	SSC 040119 On 4th Ap=132
K0040207' MAGSTORM EXPECTED	SSC 040220
B0040050 MAGALERT	SSC 042054
GE040400 MAGALERT 04	
PA041330 MAGALERT 04/05	
B0050200 MAGALERT	on 5th Ap=182
K0050135 MAGSTORM EXPECTED	
PA051400 MAGALERT 05/07	
K0060130 MAGSTORM EXPECTED	On 6th Ap=87
B0060300 MAGALERT 06/07	
GE060400 MAGALERT 06/07	on 7th Ap= 19
B0080200 MAGALERT 08/09	SSC 081341
GE080400 MAGALERT 08/09	SSC 082354 On 8th Ap= 9
PA081330 MAGALERT 08/09	
NE081200 MAGSTORM EXPECTED	
DA081328 MAGALERT 08/09	
MO081600 MAGSTORM EXPECTED	
B0090200 MAGALERT 09/10	SSC 090037 On 9th Ap=74
K0090125 MAGSTORM EXPECTED	
GE090400 MAGALERT 09/10	
PA091530 MAGALERT 09/10	
MO101600 MAGALERT	On 10th Ap=18
MO111600 MAGALERT	On 11th Ap=17
PA121300 POSSIBILITY OF WEAK MAGSTORM 12/13	

Table 3

Data on the Centimetric Flux and Spectra of the Center
(according to the data of the Toyokawa Observatory)

Date	Position	Flux		Ratio	Date	Position	Flux		Ratio
		1972 min	arc				3cm	8cm	
Jul28	E 15.9	02.7	04.4	0.60	Aug5	W 0.9	52.5	44.7	1.17
	29 E 15.7	12.3	10.0	1.35		6 W 4.2	39.6	40.5	0.98
	30 E 15.0	24.8	19.4	1.28		7 W 7.4	40.2	39.1	1.03
	31 E 13.9	40.3	25.2	1.60		8 W10.1	25.2	22.2	1.14
Aug	1 E 12.1	47.1	31.7	1.49		9 W12.4	27.7	23.2	1.19
	2.E 9.1	59.2	49.4	1.20		10 W13.7	27.2	18.8	1.45
	3 E 6.3	42.3	40.5	1.04		11 W14.4	22.6	22.2	1.02
	4 E 2.9	44.3	41.0	1.08					

These two categories of information circulate regularly on the IUWDS network thanks to the existing codes.

3. Evolution of the active center:

The prediction of the evolution of each part of the spot group contributes to the forecast of the solar events. At higher latitudes the differential rotation plays an important role for the relative evolution of the spots. However, around 13° the proper motion alone are important, and in such a complex group they are difficult to predict.

We also have to note that for a spot somewhere between the East limb and about E30, one cannot in general expect any prompt proton arrival. Thus, the forecast is usually only "Active". From W40 to the limb many events are proton producers.

Comment on the Geomagnetic Activity Forecasts

Large flares which fulfill all the usual solar criteria for a geomagnetic storm sometimes do not disturb the geomagnetic field. In that case the "way" between the interplanetary medium and the magnetosphere was not "open" for an interaction. The solar data could help to forecast the delay of the storm but we have little information for a prediction of the importance of the geomagnetic activity. Of course, a series of large events could be supposed to produce an unusual high level of geomagnetic disturbance.

Conclusion

The information circulating on the IUWDS network allowed some material which could contribute to a successful forecast of the solar activity and of the geomagnetic disturbances during this period.

REFERENCES

SIMON, P. and
P. S. McINTOSH

1972

Survey of Current Solar Forecast Centers, "Solar Activity Observations and Predictions", Progress in Astronautics and Aeronautics, 30, 343.

EVALUATION OF THE AUGUST 1972 REGION AS A SOLAR CENTER OF ACTIVITY (McMATH PLAGE 11976)

by

Helen W. Dodson and E. Ruth Hedeman
McMath-Hulbert Observatory, The University of Michigan

1. Time of McM 11976 in the 11-year solar cycle

a. Time in solar cycle 20

The active, particle-producing region of August 1972 (McMath plage 11976) with its ground-level enhancement of cosmic rays, occurred ~ 3.7 years after sunspot maximum and during a well-defined resurgence of activity or "stillstand" in cycle 20. This resurgence of activity in 1971-72 resembled closely the "stillstand" of 1950-51 in cycle 18. They both took place about four years after solar maximum, lasted for about a year, and corresponded to a level of ~ 70 in smoothed sunspot numbers. (See Figure 1.) The 1950-51 resurgence included the formation of the fourth largest known spot (CMP May 16, 1951). Resurgences or pulses of marked activity appear to be a characteristic of the declining phase of the 11-year solar cycle.

The resurgence of activity in solar cycle 20, according to monthly mean values of sunspot numbers and 10 cm flux, may have started as early as July 1971, was well established by December 1971, reached maximum values in February 1972, and then diminished irregularly throughout the remainder of the year. Accordingly McMATH plage 11976 with CMP on August 4, 1972, occurred after the maximum and near the end of the resurgence of activity in solar cycle 20 and not at the time of its peak development. (See Figure 1.)

b. Energetic particle events in the late phase of other solar cycles

The occurrence of flare-associated, high energy particle events at the earth in the declining phase of the 11-year solar cycle likewise appears to be a usual rather than an unusual aspect of solar-terrestrial relationships. The first known instances of sun-associated ground-level enhancements of cosmic rays (GLE) occurred on February 28 and March 1, 1942 during the transit of an important center of activity at the end of a small "stillstand" ~ 4.8 years after maximum in cycle 17. In cycle 18, a GLE occurred on November 19, 1949 ~ 2.3 years after maximum. The more sensitive detectors of later years recorded 8 GLE's during the declining phase of cycle 19 between July 16, 1959 and July 20, 1961 (~ 1.4 to 3.3 years after spot maximum). Table 1 brings together data relating to the five centers of activity associated with GLE's in the postmaximum phase of cycle 19 and similar information for cycle 20, including data for McM 11976.

From the solar point of view, there seems to be considerable similarity between McM 11976 of August 1972 and McM 6171 of July 1961. The two regions occurred at approximately similar times in the cycle and during intervals of comparable 2800 MHz flux and sunspot numbers. The regions had similar Active Region Indices and both produced 4-5 great flares with Comprehensive Indices >11 . Both regions were associated with extensive energetic particle emission and severe geomagnetic disturbances. These two apparently similar solar "events" differed, however, in what may be a significant circumstance. The 1961 center of activity took place in the postmaximum phase of a solar cycle famous for the height of its maximum and the level of its activity. The 1972 event occurred in the years following an average solar maximum. The interplanetary medium in the two cases may have been markedly different, and may have led to significant differences in the geophysical effects and the particle phenomena in the neighborhood of the earth.

2. Magnitude and characteristics of McM 11976

a. Comparison of McM 11976 with other regions in 1972

The active, particle-producing center of activity of August 1972 (McM 11976) was outstanding in the year 1972 on the basis of the magnetic complexity of its spots and the frequency of its production of flares of great magnitude. It was not a uniquely great center of activity when other criteria are used for evaluation.

The magnetic complexity of McM 11976 should be discussed by those who have direct access to detailed magnetic measurements. From summarized reports, the spot group seems to have been the only one in 1972 for which the magnetic classification was both γ and δ for most of the days of transit across the disk.

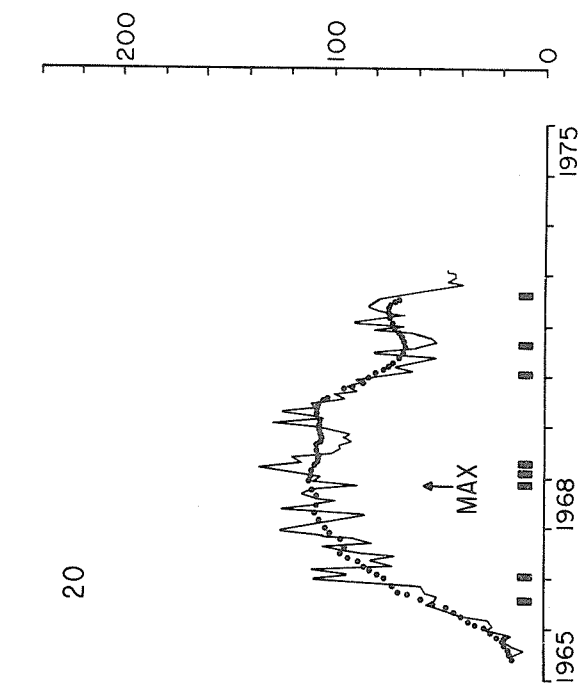
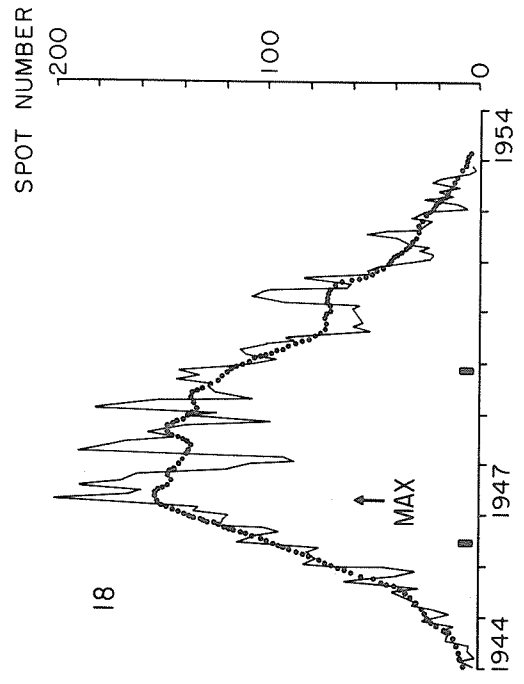
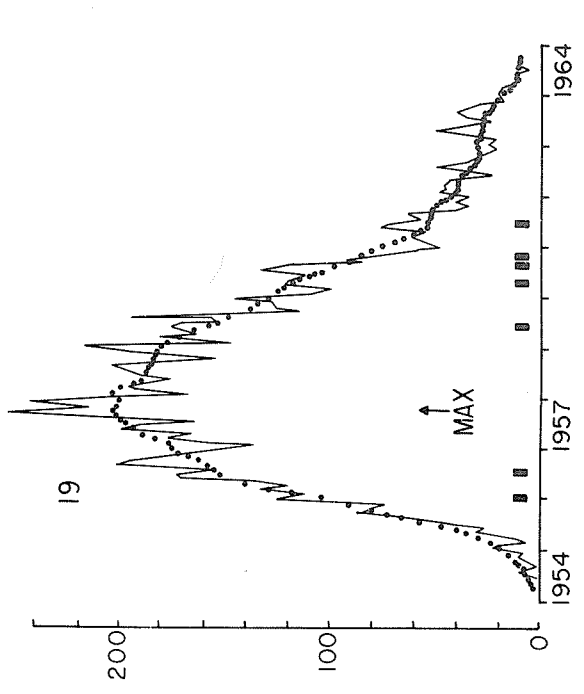
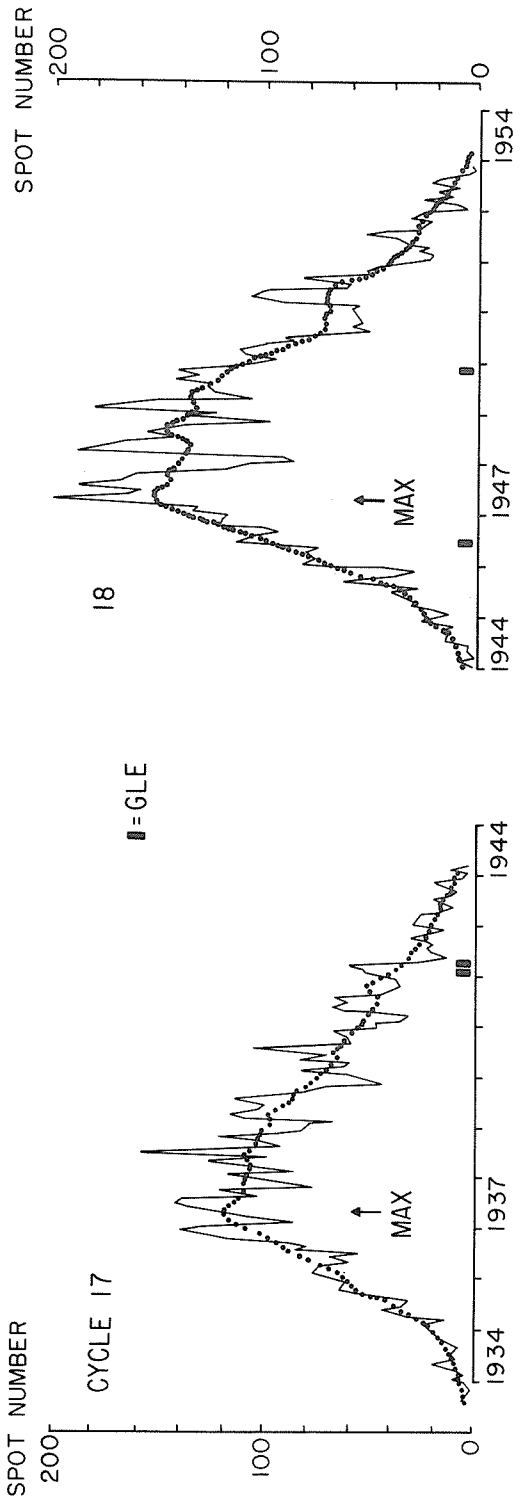


Fig. 1. Monthly mean and smoothed Zurich sunspot numbers for solar cycles 17-20. Times of sunspot maxima and ground-level enhancements of cosmic rays are indicated.

According to the flare data in SGD, No. 342 and the Quarterly Bulletin there were in McM 11976 twelve flares of importance ≥ 1 . Worldwide reports for 1972 are currently available only through August, but in this interval in 1972 three other regions had approximately similar numbers of flares of importance ≥ 1 . (See Table 2.)

The flares in McM 11976, however, included four events that were not only important optically but also were very great in ionizing and radio frequency emission. For these flares the Comprehensive Indices [see Report UAG-14 for description of this index] were ≥ 11 , a rating attained by only the very small number of flares that are great in all parts of the electromagnetic spectrum. (See Tables 2 and 3.) It is the frequent occurrence of these large H α flares with high Comprehensive Indices that made McM 11976 exceptional in 1972 and indeed in solar cycle 20.

Criteria other than magnetic complexity and great flares suggest that McM 11976 was outstanding, but not obviously unique, among the centers of activity of 1972. (See Table 2.) The calcium plage was neither larger nor brighter than that of several other regions in 1972. The included spot was not the largest of the year. The 9.1 cm flux associated with the August region was not markedly greater than that produced by McM 11748 (CMP Feb. 22) and 12094 (CMP Oct. 29). The 169 MHz flux was somewhat less than that of McM 11769 (CMP March 8). On the other hand, although McM 11976 was not the outstanding region of 1972 in these latter characteristics, it was well above average in all of them, and the Comprehensive Region Index (based on flares of importance ≥ 1 , SID's, spots, and centimetric and metric radiation) was 12, a relatively high value. This value was approximately matched in 1972 only by that of McM 11769 with CMP on March 8 and McM 12094 with CMP October 29. (See Table 2.)

TABLE 1

Data relating to Centers of Activity with Flares
associated with Ground-level Enhancement of Cosmic Rays:
Postmaximum Phase, Solar Cycles 19 and 20

Date of GLE	McM Plage Number	CMP of Region	Years after Max.	Spot		Region Index (a)	Number of Flares, Comp. Index ≥ 11 (b)	Max.2800 MHz Flux during Transit of Region
				Area	Mag. Class			
Postmaximum - Cycle 19								
1959 July 16	5265	July 14	1.3	1981	γ	13	4 (11, 12, 16, 15)	264
1960 May 4	5642	Apr. 27	2.1	1217	γ	8	1 (11)	167
1960 Sept. 3	5837	Sep. 10	2.5	832	γ	6	1 (14)	183
1960 Nov. 12) Nov. 15) Nov. 20)	5925	Nov. 12	2.7	1775	$\beta\gamma$	17	6 (11, 15, 15, 13, 16, 12)	200
1961 July 18) July 20)	6171	July 14	3.3	1512	$\beta\gamma$	13	5 (14, 16, 12, 12, 15)	147
Postmaximum - Cycle 20								
1971 Jan. 24	11128	Jan. 21	2.2	952) 627)	β_p β_p	7	2 (11, 13)	184
1971 Sept. 1 ^(c)	11482	Aug. 24	2.8	1857	$\beta\gamma$	12	0 ^(d)	154
1972 Aug. 4) Aug. 7)	11976	Aug. 4	3.7	1300	γ	12	4 (11, 14, 17, 15)	156

(a) The Region Index is based on flares of importance ≥ 1 , SID's, spots, and centimetric and metric radiation.

(b) The Comprehensive Flare Index is based on the ionizing and radio frequency emission of the flare as well as on its optical importance.

(c) Region was beyond west limb on invisible hemisphere at time of GLE.

(d) The GLE appears to have been associated with a major flare just after west limb passage. Comprehensive Index cannot be derived.

TABLE 2

Principal Centers of Activity(a) in 1972 (Jan.-Aug.) (b)

McM Plage No.	1972 CMP	Lat.	Long.	Plage		Flares			SID's	Spot		Region(d) Index
				Area	Int.	Imp. ≤1	Imp. ≥2	Comp. Index ≤11		Class	Max. Area(c)	
11693	Jan. 20	S15°	102°	5600	3.5	13	2	1	13	Bγ	500	7
11734	Feb. 16	S17°	100°	6400	3.5	10	1	0	19	Bp	550	5
11748	Feb. 22	N10°	21°	6500	4	5	1	1	32	Bp-Bγ B-Bγ	950	9
11769	Mar. 8	S08°	190°	4500	3.5	8	-	2	20	Bγ	1625	11
11827	Apr. 21	S12°	323°	5000	3	1	-	0	5	Bf-γ	575	4
11876	May 18	S05°	326°	4000	3	5	-	0	11	Bp	775	5
11883	May 20	S14°	299°	3600	3.5	5	-	0	6	Bγ	1150	9
11895	May 30	N09°	167°	3600	4	11	1	1	15	Bγ-γ	1025	9
11911	June 6	S12°	81°	4500	3.5	3	-	0	19	Bp-Bγ	625	7
11926	June 16	S13°	302°	5000	3	4	-	0	10	Bγ	?	4
11930	June 22	S10°	229°	3800	3.5	3	-	0	3	Bγ	825	4
11976	Aug. 4	N13°	10°	6000	3.5	12	3	4	17	γ	1300	12
12094(e)	Oct. 29	S12°	315°	6000	4	15	0	?	26	Bγ	2425	13

(a) Includes all centers of activity for which the Region Index was ≥ 4 , and all regions with flares with Comprehensive Index ≥ 11 .

(b) Data for later months in 1972 not yet available.

(c) Spot areas are primarily from Rome and Greenwich data.

(d) Region Index is based on number of flares, SWF's, spots, CM, and meter radiation associated with the plage.

(e) Preliminary data.

TABLE 3

Flares of Importance ≤ 1 in McM 11976, CMP August 4, 1972
(Based on data in SGD, No. 342 and Quarterly Bulletin Lists)

Date 1972	Time (U.T.)			Location	H α Imp.	Comprehensive Flare Index(a)	
	Start	End	Max.			Profile	Sum
Aug. 1	0655	- 0805	0704	N13 E48	(SN-1N?)	11-0-	≤ 2
Aug. 1	0841	- 1025	0927	N13 E47	1N	21-0-	≤ 3
Aug. 2(b)	0316	- 0800	0327 0410 0515 0739	N13 E35	(1N-2N?)	31322	11
Aug. 2	1838	- 1859	1844	N14 E26	1B	2120	≤ 5
Aug. 2	1958	- 2355	2023 2058	N13 E27	2B	22334	14
Aug. 4	0620	- 1000	0635	N14 E08	3B	33335	17
Aug. 7	0348	- 0450	0357	N15 W30	1B	1120-	≤ 4
Aug. 7	1053	- 1143	1103	N14 W34	1N	1110-	≤ 3
Aug. 7	1200	- 1230	1204	N13 W34	1B	1113-	≤ 6
Aug. 7	1443	- 1730	1500 1527	N14 W36	3B	33333	15
Aug. 11	0104	- 0127	0110	N10 W90	(1N?)(c)	010(3)-	≤ 4
Aug. 11	1217	- 1305	1221 1236	N12 W90	1B	21131	8

(a) See Report UAG-14 for description of this index.

(b) Reports for this flare are very difficult to summarize.

(c) Reported by one station only.

TABLE 4

McMath Plages in Solar Cycle 20 with at least Three Flares
with Comprehensive Flare Indices ≥ 11 , 1964-72 (August)

<u>Year</u>	<u>McM Plage</u>	<u>CMP of Region</u>	<u>Long.</u>	<u>Lat.</u>	<u>Number of Flares, Comp. Index ≥ 11(a)</u>	<u>Individual Flare Indices</u>	<u>Comp. Index of Region (b)</u>
1966	8461	Aug. 29	182°	N22°	3	(16, 13, 14)	11
1967	8818	May 25	227°	N26°	4	(12, 16, 12, 12)	15
1968	9740	Oct. 28	175°	S15°	4	(11, 12, 14, 13)	15
1969	9946	Feb. 23	60°	N16°	4	(12, 13, 12, 12)	10
	9994	Mar. 21	78°	N18°	3	(12, 14, 12)	13
	10134	June 10	87°	N17°	3	(14, 11, 12)	10
	10432	Nov. 22	74°	N11°	3	(14, 12, 13)	13
1970	10607	Mar. 5	158°	N08°	4	(11, 13, 11, 11)	9
1972	11976	Aug. 4	10°	N13°	4	(11, 14, 17, 15)	12

(a) The Comprehensive Flare Index is based on the ionizing and radio frequency emission of the flare as well as on its optical importance.

(b) The Comprehensive Region Index is based on flares of Imp. ≥ 1 , SID's, spots, and centimetric and metric radiation.

b. Comparison of McM 11976 with other regions in solar cycle 20

If the comparison is extended to all of solar cycle 20 prior to August 1972, McM 11976 continues to be unusual from the point of view of the frequency of great flares. There were only four other regions in cycle 20 which produced as many as four flares with Comprehensive Indices ≥ 11 , and in McM 11976 in August 1972 the individual flare indices, viz. 11, 14, 17, 15, were slightly higher than those in the other four regions. (See Table 4.) There was only one other flare in solar cycle 20 with an index as great as 17, the value of the index for the large flare on August 4, 1972. This was the flare on 1968 July 8d17^h08^m in McM 9503.

On the other hand, from the point of view of the general characteristics of region, McM 11976 in August 1972 appears to have been far from unique in solar cycle 20. There had been 15 centers of activity prior to August 1972 for which the Active Region Index was as great as 12, the value of the index for the August 1972 region. (See Table 5.) If, however, great-flare-occurrence and region evaluation are considered jointly, then there were only two other centers of activity in cycle 20 that were approximately equal to McM 11976 on both of these counts, viz. McM 8818 (1967 May 25) and McM 9740 (1968 October 28). (See Tables 4 and 5.) Both of these regions join McM 11976 in association with extensive particle emission and geophysical effects.

TABLE 5

Centers of Activity in Solar Cycle 20 with Active Region Indices ≥ 11 , 1966-1972

McM Plage No.	CMP of Region	Lat.	Region Index (a)	Spot		Number of Flares		Individual Flare Indices
				Class	Max. Area (b)	Imp. ≥ 1 (c)	Comp. Index ≥ 11	
8207	1966 Mar. 22	N20°	14	γ	1180	39	2	(11, 12)
8223	Apr. 3	N27°	12	$\beta\gamma$	1343	24	1	(14)
{8704	1967 Feb. 27	N23°	16	$\beta\gamma$ - δ	2040	38	1	(12)
{8740	Mar. 27	N21°	12	$\beta\gamma$	960	37	1	(12)
8818	May 25	N26°	15	$\beta\gamma$ - δ	1945	27	4	(12, 16, 12, 12)
{8905	July 28	N27°	18	$\beta\gamma$ - δ	1793	30	-	-
{8942	Aug. 26	N22°	12	$\beta\gamma$ - δ	1378	29	-	-
9184	1968 Jan. 31	N15°	16	$\beta\gamma$	2769	26	-	-
9740	Oct. 28	S15°	15	$\beta\gamma$ - δ	1382	33	4	(11, 12, 14, 13)
9994	1969 Mar. 21	N18°	13	δ	1583	24	3	(12, 14, 12)
10014	Apr. 3	N17°	11	δ	1847	4	-	-
10135	June 10	S16°	12	δ	2161	13	-	-
10385	Oct. 26	N12°	12	γ	1801	16	1	(11)
10432	Nov. 22	N11°	13	γ	1874 941	55	3	(14, 12, 13)
10789	1970 June 17	N19°	11	$\beta\gamma$	1503	31	1	(11)
11029	Nov. 14	N15°	14	$\beta\gamma$	2364	19	1	(13)
11482	1971 Aug. 24	S12°	12	$\beta\gamma$	1857	18	-	-
11769	1972 Mar. 8	S08°	11	$\beta\gamma$	1625	8	2	(12, 11)
11976	Aug. 4	N13°	12	γ - δ	1300	12	4	(11, 14, 17, 15)
12094 (d)	Oct. 29	S12°	13	$\beta\gamma$	2425	15	?	-

- (a) Based on data relating to flares, SID's, spots, and centimetric and metric radiation associated with the region.
- (b) Spot areas are primarily from Rome and Greenwich data.
- (c) For 1966 and 1967 the numbers of flares are taken from reevaluations based on total patrol hours [see UAG Reports 2 and 19]. For later years they have come from Quarterly Bulletin Data.
- (d) Preliminary data.

3. Place of McM 11976 on the solar surface

Very little is known about the relationships, if any, between the location of a great center of activity on the sun and that of prior or subsequent solar activity. In the course of development of a solar cycle, major activity appears to concentrate for relatively long intervals of time in what have been called "favored longitude zones." Additionally phase differences occur between the time of development of activity in the northern and southern hemispheres. There also is growing evidence from solar cycle 20 that there may be a sustained phase difference between activity in "favored longitudes."

McM 11976 with CMP on August 4, 1972 occurred at 13°N latitude and in Carrington longitude of $\sim 10^\circ$ (day 27 in Carrington Rotation 1590). According to our records this general portion of the sun did not produce a concentration of important centers of activity until relatively late in cycle 20. Furthermore, it was a zone of minimum activity in 1969 and again in 1971. Starting in February 1972, however, this apparently retarded portion of the sun developed a succession of above average centers of activity

which culminated in the formation of McM 11976 in the northern hemisphere in August and McM 12094 in the southern hemisphere in October. These regions were in the hemisphere of longitude $\sim 180^\circ$ away from the longitudinal zone in which activity had been concentrated in the early years of cycle 20 (1965-1967.5).

4. Summary

According to our evaluations, McM 11976 in August 1972 was a center of activity that was outstanding in solar cycle 20 because of the complexity of its magnetic fields and the frequency of occurrence of great flares. It was not a region that was uniquely great on the basis of calcium plage, sunspot, or ionizing and radio frequency emissions. It was, nevertheless, well above average in all of these latter characteristics and therefore had a relatively high Active Region Index. On the basis of both major flare production and region characteristics, McM 11976 in August 1972 was apparently similar to two other regions in the earlier years of solar cycle 20, viz. McM 8818 (CMP 1967 May 25) and McM 9740 (CMP 1968 October 28). The August 1972 center of activity occurred ~ 3.7 years after solar maximum. In solar cycle 19 there was an apparently similar active region, ~ 3.3 years after maximum, viz. McM 6171, CMP 1961 July. This latter center of activity was comparable to the 1972 August region on the basis of great flare production, region characteristics, and time in the solar cycle.

McM 11976 was located in a portion of the sun that did not develop major centers of activity until relatively late in cycle 20. It was in the longitudinal hemisphere $\sim 180^\circ$ from the part of the sun in which solar activity was concentrated during the early years of cycle 20 (1965-1967.5).

It is possible that the geophysical effects and particle emissions at the earth associated with McM 11976 in August 1972 were greater than those associated with the aforementioned similar solar centers of activity. If this is the case, part of the explanation may lie in the perhaps simpler circumstances in interplanetary space at the time of transit of McM 11976. In comparison to the other centers of activity in cycle 20, McM 11976 was late in the cycle rather than near times of maximum levels of activity. With respect to McM 6171 in 1961, it should be remembered that the 1972 August region occurred in the late phase of an average solar cycle rather than late in a cycle with the abnormally high maximum of cycle 19. In addition the specific geometry of the earth-sun system at the time of occurrence of each of the great flares also may have modified particle measurements near the earth.

Evolution of Solar Active Region MM 11976
(H α and K faculae and spots)

by

G. Godoli, V. Sciuto and R. A. Zappala
Osservatorio Astrofisico di Catania
Consiglio Nazionale delle Ricerche, Italy

The McMath region No. 11976, located at N12 and Carrington longitude 15°, was the main one during the concerned unusually active period (middle July, middle August). In Figures 1a - 1d the four transits of the active region are shown. The K and H α faculae associated with this region were first observed July 2 and 3, respectively. They lasted four rotations. The spot group associated with this region appeared July 12. It lasted three rotations. These figures were obtained from the heliograms of the K, H α and white-light Catania observations and from heliograms from the Rome Photographic Journal of the Sun.

The evolution curves of the K and H α faculae areas and of the sunspot group area are shown in Figures 2 and 3. The projected area A_p is given in 10^{-4} of the solar disk. The corrected area $A_c = \frac{1}{2} A_p \sec h$ (h = heliocentric angle) is given in 10^{-4} of the solar hemisphere. The circles indicate faculae or spots only partially visible on the disk.

The sunspot group according to Mount Wilson Observatory was a β magnetic type at its appearance on July 12 and had a δ configuration by its maximum on July 31.

From the analysis of the evolution curves the following are deduced:

- (a) the lifetime of the spot group, considering its maximum spot number, was in agreement with the mean lifetime for such groups [Kiepenheuer, 1952]. Its evolution curve is symmetric, i.e., the rise time is equal to the decay time;
- (b) before the August 7 event the K and H α faculae decreased remarkably, the H α facula reaching its minimum one day before the K facula (these observed minima are not part of the expected post meridian decrease);
- (c) K facula reached its maximum on August 8, H α facula on August 9;
- (d) the evolution curves of the H α and K faculae, compared with others of usual phenomena already studied [Godoli, Monsignori Fossi, 1967, 1968a; Godoli, Morgante, Sturiale, 1970], show no anomaly. In this case we can not argue that the facula decays quickly due to its great flare activity, as was done for the flares of August 28 and September 2, 1966 [Godoli, Monsignori Fossi, 1968b].

REFERENCES

- | | | |
|--|-------|---|
| GODOLI, G. and
MONSIGNORI B. C. FOSSI | 1967 | Sull'evoluzione delle facole cromosferiche in radiazione di calcio, <u>Lincei Mem. Serie VIII</u> , 8, 85. |
| GODOLI, G. and
MONSIGNORI B. C. FOSSI | 1968a | Evolution of Ca plage of the CSSAR active regions, in <u>Structure and Development of Solar Active Regions</u> , IAU, 326, K. O. Kiepenheuer, editor. |
| GODOLI, G. and
MONSIGNORI B. C. FOSSI | 1968b | The Ca plage of the active region No. 18521 (25N 184°) of the proton flares of August 28th and September 2nd, 1966, <u>Publ. Oss. Astrof. Catania</u> , 122. |
| GODOLI, G.,
O. MORGANTE and
M. L. STURIALE | 1970 | Evolution of the active region (H α and K faculae and spots) of the proton events of October 29 - early November 1968, <u>World Data Center A, Upper Atmosphere Geophysics, Report UAG-8</u> , 11. |
| KIEPENHEUER, K. O. | 1952 | <u>Solar Activity in The Sun</u> , Edited by G. P. Kuiper, 344. |

1972
JUL.

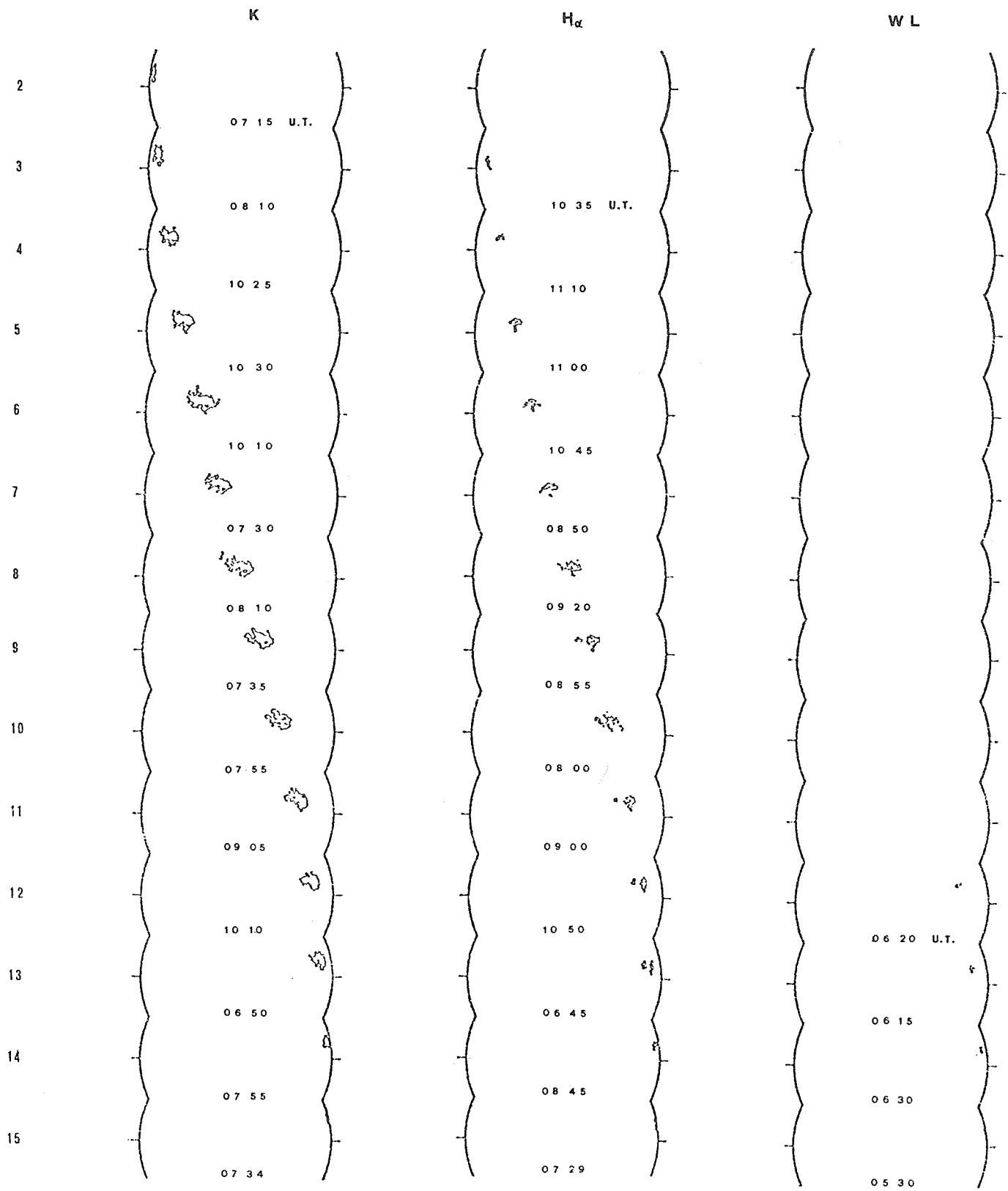


Fig. 1a. The first transit of the active region MM 11976, observed in K_{2,3,2'}, H α and white light.

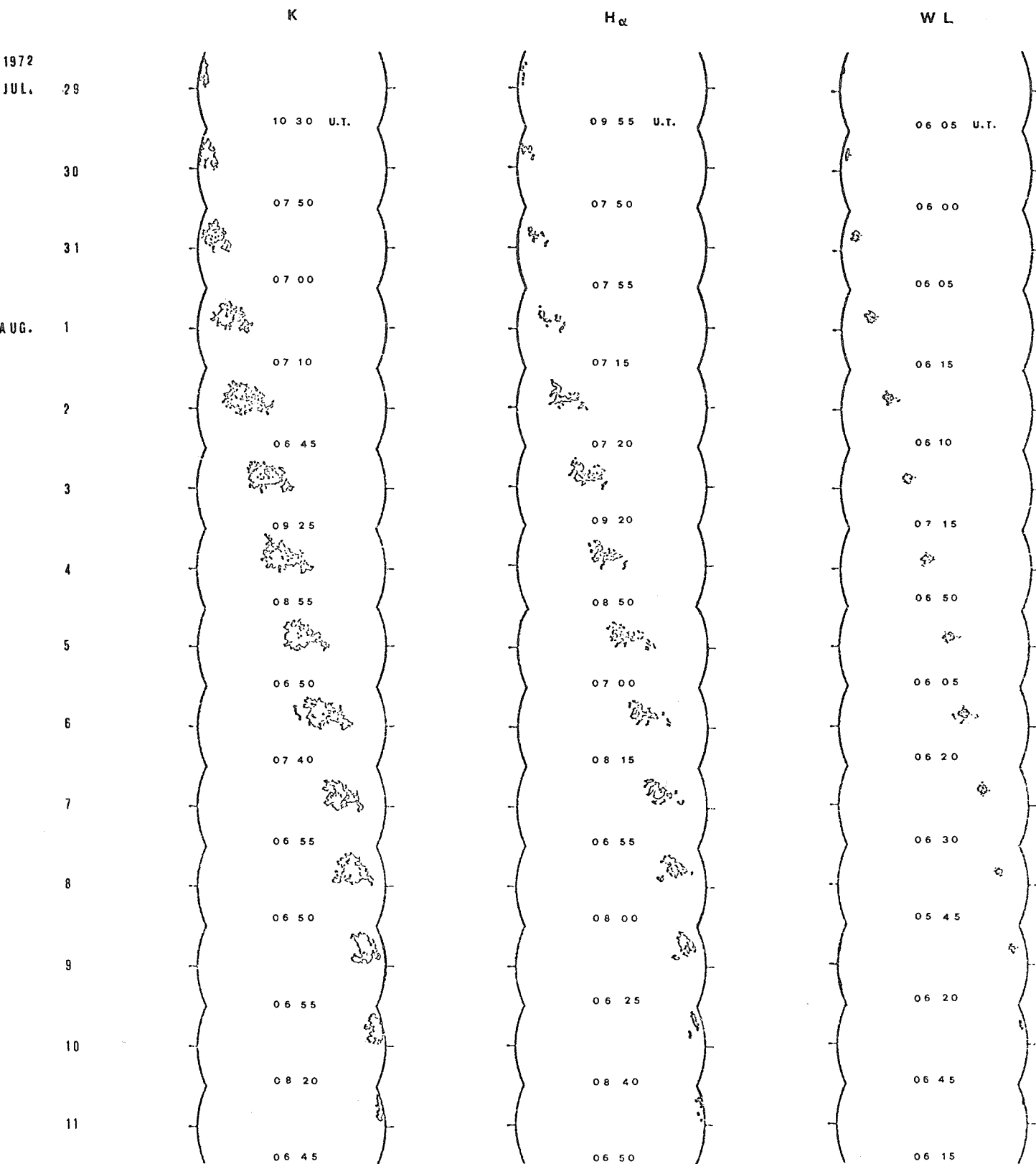


Fig. 1b. The second transit of the active region MM 11976, observed in $K_{2,3,2'}$, $H\alpha$ and white light.

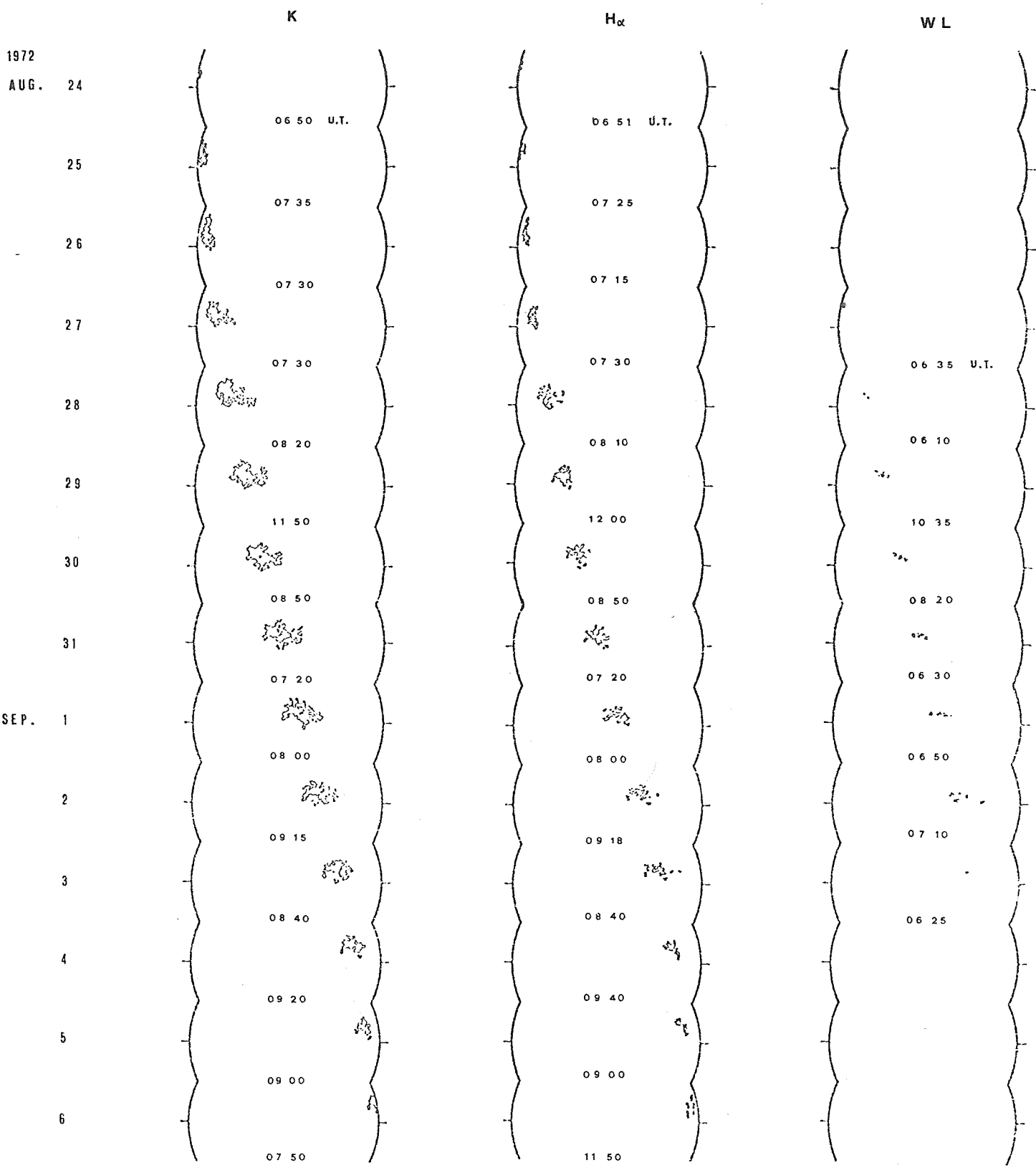


Fig. 1c. The third transit of the active region MM 11976, observed in K_{2,3,2}, H α and white light.

1972
SEP.



Fig. 1d. The fourth transit of the active region MM 11976, observed in K_{2,3,2'}, H α and white light.

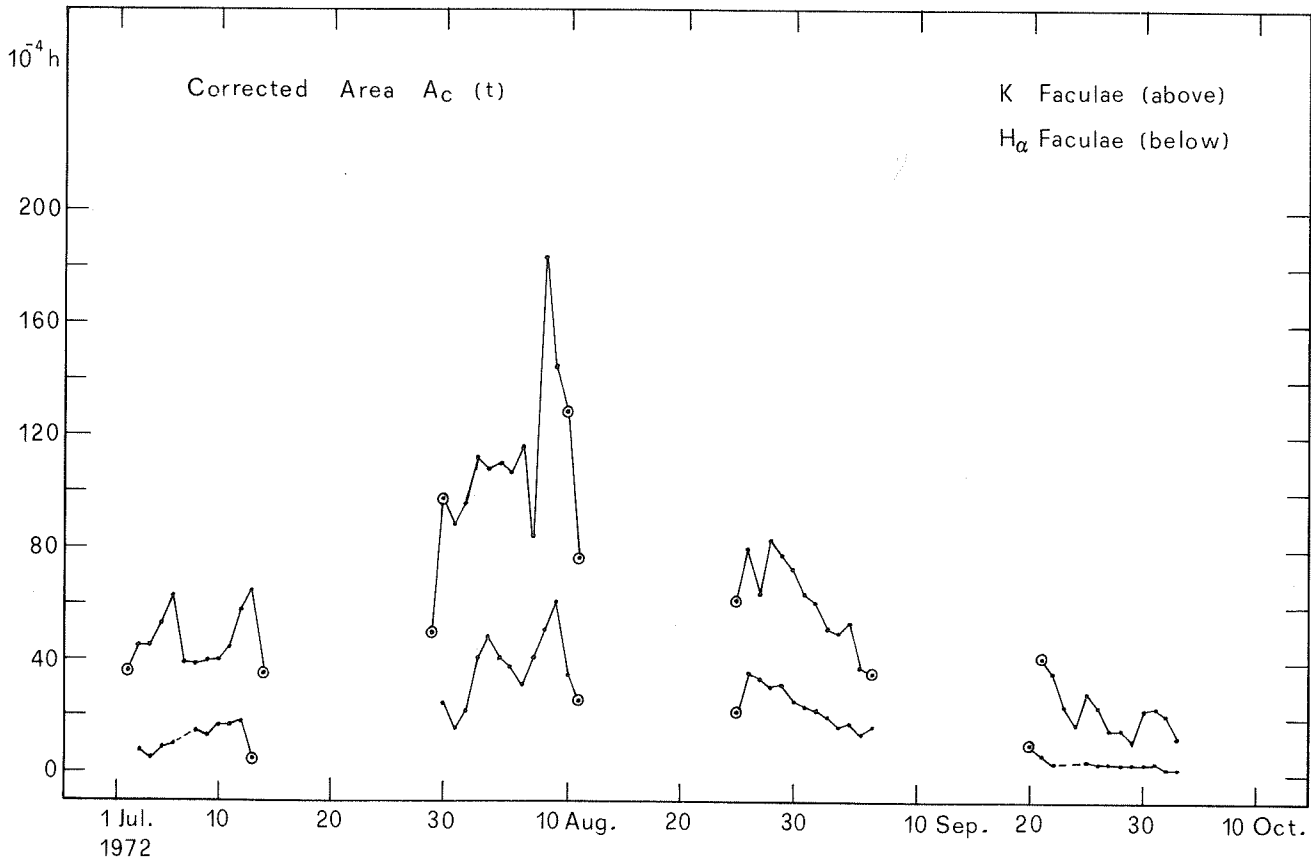
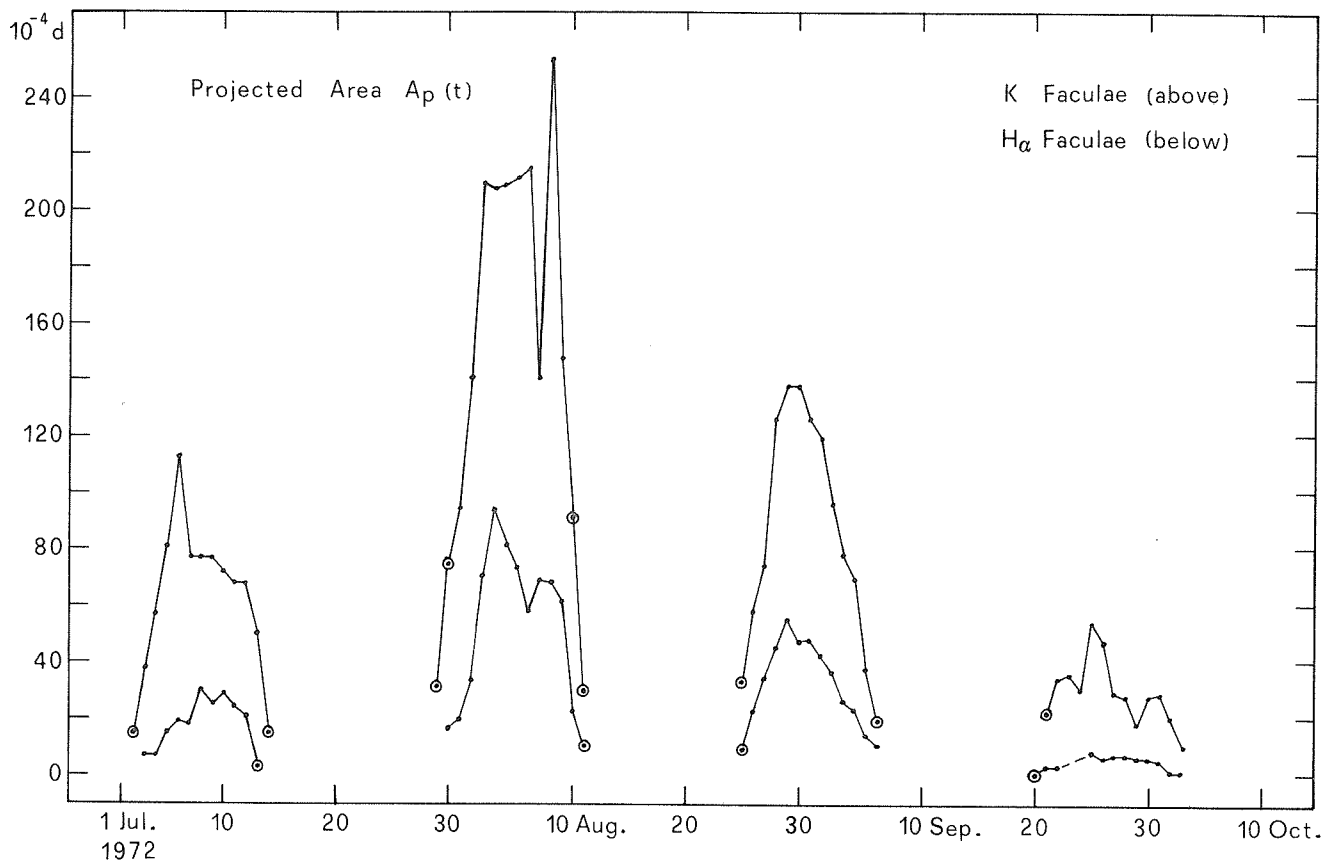


Fig. 2. Projected and corrected areas for K and H_α faculae.

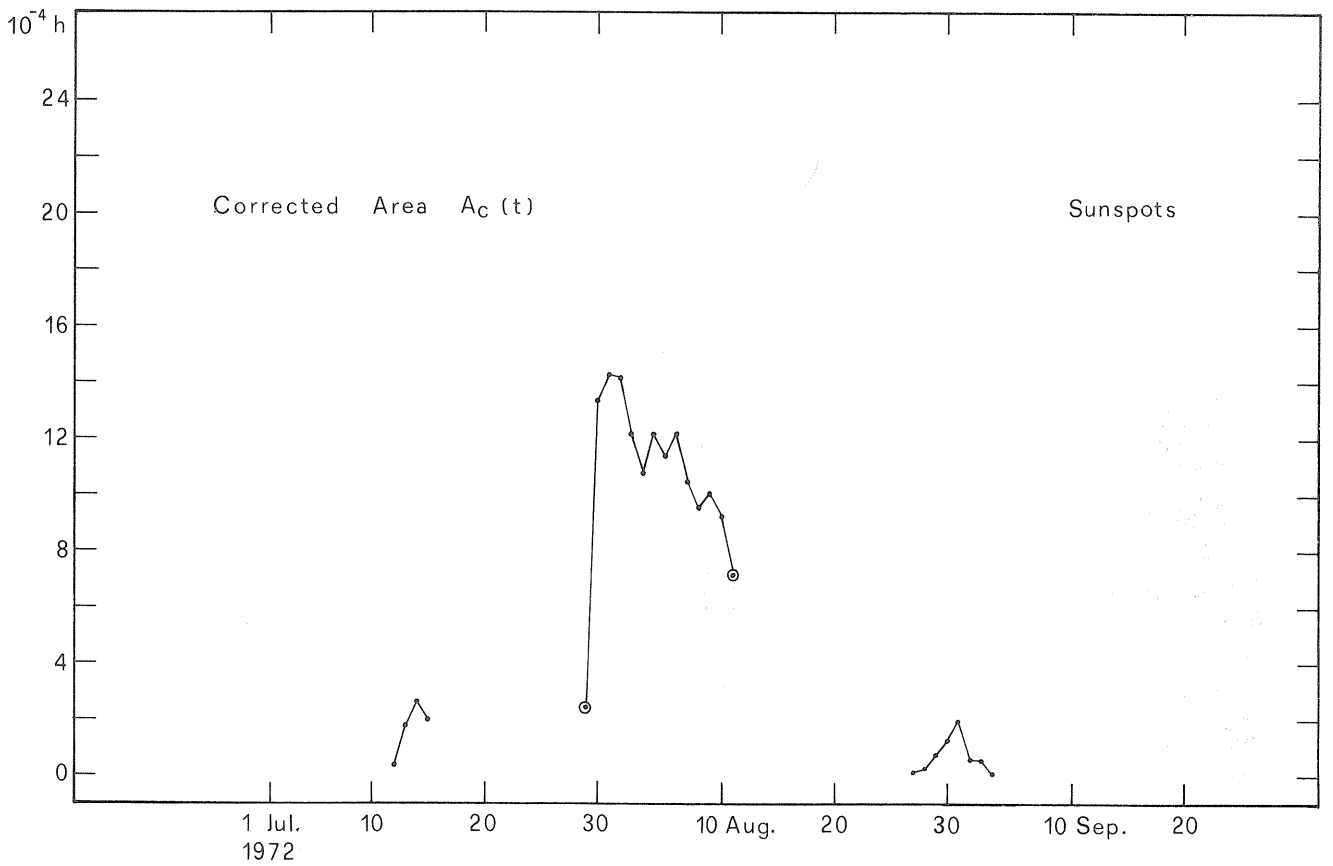
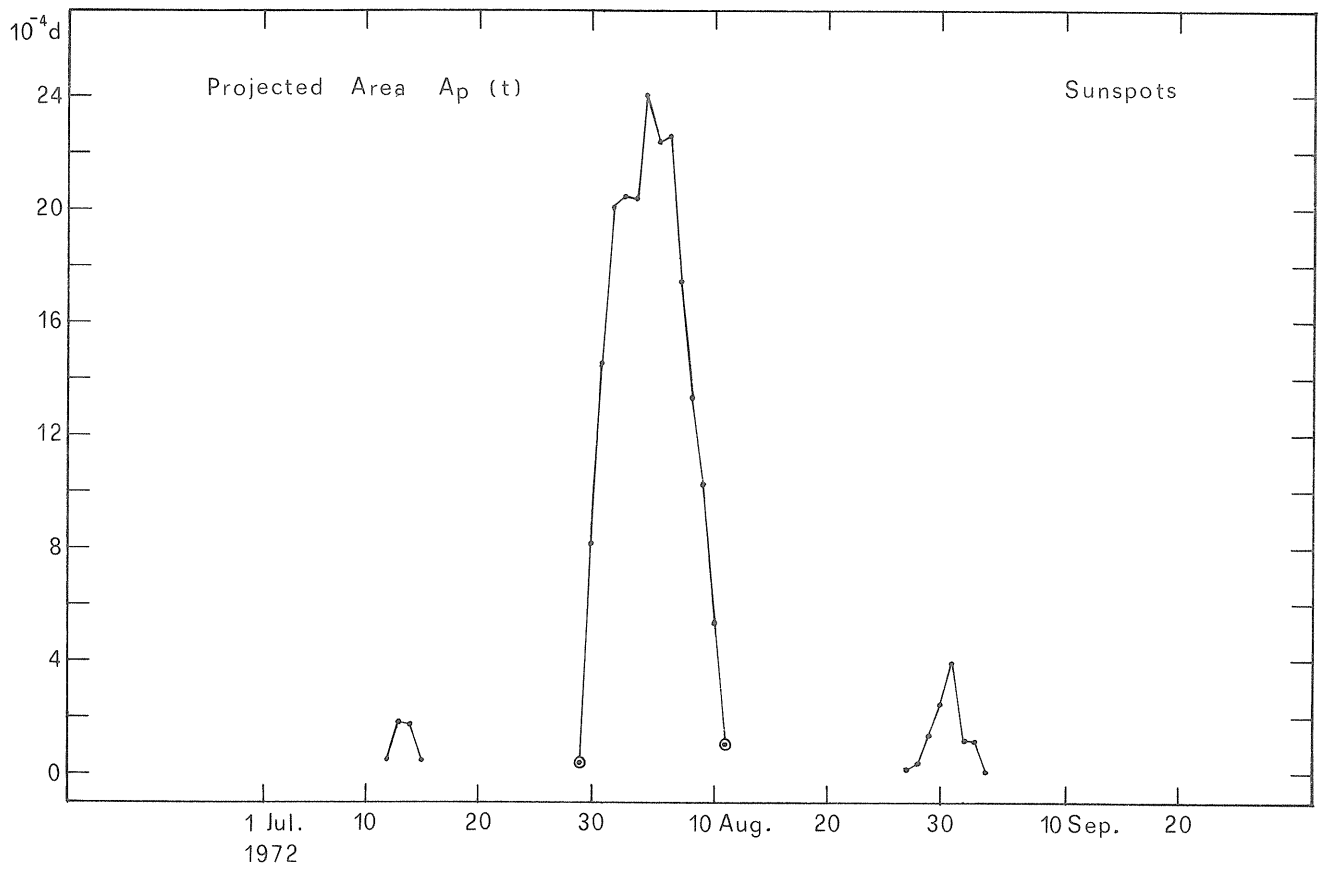


Fig. 3. Projected and corrected areas for sunspot group.

The Great Sunspot Group of August, 1972

by

Patrick S. McIntosh
NOAA Environmental Research Laboratories
Boulder, Colorado 80302

The sunspot group associated with the series of great cosmic-ray flares during August, 1972 possessed all the classic properties noted in earlier cosmic-ray active centers. The group appeared throughout its disk passage with a large total area (~1000 millionths of the solar hemisphere) invested in a single, circular penumbra encompassing all the major spots. This description was given to the typical proton-flare sunspot group by Anderson [1961] in his attempt to estimate periods "safe" from solar proton events. The magnetic field configuration illustrated in Figure 1 shows a highly convoluted longitudinal neutral line passing through the single penumbra, giving the group a magnetic classification of "delta"; i.e., there were strong spots of opposite polarity closely spaced within the same penumbra. In addition, the order of polarities from west to east was reversed from the normal order for northern hemisphere groups in the present solar cycle. Reversed polarity groups have been associated with exceptional flare activity [Smith and Howard, 1968] and delta configurations have a high correlation with proton flares [Warwick, 1966]. A careful study of the evolution of the sunspots below will show that one of the major magnetic poles was ejected from the penumbra during the period of intense flare activity, recalling the results of the study by Gopasyuk *et al.* [1963]. As in previous case histories of proton-flare sunspots, the details of the sunspot motions and growth patterns suggest a close relationship with the time and place of the major solar flares [McIntosh, 1969, 1970, 1972a, 1972b], giving additional support to the relationship of Evolving Magnetic Regions to flares [Martres, *et al.*, 1968].

The birth of the active center with McMath number 11976 occurred on 11 July on the western portion of the visible solar disk and only about five heliographic degrees east of what was then the largest active center on the solar globe. The new region continued to grow until it passed from view at west limb on 15 July, having formed a peculiar group with its dominant spot directly south of a cluster of smaller spots of opposite polarity. The coordinates of the large, leader-polarity spot (negative polarity) were N11 and Carrington longitude 009.

The appearance of the group upon its return on 29 July is shown in Figure 2. The original leader-polarity spot returned as spot C in our diagrams, with a large symmetric penumbra extending south of it. To its north were several large spots that were still increasing in size during the first days of the disk passage, suggesting that they may have formed only a few days prior to east limb appearance. It would be unusual for follower polarity spots to have survived during the entire two weeks of transit on the invisible solar hemisphere. If we can assume that spots that grow in unison are part of the same magnetic field system, then we were observing the emergence of a strong, new bipolar spot group with reversed polarities. The spots of leader polarity were spots D and E and the follower was spot B.

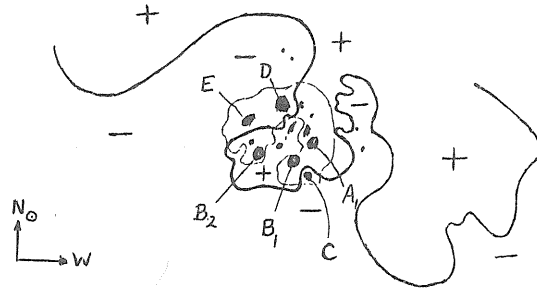
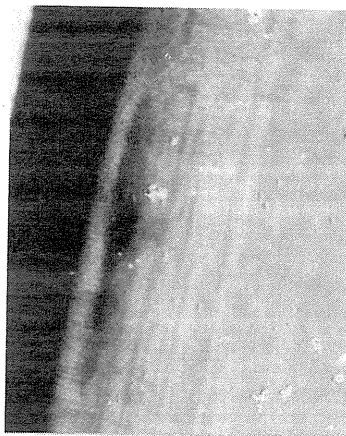
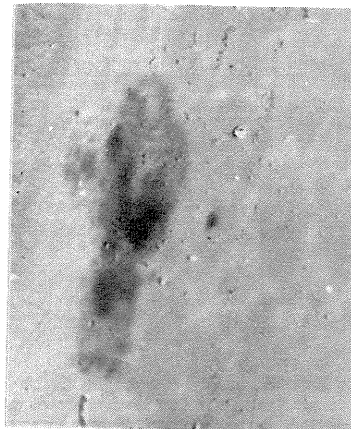


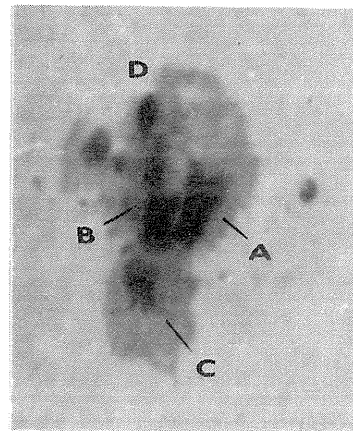
Fig. 1. The path of the longitudinal neutral line was inferred from H α structures photographed with Leinbach spectrohelioscope August 6 at 1816 UT [from McIntosh, 1972c]. The penumbra is lightly outlined.



29 July '72 1448 UT



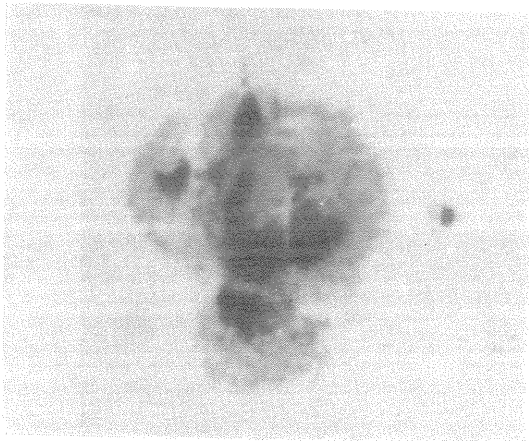
30 July '72 1430 UT



31 July '72 1548 UT

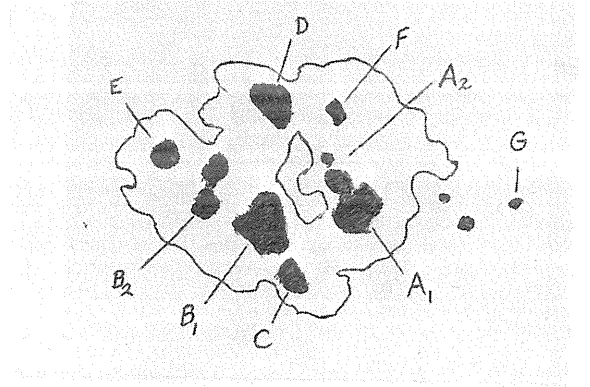
1 Arc Min

Fig. 2.



1 Aug. '72

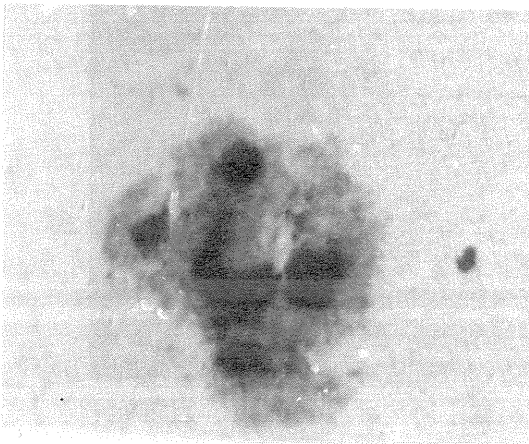
1638 UT



4 Aug. '72

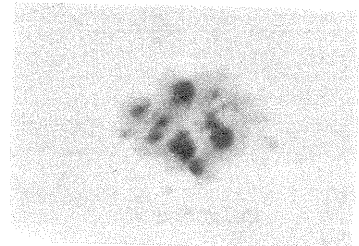
194649 UT

Tracing of low-resolution spectroheliogram at $\lambda 5169$ with Leinbach spectrohelioscope at N.O.A.A., Boulder, Colorado



2 Aug. '72

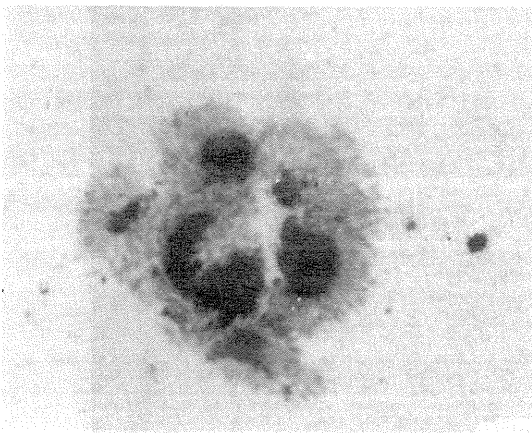
1348 UT



4 Aug. '72

2325 UT

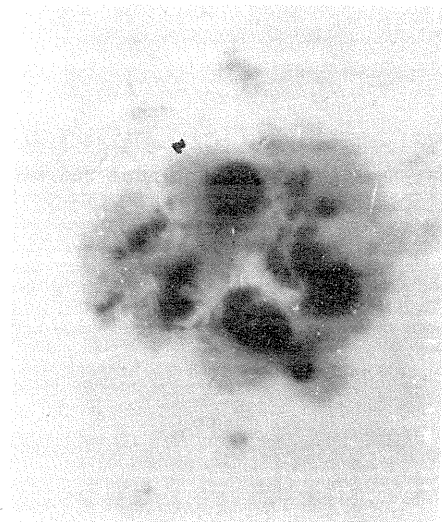
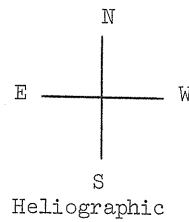
C.S.I.R.O. Culgoora Solar Observatory



3 Aug. '72

1427 UT

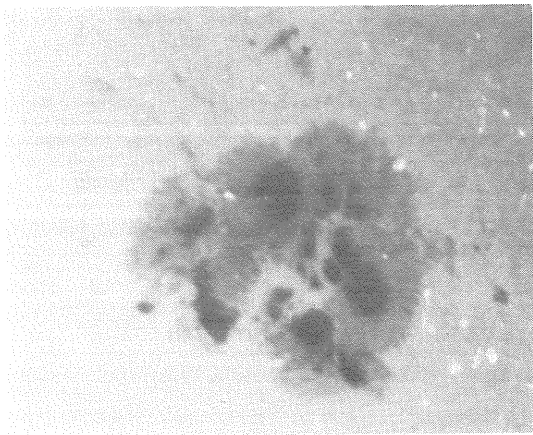
1 Arc Min



5 Aug. '72

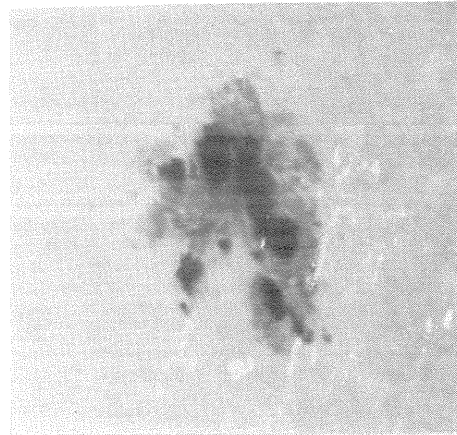
1615 UT

Fig. 3.



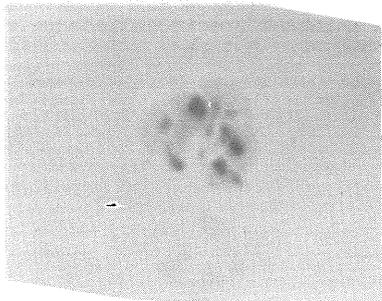
6 Aug. '72

1440 UT



8 Aug. '72

1351 UT



6 Aug. '72

2255 UT

Culgoora



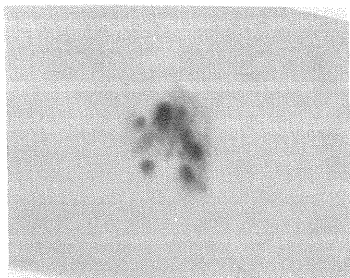
9 Aug. '72

2142 UT

7 Aug. '72

155327 UT

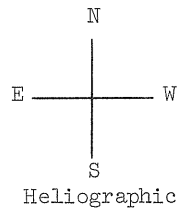
From spectroheliogram in continuum red side of λ 5169. By H. Leinbach



7 Aug. '72

2240 UT

Culgoora



10 Aug. '72

1320 UT

1 Arc Min

Fig. 4.

A study of the sunspot evolution in Figs. 3 and 4 shows that spot B split into two parts B₁ and B₂. At the same time B moved from the center of the penumbra to the southwest edge. This spot grew in unison with the growth of spots D and E and it was opposite in polarity to them; therefore, B-D-E represents a sunspot "group." The change in relative positions of these spots can be viewed as a rotation of the spot group axis in a clockwise sense, as if to turn the "reversed" orientation toward a "normal" orientation. The movements of both B and D led to increases in magnetic field gradients across longitudinal neutral lines between spots B and C and between spots D and F. The gradient D-F became the more important as spot C was diminishing in area while spot F was enlarging.

If we consider spots A, B and D as the primary poles of the sunspot group, the movement of spot B represents the expulsion of a primary pole from the group. This had the effect of changing the magnetic field configuration to a lower energy configuration. The powerful flares of August 2 occurred during the most rapid rate of movement for spot B.

Rotation of individual sunspots may have occurred. The fine structure on the southern border of spot B and on the western border of spot A was little changed during August 1-5, providing reference structure for detecting counterclockwise rotation of about 90° in both spots. This may be one of the first observational corroborations of a proposed mechanism for building energy content and instabilities in sunspot magnetic fields [Stenflo, 1969; Sturrock, 1972].

The times and locations of the several major flares, described in other contributions in this volume, were so correlated with the spot evolution that a common physical cause seems obvious. All the flares began within 10 arc seconds of the region of steep magnetic field gradient between spots D and F. The flares usually spread along the neutral line near spots B and C. The outstanding events on August 4 and 7 had initial flare segments centered over the strong umbra D. The first of the major flares occurred early on August 2, during the most rapid movement, splitting and rotation of spot B. The flares of August 4 and 6 occurred during the buildup of the gradient between D and F, with the growth of spots F and A₂ contributing more to the gradient than even the approach of spot D to these new spots.

What is the common "cause" of the flares and sunspot motions? The only conceivable force capable of moving and rotating magnetic fields of the strength and size of these spots is large-scale gas motions beneath the photosphere, where the hydrodynamic forces exceed the inertia of the frozen-in magnetic fields. The scale of these motions is such as to move and twist the magnetic fields in unison throughout the sunspot group. The shearing and twisting of magnetic fields are efficient mechanisms for storing energy and creating instabilities that suddenly release some of this energy [Sturrock, 1972].

The prediction of such flares with great geophysical effects can improve with the recognition of the structural and evolutionary similarities among proton flare sunspot groups. Effective forecasts can be made by simply recognizing the peculiar configurations of such groups. Precise prediction of flare times, locations and emission characteristics will surely require real-time analysis of sunspot growth and motions. High resolution magnetic field data, measured or inferred, is essential in this prediction process.

ACKNOWLEDGEMENTS

This descriptive report was made possible by the observations provided by the Sacramento Peak Observatory, AFCRL (Dr. J. W. Evans, Director); CSIRO Culgoora Solar Observatory (R. Giovanelli, Chief); and Dr. H. Leinbach of NOAA's Space Environment Laboratory.

REFERENCES

- | | | |
|---|------|--|
| ANDERSON, K. A. | 1961 | Preliminary study of prediction aspects of solar cosmic ray events, NASA Tech. Note D-700. |
| GOPASYUK, S. I., M. B. OGIR, A. B. SEVERNY, and E. F. SHAPOSHNIKOVA | 1963 | <u>Izv. Krymskoi Astrophys. Obs.</u> <u>29</u> , 15. |
| MARTRES, M. -J., R. MICHARD, I. SORU-ISCOVICI, and T. T. TSAP | 1968 | <u>Solar Phys.</u> <u>5</u> , 187-206. |
| McINTOSH, P. S. | 1969 | Sunspots associated with the proton flare of 23 May 1967, <u>World Data Center A, Upper Atmosphere Geophysics Report UAG-5</u> , 14-19. |
| McINTOSH, P. S. | 1970 | Sunspots associated with the proton flares of late October 1968, <u>World Data Center A, Upper Atmosphere Geophysics Report UAG-8</u> , 22-29. |

- McINTOSH, P. S. 1972a Sunspots and H-alpha plage associated with the GLE event of 24 January 1971, World Data Center A for Solar-Terrestrial Physics, Report UAG-24, Part I, 19-25.
- McINTOSH, P. S. 1972b Sunspots and H-alpha plage in McMath Region #11482, World Data Center A for Solar-Terrestrial Physics, Report UAG-24, Part II, 303-310.
- McINTOSH, P. S. 1972c August solar activity and its geophysical effects, Sky and Telescope, Vol. 44, 214-217.
- SMITH, S. F., and R. HOWARD 1968 In Structure and Development of Solar Active Regions (ed. by K. O. Kiepenheuer), D. Reidel, Dordrecht, 33-42.
- STENFLO, J. O. 1969 Solar Phys. 8, 115-118.
- STURROCK, P. A. 1972 Magnetic models of solar flares, in Solar Activity Observations and Predictions, ed. P. S. McIntosh and M. Dryer, MIT Press, 163-176.
- WARWICK, C. S. 1966 Astrophys. J. 145, 215-223.

Proper Motion in the Large Sunspot from July 30 to August 10, 1972

by

H. J. Pfister
Swiss Federal Observatory, Zürich

The large sunspot under consideration was of a type rarely found. It consisted of a large number of umbrae of different magnetic polarity. All of them were embedded in one of the same penumbra. Therefore, spots of opposite polarities were close together with large field gradients between them. This is believed to be a configuration favorable for the production of flares. The author has studied the proper motions of the individual umbrae and has proposed explanations of some of them.

The observational material shows the following characteristics:

1. On 31 July the complex spot group possesses three zones: a north section with southern polarity, a middle zone with northern polarity, and a south section with southern polarity. This magnetic field order is stable until 10 August. However, the sizes of the umbrae change. For example, the C component (Figures 1) shows considerable initial development but then becomes smaller and smaller.
2. On 6 and 7 August a very unusual observation was made. Within a bright spot in the penumbra, separate isolated umbrae were seen (this has been verified through photographs).
3. A long umbra (D, F in Figure 1) separated into two pieces from 3 to 4 August. This suggests that much activity was taking place even in the photosphere.

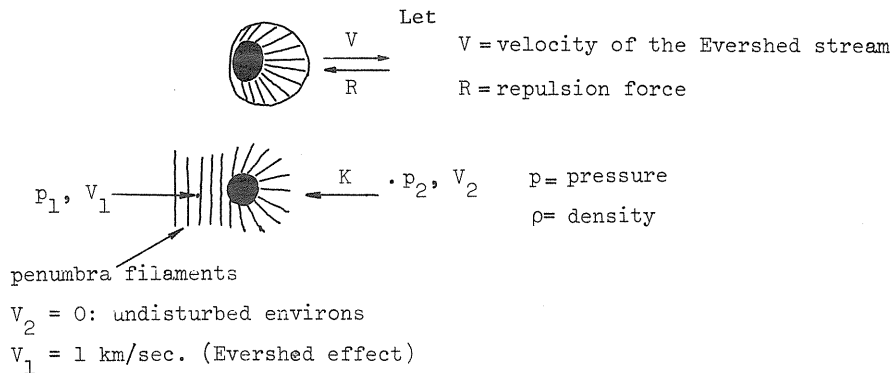


4. From a bright spot in the penumbra on 2 August a huge bay arises until 7 August. Especially from 6 to 7 August, a major form change occurs. Whether this has something to do with the massive flare on 7 August is not clear. As we shall see later, there could also be another explanation.



In Figure 2 the motions of the most important umbrae are shown. The A component is taken as stationary though the whole group shifts position about 2° northward. Umbra B shows little "real" motion ("real" motion here does not consider daily fluctuations, changes of form and inexact measurements). C moves after 5 August about 2° west. D moves eastward until 5 August, then southwestward. After 5 August E travels northwestward. The F component shows the most noticeable motion, about 3° . It moves towards the southeast after separation from spot D on 4 August.

An exceptionally good photograph of the spot group was taken on 5 August. One can easily recognize the shapes of the penumbra filaments (see Figure 3). The penumbra filaments (dark) are streams of matter which flow along the magnetic field (Evershed streams concentrate in tubes of magnetic fields). When the shape of the penumbra is irregular, i.e., the umbra is not surrounded symmetrically by the penumbra, these streams can exert forces on the spots (a comprehensive study is in preparation).



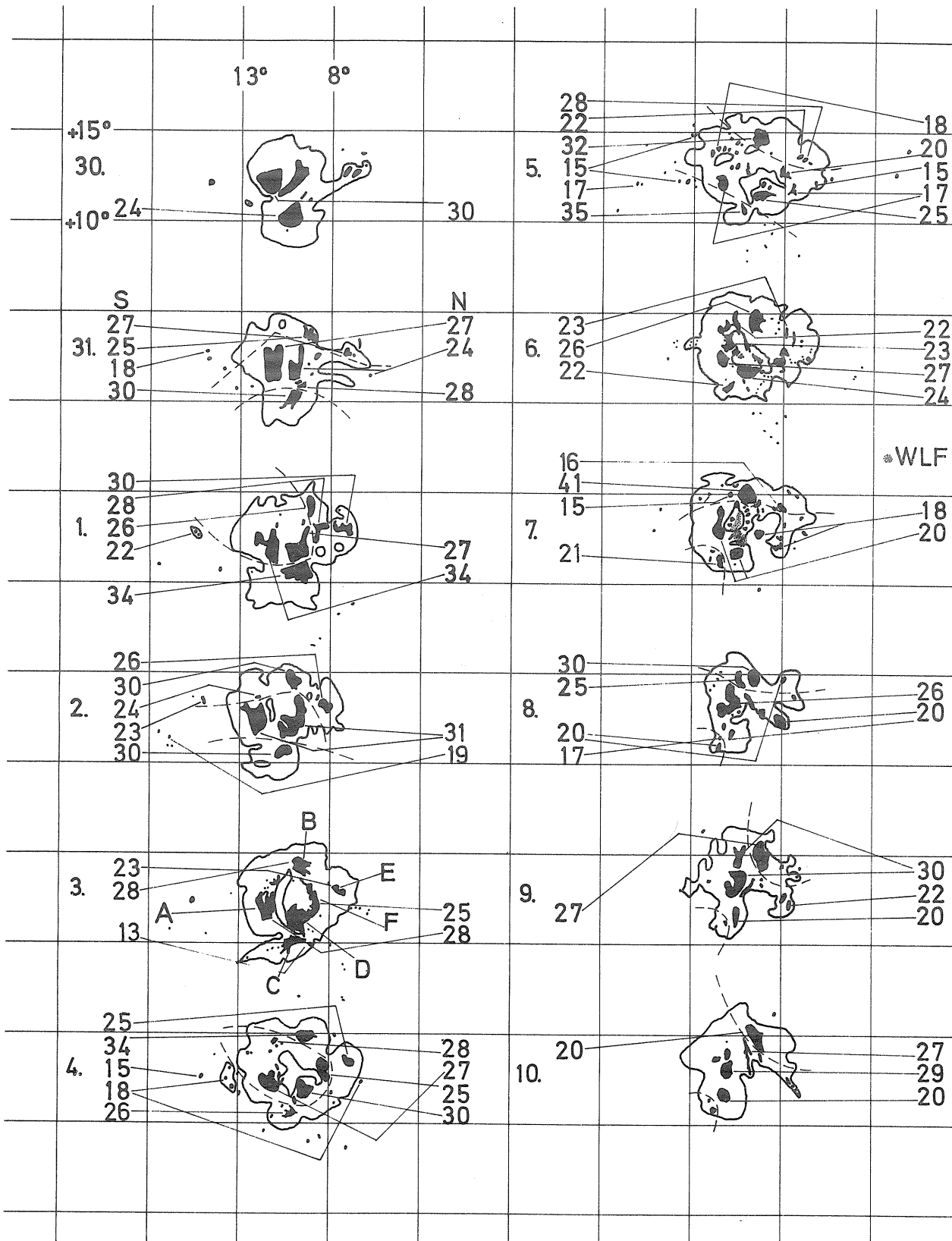


Fig. 1. In the development of the spot, north is at the top and west on the left. The magnetic field is given in units of 100 Gauss. The dashed lines separate regions with different magnetic polarities (taken from "Osservatorio Astronomico di Roma", and "Solar Data, U.S.S.R").

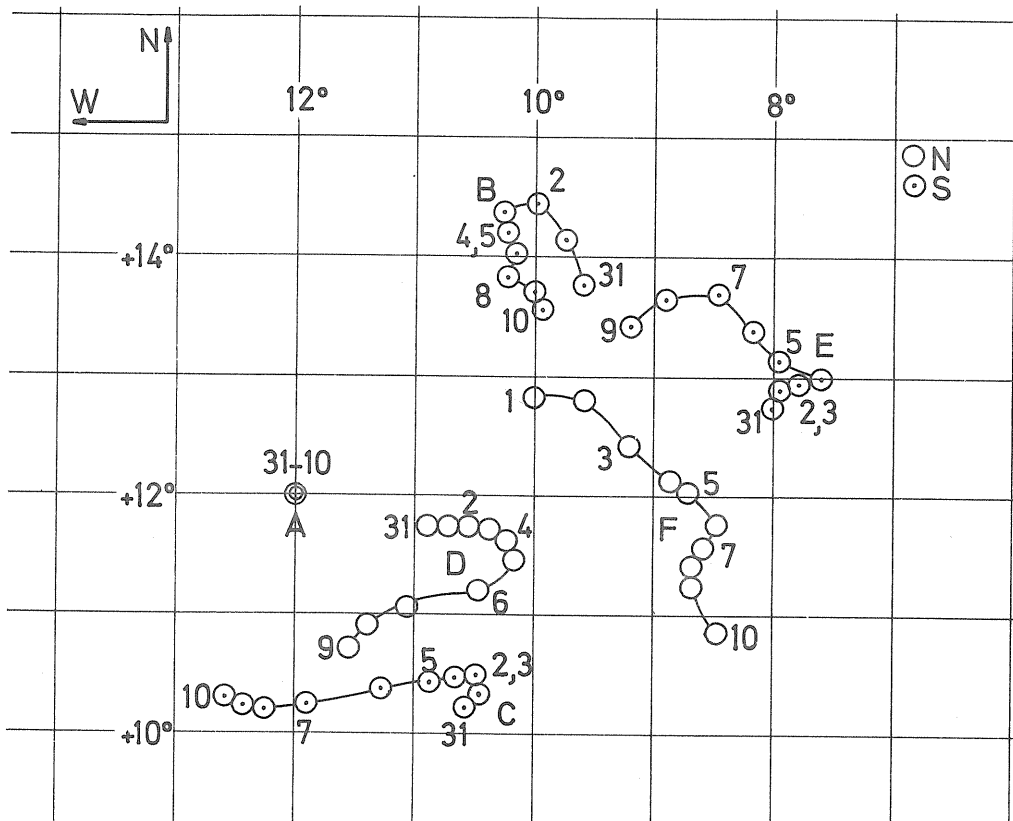


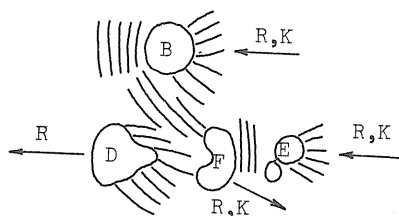
Fig. 2. Movements of the different umbrae.

Then the force due to a pressure difference is given by the Bernoulli equation:

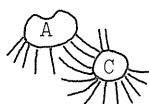
$$p_1 + \frac{\rho}{2} v_1^2 = p_2 + \frac{\rho}{2} v_2^2$$

Then $\Delta p = \frac{\rho}{2} v_1^2 \rightarrow K$

As Figure 3 shows, such situations are also found within this spot group. The origin of the bay on the southeast side is the effect of the Evershed streams as shown in the following sketch:



The umbra D recoils westwards because of the asymmetric penumbra. Meanwhile, F is moving to the east because of the asymmetric effects and the stream between F and E (the tangential tide causes a one-sided pressure reduction as the Bernoulli equation shows (K)). The result is that a bay is opened between D and F. The structure of the filaments around the E component on 5 August can be used to explain the change of direction of the motion between 3 and 5 August. A force on B in this direction is caused by the tangential filaments on the west side. The penumbra on the east side pushes this sunspot towards the west also. The flow of F towards the southeast is due to a similar situation. The westward motion of the umbra C starting on 4 August is probably due to the magnetic force of the umbra D and also a connection between C and A.



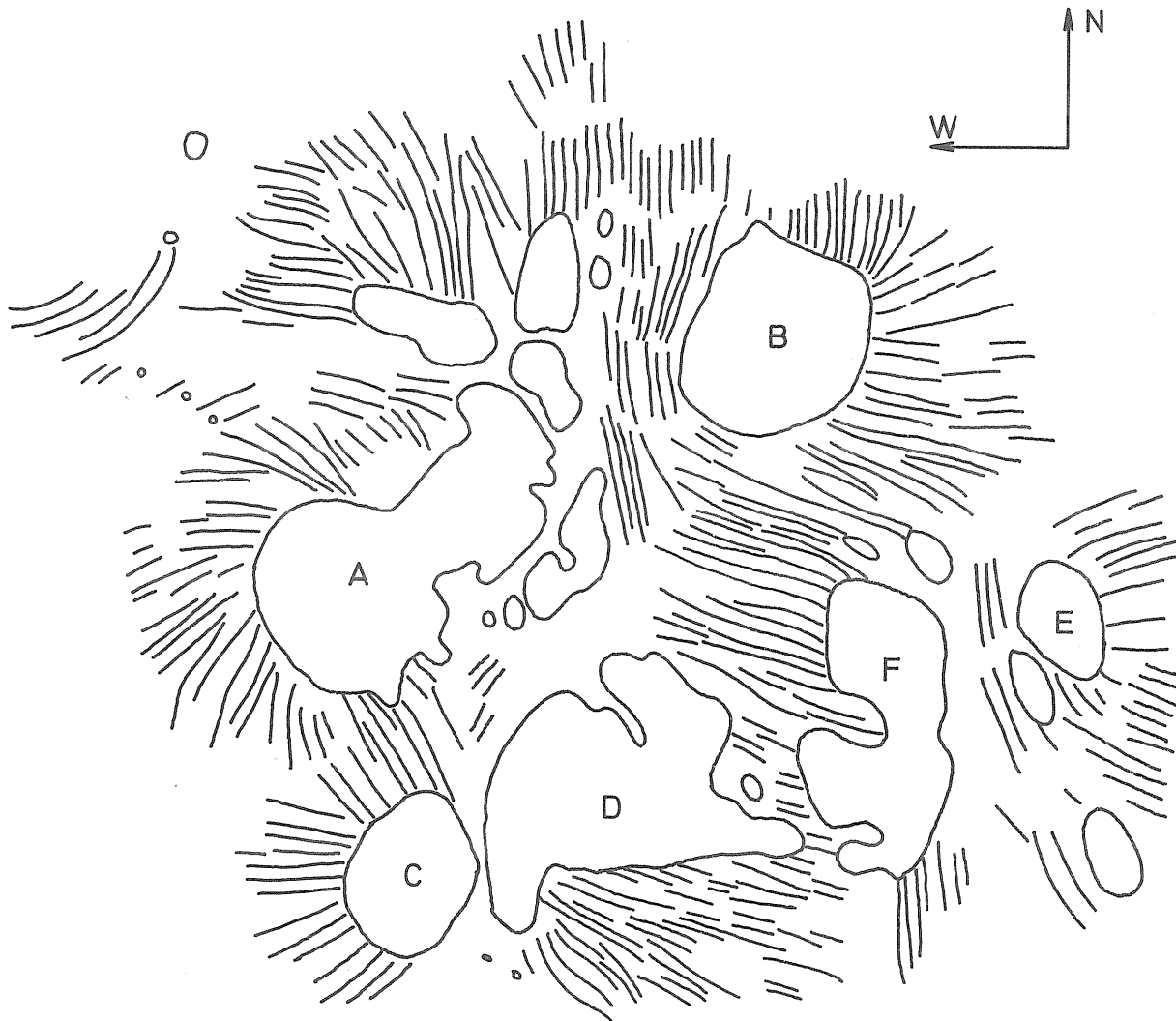
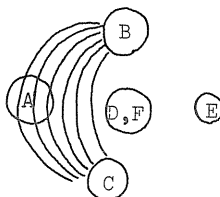


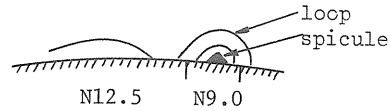
Fig. 3. The penumbra filaments drawn from a photograph in Sterne und Weltraum 10.72 (frontpage) taken on 5 August 1972.

The white light flare (WLF) which was seen on 7 August is located in two regions. One is south-east of the umbra B, exactly on the magnetic boundary line. The other is elongated and almost in the middle of the sunspot group, in a region with only northern polarity.

The next sketch shows an arch filament system [McIntosh, 1972; Rust, 1972]. Considering Frazier's description of arch filament systems [Frazier, 1972] and Figure 3, we see that at the northern foot of the arch the directions of the magnetic field are different in the chromosphere than in the photosphere. This shows that the region between the B and D, F components is magnetically unstable.



The foot points of the loop on 11 August have a heliographic latitude of N9.0 and N12.5 (1530 UT). At 1300 UT a large spicule was seen exactly in the middle of these positions.



This means that the southern foot is far outside the spot group and the northern one is near the middle of it, probably in the large bay on the southeast side.

Other sunspot groups showing penumbra filaments which are normal to the connecting line of umbrae of different polarities are also marked by much activity. Such regions must be extremely unstable.

I wish to thank Prof. Dr. M. Waldmeier for his helpful advice.

REFERENCES

- | | | |
|--------------|------|--|
| FRAZIER | 1972 | <u>SoI.Phys</u> , <u>26</u> , No. 1, 130. |
| McINTOSH, P. | 1972 | <u>Sky and Telescope</u> , <u>44</u> , No. 4, 214. |
| RUST, D. | 1972 | <u>Sky and Telescope</u> , <u>44</u> , No. 4, 226. |

Some Results of Spectrophotometric Studies of Prominences during July and August 1972

by

A. I. Kiryukhina
Academy of Sciences of the USSR
Moscow, U.S.S.R.

In July and August 1972, some prominences were observed on the solar instruments at the High Altitude Station ($h = 3000$ meters) of Sternberg Astronomical Institute near Alma-Ata. The spectrograms were obtained in the $3000 - 4400 \text{ \AA}$ region on ORWO photographic plates Blau Rapid. The solar image was about 140 mm and the spectral dispersion was about 2 \AA/mm . Simultaneously the prominences were photographed by means of the narrow band $H\alpha$ filter in the Coude refractor.

The clarity of the sky and the high optical quality of the spectrograph along with the great solar activity made it possible to obtain fine spectra. For almost all the prominences on these spectrograms the metallic lines are seen. Furthermore, the continuous spectrum in the visible region and beyond the Balmer limit was observed on the spectrograms of some of the prominences. Usually the continuous spectrum of prominences can be observed only during total solar eclipses.

Table 1 shows a list of observed emission lines of prominences. The wave lengths were taken from Rowland's table.

Table 2 provides information about the observation of 19 prominences which occurred between 26 July and 14 August. [See SGD, 1972 a, b for solar region identification.]

From the present observations it was found that the brightness of prominences, their structure, the line profiles in them and the degree of ionization as defined by the intensity ratio of the He and H lines are different for different prominences.

On Figure 1 one can see the $\text{Ca}^+ - \text{H}$ and $\text{Ca}^+ - \text{K}$ lines spectra of two different parts of the prominence near 70W on 12 August. In one of them, at 70W, the emission lines have regular forms and indicate the absence of line-of-sight motions in the prominence. Nearby there were two surges moving in the line-of-sight with velocities of 30 and 90 km/sec , respectively. In the other part of this prominence, at 65W, the emission lines show fine structure which indicates line-of-sight velocities between 30 and 120 km/sec .

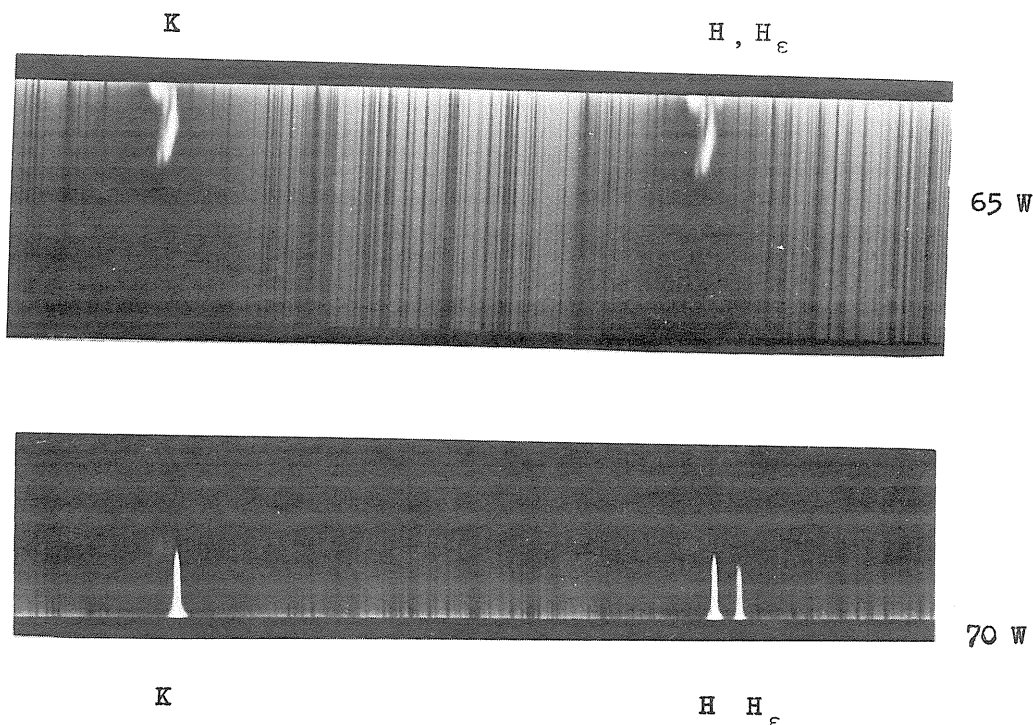


Fig. 1. H_{ϵ} , $\text{Ca}^+ - \text{H}$ and $\text{Ca}^+ - \text{K}$ line spectra of two different parts of the prominence near 70 W on 12 August.

Table 1

1	2	1	2	1	2
3066.227	Ti ⁺	3227.761	Fe ⁺	3341.835	Ti, Ti ⁺
3066.501	Fe-Ti ⁺	.809	Fe	.930	Fe
3072.115	Ti ⁺	3229.147	Fe	3342.585	Cr ⁺
3072.984	Ti ⁺	.208	Ti ⁺	3349.002	Ti ⁺
3075.239	Ti ⁺ , Fe ⁺	3229.426	Ti ⁺	.079	Cr
3078.662	Ti ⁺ , Fe ⁺	3232.290	Ti ⁺	3349.447	Ti ⁺
3088.039	Ti ⁺	3234.518	Ti ⁺	3354.390	Co, Zr ⁺
3110.704	Ti ⁺ , V ⁺	.647	Ni, Fe	3354.645	Ti
3118.656	Cr ⁺	3236.586	Ti ⁺	3358.515	Cr ⁺
3119.504	Fe	3239.052	Ti ⁺	3360.310	Cr ⁺
3120.372	Cr ⁺	3239.668	Ti ⁺	3361.193	Ti ⁺
3124.998	Cr ⁺	3242.007	Ti ⁺	.287	Ti ⁺
3128.706	Cr ⁺	3248.612	Ti ⁺ , Ti	3368.058	Cr ⁺
3132.055	Cr ⁺	.722	Ti ⁺	3372.812	Ti ⁺
3136.707	Cr ⁺ , Co	3251.857	Cr, V ⁺	3380.585	Ni
3143.242	Fe	.937	Ti ⁺	3383.765	Ti ⁺
3144.501	Fe, CH	3252.892	Ti ⁺ , Fe	3387.852	Ti ⁺ , Zr ⁺
3161.204	Ti ⁺	.970	Mn, Ti ⁺	3394.550	Ti ⁺ , Fe
3161.774	Ti ⁺	.038	OH	3403.271	Fe
3162.570	Ti ⁺	3254.261	Ti ⁺ (Fe)	.345	Cr ⁺
3168.435	Ti ⁺	3255.817	Fe ⁺	3408.779	Cr ⁺
.538	Ti ⁺	.901	Fe ⁺	3414.779	Ni
3179.342	Ca ⁺	.982	Ti ⁺	3421.221	Cr ⁺
3183.124	Fe ⁺	3261.584	Fe	3422.759	Cr ⁺
3186.752	Fe ⁺	.639	V ⁺	3433.318	Cr ⁺
.794	Fe	3276.135	Fe ⁺	3440.626	Fe
3187.713	V ⁺	3277.358	Ti ⁺	3441.019	Fe
3190.849	Fe	3278.295	Ti ⁺ , Ti	3441.982	Mn ⁺
.899	Ti ⁺	3278.935	Fe ⁺	3444.266	Ni
3192.824	Fe ⁺	3281.304	Ni	3444.331	Ti ⁺
3193.734	Fe, Fe ⁺	3281.868	Zr, Ti ⁺	3460.326	Mn ⁺
.816	Fe ⁺	3282.334	Ti ⁺	3461.499	Ti ⁺
3196.106	Fe ⁺	3287.667	Co, Ti ⁺	3474.060	Mn ⁺
3197.110	Cr ⁺ , Ni	3308.819	Ti ⁺	3475.457	Fe
3202.539	Ti ⁺	3315.329	Ti ⁺	3477.186	Ti ⁺
3209.185	Cr ⁺	3318.031	Ti ⁺	3482.909	Mn ⁺
3210.452	Fe ⁺	3321.707	Ti ⁺	3488.678	Mn ⁺
.480	OH	3322.325	Ni	3490.594	Fe
3213.311	Fe ⁺	3322.874	NH	3491.056	Ti ⁺
3214.776	Ti ⁺	.949	Ti ⁺	3492.975	Ni
3217.070	Ti ⁺	3326.777	Ti ⁺ , Zr ⁺	3504.892	Fe (Ti ⁺)
.097	V, V ⁺	3329.438	Ti ⁺ , Co	3510.846	Ti ⁺
3217.392	Fe, Cr ⁺	3332.109	Ti ⁺	3515.066	Ni
3222.855	Ti ⁺	.195	Mg	3524.536	Ni
		3335.185	Ti ⁺		
		3340.356	Ti ⁺		

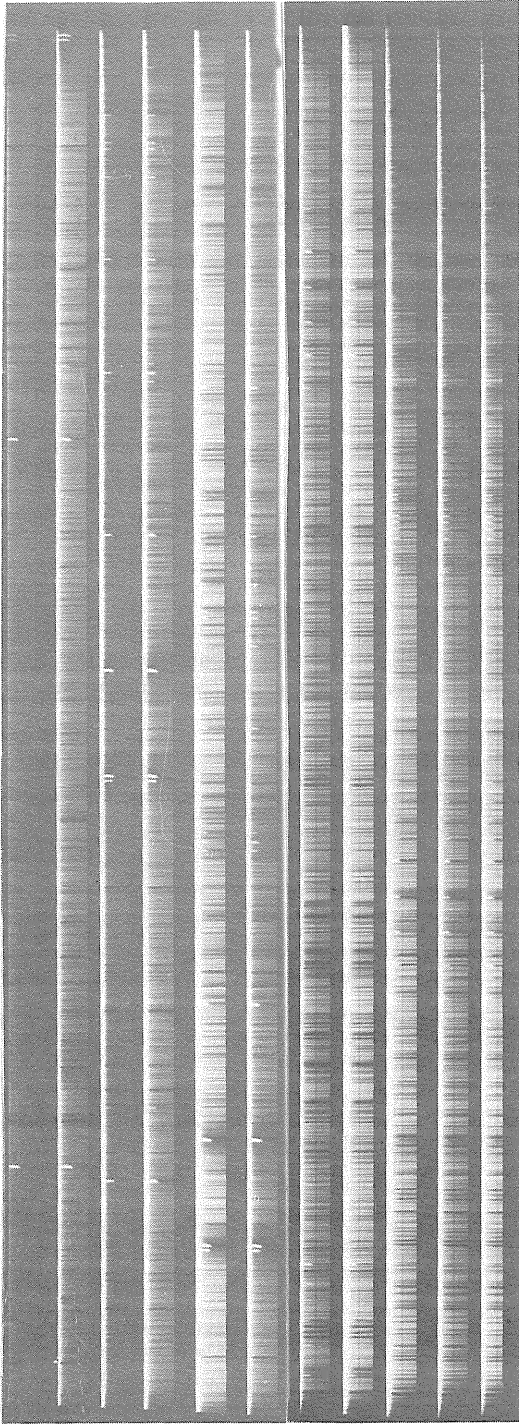
3558.532	Fe, Sr ⁺	3745.910	Fe
3565.396	Fe	3748.271	Fe
3570.134	Fe	3749.495	Fe
3572.478	Zr ⁺	3750.15	H ₁₂
.573	Sc ⁺ (Fe)	3758.245	Fe
3576.329	Sc ⁺	3759.299	Ti ⁺
.387		3761.320	Ti ⁺
3578.693	Cr	3770.63	H ₁₁
3581.209	Fe	3797.900	H ₁₀
3593.495	Cr	3815.851	Fe
3605.339	Cr, Co	3820.436	Fe
3608.869	Fe	3824.452	Fe
3613.809	Sc ⁺	3825.891	Fe
.881		3827.832	Fe
3618.777	Fe	3829.365	Mg
3619.400	Ni	3832.310	Mg
3624.839	Ti ⁺ (Fe ⁺)	3835.386	H ₉
3630.754	Ca, Sc ⁺	3838.302	Mg
3631.475	Fe, Cr ⁺	3856.381	Fe
3641.335	Ti ⁺	3859.922	Fe
3642.806	Sc ⁺	3878.580	Fe
3647.851	Fe	3886.175	Fe
3673.761	H ₂₃	.320	Ti ⁺
3676.365	H ₂₂	3888.646	He ₅
3679.355	H ₂₁	3889.051	H ₈
3682.810	H ₂₀	3900.541	Fe, Ti ⁺
3685.196	Ti ⁺	.44	
3686.833	H ₁₉	.412	
3691.557	H ₁₈	3900.836	—
3697.15	H ₁₇	3913.470	Ti ⁺
3703.86	H ₁₆	3933.682	Ca ⁺
3705.577	Fe	3944.016	Al
3709.256	Fe (Zr ⁺ , Ce ⁺)	3961.535	Al
3711.97	H ₁₅	3968.492	Ca ⁺
3719.947	Fe	3970.076	H ₅
3721.94	H ₁₄	4026.362	He
3734.37	H ₁₃	4077.724	Sr ⁺
3734.874	Fe	4101.748	H ₆
3736.917	Ca ⁺	4215.539	Sr ⁺
3737.141	Fe	4226.740	Ca
3741.645	Ti ⁺	4340.475	H ₇
3745.574	Fe		
.609	Sm ⁺ ?		

Table 2

Date 1972	Observation Time UT	Position Angle*	Prominence Lines Observed	Comparison of central intensities of He_{ζ} and H_{β}	Remarks regarding continuum spectrum
July 27	0300-0400 and 1000-1100	140 E	H, He, Mg, Ca^{+} , Ti^{+} , Fe	$He_{\zeta} \gg H_{\beta}$	all over the prominence
July 27	0400-0500	65 E	H, He, Ca^{+} , Ti^{+}	$He_{\zeta} = H_{\beta}$	in the dense part
July 29	0200-0500	140 E	H, He, Ca^{+} , Ti^{+}	$He_{\zeta} \gg H_{\beta}$	all over the prominence
July 30	0100-0530	145 E	H, He, Ca^{+} , Ti^{+}	$He_{\zeta} \gg H_{\beta}$	all over the prominence
July 30	0530-0600	70 E (near Region 976)	H, He, Ca^{+} , Mg, Ti^{+}	$He_{\zeta} < H_{\beta}$	in the dense part
				$He_{\zeta} = H_{\beta}$	in the part with fine structure
				$He_{\zeta} > H_{\beta}$	on the edge
July 31	0100-0420	85 W (over Region 972)	H, He, Mg, Al, Ca, Ca^{+} , Ti^{+} , Cr, Cr^{+} , Mn, Mn^{+} , Fe, Fe^{+} , Co, Ni, Sr^{+}	$He_{\zeta} \ll H_{\beta}$	all over the prominence
July 31	0420-0600	65 E	H, He, Mg, Ca^{+} , Ti^{+}	$He_{\zeta} = H_{\beta}$	in the dense part
				$He_{\zeta} > H_{\beta}$	on the edge
August 1	0330-0400	120 E	H, He, Mg, Ca^{+} , Ti^{+} , Cr^{+} , Fe, Fe^{+}	$He_{\zeta} < H_{\beta}$	in the dense part
				$He_{\zeta} > H_{\beta}$	on the edge
August 2	0200-0500	95-110 W	H, He, Mg, Al, Ca, Ca^{+} , Ti^{+} , Fe, Fe^{+} , Sr^{+}	$He_{\zeta} < H_{\beta}$	in the dense part
				$He_{\zeta} = H_{\beta}$	in the part with fine structure
				$He_{\zeta} > H_{\beta}$	on the edge
August 4	0200-0400	100 W	H, He, Mg, Ca^{+} , Ti^{+} , Cr^{+} , Fe, Fe^{+} , Ni	$He_{\zeta} < H_{\beta}$	in the dense part
				$He_{\zeta} = H_{\beta}$	in the part with fine structure
				$He_{\zeta} > H_{\beta}$	on the edge
August 10	0200-0500 and 0930-1100	120-130 E	H, He, Ca^{+} , Ti^{+}	$He_{\zeta} > H_{\beta}$	all over the prominence
August 10	0500-0800	75 W (near Region 976)	H, He, Mg, Al, Ca^{+} , Ti^{+} , Cr^{+} , Fe, Fe^{+} , Ni, Sr^{+}	$He_{\zeta} = H_{\beta}$	in the dense part
				$He_{\zeta} > H_{\beta}$	on the edge
August 12	0200-0500 0515-0600	70 W (near Region 976)	H, He, Mg, Al, Ca, Ca^{+} , Ti^{+} , Cr^{+} , Fe, Fe^{+} , Ni, Sr^{+}	$He_{\zeta} = H_{\beta}$	in the dense part
				$He_{\zeta} > H_{\beta}$	on the edge
August 12	0635-0800	75 E	H, He, Mg, Al, Ca, Ca^{+} , Ti^{+} , Cr^{+} , Fe, Fe^{+} , Ni, Sr^{+}	$He_{\zeta} < H_{\beta}$	all over the prominence
August 12	0840-0900	140 E	H, He, Ca^{+}	$He_{\zeta} > H_{\beta}$	all over the prominence
August 13	0300-0500	80 E	H, He, Mg, Al, Ca, Ca^{+} , Sc^{+} , Ti^{+} , V, Cr, Cr^{+} , Mn, Mn^{+} , Fe, Fe^{+} , Co, Ni, Sr^{+} , Zr^{+}	$He_{\zeta} < H_{\beta}$	all over the prominence
					continuum in visible region, Balmer continuum
August 13	0530-0600	140 E	H, He, Ca^{+}	$He_{\zeta} \gg H_{\beta}$	all over the prominence
August 14	0200-0430	85 E	H, He, Ca^{+} , Mg, Ti^{+}	$He_{\zeta} < H_{\beta}$	all over the prominence
August 14	0500-0515	65 E	H, He, Ca^{+}	$He_{\zeta} > H_{\beta}$	all over the prominence

* Position angle is measured from North to South along the East and West solar limbs.

$\lambda 4400\text{\AA}$



$\lambda 3050\text{\AA}$

Fig. 2. The spectrum of the bright prominence on 31 July over Region 972 at 85 W.

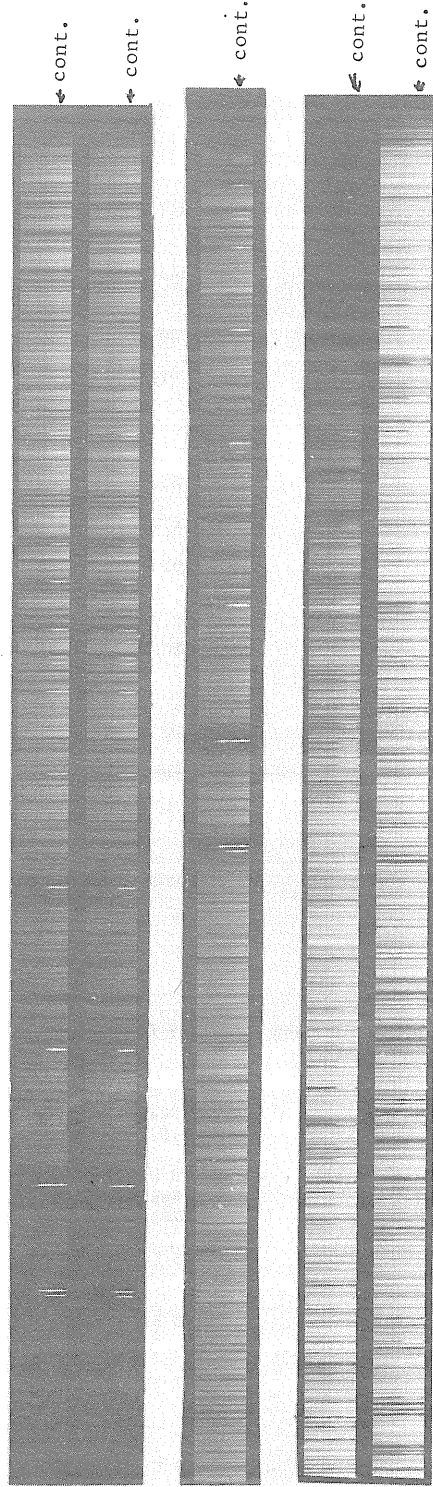


Fig. 3. The spectrum of the prominence on 13 August at 80 E, with continuum in the visible region and at the Balmer limit.

Figure 2 shows the spectrum of the bright prominence at 85W on 31 July over Region 972 [SGD, 1972a].

Figure 3 shows the spectrum of the prominence on 13 August at 80E. In the spectrum of this prominence it is obvious that one can see all the lines given in Table 1, including the Balmer lines from $H\gamma$ to H_{23} . Besides, continuum was observed in the visible region and at the Balmer limit.

Figure 4 shows the spectrograms of several prominences in the He_{ζ} and H_{δ} lines.

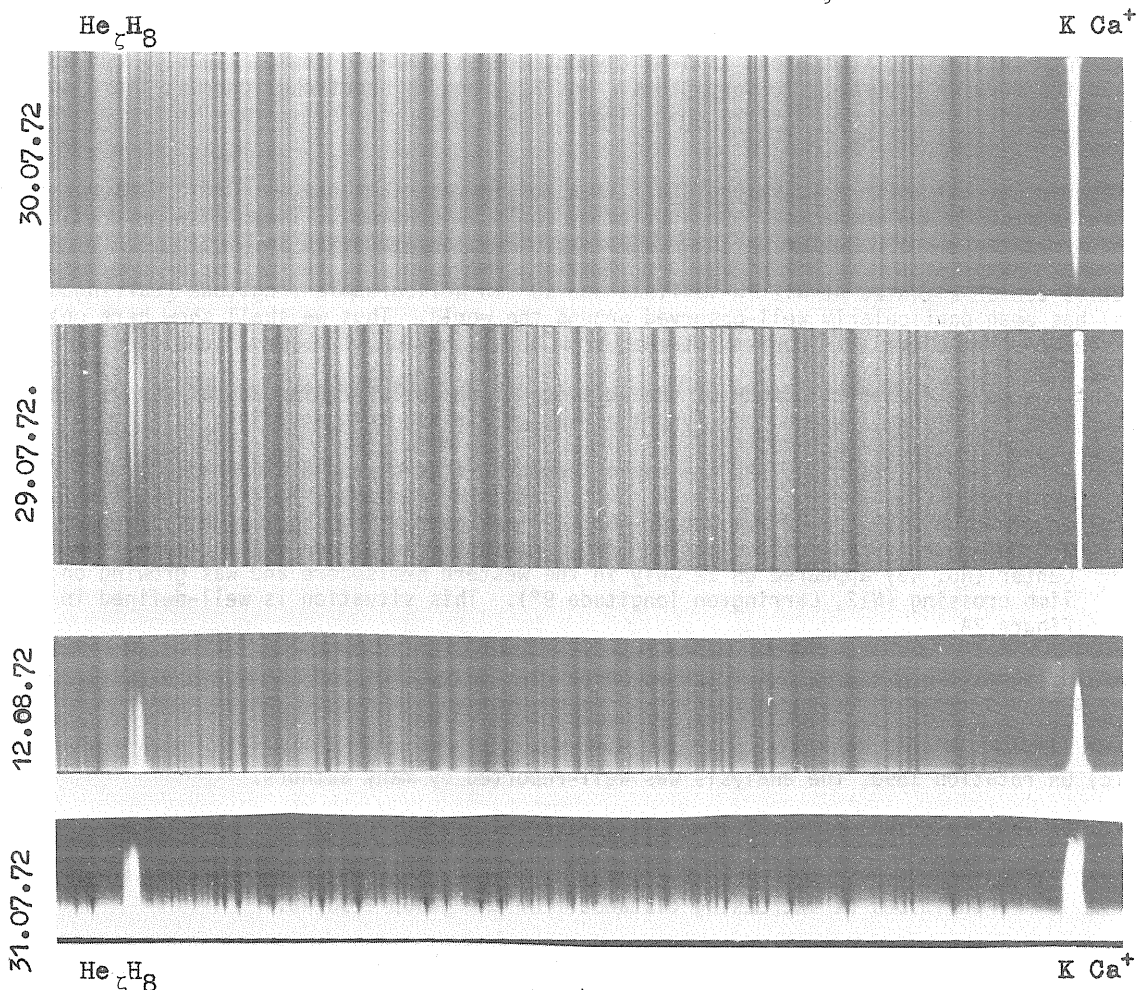


Fig. 4.

On the basis of these observations we should like to study whether the intensity ratio of the He_{ζ} and H_{δ} lines depends on the kinetic temperature or only on the fine structure of the prominence. The preliminary results of this study have shown a clear correlation between the ratio of He_{ζ} to H_{δ} and the fine structure of the prominences. Fine structure is noted in prominences where the He_{ζ} line is brighter than the H_{δ} line. On the contrary, in dense prominences, the H_{δ} line is brighter than the He_{ζ} line.

In the future we intend to investigate the profiles of emission lines in different prominences and to determine the kinetic temperature from the halfwidths of these lines and their variations inside a prominence.

Furthermore, we should like to define the kinetic temperature by studying the energy distribution in the continuum at the Balmer limit. Additionally, the central intensities and equivalent widths of the prominence emission lines will be measured.

REFERENCES

- | | |
|--------|--|
| 1972 a | <u>Solar-Geophysical Data</u> , 337, Part I, September 1972, U.S. Department of Commerce, (Boulder, Colorado, U.S.A. 80302). |
| 1972 b | <u>Solar-Geophysical Data</u> , 338, Part I, October 1972, U.S. Department of Commerce, (Boulder, Colorado, U.S.A. 80302). |

Contribution of Meudon to the Observations of the August Solar Events

by

M. J. Martres
Observatoire de Meudon
Meudon, France

During August 1972, the favorable weather in Meudon allowed a great number of optical observations on the very interesting spot group 1590-42 (Synoptic Maps), McMath region 11976. Most were obtained with the routine program of observations: $H\alpha$, K_{1V} , and K_3 spectroheliograms; flare patrol films; maps of Doppler and Zeeman effects; white light images of spots; heliograms in three wavelengths; automatic patrol in the $H\alpha$ line.

The gathering of all these data by one staff is a considerable advantage. Radio data recorded at Nançay are kept at Meudon where they are studied by radio astronomers. They allow an early analysis and comparison, and a posteriori comprehensive study and synthesis work.

The active center situated at N12 in latitude and 10° in heliographic longitude (Carrington coordinates) has been particularly well-observed around the world. Thus we shall show here only two examples of information about this center obtained from a combination of observations.

The first one is an historical study of the activity of the solar region and of the evolution of the center itself. Figure 1 drawn from Synoptic Maps summarizes the situation:

- (a) At the end of rotation 1588 the region appeared free of any disturbance.
- (b) On rotation 1589, an Active Center (No. 42) was born on the back side of the sun and decreased during disk crossing (N10, Carrington longitude 12°). Another active Center (No. 43) appeared on 12 July in the western hemisphere and was growing on its limb crossing (N12, Carrington longitude 9°). This situation is well-defined in Figure 2A.

At this latitude, the differential rotation being near zero, the conditions are present for the existence at the East limb, thirteen days later, of a complex active region issued from the interaction of the two mixed centers [Martres, 1968].

- (c) On rotation 1590, the analysis was well-reported by many authors.
- (d) On rotations 1591 and following, it is interesting to note:
 1. The appearance, successively, of many juxtaposed active centers and their positions at increasing distance from the group 1590-42.
 2. The duration of the whole perturbation of the region which lasts about 7 rotations.

The second example is an attempt to compare the three main flares observed during rotation 1590, on 4, 7 and 11 August.

Let us pay attention to several points:

- (a) The two very bright points or ribbons from which the flash phase starts are always exactly situated at the same mean coordinates: N13, Carrington longitude 10° , that is to say at the right point of the contact between the two centers No. 1589-42 and 43 (points marked by arrows on Figures 3 and 4).
- (b) Note how poorly the transformations are reflected by the faculae and the filaments (Figure 2B). No "disparition brusque", even transitory, is observed. The greatest modifications are those which concerned the relative dimensions of the umbrae of the spots and their relative disposition. In the long term, it is necessary to take into account the appearance to the South of the "filaments-sourcils" and their growing distance to the spots.
- (c) The recording of the flare which occurred on 11 August on the West limb seems particularly interesting (Figure 5). Each minute we recorded three successive images with the three wavelength automatic patrol, in the center of the line and at $\pm 0.7 A$, with a three second delay between successive images.

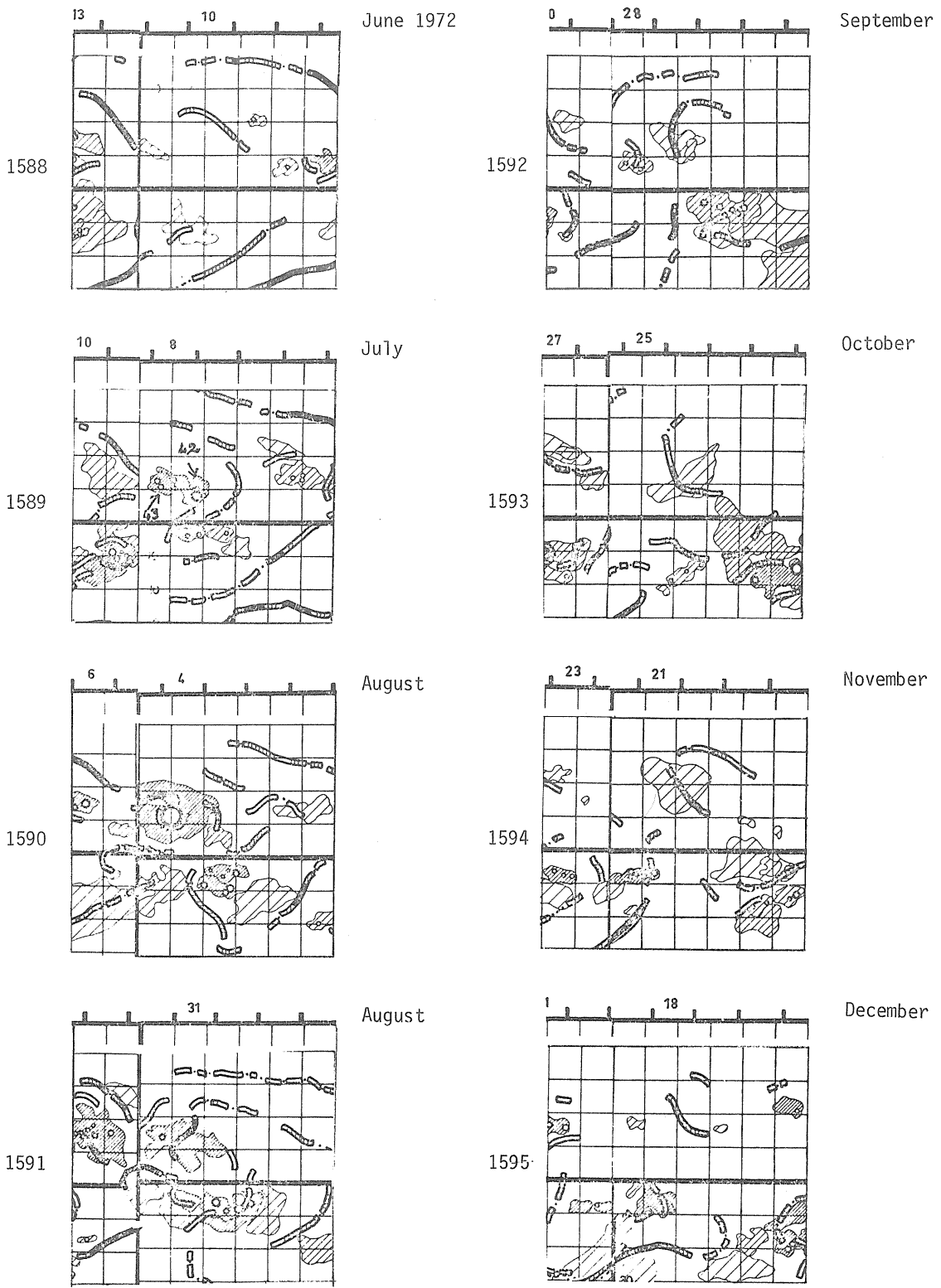


Fig. 1. Historical synopsis of solar activity for June-December 1972 for the region at N12, 10° Carrington longitude drawn from Synoptic Maps.

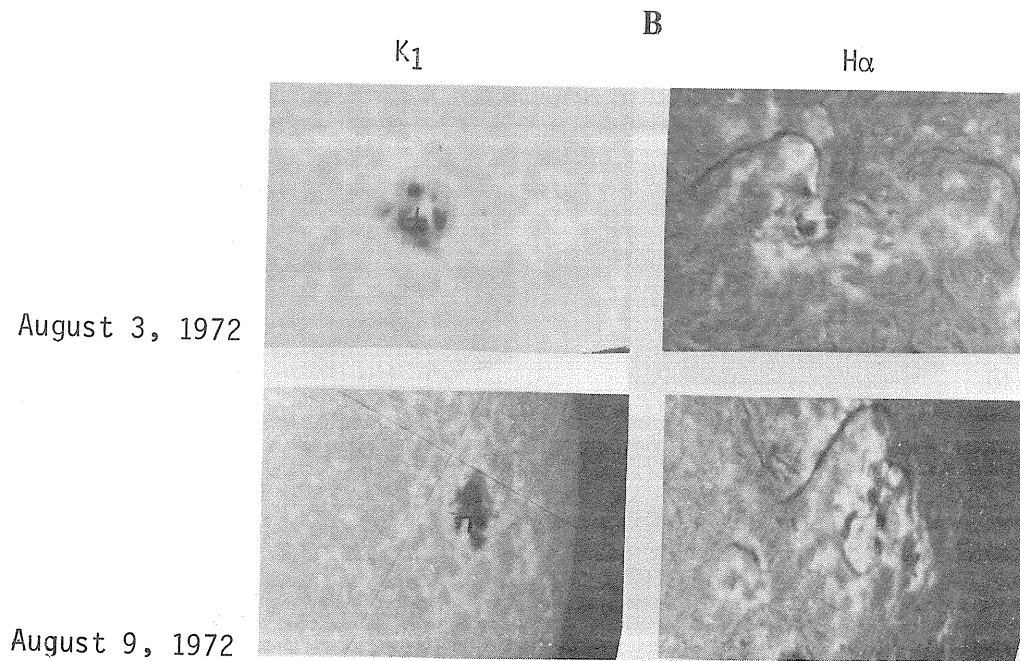
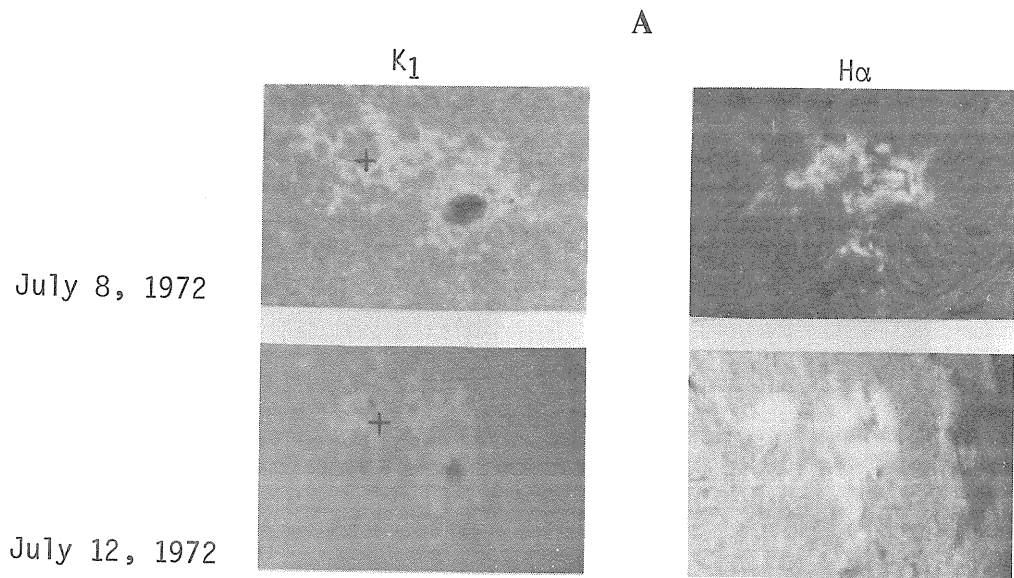


Fig. 2A and 2B. K_1 and $H\alpha$ Spectroheliograms taken at the Meudon Observatory for heliographic latitude N12 and 10° Carrington longitude.

August 4, 1972

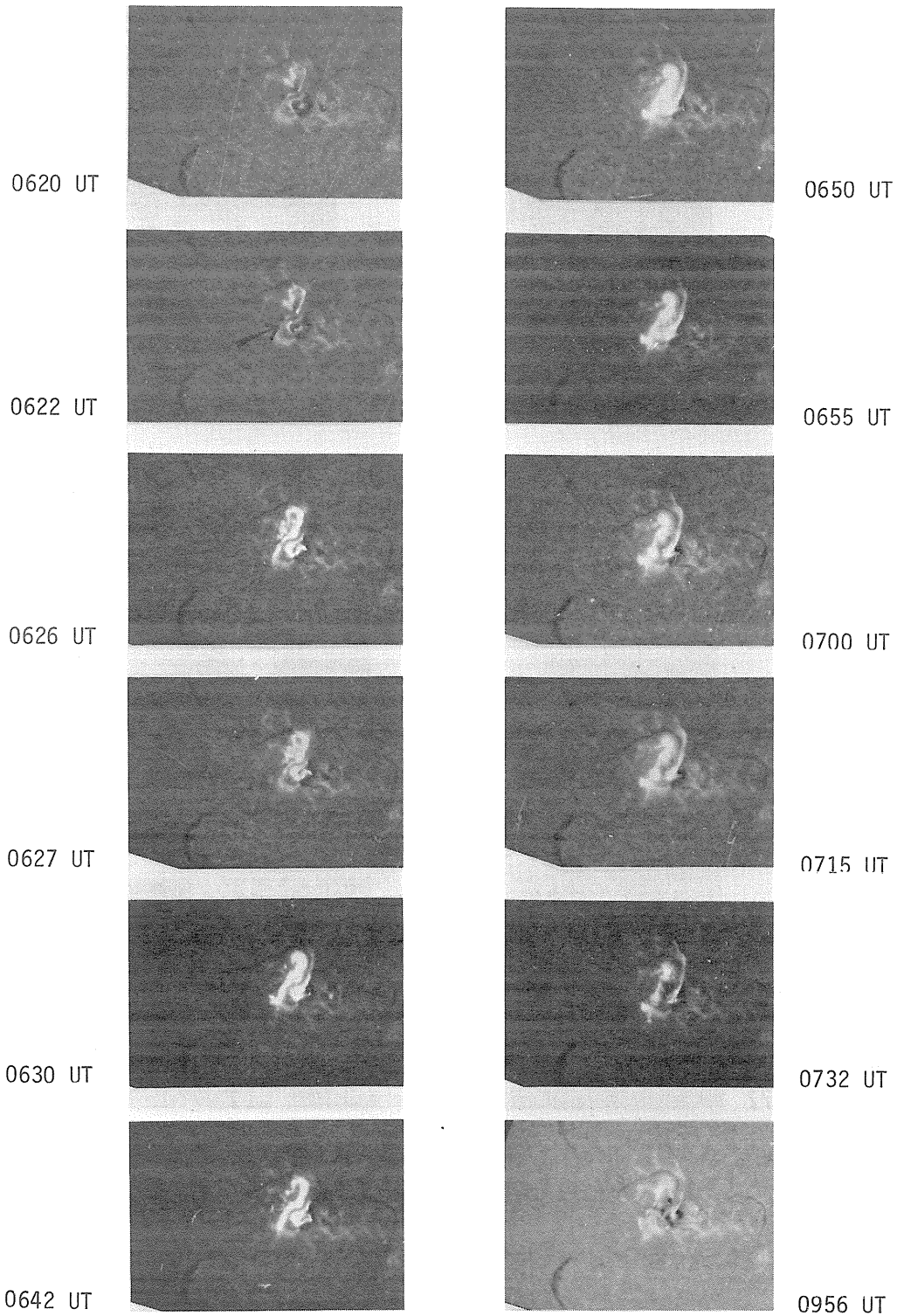


Fig. 3. Heliographic photographs taken at Haute Provence Observatory

August 7, 1972

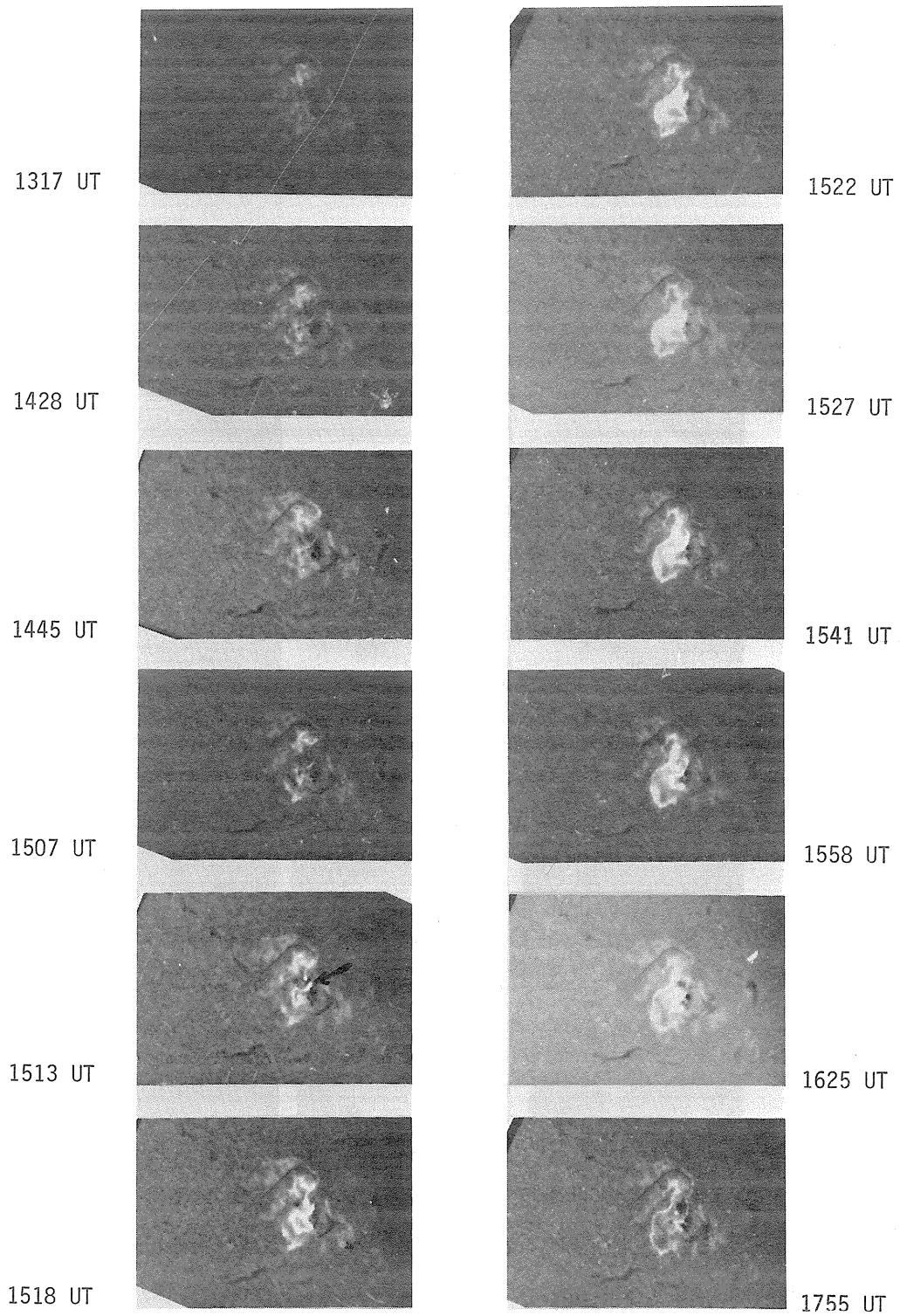


Fig. 4. Heliographic photographs taken at Haute Provence Observatory.

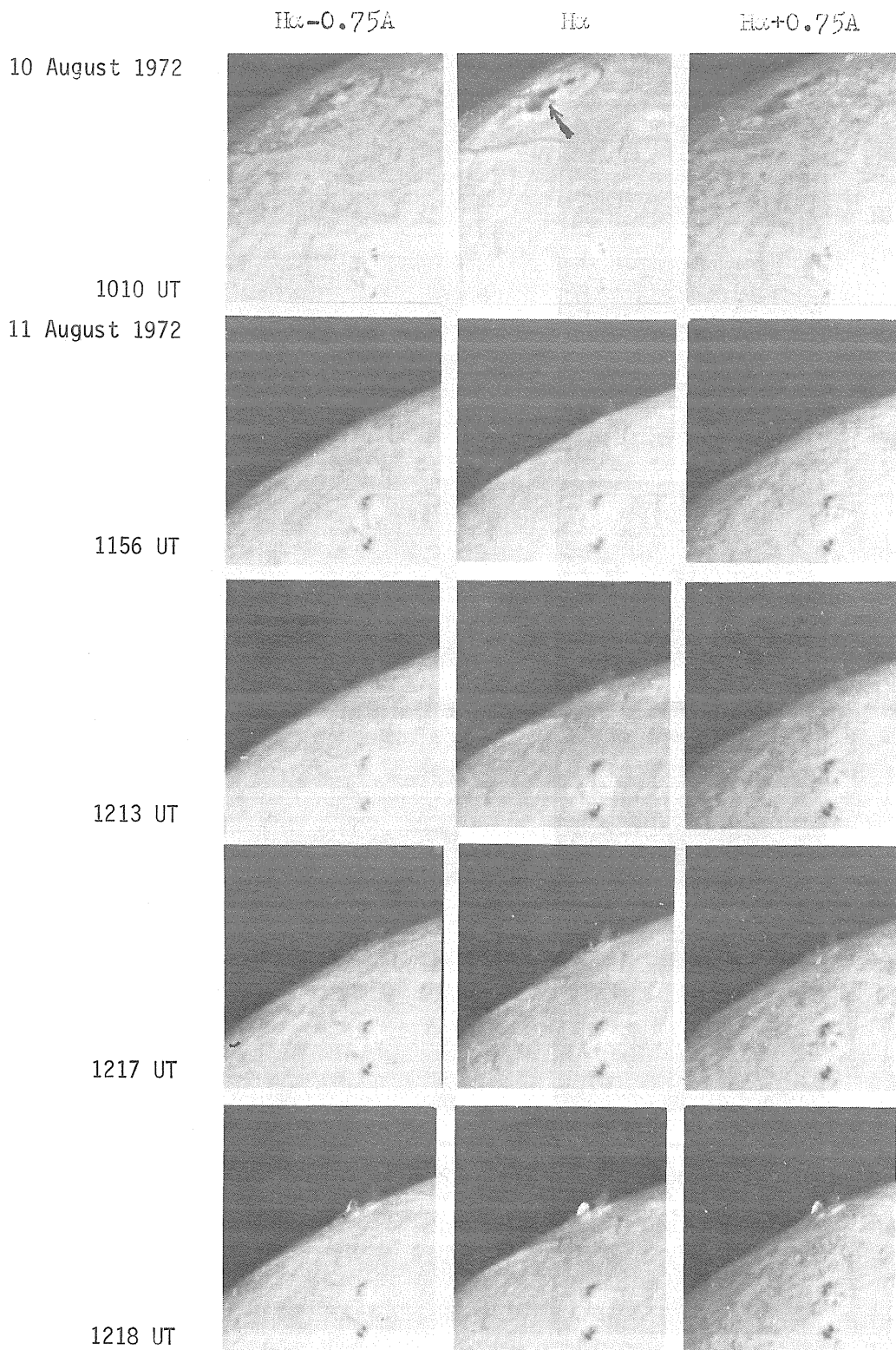


Fig. 5-1. Heliographic photographs in variable wave-lengths taken at Meudon.

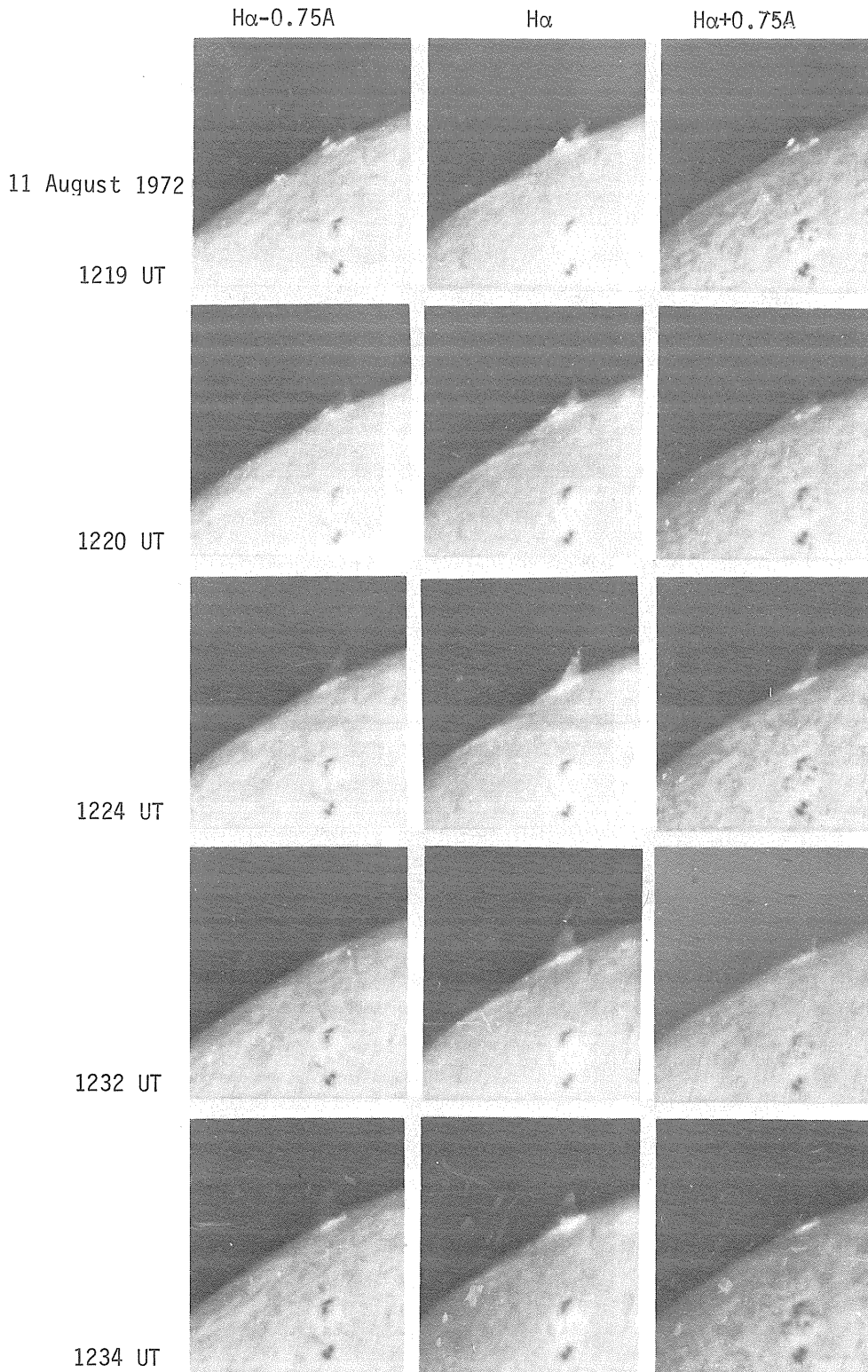


Fig. 5-2. Heliographic photographs in variable wave-lengths taken at Meudon.

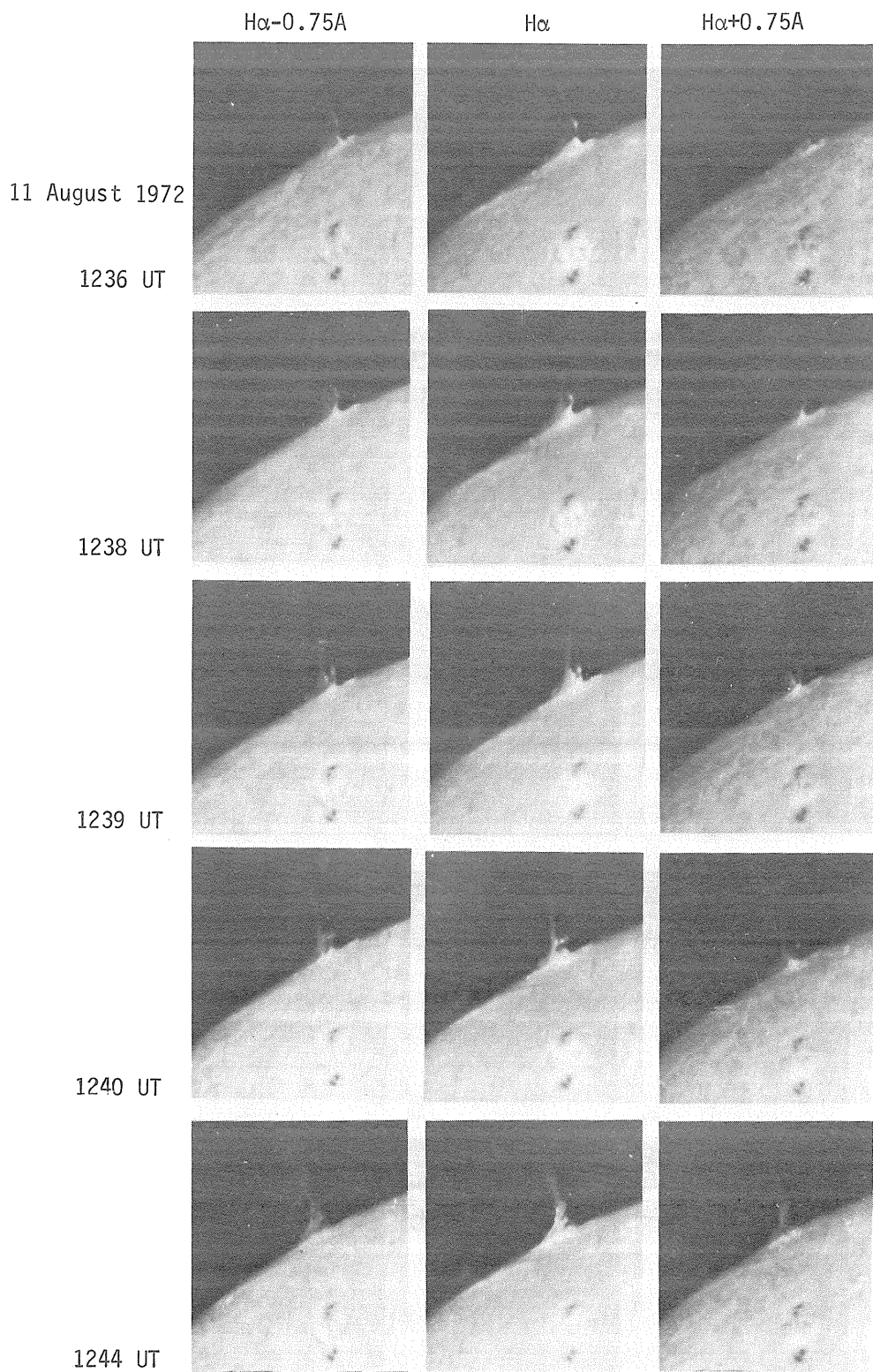


Fig. 5-3. Heliographic photographs in variable wave-lengths taken at Meudon.

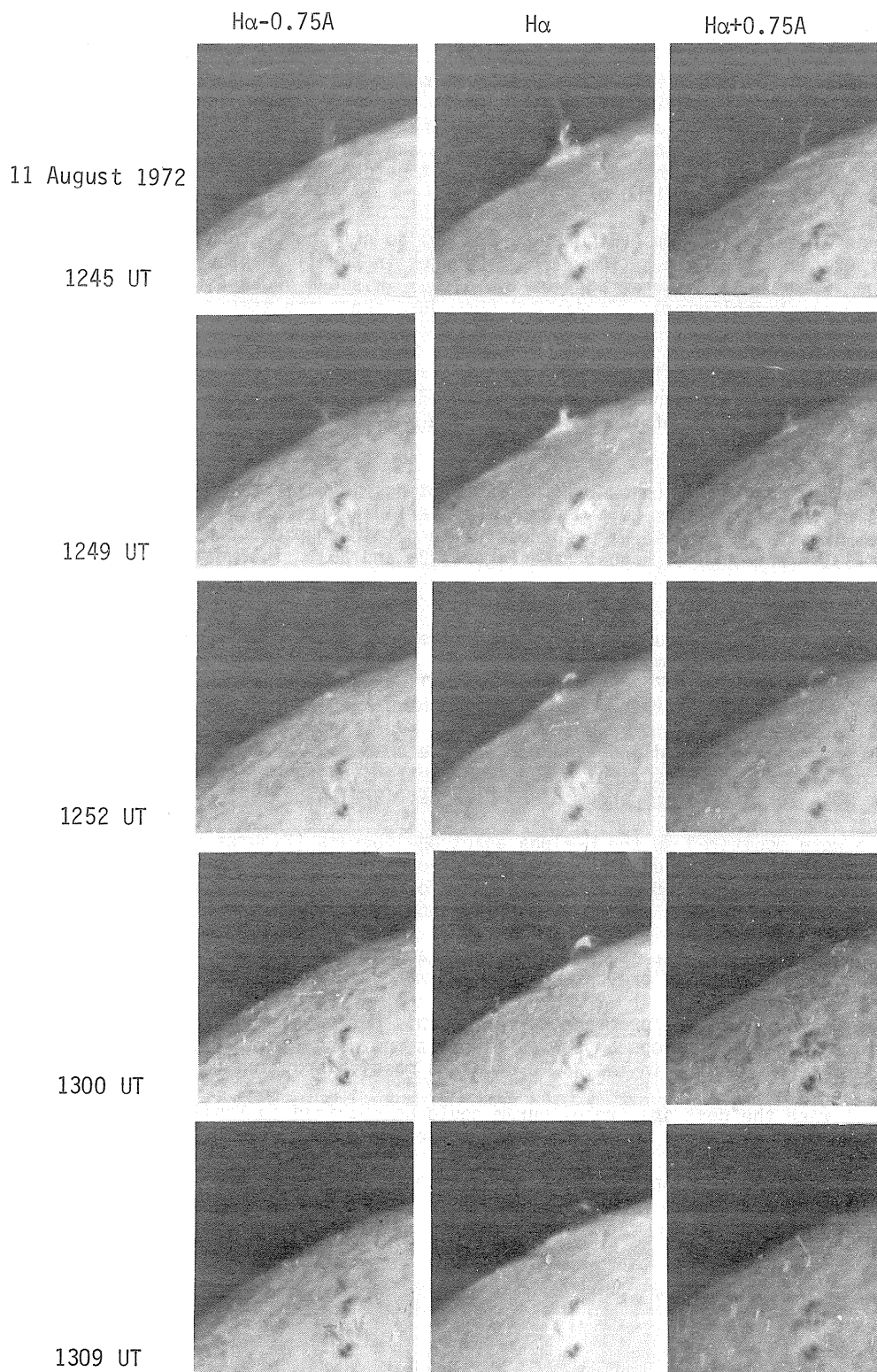


Fig. 5-4. Heliographic photographs in variable wave-lengths taken at Meudon.

A Photographic Record of Solar Activity from 5 to 13 August 1972 at Manila Observatory

by

Francis J. Heyden, S.J.
Manila Observatory, Republic of the Philippines

Weather conditions in the Philippines during the months of June and July of 1972 will be memorable for the unusual amount of rainfall, especially in the region of the island of Luzon just north of the city of Manila. Observations of the sun kept the staff of Manila Observatory on the alert for the brief random intervals between clouds when the sun could be observed. The following photographs show most of the results that were obtained just before and after the flare of importance 3B which occurred on 7 August at 1500 UT.

The hydrogen alpha filtergrams (Figures 1a and 1b) do not show extensive changes until about twelve hours after the occurrence of the flare. Changes in the filaments are evident, especially in the large one in the north central part of the disk. This one broadens and darkens appreciably on 9 August. The spectroheliograms (Figure 1c) show just about the same details but with better resolution.

The calcium II (K) spectroheliograms in Figure 2 reveal this same large filament and its invasion into the plage area around the spot group 331 on 8 and 9 August. The general brightening of the plage areas over the center of the disk may be due more to photographic effects and sky transparency conditions than to actual changes on the sun.

Moreton's lapsed time films (shown at the IAU meetings in California in 1960) of solar flares showed the sensitivity of sunspots to a wave of fast particles from a solar flare. Fortunately, observers at both Manila and Baguio were successful in obtaining photographs of the very large group of spots (331) from 5 to 11 August (see Figures 3a and 3b). The weather during this period was mostly overcast.

Changes in the internal features of the group were obvious as might have been expected with such a violent flare occurring almost in coincidence. The greatest differences appear in the photographs of 0030 UT and 2248 UT on 7 August. The overall penumbra shows an extensive change, especially in the northeast. The entire group appears to have been drifting southward in latitude until stopped by the flare. It paused for about twenty-four hours and then resumed its downward trend. All umbrae seemed to move eastward and then to continue downward. Figure 4 and Table 1 show roughly this trend of the members of the sunspot group. The letters designating the individual umbrae have been taken from NOAA Technical Memorandum of 22 December 1972, page 109.

Prominences were monitored in the H-alpha spectroheliograms (Figures 5a, 5b, 5c and 5d). Both of the bright plage areas, 331 and 337, were associated with moderate activity on the NW limb. Later, a large mound prominence persisted over the area 331 for more than two days. A large array of loops appeared over 337 on 8 August and lasted apparently about twenty-four hours.

These were not visible on the spectroheliograms made at Manila on 6 and 7 August. The weather on these days was quite windy and prevented a steady image during the scan in H-alpha.

The greatest activity of the prominences during this period appeared on 13 August at about 0133 UT. At this time two pairs of loops appear on the east and west limbs of the southern hemisphere. The remarkable active prominence in the WSW produced a massive eruption.

On 15 August when the next spectroheliogram could be obtained in Manila, a very large loop prominence hovered over the WSW limb, while the rest of the solar limb seemed to remain very quiet.

Observers Angel Ambion and Anthony Medrano have contributed much time and effort in preparing the photographs presented in this report.

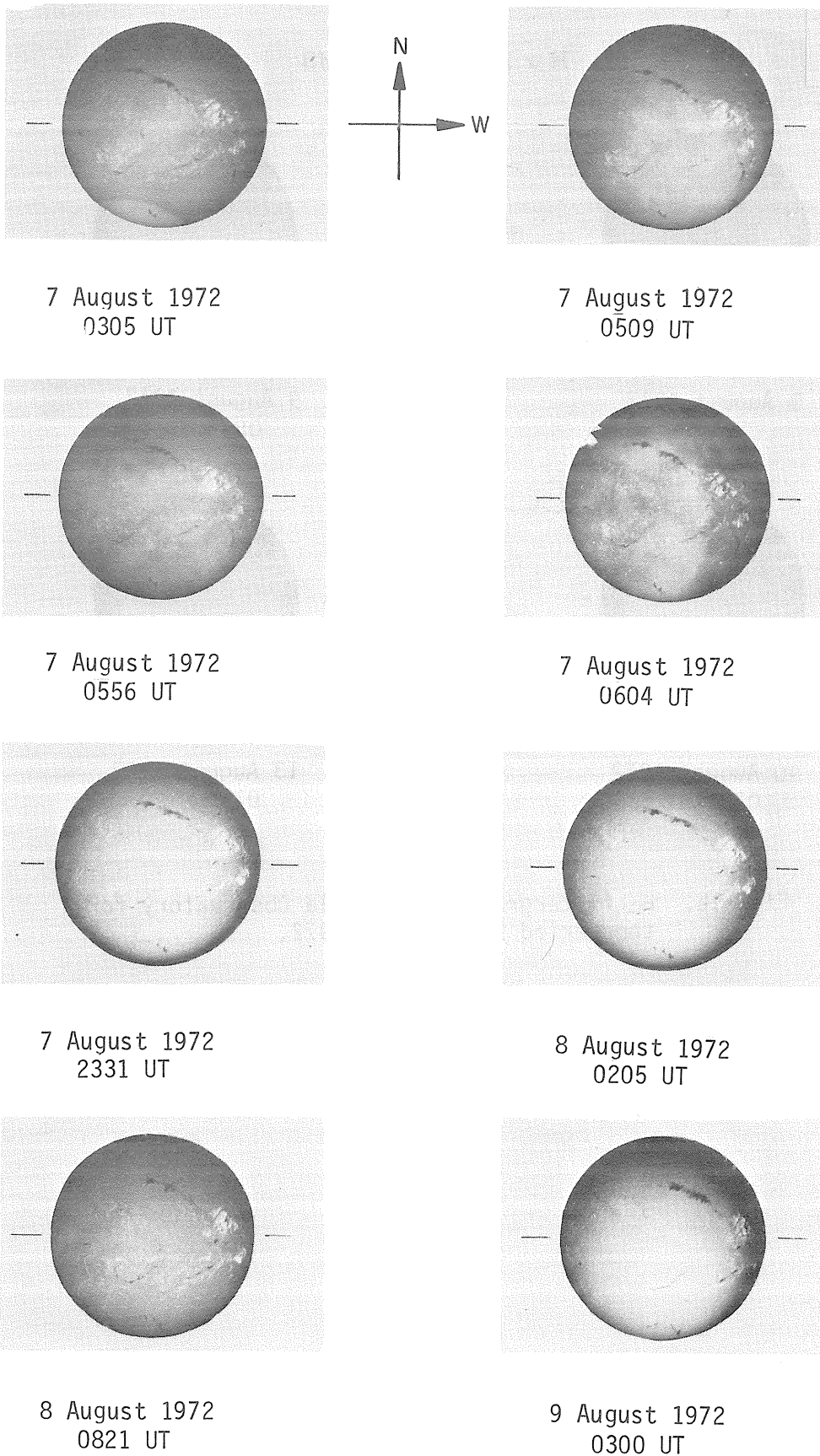


Fig. 1a. $H\alpha$ filtergrams from Manila Observatory for the period 7-9 August 1972.

H α FILTERGRAMS

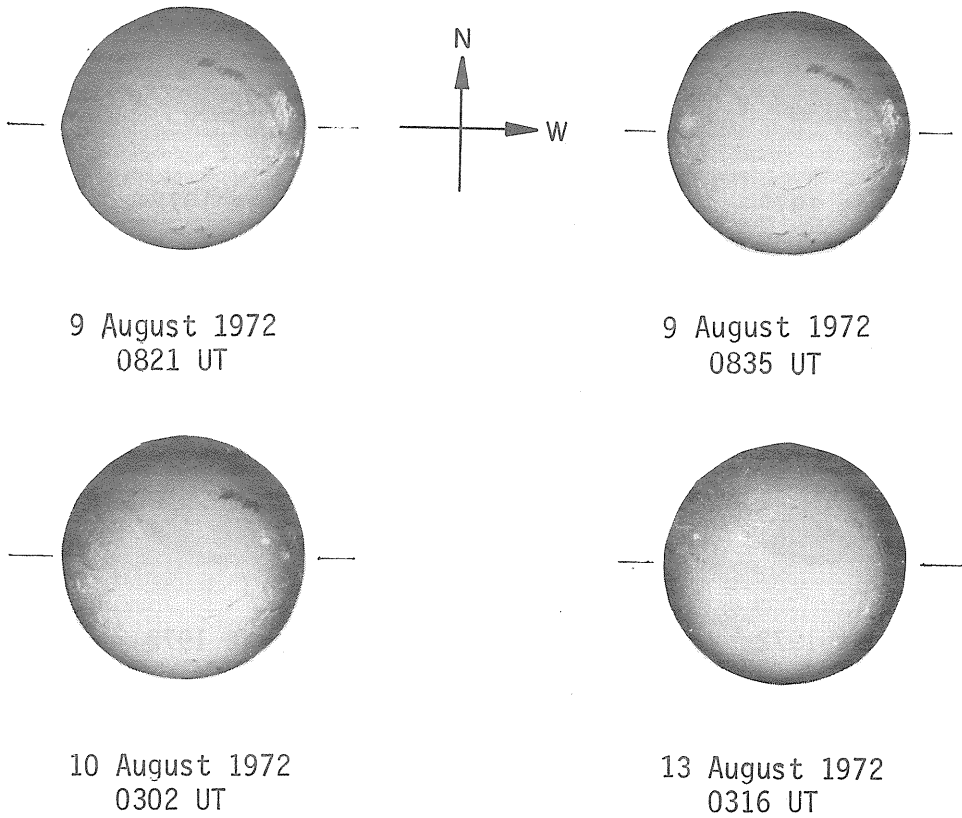
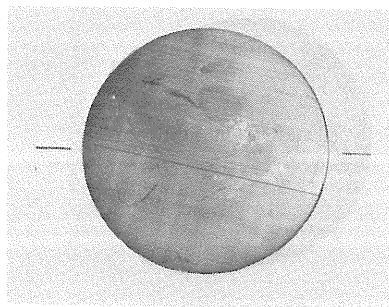
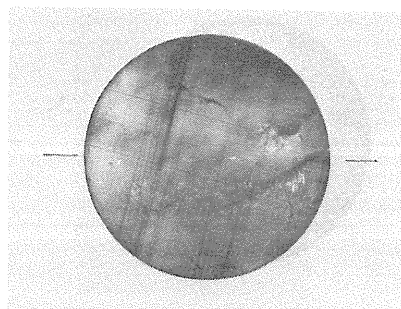
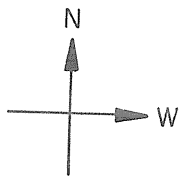


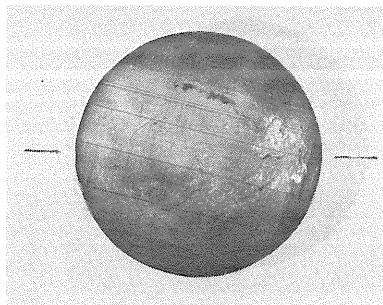
Fig. 1b. H α filtergrams from Manila Observatory for the period 9-13 August 1972.



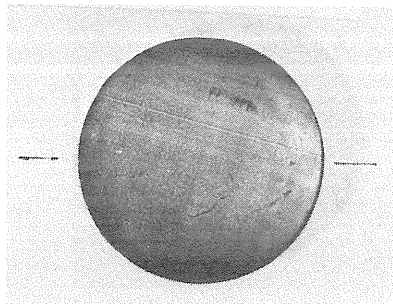
6 August 1972
0655 UT



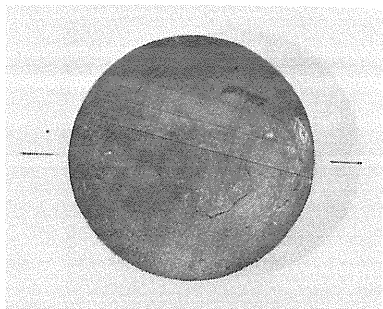
7 August 1972
0515 UT



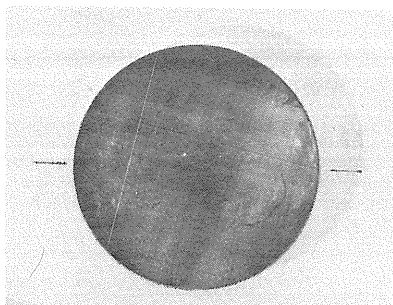
8 August 1972
0145 UT



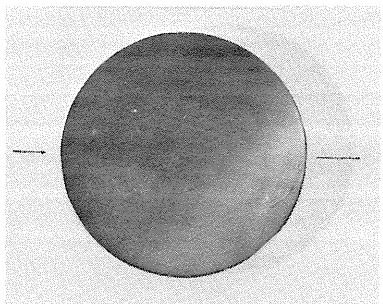
9 August 1972
0055 UT



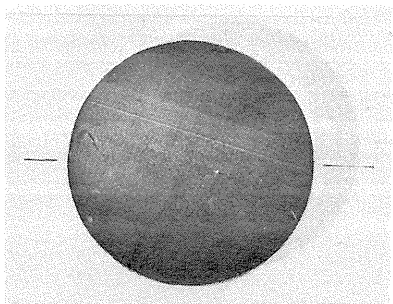
10 August 1972
0105 UT



11 August 1972
0652 UT

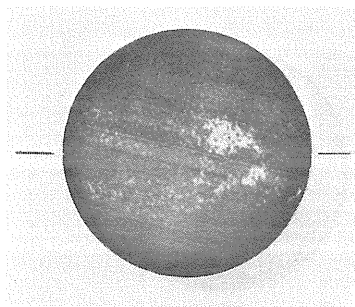


13 August 1972
0133 UT

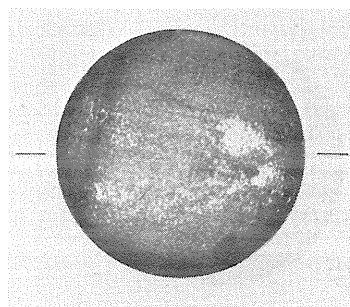
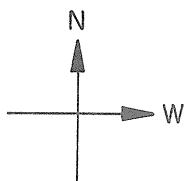


15 August 1972
0805 UT

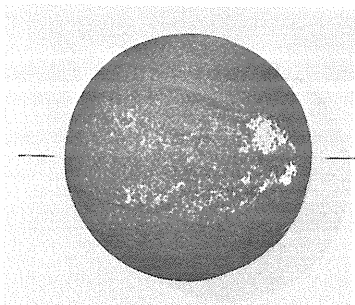
Fig. 1c. $H\alpha$ spectroheliograms from Manila Observatory for the period 6-15 August 1972.



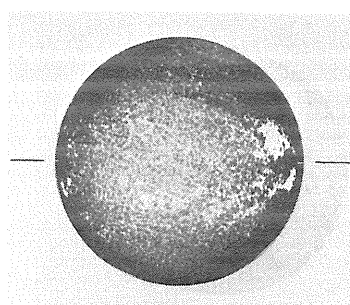
6 August 1972
0625 UT



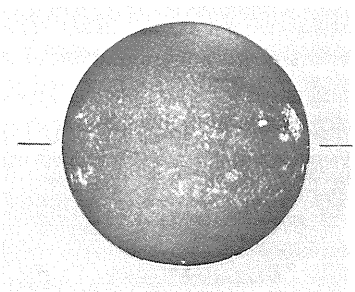
7 August 1972
0025 UT



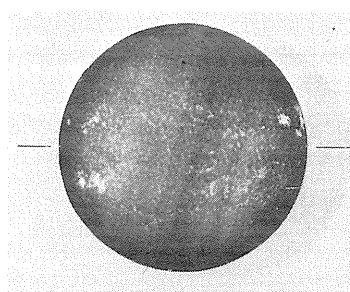
8 August 1972
0002 UT



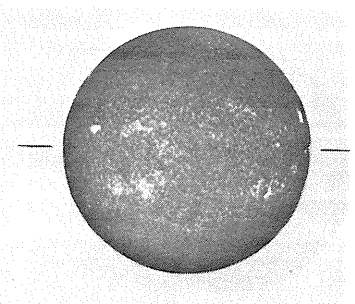
9 August 1972
0040 UT



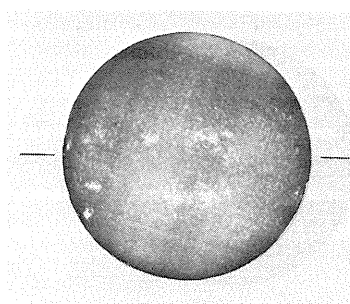
10 August 1972
0200 UT



11 August 1972
0550 UT

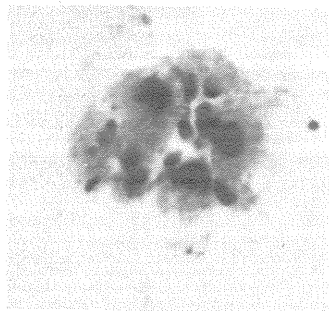


13 August 1972
0122 UT

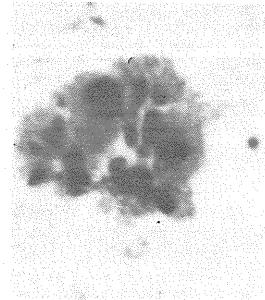
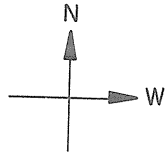


15 August 1972
0755 UT

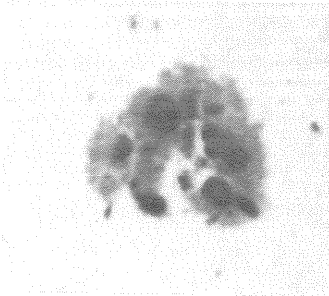
Fig. 2. Calcium II (K) spectroheliograms from Manila Observatory for the period 6-15 August 1972.



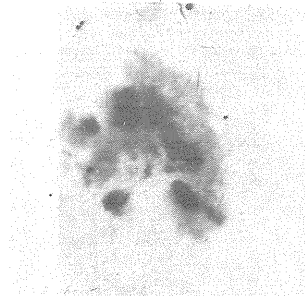
5 August 1972
2330 UT (Manila)



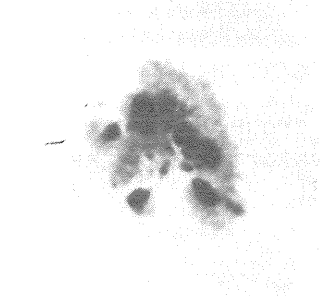
6 August 1972
0110 UT (Manila)



7 August 1972
0030 UT (Manila)



7 August 1972
2248 UT (Baguio)



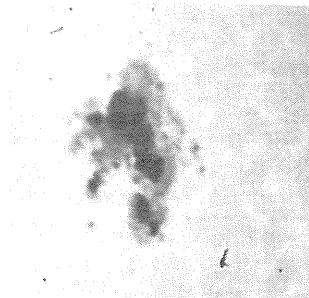
8 August 1972
0000 UT (Manila)



8 August 1972
0113 UT (Baguio)

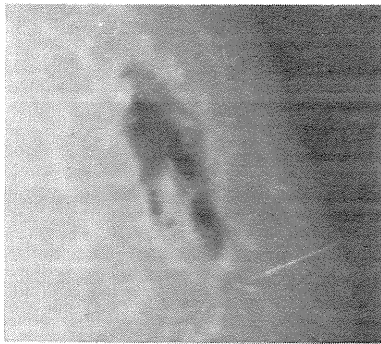


8 August 1972
2236 UT (Baguio)

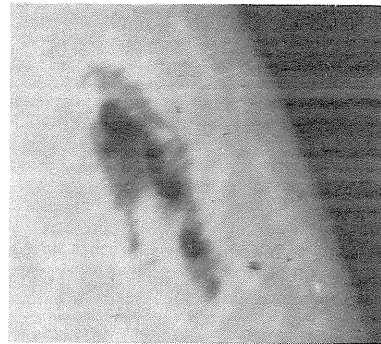
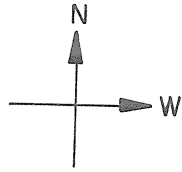


8 August 1972
2244 UT (Manila)

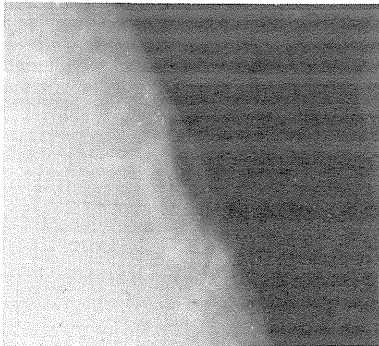
Fig. 3a. Sunspot observations of group 331 from Manila and Baguio Observatories for the period 5-8 August 1972.



10 August 1972
0027 UT (Manila)



10 August 1972
0110 UT (Baguio)



11 August 1972
0157 UT (Baguio)

Fig. 3b. Sunspot observations of group 331 from Manila and Baguio Observatories for the period 10-11 August 1972.

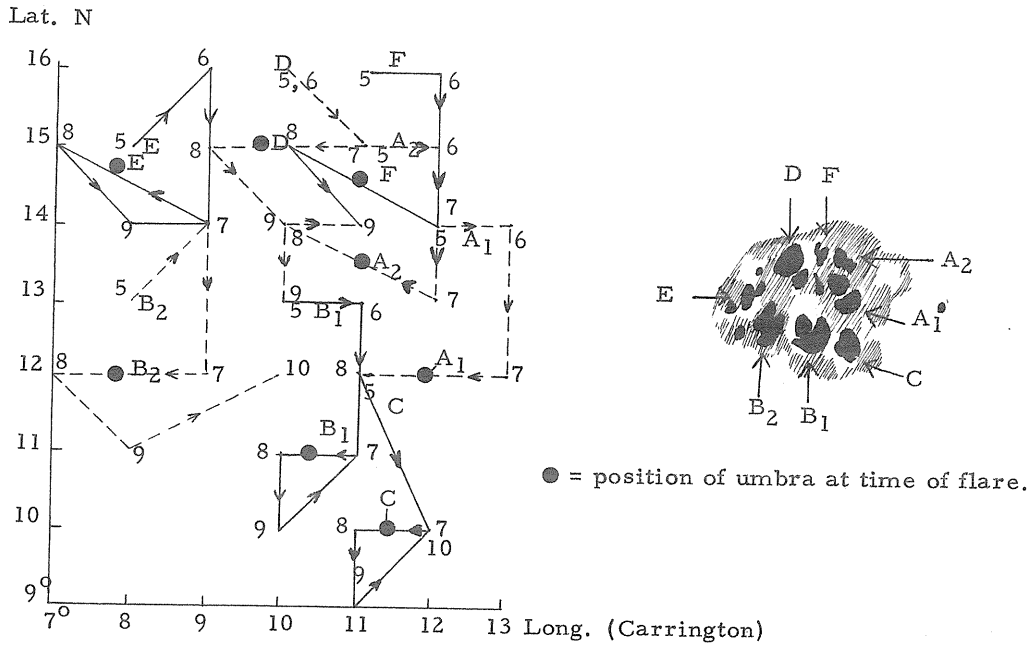


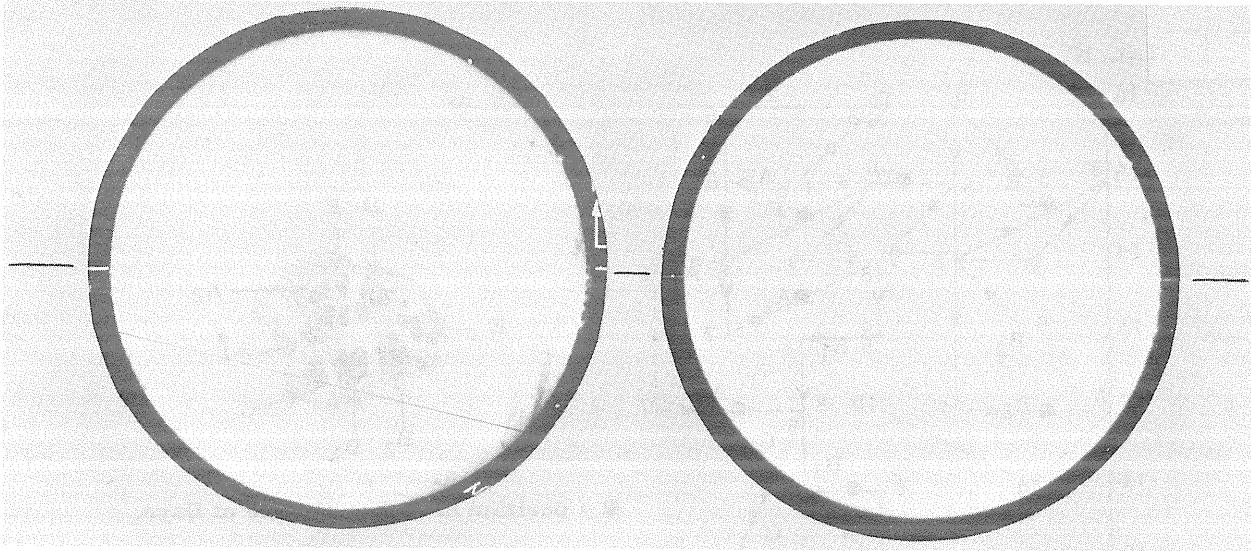
Fig. 4. Complex movement of spots in spot group 331 during the period 5-10 August 1972. 3B flare occurred 1500 UT 7 August 1972.

Table 1

(Carrington longitude is used)

1972 August	Umbr Position		A ₁		A ₂		B ₁		B ₂		C		D		E		F	
	Lat	Long	Lat	Long	Lat	Long	Lat	Long	Lat	Long	Lat	Long	Lat	Long	Lat	Long	Lat	Long
5	N14	12	N15	11	N13	10	N13	8	N12	11	N16	10	N15	8	N16	11		
6		14 13		15 12		13 11		14 9		12 11		16 10		16 9		16 12		
7		12 13		13 12		11 11		12 9		10 12		15 11		14 9		14 12		
8		12 11		14 10		11 10		12 7		10 11		15 9		15 7		15 10		
9		12 11		13 10		10 10		11 8		9 11		14 10		14 8		14 11		
10		12 11		13 11		11 11		12 10		10 12		14 11		14 10		14 11		

Latitude and longitude estimates to nearest degree.

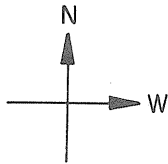


8 August 1972
0145 UT

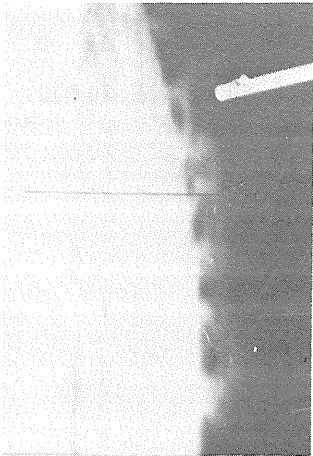
9 August 1972
0055 UT



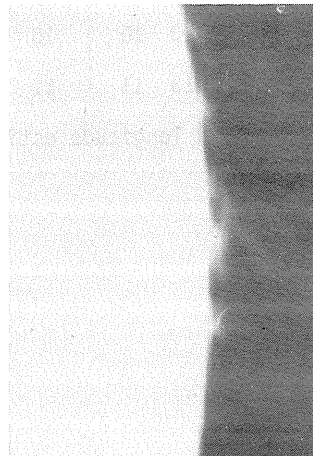
WNW



WNW

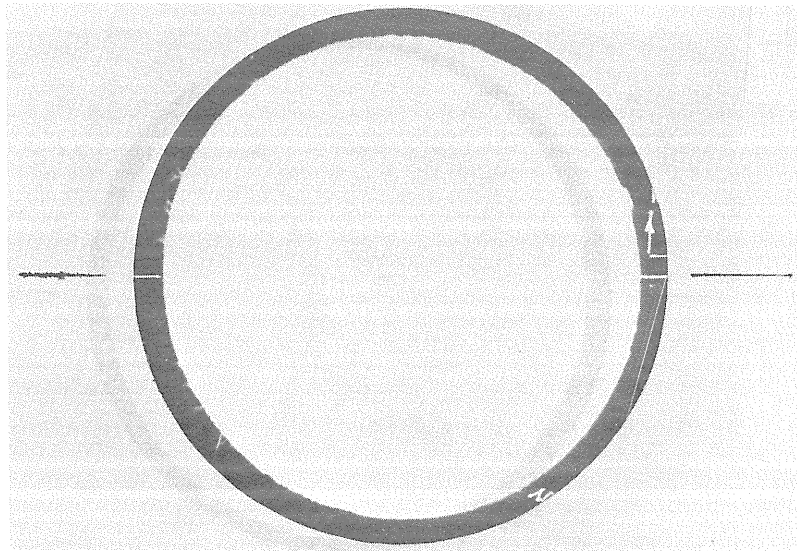


W



W

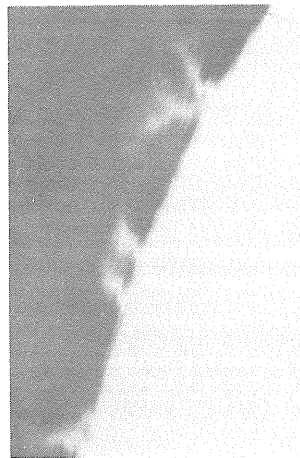
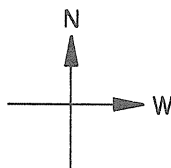
Fig. 5a. H-alpha spectroheliograms showing prominences during the period 8-9 August 1972.



11 August 1972
0652 UT



WNW



ENE

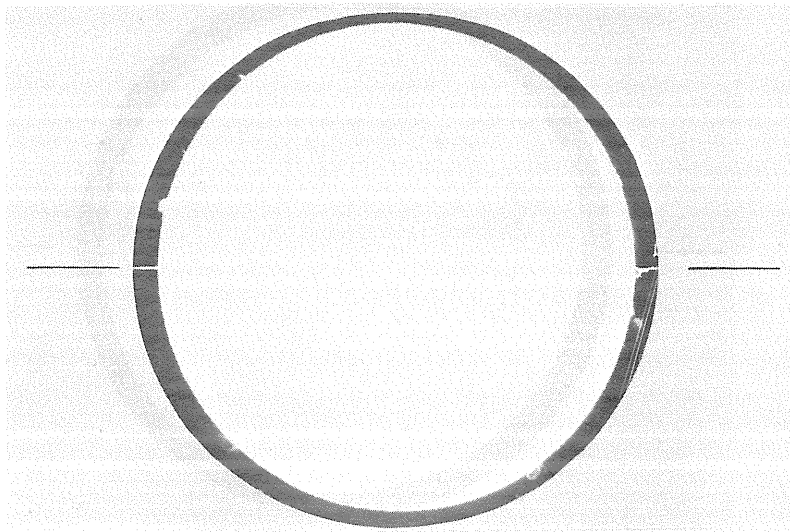


SE

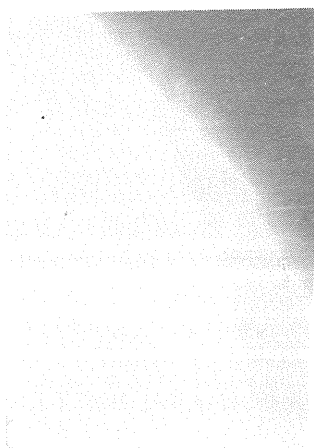


NE

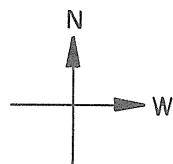
Fig. 5b. H-alpha spectroheliograms showing prominences during the period 11 August 1972.



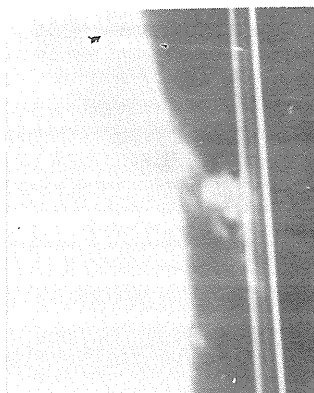
13 August 1972
0133 UT



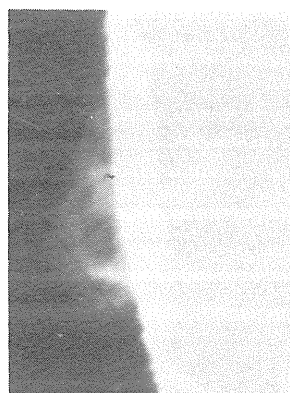
WNW



SW



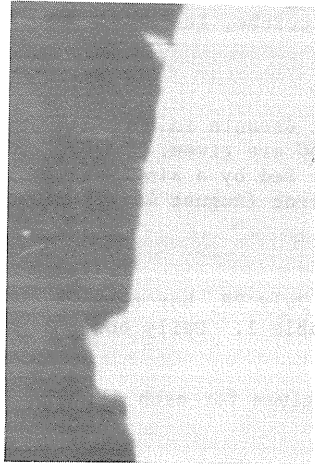
WSW



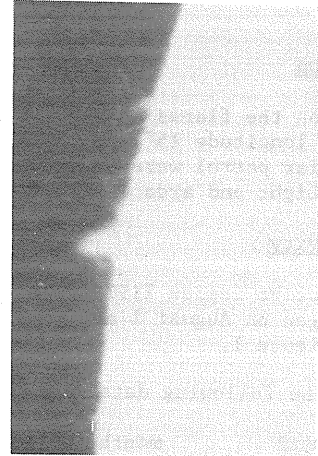
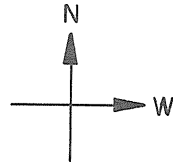
SE

Fig. 5c. H-alpha spectroheliograms showing prominences during the period 13 August 1972.

13 August 1972



ENE



NE

Fig. 5d. Continuation of Figure 5c.

Flares and Active Prominences Observed at Catania from
July 26 to August 14, 1972 in the MM1976 Region

by

G. Godoli, V. Sciuto, and R. A. Zappala
Osservatorio Astrofisico di Catania
Consiglio Nazionale delle Ricerche, Italy

Introduction

Data on the flares and active prominences observed at Catania in the MM1976 region (N12, Carrington longitude 15°) in the July 26 - August 14 period are given. Observations made during the Catania solar patrol were performed with a Zeiss H α filter fed by a single aspherical lens (15 cm/222 cm). Light and area curves of the greatest optical event (August 4) are given.

Flare Activity

The active region 11976 appeared on the east limb on July 28, but flare activity observed at Catania began on August 1 and continued as indicated in Table 1. Daily hours of observation are shown in Figure 1.

The following data, computed on a CDC 6600, are given for each flare in Table 1:

DATE		month, day
TB	F	UT of the beginning of the flare
	O	UT of the beginning of the observation
TE	F	UT of the end of the flare
	O	UT of the end of the observation
TM		UT of the maximum of the flare
LAT		heliographic latitude
L		heliographic longitude
IMP		flare importance according to the international rules
O	P	partial observation
	C	complete observation
T		UT of the measurements
AP		projected area at maximum in millionths of the solar disk
AC		corrected area in square degrees (if the heliocentric angle is smaller than 65 degrees)
F		maximum intensity referred to the local undisturbed chromosphere
R		remarks according to the international rules

Table 1

Flare Activity Observed at Catania

DATE	TB	TE	TM	LAT	L	IMP	O	T	AP	AC	F	R
07 31	O 0700	O 0710	0700	15	-63	SN	P	0700	0022.5	00.56	1.91	
08 01	F 0705	O 0830	0705	13	-47	1B	P	0705	0224.8	03.55	2.19	TZ
	F 0920	F 1215	0935	13	-45	1B	C	0935	0179.9	02.74	3.02	TZ
08 02	O 0505	F 0800	0515	13	-35	2B	P	0515	0674.5	08.86	2.88	Z
08 04	F 0525	F 0905	0633	15	-08	3B	C	0633	1461.5	16.03	5.37	Z
	F 1310	O 1340	1315	03	01	SB	P	1315	0134.9	01.40	2.34	
08 05	F 0655	F 0705	0655	13	04	SN	C	0655	0067.5	00.72	1.66	
	F 0710	F 0725	0710	15	11	SN	C	0710	0084.3	00.93	1.78	
	F 0820	F 0840	0820	16	11	SN	C	0820	0078.7	00.87	1.86	
	F 1245	F 1310	1245	17	08	SN	C	1245	0056.2	00.62	1.86	
08 06	F 0825	O 0845	0830	12	18	SN	P	0830	0039.3	00.44	1.95	
08 07	O 1055	F 1155	1105	15	34	1B	P	1105	0382.2	05.03	2.14	
	F 1200	F 1240	1205	14	33	1B	C	1205	0252.9	03.27	2.51	
	F 1445	O 1505	1455	13	35	1B	P	1455	0196.7	02.59	2.24	
08 09	F 1025	F 1035	1025	17	65	SB	C	1025	0016.9	00.45	2.19	
08 11	F 0550	F 0600	0550	14	90	1B	C	0550	0056.2	-----	2.75	
	F 0800	F 0805	0800	14	90	SN	C	0800	0039.3	-----	1.74	
	F 1235	O 1240	1235	13	90	1B	P	1235	0112.4	-----	3.09	

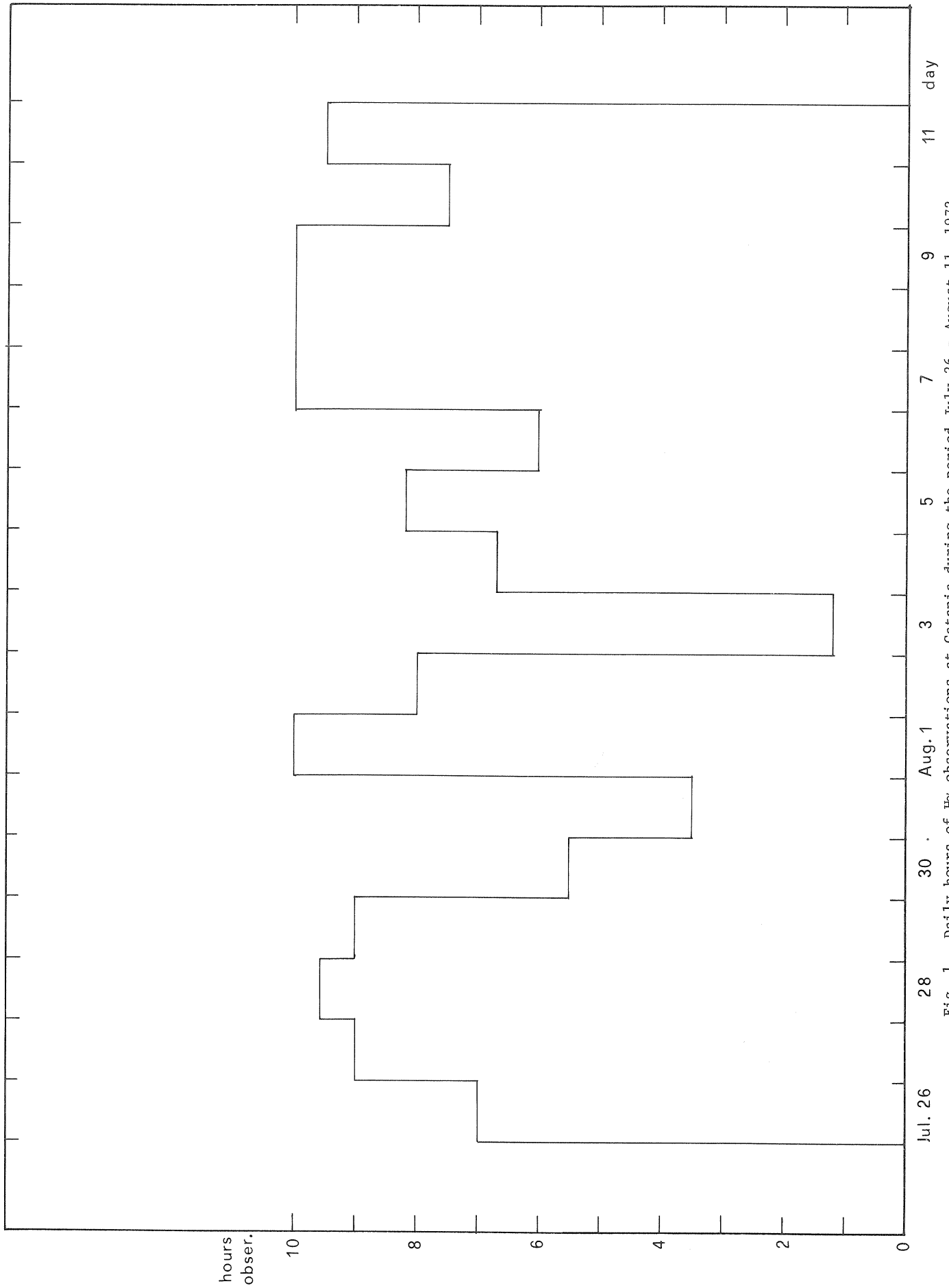


Fig. 1. Daily hours of H α observations at Catania during the period July 26 - August 11, 1972.

Prominence Activity

Active prominences associated with region 11976 were observed at Catania on July 28, 29, and August 10, 11 as indicated in Table 2.

The following data are given for each phenomenon in Table 2:

DATE		month, day
TB	P	UT of the beginning of the phenomenon
	O	UT of the beginning of the observation
TE	P	UT of the end of the phenomenon
	O	UT of the end of the observation
LAT		heliographic latitude
L		heliographic longitude
I		importance according to the international rules

Table 2

Active Prominences Associated with Region 11976

DATE	TB	TE	LAT	L	I
07 28	O 1405	P 1415	10	-90	1-
07 29	P 0600	P 0725	12	-90	1-
	P 0845	P 0925	10	-90	1
	P 1045	P 1055	14	-90	1-
	P 1135	P 1145	11	-90	1-
	O 1315	P 1335	10	-90	1-
	P 1445	O 1505	11	-90	1-
	P 1455	O 1500	10	-90	1
08 10	P 1240	P 1310	12	90	1-
08 11	O 0520	P 0605	14	90	1-
	O 0625	P 0630	11	90	1-
	P 0735	P 0950	12	90	2
	P 1035	P 1200	10	90	2
	P 1220	O 1505	12	90	3

August 4 Optical Event

The $H\alpha$ flare had two ribbons, shown in Figure 2. The configuration is typical for proton flares.

The first ribbon of the flare is located outside the sunspot penumbra, while the second is located on the penumbra. The two ribbons were studied separately.

In Figure 3 the projected area measured from prints (solar diameter 24.5 cm) is given versus time for the two parts of the flare. We note that the area of ribbon 1 is always greater than that of ribbon 2. We note also that there is a shift of 10 minutes between the maxima of the two curves.

The intensity behavior of the flare was studied with the Catania Astrophysical Observatory's Jena microphotometer. From this study we deduced the presence of several knots having shifted light curves. In Figures 4a and 4b the light curves of the most active knots of the two ribbons are given. The intensity of the two knots was measured placing the microphotometer slit on the two circles drawn on the ribbons in Figure 2.

We note from the two light curves that the smaller ribbon has on the average the same intensity as the greater and that the two light curves do not show the shift in time of the maxima shown by the area curves.

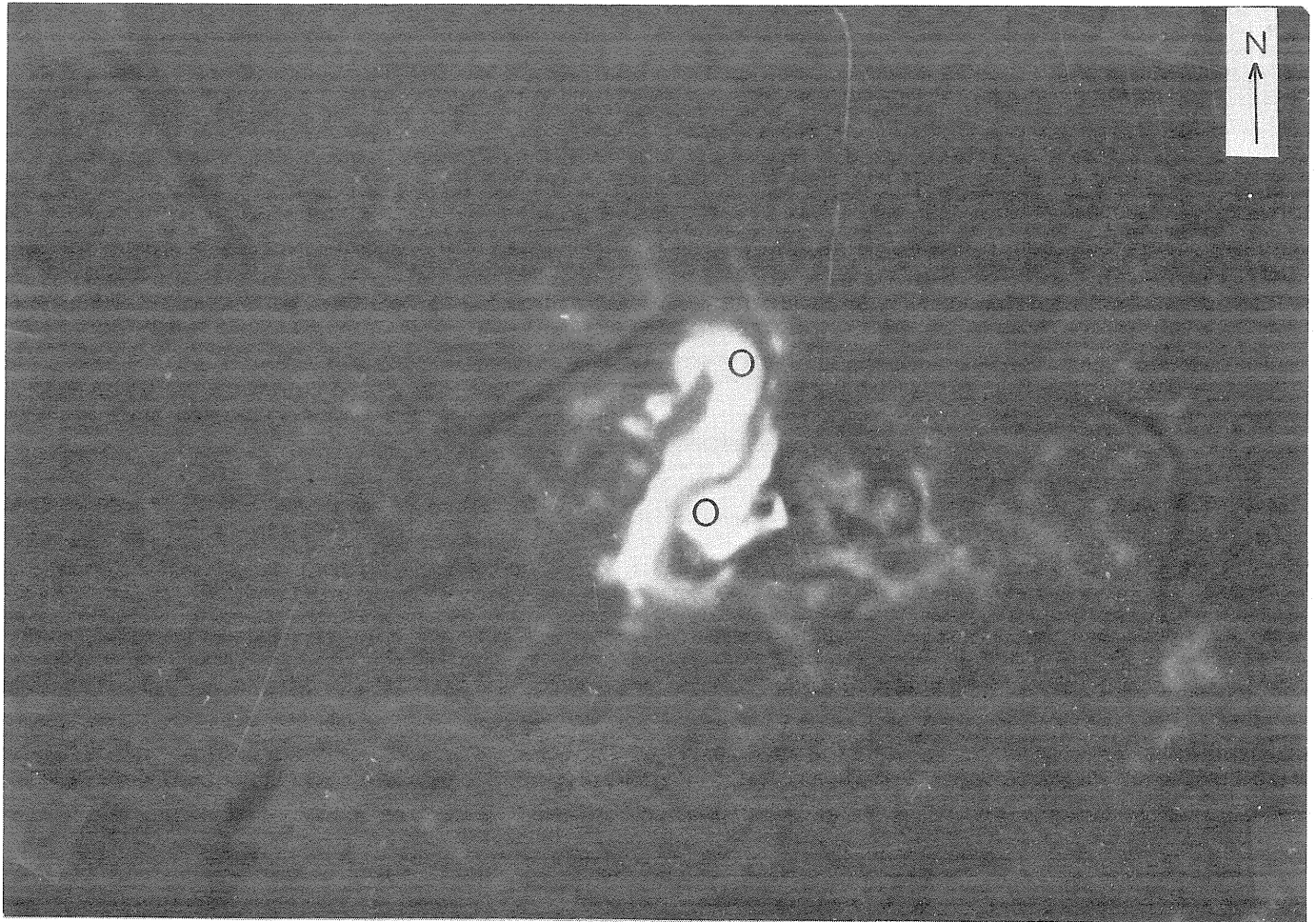


Fig. 2. Picture of the H_{α} flare of August 4 near maximum; circles show the position in the two ribbons in which intensity measurements were taken (0635 UT; \emptyset 48 cm).

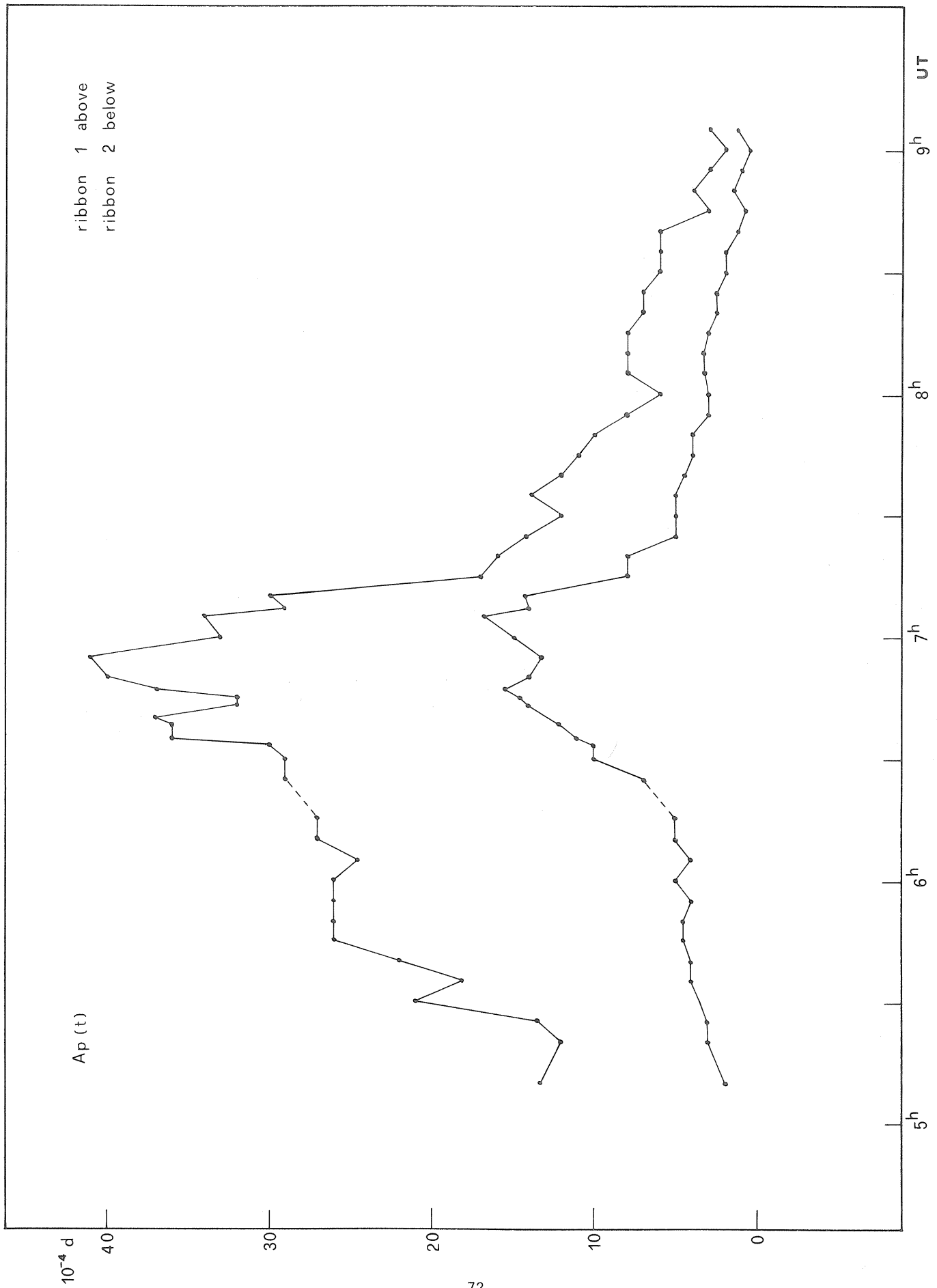


Fig. 3. Projected area of the two ribbons of the August 4 flare versus time.

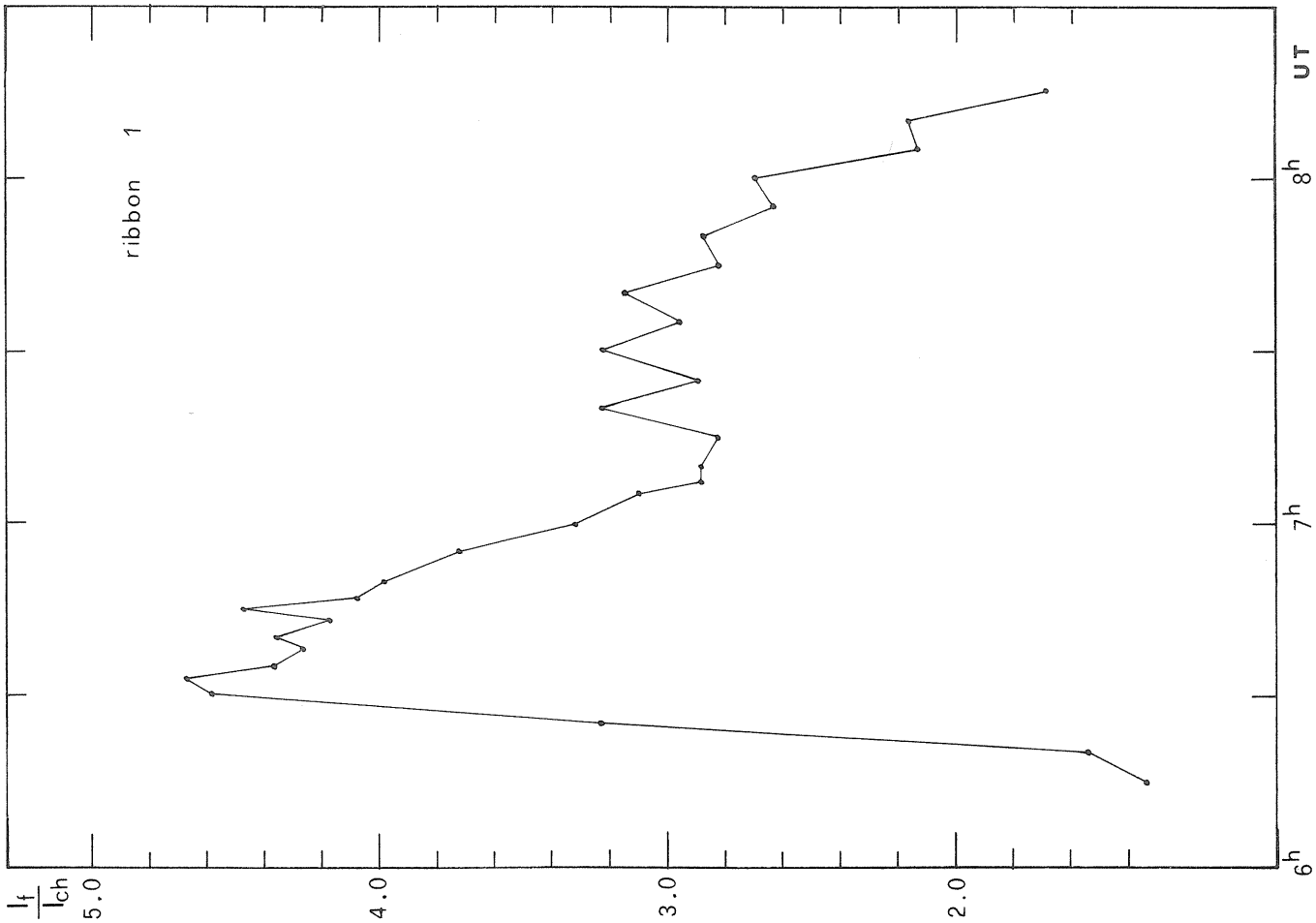


Fig. 4a. Intensity of ribbon 1 of the August 4 flare versus time. Intensities are referred to the local undisturbed chromosphere.

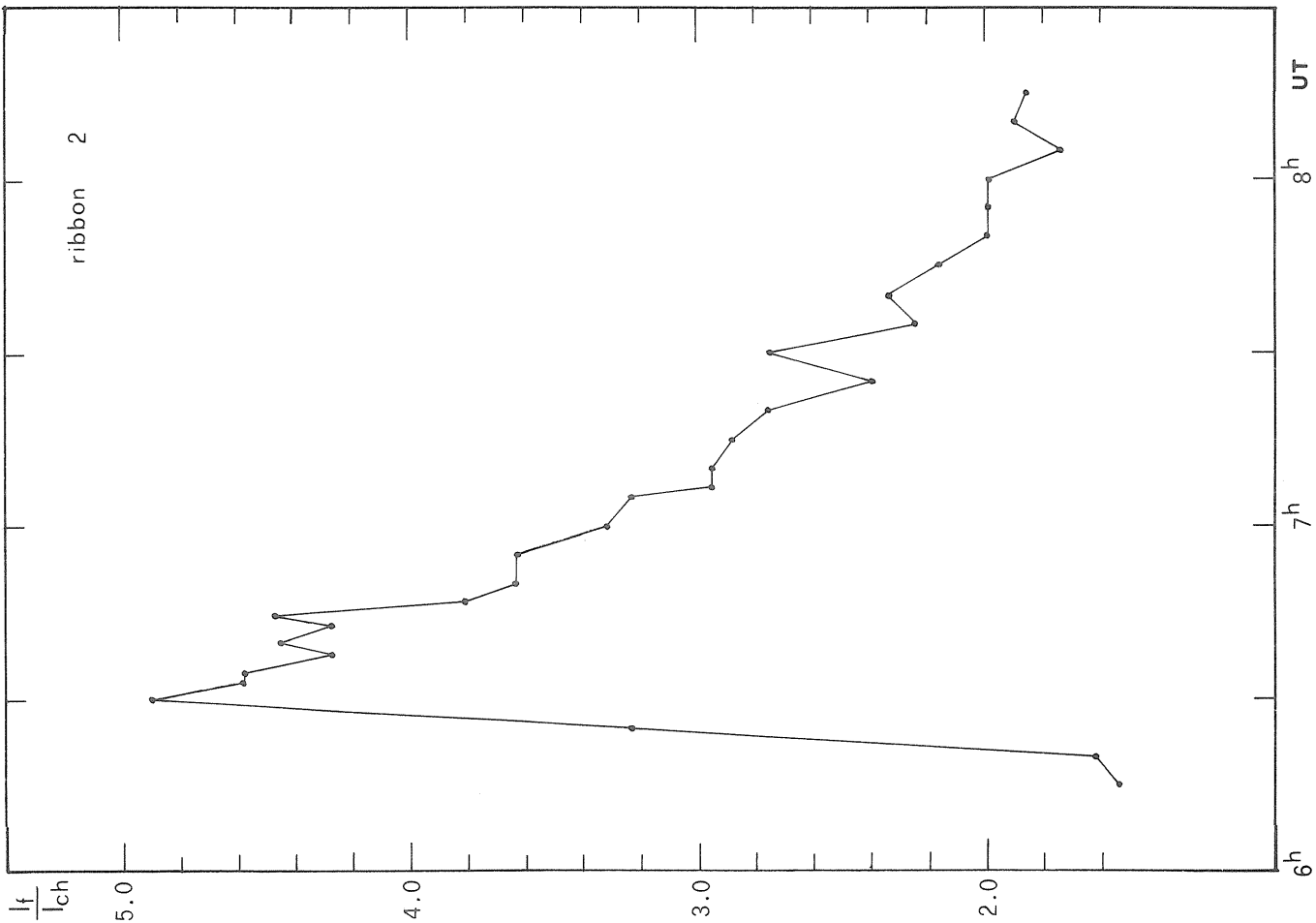


Fig. 4b. Intensity of ribbon 2 of the August 4 flare versus time. Intensities are referred to the local undisturbed chromosphere.

Coronal Magnetic Field Maps, before, during, after the
Period 26 July to 14 August 1972. (Current-free approximation).

by

M. D. Altschuler and D. E. Trotter
High Altitude Observatory
National Center for Atmospheric Research
Boulder, Colorado 80302

Using the line-of-sight magnetic fields measured by the magnetograph of the Hale Observatories, we have calculated the coronal magnetic fields for the period 26 June to 1 September 1972 in the current-free approximation. The method used is described in Altschuler and Newkirk [1969] (see in particular Section 6).

The accompanying figures show the contributions to the coronal magnetic field of the strongest photospheric magnetic regions. Both polar views looking down on the north pole of the solar rotation axis and stereo views from a vantage point in the plane of the solar equator are shown.

We note that after the flares, the strong magnetic fields (both photospheric and coronal) to the east of the flare region have disappeared. We suspect from these results that the August 1972 flares had a large-scale (global) effect on the solar magnetic field.

REFERENCE

ALTSCHULER, M. D. and
G. NEWKIRK, JR.

1969

Solar Phys., 9, 131

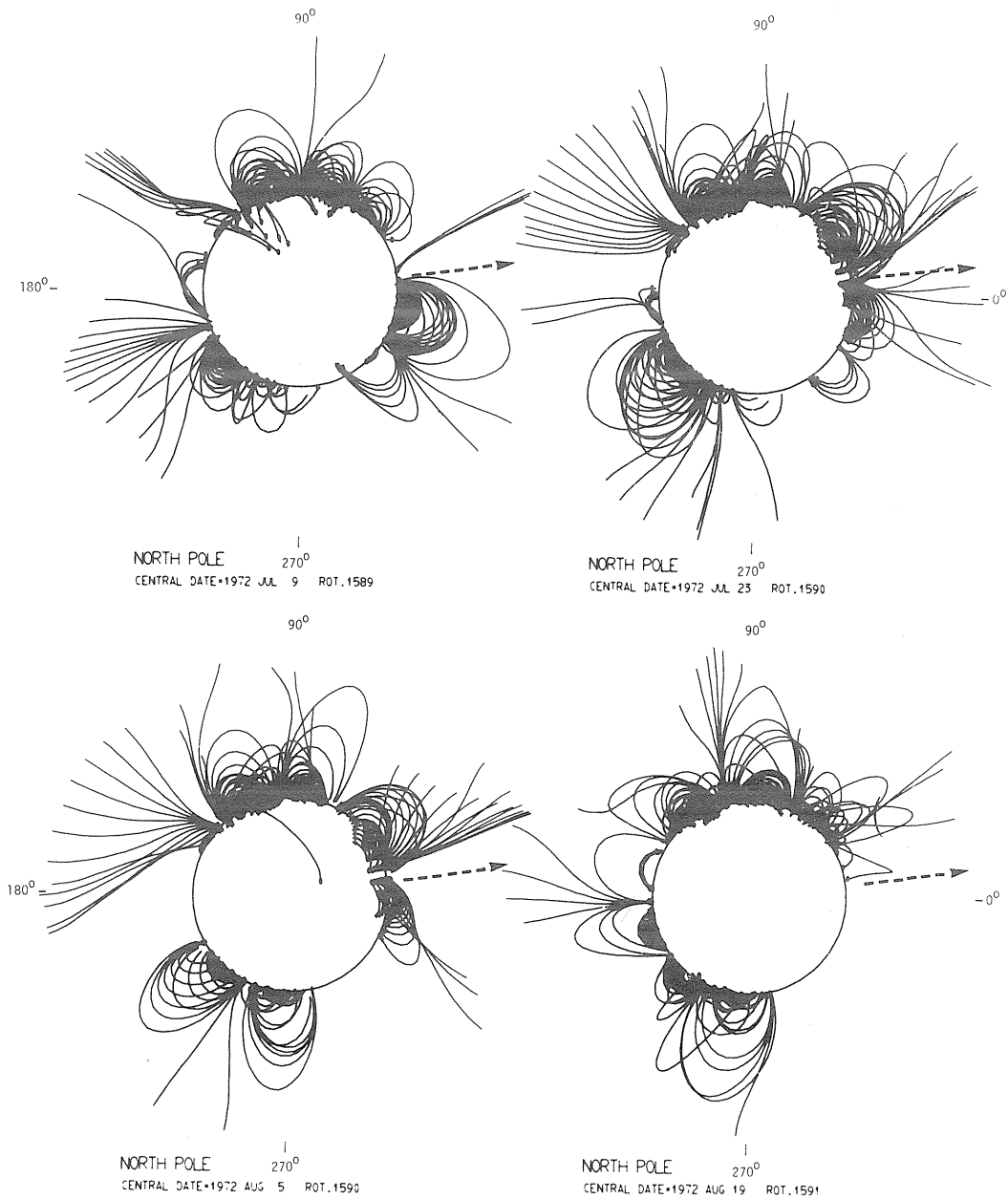


Fig. 1. Potential coronal magnetic fields as viewed from above the north pole of the sun at two week intervals between 26 June and 1 September 1972. Carrington longitudes are indicated around the circumference of each picture. The arrow shows the longitude at which the August 1972 flares occurred.

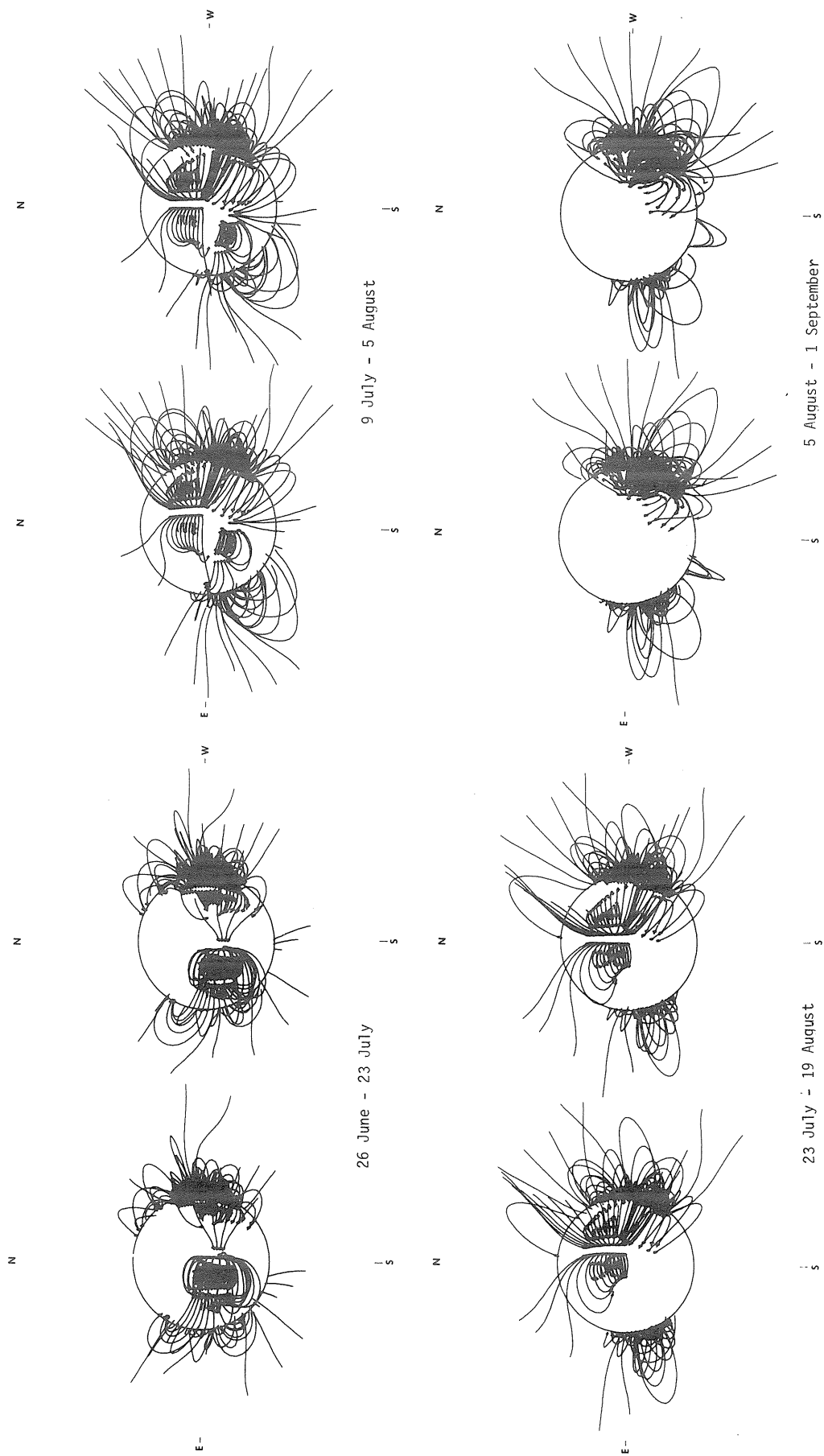


Fig. 2. Four stereoscopic pairs showing the coronal magnetic field in the current-free approximation. Data periods for the magnetic maps are 26 June to 23 July, 9 July to 5 August, 23 July to 19 August, and 5 August to 1 September 1972. The north-south rotation axis

is vertical. For all the stereo pairs, the central meridian Carrington longitudes are 0° in the left picture and 10° in the right picture. The flare occurred at 9° Carrington longitude.

Occurrence of the August 1972 Proton-Flare Region in the
Frame of the Large-Scale Magnetic Field Regularities

by

V. Bumba

Astronomical Institute of the Czechoslovak Academy of Sciences
Ondrejov, Czechoslovakia

In connection with the occurrence of the August 1972 proton-flare region, we would like to present a short comment on a complex figure representing the time-series of large-scale photospheric magnetic field development in the form of synoptic charts. The negative and the positive polarity fields are shown on separate charts.

There exists a number of papers and notes [Bumba, Krivsky, Sykora 1972; Bumba 1972 a, b; Bumba, Sykora 1972 a, b] which try to show that the location of large particle emitting flares is closely related to a characteristic large-scale pattern in magnetic field distribution with life-time of the order of 8 - 10 solar rotations. These regular features are seen in the negative as well as in the positive polarity, although their visibility seems to be better in the negative polarity where their forms are more pronounced without respect to the activity cycle. The form alternates with the location in the northern or the southern solar hemisphere due to the mutual relations of both polarities and individual active regions, and to the influence of differential rotation which is smaller in lower and greater in higher heliographic latitudes.

This situation may be seen again in the case of the August 1972 proton-flare region in relation to the large-scale magnetic field distribution development, as shown in Figure 1. The preliminary synoptic charts used in this figure have been drawn from the daily Mt. Wilson magnetic maps. The first appearance of the pronounced elliptical body in both negative and positive polarity fields may be seen during rotations 1585 and 1586. This elliptical feature is extended for about 70° in heliographic longitude and occupies both hemispheres. The second eastward ellipse visible in the negative polarity field in the northeast part of which the proton-flare region developed, started to develop at the same time but reached its best visibility only during the time of the proton-flare region occurrence. The whole characteristic body of negative polarity extends more than 100° in heliographic longitude. Although the negative polarity is the leading one in the northern hemisphere both ellipses are extended toward the northern higher latitudes.

These features are not as visible in the positive polarity field distribution, however, their development may be followed throughout all rotations. The positive polarity extension is toward the southern higher latitudes.

As in practically all of the cases yet studied, it is characteristic that the whole pattern disintegrates rapidly during the one or two solar rotations following the rotation with the proton-flare region.

If we could succeed in having the magnetic synoptic charts promptly, the formation of such characteristic large-scale magnetic field patterns could be used as a predictor of the development of particle-emitting flare regions. Because of the relatively long life-time of these features such forecasts could be made well in advance.

REFERENCES

- | | | |
|--|--------|--|
| BUMBA, V. | 1972 a | Large-Scale Negative Polarity Magnetic Fields on the Sun and Particle Emitting Flares, <u>Solar Wind</u> , Ed. by C. P. Sonett, <u>et al.</u> , NASA, Washington, 31. |
| BUMBA, V. | 1972 b | Solar Large-Scale Positive Polarity Magnetic Fields and Geomagnetic Disturbances, <u>Solar Wind</u> , Ed. by C. P. Sonett, <u>et al.</u> , NASA, Washington, 151. |
| BUMBA, V.,
L. KRIVSKY, and
J. SYKORA | 1973 | Development and Spatial Structure of Proton-Flares near the Limb and Coronal Phenomena. IV. Proton-Flare from Nov. 2, 1969 and its Active Region, <u>Bull. Astron. Inst. of Czech.</u> <u>23</u> , 85. |
| BUMBA, V. and
J. SYKORA | 1972 a | Development of the Large-Scale Situation in which the Proton-Flare of January 24, 1971 Took Place, <u>Report UAG-24, Part I</u> , 43. |
| BUMBA, V. and
J. SYKORA | 1972 b | Large-Scale Magnetic Field and Activity Distribution Connected with the Proton-Flare of September 1, 1971 Region, <u>Report UAG-24, Part II</u> , 311. |

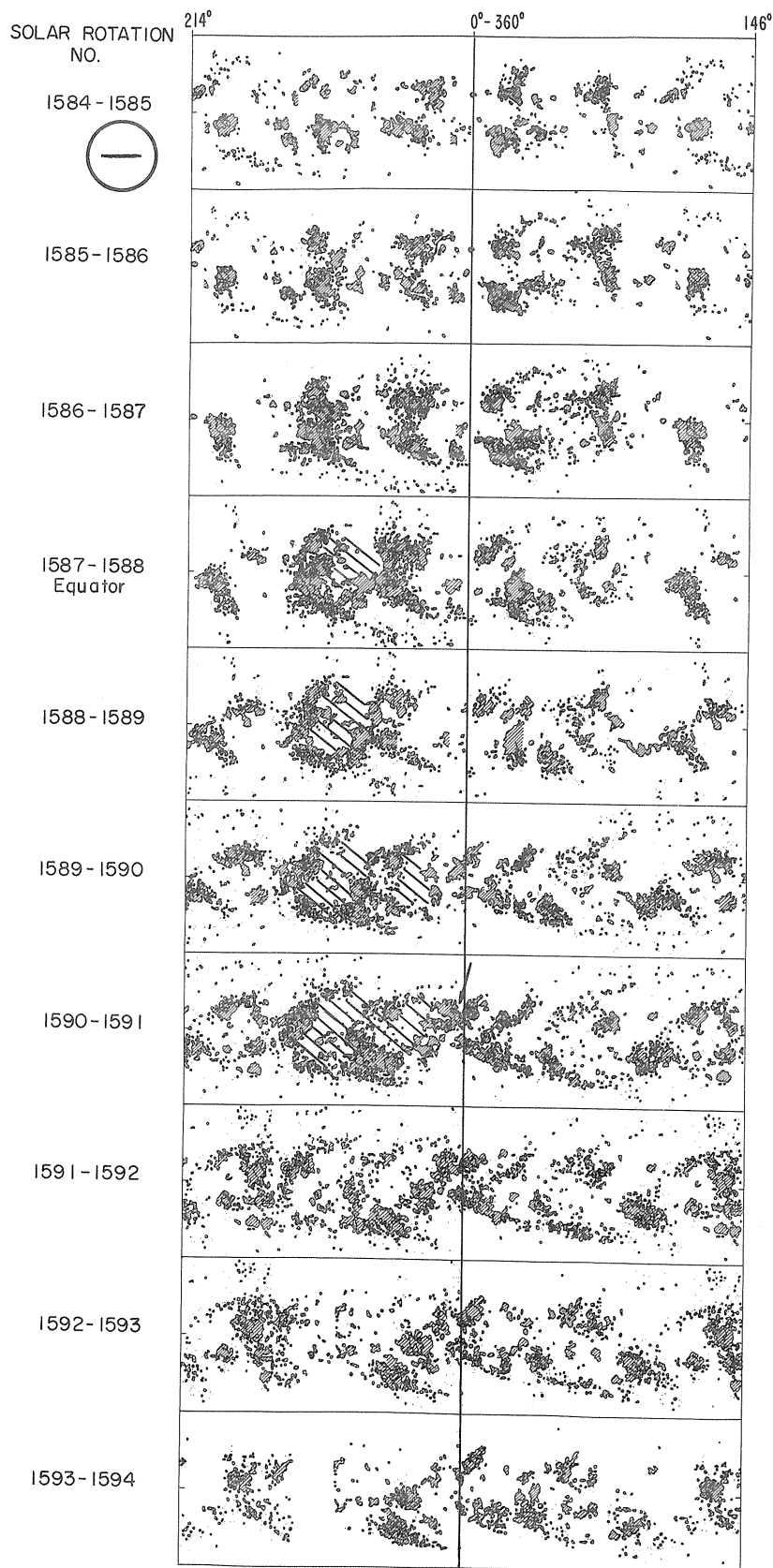


Fig. 1a. Series of consecutively mounted magnetic synoptic charts of negative polarity for rotations Nos. 1584-1594. For integration two consecutive maps, one of which is repeated, are overlapped. The position of the proton-flare region which occurred in rotation 1590 is shown by the arrows.

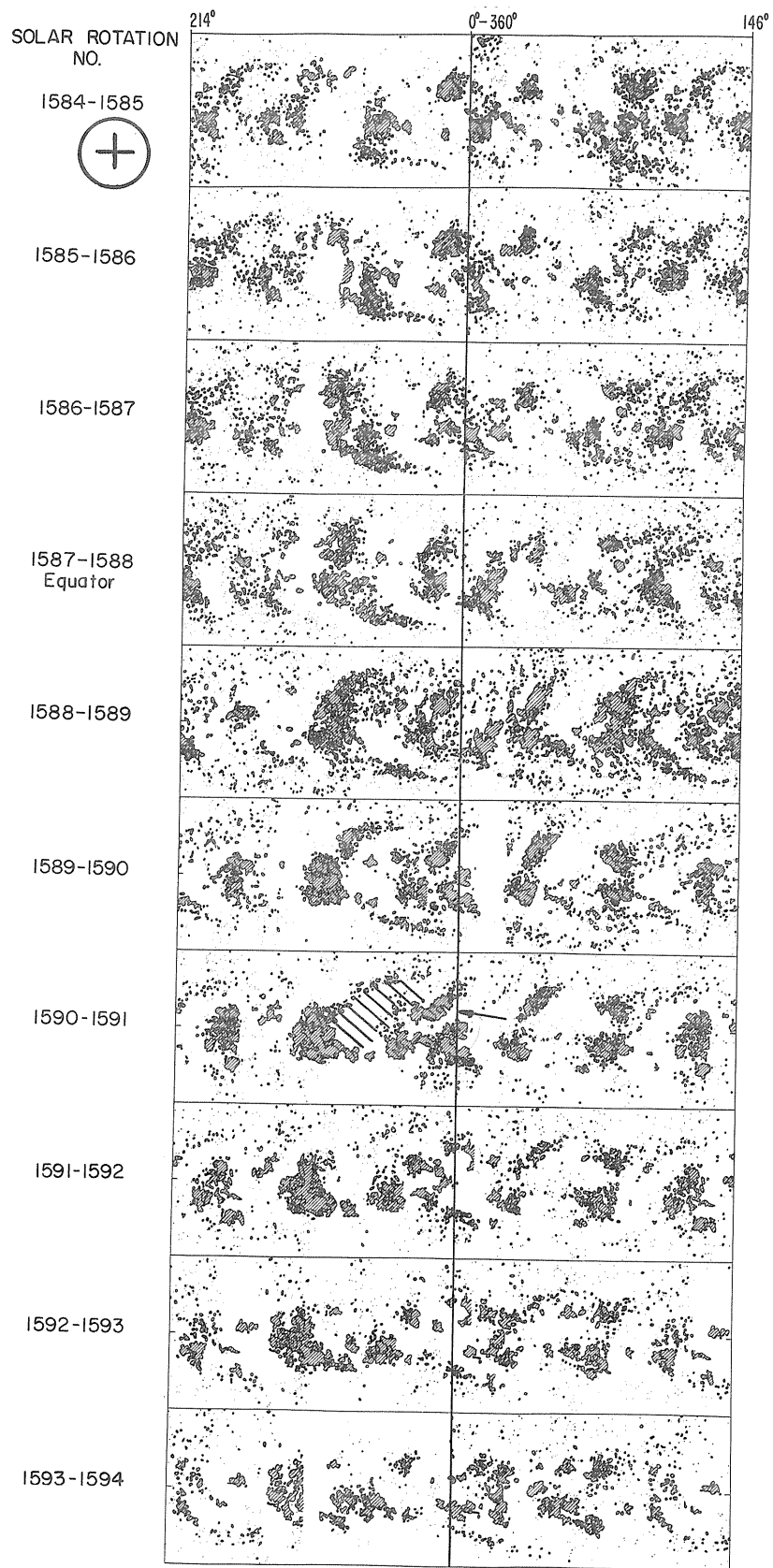


Fig. 1b. The same series of consecutively mounted synoptic charts as in Fig. 1a for positive polarity fields.

Magnetic Field Development of the August 1972 Proton-Flare Region

by

V. Bumba

Astronomical Institute of the Czechoslovak Academy of Sciences
Ondrejov, Czechoslovakia

Introduction

Several times [Bumba, Krivsky, Sykora 1972; Bumba 1972 a, b; Bumba, Sykora 1972 a, b; Bumba 1973] we have tried to demonstrate that a characteristically long-lived, regular, large-scale (occupying practically half of the solar surface) magnetic field feature is needed for a proton-flare region to be formed in a certain position of the field pattern. In the present note we would like to do a similar treatment to show, on a much smaller scale involving only one active region, the development of the proton-flare region magnetic field throughout the course of several solar rotations.

It has already been found [Bumba, et al., 1968 a; Bumba, et al., 1968 b] that the formation of a "gulf" on a boundary of the two polarities of an active region magnetic field, observed with a relatively low resolution of 10" - 20", which takes place usually in the center of a sunspot group having the Zurich classification type of at least C complexity, is as a rule related to a sudden increase of the group flare activity. The proton-flare region of August 1972 may be used as an example of such a situation development.

We obtain still more information by comparing the distribution of photographically estimated magnetic fields in visible sunspots with magnetic fields measured photoelectrically for the whole region.

Observational material used

The available daily Mt. Wilson Observatory magnetograms have been used as the basic observational material. For the estimation of magnetic polarity distribution in the sunspot group itself on sunspot photographs, we took the "Longitudinal sunspot magnetic fields" measured at the Roma Astronomical Observatory and published in the Solar Phenomena Monthly Bulletin, as well as the "Magnitnie polja solnethnykh platen" published by the Main Astronomical Observatory of the Academy of Sciences of the U.S.S.R. in Pulkovo.

Results

A. Magnetic field changes during eight rotations

Figure 1 represents the magnetic field configuration development during several passages of the studied part of the sun across the visible solar disk. Contrary to the previous paper [Bumba, 1973] more details in magnetic field distribution changes and in appearance and disappearance of magnetic flux with relatively low resolution (17" by 17") may be followed.

One very interesting behavior of the magnetic field situation may be noted: during rotations 1587 and 1588 in this part of the sun there is the normal distribution of the leading (negative) and following (positive) polarities in the northern hemisphere. During rotation 1587 there are two large, old, widely dispersed regions of both polarities with small inclusions of new negative polarity formations in the old positive fields. During rotation 1588 the situation does not seem to change very much, although there is a large gap in the observational material. The growing importance of the positive polarity seems to be detectable. During rotation 1589, one rotation before the proton-flare region appearance, the observed area is covered mostly by the positive polarity, but there are some remnants of the older negative polarity from an active region clearly visible one rotation before. This older negative polarity area, which is the remainder of the leading part of a bipolar region, is located eastwards from the main body of the mentioned positive polarity at a relatively large distance. No rotations of both polarities in this part of the observed area seem to be detectable; therefore, there does not exist any place with magnetic field gradient in the horizontal direction. In the western part of the positive polarity body the new formation of a bipolar region is clearly visible.

During the most important passage (rotation 1590) of the region across the visible disk the change in polarity distribution is striking: both polarities we observed one rotation before as widely separated are now pushed together with the main boundary between them being tilted to the equator. The positive polarity is now in the leading position. The main part of the negative polarity, in which the studied sunspot group developed as an island of positive polarity, now plays the role of a following polarity. One has to say that a weaker negative polarity area, the remainder of a bipolar region from the previous rotation, is still visible at the right position for a leading polarity south-west from the main positive polarity body.



CMP
Day

Fig. 1. Solar magnetic field development during eight solar rotations. The proton-flare activity occurred during rotation No. 1590. Positive polarity fields are shown as darker than the negative polarity fields.

During the next rotation, No. 1591, the magnetic situation does not show great changes except for the decrease of gradients, the joining of the island with the main positive polarity area, and the development of a new positive polarity island. During rotation 1592 the distribution of polarities due to several renewals of activity is again normal. Renewals of activity are still weaker. In the studied area not only the divergence of both polarities, but also fast disintegration and very soon the disappearance of practically all magnetic fields is again striking. This may be seen especially during rotation No. 1594, where this time the remains of the negative polarity prevail.

B. Changes during the disk passage of the proton-flare occurrences

The formation of a gulf on the main boundary of polarities and the formation of an island of one polarity in the other polarity area seem to be very characteristic not only for the proton-flare region development, but they are also generally associated with the increase of flare activity in all regions demonstrating such magnetic field configurations [Bumba, et al., 1968 a; Bumba, et al., 1968 b; Rust 1968; 1972]. Only by proton-flare regions may such an island be represented by nearly all sunspots of the group.

Following the development of the described situation throughout the whole passage of the region from the eastern to the western limb we may see that the formation of a positive polarity island is very probably related to the remnants of the main positive polarity body seen one rotation before. With the appearance and growth of this island we must also anticipate the occurrence of a new system of magnetic lines of force which must be orthogonal or even antiparallel to the older system of lines of force joining the main opposite polarity bodies.

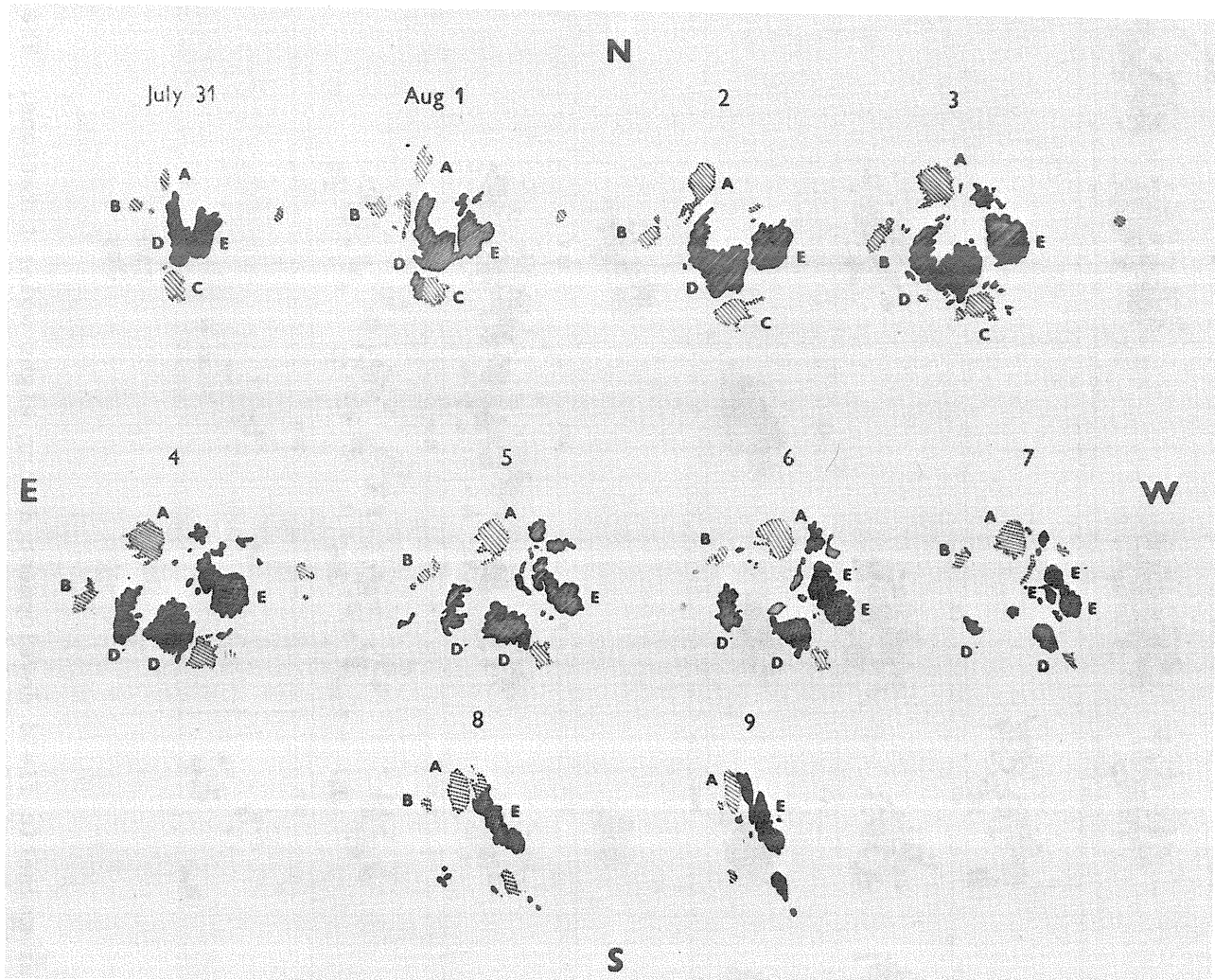


Fig. 2. The outlines of the visible sunspot nuclei in the proton-flare group drawn from high-resolution photographs. The polarity estimations are taken from the Roma and Pulkovo observations. The positive polarity is the darker one. The nuclei with vertical hatching are those without polarity estimations.

C. Development of magnetic polarity distribution in the visible spots of the proton-flare group

The development of the positive polarity island described above is demonstrated in more detail on Figure 2. The figure represents the outlines of the visible sunspot nuclei in the proton-flare group drawn from the high resolution photospheric photographs. The data concerning the polarity of individual sunspots are taken from photographic measurements (see Section B). Therefore, it is sometimes difficult to say whether the whole spot has the same polarity. The greatest difficulties were with the estimation of polarities in small, fast changing nuclei in the center of the group.

The figure presents the unusual situation in the polarity distribution and the fact that the greatest number of visible spots have the positive (following) polarity. During the whole disk passage only small changes in the negative (leading) polarity spots are seen, while the greatest and fastest changes involve the positive polarity spots, where their continuous divergence and diminution is apparent. In the same time the most stable magnetic field with the highest intensity has the negative polarity spot.

More time is needed for evaluation of all our high resolution photographs and magnetic field photographic and photoelectric measurements concerning the study of the past variations of the spot and possibly the field configuration in the center of the spotgroup.

D. Comparison with flare activity

Studying the development of the magnetic as well as the photospheric situation during the passage of the group across the visible disk, there seem to be three important moments in the life history of the group: 1. during August 1, when the development of new formations in the north-west part of the group started (northward from the spot E), 2. during August 4 or 5 when the development reached its maximum, and 3. during August 7 when the fast disintegration of the group began. This is in good agreement with Krivsky's results [Krivsky, 1974] as may be seen on Figure 3 representing the integral curves of the H α and X-ray flare activity. The slope of both curves changed for the first time during August 1, when a fast increase of flare activity occurred. Then starting with the end of August 4 the flare activity throughout August 5 and 6 was relatively small and increased again during August 7. From August 8 it was small again. The method of construction of an integral flare activity curve has been recently described [Krivský, 1973].

REFERENCES

- | | | |
|--|--------|---|
| BUMBA, V. | 1973 | Elsewhere in this compilation |
| BUMBA, V., R. HOWARD,
M. J. MARTRES, and
I. SORU-ISCOVICI | 1968 a | Structure and Development of Solar Active Regions,
<u>I.A.U. Symposium, No. 35</u> , Kiepenheuer (ed.), 13. |
| BUMBA, V., L. KRIVSKY,
M. J. MARTRES, and
I. SORU-ISCOVICI | 1968 b | Structure and Development of Solar Active Regions,
<u>I.A.U. Symposium, No. 35</u> , Kiepenheuer (ed.), 311. |
| KRIVSKY, L. | 1973 | <u>Bull. Astron. Inst. Czech.</u> , <u>24</u> , in print. |
| KRIVSKY, L. | 1974 | <u>Bull. Astron. Inst. Czech.</u> , <u>25</u> , in print. |
| RUST, D. M. | 1968 | Structure and Development of Solar Active Regions,
<u>I.A.U. Symposium, No. 35</u> , Kiepenheuer (ed.), 77. |
| RUST, D. M. | 1972 | <u>Solar Physics</u> , <u>25</u> , 141. |

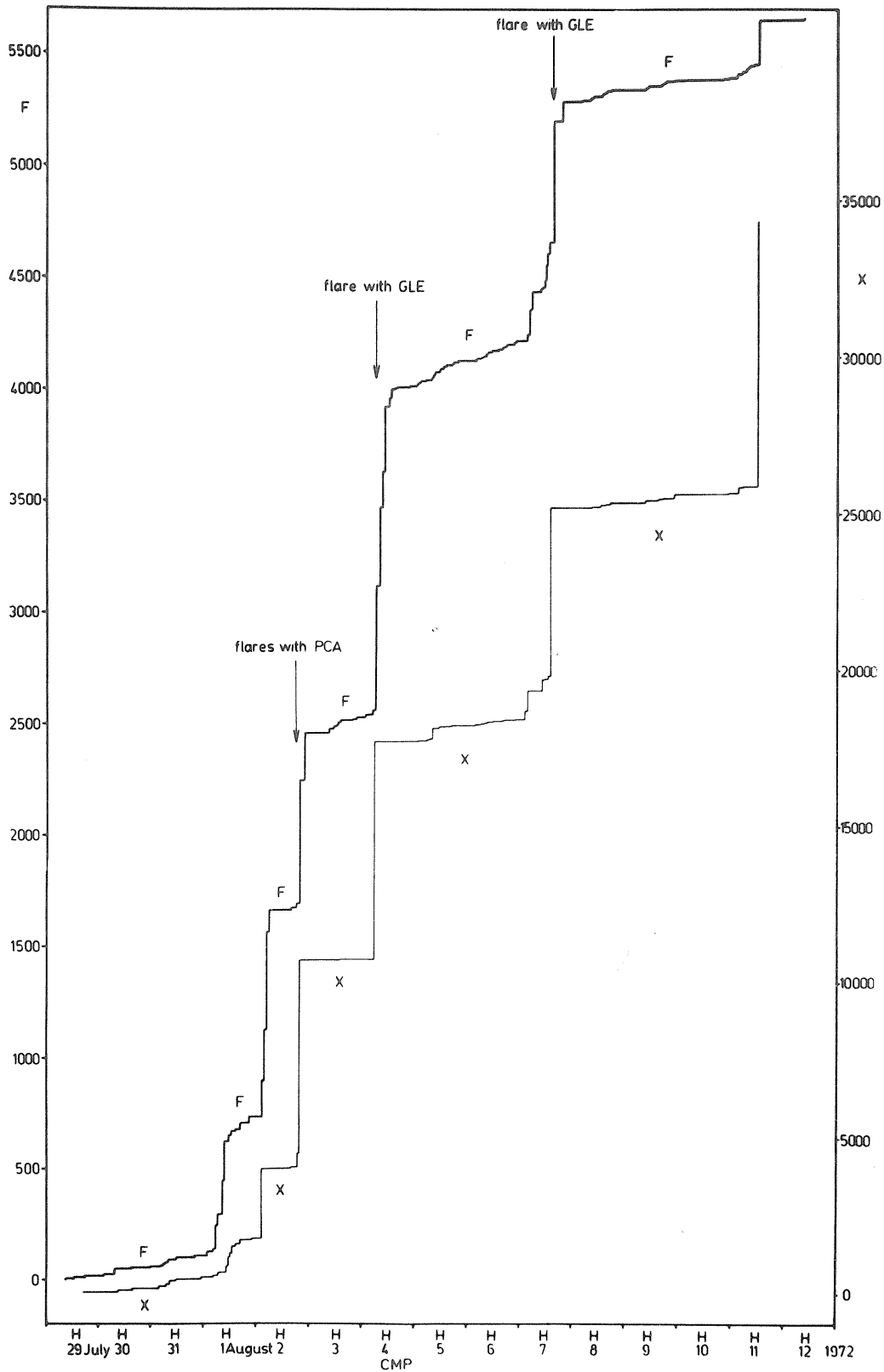


Fig. 3. Krivsky's results [Krivsky, 1974] representing the integral curves of H_{α} and X-ray flare activity. [See Krivsky, 1973, for the method of curve construction.] Values of the H_{α} flare index (darker curve) is to the left, the X-ray flare index to the right.

Observations of the Magnetic Fields of the August 1972 Sunspot Group

by

G. A. Chapman
San Fernando Observatory
Space Physics Laboratory
The Aerospace Corporation
Los Angeles, California

The magnetic field observations reported here were obtained with the 61 cm vacuum telescope and 3 meter spectroheliograph of the San Fernando Observatory and show the line of sight component of the magnetic field. All figures are to the same scale except Figure 4c. The spatial resolution varies from a typical value of about 3 arc-seconds to as high as about 1.5 arc-seconds on 5 August (Fig. 4). The cancellation for 8 and 9 August has higher background noise and reduced magnetic signal as well as loss of spatial resolution in the magnetic field. These difficulties are caused primarily by a wavelength separation between the two channels of the spectroheliograph [cf. Vrabc, 1971, for a description of the cancellation process]. Along with each magnetogram is presented a "wing sum" picture in which the magnetic signal is suppressed. These wing sum pictures will serve to show the penumbral structures clearly and thereby allow one to better interpret the corresponding magnetogram. Since they are from the same photograph used for the magnetogram, they have the same resolution and distortion.

The magnetograms compare favorably with those obtained by others [Livingston, 1973; Zirin and Tanaka, 1973]. The minimum detectable signal is about 30 Gauss/resolution element on 5 August and somewhat higher on other days. The observations of 5 August are the best of the series from 2-9 August in resolution, especially within the sunspot itself. Figure 4a shows the very complex field geometry that must have existed in this sunspot. There are numerous areas in and near the light bridges (Fig. 4b) where the longitudinal magnetic field apparently disappears over a small area of several arc-sec extent. (The gray umbrae have no magnetic signal and should be disregarded.) The crooked feature in the NW part of the sunspot is apparently real, lying within the penumbra. These irregularities are quite unusual. The typical penumbral magnetic field pattern is more like that of the large sunspot on the north side of the group. The irregular field patterns suggest that the magnetic field is highly curved in places and has strong local variations in strength in other places.

A time-lapse movie 1650 to 0035 UT on 5/6 August shows extensive outflow of magnetic structures at the edge of and somewhat beyond the penumbral boundary, especially on the west (right) side.

During the period 2-6 August, while the sunspot group changes greatly, a moderate-sized pore can be seen just west of the main group of sunspots. This pore does not change position very much, and the nearby network magnetic fields preserve some of their identity during this same period. Therefore, it is concluded that the large sunspot group is like an isolated system having little or no interaction with the surrounding network magnetic fields.

The photographic cancellation and printing was done mostly by R. Maulfair. This work was supported by the company-financed research program of The Aerospace Corporation.

REFERENCES

- | | | |
|-------------------------|------|---|
| LIVINGSTON, W. L. | 1972 | Private communication. |
| RUST, D. M. | 1972 | The great solar flares of August, 1972, <u>Sky and Telescope</u> , 44, 226-230. |
| VRABEC, D. | 1971 | Magnetic field spectroheliograms from the San Fernando Observatory, <u>IAU Symp.</u> , 43, 329-339. |
| ZIRIN, H. and K. TANAKA | 1973 | The flares of August 1972, <u>BBSO preprint No. 128</u> . (Abstract appears in this compilation.) |

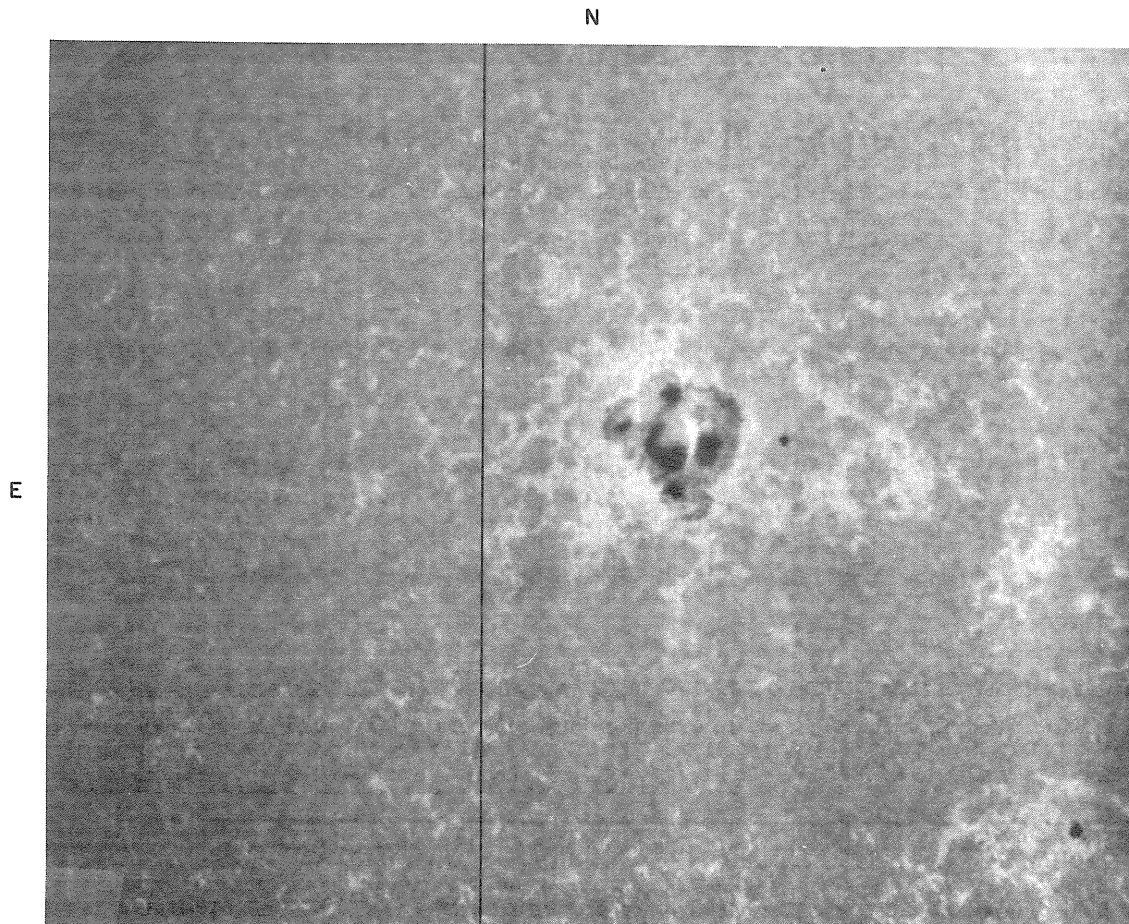


Fig. 1. Photospheric Network (unpolarized) seen in the wing of the MgI 5184Å on 2 August 1972 at about 2350 UT. This network shows the location of the photospheric magnetic field. The correct polarity must be determined from other sources.

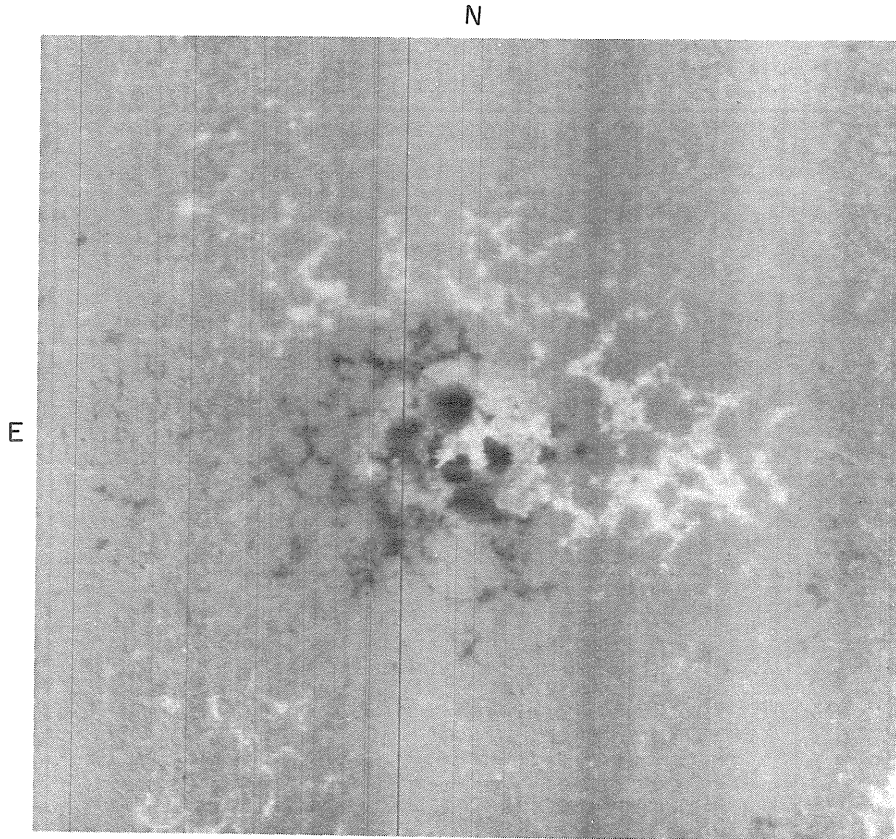


Fig. 2a. 6103\AA Magnetogram on 3 August 1972 (4 Aug., 0110 UT). White polarity is plus. North is up and east is to the left in heliocentric coordinates.

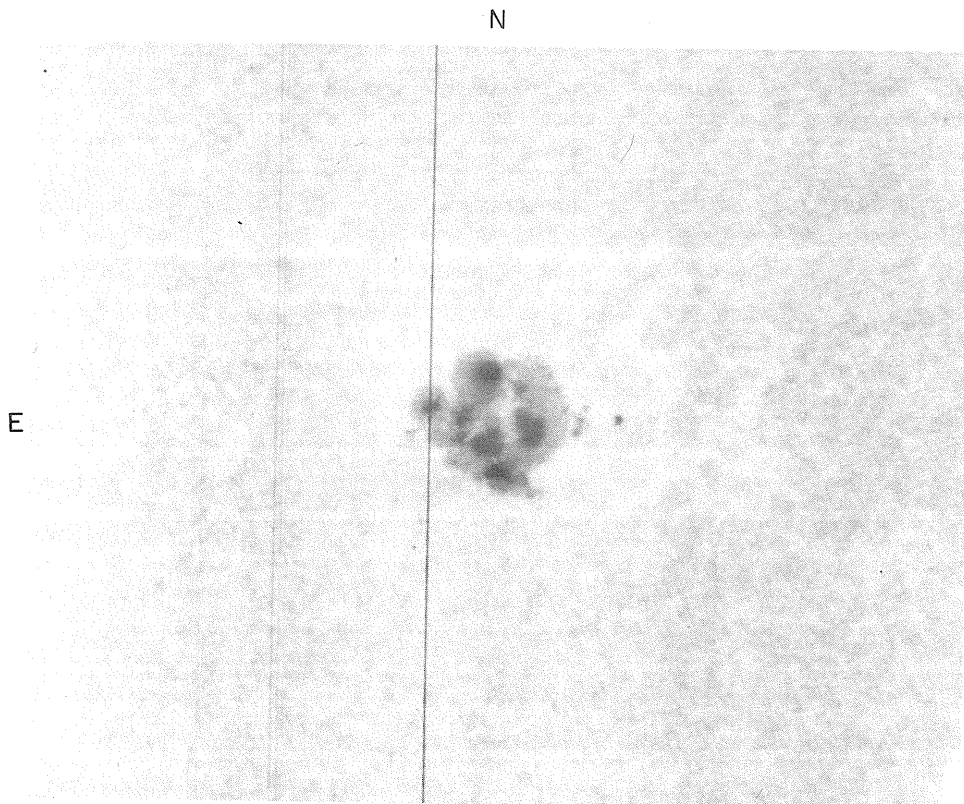


Fig. 2b. The scale is nearly the same in all figures and is shown in Figure 5a. 6103\AA wing sum on 3 August 1972. The contrast has been kept low in order to show the umbra-penumbra boundary.

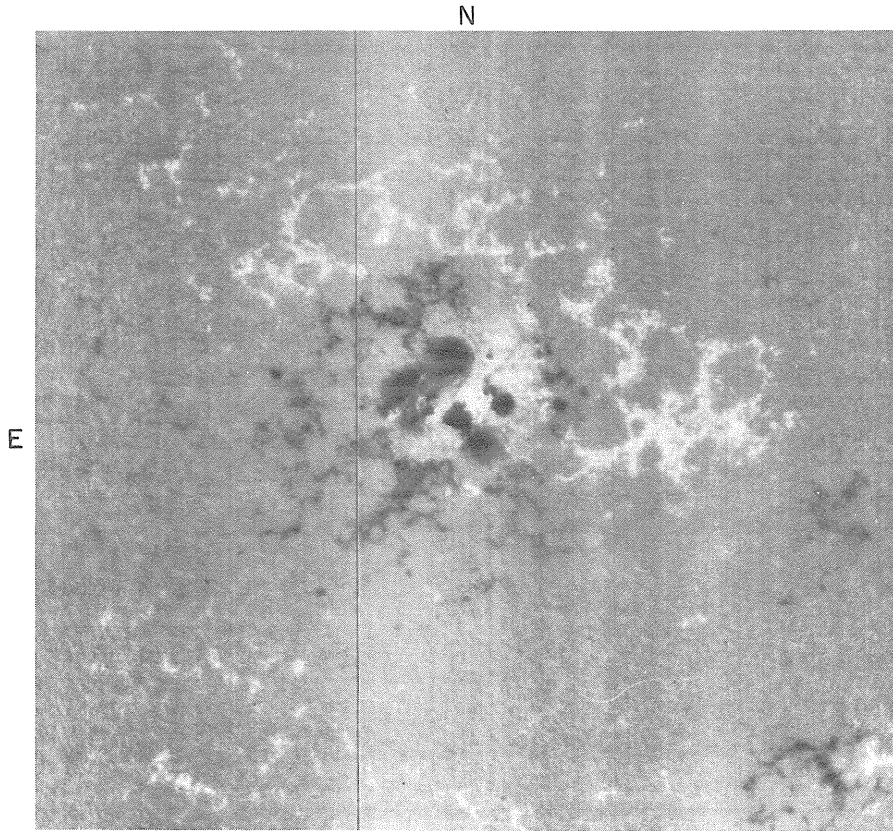


Fig. 3a. Magnetogram in 6103\AA on 4 August 1972 at 2234 UT.

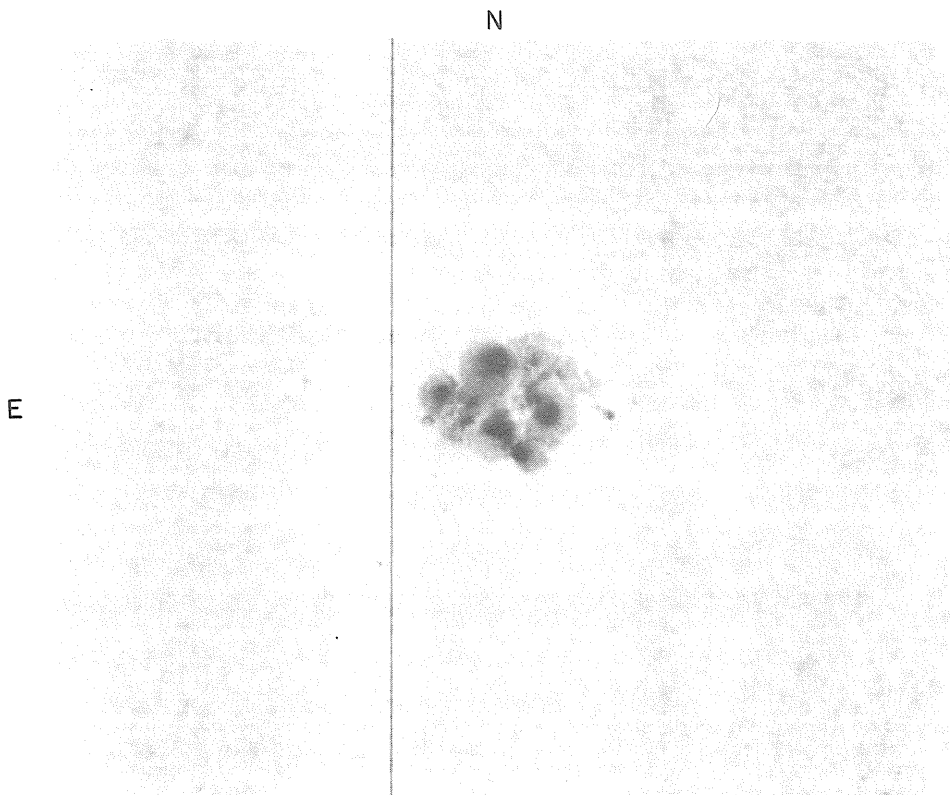


Fig. 3b. Wing sum in Ca I 6103\AA on 4 August 1972.

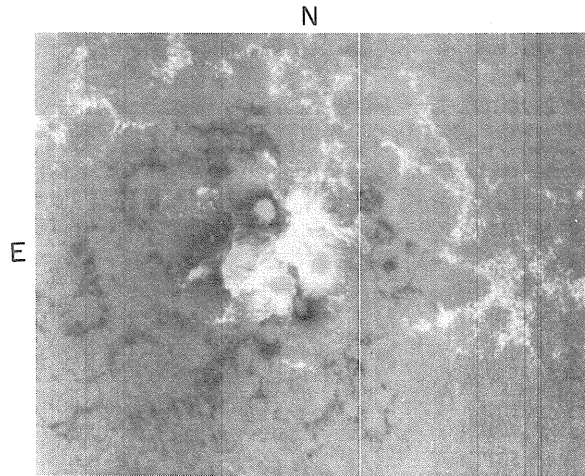


Fig. 4a. Magnetogram in 6103\AA on 5 August 1972 at 1730 UT.

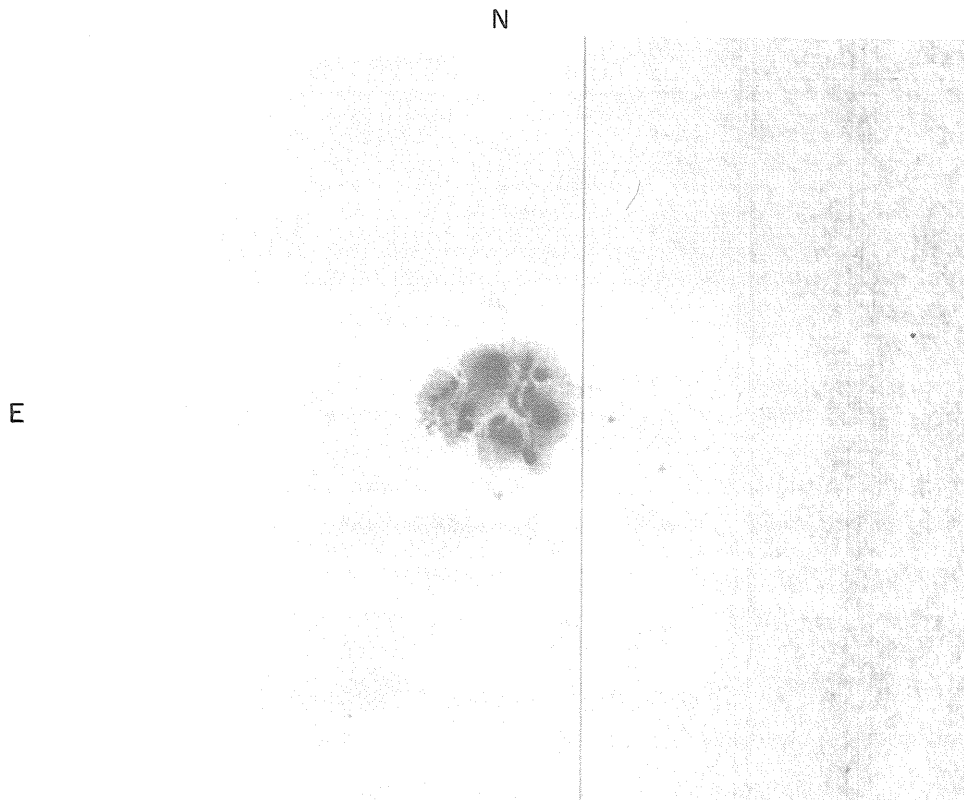


Fig. 4b. Wing sum in 6103\AA on 5 August 1972.

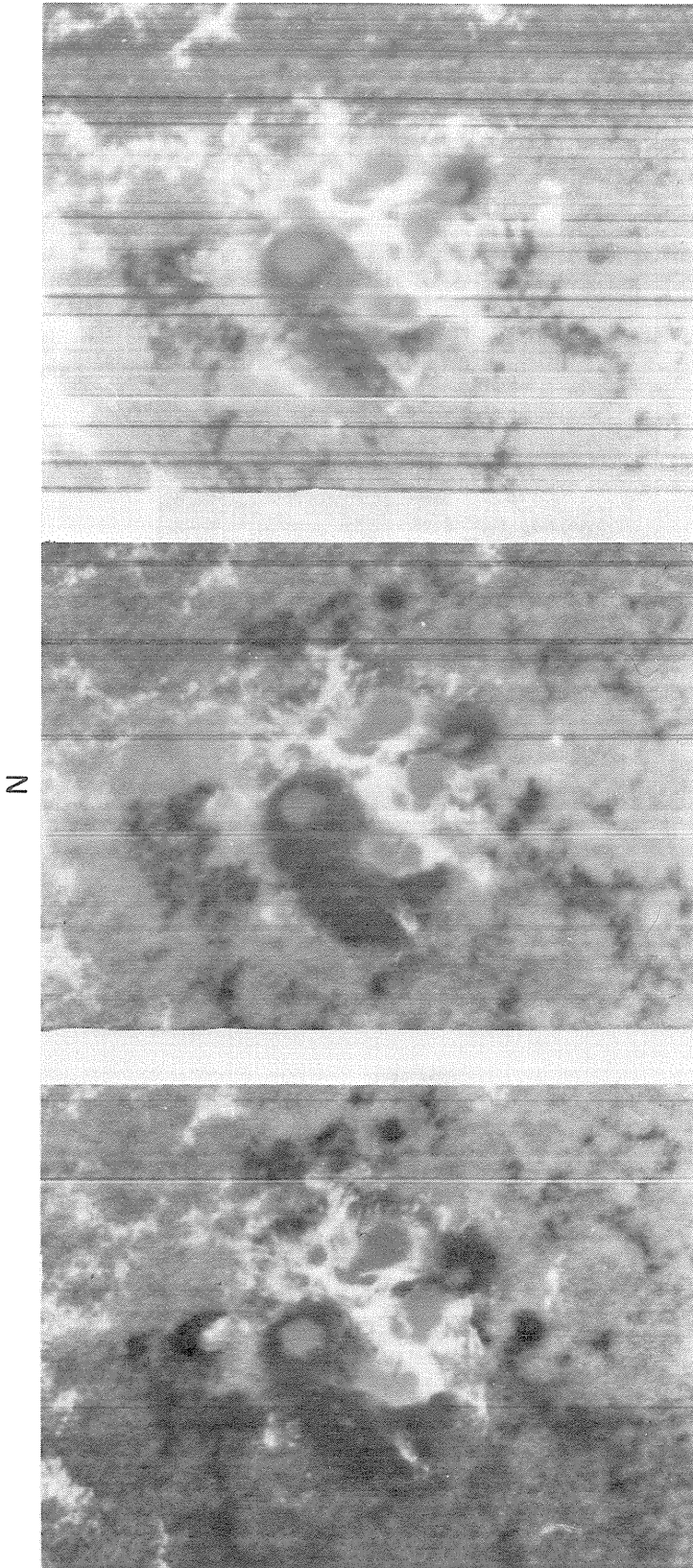


Fig. 4c. Magnetograms separated by about 2 1/2 hours between each. The times are, from left to right; 1735 UT, 2030 UT, and 2345 UT. These frames have been selected from 46 integrated magnetograms covering 8 hours on 5 August 1972.

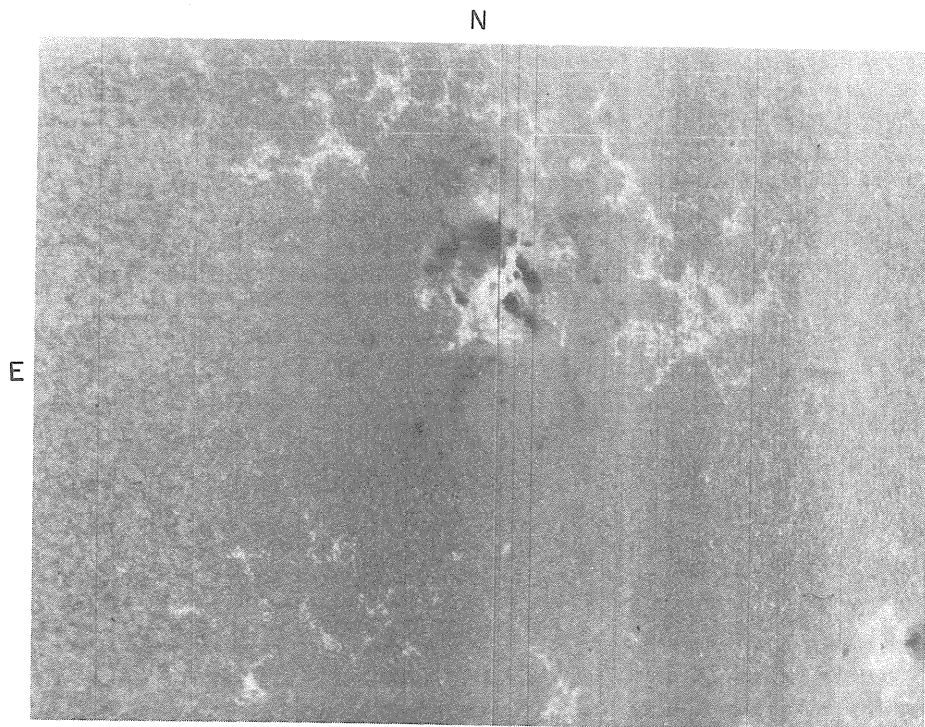


Fig. 5a. Magnetogram in 6103\AA on 6 August 1972 at 1947 UT. The two channels were not at the same position in the line resulting in uneven cancellation and high background noise.

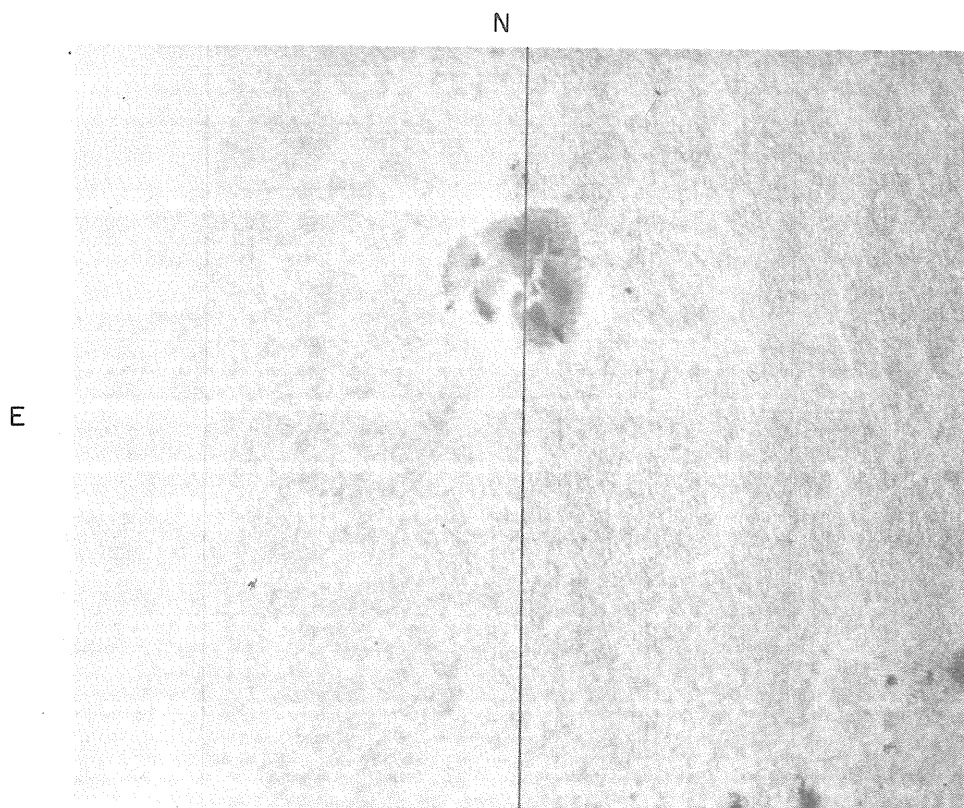


Fig. 5b. Wing sum in 6103\AA on 6 August 1972.

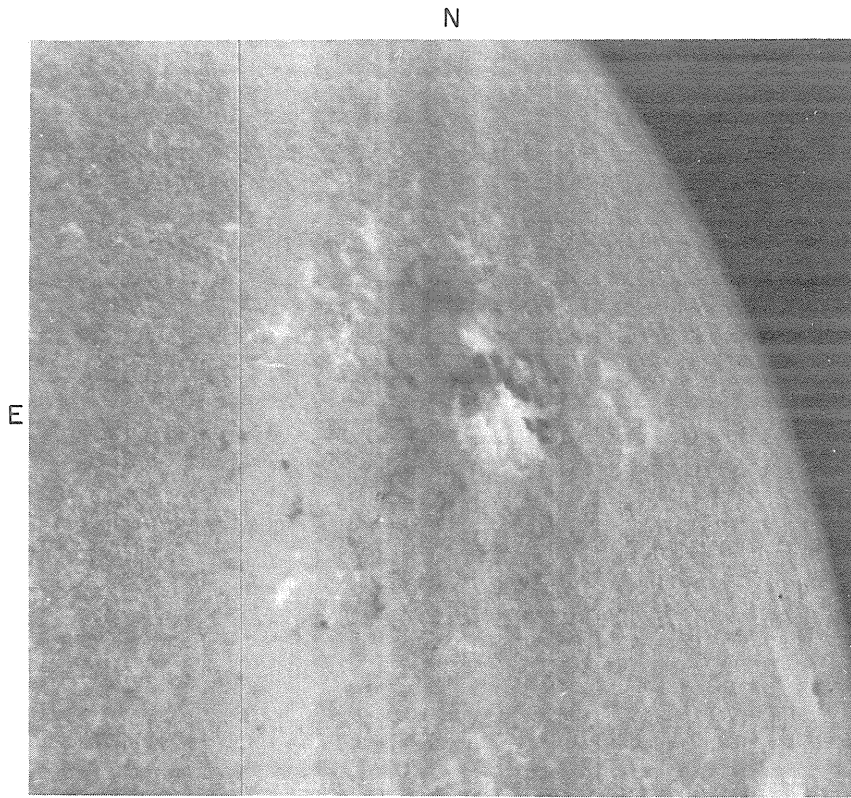


Fig. 6a. Magnetogram in 6103Å on 8 August 1972.

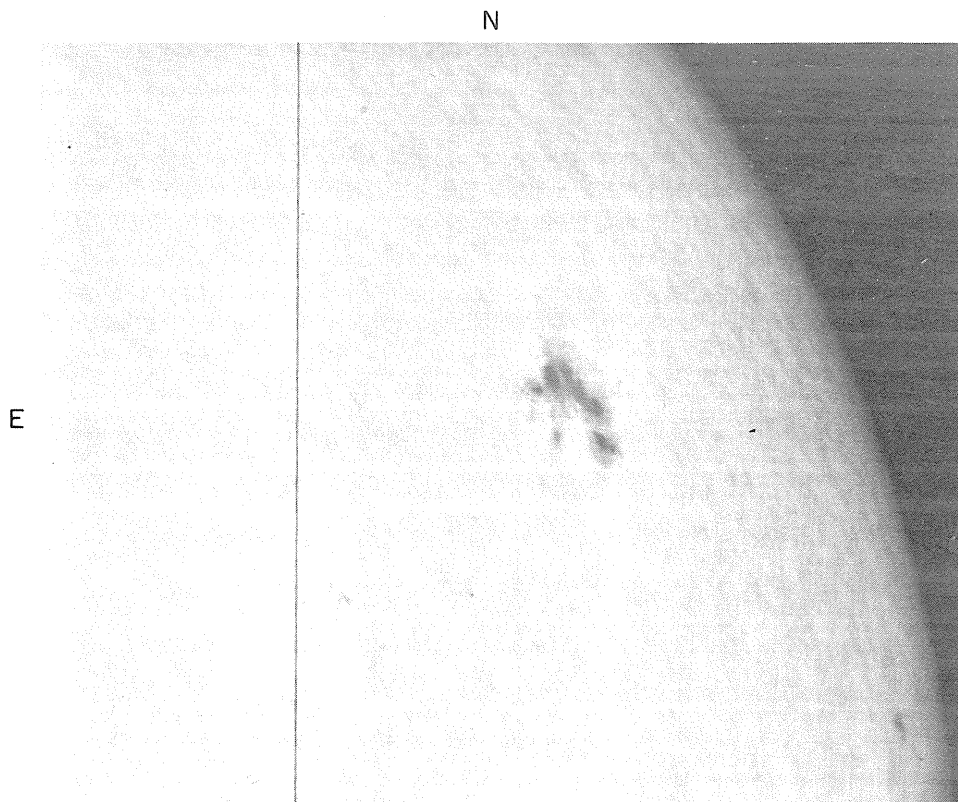


Fig. 6b. Wing sum in 6103Å on 8 August 1972.

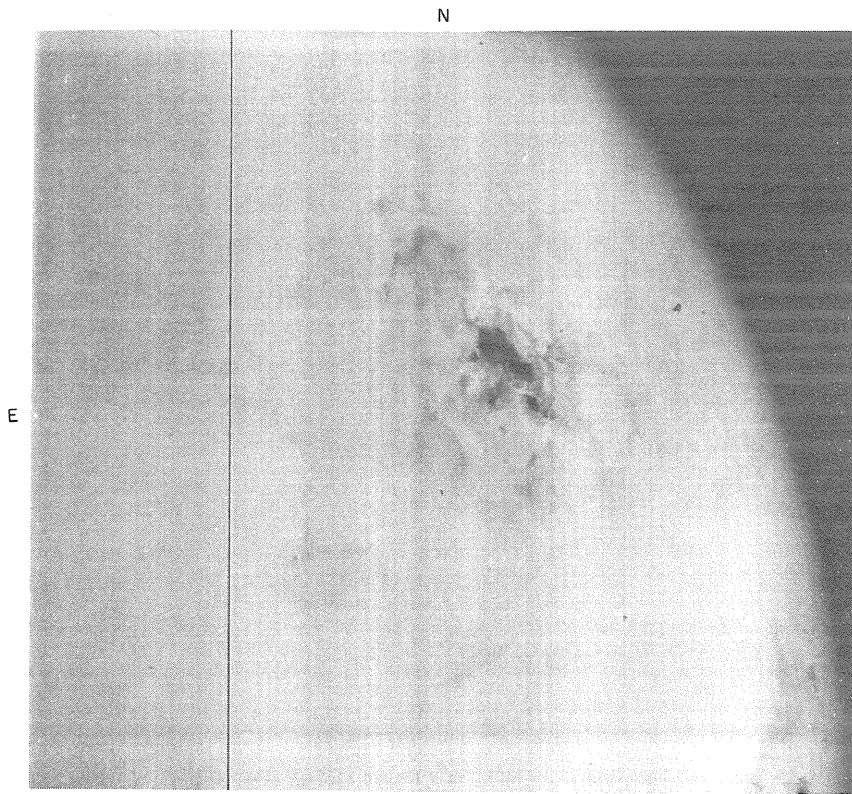


Fig. 6c. Continuum - He D₃ on 8 August 1972 at 2211 UT.

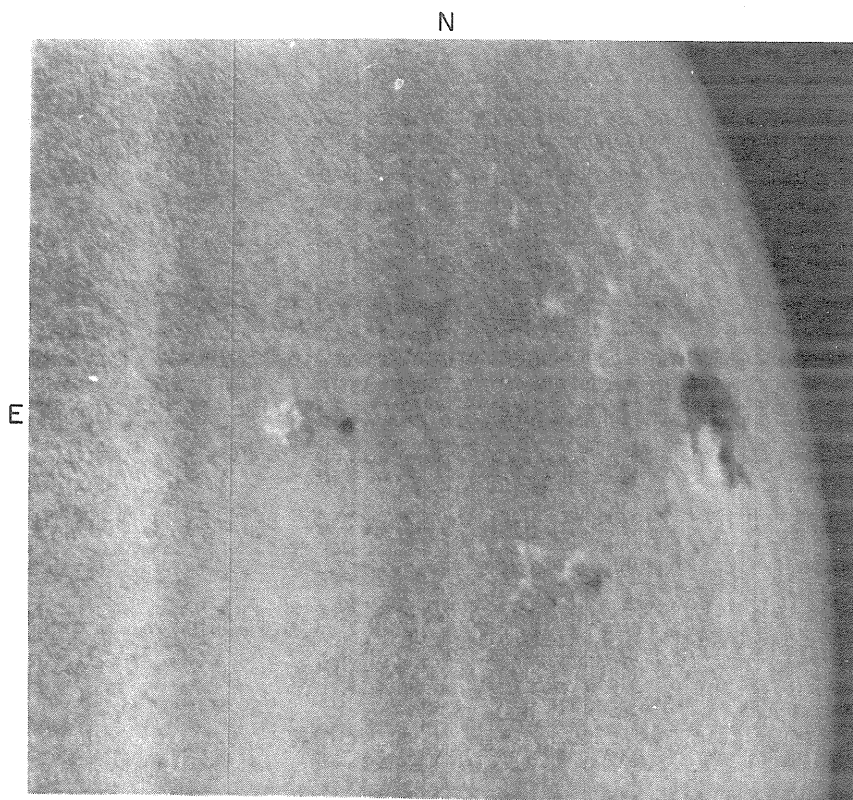


Fig. 7a. Magnetogram in 6103Å on 9 August 1972 at about 2130 UT.

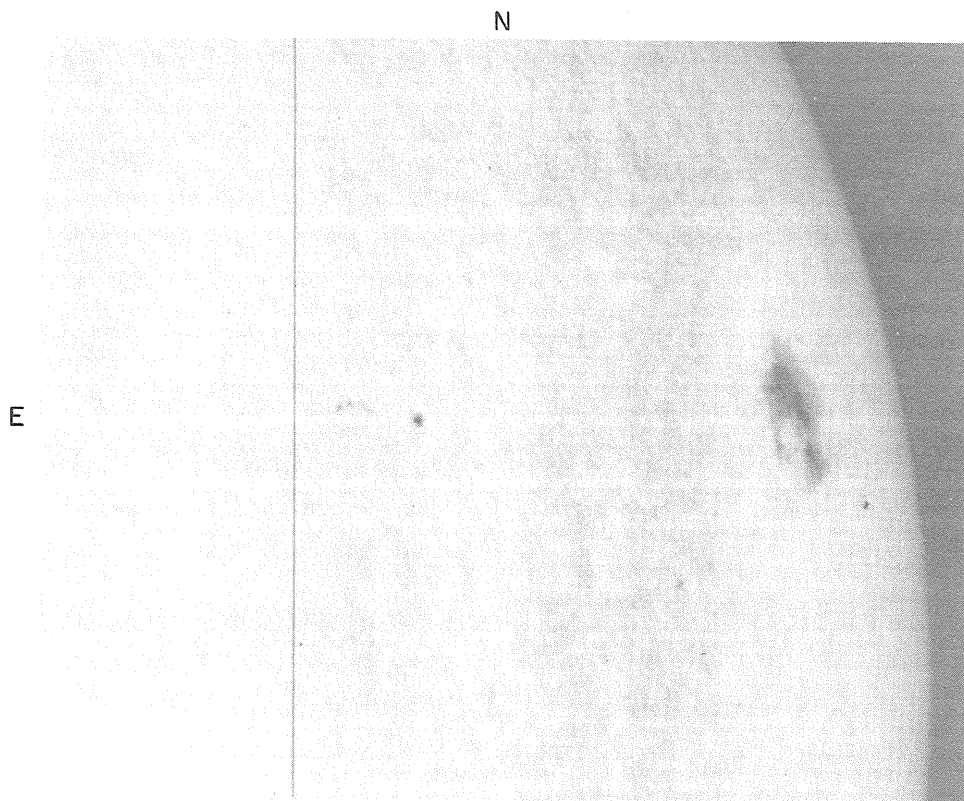


Fig. 7b. Wing sum in 6103Å on 9 August 1972.

Photospheric and Chromospheric Magnetograms Related to the 3B Flare of 4 August 1972

by

W. C. Livingston
Kitt Peak National Observatory
Tucson, Arizona

Kitt Peak does not maintain a daily solar patrol and it was only by chance that the events of 2 - 4 August were covered. The magnetograph was scheduled for those three days and the uniqueness of McMath #11976 commanded our attention. Occasional full-disk magnetograms, taken in connection with other programs, provide a fragmentary but useful picture of the general birth, evolution, and decay of the region.

THE OBSERVATIONS

Table I catalogues our magnetograph data on #11976. Our photospheric magnetograms are derived from the Zeeman effect in the wings of Fe I $\lambda 5233$, a medium strong, high excitation Fraunhofer line [Livingston and Harvey, 1971]. The profile of Fe I $\lambda 5233$ shows negligible changes between quiet photosphere, faculae, and penumbra conditions and magnetograph response is linear to greater than 3000 G. However, in a sunspot umbra Fe I $\lambda 5233$ deepens and becomes contaminated with molecular lines causing a signal saturation at about 1200 G. Observational points for umbral light are thus cut off at the 1200 G level.

Magnetograms are presented either as contoured isogauss maps or as CRT produced intensity plots. Isogauss maps are useful for estimating field gradients, position of the neutral line, and other quantitative but low resolution aspects. Intensity pictures convey best the structural details, particularly when the achieved resolution is high. Positive flux is indicated bright, negative dark. As the magnetic information and mean brightness are derived simultaneously from the spectrum line wings, the corresponding maps coincide exactly.

COMMENTS AND CONCLUSIONS

Birth of McMath #11976

The region emerged on 10 July as a just detectable bit of negative flux within the extensive field of positive flux making up the "following" field of #11947. This position of emergence can be identified on the previous day as being on the edge of a remarkably unipolar, well-developed network cell. By 11 July this EFR had developed a definite bipolar character having normal polarities. Our records then jump to 14 July when the region had greatly expanded and assumed the reversed polarity which then persisted over its subsequent life.

Evolution During 2 - 4 August

Isogauss maps for 2, 3, and 4 August are reproduced as Figures 1, 2, and 3. Notable is the growth of fields related to the NE spot and the intrusion of these negative fields into the lower latitude positive flux. This intrusion produced a monotonic increase of the line-of-sight gradients over the dates covered, not withstanding intervening major flare activity. On 2 August we deduce a maximum gradient of 0.4 G/km, on 3 August 1.0 G/km, and on 4 August 1.5 G/km. Of course, these observed gradients, being uncorrected for image smear, depend very much on atmospheric seeing.

Magnetic Fields and the 4 August Flare

The great flare of 4 August began at 0621 UT, around midnight local time. Fortunately, quality magnetograms were obtained of the region late the previous afternoon and early the following morning, providing a coverage of $\pm 7 \frac{1}{2}$ hours of the event.

A comparison of these pre- and post-flare magnetograms indicates no significant diminution or simplification of the fields as has been reported in connection with other great flares. In fact, because of improved seeing the post-flare magnetogram shows stronger, more complex field structure than pre-flare. We conclude that if a flare induced alteration of the magnetic field does exist, its detection requires better time resolution and a more uniform spatial resolution than allowed by our records.

TABLE I

Available Longitudinal Magnetograms

Date	UT	Type	Line	Comment
9 July	1343	full disk ¹	Fe I λ 5233	good seeing, no evidence of #11976
10 July	1534	full disk	Fe I λ 5233	#11976 as EFR
11 July	1534	full disk	Fe I λ 5233	#11976 as EFR
14 July	1601	full disk	Fe I λ 5233	#11976 definite polarity reversal
2 Aug.	2118	area ²	Fe I λ 5233	post max. flare in progress
2 Aug.	2127	area	Fe I λ 5233	post max. flare in progress
2 Aug.	2140	area	Fe I λ 5233	post max. flare in progress
2 Aug.	2207	area	Fe I λ 5233	post max. flare in progress
*3 Aug.	2309	area	Fe I λ 5233	~7 ^h before 0621 flare
*4 Aug.	1408	area	Fe I λ 5233	~7 ^h after 0621 flare
*4 Aug.	1437	area	Fe I λ 5233	exceptional quality
*4 Aug.	1511	area	H β λ 4861	chromospheric
	1605	area	Mg λ 5173 wing	upper photosphere
	1713	area	Mg λ 5173 core	extreme lower chromosphere
	1809	area	Fe I λ 5233	
	1905	full disk	Fe I λ 5233	
6 Sep.	2346	full disk	Fe I λ 5233	
27 Sep.	1753	full disk	Fe I λ 5233	CMP of old #11976

Notes: * Reproduced herein

¹ All full disk scans are made with scanning element area $\Delta s = (2.4 \text{ arc-sec})^2$

² Local area scans are centered on spot group. The size: $\Delta\alpha = 9 \text{ arc-min}$; $\Delta\delta = 8 \text{ arc-min}$; the element area $\Delta s = (1.2 \text{ arc-sec})^2$ (except 1437: $\Delta\alpha = 4.5 \text{ arc-min}$; $\Delta\delta = 4 \text{ arc-min}$; $\Delta s = (0.6 \text{ arc-sec})^2$).

This instrument resolution is further degraded in variable amounts by atmospheric "seeing", imperfections in optical focus, etc.

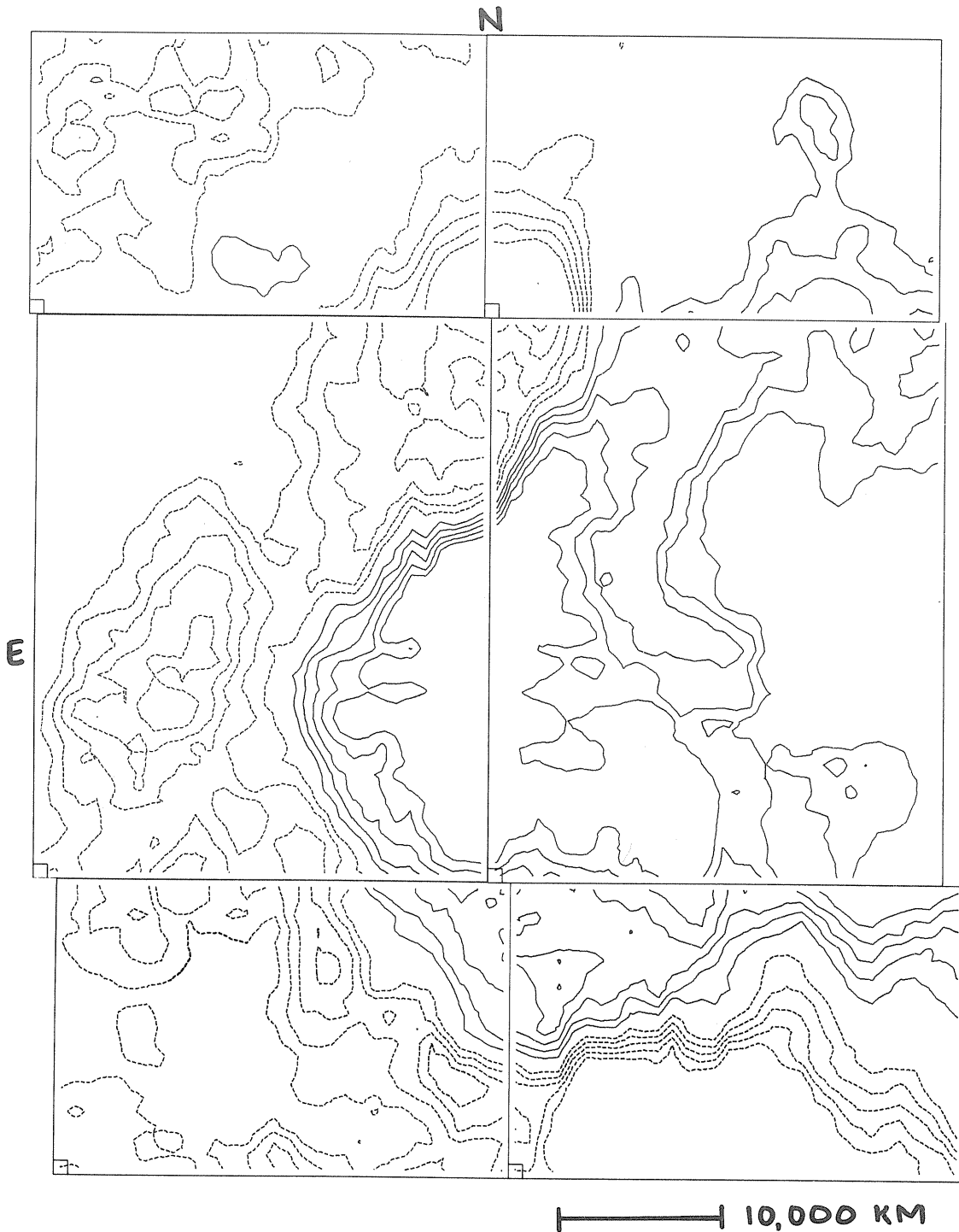


Fig. 1. Low resolution photospheric isogauss map of McMath #11976 for 2 August, 2118 UT. Solid contours are positive fields, dashed negative. Contour interval is 100 gauss. The zero gauss line has been deleted, as well as fields in excess of 500 G. North is at top, east at left.

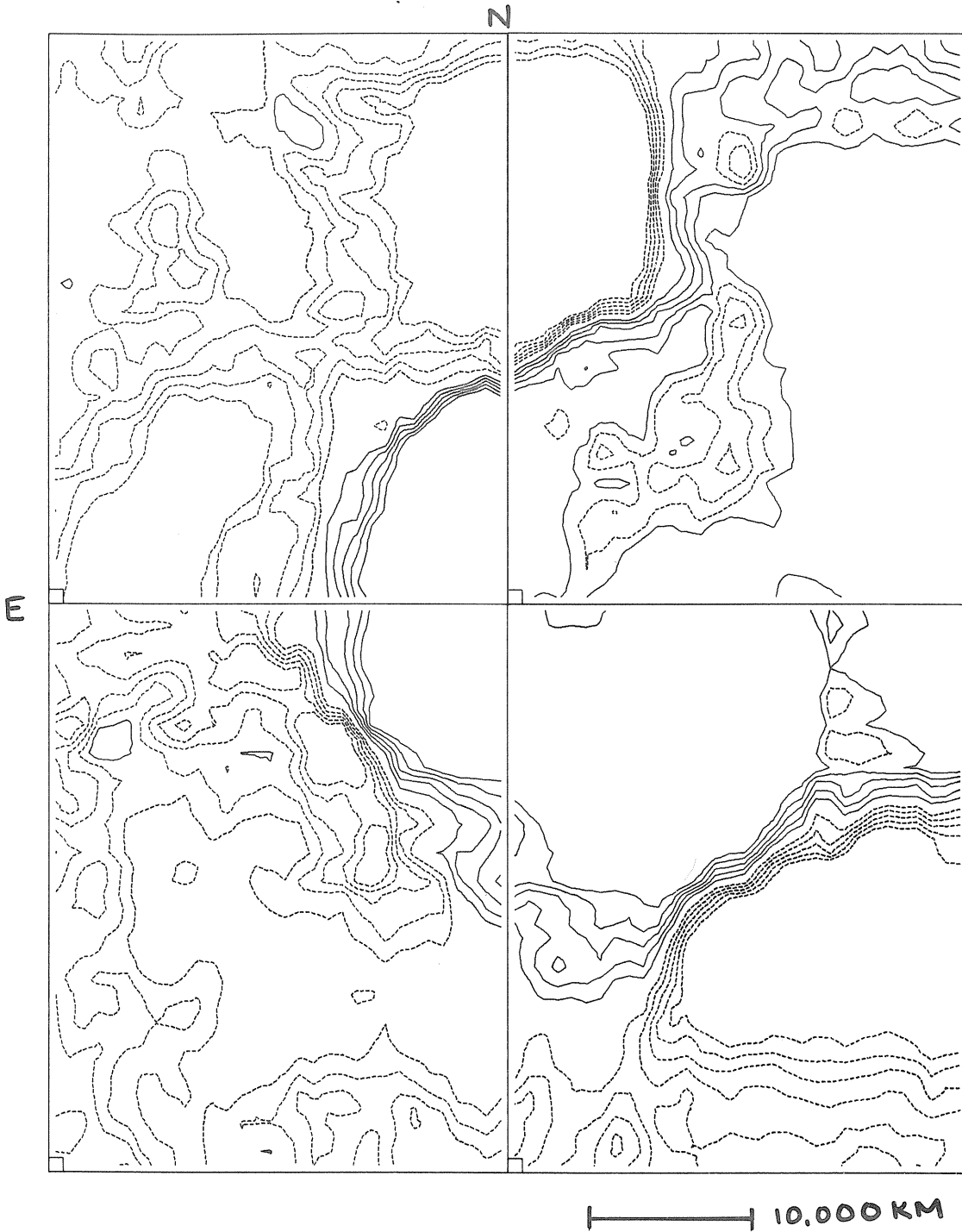


Fig. 2. Same as Fig. 1 except 3 August 2309 UT.

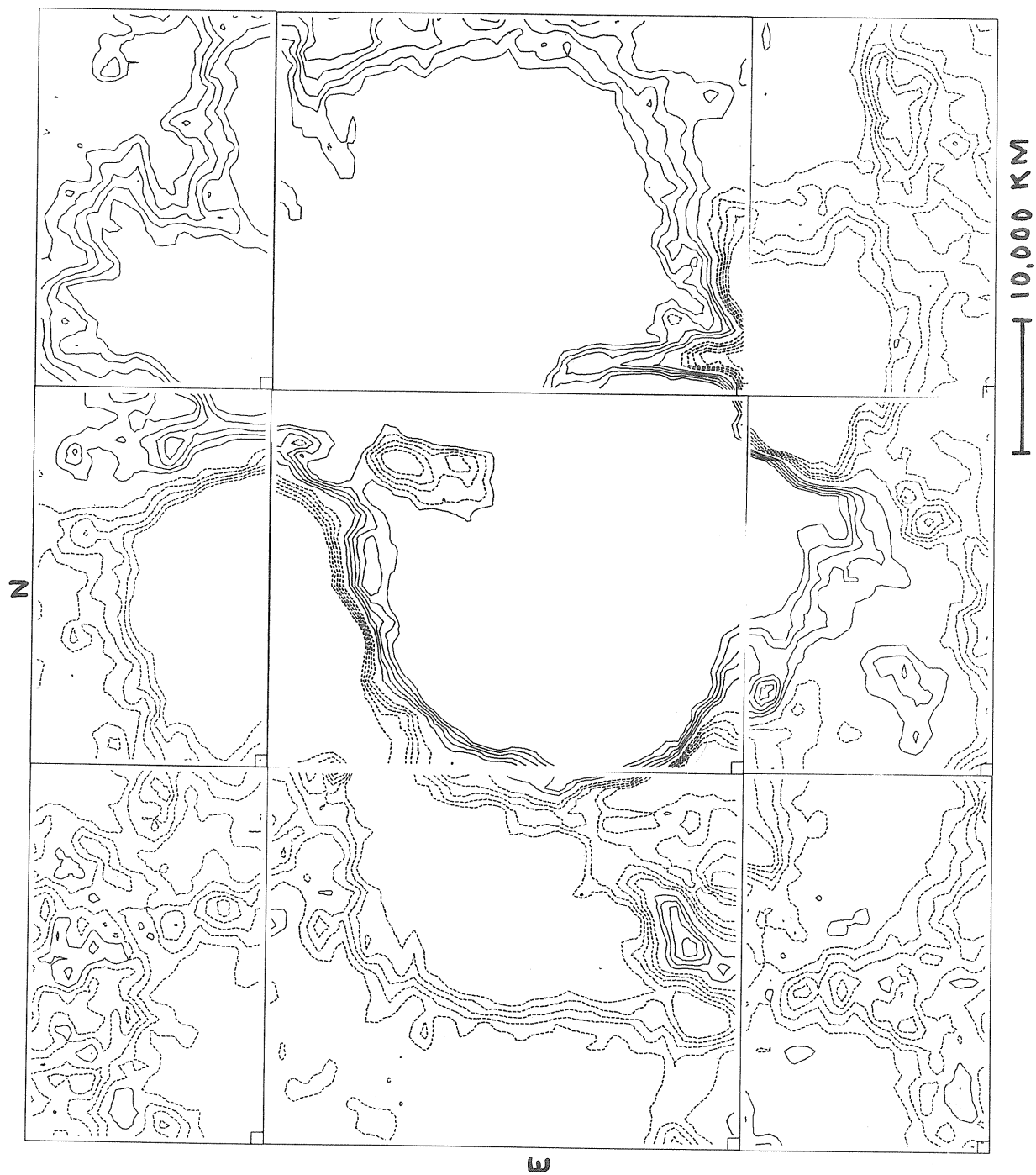


Fig. 3. Same as Fig. 1 except 4 August 1408 UT.

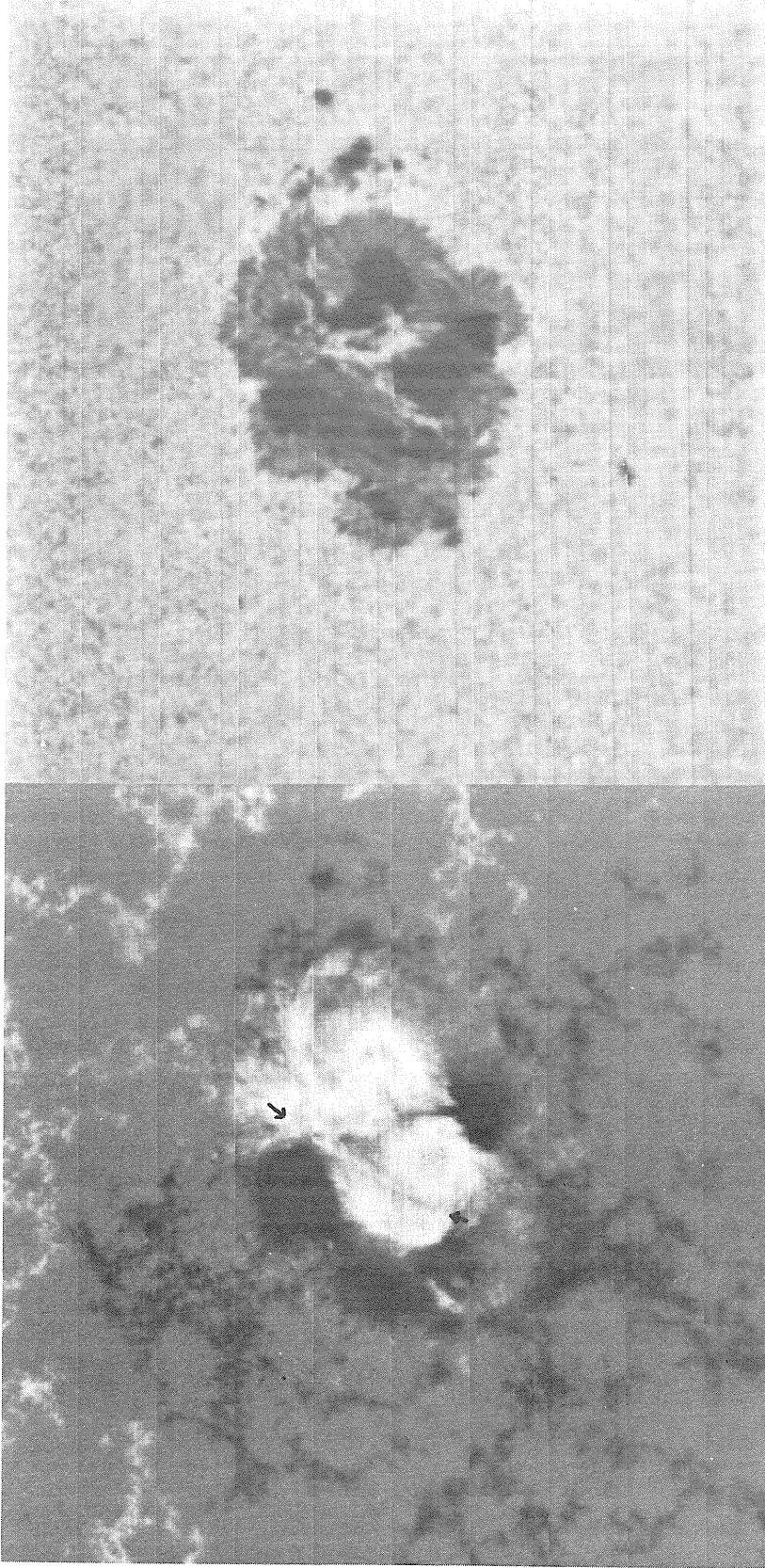


Fig. 4. High resolution photospheric magnetogram and simultaneous brightness map, 4 August 1437 UT. In the magnetogram bright features represent positive fields, dark negative. Fields in excess of 1200 G are displayed at constant intensity. Arrows indicate field anomaly discussed in text.

One curious field anomaly is noted on the 4 August records (see arrow, Figure 4). Spanning a fair portion of the positive flux is a feature describable as a double furrow, i.e., a linear alignment of enhanced flux bordered by troughs of reduced strength. Unlike the umbral related flux, this double furrow does not correlate in detail with any brightness (white light) formation. The double furrow was not distinctive on pre-flare magnetograms, and by 6 August had broken up according to an excellent Aerospace magnetogram (courtesy G. Chapman). A superposition of H α flare films taken at Tel Aviv (courtesy H. Zirin), show that the double furrow best matches the positive field side of the two strand flare.

J. Harvey has suggested that the double furrow may represent the establishment of conditions for a current sheet. Presumably the surrounding umbral fields are interconnected and closed. However, the central enhancement between the furrows is conjectured to be a source of open field lines.

On 4 August magnetic observations were also obtained in Mg λ 5173 and H β in an effort to determine the height dependence of the fields. The Mg λ 5173 maps are identical with the photospheric maps within the limitations imposed by seeing. However, the H β record does have distinctive characteristics. In general the chromospheric magnetic elements are diffuse compared to photospheric, possibly indicating a general divergence with height. Of initial interest was the apparent almost point-like reversal of field over the NE umbra seen in Figure 5 [Livingston, 1972]. However, magnetograph response in H β depends critically on Doppler error, and a displacement corresponding to 10 km/s downward will produce the observed reversal. Indeed, multislit spectra obtained for this region at Lockheed Solar Observatory (courtesy H. Ramsay and S. Smith) indicated umbral downflows of this magnitude. Therefore, the field reversal hypothesis was rejected.

Decline of McMath #11976

The interval 2 - 4 August saw the increasing emergence of negative flux along the western, or preceding, edge of the region. Had this trend continued the group would have reverted to a normal sense of polarity. This seems not to have happened. The CMP of #11976 on 27 September shows dissipated fields that continue to have a sense of reversed polarity.

SUMMARY

1. McMath #11976 emerged between 9 and 10 July. The polarity appeared at first normal but soon reversed.
2. Within our time resolution of 7 hours the flare of 4 August produced no diminution or alteration of field structure.
3. A field anomaly has been identified, possibly as the source of a current sheet connected with the western side of the double strand flare of 4 August.
4. An apparent chromospheric field reversal with height above the NE umbra was an instrumental effect.
5. The overall reversed polarity aspect of #11976 continued through its declining stages.

ACKNOWLEDGMENTS

Our interpretation of the Kitt Peak data has depended strongly on the more extensive patrol coverage provided generously and expeditiously by other observatories, especially Sacramento Peak, Lockheed, Big Bear, and NOAA. Mr. L. Ramsey measured the multislit spectra.

REFERENCES

- | | | |
|---------------------------------|------|---|
| LIVINGSTON, W. C. | 1972 | Solar Magnetic Fields of McMath #11976, <u>Trans. Amer. Geophys. Union EOS</u> , <u>53</u> , 1052. |
| LIVINGSTON, W. and
J. HARVEY | 1971 | The Kitt Peak Magnetograph IV. 40-Channel Probe and the Detection of Weak Photospheric Fields, in <u>Solar Magnetic Fields</u> , R. Howard, ed., (D. Reidel Publishing Co.), 51-61. |

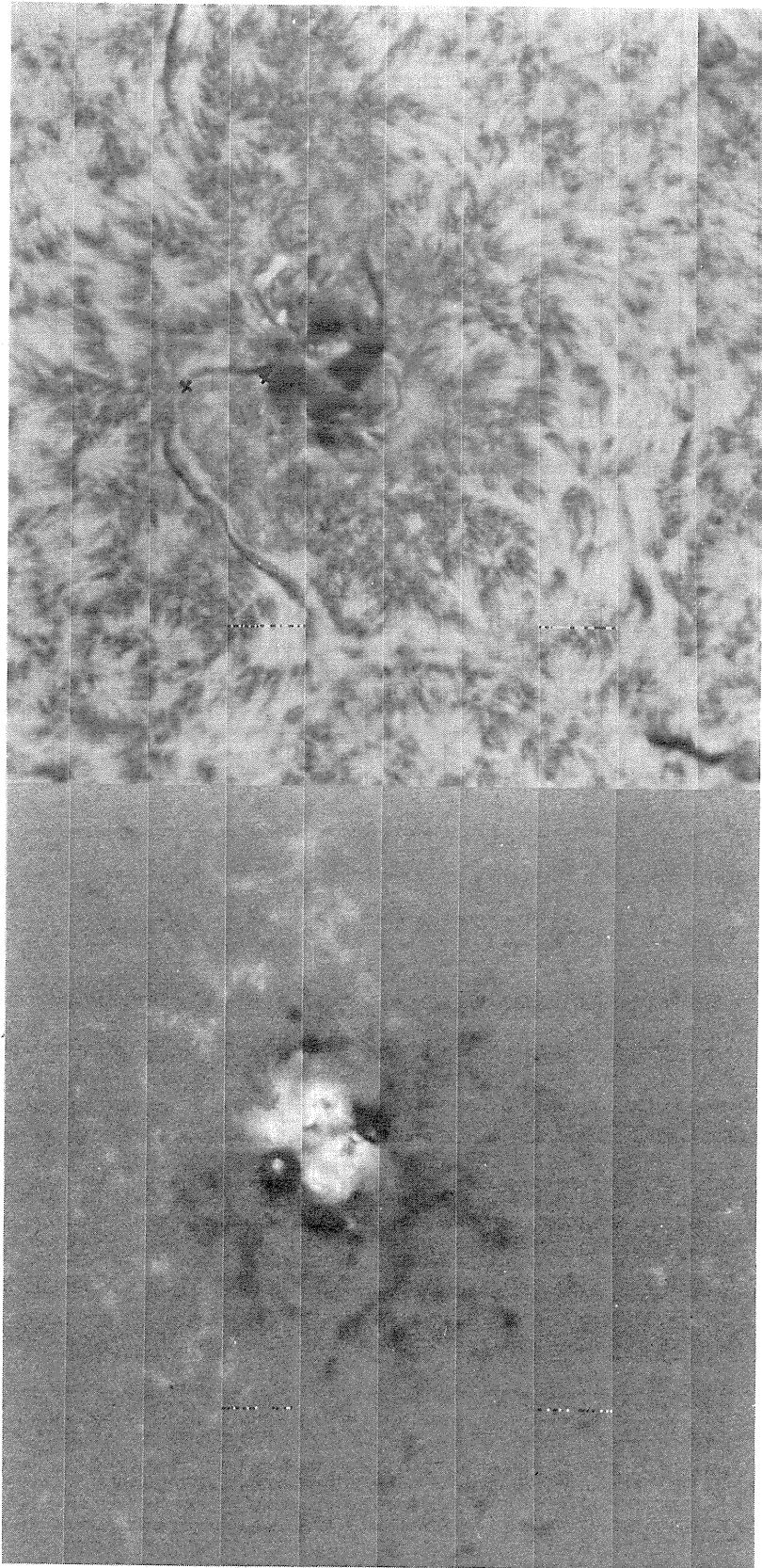


Fig. 5. Medium resolution chromospheric ($H\beta$) magnetogram and brightness picture, 4 August 1511 UT. Magnetograph response will reverse sign in regions where $H\beta$ goes into emission, or as discussed in text, where large Doppler shifts occur. The first perceptible brightening was seen at the points marked x (from Carnarvon Films, NOAA). Presumably these are the impact sites for high energy electrons originating in the unseen flare kernel, channeled by magnetic flux in a plane along the neutral line coincident with the filament.

Observation of the Flares of August 1, 2, and 4, 1972

by

G. F. Sitnik, A. I. Kirjukhina, O. N. Mitropolskaja, I. F. Nikulin, G. A. Porfirjeva,
V. S. Prokudina, E. M. Roschina, A. I. Khlistov, T. P. Khromova, and G. V. Jakunina
Academy of Sciences of the USSR
Moscow, U.S.S.R.

Spectra and filtergrams of the major flares of August 1, 2, and 4, 1972 were obtained by the three stations of the Solar Department of the Sternberg Astronomical Institute. Details of these stations are given in Table 1.

With the first instrument (see Table 1) spectra of the studied flares in 3850-3960Å, 4250-4350Å, 4770-4900Å, 5090-5208Å, and 6400-6640Å regions were obtained. The last one was photographed with a 1.6Å/mm dispersion. Exposure times were from 1 to 30 seconds.

The flares developed in a complex group of sunspots and extended over a large area around the group. Dark ejections were observed in some parts of the H γ line. The spectrograph slit was set in different parts of the active region, and its position was accurately fixed.

Upon examining the spectra of the flares, we noticed some interesting details which one can see without detailed analysis. In spectra taken on August 1, 2, and 4, 1972, an emission in the H ϵ and H δ -lines can obviously be seen (see Fig. 1). The emission is situated over the sunspots in such places where there is not a double emission in the center of the H and K-lines of Ca⁺. Outside the sunspot region, where the central emission in the H- and K-lines clearly doubles, the emission in the H ϵ - and H δ -lines cannot be noticed, but an additional emission in continuous spectrum seems to have taken place.

Table 1

Information about the Instruments

Instrument	Location	Diameter of solar image (mm)	Focal length of camera (mm)	Dispersion (2 order of spectrum)	Resolution	Receiver of radiation
1. Solar tower with diffraction grating	Moscow, Sternberg Astronomical Institute	140	10,000	0.8Å/mm	180,000	Isopanchromatic film
2. Horizontal solar telescope with diffraction spectrograph	Kuchino, Astrophysical Observatory	140	5,000	1.6Å/mm	144,000	Photomultiplier
3. Horizontal solar telescope with diffraction spectrograph	High-Altitude expedition near Alma-Ata	140	4,000	2.0Å/mm	144,000	ORWO plate blau-rapid
4. Coude-refractor "Opton" with H γ -monochromator Lyot ($\Delta\lambda=0.25\text{\AA}$)	"_"	22				film

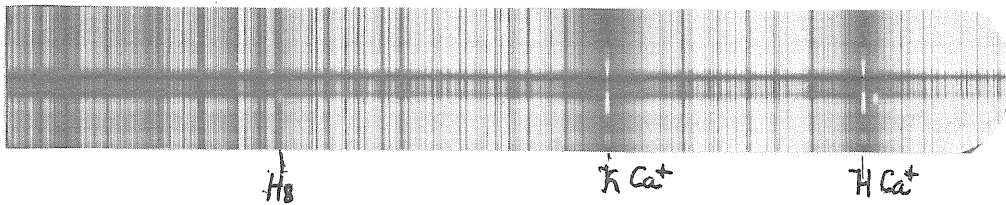


Fig. 1a. Aug. 1, 0912 UT

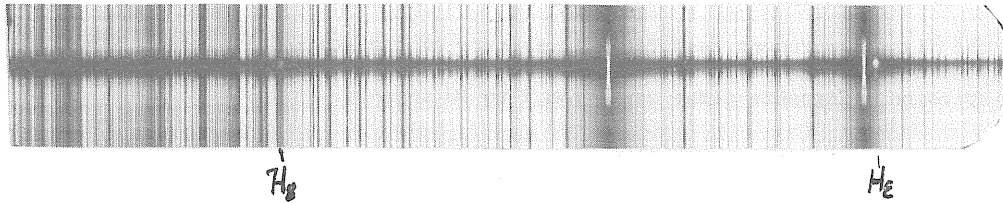


Fig. 1b. Aug. 1, 0915 UT

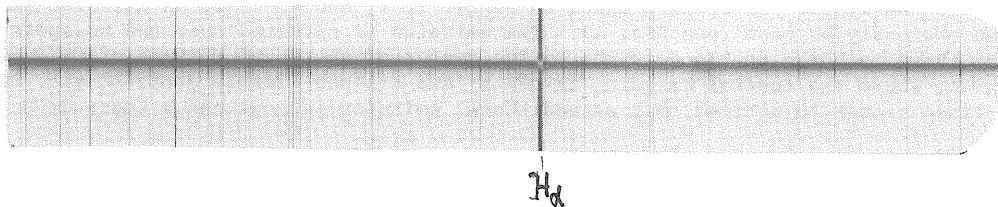


Fig. 2. Aug. 1, 0919 UT

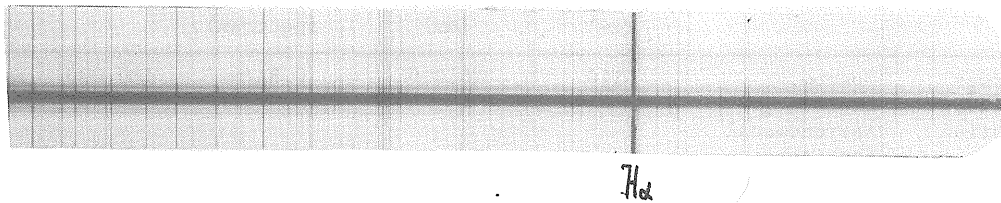


Fig. 3a. Aug. 2, 0830 UT

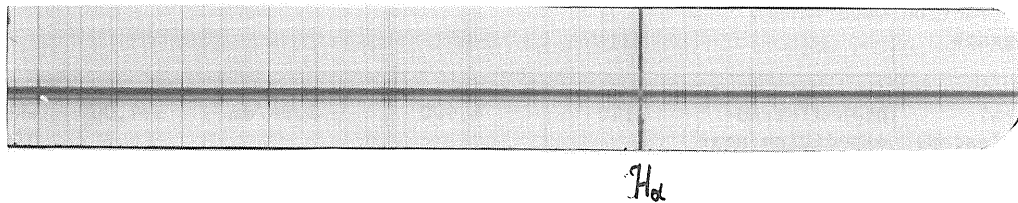


Fig. 3b. Aug. 2, 0832 UT

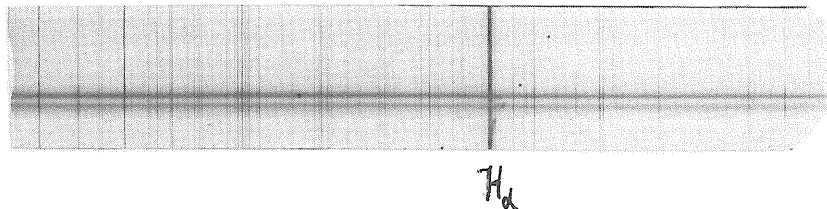


Fig. 3c. Aug. 2, 0835 UT

Figure 2 shows the spectrum in the H α region at 0919 UT on August 1, 1972. Above the sunspot the emission in the H α line happened to be double. Such doubling can also be seen in the spectrum obtained on August 2 at 0832 UT at nearly the same place where the spectra of August 1 were observed (Fig. 3a, b). At a distance of 68" from the emission in H α line (Fig. 3a, b) a dark ejection with a red shift corresponding to a line-of-sight velocity of about 60 km/sec (Fig. 3c) appeared. The image of the spectrum shown in Figure 3c was obtained three minutes after that in Figure 3b. On this spectrum one can notice great variations: first, the dark ejection is displaced from the H α line and its shift corresponds to a somewhat larger velocity (75 km/sec); second, a new dark ejection with a red shift corresponding to the velocity of 220 km/sec appeared above the smaller sunspot.

On August 2, 1972 we obtained spectra with different positions of the spectrograph slit relative to the image of the sunspot group (Fig. 4a, b, c, d). In the H α line several emission knots of various forms were noticed. The shifts of the lines caused by the dark ejections correspond to velocities of 100-200 km/sec. By their appearance these dark ejections (Fig. 4a, b) were very similar to those observed one hour later under the original position of the spectrograph slit. It is characteristic that the dark ejections produce a red shift of the H α line everywhere except for the case when the slit happened to be in the place free of sunspots. In the latter place in addition to the weak H α emission there is a violet shift corresponding to the velocity of 75 km/sec. (Fig. 4d.)

At 0715 UT on August 4, 1972 the spectrum of the flare was obtained from nearly the same regions as on the previous two days (Fig. 5). The emission of the H α line became broader, more intense, and very complex and could also be seen outside the sunspot group. One can notice dark ejections which give red shifts of almost the same order as on August 2. In the photographs obtained from 0717 to 0730 UT (see Fig. 6) there is complex emission in the H α line, the dark ejection increased giving a red shift corresponding to a velocity of 180 km/sec. On the photograph of the spectrum obtained at 0750 UT on August 4 one can see the emission in the H γ line and notice a dark ejection with the shift corresponding to a velocity of 100 km/sec (see Fig. 7). On the photographs obtained at 0800-0830 UT emission in the H β , H γ , and H ϵ lines (see Figs. 8-10) was observed. No noticeable changes in the lines of the Mg-triplet were detected with the same slit position (see Fig. 11).

On the Figures 12-15 the images of the spectra in the regions H γ (0740 UT), H and K Ca⁺ (0745 UT), H β (0820 UT), and H α (0710 UT) are shown. The general features of the emissions in these lines are very similar to those described before.

We note with special attention the peculiarity of the spectra in Figure 13. In the K Ca⁺ line there is a dark ejection of about 120 km/sec toward the red in the same direction as in the case of the dark ejection in the H α line. A dark ejection in the H α line is observed at the same place where emission in H ϵ and H δ lines occurs. When the slit was placed away from the group of sunspots we observed neither the emission nor the dark ejection in the H α line (Fig. 16).

On instrument 2 (see Table 1) on August 1 and 4, 1972 we obtained photoelectric records of spectra of the active region with different positions of the slit relative to the image of the sunspot group. The height of the entrance slit was 3 mm and its width was 0.04 mm. The time of observation on August 1 was from 0805 to 0934 UT. The slit was set in four positions. On August 4 photoelectric records were registered from 0852 to 0947 UT by setting the slit in two positions relative to the image of the group. The spectral region 3909-4009Å was recorded. As shown in Figure 17 there is conspicuous emission in the center of the K Ca⁺ line.

With instrument 3 (see Table 1) on August 4 from 0730 to 0800 UT, 28 spectrograms of an active region were obtained. The spectral region 3050-4350Å was photographed. The hydrogen emission lines H γ -H δ and H, K Ca⁺ were observed. Figure 18 also shows that the more intense hydrogen emission was observed in the places where the central emission in the H and K Ca⁺ doubled.

In the region where hydrogen emission was observed, the presence of a weak continuous spectrum was noticed. In the spectral region 3450-3050Å a bright continuum was photographed. The intensities and the form of the profile of emission line strongly varied from one place to another.

With instrument 4 (see Table 1) the active region was photographed in the different parts of the H α line. The active region which produced the flares of August 2 and 4, 1972, had on the previous rotation consisted of one large spot and several satellite pores. On the chromospheric level a characteristic vertical structure was observed.

On July 29, 1972 this region appeared once again on the eastern limb accompanied by very bright active prominences. On August 1 the flare started about 0920 UT and continued about 50 minutes. It had the form of two large strips almost perpendicular to one another and beginning in the center of the group.

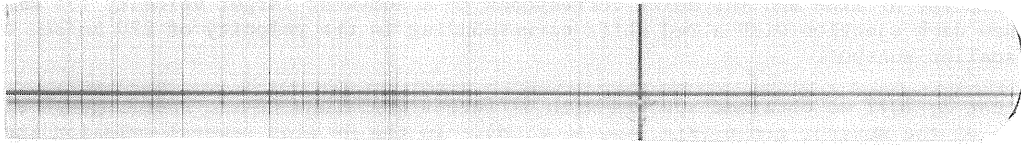


Fig. 4a. Aug. 2, 0821 UT

H_{α}

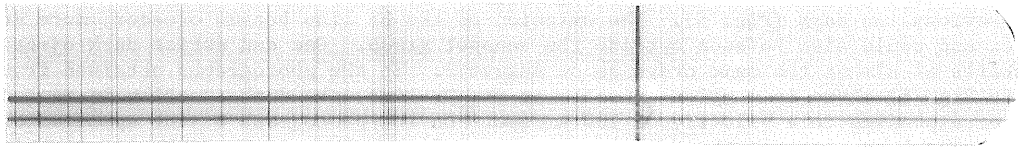


Fig. 4b. Aug. 2, 0822 UT

H_{α}

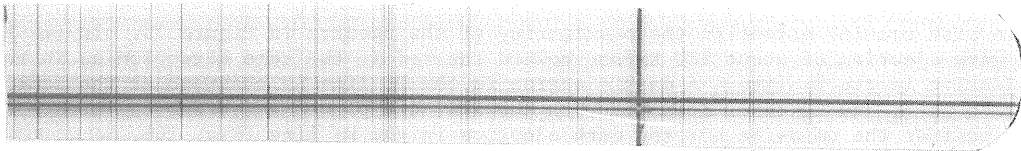


Fig. 4c. Aug. 2, 0823 UT

H_{α}



Fig. 4d. Aug. 2, 0825 UT

H_{α}

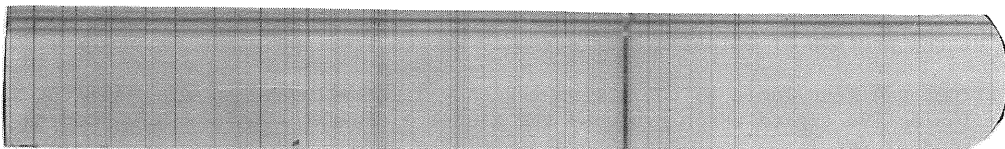


Fig. 5. Aug. 4, 0717 UT

H_{α}

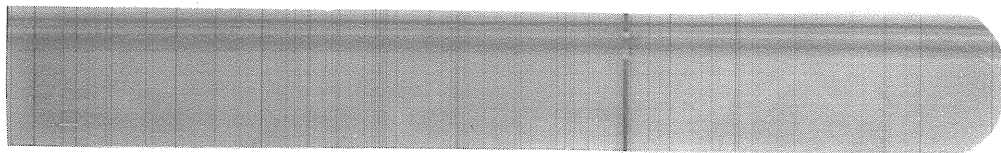


Fig. 6a. Aug. 4, 0720 UT

H α

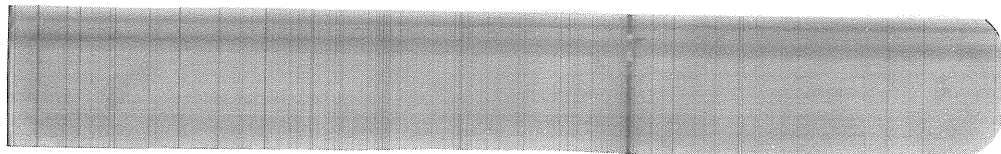


Fig. 6b. Aug. 4, 0725 UT

H α

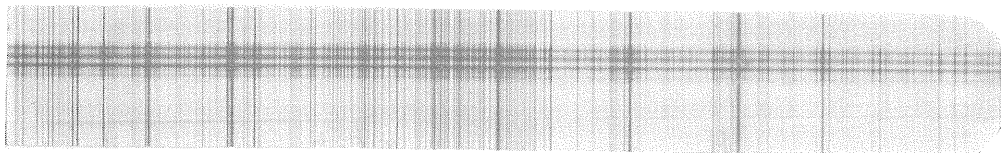


Fig. 7. Aug. 4, 0750 UT

H γ

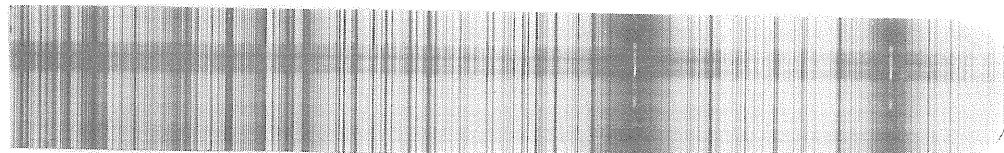


Fig. 8. Aug. 4, 0800 UT

KCa⁺

HCa⁺

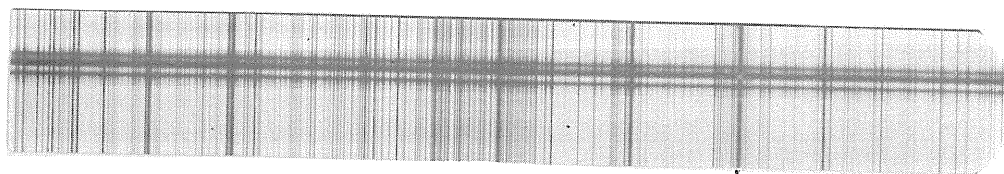


Fig. 9. Aug. 4, 0815 UT

H γ

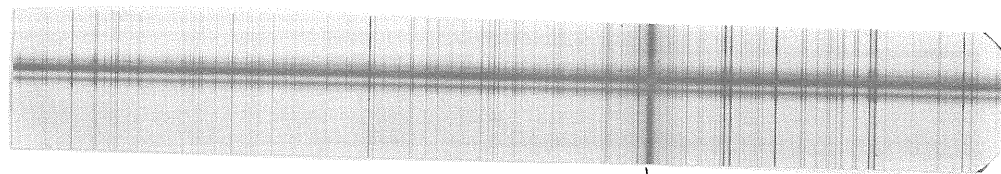


Fig. 10. Aug. 4, 0825 UT

H β

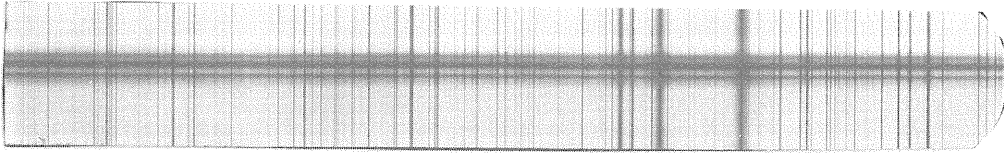


Fig. 11. Aug. 4, 0830 UT

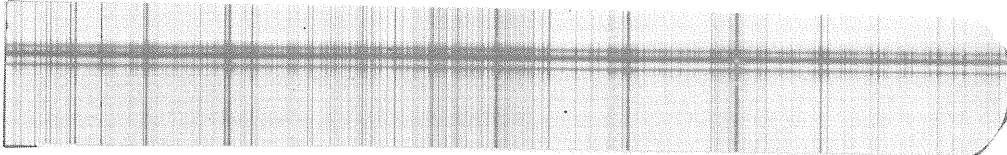


Fig. 12. Aug. 4, 0740 UT

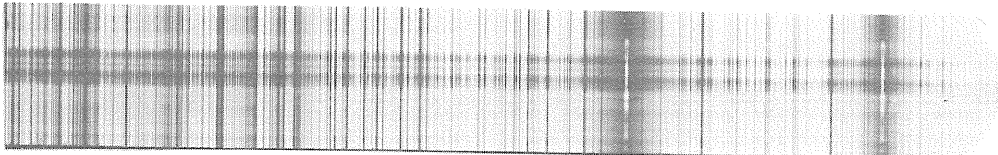


Fig. 13. Aug. 4, 0745 UT

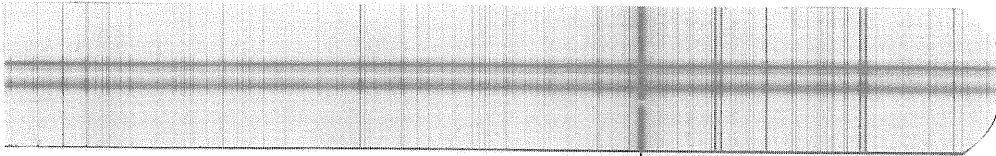


Fig. 14. Aug. 4, 0820 UT

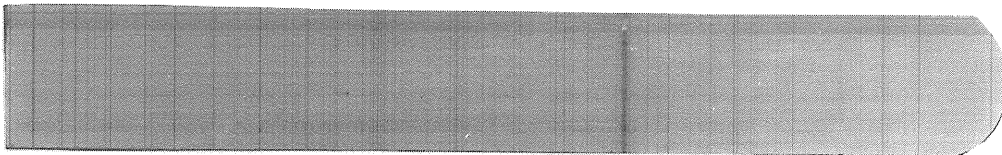


Fig. 15. Aug. 4, 0710 UT

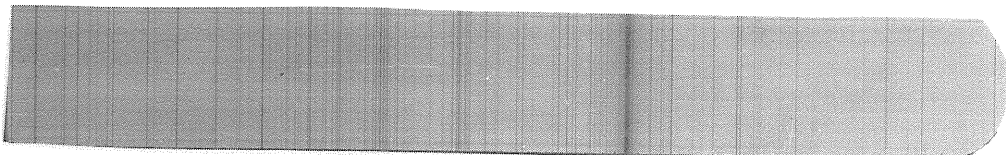


Fig. 16. Aug. 4, 0700 UT

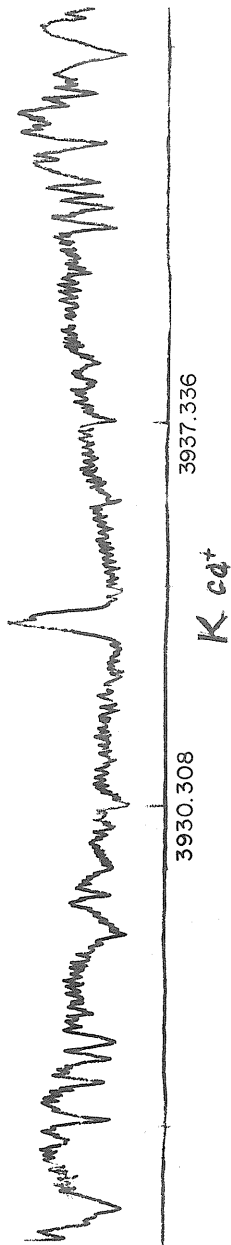


Fig. 17. The photoelectric record in the region of the $K Ca^+$ line.

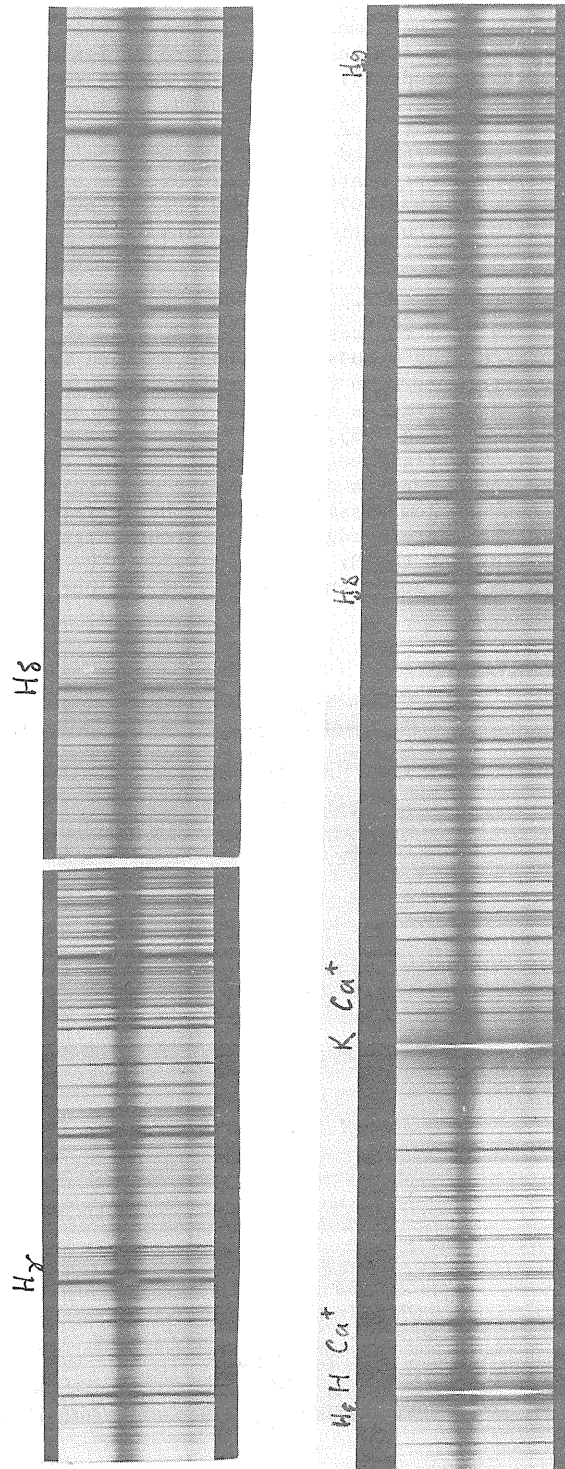


Fig. 18. The $H\gamma - H_{10}$ region. Aug. 4, 1972.

In the $H\gamma$ wings the flare was observed up to $\pm 1.5\text{\AA}$ from the center of the line. On August 2 three flares were registered during the time-intervals 0330-0430, 0430-0515, 0550-0630 UT (it was probably one flare with three local maxima).

Figure 19 shows the flare on the disk at 0340 UT in the center of the $H\gamma$ line. Figure 20 shows the enlarged image of the flare at 0346 UT. Similar to the flare of August 1 the flare of August 2 consisted of two bright compact strips one of which crossed the center of group and the other began in it. In the wings of the $H\gamma$ line these strips were seen as bright up to $\pm 1.5\text{\AA}$ from the line center (see Fig. 21 and 22). Figures 23 and 24 (0410 UT) show the first stages of the formation of absorption ejection from the flare region. Figures 25-27 (0433-0436 UT) show the flare at maximum development at the center of $H\gamma$ and in the wings at $H\gamma \pm 0.5\text{\AA}$. On Figure 29 (0446 UT) one can see arc-like ejection at the red wing of the $H\gamma$ line ($+1.5\text{\AA}$), however, at the violet wing (Fig. 28) it was essentially weaker. Later, at 0620 UT, the ejection at $+1.5\text{\AA}$ transformed into the system of arcs (Fig. 30). By about 0715 UT some breakup of the system has occurred. The phenomenon was accompanied with the formation of two jets (Fig. 31) which were seen in the wings up to $\pm 2.5\text{\AA}$ from the center.

On August 4, 1972 photographs were obtained every 15 minutes in both center and the wings of $H\gamma$ at the distances from the center of ± 0.5 , ± 1 , ± 1.5 , ± 2.0 , $\pm 3.0\text{\AA}$. The observations were carried out through the cirrus clouds up to 0830 UT when weather prohibited observations. At the beginning of the observations at 0200 UT the active region was quiet (Fig. 32), however, in the wing up to $+2.0\text{\AA}$ there was noticed a weak ejection which apparently represented the last stage of the previous flare. At 0435 UT (Fig. 33), 1.5 hours before the flare at about 0600 UT, bright emission appeared in the region. The flare began at about 0600 UT and brightened very quickly during the first 10 minutes. The configuration of this flare was typical of the "proton-type." There were two parallel strips with one of them passing through the center of the group and the other, which had a larger area, crossed the eastern edge of this group (Figs. 34-36). Figures 37-38 show the image of the flare in the wings of the $H\gamma$ line at $\pm 0.5\text{\AA}$. The maximum area of the flare occurred at about 0640 UT. In the future we are going to study all of the obtained data in detail.

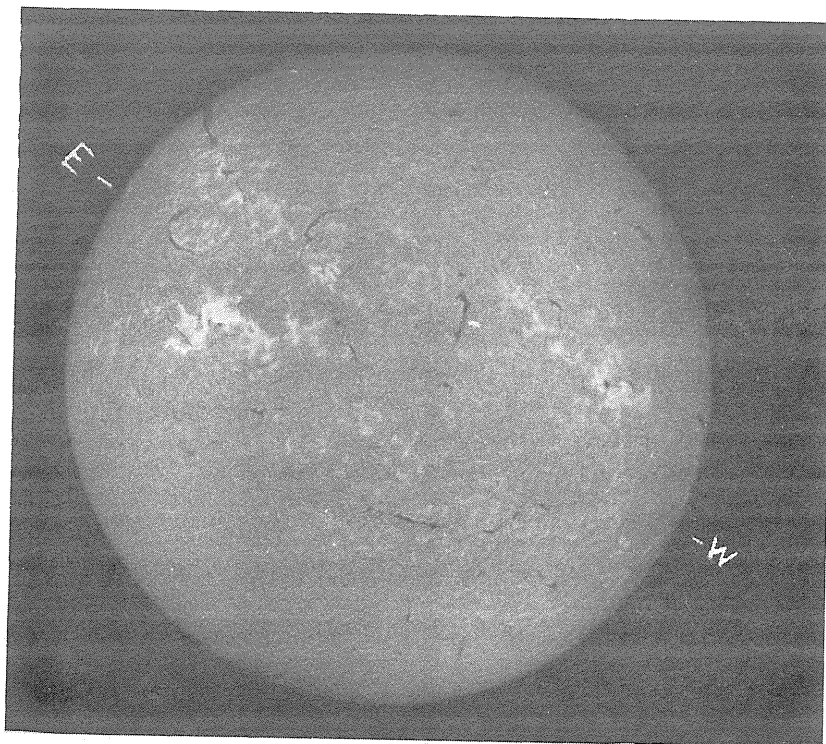


Fig. 19. $H\gamma$ line center. Aug. 2, 0340 UT.

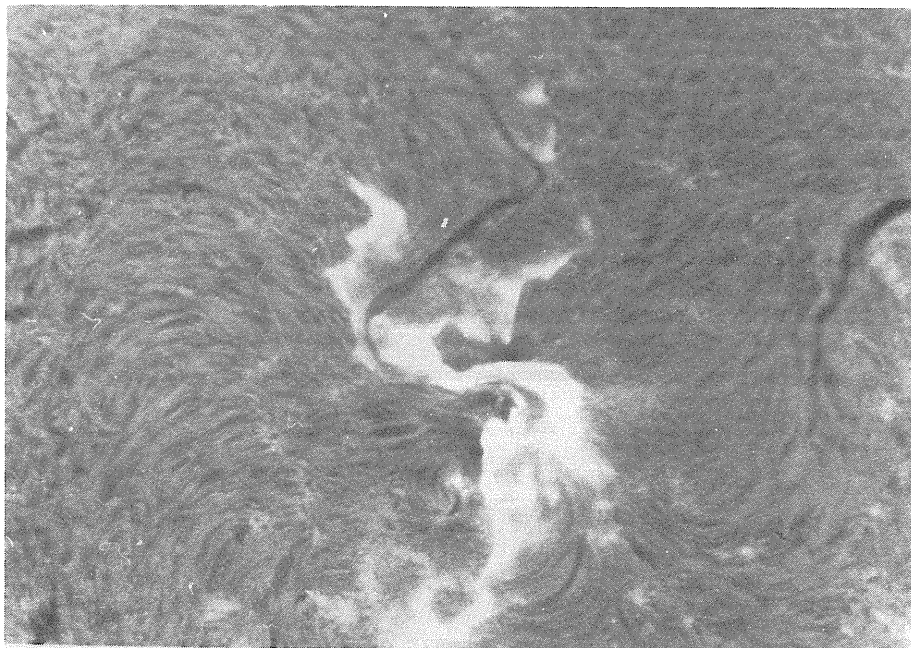


Fig. 20. $H\gamma$ line center. Aug. 2, 0346 UT.

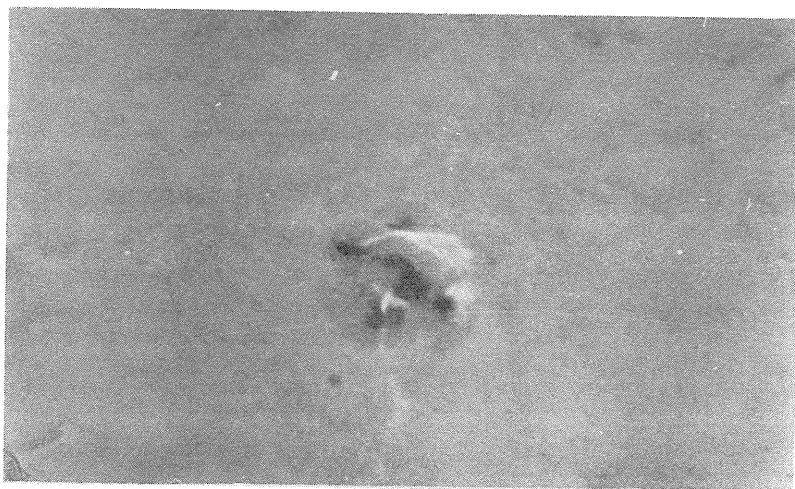


Fig. 21. $H\gamma - 1.0\text{\AA}$. Aug. 2, 0355 UT.



Fig. 22. $H\alpha + 1.0\text{\AA}$. Aug. 2, 0356 UT.



Fig. 23. $H\alpha - 1.0\text{\AA}$. Aug. 2, 0410 UT.

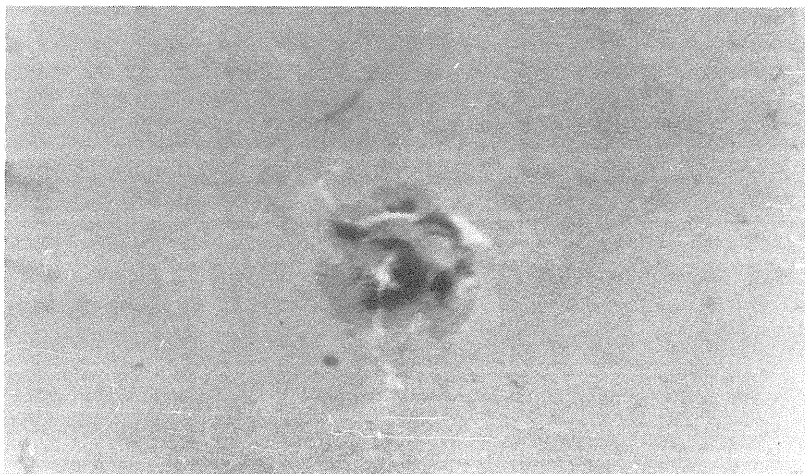


Fig. 24. $H\alpha + 1.0\text{\AA}$. Aug. 2, 0412 UT.

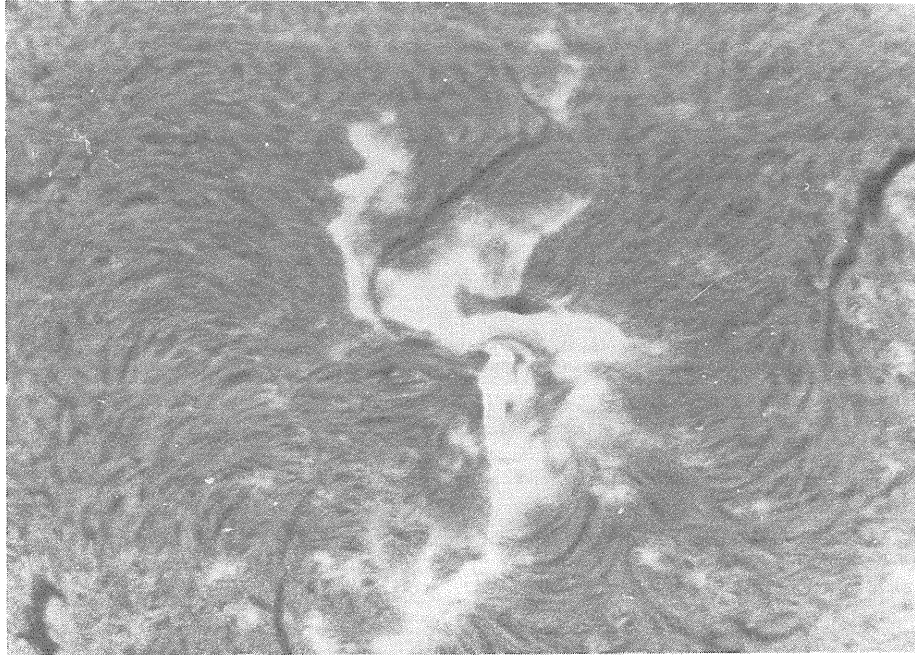


Fig. 25. $H\alpha$ line center. Aug. 2, 0433 UT.

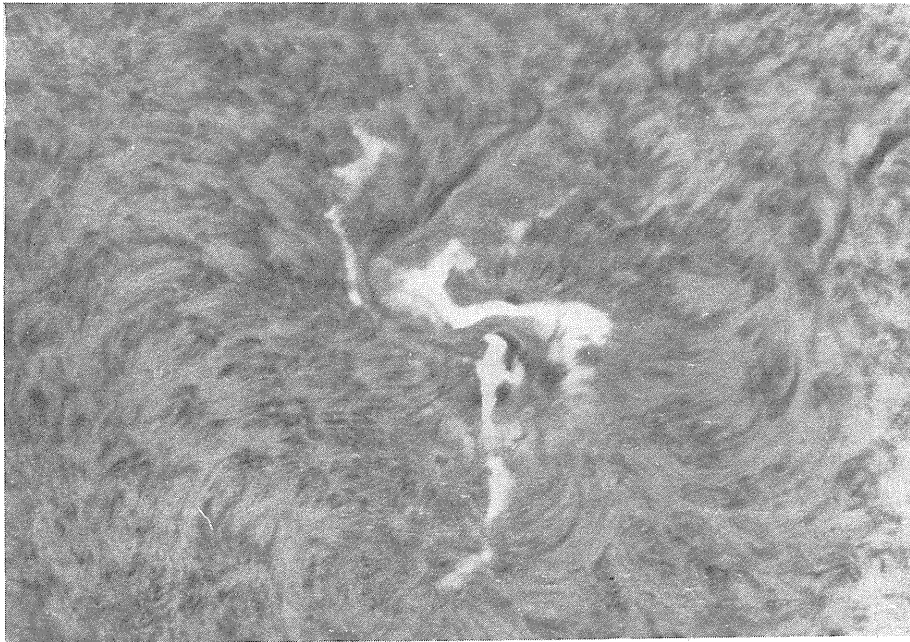


Fig. 26. $H\alpha - 0.5\text{\AA}$. Aug. 2, 0435 UT.

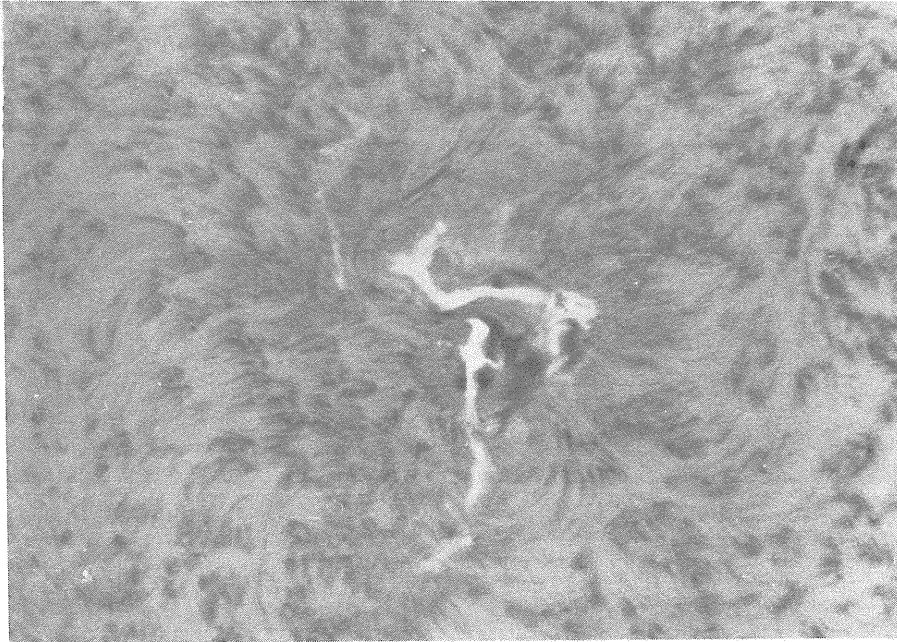


Fig. 27. $H\alpha + 0.5\text{\AA}$. Aug. 2, 0436 UT.

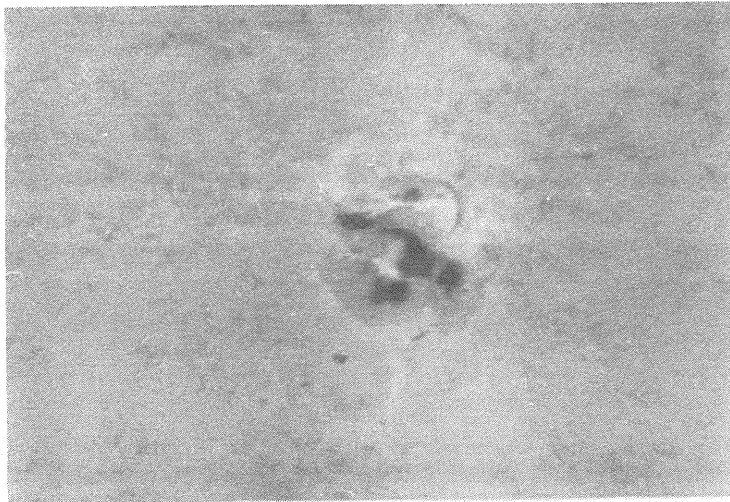


Fig. 28. $H\alpha - 1.5\text{\AA}$. Aug. 2, 0445 UT.



Fig. 29. $H\alpha + 1.5\text{\AA}$. Aug. 2, 0446 UT.

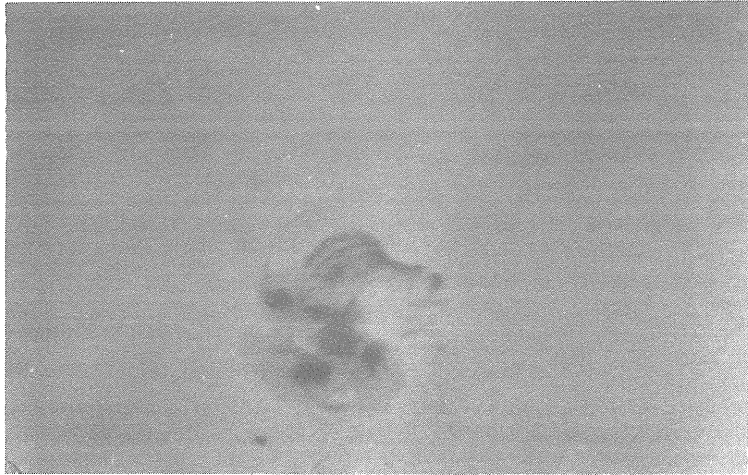


Fig. 30. $H\alpha + 1.5\text{\AA}$. Aug. 2, 0620 UT.

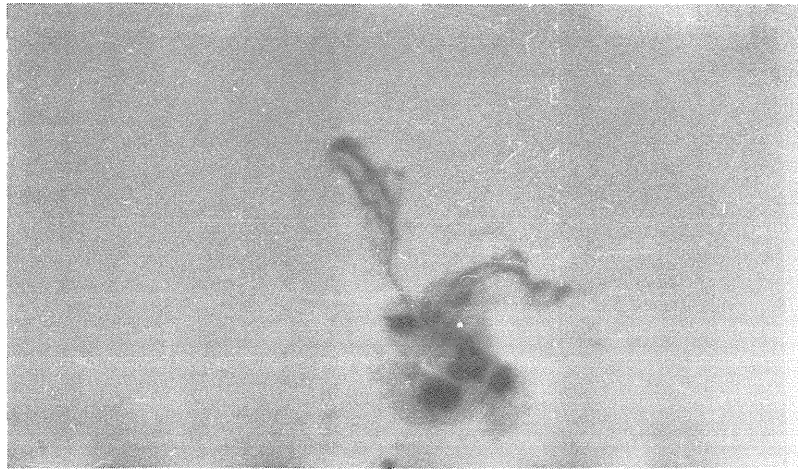


Fig. 31. $H\alpha + 1.5\text{\AA}$. Aug. 2, 0720 UT.

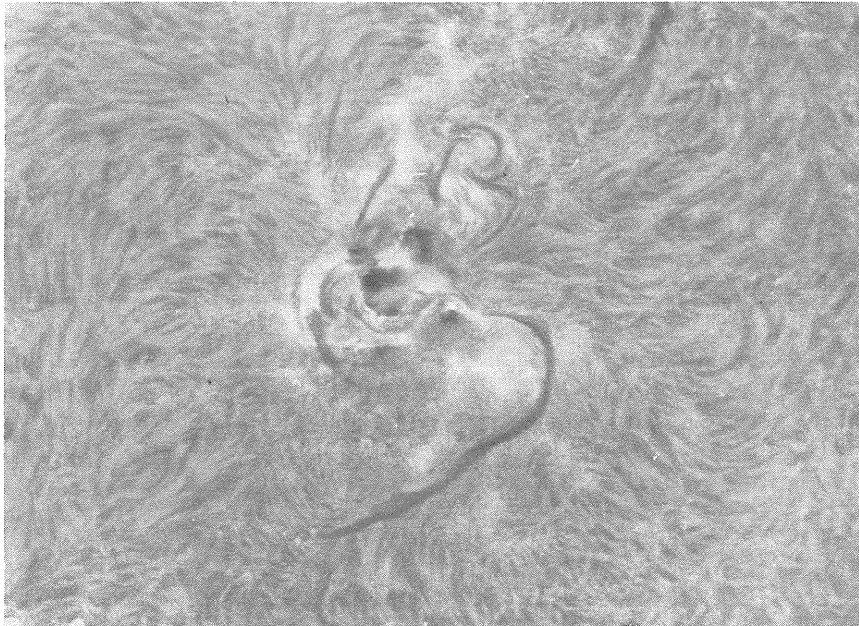


Fig. 32. $H\alpha$ line center. Aug. 4, 0200 UT.

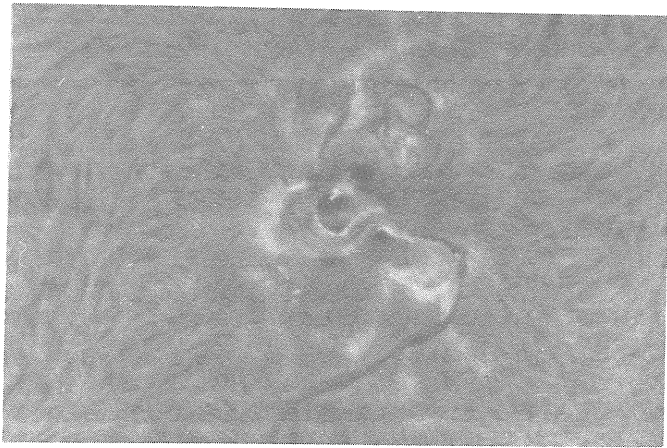


Fig. 33. H α line center. Aug. 4, 0435 UT.

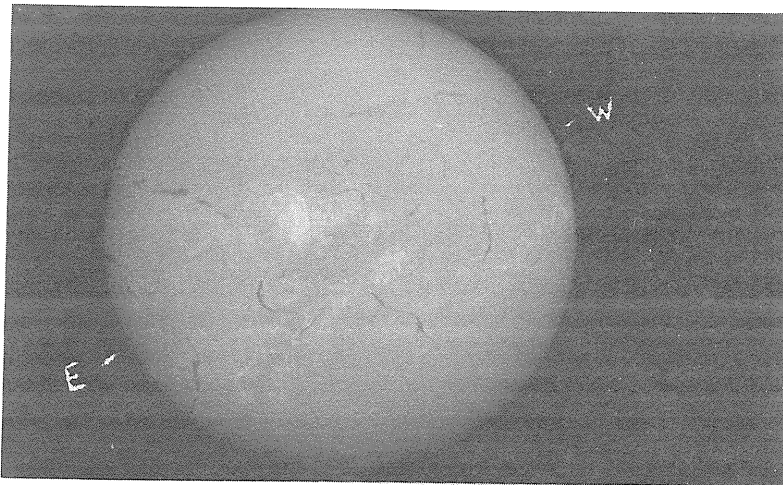


Fig. 34. H α line center. Aug. 4, 0705 UT.

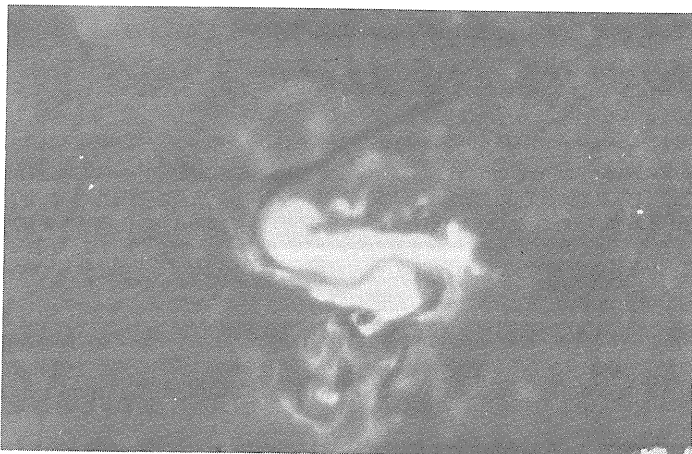


Fig. 35. H α line center. Aug. 4, 0615 UT.

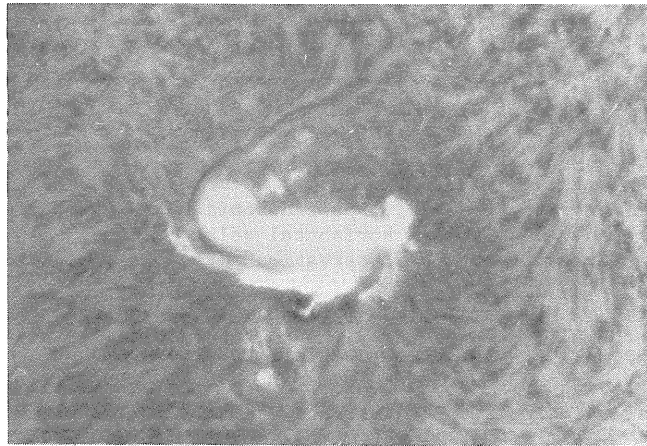


Fig. 36. $H\gamma - 0.5\text{\AA}$. Aug. 4, 0646 UT.

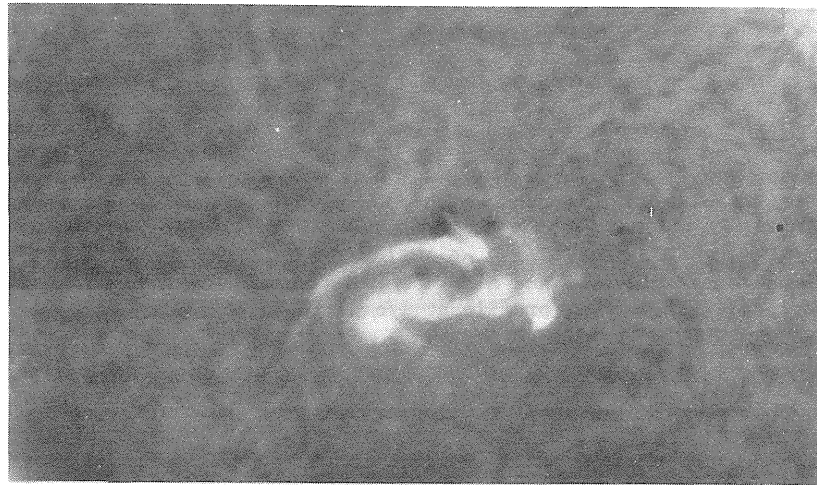


Fig. 37. $H\gamma - 0.5\text{\AA}$. Aug. 4, 0711 UT.

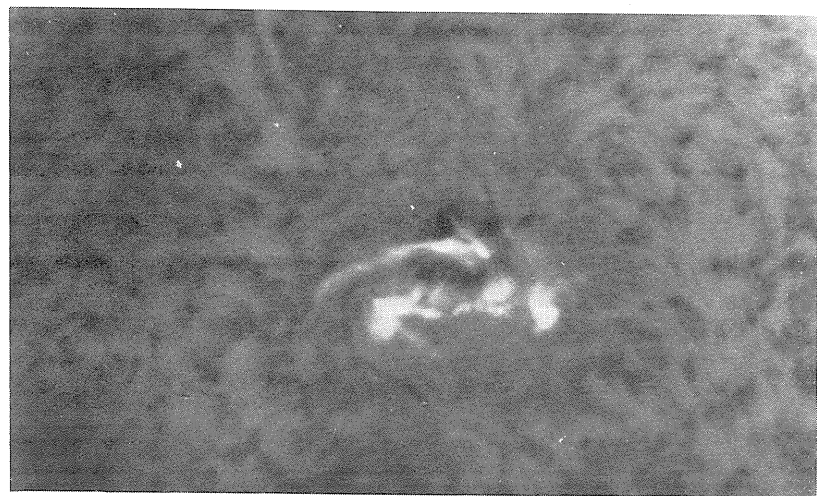


Fig. 38. $H\gamma + 0.5\text{\AA}$. Aug 4, 0712 UT.

A Flare of August 2, 1972

by

J. Kubota, H. Kurokawa and T. Kureizumi
Kwasan and Hida Observatories
Yamashina, Kyoto, Japan

On August 2, 1972 a large two ribbon type flare occurred at N12 E34 in an H-type spot group. As indicated in a preliminary report [1972], spectroscopic and H α monochromatic observations were performed at the Kwasan Observatory with a horizontal solar telescope (50 cm aperture and 20 m focal length) and helioscope camera system. The observation period is from 0508 to 0708 UT.

Figure 1 shows H α images of this flare event photographed at 0515 and 0708 UT, and a white light image of the spot group at 0616 UT. The dark line on the H α image in Figure 1 indicates the position of the entrance slit of the spectrograph. In Figure 2 thick lines show the bright region of the flare, dotted lines the filament, and thin lines the boundary of the spot group. Hatched areas illustrate the umbra, and straight lines the direction of the entrance slit of the spectrograph.

The flare appeared on both sides of a stable filament. However, the two ribbons and the filament were not parallel. The ribbon "a" (Figure 2) elongated eastward, crossing over the umbra. The flare was fairly stable as a whole during our observed period, except for the southern part of ribbon "b", where serious deformations of the bright region, many eruptions and loop prominences were detected.

The non-thermal motions of the matter in this flare were studied with a time sequence of the spectra of metallic lines Fe II 5169Å, Mg I b and Na I D. These spectra were taken at a fixed point in the bright part of ribbon "a" with exposure time of 2 seconds. Dispersion of the spectra was about 0.18Å/mm.

Bright fine structures or knots can be seen on the spectra of the Fe II (5169Å) line, while neutral metallic lines, Mg I and Na I, show ordinary flare emission without conspicuous structures.

Figure 3 indicates the time variation of $\Delta\lambda_e/\lambda$ values of the Fe II(5169Å) line, measured at bright points of the Fe II emission, and also the corresponding variation for the case of the Na I D lines. $\Delta\lambda_e$ is the half width of the profile at 1/e of the central intensity and gives the true Doppler width in the optically thin case.

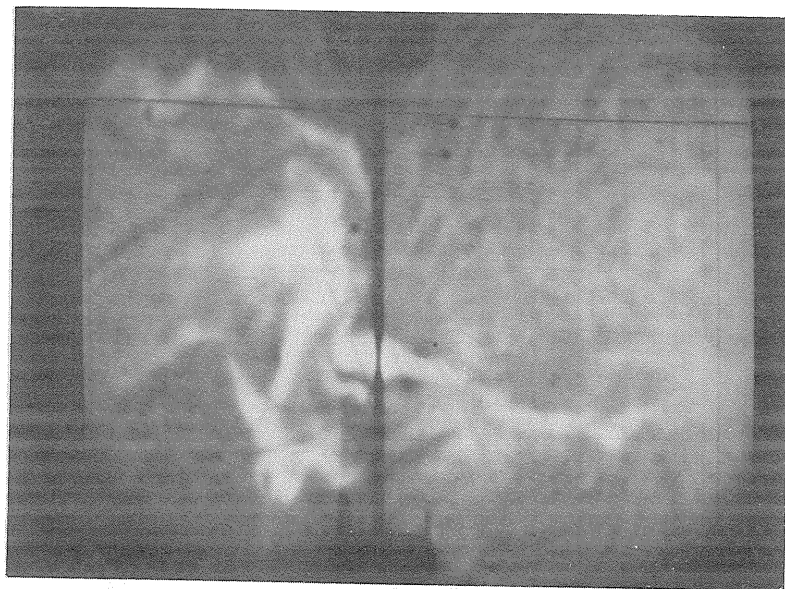
Profiles of these lines are symmetric and very narrow, corresponding to a range of random non-thermal velocity between 4.5 and 6.5km/sec. The non-thermal velocity obtained from the Fe II line changes slightly with time compared with that from the Na I lines. The latter is nearly constant during the observed period. This fact may suggest that the Fe II emission originates in a different region than the Na I line.

REFERENCES

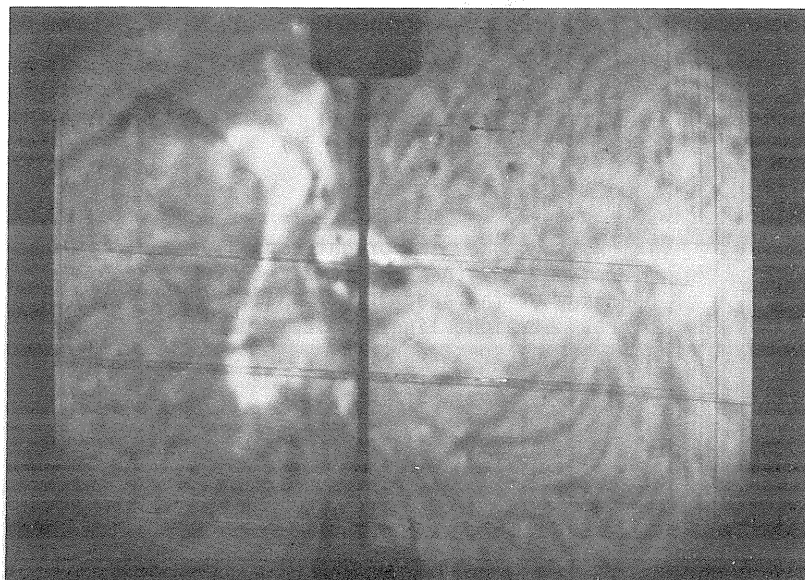
1972

Report of Ionospheric and Space Research in Japan, 26.

0515
UT



0708
UT



0616
UT



Fig. 1. $H\alpha$ images of the August 2, 1972 flare taken at 0515 and 0708 UT, and white light photograph of spot group taken at 0616 UT at the Kwasan Observatory. Heavy line on $H\alpha$ images indicate position of entrance slit of the spectrograph.

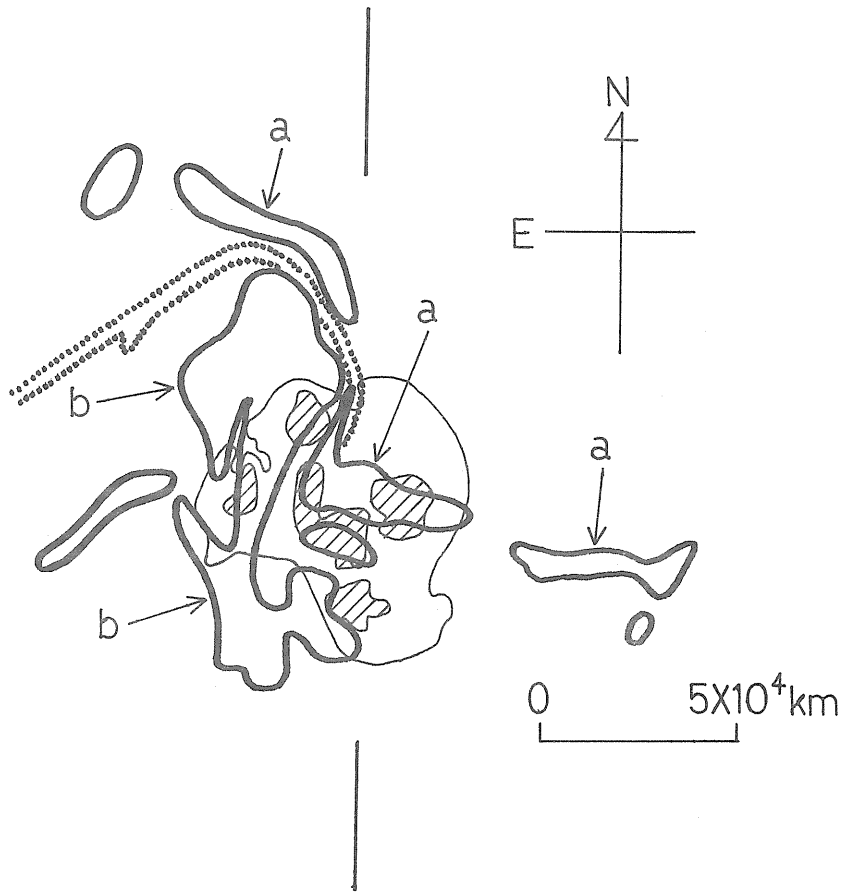


Fig. 2. Thick lines show the bright region of the August 2, 1972 flare; dotted lines the filament; and thin lines the boundary of the spot group. Hatched areas indicate umbra. Straight lines indicate direction of the entrance slit of the spectrograph.

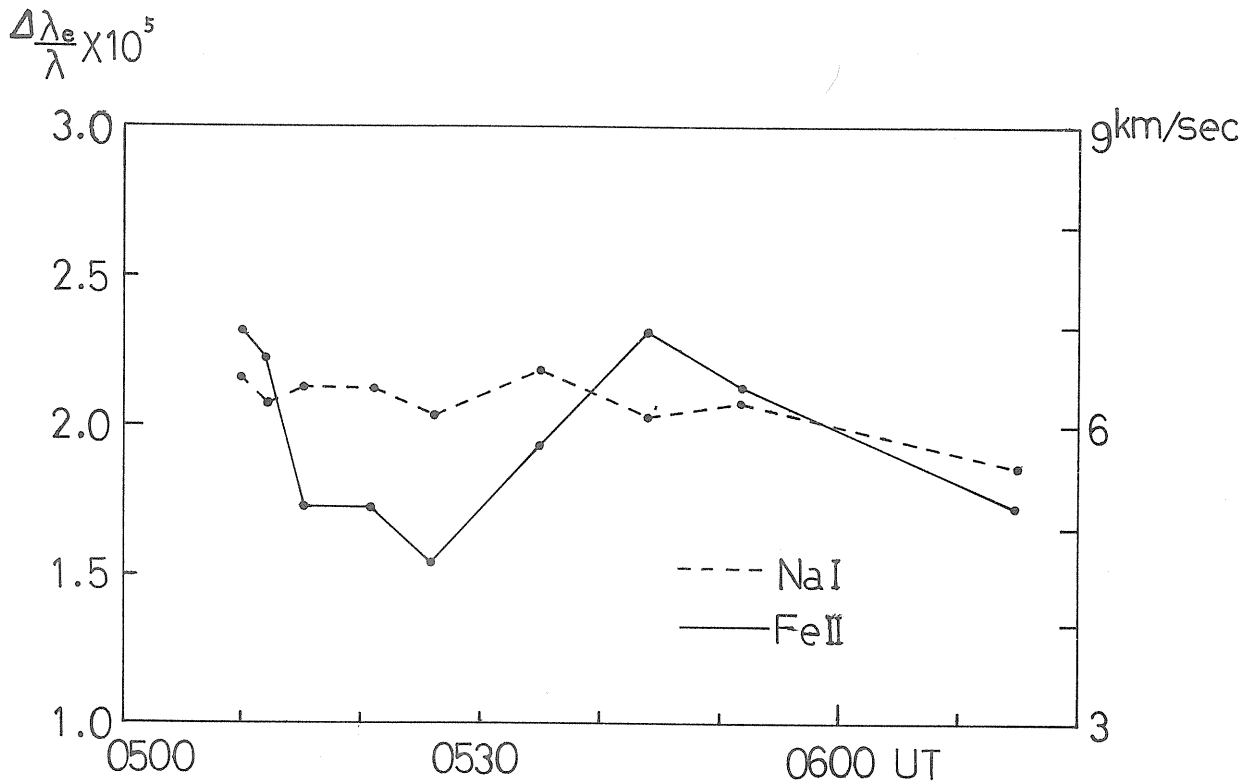


Fig. 3. Time variation of $\Delta\lambda_e/\lambda$ values of the Fe II (5169Å) and Na I D lines for the August 2, 1972 flare.

The Flares of August 1972

by

Harold Zirin and Katsuo Tanaka
Big Bear Solar Observatory, Hale Observatories
California Institute of Technology
Carnegie Institution of Washington

Editors' Note: Only a section of the article, "The Flares of August 1972" by H. Zirin and K. Tanaka, appears here. This section covers mainly the August 2, 1972 solar flares, though the entire abstract, introduction and conclusions of the article are included. The entire article which also covers the development of the region and the great flare of August 7 will appear in a future issue of Solar Physics, D. Reidel Publishing Company, Dordrecht, Holland. Permission has been received from the authors and Journal to reprint sections of this article.

ABSTRACT

We present the analysis of observations of the August flares at Big Bear and Tel Aviv, involving monochromatic movies, magnetograms and spectra. In each flare the observations fit a model of particle acceleration in the chromosphere with emission produced by impart and by heating by the energetic electrons and protons. The region showed twisted flux and high gradients from birth, and flares appear due to strong magnetic shears and gradients across the neutral line produced by sunspot motions. Post flare loops show a strong change from sheared, force-free fields parallel to potential-field-like loops, perpendicular to the neutral line above the surface.

We detected fast (10 sec duration) small (1 arc sec) flashes in 3835 at the footpoints flux loops in the August 2 impulsive flare at 1838, which may be explained by dumping of >50 keV electrons accelerated in individual flux loops. The flashes show excellent time and intensity agreement with >45 keV X-rays. In the less impulsive 2000 UT flare a less impulsive wave of emission in 3835 moved with the separating footpoints. The thick foil model of X-ray production gives a consistent model for X-ray, 3835 and microwave emission in the 1838 event.

Spectra of the August 7 flare show emission 12 Å FWHM in flare kernels, but only 1 to 2 Å wide in the rest of the flare. The kernels thus produce most of the H α emission. The total emission in H α in the August 4 and August 7 flares was about 2×10^{30} ergs. We believe this dependable value more accurate than previous larger estimates for great flares. The time dependence of total H α emission agrees with radio and X-ray data much better than area measurements which depend on the weaker halo.

Absorption line spectra show a large (6 km/sec) photospheric velocity discontinuity along the neutral line, corresponding to sheared flow across that line.

Introduction

The active region McMath 11976, which produced the great flares of August 1972, produced an unparalleled opportunity for the study of solar activity. We present optical observations made at the Big Bear Solar Observatory and its station at Tel Aviv University, and comparisons with data kindly made available by various colleagues.

The data at Big Bear Lake were made with a battery of telescopes on a single mount. Two 10-inch refractors produced large scale cinematographic data in various wavelengths, mostly H α and H $\alpha \pm 1/2$ Å, but also on August 2 with a Chapman filter [Chapman, 1971] 15 Å wide, centered on 3835 Å. Observations of the full disk in H α were made with an 8.6-inch vacuum refractor, white light full disk observations with a 6-inch refractor. Magnetograms were made with the Leighton-Smithson magnetograph, time sharing in one of the 10-inch refractors, and spectrograms, with the 5 meter Coude spectrograph fed by a third 10-inch refractor. At Tel Aviv, observations were made with a 5-inch photoheliograph used in the center of H α . We were fortunate in that not only was the birth of the region observed in July, but all of the large flares were picked up on either the Big Bear or Tel Aviv photoheliographs. The principal large flares occurred at 0330 UT August 2 (only observed in progress), 1838 UT August 2, 2005 UT August 2, 0620 UT August 4, 1516 UT August 7, and 1216 UT August 11 (only late phases).

The highlights of the observations are the following: the region showed inverted polarity from its inception on July 11; the great activity was due to extremely high shear and gradients in the magnetic field, as well as a constant invasion of one polarity into the opposite; observations in 3835 show remarkable fast flashes in the impulsive flare of 1838 UT on August 2 with lifetimes of

of 5 seconds, which may be due to dumping of particles in the lower chromosphere; flare loops show evolutionary increases of their tilts to the neutral line in the flares of August 4 and 7; spectroscopic observations show red asymmetry and red shift of the $H\alpha$ emission in the flash phase of the August 7 flare, as well as substantial velocity shear in the photosphere during the flare, somewhat like earthquake movement along a fault; finally the total $H\alpha$ emission of the August 7 flare could be measured accurately as about 2.5×10^{30} ergs, considerably less than coarser previous estimates for great flares. A preliminary report on our data has appeared [Tanaka and Zirin, 1973] and we present here our comprehensive analysis of the wealth of material obtained.

IV. Flares of August 2

Major activity began in the region on August 2 with a remarkable series of complex flares. The first great flare was reported at 0316 UT by Teheran; the later phases or perhaps a resurgence (two flares were reported but only one radio burst) are visible on our Tel Aviv photograph of 0547 UT (Figure 8). This shows a large flare with bright strands covering all the spots, the brightest portion being over f_2 . It differed from the later flares in that the p emission was confined to the spots and an area directly west. The long, dark filament following the group had disappeared, blown away by the flare. It reformed in bits and pieces, was blown away again by the later flares, and was whole again on August 3. By contrast, the great flares of August 4 and 7 only made it wave about.

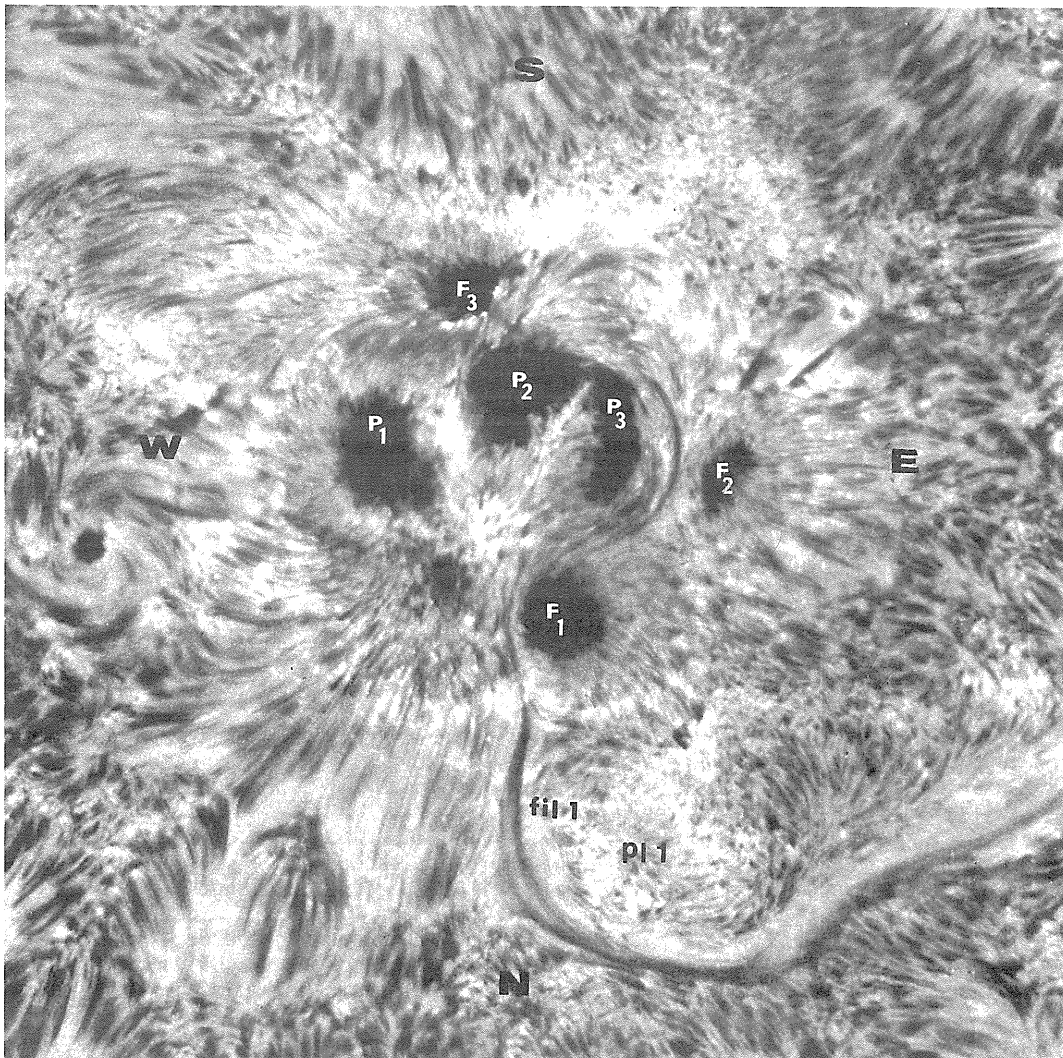


Figure 7 *

An enlarged frame 8/3, with various sunspots and areas marked to facilitate reference in the text. Note the strongly twisted penumbral structures.

* Figure included for clarity in the following discussion:

"p" refers to preceding spot with S polarity,
 "f" refers to follower spot with N polarity.

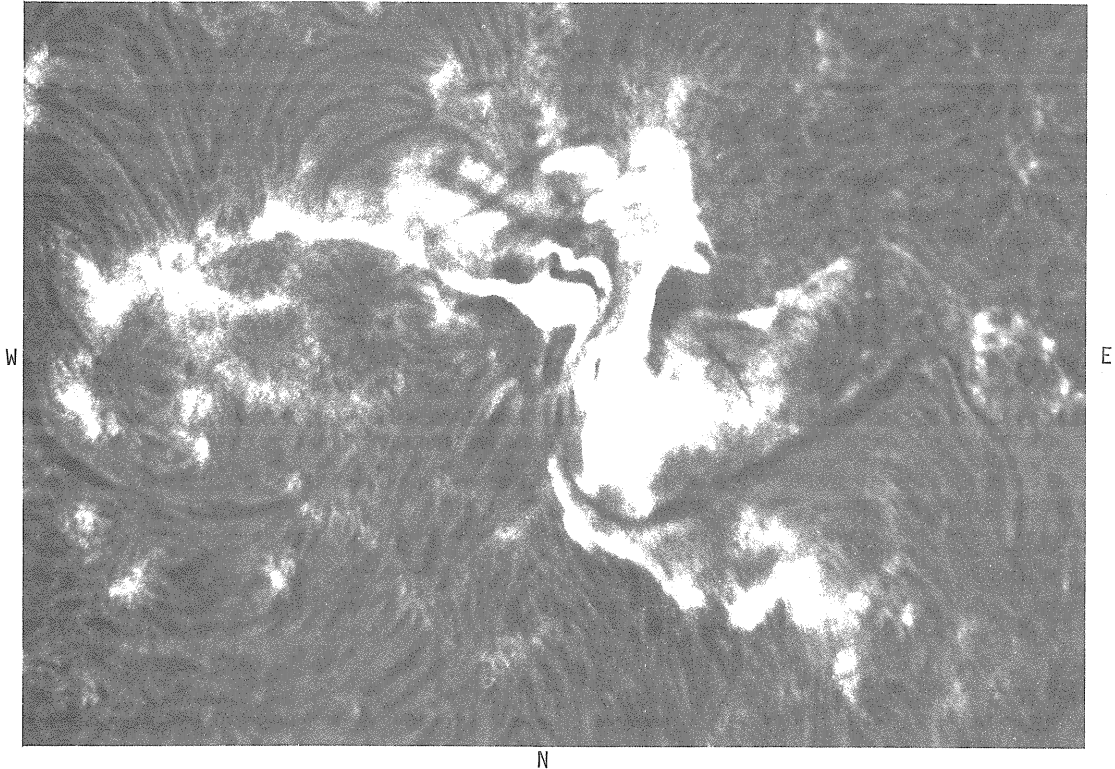


Figure 8

First flare, August 2, photographed at Tel Aviv, dawn, by Shlomo Hoory in H α centerline. This photo at 05:43:38, more than two hours after the flare began, shows that it was similar to the later great flare.

Whether or not the flare was associated with changes in the magnetic field structure, there were definite changes on August 1 and 2; the spot f_1 grew, and the spots f_2 and f_3 shrank, so that at August 2, 1600 UT, f_1 was bigger than the other two (eventually f_1 became the largest spot in the group). Spot f_1 also pushed ahead (W) relative to the other spots, as can be readily seen from the illustration (Figures 3 and 4); by August 2 the neutral line marked by the filament was directly beneath (N) of the p spots. A remarkable change also occurred in the fibril structure preceding the spot f_3 . On July 31, this was directly above (S) of p_1 and very close to f_3 , almost along the neutral line dividing p_1 and f_3 ; on August 2 (after the first flare), the fibril on the neutral line had moved considerably ahead (W) of f_3 and a new fibril system connected f_3 to p_1 , with f_3 rapidly decaying. We have noted before that a sheared neutral line can be replaced by shorter lines going directly across the neutral line to the nearest opposite polarity; this appears to occur in this case. The flux in f_3 can disappear by shortening and eventual subsidence below the surface of the flux loops. The energy released in this flare would presumably be the difference between the elongated sheared lines and the shorter field lines of the final configuration. This difference was actually observed during later flares; for example, in the flare 1838 UT August 2, a rapid break-up of the filament into shorter fibrils occurred at 1837 UT, one minute before the brightening started (Figure 9). For the flares of August 4 and August 7, we could see the bright flare loops cross the neutral line with increasing tilts, late in the flash phases (Figures 18 and 19). If there is a further contraction involved in the subsidence of field lines below the surface, this energy too is available for the flare. In succeeding days f_3 moved considerably closer to p_1 and thus lowered the total energy.

On August 2, Big Bear observations were made in H α centerline and 3835 Å. After a small flare along the neutral line at 1601, a brilliant impulsive flare began at 1838 UT. Its development is shown in dark prints in Figure 9 and in normal prints in Figures 11a and 11b. The flare occurred along the neutral line between f_1 and p_3 following a break-up of fibrils on the neutral line (Figure 9, 1837 UT) and spread rapidly along that line; there was a fast increase at 1839:02 UT and another rise to a peak at 1839:36 UT; these coincide with an early hard X-ray peak at 1839:00-10 UT and a main peak at 1839:30-40 UT. The dark prints, Figures 9d and 9e, and the negative print, Figure 9f, show the structure of the kernel. (The kernel consists of chains of bright points along the neutral line with an area of $3.8 \times 10^{17} \text{cm}^2$ and a diffuse halo with an area of $2.1 \times 10^{18} \text{cm}^2$.) This was the most brilliant flare we have yet seen in H α , although its limited area kept the total fluxes down. This was not a classic two-ribbon flare; however, in the late phase (1845 UT) two emission strands were seen with a large shear, confined in the inner edges of f_1 and p_3 . The two ribbons may have

S

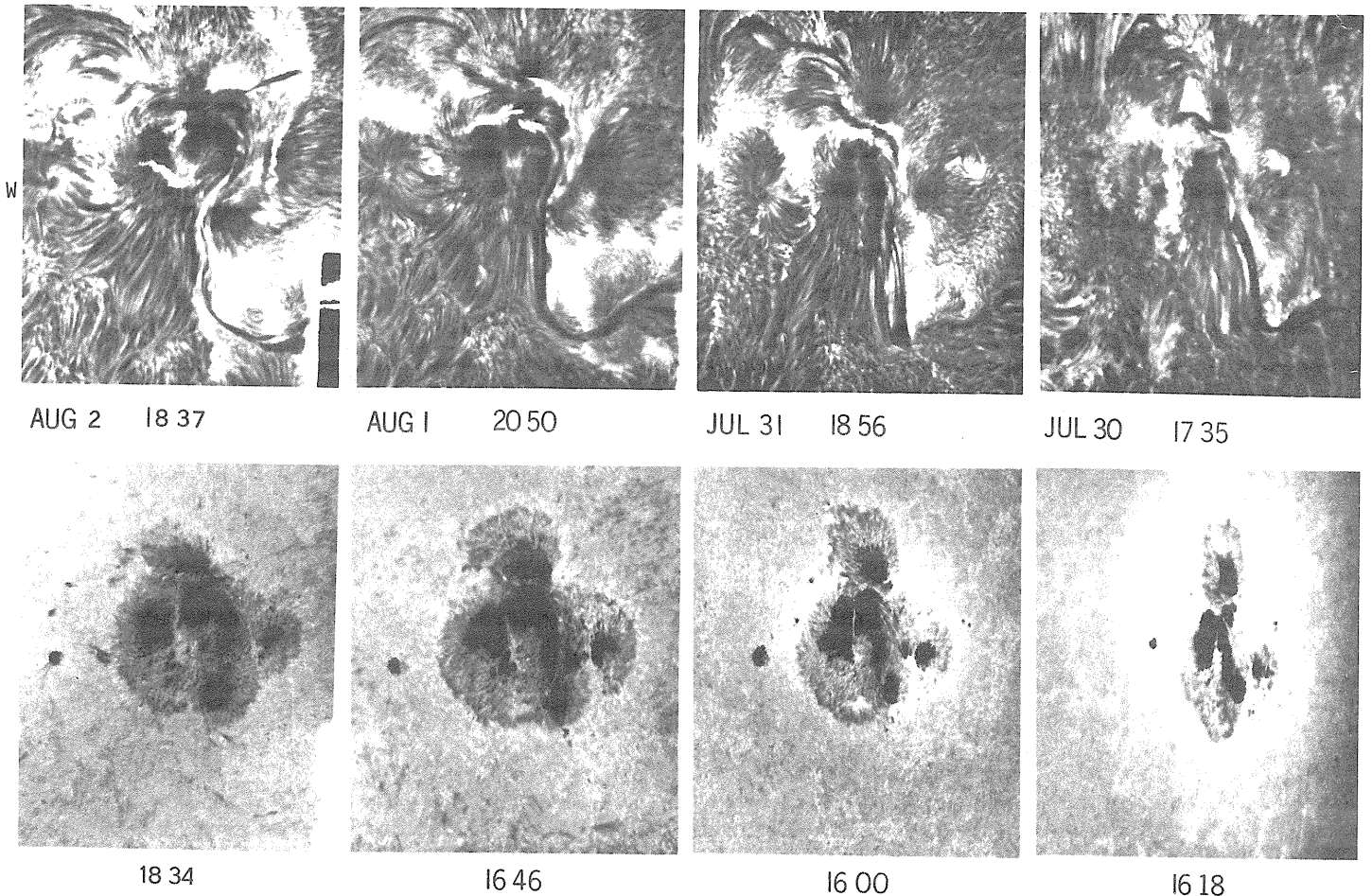


Figure 3

Synoptic series 7/30 - 8/2, with $H\alpha$ centerline, best for plages and filaments, above, and $H\alpha - 1.0 \text{ \AA}$, best for sunspots, below. Note the rapid growth of the lower spot, designated f_1 , and the increase of twist in the neutral line between f_1 and p_3 .

expanded, but the wall of the strong fields in f_1 and p_3 would have prohibited further expansion across the umbras. At 1841 UT fast ejection of material was observed along the neutral line to the north of f_1 .

Figure 10 shows how a sequence of brilliant fast flashes along the neutral line occurred in 3835. They occurred precisely at the W edge of umbra f_1 and the E edge of umbra p_3 , showing how close to the edge of the umbrae the field became horizontal; flashes above either umbra or penumbra would probably have been visible, but were not seen. The average lifetime of the points was 5 to 10 sec (frame rate was 5 sec) and their individual size can be seen to be less than 1 arc sec, although some appeared in groups and had larger area (for example, Figure 10 (a), (b) and (c) at 1839:44 UT). The double bright strands (d) in Figure 10 mark the $H\alpha$ center, and presumably correspond to the usual p and f polarity strands, but are much closer. The strands (d) and point (b) rose with the first X-ray pulse, then broke up into faint points; a new bright point appeared at 1839:24 UT, as the flux rose. It faded in 10 seconds, and a row of points flashed into view at the X-ray maximum, 1839:34 UT. The points appeared in symmetric pairs such as points (a) and (e); the lower points are less visible. As time passed, more points appeared to the north edge of f_1 . By 1840:00 UT, no more flashes were seen except for the lingering of point (f), which was under a long-lived $H\alpha$ flare knot.

We interpret the 3835 flashes as occurring at the intersection of flux loops with the surface; the emission must be due to the heating of the lower atmosphere by energetic electrons as they are accelerated in individual flux tubes and give up their energy at the surface. Thermal conduction from the flare above as an alternative source of heating would not be able to explain the fast time variation and limited extent of the flashes; the collision frequency at these densities is sufficient to produce conductivity across the field line which would rapidly homogenize the temperature in the source region, making difficult selective and time-dependent heating of the lower atmosphere, as well as spreading the emission area. Detailed discussions of the 3835 flashes related to the X-ray and radio bursts will be given in the next chapter.

S

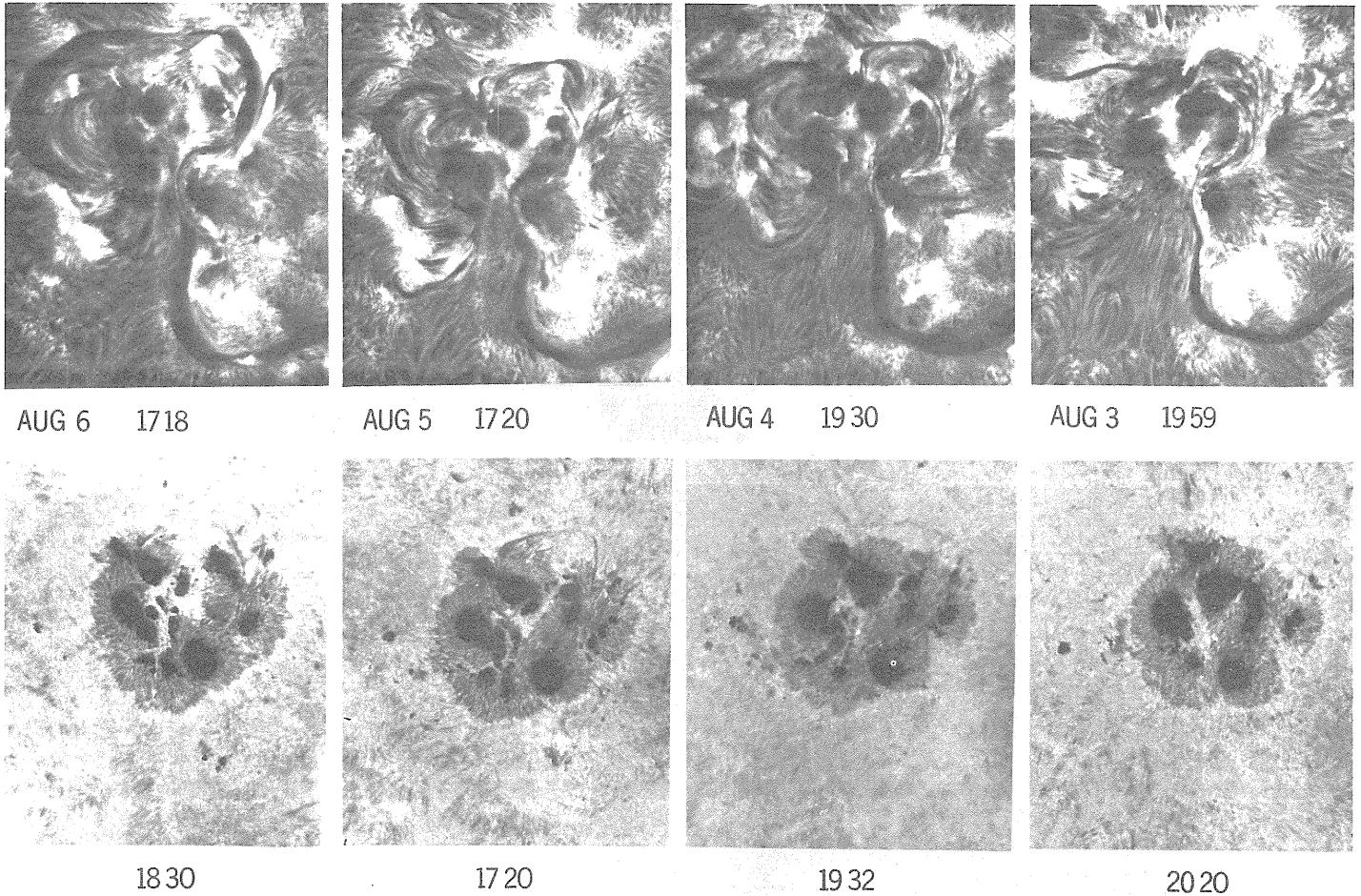


Figure 4

Further development, 8/3 - 8/6. Note the filament development and the E-W separation of the p spots. Note also the further increase of shear in the neutral line between f_1 and p_3 . On 8/6 a complex double ring exists around f_2 in the main flare area.

The activity of August 2 was not yet over; more flares were to come. Although the filament *fil 1* was disrupted, it reformed and straightened again; bright areas resulting from the flare remained, particularly of the f edge of *fil 1*. At 1957 UT the area below spot f_1 brightened slowly, then more rapidly after 2001 UT (Figure 11c). A weak brightening in 3835 appeared at the most intense portion of the $H\alpha$ flare. This flare reached maximum around 2005 UT and remained stable; it produced a modest hard X-ray burst, but little radio emission; at 2020 UT a new increase in area and brightness began on both sides of *fil 1* and at 2030 UT yet another wave of brightening spread south from *fil 1*; this was matched by a bright region (Figure 12) in 3835 (twice the photospheric intensity) just at the edge of the advancing bright $H\alpha$ front. At the same time the entire p side of *fil 1* brightened as well. The 3835 emission in this flare was not impulsive at all, lasting more than 15 minutes, although the lifetime at any point on the surface was only a few minutes. Again it appears to mark the footpoints of flux loops containing the energetic material (this time thermal conduction can be the heat source). The hard X-ray flux increased again and a large 6600 sfu, 8800 MHz burst occurred. The $H\alpha$ front spread steadily on to a maximum at 2050 UT (Figure 11d); the 3835 emission moved south with a constant velocity of 12 km/sec and changed its direction to northeast when it hit the edge of penumbra f_1 as if it was reflected by the spot field. The 3835 emission could be followed till 2105 UT, but by now the $H\alpha$ emission near the filament was dying out and the whole flare faded, accompanied by fine dark loops. But the last bright parts of this flare, spreading over p_2 and f_1 (Figure 11e, f), produced at 2140 UT the greatest peaks of radio and X-ray flux. Weak 3835 emission appeared at this time over the penumbra of p_2 . Note that this is different from the decay of other flares, which leave two widely separated strands on the flare perimeter; the emission actually shifted to a different place, and was strong in off-band (Figure 11e), indicating broad $H\alpha$ profile, and showed 3835 emission. So there was a real flare resurgence, particularly over the main umbra. The UCSD X-ray data shows a small resurgence of X-ray emission above 10 keV but less than the peak of 2050 UT. So there were no more harder electrons, just a stronger magnetic field.

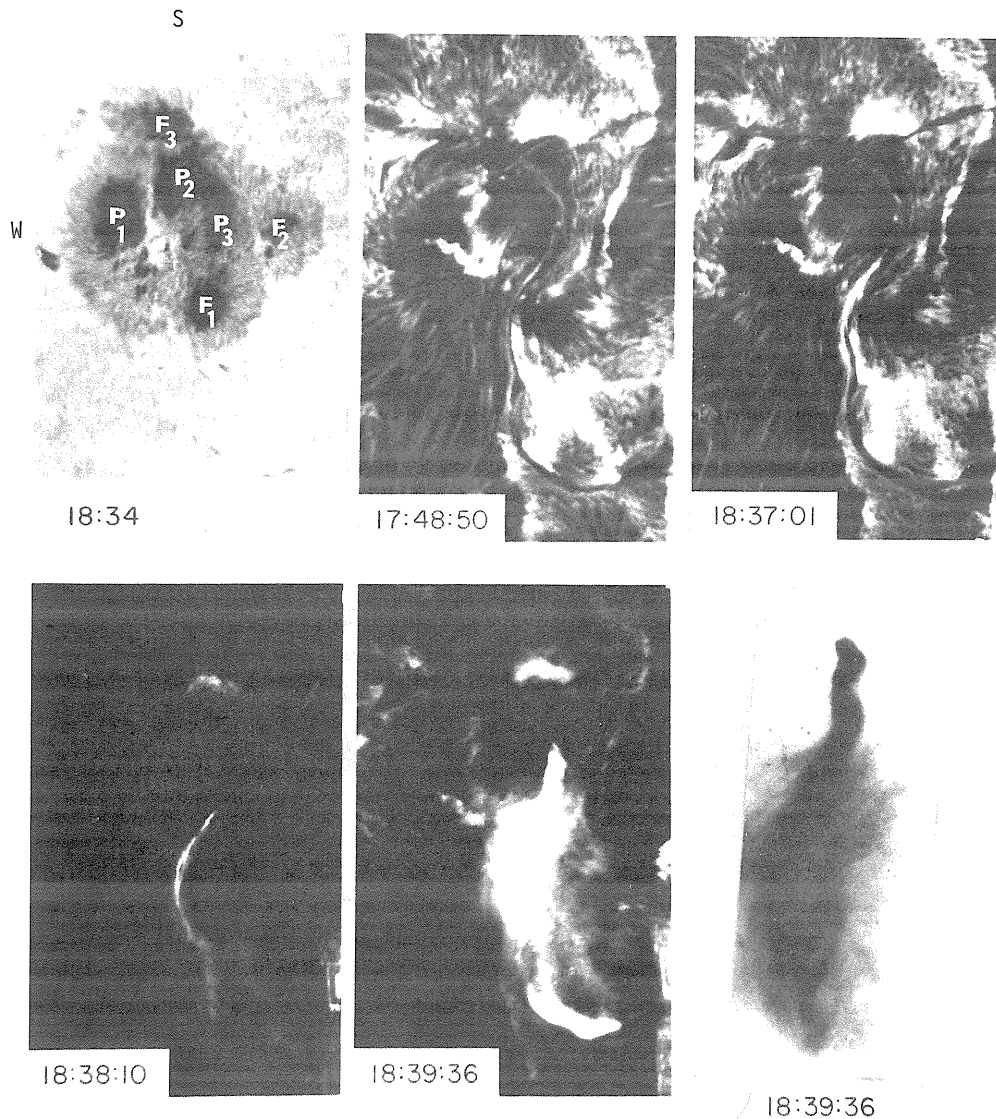


Figure 9

A series of prints made to show varied aspects of the 18:38 flare (18:34) $H\alpha + 1 \text{ \AA}$, showing spot structure, with spots marked. Note that all the spots lie in one penumbra, and the umbrae and penumbrae of f_1 and p_3 are twisted to follow the horizontal lines of force, rather than the normally radial structure.

- (17:48:50) - $H\alpha$ before the flare. Note that the filament is sharp.
- (18:37:01) - The filament begins to break up into shorter fibrils.
- (18:38:10) - Dark print of flare beginning.
- (18:39:36) - Brilliant halo around the flare, probably $H\alpha$ scattered by surrounding chromosphere.
- (18:39:36) - Light negative print, heavily dodged to show the structure of the flare kernel.

The varied aspects of the August 2 flares present an excellent opportunity to compare different flares in the same region. The comparison between the impulsive 1838 UT flare--small, violent, short-lived--and the large, long-lived, slowly-rising flares at 0310 and 2000 UT is most instructive. The first was physically low in the atmosphere, confined to the neutral line in a small region, and by far the most brilliant and concentrated. It also produced the short-lived, intense hard X-ray burst with a spectrum proportional to $\nu^{-3.5}$. The 3835 observations show the impulsive nature very well. Radio emission was low below 2700 MHz, indicating a low source height (because of plasma cut-off or other high density absorption). The 0310 and 2000 UT flares were by contrast complex and slow, with longer rise times both for $H\alpha$ and energetic electrons, and radio emission appeared at low frequencies, showing that the events reached high in the atmosphere. Since radio flux and X-rays are proportional to the total number of electrons, we can see how the large volume involved produced the huge radio bursts. However, these large events were less impulsive and had a steeper electron spectrum, so high

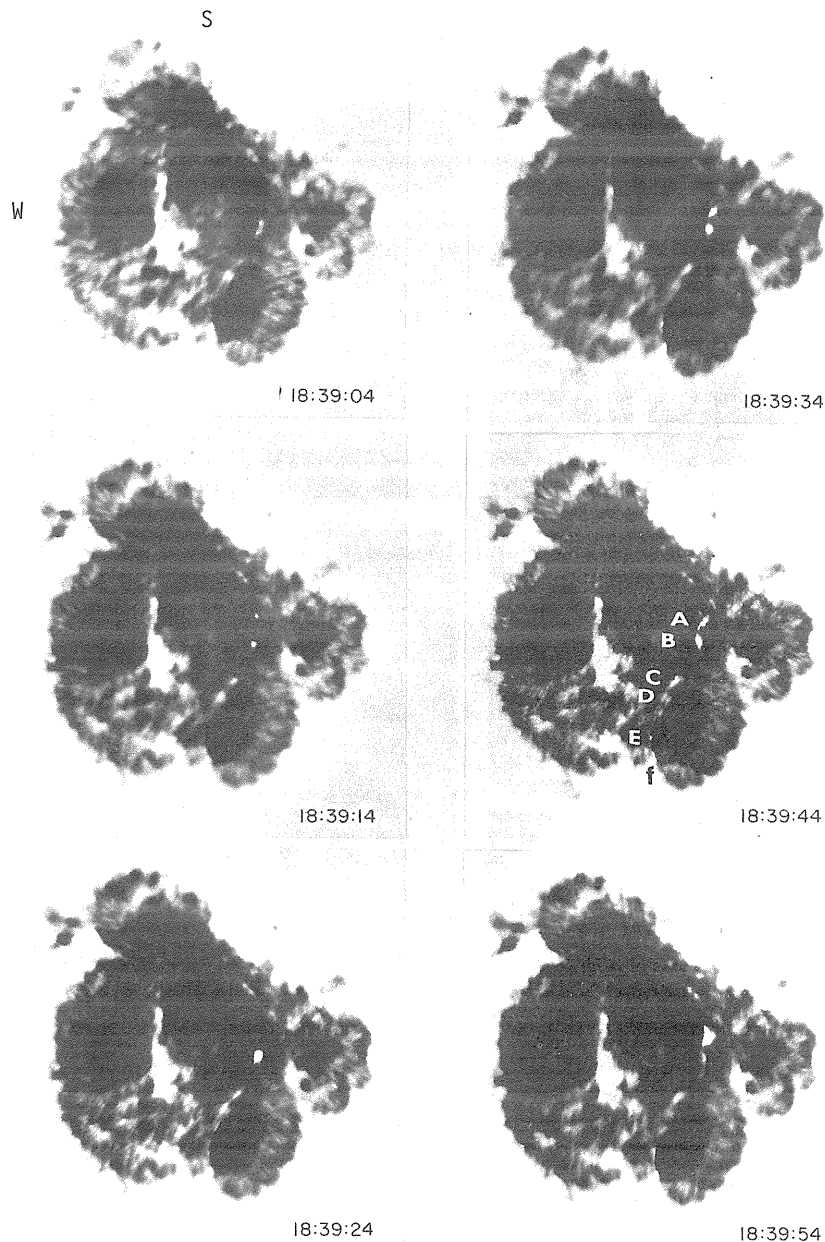


Figure 10

Dark prints showing the flashes in 15 Å band centered at 3835 Å. The point D (18:39:44) at the two bright strands on the left edge of the spot coincide with the H α maximum. All flashes occur precisely at the edge of the umbras, where the field lines turn and intersect the surface. These pictures are taken with a corrector designed by the late Professor I.S. Bowen to remove the aberration of the singlet lens; unfortunately it was not properly adjusted and there is some astigmatism.

frequency radio emission was less; for example, at 35 GHz the 2140 UT peak is only slightly higher than the 1839 UT peak, although it is 20 times higher at 8.8 GHz. We may conclude that slow events may accelerate particles quite well, but that impulsive, low-lying flares produce the hardest spectra. Finally we have the peculiar effect of the greatest radio burst occurring late in the event without an accompanying large change in the optical flare; apparently once the hard electrons are produced, phenomena over the greatest spots can produce great fluxes of radio emission (because the emission is proportional to B).

Huancayo polarization data published by Lincoln and Leighton [1972] show a sharp variation from left to right hand circular polarization at 9400 MHz, then back to left, in the 1838 UT flare, whereas the 2100 UT flare shows only right hand polarization. This corresponds to the fact that the later

BIG BEAR SOLAR OBSERVATORY
 S MULTIPLE FLARE 8/2/72

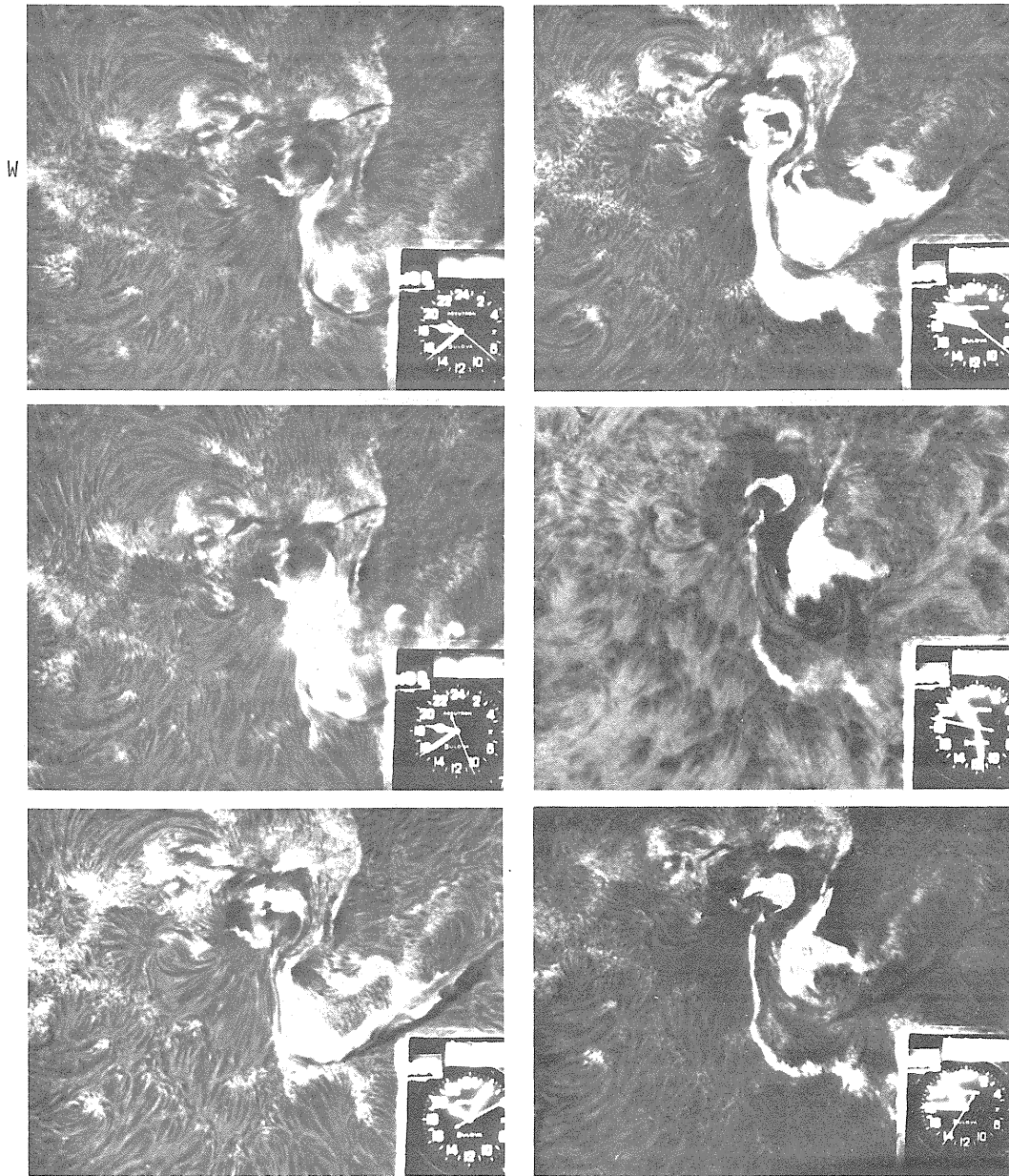


Figure 11

An $H\alpha$ centerline sequence of the flares after 18:38. The fifth frame (21:28) shows an $H\alpha + 0.5 \text{ \AA}$ picture which reveals the loops raining down after the flare; the last frame (21:45) shows the peak of the radio burst; note that the emission has shifted to an entirely different location from the fourth frame (20:47) and both f_1 and $p_2 - p_3$ are covered by emission.

flare occurred primarily in the following (= N polarity = rhc polarization) part of the group (see Figure 11e, how f area is large compared to p area), while the impulsive flare was on the neutral line where changes in the polarity balance could easily occur. The August 7 flare was also found by Huancayo to show such a L-R-L shift in the impulsive phase. In both cases, the largest sunspot in the flare region was f_1 , so that following polarity would dominate the radio propagation.

V. The 3835 Flashes and Impulsive Bursts of X-Rays and Microwaves

The 3835 flashes in the 1838 UT flare of August 2 occurred simultaneous with the impulsive hard X-rays and radio bursts. Since good data were obtained in UCSD X-ray experiments and at Sagamore Hill for microwave bursts, it would be useful to compare these three wavelengths for better understanding of electron accelerations in the impulsive phase.

Figure 13 shows comparison of the light curves of several 3835 flashes with X-rays and radio bursts. Each light curve was made by measuring the brightness of a 3 arc sec² area which showed several resolved and/or unresolved flashes in the whole lifetime (1 minute) of the flashes with a mean lifetime of an individual flash less than 10 seconds. (For example, in Figure 10 point (a), the topmost at 1839:44 UT, is made up of at least 5 points.) One can see that the intensity of the optical flashes peaked around the same time as the X-ray and radio bursts and that the light curves are more similar to the X-ray bursts above 50 keV than to the 14-20 keV X-rays or radio bursts at 5000 MHz. In addition, Figure 10 shows that the first flashes appear at 1839:04 UT simultaneous with the first X-ray spike, and the most flashes were seen at the peak around 1839:40 UT. The X-ray spectrum was proportional to $\nu^{-3.4}$ at the peak and softening of the spectrum began from 1840:10 UT [Datlowe, private communication].

The observed intensity of the 3835 flashes can be explained by Balmer line (H α) emission centered at 3835 Å. When we look at spectra taken in another large 2B flare, November 18, 1970, observed by Tanaka (unpublished) at Okayama, we find wide and large emission of H α , which has 4 equivalent Å of the mean intensity level of 3835 region (20% of the true continuum). We require, in this intense flash, emission of H α greater by a factor of two than the above flare; if we equate the observed flux at the peak of the flash (equal to the intensity of 3835 Å in quiet region) to $n_0 A_{g2} h\nu H / 4\pi$ (H: thickness of the emitting layer; A_{g2} : rate of spontaneous emission; n_0 : number density of level 9) we get $n_0 H \sim 1.7 \times 10^{14} \text{ cm}^{-2}$. Assuming the Saha-Boltzman distribution with a temperature of 10^4 K , we have $n_e n_p H \sim 4.2 \times 10^{33} \text{ cm}^{-5}$ at the peak (n_e , n_p are electron and ion number density, respectively). The total flux emitted by the flashes may be estimated by adding line emissions, free-bound and free-free continuum emissions radiated from this $n_e n_p H$. With a mean area of the flashes $6 \times 10^{16} \text{ cm}^2$ (= 10 flashes) we have $2.6 \times 10^{27} \text{ ergs/sec}$ at the peak. Note that half of this energy flux is radiated in H α . Actually in dark prints of H α , we could see H α brightening simultaneously with the 3835 flashes, but they remained bright after the latter disappeared because of the large opacity of H α ; precipitation of low energy electrons below 20 keV, which existed till late as Figure 11 shows, or thermal conduction produced continued heating of the upper layer emitting H α .

It can be shown from the X-ray flux that electrons above 45 keV in the thin foil model and above 60 keV in the thick foil model have the same total energy as the optical flux estimated above. 50 keV electrons can penetrate the column density $n_p H \sim 10^{20.4}$ as the theory of Coulomb collision shows [Schatzman, 1965; Syrovatskii and Shmeleva, 1972; Brown, 1972]. Also from the observed production rate of 50 keV electrons in the thick foil model ($= 1.0 \times 10^{35} \text{ sec}^{-1}$) it turns out that these electrons penetrating the chromosphere can ionize $7 \times 10^{20} \text{ atoms/cm}^2 \text{ sec}^{-1}$ by making an ion pair every 33 keV [Fermi, 1949; Hudson, 1972]. Therefore we can explain reasonably the heating and ionization of the layer responsible for the 3835 flashes ($n_e n_p H \sim 4.2 \times 10^{33}$) by the dumping of the electrons above 50 keV. We have $n_e \sim 10^{13.2} \text{ cm}^{-3}$ and $H \sim 10^{7.2} \text{ cm}$ for the emitting layer. Similarity of time profiles between the 3835 flashes and X-ray bursts above 50 keV (Figure 13) would support this explanation. Because of confusion with the other flares we do not know if there was any proton production involved in this fast event, but the fact that γ -rays were not detected gives an upper limit of proton flux less than $3 \times 10^{26} \text{ ergs/sec}$, below the energy flux of the optical flashes.

Optical evidence of electron precipitation seen in the 3835 flashes would give a more realistic image of acceleration; impulsive acceleration of electrons occurs in each individual flux loop with a time constant less than 10 sec and the place of acceleration moves around with the same time scale. Since the flux loops have small cross sections at their ends (0.5", size of the flashes) and stretch flat on the surface as H α fibrils structure shows, the acceleration must have taken place at a low height ($h < 10^9 \text{ cm}$) and in limited regions. Thick target emission of X-rays [Hudson, 1972] is realistic since most of the electron energy is dumped in a short time at the high density layer. Even if trapped electrons exist and emit X-rays by thin foil, the emission must be small compared to the observed flux, which could be emitted in denser layers by electrons needed to explain the optical flashes.

Radio spectra observed by Castelli (Figure 14) show an increase of flux from 15 GHz to 35 GHz with a dip around 15 GHz. In coincidence with the end of the 3835 flashes and the X-ray flux in the hardest channels the flux at 35 GHz decreased appreciably showing a single peak spectrum by 1840:40 UT. If the dip in the otherwise flat spectrum is not an observational effect, it might be explained by free-free absorption due to hot ambient plasma, which has been proposed by Zirin *et. al.* [1971] and by Ramaty and Petrosian [1972] to explain flat type spectrum. In order to realize a dip in the spectrum, it turns out that there must be an optically thick plasma for free-free absorption at the frequency at least 40 GHz. Since hot plasma emitting soft X-rays is transparent for free-free absorption down to 4 GHz as the observed emission measure and temperature show, lower temperature material such as produced the XUV flash must be invoked for the absorption in this model. The double-

peaked spectra may also be interpreted as originating from two sources; one at the top of the flux loops, where acceleration takes place with lower magnetic field and plasma density and giving a peak at 5000 MHz, and the other is located at a lower height near the mirror points with a stronger magnetic field and a peak beyond 35 GHz; the flux around 15 GHz may have been depressed due to cut off by plasma frequency or Razin effect or free-free absorption of low-temperature material. These two sources may well correspond to H α bright points and diffuse halo, respectively (Figure 9).

For these two models we may estimate the number of electrons needed to explain the radio fluxes and compare these with X-ray observations. In the case of a homogeneous source model with a free-free absorption, we have a total number of electrons above 100 keV (denoted as N_{100}) equal to $10^{34} - 10^{35}$ by fitting the observed spectra to those calculated by Ramaty and Petrosian [1972]. This number is not inconsistent with $n_i N_{100} \sim 10^{45.6} \text{ cm}^{-3}$ derived from the X-rays by assuming thin foil although

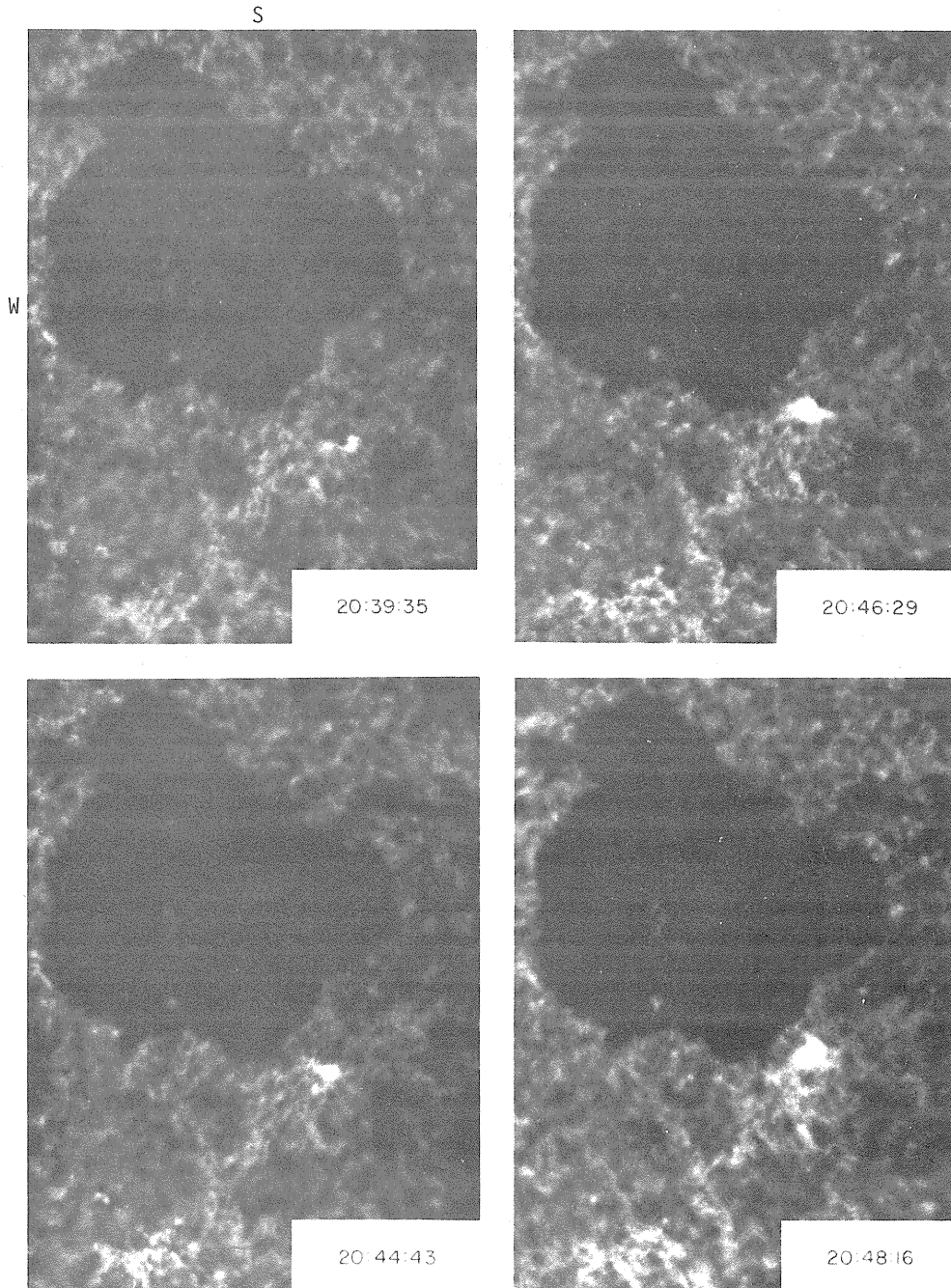


Figure 12

Dark prints showing the drift of bright points in the 3835 bands in the 20:35 flare of August 2. The bright points coincide with the H α bright front (the fourth picture of Figure 11) and move toward spot f_2 with a velocity of 12 km/sec.

although the thin foil model is not realistic for explaining the 3835 flashes. In the thick foil $\frac{dN_{100}}{dt} \sim 1.6 \times 10^{33} \text{ sec}^{-1}$; so accumulation of injected electrons for 10 seconds or more is necessary.

This does not agree with the thick foil picture. On the other hand, when we consider a flux loop model in which acceleration takes place continuously for 10 seconds or less at the top, and electrons dump at the two ends of the loop emitting X-rays there by thick foil, the total number of electrons in the flux loop at any instant can be determined by the continuity equation along the flux loop:

$v \frac{N_{100}}{L} = \frac{dN_{100}}{dt}$, where L is a length of flux loop. With $v \sim \frac{c}{2}$ and $L \sim 2 \times 10^9 \text{ cm}$ (observed mean distance between pair flashes) as well as $\frac{dN_{100}}{dt}$ from the thick foil model we have $N_{100} \sim 2.1 \times 10^{32}$, in agreement with $N_{100} \sim 10^{32}$ obtained for the 5000 MHz peak of two source models. To derive the latter number, optically thin gyrosynchrotron emission is assumed with the peak emission occurring at $3\nu_p$ [Takakura, 1967] since self-absorption would be negligible in a small cross section of a flux loop such as is considered here. ($N_{100} = 10^{32}$ together with $B = 500 \text{ G}$ and $A = 2 \times 10^{18} \text{ cm}^2$ gives a self-absorption factor $\frac{N}{BA} \sim 10^{11}$, which agrees approximately with the calculated curve by Ramaty and Petrosian [1972] if we adopt the electron power equal to 4.5 obtained from the thick foil in this case.) For the higher frequency peak we get a similar value for a magnetic field larger than 1000 G

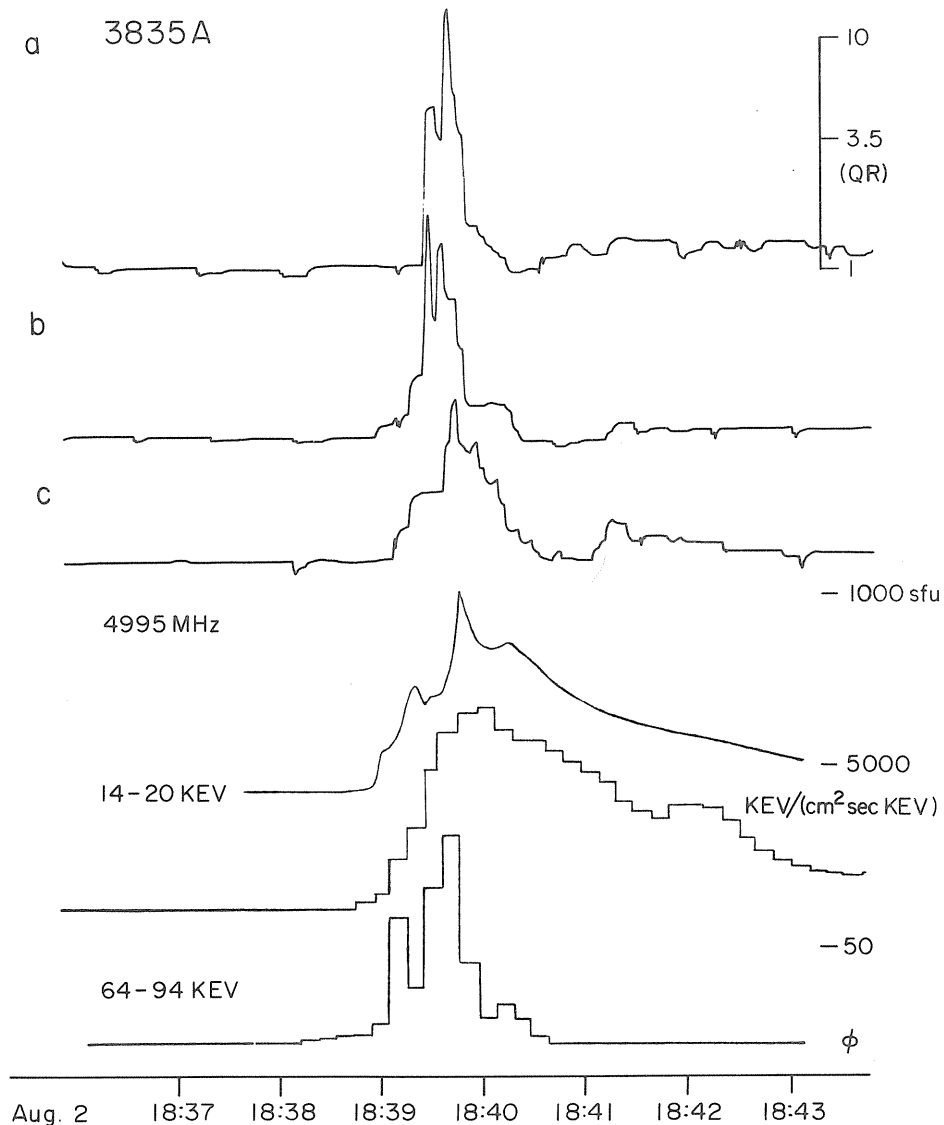


Figure 13

Light curves of the 3835 flashes measured at three positions (see Figure 10 for identifications of positions). The lower three curves show a microwave burst (Sagamore Hill) and two channels of hard x-rays (UCSD). Note that the time histories of the 3835 flashes are most similar to the 64-94 KeV burst.

Radio Spectrum

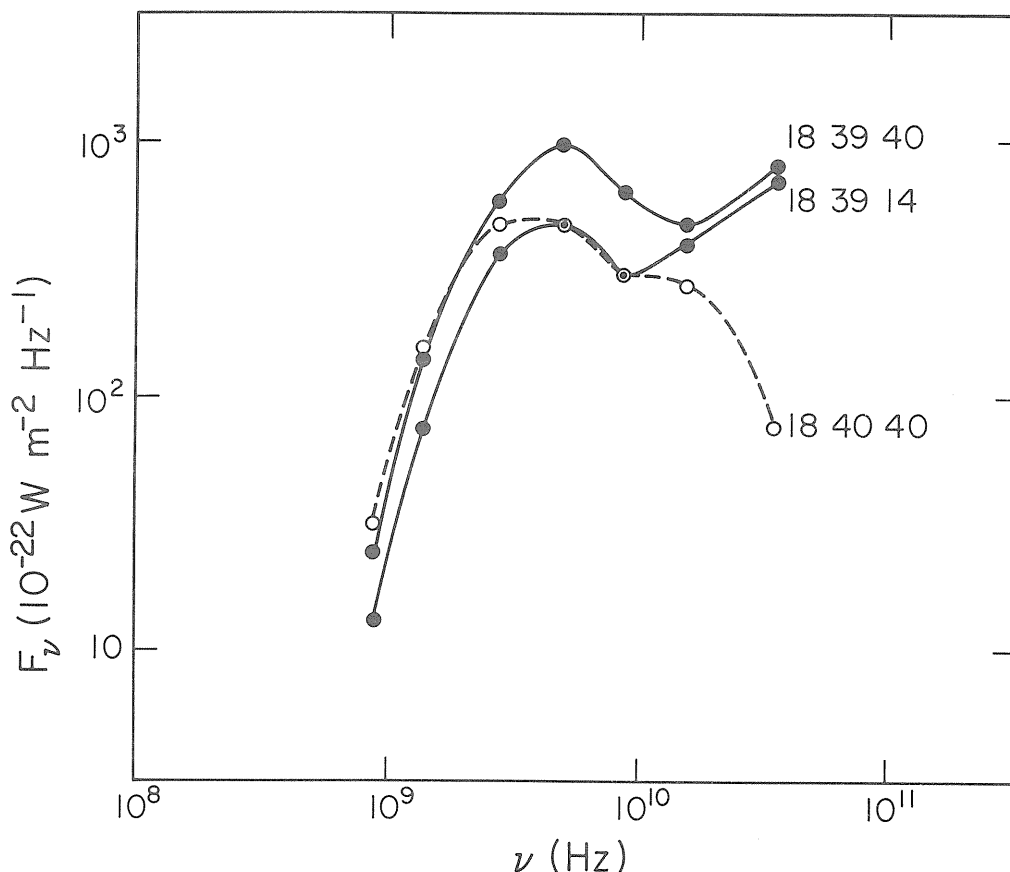


Figure 14

Microwave spectrum for the 18:38 flare of August 2 obtained by Castelli. Note the rapid decrease of the flux at 35 GHz after 18:40, which was in coincidence with the end of the 3835 flashes.

although we don't know the exact frequency and flux of the peak. Thus we can explain the radio flux in this simple model of a flux loop consistently with thick foil X-ray emission and the 3835 flashes. It is to be noted that the electron distribution exponent γ ($N(E) \propto E^{-\gamma}$) derived from the high frequency slope of the radio spectrum at 1840:40 UT (single peak) is equal to $\gamma = 4.7$, in agreement with $\gamma = 4.9$ derived from the hard X-ray spectrum assuming thick foil. In the thin foil model, on the other hand, we have $\gamma = 3.0$, inconsistent with the radio value.

XI. Conclusions

- (1) The region exhibited twisted magnetic flux and high gradients from its birth.
- (2) The flare occurred because of large shear of the neutral line and high field gradients.
- (3) The motions and growths of sunspots occurred producing the invasion of f spot to p area and increasing the shear of the neutral line.
- (4) Development of the post-flare loops revealed sheared structure magnetic field lines above the neutral line; the lowest field runs parallel to the neutral line and the higher field runs more and more perpendicular to it. The flares occur in the transition from the sheared field to the potential field.

- (5) The H α flux of the large flares comes mainly from kernels whose emission peaks with radio and X-rays. The total H α emission from the great flares of August 4 and August 7 was 2.0×10^{30} and 2.5×10^{30} ergs, respectively.
- (6) The H α emission is 12 Å wide in the flare kernels and only 1 to 2 Å wide in the rest of the flare. This flare halo makes up most of the area and thus determines the assigned "importance" but only produces 1/4 of the H α emission.
- (7) In 3835 band we detected rapidly varying emission at the edges of the flux loops. The emission can be explained by the dumping of the 50 keV electrons accelerated in individual flux loops.
- (8) Comparison of the 3835 flashes with the X-rays and microwave emissions shows that thick foil models of X-ray emission are more consistent than the thin foil model for the impulsive flare.
- (9) We observed the large velocity shear of absorption lines in the flare region. This explains the rapid change of the fibril orientation observed in the penumbra which may be related to the cause of the flare.

Acknowledgements

We are indebted to many colleagues who supplied their data for this study, in particular to Dr. Dayton Datlowe, UCSD, and Dr. John Castelli, AFCRL, and James Mosher. We thank also Drs. H. Hudson and S. Enome for discussions. The Big Bear observations were made by James Mosher, Tom Pope, David Glackin, James Dominy, David Brin, John Morgan, Douglas Rabin and the authors. A 16 mm film of the flares is available at cost (\$30.00).

This work has been supported by NASA under NGR 05 002 034, NSF Atmospheric Sciences program under GA 24015, and AFCRL under FI9628-73-C-0085.

REFERENCES

- | | | |
|--|------|---|
| BROWN, J. | 1972 | <u>Solar Phys.</u> , <u>26</u> , 441. |
| FERMI, E. | 1949 | <u>Nuclear Physics P.</u> , The University of Chicago Press. |
| HUDSON, H. S. | 1972 | <u>Solar Phys.</u> , <u>24</u> , 414. |
| LINCOLN, J. V. and
H. LEIGHTON | 1972 | <u>World Data Center A for Solar-Terrestrial Physics, Report UAG-21</u> , November, 1972, 80. |
| RAMATY, R. and
V. PETROSIAN | 1972 | <u>Ap. J.</u> <u>178</u> , 241. |
| SCHATZMAN, E | 1965 | <u>The Solar Spectrum</u> , de Jager ed., p 313, D. Reidel Publishing Company, Dordrecht-Holland. |
| SYROVATSKII, S. I. and
O. P. SHARAF | 1972 | <u>S.A.J.</u> <u>16</u> , 273. |
| | 1967 | <u>Solar Phys.</u> <u>1</u> , 304. |
| TAN
H. ZIRI | 1973 | <u>The Symposium on High Energy Phenomena on the Sun</u> , in press. R. Ramaty and R. Stone, editors. |
| ZIRIN, H.,
G. PRUSS and
J. VORPHAL | 1971 | <u>Solar Phys.</u> <u>19</u> , 463. |

The Flare of August 4, 1972

by

K. Maeda and N. Oda
Hyogo College of Medicine, Hyogo 663, Japan

and

K. Nakayama
Kwasan Observatory, University of Kyoto
Kyoto 607, Japan

and

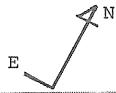
M. Shimizu
Okayama Astrophysical Observatory
University of Tokyo, Tokyo, Japan

The active region McMath 11976 produced great flares in August 1972. We observed the flare on 4 August at Okayama Astrophysical Observatory. The flare was 2B at 0634 UT. Continuous photographic observations were made with a birefringent filter having a pass band of 0.5Å at the center of the H α line. Observation started at 0557:59 UT (about 30 minutes before the onset of the flare) and lasted about two and a half hours. Photographs were taken every one minute after the maximum phase, totalling ninety-two negatives of the flare.

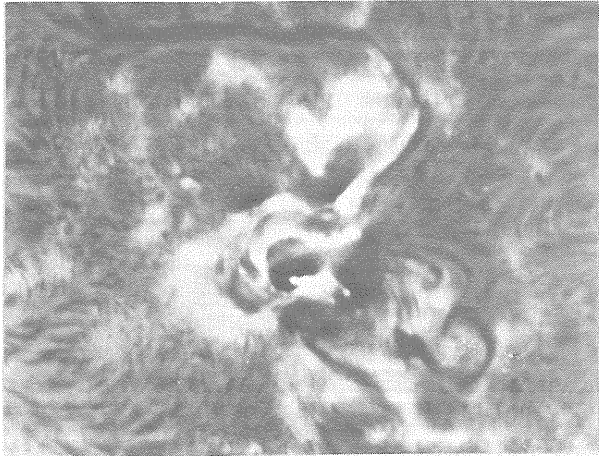
Figures 1a and 1b show the development of the flare. Isodensity maps of No. 1, 5, and 9 (Figure 1) were made using the JOYCE-LOBEL auto-densitometer (Figure 2).

The widths of the flare ribbons expanded outwards at a rate of about 25 km/sec which is several times as large as the average values observed in two ribbon flares (Figure 3).

Figure 4 shows the time variation of H α area obtained by a visual estimate.



BEFORE THE FLARE



No. 1. 0600 UT

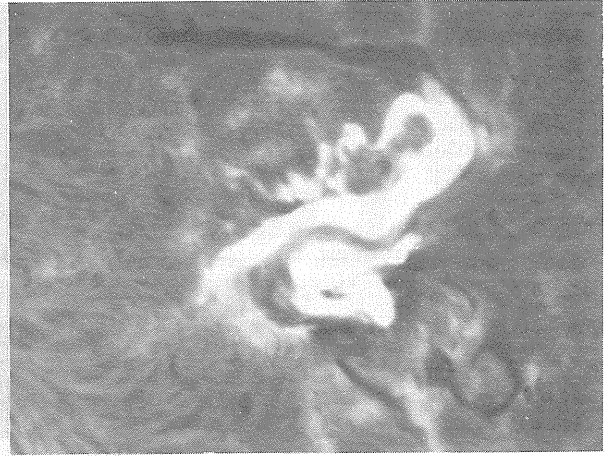
50"
└──────────┘



2. 0624 UT



3. 0626 UT



4. 0628 UT



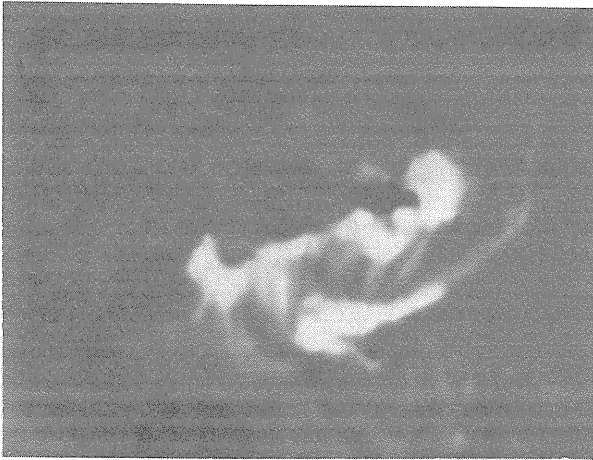
5. 0634 UT MAXIMUM



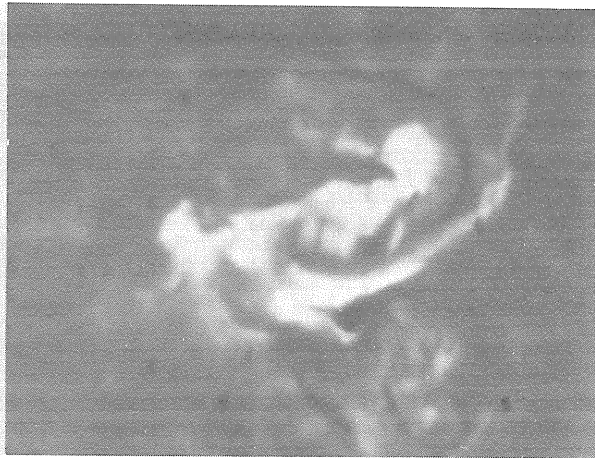
6. 0649 UT

Fig. 1a. Development of the flare on August 4.

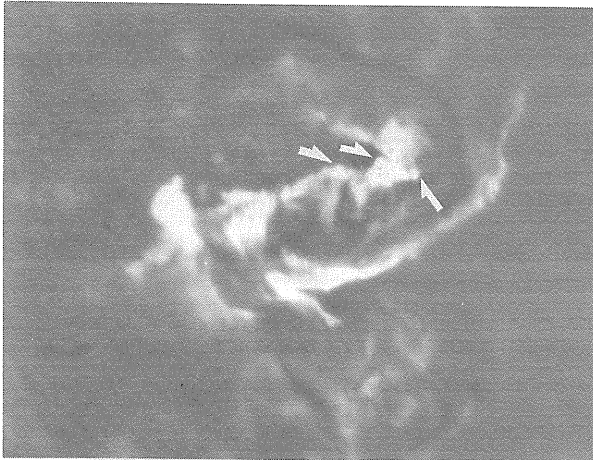
1. Note the loops between two strands of plage regions and the two bright points on spots.
4. Inner boundaries of the flare ribbons do not spread.
6. Note the emission and absorption loops radially extended from the lower flare ribbon.



7. 0655 UT



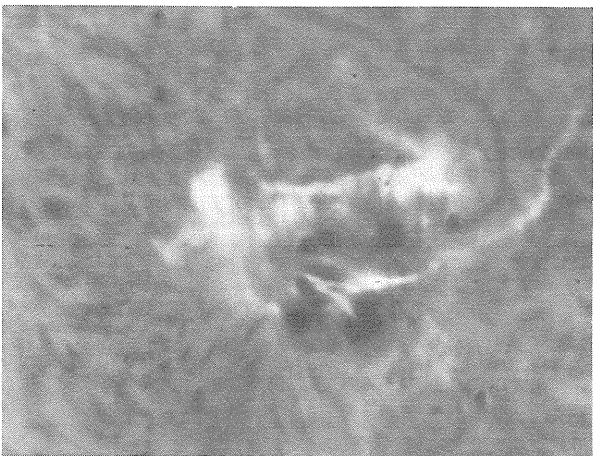
8. 0701 UT



9. 0718 UT BRIGHT POINTS APPEARED



10. 0732 UT



11. 0739 UT $H_{\alpha} - 0.5\text{\AA}$



12. 0815 UT

Fig. 1b. Continuation of Figure 1a.

9. Three bright points indicated by arrows appeared at 0717 UT at the same time an impulsive burst in radio frequencies was observed.
10. Loops are nearly parallel.
11. Note the location of the flare ribbons relative to the spots.

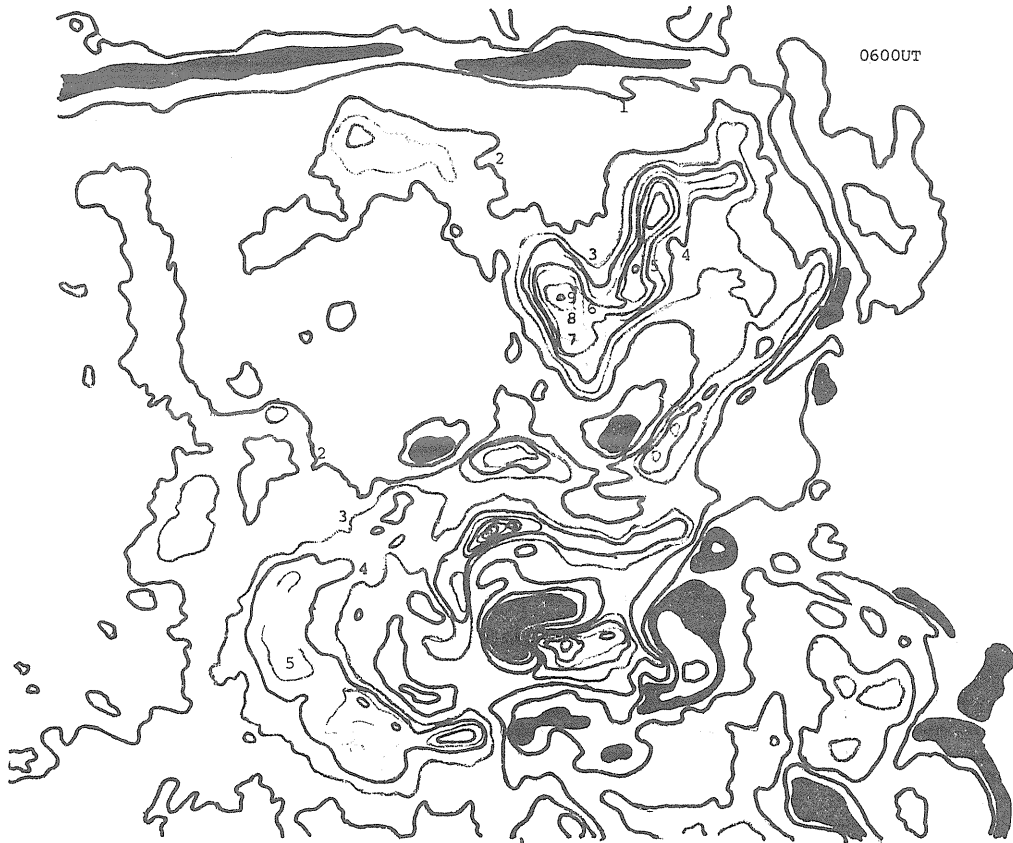


Fig. 2a.



Fig. 2b.



Fig. 2. Isodensity maps for 0600, 0634, and 0718 UT are shown. Numbers are density scales. Density interval of one step equals 0.22. The same number in different maps does not indicate the same absolute intensity.

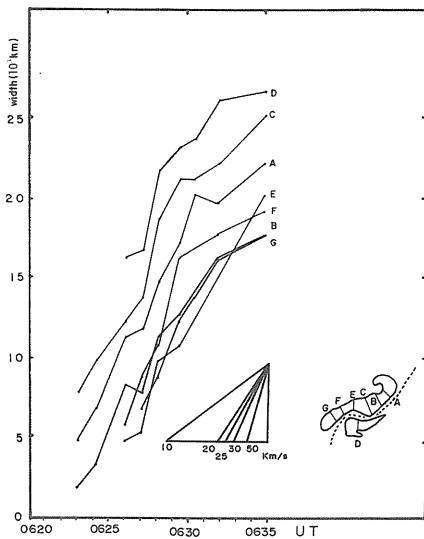


Fig. 3. Time variations of the widths of the flare ribbons are presented. Expanding velocity is about 25 km/sec in the flash phase of the flare and about 10 km/sec just before the maximum.

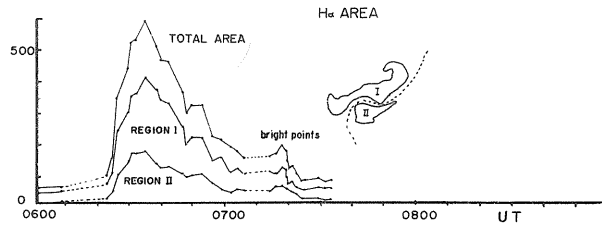


Fig. 4. Time variations of the H_{α} area of the flare ribbons measured in units of $5.97 \times 10^6 \text{ km}^2$ are presented.

On the Dynamics of the Proton Flare of August 4, 1972, at IZMIRAN

by

E. I. Mogilevsky
Institute of Terrestrial Magnetism, Ionosphere and
Radiowave Propagation of the Academy of Sciences,
Moscow, U.S.S.R.

During a number of days of the active period of 29 July - 11 August 1972, on the solar tower telescope IZMIRAN regular filming with $H\alpha$ -filter of the Firm "Opton" ($\Delta\lambda = 0.25 \text{ \AA}$, $\delta\lambda_0 = \pm 16 \text{ \AA}$) was made of the group No. 223 (according to *Solar Data*, USSR, or McMath 11976 according to *Solar-Geophysical Data*, NOAA), and its neighborhood (dimensions of the filmed region $\approx 160'' \times 250''$). The filming was made with discrete movement (every 0.2 \AA) of the pass-band along the profile of $H\alpha$ line wings within the limits $\pm (0.8 \text{ to } 1.0) \text{ \AA}$ (if there were eruptions - the band movement was limited to $2.5 \text{ to } 3.5 \text{ \AA}$). The complete filming cycle along the line profile took ≈ 30 s. Prolonged filming was completed by obtaining a number of polarization spectrograms for photographic measurements of magnetic fields of sunspots. The summary of obtained data is given in Table 1.

Table 1

Observations of the active region with the spot group no. 223 from
29 July to 12 August 1972 at the tower telescope of IZMIRAN

Date	UT Time of chromospheric observations	UT Time of photographic measurements of magnetic fields of spots	Atmospheric conditions of observations
29 July	1000-1100 1435-1525	- -	Satisfactory "
30 July	0725-0800 1510-1540	0530-0650 1405-1425	Good "
31 July	1425-1530	0749-0810	Good
1 August	0720-0845 1445-1529	0530-0600 -	Good "
2 August	0717-0951	1325-1357	Good
3 August	1715-1740	-	Satisfactory
4 August	0500-0900 1503-1516	0904-0936	Good
6 August	0445-0510 1504-1516	0600-0708 1405-1535	Satisfactory "
7 August	1405-1410	1208-1322	Satisfactory
8 August	0930-1210	-	Good
10 August	0655-0851	1155-1210	Good
11 August	0728-0844 1418-1540	-	Good
12 August	0617-	-	Satisfactory

We succeeded in filming the development of the large proton flare according to above mentioned program from 0550 to 0900 UT. The image was on the whole good, so that the chromosphere fine structure at different levels was fixed with resolution of $\leq 2 \text{ to } 3''$. The preliminary results of the analysis (without measuring the Doppler velocity and photometry) and detailed data on active region magnetic fields are considered below.

Group No. 223 that appeared from behind the E-limb as a group of "δ" magnetic configuration, retained its total area almost invariable, though the changes in the umbras and penumbras were considerable. When the number or size of the umbras changed considerably (often suddenly), there remained an almost threefold excess of N polarity magnetic flux over the flux of umbra of S polarity. The magnetic field of the group and neighboring regions formed two systems of quasi-dipole magnetic fields: an eastern system in which the flare flocculi developed, and the "stable" filament was situated along the line $H_{II} = 0$; and the western system where the activity was considerably lower (see Figure 1). The comparison of photoheliogram of the group taken late in the evening on August 3 at IZMIRAN and photoheliograms of Ussurijsk, Irkutsk and Tashkent observatories obtained at the end of August 3 and at the beginning of August 4, showed that a successive separation of two new umbras of N-polarity occurred in the central umbra of N-polarity. In the presence of very large magnetic field gradients (in many places ≥ 0.4 to 1.0 G/km) such a break of the main umbras showing the trend of total movement clockwise in the center of the spot* could determine the large intensity of the proton flare on August 4.

The development of the proton flare of August 4 can be conditionally divided into two typical phases: "emission" and "eruption." Similar phases can also be observed in the flares of August 2, 7, and 11 as well as in a number of other proton flares, i.e., our conditional division may have a more profound physical sense.

Emission Phase. From the beginning of our observations (0550 UT) a bright emission in the form of very small (≤ 3 to $5''$) points and thin (2 to $3''$) filaments was registered inside the spot (between the umbras of the same polarity) as well as outside it (along the filament boundary and away from the western S-nucleus) (Figure 2). It was along these "emission paths" that a

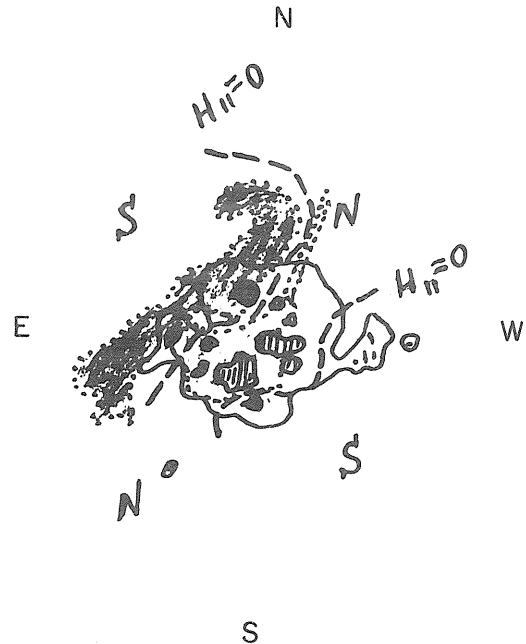


Fig. 1. Scheme of magnetic fields and two ribbons distributions during the flare of 4 August 1972.

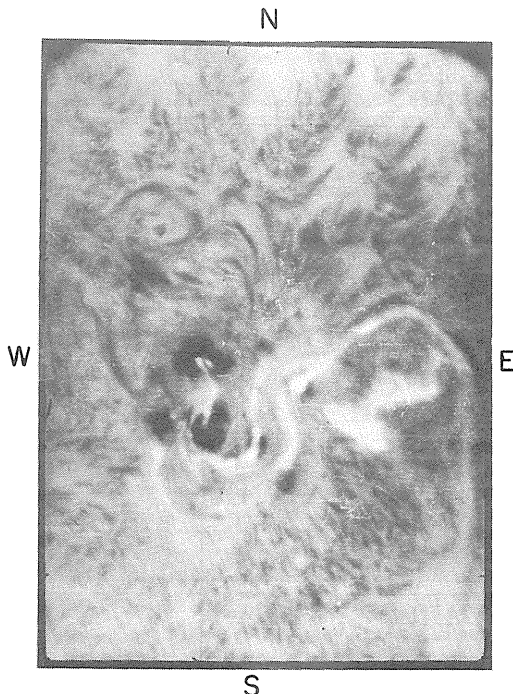


Fig. 2. Pre-flare emission in the active region.
 $\Delta\lambda = 0.25 \text{ \AA}$, $\delta\lambda_0 = 0.4 \text{ \AA}$, $t = 0600 \text{ UT}$.

sharp growth of brightness occurred at 0619 UT and it could be taken for the beginning of proton flare. Two very bright parallel flare-filaments were initially observed in the form of thin discrete ribbons, then they turned into powerful S-shaped parallel bright flare-flocculi, covering separately some of umbras. These two ribbons were situated only along N or only along S spot magnetic field and the surrounding field **. The brightness of these flare flocculi in the center of $H\alpha$ decreased only 2 to 3 times in the filtergrams taken in the wings $H\alpha \pm 0.8 \text{ \AA}$. The intensity of these two ribbons increased rather slowly to $\approx 0638 \text{ UT}$, and then began slowly decreasing (Figure 3). The noncontiguity of the flare-filaments, situated over N and S magnetic polarity, is a typical peculiarity of the emission flare phase.

* The vortex location of photospheric filaments of the spot penumbra points to the same movement.

** Even approaching to the maximum, when their area considerably increased and in some places their boundaries drew close together, this rule of noncontiguity of N and S lines held strictly.

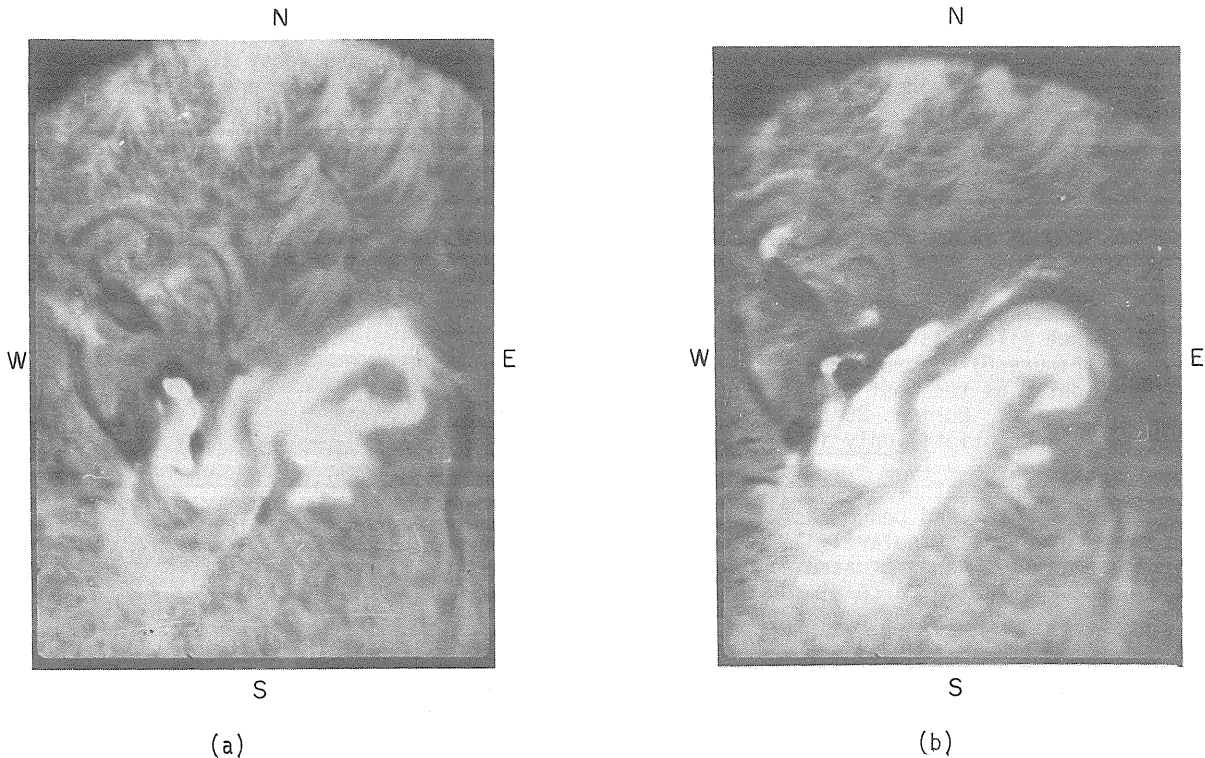


Fig. 3. Development of the emission phase of the flare
 (a) $\Delta\lambda = 0.25 \text{ \AA}$, $\delta\lambda_0 = -0.4 \text{ \AA}$, $t = 0620 \text{ UT}$
 (b) $\Delta\lambda = 0.25 \text{ \AA}$, $\delta\lambda_0 = -0.4 \text{ \AA}$, $t = 0637 \text{ UT}$

Another peculiarity of $H\alpha$ - flare emission - consists in its strikingly thin structure; which was especially well visible in the western and southern large umbras of N-polarity. Separate emission "points" ($\lesssim 2$ to $3''$) and a thin emission bridge between these nuclei suffered marked changes (Figure 4). Their life-time was $\lesssim 2$ to 3^m . They were observed symmetrically in both wings of $H\alpha$. However, such thin emission bridges between these umbras, thread-like fringes of separate umbras and umbras "points" and the splitting of the main flare flocculi of the emission into thin ribbons were observed even at the end of the flare.

The third feature of the flare development consists in original quasi-wave movements along "undisturbed" filament*. The discrete filming along the $H\alpha$ - line profile allowed one to establish that some parts of the filament $l \gtrsim 20''$ during ~ 5 to 7 s could be observed either in the red or in the blue wing. From such pairs of filtergrams we can infer the existence of a quasi-periodic fluctuation of V_D along the filament. The estimates showed that velocity in these parts of the filament reached $V_D \sim 25$ km/sec. Such movements (of the type of "stationary waves") were clearly observed during the first flare phase and with less intensity during the second phase.

We should also note that considerable changes were observed in the location of the elements of chromospheric structure. They were especially large between two ribbons and in NW part of the active region, where a separate small spot-pore of S-polarity was situated and where typical arched absorption ejections were observed for a long time.



Fig. 4. Fine structure of the flare emission
 $\Delta\lambda = 0.25 \text{ \AA}$, $\delta\lambda_0 = -0.8 \text{ \AA}$, $t = 0621 \text{ UT}$

* It was noted that these filaments, which began in the large NE umbra of S-polarity, were observed on the disk all days, and when the umbra reached the W-limb we could observe an active prominence often with great eruptions.

Flare Eruption Phase started after the emission phase maximum, at the decay of brightness of two flare ribbons. Let us consider some features of flare development, that permit one to mark out the second eruption phase.

In contrast to what was observed during the emission phase, beginning from the moment 0645 UT in the southern part of the separation between two ribbons, there appeared narrow emission ribbons that joined them (Figure 5). These ribbons crossed the line $H_{||} = 0$ with a considerable angle. From this time up to the end of the flare there was observed a slow formation on their outside boundary of the systems of thin short branches directed at a large angle to the line $H_{||} = 0$.

The appearance of the absorption system of thread-like arched filaments (AFFS-Arch Filament Flare System) (Figure 6) of prolonged existence should be considered as the most typical feature of the eruption phase. During ~25 to 30^m this AFFS was observed (in absorption!) only in the red wing $H\alpha$ (up to the distance 2.5 to 3 Å). Thread-like arches closely driven together at the beginning joined accurately umbras and penumbras with magnetic fields of opposite polarity in the western part of the spot, i.e., were situated along the magnetic lines. Eventually, arch dimensions and their number grew, they already crossed the eastern (S-polarity) flare floccula and by the end of the flare there remained only several arches (AFS-Arch Filament System). In contrast to the arches of the initial period they could be observed in both wings of the line $H\alpha$. A similar (but, preprolonged) phenomenon of nonstationary AFFS was filmed by us in detail at the phase of flare decay (1b) on the second of August. Thin (≈ 1 to 3") thread-line arches, joining magnetic fields of opposite polarity, were visible only on filtergrams taken in the red (up to $\delta\lambda_0 = 3.4 \text{ \AA}$!) wing (Figure 7). That fact that AFFS stood out clearly against the background of bright flare flocculi as well as far away from the line center, pointed to a relatively large density of the moving material down at both ends of the arch at the rate of $V_D \approx 200$ to 250 km/sec (!). The velocity along field lines was nearly monochromatic ($\Delta V_D \leq 15$ km/sec). A similar phenomenon after the maximum flare was observed in the flares of August 2 and 7 and 11 as well as in other proton flares [Roy, 1972]. AFFS have a great deal of similarity with AFS, studied by Bruzek [1969] for weakly disturbed active regions. However, AFFS considerably differ by dimensions, velocity (for AFS $V_D \leq 50$ km/sec) and extreme instability: the existence time of particular filaments was of the order of 2 to 3 minutes. But new ones appeared again along the same trajectories. The difficulty involved in understanding of AFFS nature consists in the fact that for observed velocity magnetic Mach-number was ≈ 15 to 20 but at the same time there remained a strict nonturbulent thread-like structure of the filament. The kinetics of these arches and why they are visible only in the red wing $H\alpha$ is not clear. The total energy (even by a rough estimate) of the substance movement in all the arches AFFS during the whole eruptive phase of the flare exceeds the flare energy by a factor of ≤ 1 to 2 orders. It means that during the eruptive phase an additional comparative flow energy generation that was not taken into account in accepted theoretical flare models must take place.

The flare eruption phase started when the microwave part ($\lambda < 10$ cm) of the IV type burst finished. However, a new sharp rise of intensive "stationary" (in the meter and dekameter range) component of the burst of IV type is connected with the eruption phase. Let us note that radiophenomena of this kind in the meter and dekameter range often followed chromospheric material ejections into the corona as observed optically.

In addition to the above mentioned unstable phenomena of the eruption phase we can add the following: the discovery of γ -radiation in particular lines of the flares of August 4 and 7 not only in the initial phase but also after the maximum of brightness $H\alpha$ [Forrest et al., 1972]; X-ray emission for a long time and a long generation of solar cosmic rays having energy spectrum which differs from the initial (impulse) one. It also points to the fact that besides an impulse process there is a non-thermal process of energy generation, which evidently operates at high altitudes and during almost the whole flare.

It should be noted that the comparison of $H\alpha$ filtergrams for flares of August 2, 4, and 7, characteristics of X-ray bursts and radio-wave radiation spectra leads to the preliminary conclusion of their homology.

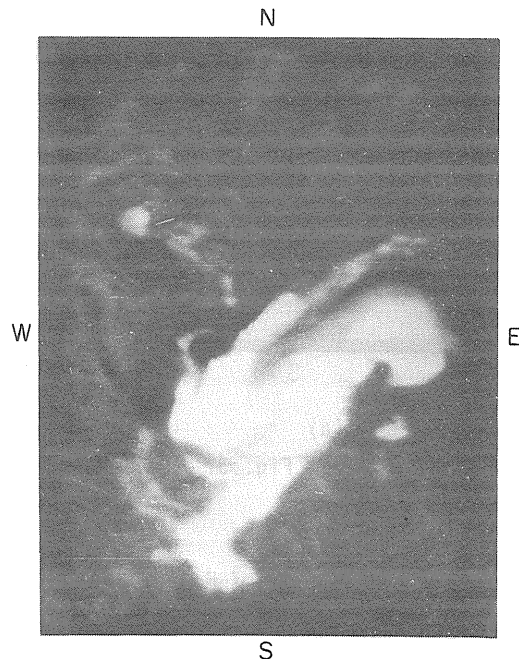


Fig. 5. Coupling of two ribbons in the eruptive phase of the flare. $\Delta\lambda = 0.25 \text{ \AA}$, $\delta\lambda_0 = -0.4 \text{ \AA}$, $t = 0643 \text{ UT}$

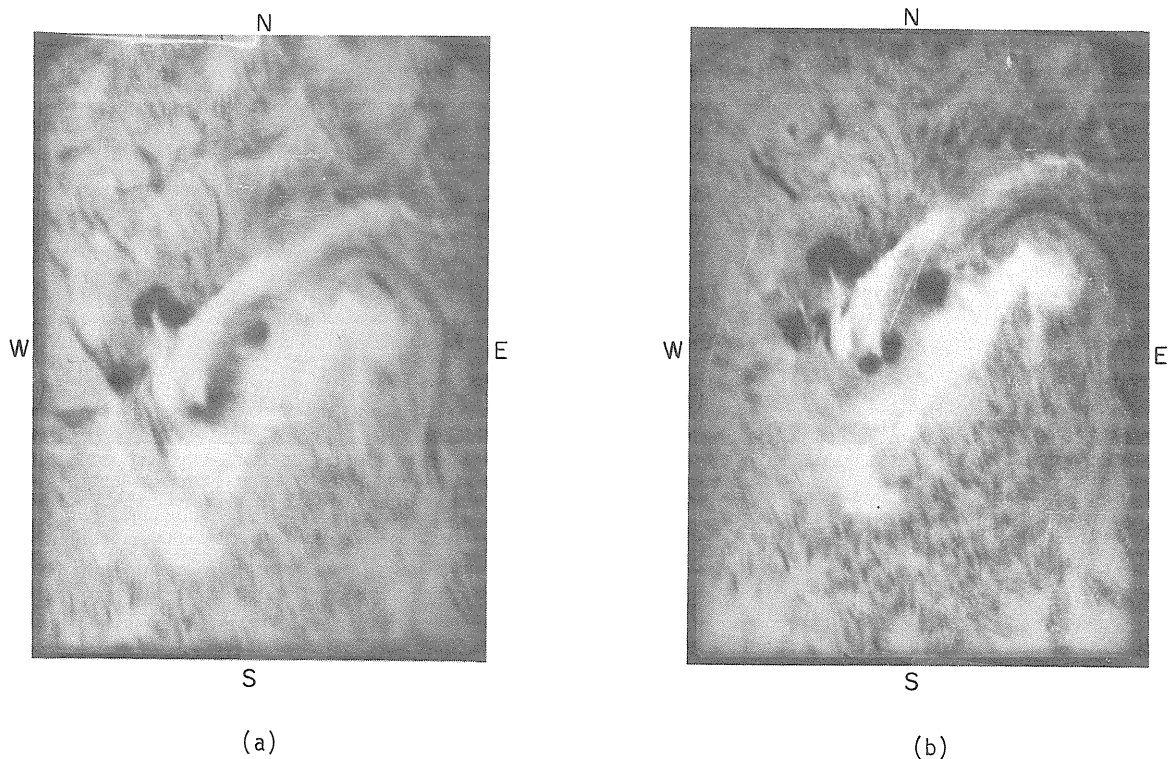


Fig. 6. AFFS Phenomenon
 (a) Filtergrams in red wing. $\Delta\lambda = 0.25 \text{ \AA}$, $\delta\lambda_0 = + 0.6 \text{ \AA}$, $t = 0658 \text{ UT}$
 (b) Filtergrams in blue wing. $\Delta\lambda = 0.25 \text{ \AA}$, $\delta\lambda_0 = - 0.6 \text{ \AA}$, $t = 0658 \text{ UT}$

On the other hand, proton flares in the August group have a number of analogies to the past. For example, the proton flare group observed in July 1959 (10, 14, and 16 July) had much in common with the August flares. The spot group in this case was similar to group No. 223 by its appearance and magnetic class (" δ " configuration). A considerable analogy can be established as well in the character of flare development, location and shape of flare flocculi, and so on. It is interesting that in the development of the complex of geophysical phenomena, caused by flares, in this case there is also much in common. We should like to stress with it that above mentioned features of the development of the proton flare of August 4, may have a more general character.

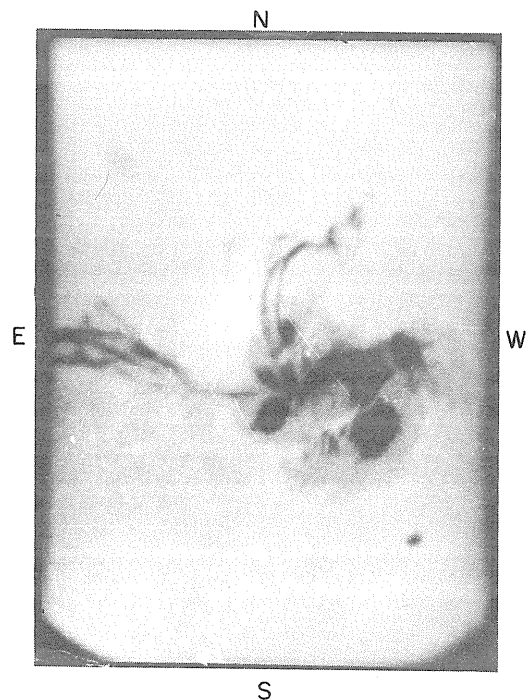


Fig. 7. AFFS phenomena during the flare Importance 1b of August 2, 1972.
 $\Delta\lambda = 0.25 \text{ \AA}$, $\delta\lambda_0 = + 1.6 \text{ \AA}$, $t = 0736 \text{ UT}$.

REFERENCES

- | | | |
|--|------|--|
| BRUZEK, A. | 1969 | <u>Solar Phys.</u> , <u>8</u> , 29 |
| FORREST, D. J.
E. L. CHUPP,
A. N. SURI,
P. R. HIGLE, and
P. DUNPLY | 1972 | <u>Trans. Amer. Geophys. Un.</u> , <u>53</u> , N11, 1053 |
| ROY, J. R. | 1972 | <u>Solar Phys.</u> , <u>26</u> , 418 |

Observations of the August 4, 1972 Chromosphere Flare at Abastumani

by

M. Sh. Gigolashvili and E. I. Tetrushvili
Academy of Sciences of the U.S.S.R.
Moscow, U. S. S. R.

An intensive chromosphere flare (importance 3; coordinates: $\varphi = N 14^\circ$, Carrington long. = 9°) has been observed simultaneously with the photosphere-chromosphere telescope, the horizontal telescope AIIV-5 [Nikolsky and Khetsuriani, 1969] and the Lyot type coronagraph [Tetrushvili, 1967].

The photographs taken with the photosphere-chromosphere telescope are given in Figure 1: (a) the sunspot group; (b) the flare in the $H\alpha$ line at 0646 UT on August 4, 1972.

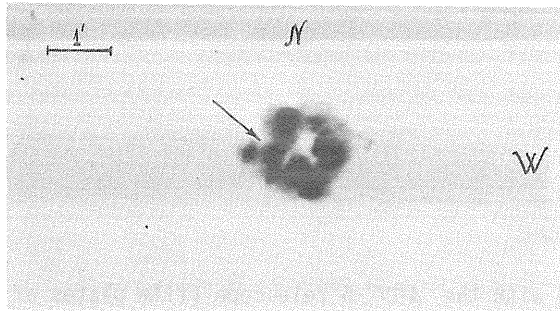


Fig. 1a.



Fig. 1b.

Fig. 1. Photographs obtained with the photosphere-chromosphere telescope: (a) The sunspot group; the arrow points to the location where the main spectrograms were obtained with the horizontal telescope AIIV-5 and the Lyot type Coronagraph; and (b) the flare in the $H\alpha$ line at 0646 UT, August 4, 1972.

The flare spectrum has been obtained in the wavelength range from 6600 Å to 3300 Å with the telescope AIIV-5 and from 6600 Å to 4800 Å with the coronagraph in the time interval from 0650 to 0830 UT. The emission lines observed are given in Table 1.

Table 1

Wavelength	Element	Wavelength	Element
6562.81	$H\alpha$	3829.36	Mg I
5895.94	Na (D_1)	3824.45	Fe I
5887.97	Na (D_2)	3820.44	Fe I
5875.64	He (D_3)	3761.43	Fe I
4861.53	$H\beta$	3761.32	Ti II
4101.74	$H\delta$	3759.30	Ti II
3968.49	H CaII	3749.50	Fe I
3933.68	K CaII	3748.27	Fe I
3930.31	Fe I	3745.67	Fe I
3922.92	Fe I	3745.61	Sm II
3905.53	Si I	3737.14	Fe I
3889.05	$H\gamma$	3736.92	Ca II
3886.29	Fe I	3734.87	Fe I
3859.92	Fe I	3733.33	Fe I
3838.30	Mg I	3719.95	Fe I
3832.31	Mg I	3706.04	Ca II

Absorption in the D_3 He line was also present.

The following lines have been analyzed: $H\alpha$, $H\beta$, $H\epsilon$, H and K Ca^+ , D_1 and D_2Na and D_3He . The prints of the spectral regions close to $H\alpha$, $H\beta$, H and K Ca^+ , D_1 and D_2Na and D_3He obtained with the horizontal telescope, and the prints of D_1 and D_2Na and D_3He obtained with the coronagraph are given in Figures 2 and 3, respectively. P_i points indicate the places of photometric sections. The corresponding line contours represented in Figures 4 and 5 are drawn as intensities expressed in the units of the solar disk continuum spectrum.

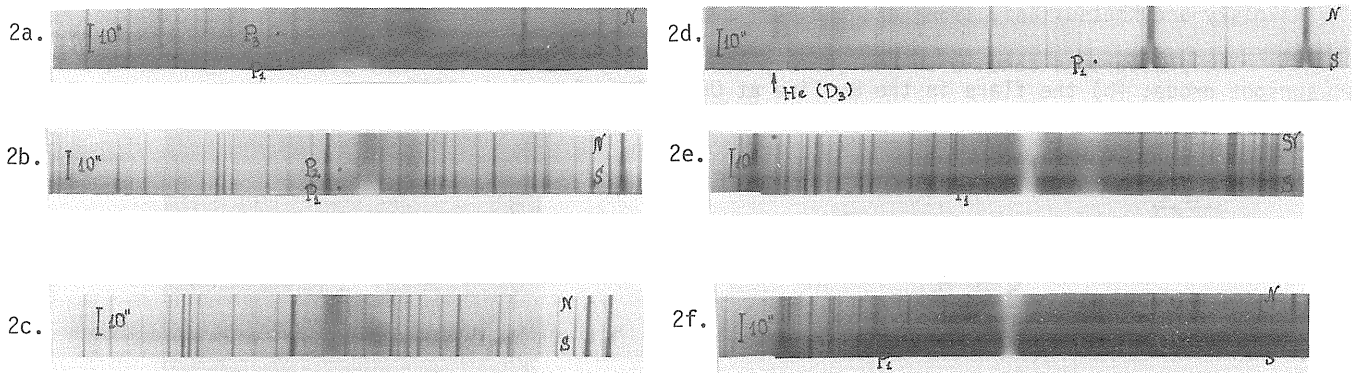


Fig. 2. The prints of the spectrophotograms obtained with the AIIV -5 telescope (film plates of ORWO Rot rapid WP-1, exposure from 2 sec to 8 sec): 2a. in $H\alpha$ line; 2b. $H\beta$ in emission; 2c. $H\beta$ in absorption; 2d. the region of D_1 and D_2Na and D_3He ; 2e. H Ca II and $H\epsilon$; 2f. K Ca^+ . The points (P_i) show the places of photometric sections.

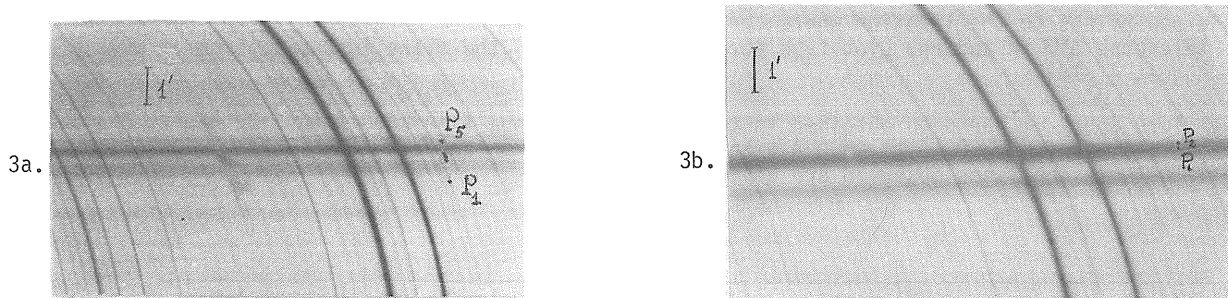


Fig. 3. The prints of the spectrophotograms obtained with the Coronagraph: 3a. the region D_3He with large radial velocities in absorption (0650 UT, the film $P\Phi-3$, exposure 1/250 sec); 3b. the region of D_1 and D_2Na and D_3He in emission (0655 UT, the film $P\Phi-3$, exposure 1/30 sec). The points (P_i) show the places of photometric sections.

In the $H\alpha$ and $H\beta$ lines (Figures 4a and 4b), besides the main emissions, the centers of which are not displaced, one can separate discrete emissions having Doppler velocities +42 km/sec and +40 km/sec, respectively.

During the course of the flare the motion of dark matter with large radial velocities was observed. Upon measuring the spectrophotograms, the presence of such a displacement towards the red end of the spectrum was confirmed.

The results of radial velocity measurements for $H\alpha$, $H\beta$ and D_3He are given in Table 2. The radial velocity measurements are accurate to ± 2 km/sec. (Table 2). In the emission of the D_3He line (Figure 5b, sections P_1 and P_2), $\Delta\lambda_{D_1} = 0.28\text{\AA}$ and $\Delta\lambda_{D_2} = 0.27\text{\AA}$. The equivalent widths $W_1 = 39m\text{\AA}$ and $W_2 = 23m\text{\AA}$ have been determined correspondingly (the half-widths and intensities are corrected for the red component of the D_3 triplet; the contours of D_3He are Gaussian).

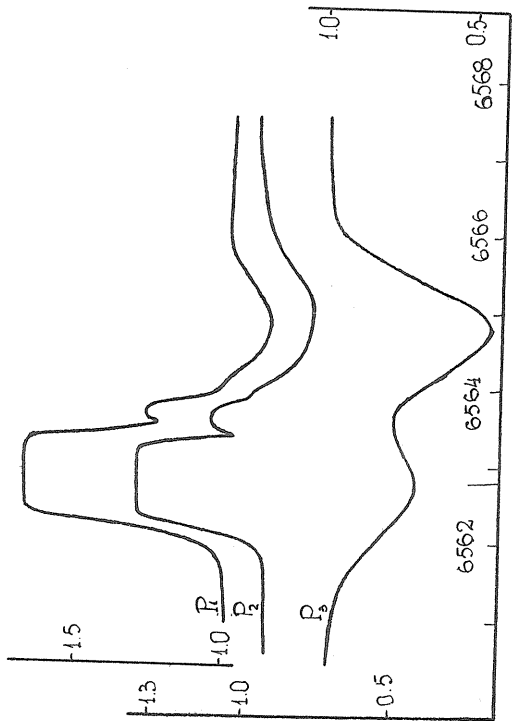


Fig. 4a.

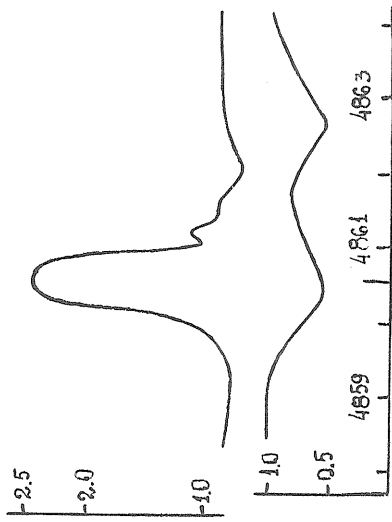


Fig. 4b.

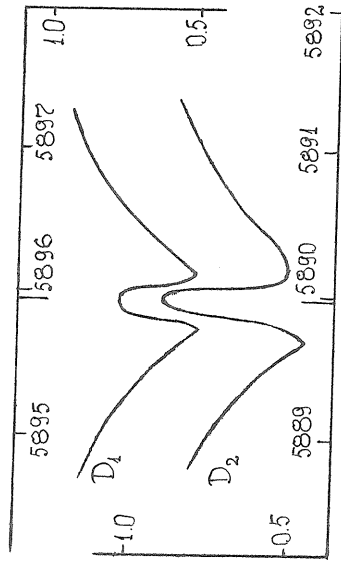


Fig. 4c.

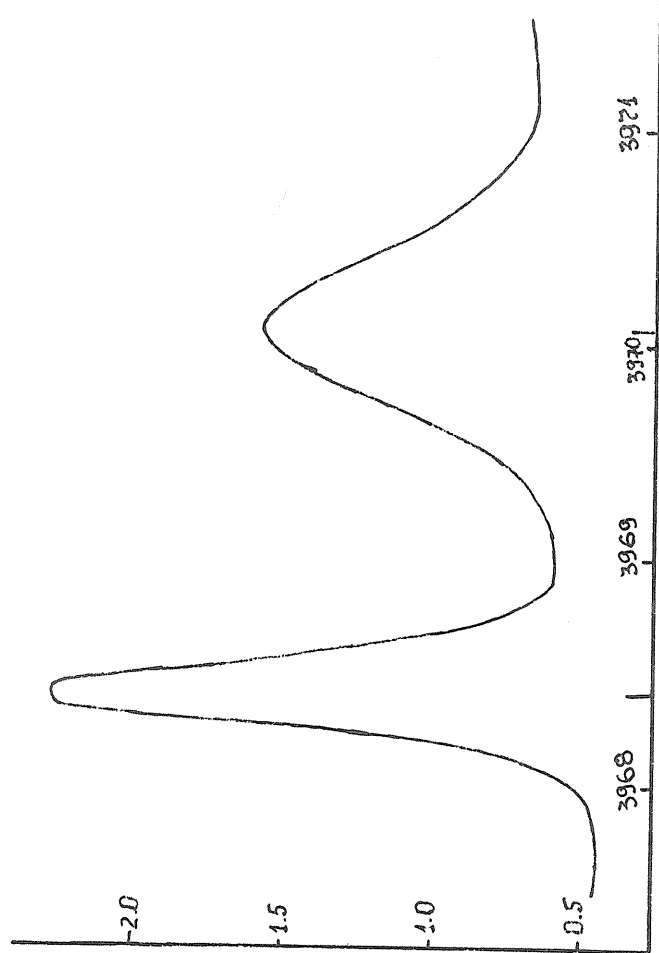


Fig. 4d.

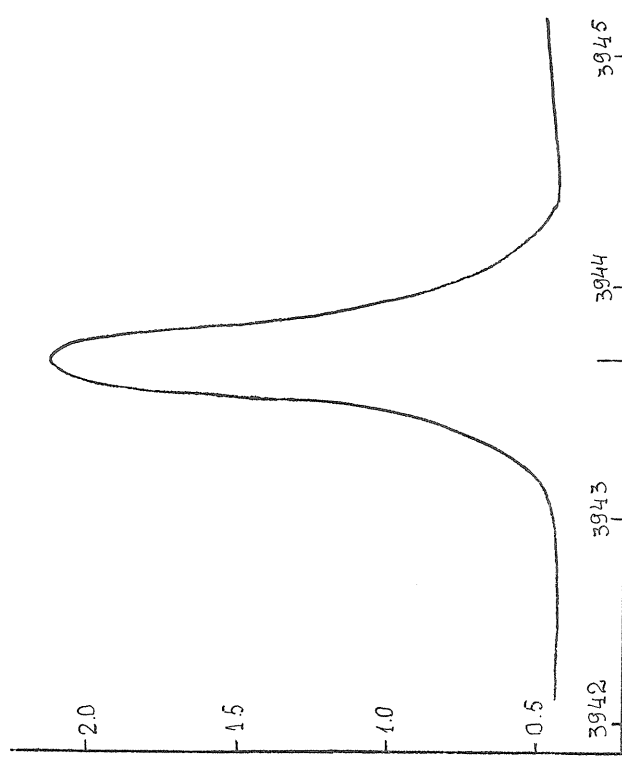


Fig. 4e.

Fig. 4. The contours drawn from the analysis of the spectrophotograms of AlIV -5: 4a, the contour of H α line; 4b, H β ; 4c, D $_1$ and D $_2$ Na; 4d, H Ca II and He; 4e, K Ca II.

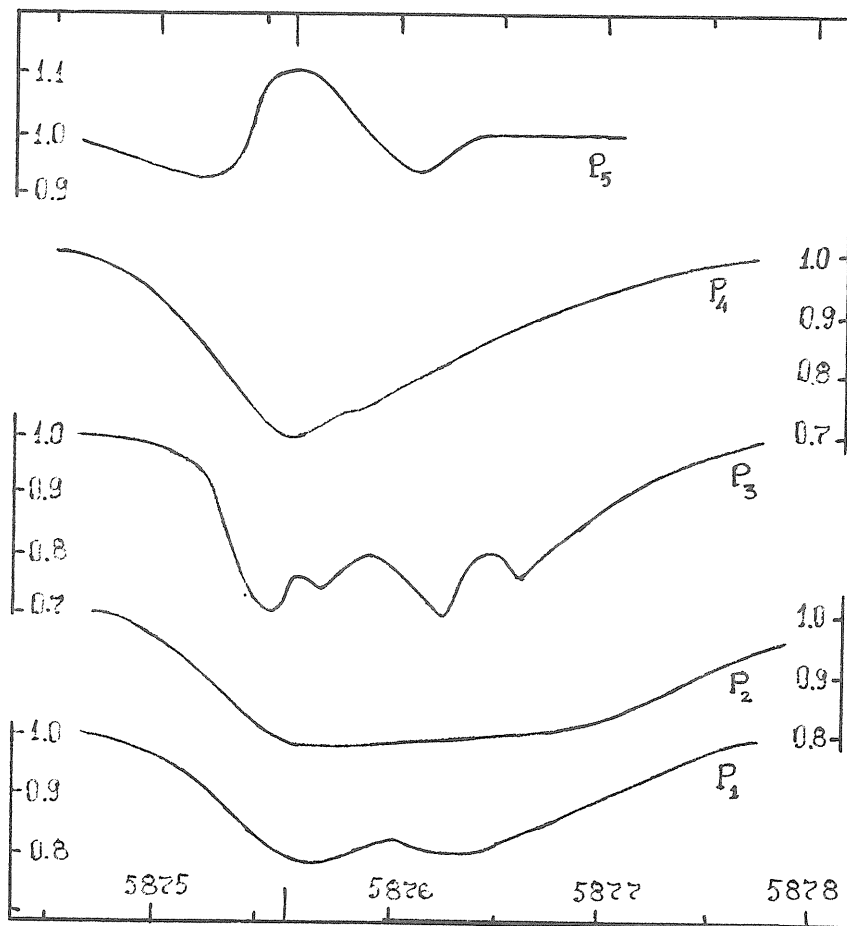


Fig. 5a.

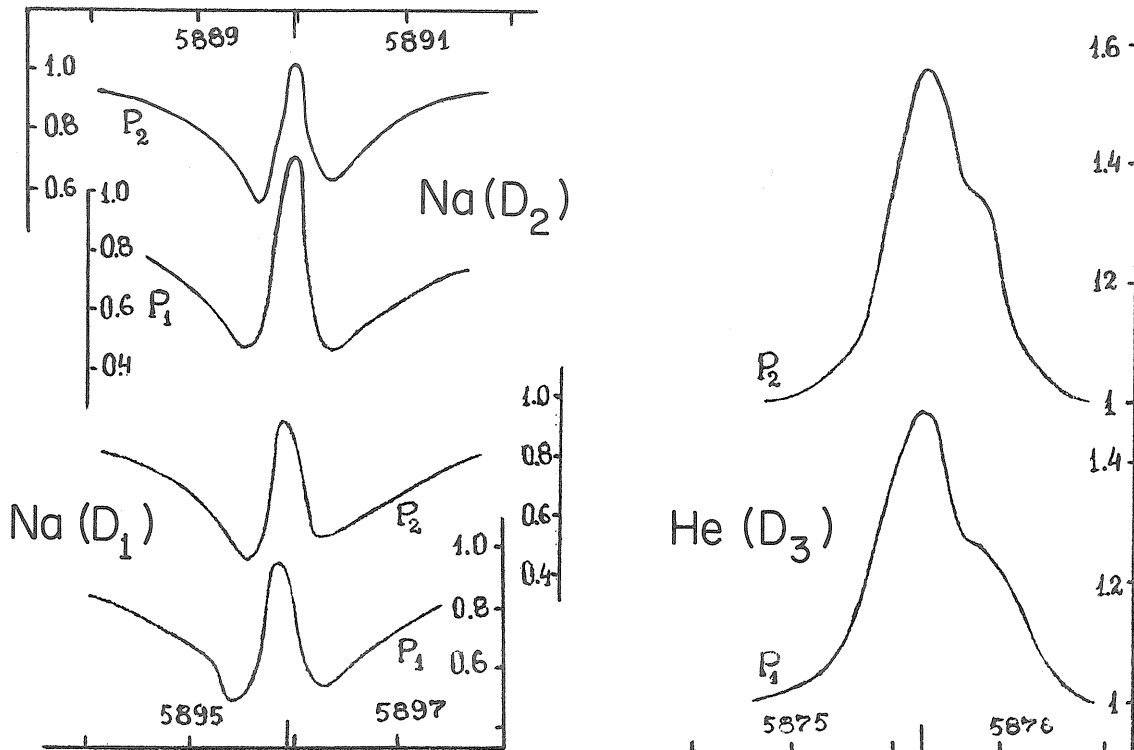


Fig. 5b.

Fig. 5. The contours drawn from the analysis of the coronagraph spectrophotograms: 5a. the contour of $D_3\text{He}$ line (0650 UT); 5b. the contour of D_1 and $D_2\text{Na}$ and $D_3\text{He}$ lines (0655 UT).

Table 2

Element	Doppler velocities in emission km/sec	Doppler velocities of dark matter km/sec
H α	+42	+95; +103
H β	+40	+98; +104
He (D ₃)	0	+36; +40

REFERENCES

- NIKOLSKY, G. M. and Ts. S. KHETSURIANI 1969 Soviet Astron. - A. J., 5, 46.
- TETRUASHVILI, E. I. 1967 Bull. Solar Data, 12, 98.

by

Juan M. Fontenla and Jorge R. Seibold
 Observatorio Nacional de Física Cosmica
 San Miguel - Argentina

Introduction

The D₃ (He I) line is a triplet originated between the 2³p and 3³D levels whose wavelengths correspond to 5875.618 Å, 5875.650 Å and 5875.989 Å and whose relative intensities are 5, 3, and 1, respectively. The two first components are equivalent to a line of 5875.63 Å with a relative intensity of 8. Thus, we can consider two components of wavelengths of 5875.63 Å and 5875.989 Å and relative intensities 8 and 1, respectively. Two telluric lines can be found at 5875.596 and 5875.769 Å. The D₃ line is invisible in the normal atmosphere of the Sun. It appears weakly in absorption in facular areas, and its behavior is quite complex in flares, appearing either in absorption or in emission or in both at the same time in different places of the flare, depending on the phase of the flare [Smith and Smith, 1963, and others].

Observations

The flare of August 7, 1972 was of importance 3B at N14 W37. It developed from 1449 UT to 1721 UT having its maximum around 1534 UT [NOAA, 1973]. Our spectrum was obtained in the San Miguel Spectrograph, after the maximum, at 1613 UT with an exposure of 0.8 sec. and a 1 Å/mm dispersion in the third order. An Agfa Avi-Phot plate was used. Structures of two seconds of arc can be spatially distinguished on the plate. An emission zone on the umbra of the subjacent spot, and an absorption zone on the penumbra are distinctly recognized in our record (Fig. 1). We have drawn four profiles (Fig. 2). The first one is on the emission zone that covers the umbra. The second is on the penumbra at 2,100 km from the umbra. The third one is on the penumbra at 4,200 km from the limit of the umbra, and the fourth is at 6,300 km.

The characteristics of these profiles will be discussed later.

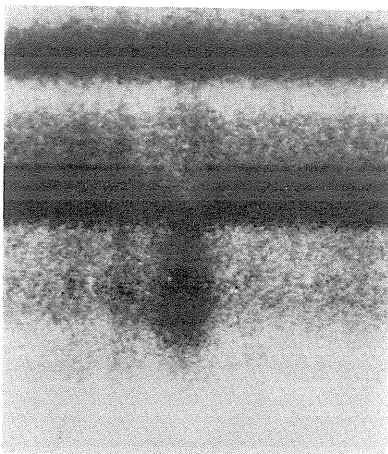


Fig. 1. Flare spectrum of the D₃ region. Higher wavelengths are to the left.



Fig. 2. Line profiles. Numbers 8 and 1 indicate the components of relative strength 8 and 1, respectively. The letter A indicates atmospheric lines. The ordinate values correspond to the intensities relative to the local continuum.

Determination of Optical Depth and Doppler Width

Using the equation [Svestka, 1972]

$$I(\lambda) = I_0(\lambda) \exp[-\tau(\lambda)] + \int S(\lambda, t) \exp[-t(\lambda)] dt \quad (1)$$

and assuming that $S(\lambda, t) = S$ we have

$$I(\lambda) = I_0(\lambda) \exp[-\tau(\lambda)] + S (1 - \exp[-\tau(\lambda)]) \quad (2)$$

that is equivalent to:

$$\frac{I(\lambda)}{I_0(\lambda)} = 1 + \left(\frac{S}{I_0(\lambda)} - 1 \right) (1 - \exp[-\tau(\lambda)]) \quad (3)$$

If the intensity observed in the line of relative intensity 8 is called I_8 , and if the relative intensity 1 is called I_1 , and likewise with τ_8 and τ_1 , then

$$\tau_1 = \tau_8 \left(\frac{1}{8} + \exp \left[- \left(\frac{0.36}{\Delta \lambda_D} \right)^2 \right] \right).$$

Since $S_8 = S_1 = S$, if we replace them in (3) we have the relation:

$$\frac{\frac{I_8(\lambda)}{I_0(\lambda)} - 1}{\frac{I_1(\lambda)}{I_0(\lambda)} - 1} = \frac{1 - \exp(-\tau_8)}{1 - \exp(-\tau_1)} \quad (4)$$

Taking account of the violet wing of the 8 component and by an iterative procedure we can obtain the values of $\Delta \lambda_D$ and τ_8 which better approximate the observed profile. In Table I we present the obtained values of τ_8 and $\Delta \lambda_D$ in the four profiles. These values show an interesting result: the optical depth decreases when going towards the umbra. This result is in accordance with those obtained by Machado and Seibold [1973] when studying flares over spots in the H and K regions of Ca II. This leads us to think that the emission of the flare is more diluted in the region located over the sunspots. Our results also show that optical thickness is not too high, in accordance with Kubes [1965], Steshenko & Khokhlova [1960, 1962], Jefferies [1957], and Severny [1959]. It is necessary to remark that these results have been obtained with the assumption of a constant source function.

TABLE I

Profiles	τ_8	$\Delta \lambda_D$ (A)	$T_K(\text{max})$ (°K)	S ($\times 10^6$)	$N(2^3P)$ cm^{-2}	$N(3^3D)$ cm^{-2}
1	0.8	0.24	34,000	0.77	2×10^{12}	1.5×10^{10}
2	2	0.18	19,000	1.15	3.7×10^{12}	4.2×10^{10}
3	4.2	0.14	12,000	1.50	6.1×10^{12}	9.0×10^{10}
4	~ 5.3	~ 0.15	-	~ 1.86	-	-

Estimation of the Kinetic Temperature

The asymmetrical profile of the line can be explained by the presence of the two components as shown in the theoretical profiles in Figure 3 which were drawn from the formula

$$I_{\lambda} = A (1 - e^{-\tau_{\lambda}})$$

with

$$\tau_{\lambda} = \tau_8 \left(\exp \left[- \left(\frac{\Delta\lambda}{\Delta\lambda_D} \right)^2 \right] + \frac{1}{8} \exp \left[- \left(\frac{\Delta\lambda - 0.36}{\Delta\lambda_D} \right)^2 \right] \right).$$

The violet wing is in accord with the Doppler profile (taking account of the autoabsorption) in the central parts of the line. Assuming that the widening is exclusively thermic, we can find the upper limit of the kinetic temperature applying the formula

$$\frac{(\Delta\lambda_D)^2}{\lambda_0} = \frac{2kT_K}{mc^2}.$$

In Table I we show the resulting values of maximum T_K .

In profile 4 (Fig. 2) the relative intensity component 8 (5875.634) is doubled towards the red at a displacement equivalent to 6 km/s and the relative intensity component 1 (5875.989) is also doubled at the same displacement. This effect can be explained as a relative motion of two parts of the flare region or by the existence of a moving filament above this part of the flare.

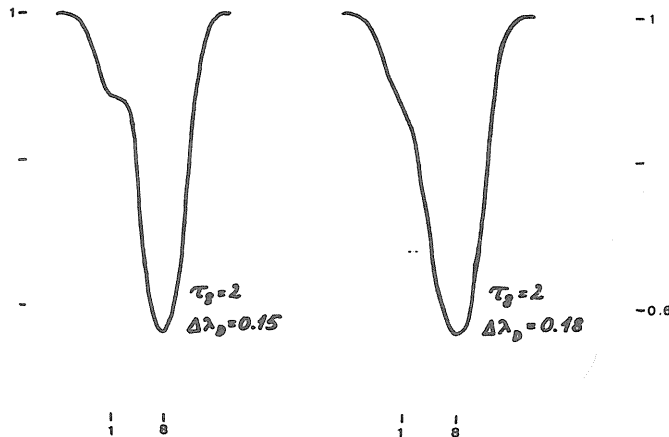


Fig. 3. Theoretical resultant profiles from the two components.

Determination of the Source Function

The S value can be deduced from (3) once we have introduced in it the values obtained from τ for the center of the considered line and the observed values of $\frac{I(\lambda_0)}{I_0}$. The values obtained for the different profiles are:

Profile 1:	$S = 1.30 I_u$
Profile 2:	$S = 0.63 I_p$
Profile 3:	$S = 0.70 I_p$
Profile 4:	$S = 0.79 I_p$

Where I_u is the intensity of the local continuum on the umbra and I_p is the intensity of the local continuum in the penumbra.

We obtain the continuum intensity from Allen [1963] interpolating between 5500 Å and 6000 Å and calculating I_0 for the θ angle corresponding to the flare over the disk. Assuming that the values

$$\frac{I_u}{I_0} = 0.17 \quad \text{and} \quad \frac{I_p}{I_0} = 0.76$$

we obtain the values of Table I. This would indicate that S also decreases towards the umbra together

with τ . The values of this source function will allow us in the following section to estimate the populations of the upper level of D_3 transition.

Determination of the Populations of 2^3P and 3^3D Levels

The 2^3P level population can be calculated by using the known expression of optical depth for a Doppler profile

$$\tau_o = \frac{\sqrt{\pi} e^2 \lambda^2 f N(2^3P)}{mc^2 \Delta\lambda_D} = 9.56 \times 10^{-22} \frac{1}{\Delta\lambda_D} N(2^3P)$$

For the profiles 1, 2, and 3 we introduce the τ and $\Delta\lambda_D$ values obtained before. Thus, we have the values of Table I.

$N(3^3D)$ is found using the values of the source function corresponding to the flare over the penumbra and the population $N(2^3P)$ previously found. Starting from the general expression of the source function [Jefferies, 1968].

$$S = \frac{2hc^2}{\lambda^5} \left(\frac{n_1}{n_u} \frac{g_u}{g_l} - 1 \right)^{-1} = \frac{2hc^2}{\lambda^5} \frac{n_u}{n_1} \frac{g_l}{g_u}$$

where $zn_u = N(3^3D)$
 $zn_1 = N(2^3P)$

where z = height of the column.

Then, $S = 1.02 \times 10^8 \text{ (erg cm}^{-2} \text{ A}^{-1} \text{ s}^{-1} \text{ ster}^{-1}) \frac{N(3^3D)}{N(2^3P)}$

Replacing S and $N(2^3P)$ from Table I by profiles 1, 2, and 3 we obtain the values of $N(3^3D)$.

The values obtained for $N(2^3P)$ and $N(3^3D)$ are one or two orders of magnitude lower than those obtained by Steshenko and Khokhlova [1960] but our spectrum was taken after the flare maximum so that lower values for the population of these levels can be expected.

Estimation of the Electron Density

The Boltzmann-Saha formulae, taking account of the departures from LTE is

$$n_2/n_3 = (b_2/b_3) (g_2/g_3) \exp (hc/k\lambda T_e)$$

As the relation n_2/n_3 is known for what was stated previously, we can calculate the empirical values for b_2/b_3 with different electron temperatures. The b_2/b_3 results are shown in Table II.

In Table III we show the values calculated by Athay [1963] where his values have been changed by the factor which corresponds to the statistical weight of the D sublevel in the third level. Upon examining Table III it can be seen that the empirical values of profile 2 corresponds to the theoretical with $n_e = 10^{11} - 10^{12} \text{ cm}^{-3}$ and the profile 3 with $n_e = 10^{12} - 10^{13} \text{ cm}^{-3}$. This leads us to think that the most suitable temperature and density for our flare from profiles 2 and 3 would be T_e between 10^4 and 2×10^4 and $n_e \approx 10^{12} \text{ cm}^{-3}$ if we assume that Athay values can be applied, but probably his calculations are not exact for a flare, due to the enhancement of the UV radiation density in the flare region. With respect to profile 1, it has special characteristics and it seems to correspond to a lower electron density. These values of electron density are reasonable for the post-maximum phase of the flare [Svestka, 1972].

TABLE II

Profile	T_e		
	$10^4 \text{ }^\circ\text{K}$	$2 \times 10^4 \text{ }^\circ\text{K}$	$3 \times 10^4 \text{ }^\circ\text{K}$
1	22	67	102
2	15	45	69
3	11	34	53

TABLE III

n_e (cm^{-3})	Te		
	$10^4 \text{ }^\circ\text{K}$	$2 \times 10^4 \text{ }^\circ\text{K}$	$3 \times 10^4 \text{ }^\circ\text{K}$
10^{11}	15	52	78
10^{12}	15	40	55
10^{13}	9	16	19

REFERENCES

- ALLEN, C. W. 1963 Astrophysical Quantities, 170 and 172, Althone Press, London.
- ATHAY, G. 1963 Excitation of Chromospheric He I, Ap. J., 137, 931.
- JEFFERIES, J. T. 1957 Temperatures and Electron Densities in Flares as Derived from Spectroscopic Data, Mont. Not., 117, 493-503.
- 1968 Spectral Line Formation, 42, Blaisdell, Waltham, Massachusetts, U.S.A.
- KUBES, P. 1965 D₃-Line in Solar Flares, in 13th Consultation on Solar Physics and Hydrodynamics, Tatranska, Lomnica, CZECH. Acad. of Sc. Astr. Inst., 51, 89.
- 1973 Solar-Geophysical Data (comprehensive reports), 342, Part II, U.S. Department of Commerce, (Boulder, Colorado U.S.A. 80302).
- MACHADO, M. and J. SEIBOLD 1973 Spectral Analysis of Sunspot Flares, Solar Physics, in press.
- SEVERNY, A. B. 1959 An Investigation of the Spectra of Great Flares. Izv. Krym. Astr. Observ., XXVII, 120.
- SMITH, H. J. and E. V. P. SMITH 1963 Solar Flares, 153, MacMillan Co., New York, U.S.A.
- STESHENKO, N. V. and KHOKHLOVA 1960 Helium Emission of the Chromospheric Flare of September 14, 1958, Izv. Kryms. Astr. Observ., XXIII, 322.
- 1962 He I Excitation in Chromospheric Flares, Izv. Kryms. Astr. Observ., XXVII, 120.
- SVESTKA, Z. 1972 Spectra of Solar Flares, Annual Rev. of Astr. and Astroph., 10, 4.

Changes in the Photosphere around the Locations of the Knots of the August 7, 1972 White-Light Flare

by

V. Bumba and J. Suda
Astronomical Institute of the Czechoslovak Academy of Sciences
Ondrejov, Czechoslovakia

Introduction

The problem of magnetic field variations or structural changes in the photosphere and chromosphere related to the occurrence of flares is still a very actual one. During the existence of the large August 1972 proton-flare region we succeeded in obtaining a relatively good series of photospheric pictures which cover the period preceding and following the large white-light flare of August 7. Having the exact position of the white-light flare knots during the phase of maximum brightness from the photograph taken at the Sacramento Peak Observatory [Rust, 1972], we were able to search for the changes in the organization of photospheric fine structure elements in the neighborhood of these knots.

Observational material

During August 7, 21 series of photospheric photographs (several hundred pictures) were taken concerning the large sunspot group. The instrument used and the method have already been described [Bumba et al., 1973]. The first picture was made at 05h 31m 00s UT and the last one at 15h 48m 10s UT. The intervals between series varied from about 20 to 30 minutes, with two exceptions which were 47 and 48 minutes. The quality of photographs varied during the day too, but in the majority of picture-series good quality photographs with resolution around 1" or better may be found.

The time interval between the last picture from August 7 and the first of August 8 was 13h 29m. On August 8, 1972, the first picture was taken at 05h 17m 33s UT. During August 8, again, many series of photographs were obtained.

Results

For better orientation in the sunspot group on Figure 1 the individual greater spots are indicated by capital letters in the same manner as in another paper in this compilation [Bumba, 1973, Figure 2]. The knots of the white-light flare which are concentrated in the northern part of the group between spots with prevailing northern polarity we shall call region A, and those in the center of the group close to the spots E, E' and D' we shall denote as region B.

Relation to the magnetic field distribution and H α flare

Comparing the position of flare knots with the magnetic situation we may see that they coincide well with the boundary of magnetic field polarities as they are estimated from photographic measurements (Pulkovo, Roma). Even in the region A between the spots A and B there is an inclusion of positive polarity as may be seen from the course of fibrils in the penumbra fine structure [Bumba, 1973, see Figure 2] and as was also recorded on August 6 by photographic field measurements at Pulkovo.

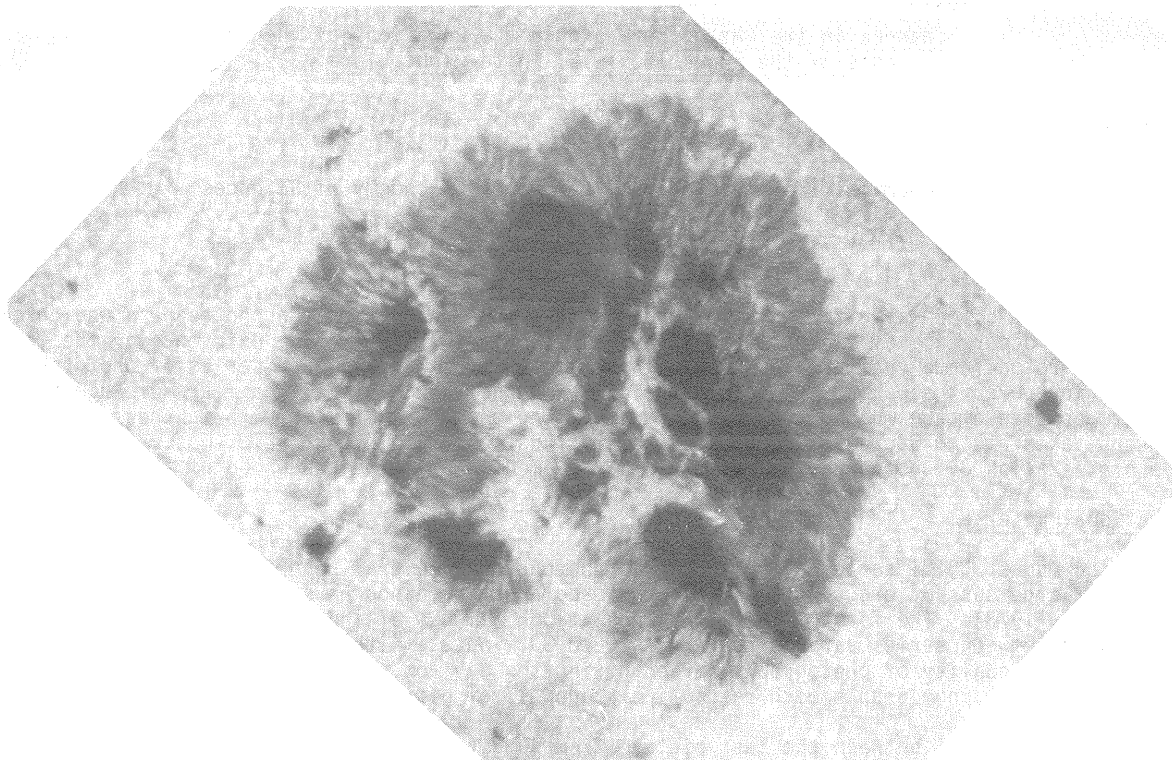
Region B of the flare parallels a light bridge having a specific form, which not only seems to form the boundary between polarities, but there also seem to be great changes concerning the magnetic field distribution especially in the northern part of the bridge itself. More detailed studies on the basis of Ondrejov magnetic field photographic and photoelectric measurements are in preparation.

The knots of the white-light flare also coincide very well with the brightness maxima of the monochromatic picture of the flare in the H α line.

Changes of photospheric structure

If we try to characterize the general trend of the group development comparing the photographs obtained during an interval of several days we have to state that generally there were small changes in the group between the fifth and sixth of August, but there were changes between the sixth and seventh of August such that several spots diminished in area (spots B, D', E, E', D, C) and the influence of a process of spot disintegration may be observed (see Figure 2).

In the northern part of the group (region A of the flare) this process of disintegration, especially of the spot D' which has an opposite polarity to the neighboring spot B (see August 6), may be seen. The inclusion of positive polarity between the spots B and A connected as we assume, with a bright light bridge and several small spot nuclei, may be possibly related to this process. With the disintegration of spot D' the area of penumbra between the spots B, D', and A diminished and another light bridge which was clearly visible during August 5 and 6 between the spots D' and D was transformed



N

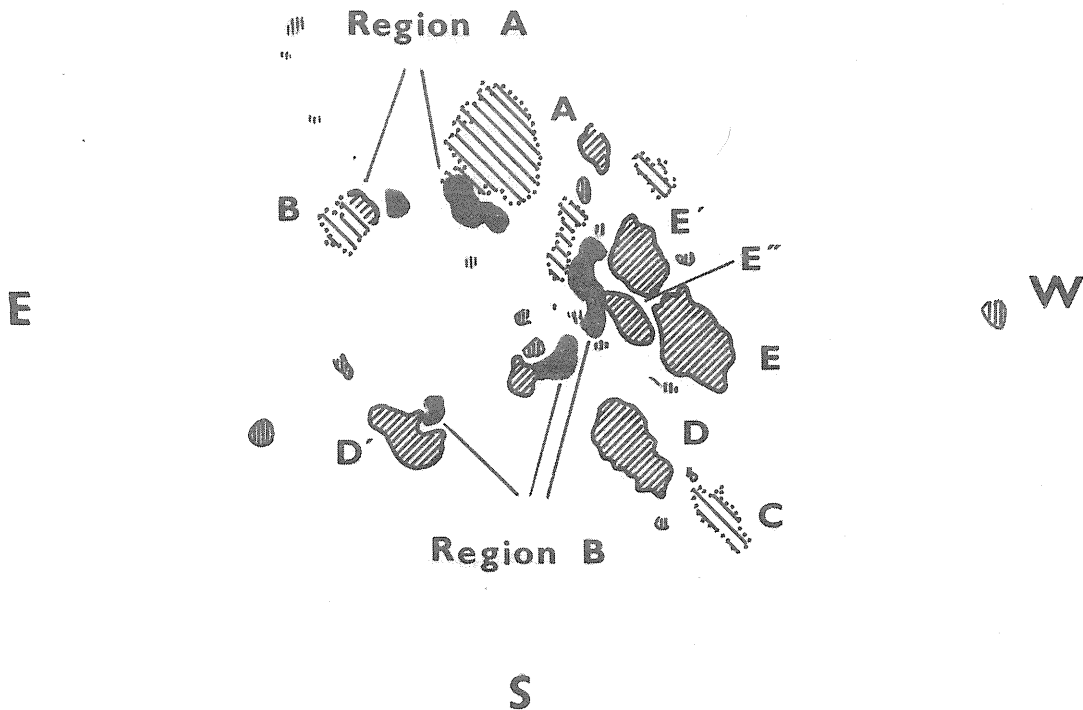


Fig. 1. Photograph of the proton-flare sunspot group from August 7, 1972 (06h 03m 53s UT), with the scheme of spot nuclei distribution. The polarity estimations are taken from Roma and Pulkovo observations. The positive polarity is the darker one. The nuclei with vertical hatching are those without polarity estimations. The positions of white-light flare knots are indicated as completely dark areas. The individual greater spots are specified by capital letters.

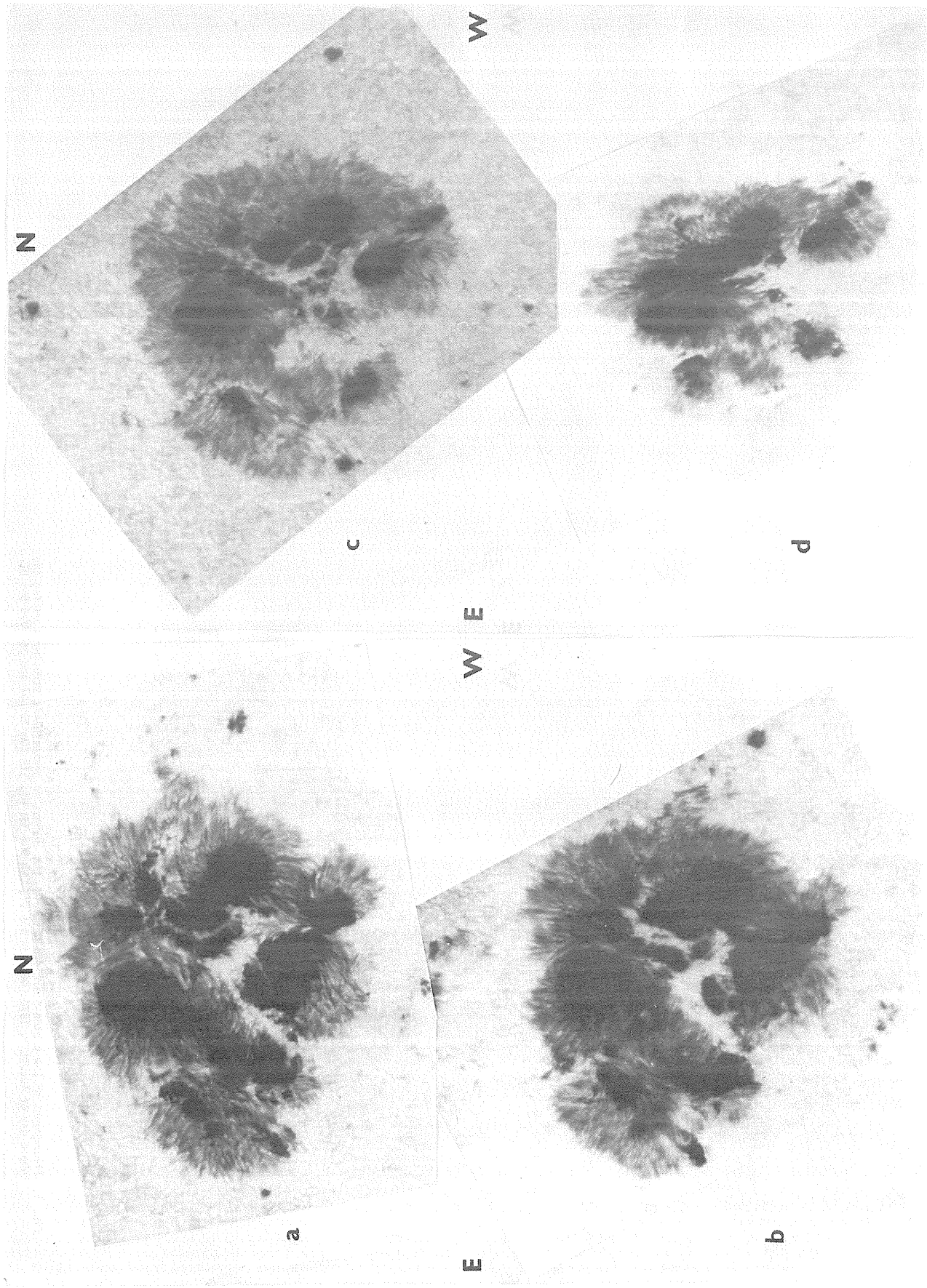


Fig. 2. Photographs demonstrating the development of photospheric structures in the group during the four subsequent days: August 5 (13h 34m 15s UT), August 6 (07h 23m 46s UT), August 7 (06h 03m 53s UT) and August 8, 1972 (06h 16m 21s UT).

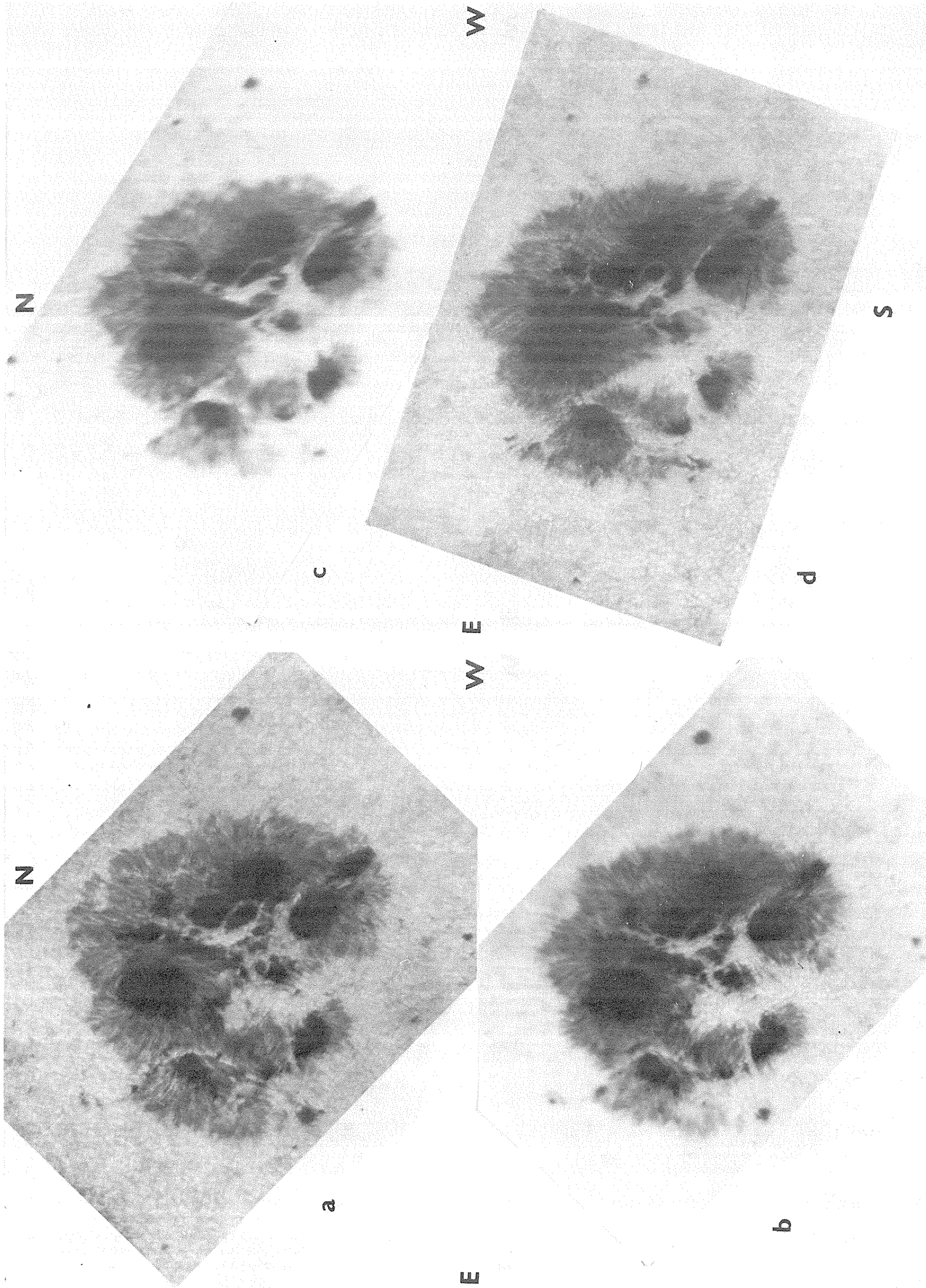


Fig. 3. Photographs of the proton-flare group showing the changes in photospheric structures during the whole day of August 7, 1972: 06h 03m 53s UT, 09h 00m 31s UT, 11h 59m 13s UT and 15h 09m 36s UT.

into a region of normal photosphere. This region of photosphere continuously enlarged in area throughout the whole day of August 7. The fastest changes may be seen in the northern part of the group on the photographs taken at 1159 and 1509 UT (see Figure 3), where instead of the original light bridge around the spot B a strip of rudimentary penumbra with elements similar to photospheric granulation may be seen as a prolongation of a gulf of the photosphere from both northern and southern sides of this strip.

This region also coincided well with the area where the relatively large photospheric radial velocities change their direction from upward to downward [Bumba et al., 1973].

In the center of the group where the brightest knot of the white-light flare (region B) was situated the changes seem to have a different character. In this place during the preceding days a very fast development of a double chain of small nuclei and of a spatial form light bridge took place. It has not yet been possible to estimate in detail the magnetic polarity of the individual nuclei. The whole process of development of this specific situation must be studied separately. The form of this region did not change very much from August 6 to August 7, only the influence of a disintegration process may be seen again. Near this region, in the southern part of the group a strong magnetic field gradient was observed between the spots C and E, visualized by the distribution of penumbra fibrils between these two spots (see Figure 2). The gradient seems to be largest on August 5 and afterwards it seems to decrease. On August 7 it seems that there is only the remnant of this gradient, visible now mostly between the spots C and D, but there is still a singularity in the magnetic field observed spectrographically as disturbances in a normal magnetic line splitting [Bumba et al., 1974].

Small nuclei surrounding the brightest knot of the flare demonstrated small changes in form, position and area (see Figure 3). Those which are located just westwards from the main flare-knot especially diminished in area. There were changes in the form of the light bridge separating the spot E'' from the main body of double spot E, E'. This bridge which was already in the form of an arc on August 5 and 6 changed so that it split the spot E'' into two smaller nuclei. The indication of this splitting may be seen during the morning hours as a brighter region in the umbra. On the pictures taken around 1509 UT the spot E'' is divided into two parts, although on the photograph obtained around 1159 UT the separation seems to be indicated only.

Again, close by, a small region with radial motions in both directions was detected. A large region with downward radial velocities was found in the north-west part of the group, northward and westward from the spots E' and E [Bumba et al., 1974]. In this region, small configuration and position changes in the nuclei and light bridges may be observed during August 7.

The most evident changes occurred in the group during the night of 7-8 August. The most interesting fact is that the changes in the region A led practically to the restoration of the situation to the stage which was observed during the morning hours on August 7 (see Figure 2). In region B the very complicated figure of the light bridge and small nuclei simplified so much that the mutual merging of spots A, E', and E with the new formations which developed mostly during August 4 in the northern part of the group between the spots A and E may be seen. Again, only very small changes concerning the situation in the southern part of the group, between the spots D, C, and E which means outside the main white-light flare regions are detectable.

Conclusions

To summarize the results again as in so many cases we can only say that there were changes in the position, form, direction and area of photospheric structures, but these changes were observed before as well as after the flare occurrence. They are located very close to the position of the main flare knots, and they have to be connected with magnetic field configuration and strength variations, but we still do not know the physics of these relations.

REFERENCES

- | | | |
|---|------|---|
| BUMBA, V. | 1973 | Elsewhere in this compilation |
| BUMBA, V.,
P. RANCINGER, and
J. SUDA | 1973 | <u>Bull. Astron. Inst. Czech.</u> , <u>24</u> , 22. |
| BUMBA, V., L. HEJNA,
M. KLVANA, L. KRIVSKY,
P. MACAK, J. SUDA,
A. TLAMICHA, and
B. VALNICEK | 1974 | <u>Bull. Astron. Inst. Czech.</u> , <u>25</u> , in print. |
| RUST, D. M. | 1972 | <u>Sky and Telescope</u> , <u>44</u> , 2. |

The Limb Flare of August 11, 1972

by

M. Waldmeier
Swiss Federal Observatory, Zurich

The large sunspot group that crossed the sun's disk from July 29 to August 11 was the site of major flares on August 2, 4, 7 and 11. Characteristically, the interval between consecutive flares increased during the development of the spot group. The last of this series of flares occurred when the group was almost exactly on the western limb. This situation allowed optical observation of the coronal disturbances connected with the flare.

H α Records

In the time history of the August 11 flare five phases can be distinguished:

1. The pre-flare phase: A spicule-like prominence which existed for more than two hours in an unchanged state, began to brighten at 1210 UT.
2. The flash phase: At 1216 UT the prominence had reached flare-brightness. It expanded in height and width. Between 1216 and 1228 UT the top of the flare was rising at a speed of 32 km/s.
3. The spray phase: At 1228 UT several blobs were ejected with high speed. One of them could be followed on ten consecutive pictures. In eight minutes its vertical speed increased from 165 km/s to 745 km/s with a nearly constant acceleration of 1.32 km/s².
4. The surge phase: At 1235 UT a surge ejected out of the flare. It reached its full development at 1250 UT with the uppermost knot 400,000 km above the solar limb. Afterwards, its matter fell back and faded. The surge came to an end at about 1310 UT.
5. Post flare loops: At 1300 UT before the surge had disappeared completely a bright filament was seen rising, forming a loop. Initially the velocity of ascent was 4.2 km/s and decreased to 1.8 km/s after 1600 UT. At the end of the observation (1630 UT) the loop had reached a height of 46,400 km.

Coronal Observations

Coronal observations were begun at 1325 UT at which time the flare and the surge were already over. Thus, the observations concern only the last stage, the loop phase. Surprisingly, the intensity of the line 5303 Å decreased from 140 (unit = 10⁻⁶ of 1 Å of the solar continuum) before the flare to 38 at 1325 UT. At 1332 UT when the loop was already in full development, the line was still remarkably weak (I=39). But then the intensity in the loop increased strongly. At 1345 UT it amounted to 118, at 1347 UT to 174 and at 1350 UT to 220, decreasing gradually to 200 at 1400 UT and to 180 at 1430 UT.

At 0640 UT the line 5694 Å was visible with low intensity (I=39) above the spot group. This emission came from the permanent condensation that covered the whole center of activity. After the flare, the intensity increased very strongly. It amounted to 200 at 1332 UT, 240 at 1345 UT, 220 at 1347 and 1350 UT, 150 at 1400 UT and still to 110 at 1430 UT. We have the unusual case that the line 5694 Å reached a higher intensity than the line 5303 Å. Furthermore, the yellow line reached its brightness maximum earlier than the green line. The intensity ratio I₅₆₉₄ / I₅₃₀₃ amounted to 0.3 at 0640 UT, 4.7 at 1325 UT, 5.1 at 1332 UT, 2.0 at 1345 UT, 1.3 at 1347 UT, 1.0 at 1350 UT, 0.7 at 1400 UT, and 0.6 at 1430 UT. This variation demonstrates that the temperature of the loop was very high at the beginning, decreasing gradually in the course of development.

X-ray Emission

The flare began at 1216 UT, reached its maximum brightness at 1230 UT and came to an end around 1300 UT. The X-ray burst started simultaneously with the flare. Maximum intensity occurred at 1219 UT in the spectral region 0.5 to 8 Å, but not before 1307 UT in the region 8 to 20 Å. The burst lasted until 1539 UT, thus being of unusually long duration. It not only persisted during the flare phase, but also during the much longer loop phase. The ionospheric disturbances produced by the X-ray emission started at 1217 UT, reached their highest intensity between 1225 and 1245 UT and lasted until 1400 UT, thus one hour longer than the flare. This post flare disturbance coincides with the loop phase. Both the post flare X-rays and the post flare ionospheric disturbances indicate that the loop is also a source of intensive X-ray emission.

Radio Bursts

In radio spectra the sun was completely quiet during the hours preceding the flare. The first strong bursts occurred at 1210 UT at the time when the micro-prominence began to brighten. Further bursts occurred at 1216 UT, thus at the beginning of the flare, and at 1222 UT. All those bursts were restricted to frequencies >1000 MHz. A series of bursts of type II and III appeared in the spray phase between 1230 and 1240 UT. More bursts were recorded at 1313 UT at the beginning of the loop phase. Weaker bursts appeared around 1345 and 1418 UT when the loop was still in progress.

A more extended report on this flare will appear in "Solar Physics".

The Great Limb Phenomenon of August 11, 1972

by

Claes Bernes and Ulf Kusoffsky
Swedish Astrophysical Station
Anacapri, Italy

Introduction

At 1216 UT on August 11, immediately before passing the west limb, McMath region 11976 produced the last visible great flare in the series starting on August 2. At the Swedish Astrophysical Station in Anacapri we observed the flare and the related surge and loop system with our patrol instrument, fitted with a 0.7 \AA $H\alpha$ filter. An $f/100$ 20-cm horizontal telescope with a Babcock grating was used to obtain spectra at $H\alpha$ in the fourth order, giving a linear dispersion on the film of 1.4 \AA/mm .

50 filtergrams at the $H\alpha$ center as well as in the wings were taken of the surge between 1227 and 1259 UT. During the same time interval, 26 spectra with simultaneous slit-jaw pictures were secured. The subsequent loop system was covered with 9 filtergrams and 4 spectra.

Morphological Description

Small scale prominence activity at N10 W90 started at 0704 UT (flare patrol began at 0555 UT). Enhanced activity was noted at 1205 UT and was followed by a brilliant limb flare, temporally coincident with radio bursts and X-ray peaks, and starting at 1216 UT. By 1222 UT the intensity had decreased, and the initial phase of the surge began.

In Figures 1a-d, the outlines of the surge have been sketched at 1232:35, 1239:10, 1244:15 and 1252:15 UT, respectively. The positions of 28 selected condensations are plotted at half-minute intervals (note that condensation No. 1 can be seen both in Figure 1a and 1b, and No. 6 both in Figure 1b and 1c).

Figure 1a shows the initial phase when the ejection was confined within a tube inclined $40\text{--}45^\circ$ to the radial direction, measured in the tangential plane. Spectra taken at that time (Figure 3a; slit position indicated in Figure 1a) show velocities in the line-of-sight direction that are small at the base of the surge but increase with height. Condensations 2-5 which were then ejected could thus only be followed to a height of 120,000 km, where line-of-sight velocities away from us of about 150 km/s placed them outside the passband of the filter.

The inclination of the main stem of the surge changed very rapidly towards the radial direction, as can be seen from the Figures. Condensation No. 1, which appeared at the very beginning of the surge, could be followed for 22 minutes out to a distance of about 400,000 km or $0.58 R_\odot$ from the limb (1244 UT). Six minutes later, a small knot above condensation No. 15 reached about the same height.

Condensation No. 1 was large and brilliant compared with the other ones. As judged from spectra, this plasma cloud showed clumpiness and internal motions. It also had the highest acceleration and reached a maximum tangential velocity of 750 km/s. The velocity curve is drawn in Figure 2.

Between 1239 and 1247 UT the general appearance of the surge remained fairly unchanged. The main stem reached 150,000 - 200,000 km above the surface. The knots in this part of the surge could only be traced over relatively short distances, so the velocity estimates are uncertain, but the measurements seem to indicate that the visible condensations in the stem moved with nearly constant or slightly increasing velocities, as can be seen from Figure 2. The higher condensations in the stem generally moved faster than the lower ones. This velocity pattern can also be derived from the spectra c and d in Figure 3, which were obtained at 1247 UT simultaneously with Figure 4. The slit was orientated parallel to the surge. Spectrum c shows the base and spectrum d shows the medium part of the surge. As can be seen, the average velocity increases with height, mainly in the direction towards us. The complicated plasma structure is also clearly demonstrated. The existence of broad emission features, some of them tilted, with differential velocities implies a hot, dense and turbulent plasma. The complicated nature of the phenomenon is again shown in Figure 3b, taken at 1240 UT at a height of 80,000 km with the slit oriented perpendicular to the surge. The position of the slit is indicated in Figure 1b. The condensations above the main stem show a deceleration more or less of the order one can expect in a purely gravitational field.

At 1247 UT a splitting of the surge could be discerned (knots 10 and 12 in Figure 1c). Most of the surge above 100,000 km was broken up at 1252 UT. This breaking-up process continued during the rest of the lifetime of the surge (Figure 1d). The last remnants disappeared at 1320 UT.

33 minutes after the beginning of the flare, a loop system started to develop at the base of the surge. The tops as well as the legs of the loops were extremely brilliant. Spectrum 3e, taken at 1249 UT at the top of the loop, shows very bright emission, and a weak continuous emission is clearly visible on the negative. This type of post-flare loop appeared also in connection with the flares of August 4 and 7 in the same region.

× UT 12 32:30
▲ 12 38:30

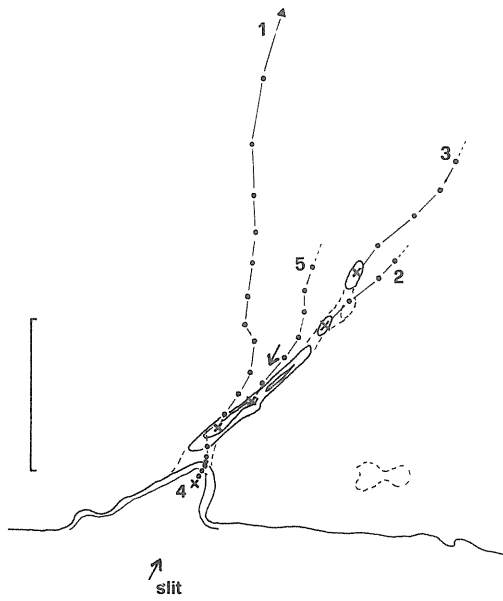


Fig. 1a.

× UT 12 39:00
▲ 12 44:00

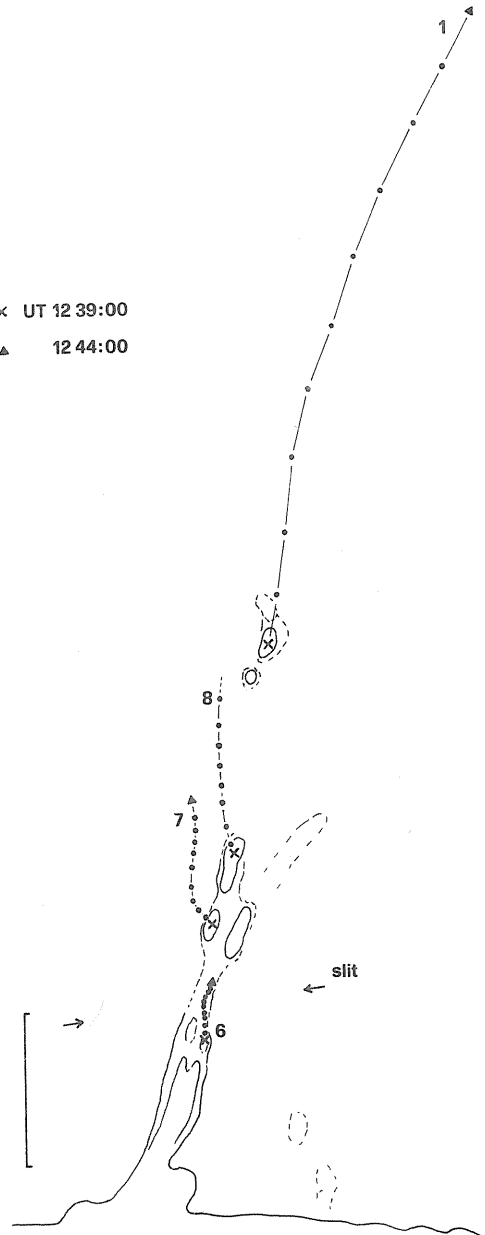


Fig. 1b.

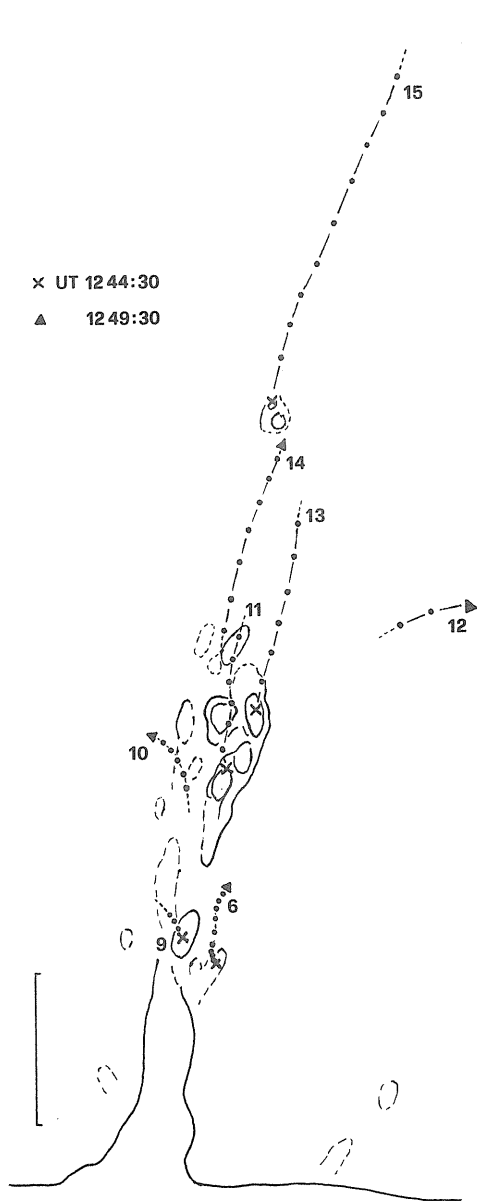


Fig. 1c.

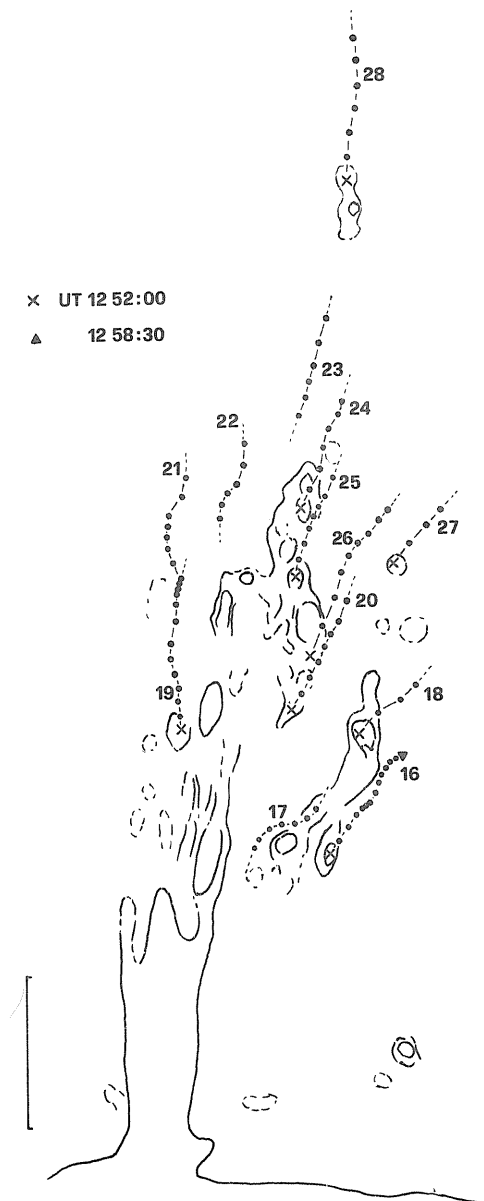


Fig. 1d.

Fig. 1. Figures 1a-d show the outlines of the surge at 1232:35, 1239:10, 1244:15 and 1252:15 UT, respectively. The trajectories of 28 knots are plotted. The dots in the diagrams are separated by half-minute intervals. The vertical lines represent 50,000 km. Slit positions for the spectra shown in Figures 3a-b are indicated.

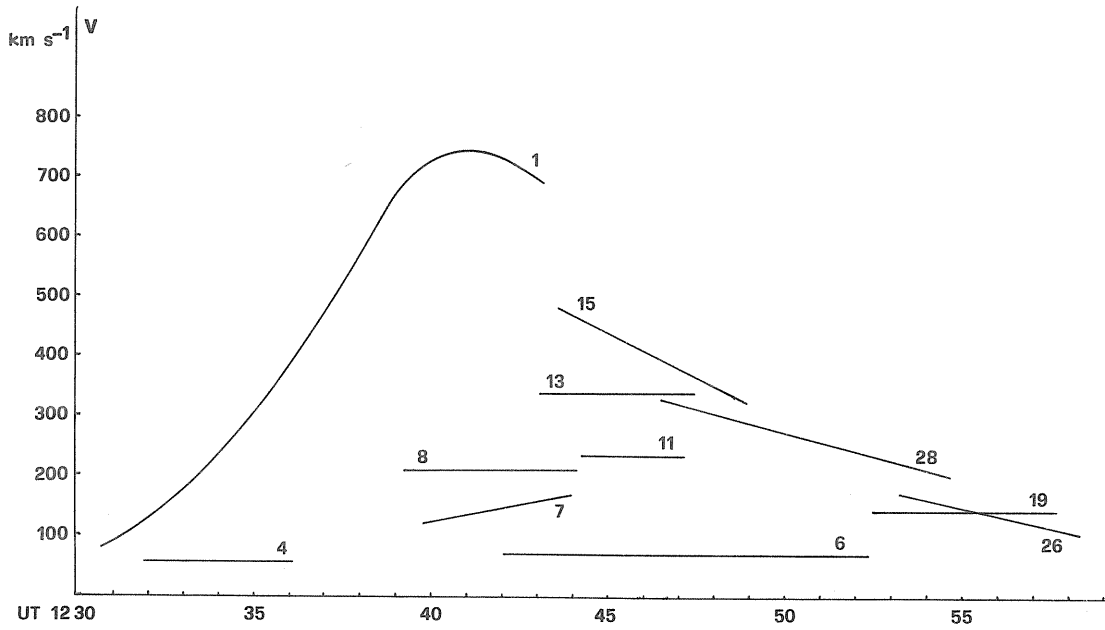


Fig. 2. Velocity vs. time diagram for some surge fragments.

Discussion

The loop system consisted of downfallen material from the surge. Assuming that matter, after having faded from view, was affected by gravitational forces only, but returned along the same path, and calculating the time between last sighting and fall-back, we found that the time of the first arrivals of downfalling matter at the upper chromosphere should be approximately 1250 UT. Many condensations could be expected to fall back around 1320 UT, and the downfalling would go on for hours. Only one condensation (No. 1) was observed to reach the escape velocity.

The result of the calculations mentioned above is well in accordance with the behavior of the loop system.

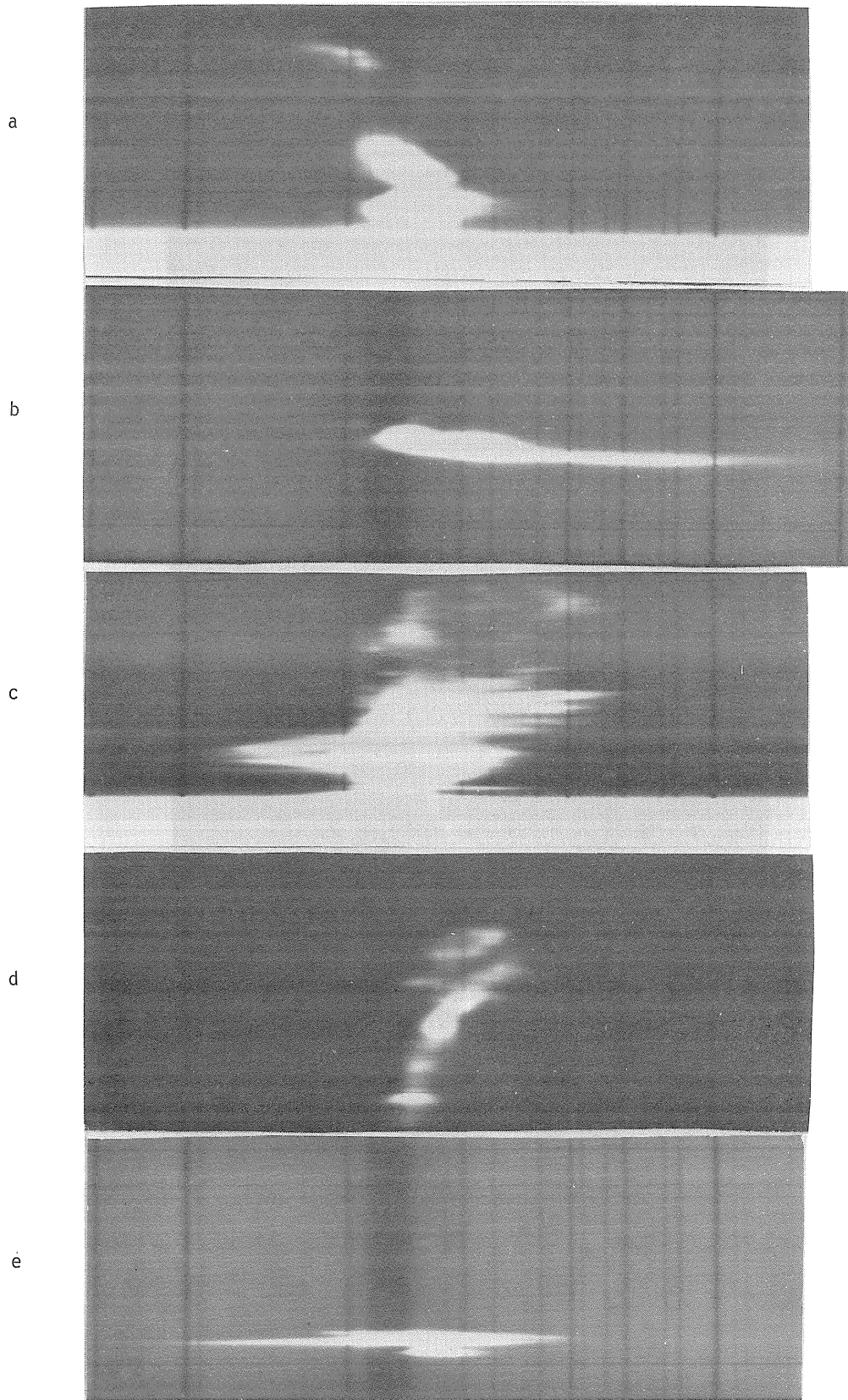


Fig. 3. $H\alpha$ spectra taken at 1232:35, 1240, 1247, 1247 and 1249 UT, respectively. See text for explanations.

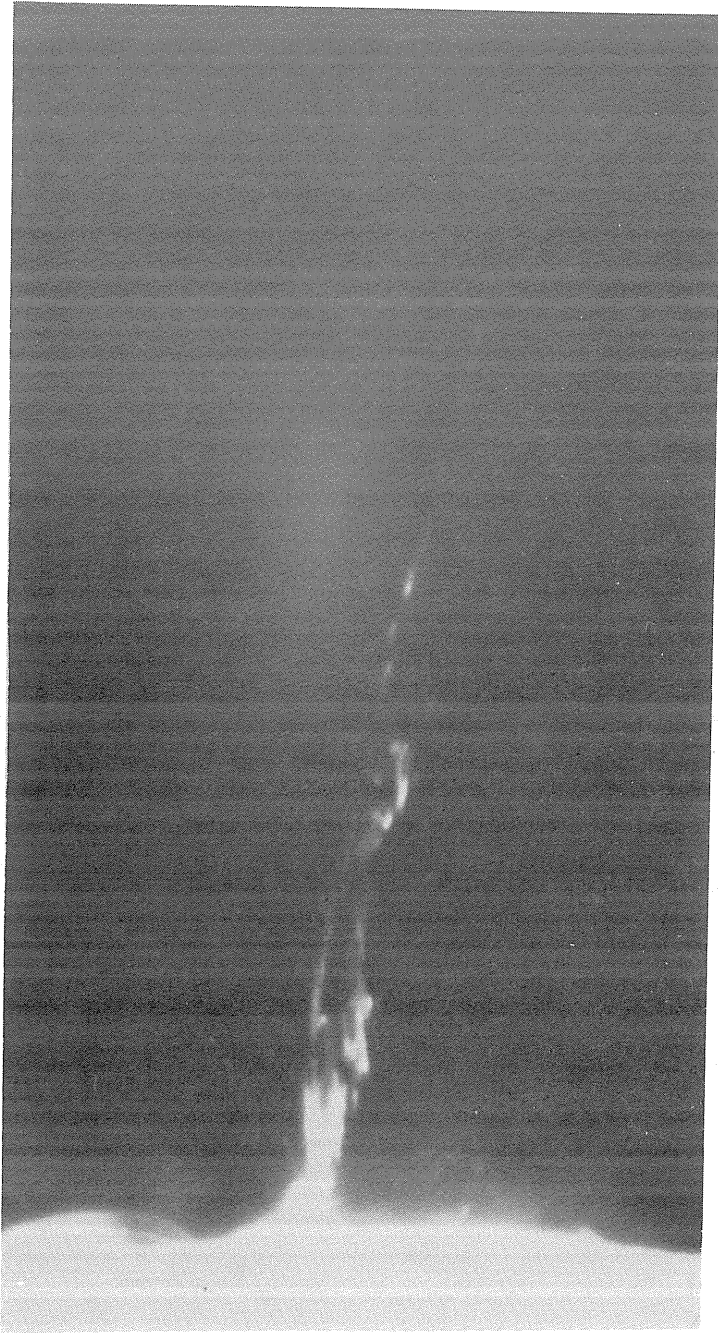


Fig. 4. Filtergram obtained at 1247 UT, simultaneously with Figure 3c and d. At this time the surge shows the first tendencies of splitting and also a twisted shape.

3. SOLAR RADIO DATA

Summary on page 4

Total Flux and High Resolution Fan Beam Observations
of the 2800 MHz Solar Activity in August 1972

by

A.E. Covington and M.B. Bell
Astrophysics Branch
National Research Council of Canada
Ottawa

Detailed records of the total solar flux at 2800 MHz from August 1 to August 16, 1972 show various kinds of bursts with intensity ranging from a few flux units (10^{-22} watts/M²/hz) to values of 4500 and 9700 for the Great events of August 2 and August 7. The usual value for the quiet daily flux level for August 7 is not obtainable. The slowly varying component has a period of 28 days with a sudden and permanent advance in phase of 4 days after the activity of August 7. High resolution drift curves were obtained with fan beams of 1.5 min and 0.5 min arc during the post-burst enhancement of August 7 and located the radio emission within McMath-Hulbert region no. 11976. The radio visibility of this region across the disc is compared with the cosine curve. Central meridian passage occurs on August 4 when a flux of 34 units was reached, and the E.-W. half power extent of the region is 1.9 min arc. On the assumption of similar N.-S. extent the equivalent temperature is 4.8×10^6 °K. A "cool region" appeared in the quiet solar disc background on the 7th and 8th.

Introduction

The total solar radio flux at 2800 MHz is measured regularly with a 1.8 meter reflector at Algonquin Radio Observatory (ARO), Lake Traverse, Ontario and the results published monthly in two parts: one part gives values of the flux representing the combined emissions from centers of activity and from the undisturbed solar background while the second part gives numerical values to describe the characteristics of the enhanced flux associated with flares. Records are also taken on a frequency of 2700 MHz with similar equipment at the Dominion Radio Astrophysical Observatory (DRAO), Penticton, British Columbia and intercompared with those taken at ARO. The records are visually examined to eliminate various spurious signals such as those from atmospheric scintillations, multipath interference between the direct and indirect rays, radar and other kinds of interference and confirm many burst features which would otherwise be ignored. In addition to the total flux measurements, single strip scans of the sun are regularly made at local noon at ARO with fan beams 1.5 min arc and 0.5 min arc E.-W. Only the broad beam scans are regularly reported with reduced scales in Solar-Geophysical Data, N.O.A.A., Boulder, Colorado. These records will be studied for a period of the declining sunspot cycle which includes two remarkable flares and is not intended to be complete in all details. Only those associations with the regularly published optical features will be made to draw attention to the unique characteristics derivable from the radio sources in the hope that these will contribute significantly to the understanding of the release of solar energy.

Description of the Records of Total Flux

The total flux records from ARO and DRAO for the period August 1-16 are presented in detailed graphical forms in Fig. 1a and Fig. 1b. The traces have been copied from the slow speed records taken at a speed of 1 1/2 in. per hour without regard to the intrinsic quiet sun level and edited to remove any operational shifts in levels or other unwanted operational marks. Such continuous records provide easy intercomparison and are of approximately equal sensitivity as indicated by the calibrations in flux units per small division entered on the left hand side of the figures. Other high speed records are available but are not given as illustrations. No correction has been made for the varying atmospheric attenuation which becomes dominant at sunrise and sunset and in the absence of solar activity accounts for the droop usually present at these times. This is particularly evident in the ARO records but is less pronounced in the DRAO records because the effect is masked by nearby mountains. Two styles of tracing have been employed; those for August 1 and 4 have been made with a smoothly changing line drawn to remove unwanted variations and thereby leaving what can be considered as a true solar variation, while the remaining records have been drawn to show all small variations and thereby duplicating as closely as possible the actual record. On August 8, the two copies of the DRAO records have been made on either side of the ARO trace and indicate how effective this method of reproduction has been. Only the common variations in the two curves are regarded as real and indicates that other variations are likely to be spurious. In the absence of bursts, the daily flux is steady or slowly varying (S.V.) and its magnitude is measured regularly with standard procedures at 14, 17, and 20 hours U.T. Such times as these away from

Solar Noise Variations at 2800 MHz and 2700 MHz copied from records made at Algonquin Radio Observatory - ARO - and from Dominion Radio Astrophysical Observatory - DRAO.
(Records 1½ inch per hour)

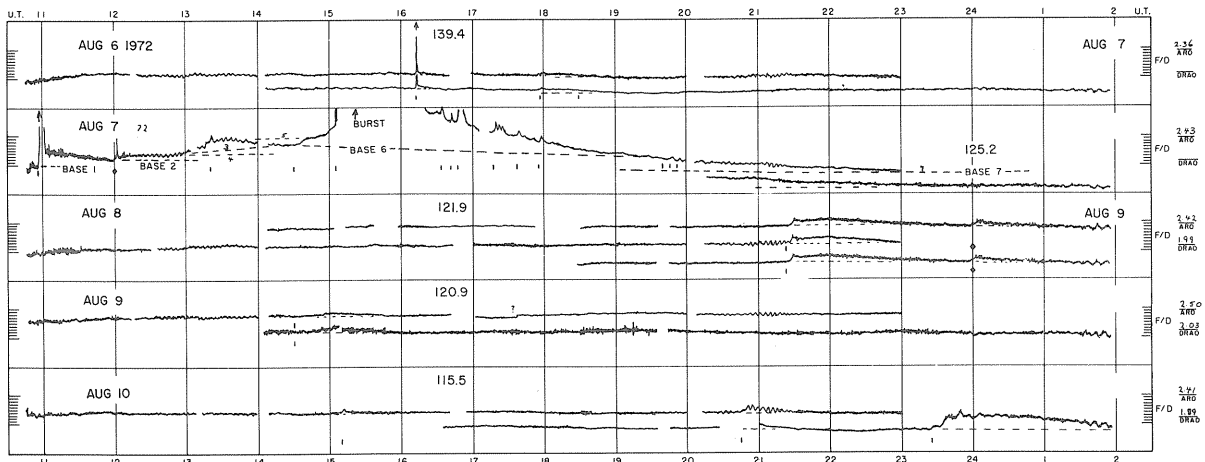
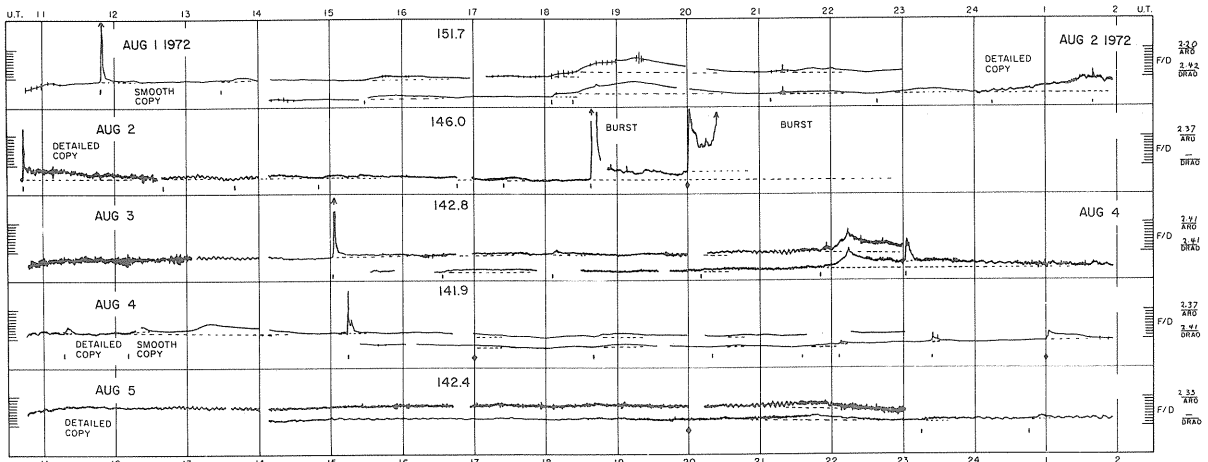


Fig. 1a. 2800 MHz and 2700 MHz total flux records from ARO and DRAO for Aug. 1-10, 1972. Legend given in fig. 1b.

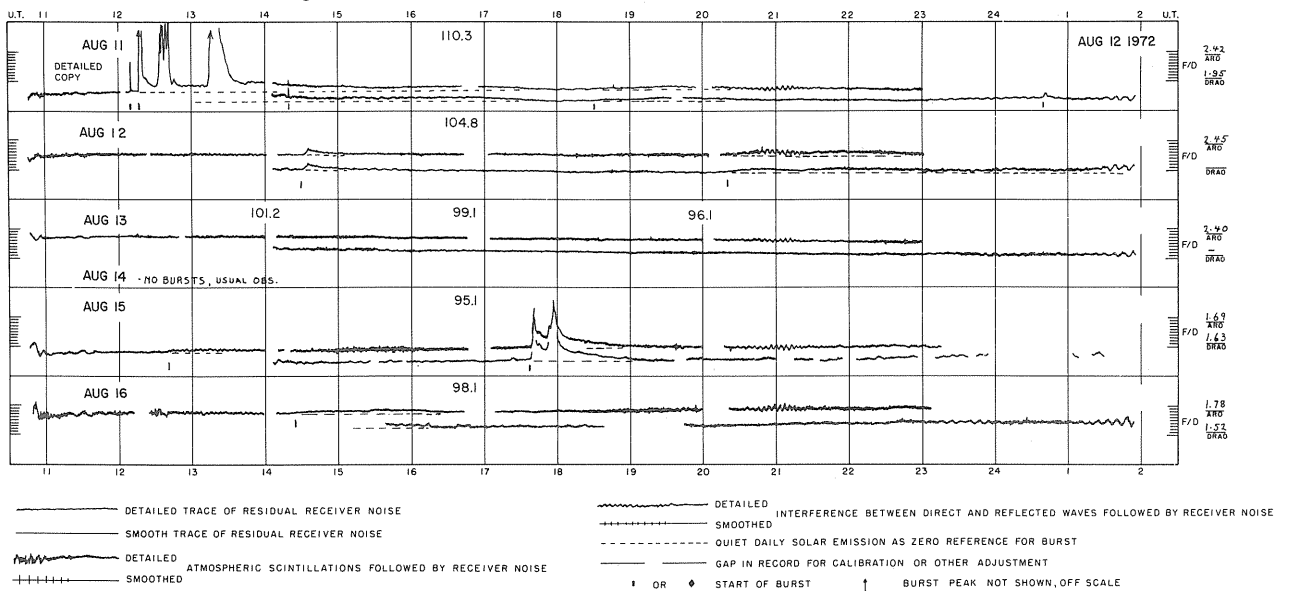


Fig. 1b. 2800 MHz and 2700 MHz total flux records from ARO and DRAO for Aug. 11-16, 1972, with legend for symbols.

solar patrol appear as gaps in the records. Since one reading is usually adequate to describe the solar flux level for the day, only values observable at 17 U.T. or local noon at the observatory have been entered as a number in each panel in Fig. 1. If a burst occurs during calibration, the quiet sun level before and after the burst is interpolated and may be indicated by a dashed line. The dashed line is also used to separate the burst from the daily level and is the zero for the burst intensity scale. The burst profiles recorded on the slow speed records as well as on the higher speed records have been examined and classified according to the prototypes presented in the Descriptive Text for Solar-Geophysical Data. A tabulation of events is given in Publications of the Astrophysics Branch #3 [1973]. The profiles for the indicated major off-scale burst events of August 2 and 7 have been reconstructed from other channels and shown in Fig. 2a, 2b, and 2c.

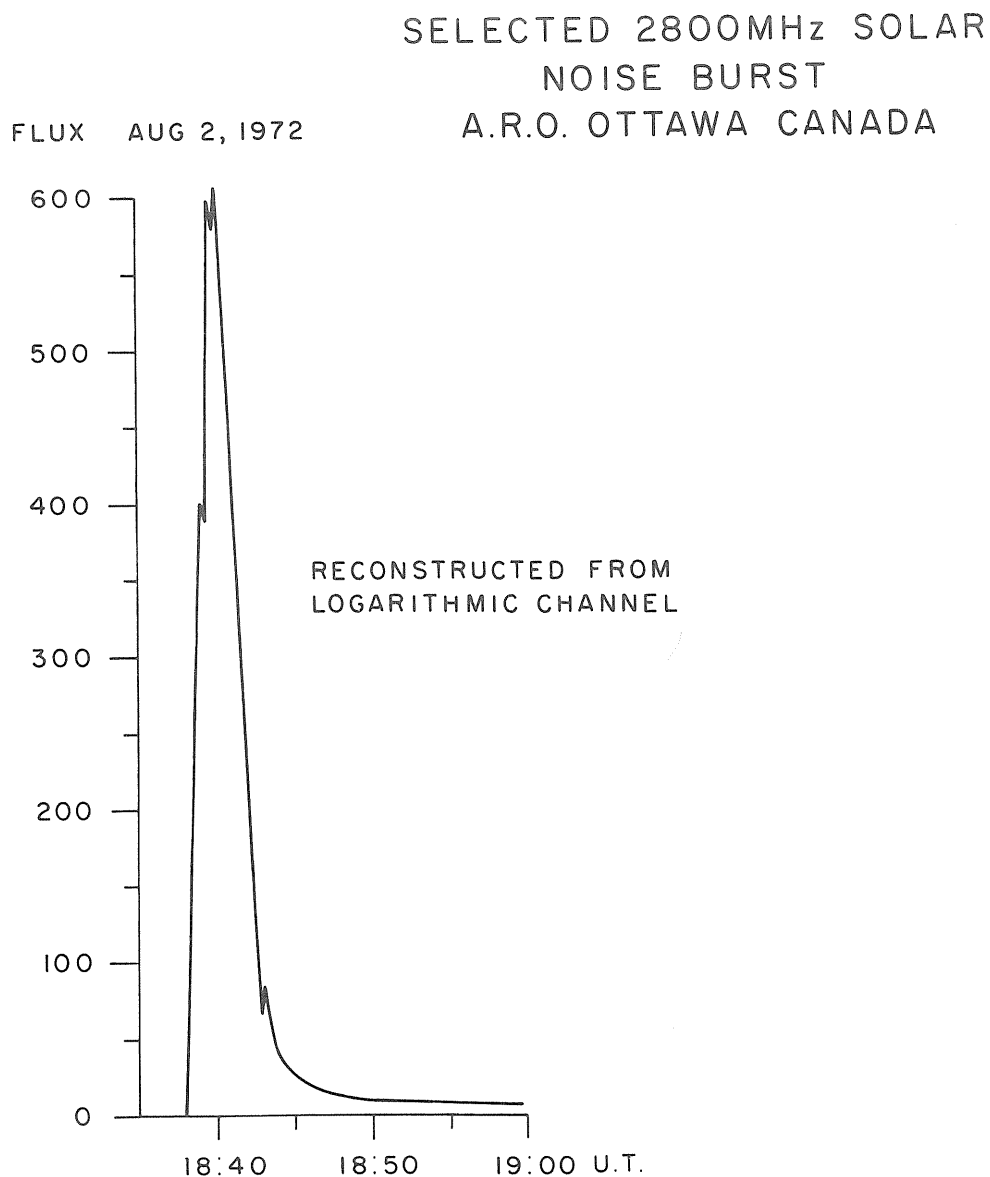


Fig. 2a. Impulsive, narrow profile component of Great Radio Burst of Aug. 2, 1972 commencing at 18:38 U.T.

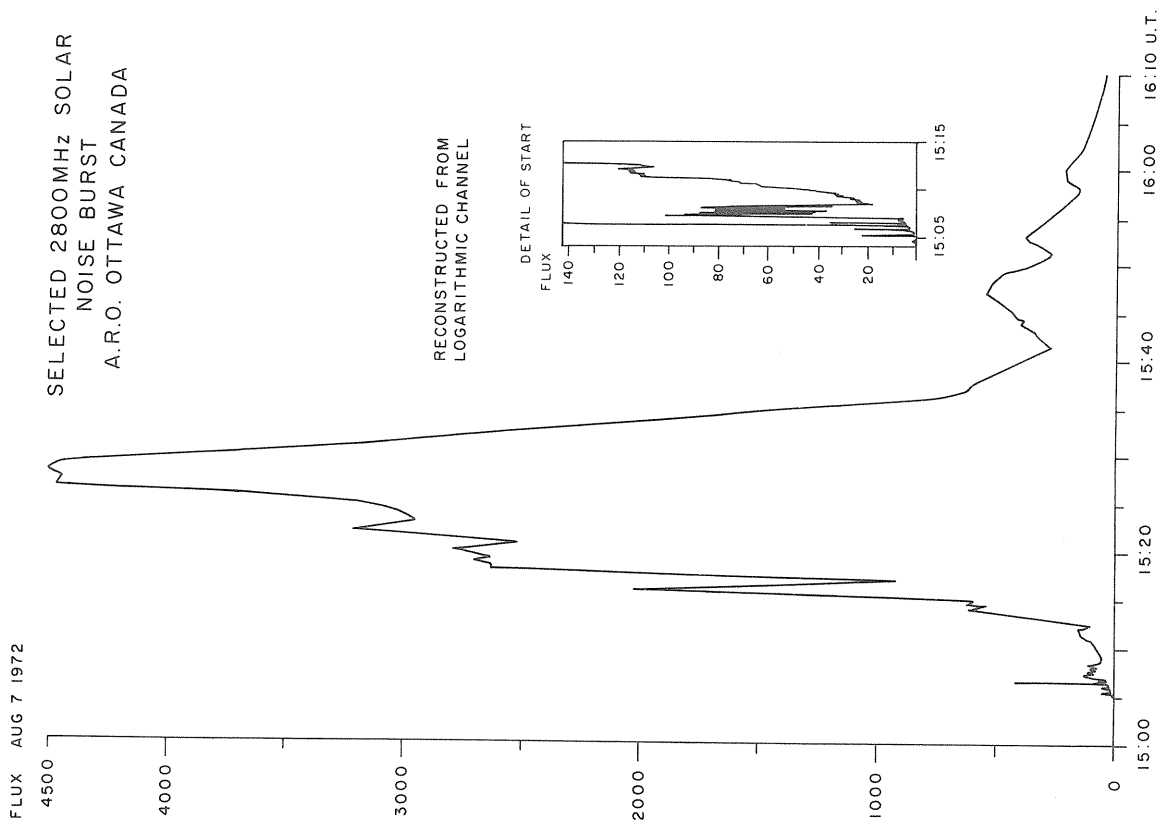


Fig. 2c. Profile of Great Burst of Aug. 7 commencing at 15:05 U.T. which has been separated from a simultaneously occurring Gradual Rise and Fall event which started at 12 U.T. and ended at 23 U.T.

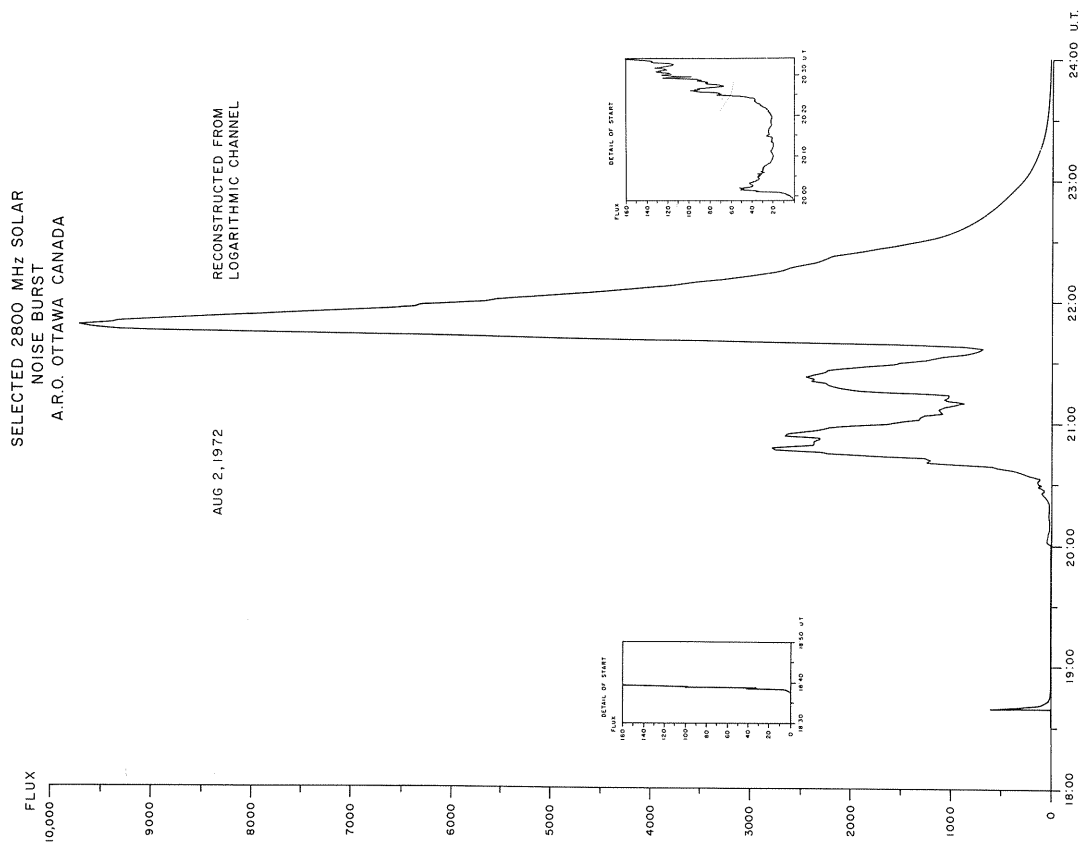


Fig. 2b. Profile of Great Burst of Aug. 2 showing initial narrow profile burst followed by three broad profile impulsive bursts.

Description of the Bursts for August 2 and August 7, 1972

The separation of the burst from the daily level as observed in a record of total flux is unambiguous when the pre- and post-burst levels can be established and have the same intensity. This indicates that within the errors of measurement the mechanism responsible for the burst has little effect on the steady emission from the steady state of the center. An exception is the post-burst enhancement which decays slowly over several hours and its termination may be difficult to determine because of other variations arising from solar rotation or the natural evolution of regions. Studies of bursts in relationship to flare brightenings also draw attention to the corresponding situation which exists for the separation of a flare brightening from a plage brightening. The factors involved in the separation relate to the determination of the brightening of some pre-existing feature, the emergence of completely new features, dynamic aspects and sympathetic brightenings in remote places. Some of these factors have been investigated by Covington and Harvey [1961] and by Saito and Covington [1963]. As a result of these and other studies, it is the practice to commence the burst as soon as the flux departs from the pre-burst level by an amount equal to the residual receiver noise. This is of the order of 1 flux unit.

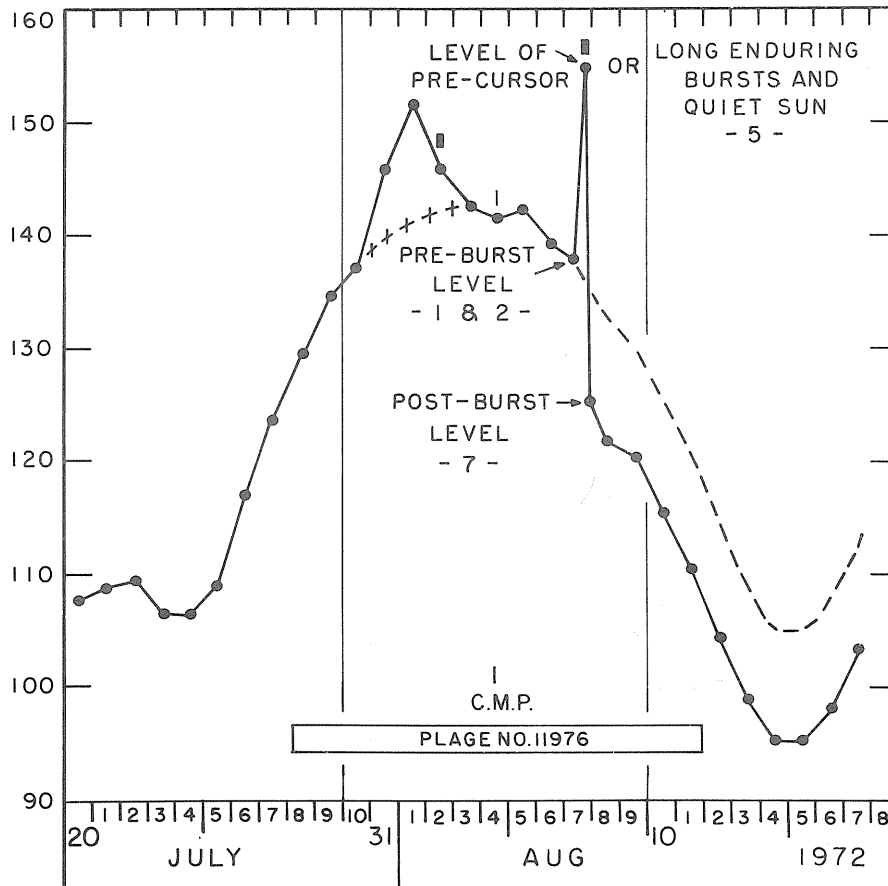
For the intense bursts associated with solar protons detected in the vicinity of earth during the years 1956-1961, Fletcher [1964] was able to derive a model profile using slightly different terms for the components such as pre-burst and major burst. These two characteristic variations are important in Great radio centimeter bursts and were recognized by Harvey [1965] in a later study as impulsive bursts in which differences in duration were found and described as narrow and broad profile impulsive bursts. The post burst increase seen after many bursts is nearly always present with Great bursts and appears to be associated with post-flare loop prominences. These characteristics are recognized in the Great event of August 2 with the first narrow impulsive burst occurring at 18:38 U.T. and with the second part consisting of three broad impulsive bursts occurring at 20:30, 21:10 and 21:40 U.T. with different peak intensities. The repetition of the three similar radio profiles suggest a repetition of the same phenomenon. The profile of August 7 differs from that of the 2nd in two aspects, firstly there is difficulty in establishing a daily quiet sun reference level, and secondly the narrow impulsive burst profile appears to be missing. On this day, the records of the total flux show that burst activity started a few minutes after sunrise with a normal impulsive burst occurring at 10:50 U.T. This was followed by a post-burst enhancement and other activity as seen in Fig. 1. The irregular activity terminated at 18 U.T. and a steady decrease set in until it too, terminated at 23 U.T. when a steady level of 125 flux units was reached. The extension of pre-burst level 1 into the period of burst activity is guided by reference to the normal quiet sun variations seen at sunrise on August 6 and 8. The transfer of these variations shows that level 1 continues into and appears as level 2 near 12 U.T. Since the preceding burst and its post burst increase is normal, the commencement of the enhanced activity which preceded the Great burst will be taken as the small increase seen at 12 U.T. with reference to base 2. These bases, 1-2 have been found to have a level of 136 flux units. The linear continuation of base 2 into level 7 provides the usual quiet sun level for burst analysis and is only partially represented by a dashed line. This emphasises the fictitious nature of the usual burst reference zero since it does not take into account the radio emission from the active center.

The rise at 12:00 U.T. base 2, was originally listed as the beginning of a Simple 3A burst of duration greater than 2 1/2 hours. It has been reconsidered as extending to provide a smooth, slowly changing enhancement which includes base lines 3 and 6 and lasts until 23 U.T., thereby having a duration of 11 hours. Base line 3 was introduced during the rise so that a shorter duration, long enduring burst or other non linear variation could be recognized as starting at 13 U.T. and ending at 14 U.T. The peak intensity of the major long enduring burst was reached at 14:30 and is 16 flux units above base line 2-7. At this time, another secondary base line 6 was introduced to serve as the reference for any subsequent short duration burst. In this case, the events are a precursor which occurred at 14:30 and the great event at 15:05. Base line 6 also provides the reference for the post-burst decay of the great burst before the decline of the long enduring burst becomes evident at 20 U.T. The termination of this decline can only be judged from the extra observing time of 3 hours obtainable from the DRAO records and has been taken as 23 U.T. when a flux level of 125 units was reached. Other base lines, 4 and 5, are introduced to draw attention to a possible absorption feature or to the precursor for the off-scale burst. The large number and complexity of the small events should not detract from two important aspects, namely the long enduring burst of modest intensity which makes it impossible to define the daily quiet sun and the superimposed great impulsive burst with a broad profile. The first part or narrow profile is missing but could be supplied by regarding the unusually short duration spike or burst of great intensity as that component. For the long enduring event, solar rotation introduces other modifications.

The Slowly Varying Component Associated with McMath-Hulbert Region No. 11976

The daily values of the observed solar radio flux taken at 17 U.T. have been plotted for the period July 20 to August 17 in Fig. 3 and show the variation of the S.V. component from one minimum to another. The days on which region 11976 are visible are also indicated and are symmetrically placed with respect to the radio minimum. From this it is concluded that most of the radio emission from the single pulse originates from, or is associated with this region. Central meridian passage occurred on the 4th. On the 7th it was necessary to use three levels for an adequate description of the S.V. component; at 11 U.T. a preburst level of 136 units, at 14:30 U.T. a combined level of quiet sun and long enduring bursts of 155 and at 23 U.T. a post "post-burst" level of 125 units. Their inclusion in the plot of daily flux values (Fig. 3) shows immediately a discontinuity of 10 flux units with reference to the dashed line which depicts the day-to-day variation of flux of an assumed stable region with intensity to match the pre-burst level. It is derived by shifting the post-burst levels the proper amount to obtain a continuous curve. The decrease in emission of 10 units is identical, to within the errors of reduction, to the decrease observed from level 2 to level 7 observed on August 7. A recovery during the night is unlikely, and even if it did occur, it would only be temporary. Thus the three hour decrease in radio emission of the S.V. component can be extended to seven days until the minimum value is reached.

OBSERVED
SOLAR FLUX



- GREAT BURSTS
- DAILY QUIET SOLAR FLUX, JULY 20 TO AUGUST 18, 1972
- ASSUMED DAILY QUIET SOLAR FLUX LEVEL IF GREAT BURST ON AUGUST 7 HAD NOT OCCURRED
- +++ ASSUMED DAILY QUIET SUN TO SEPARATE A LONG ENDURING BURST ASSOCIATED WITH BURST ON AUGUST 2.

Fig. 3. Plot of observed daily quiet flux values observed at 17 U.T. with modifications to show a visibility curve for a stable center of radio emission.

The minimum of the assumed stable region given by the dashed line has the interesting feature that its magnitude of 105 flux units approximates the magnitude of the preceding minimum reached on July 24-25. This equality justifies the assumption that the curve depicts the visibility of a stable center and draws attention to a further asymmetry produced by the enhanced flux for July 30 to August 3. This can be removed by assuming values for the quiet sun level on these days as indicated by the crosses and thereby providing the reference emission of a hypothetical stable center for one disc passage from July 24 to August 15. This reference curve has symmetry with respect to the C.M. passage of the August 4 and is very similar to the average curve derived by Waldmeier [1953]. The four days of excess emission can be regarded as the occurrence of a very long enduring burst with peak intensity of 12 flux units. The impulsive burst of August 2 occurred during the decline of this event, and there is no trace of a permanent change in the daily levels of flux such as appears to have happened after the 7th.

The extension of the post-burst decrease to several days places the event outside the class of those events whose duration is typified by the event of May 19, 1951, Covington and Dodson [1953]. Analysis of that relatively short duration absorption showed that it was necessary for ejected dark flocculus to lie over a bright plage. It is here suggested that the decline of many days duration reflects a permanent diminution of activity in one or more of the centers of activity. When a longer plot of daily flux levels for this period is examined, it will be noticed that the minima occur with regularity for three months before and for three months after August, and that the average value of the lower envelope of flux adjusted for 1 A.U. shows a decrease of 18 flux units. Of this amount, 10 units can be assigned to the lowered level observed 11 hours after the commencement of the long enduring burst. A superposition of minima has been made with reference to a 28 day wave and the result plotted in Fig. 4. The dashed line and the specified days denote the 28 day reference wave. In addition to the change in amplitude of the minima, a phase advance of 4 days can be clearly seen for those occurring after the August events. Interestingly, the minima of July partakes of both the pre- and post-burst positions. The presence of the S.V. Component outlines two hemispheres upon the solar surface, one with minimum emission and the other with maximum emission. The phase shift of four days in the center of gravity of these two areas is directly related to the flare of August 7 and could be a measure of the energy supplied by the event as well as a clue for the storage of the energy.

ADJUSTED
SOLAR
FLUX

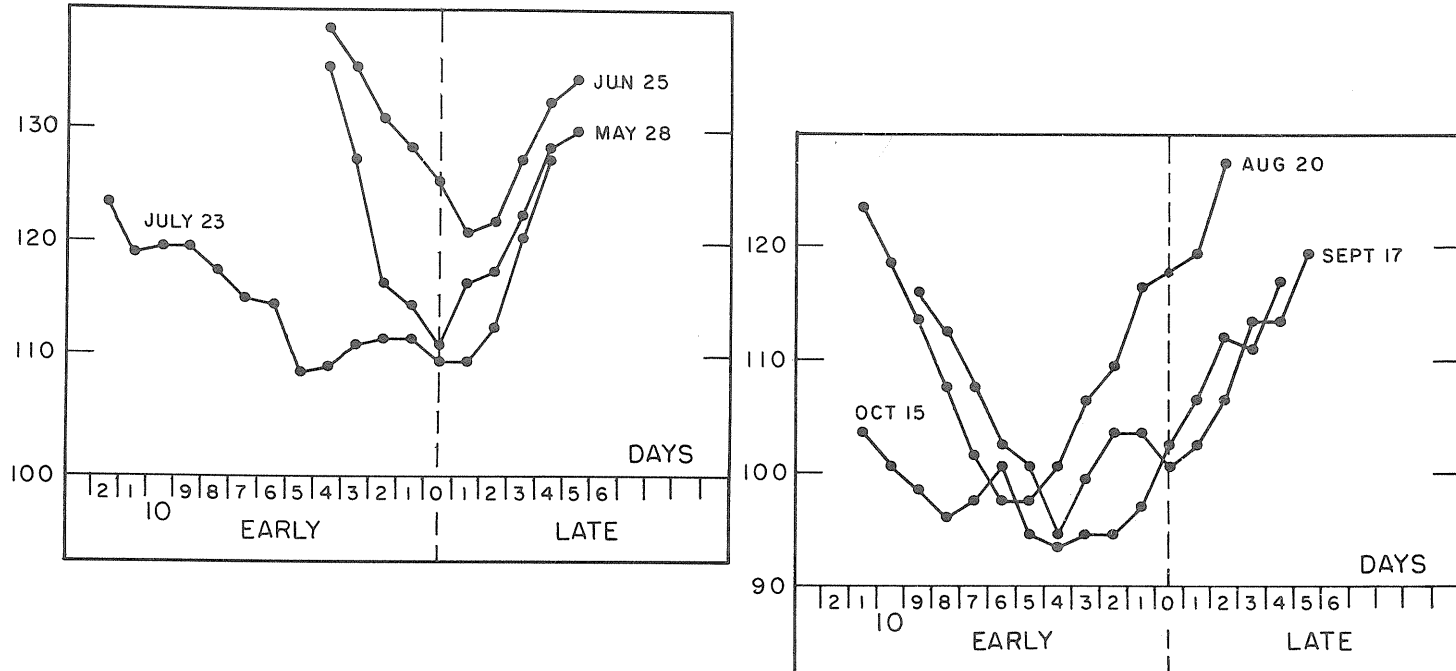


Fig. 4. Superimposed plots of the minimum values of the Slowly Varying component of solar flux for a 6 month period centered on Aug. 1972 and based upon a 28 day period starting on May 28, 1972. The various minima are identified by the recurrence of the period and not the associated minima. Upper plots for minima before the flares in August, lower plots for minima afterwards.

Other Burst Features of Interest

Other features of interest can be found in the records of total flux during the period of August 1-16. When the active hemisphere was disappearing from view on August 13, (Fig. 1b) the daily traces are particularly free from spurious fluctuations and no bursts occurred during the combined daily observing period. The measured flux values at 14, 17 and 20 U.T. were 101.2, 99.1 and 96.1 flux units and are corrected for atmospheric absorption. Such a decline is in contrast to the post-burst decrease seen after the impulsive burst at 10:45 U.T. on August 2 in which a series of weak Gradual Rise and Fall events are tabulated as starting at 12:40, 13:40 and 14:50 U.T. The "fall only" reported at 16:45 U.T. was listed since the level before the calibration was 2 flux units higher than afterwards. It could equally well be regarded as the end of the post-burst decrease for the impulsive burst. The succession of Gradual Rise and Fall events in the Ottawa records has been noted by Kaufmann [1972] and he has suggested that they be associated with oscillations sometimes seen in prominences. After the Great burst of August 2, on the morning of August 3, unusually heavy scintillations were recorded after sunrise and terminated abruptly. These are presumed to occur in the earth's atmosphere from local weather conditions. Other examples can be seen on the traces on August 5 from 22 to 23 U.T. and on August 9 from 14 to 16 U.T.

High Resolution Fan Beam Scans

Simultaneous strip scans of the sun are made with two fan beams positioned along the local meridian at ARO with E.-W. widths of 1.5 min arc and 0.5 min arc. When proper consideration is given to the coefficients for the angular variable in the function describing the antenna profile, the low resolution antenna has the profile given by $(\sin x/x)^2$ while the higher resolution has the profile given by $\sin x/x$. A study in the differences in the scans of elementary sources made with these two types of antenna patterns and their interpretation has been made by Covington and Harvey [1959]. Observations with the lower resolution beam are regularly presented in Solar Geophysical Data and here reproduced as the upper curves in Fig. 5 for August 6, 7 and 8. The higher resolution scans have only recently been commenced, Bell *et al.* [1973], and are normally taken simultaneously with the lower resolution ones. Only those for the x^2 vector are available for this period and the records reproduced as the lower curves in Fig. 5. In these drift curves, the extent of the photosphere has been indicated by a properly placed bar. Examination of the curves show immediately that the increased resolution reveals unexpected structure for the radio spots, which may arise from two or more separated sources since there is possible confusion from the wide extent of the N.-S. beam.

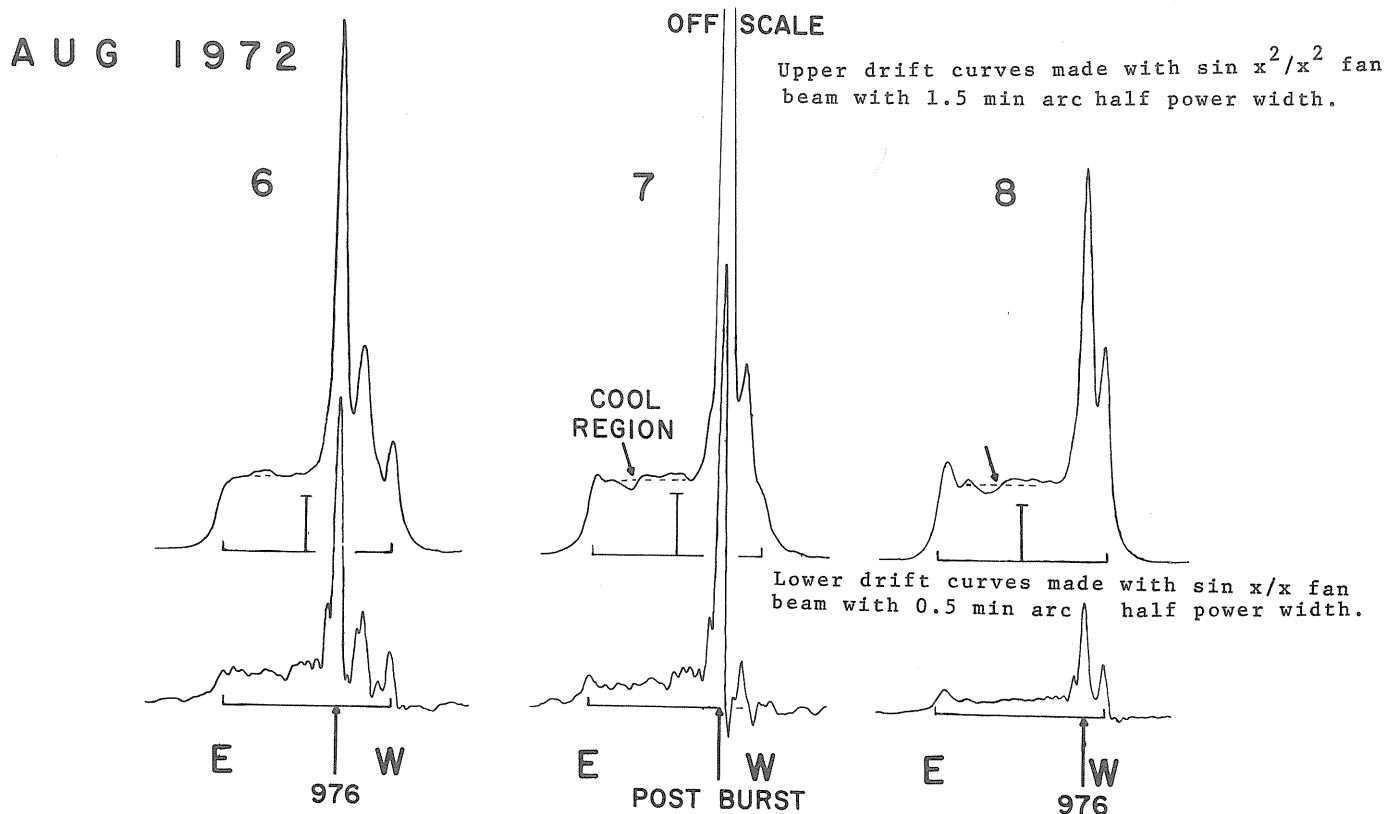


Fig. 5. Simultaneous drift curves made with high resolution fan beams on Aug. 6, 7, and 8, 1972.

On August 7, the scans occurred during the post-burst enhancement and resulted in an off-scale registration for the lower resolution beam but not for the higher resolution one. This observation enables the main peak of the high resolution scan of the centrally placed radio region to be identified with McMath-Hulbert plage region #11976 and not the smaller radio component which is located to the East some 2 minutes of arc. Here the gain in information from the higher resolution curves applies only for the radio sources and not the quiet sun since the unprocessed interferometer records emphasize residual errors in the phasing of the antenna and the side lobe response from intensive radio spots or other gradients which are superimposed upon the quiet solar background. Without further technical adjustments or processing of data, these curves will be used for the radio regions and not the quiet solar background. Only the low resolution drift curves are calibrated from the total flux found each day from the solar patrol with a procedure which places the level of the emission from the quiet solar disc found at sunspot minimum. This corresponds to a value of 67.2 flux units as observed in 1964. The fluxes for individual radio emissive regions are found with respect to a lower envelope which is established over a period of time by solar rotation tracing out the successive levels of regions of the solar background which appear free from intensive radio regions. It is generally symmetrical with respect to the center of the drift curve. Parts of the lower envelope which appeared on the 6, 7 and 8 are indicated by the dashed line, and the associated flux from this envelope was found to have a value of 83 units. A localized depression below the lower envelope appeared during the post-burst decrease on August 7, was present during the scan on the 8th and disappeared by the 9th. It has been designated a "cool region"* and was not included in the determination of the lower envelope. The feature is unusual and has not been associated with the usual solar features especially published for August [McKinnon, 1972]. Since many studies of the variations of the 10 cm solar flux have shown excellent correlations with the x-ray and x uv solar emissions, it is suggested that the cool region in the solar background may be related to the coronal holes which have been found from satellite observations.

The positions of many of the radio sources can be followed for several days and give confidence that isolated regions are being studied. The large component spot identified with the post-burst enhancement in plage No. 11976 appeared without confusion on the eastern limb on July 26. The position line with respect to the solar disc indicates that the region is located in northern latitudes and consequently a value of 15° has been assigned to it from the optically associated center. Two days later on the 28th, a companion radio spot, or follower, appeared to the east of the region and is evident in all subsequent drift curves. Its appearance on the Eastern limb coincides with the appearance of plage 11977 and it could be tentatively identified by this association which would place it in the southern hemisphere. However, examination of the position lines on a number of days indicates that they do not pass through any prominent optical feature in this plage and it could be that the satellite region is a follower to the main region at latitude 15° N. This association is preferred since other follower components in radio profiles have been noted before, for example, in Fig. 3 and Fig. 8 in Covington *et al.* [1962] and more recently in the radio profile of the centrally located region on June 21, 1972 shown in Solar-Geophysical Data [No. 335, part 1, page 16]. Unfortunately, the follower and other regions of interest cannot be separated when they disappear because of E.-W. pileup and N.-S. confusion. When valid, the low resolution composite profile has been analysed to give the total flux which originates on various days from the two close radio sources; one associated with plage 11976 and the other designated a follower. Separation of the flux between these two regions is done by use of the high resolution profiles (Fig. 6). Other radio parameters associated with the plage 11976 are the longitude of the radio peak at the assumed latitude of $N 15^\circ$, the E.-W. extent of the half power width and the equivalent temperature based upon an assumed square emitting region and are presented in Table I.

The day to day variations in the radio parameters associated with the regions of interest are plotted in Figs. 7 and 8. In the absence of an established average visibility curve for a radio source traversing the solar disc, a cosine variation has been accepted for reference and plotted to pass through the rising and falling parts of the total flux from the two sources (Fig. 7). This places the peak on the day of central meridian passage of August 4 such that the observed level of daily flux falls below. It is noted that three major bursts were observed during this period and suggested that the deficit from the visibility curve may be an indication of the energy lost by the flare mechanism during this period. The burst of August 2 is at the beginning of this period while the burst of August 7 is at the end. The appearance of the long enduring, post-burst decrease suggested from the earlier study of the total flux records is not supported by this interpretation. It is also not supported by the variations seen in the observed E.-W. extent and the flux from the radio region associated with M 11976 plotted in Fig. 8.

* Measured flux is -1.2 units.

Table 1

DATE 1972	OBS TOTAL FLUX 17 U.T.	1.5 MIN ARC FAN		0.5 MIN ARC FAN				
		SOURCES IN M11976 & FOLLOWER	ALL OTHER SOURCES	FLUX		REGION M 11976		
				M 11976	FOLLOWER	LONG AT 15°N	E.-W. EXTENT MIN ARC	TEMP. X 10 ⁶ EW=NS
July 20	107.4							
21	108.2							
22	108.1							
23	106.1							
24	106.1							
25	108.9			0.0				
26	116.9	- (b)		1.0 (b)	0.0	- (d)	1.0	0.5
27	123.4	(b)		2.0 (b)	0.0	- (d)	1.2	0.7
28	129.3	6.4	41.8	5.7	0.7	- (d)	1.4	1.4
29	134.9	16.2	33.7	14.7	1.5	- (d)	1.4	3.7
30	137.0	20.0	33.5	16.3	3.7	- (d)	1.5	3.7
31	145.7	27.8	37.3	24.1	3.7	E60	1.6	4.3
Aug. 1	151.7	39.1	28.7	36.6	2.5	E45	1.7	7.0
2	146.0	36.9	27.9	31.9	5.0	E34	1.9	4.5
3	142.8	38.8	24.7	34.5	4.3	E17	1.9	4.8
4	141.9	38.2	22.3	34.0	4.1	W 3	1.9	4.8
5	142.4	41.2	15.6	36.3	4.9	W11	1.7	6.2
6	139.4	38.5	15.6	34.3	4.2	W25	1.6	6.2
7	Burst (a)	-	-	42.2 (e)	4.8 (e)	W35	1.3(e)	12.2 (e)
8	121.9	27.6	11.3	23.7	3.9	W48	1.4	5.7
9	120.4	24.8	12.7	21.3	3.5	W60	- (c)	
10	115.5	20.9	3.3	- (c)	- (c)	W71	- (c)	
11	110.3	- (c)		- (c)	- (c)	- (c)	- (c)	
12	104.8	- (c)		- (c)	- (c)	- (c)	- (c)	
13	99.1							
14	95.4							
15	95.1							
16	98.1							
17	103.8							

(a) Preburst at 11.00 U.T. - 136
 Quiet sun and active centre at 14.30 U.T. - 155
 Post "post burst" at 23.00 U.T. - 125

(b) Unresolved with 1.5 min fan, resolved with 0.5 min fan

(c) Severe confusion with other regions

(d) Appears off solar disc

(e) Post burst enhancement

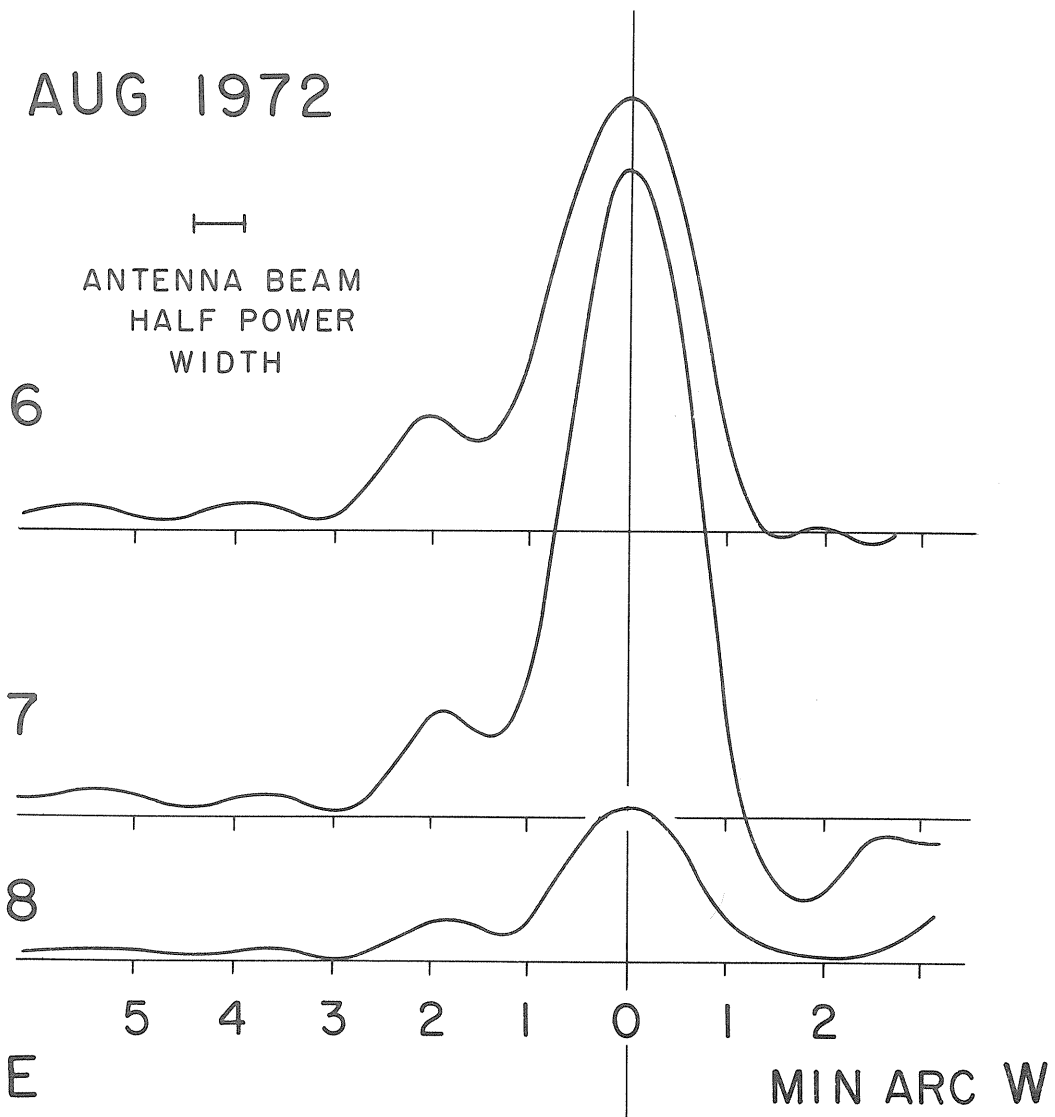
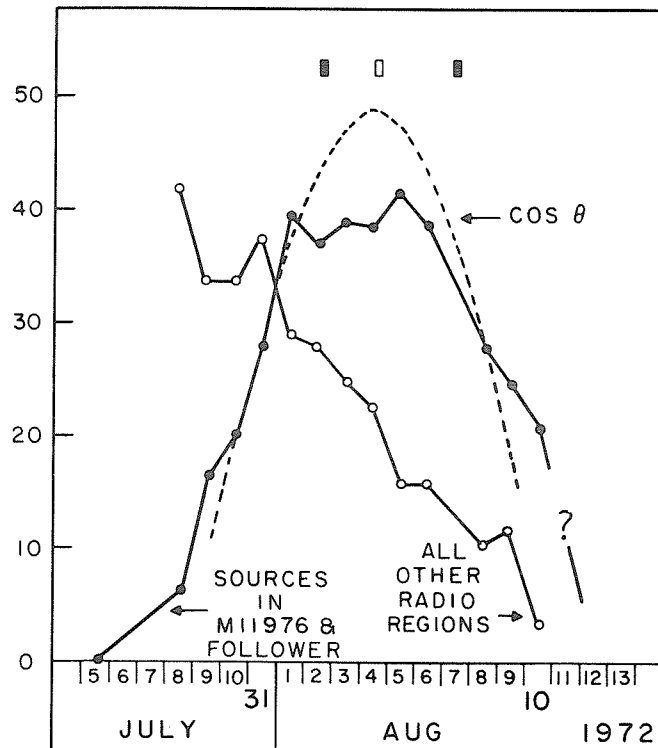


Fig. 6 High resolution drift curves of radio region associated with plage M #11976 and its follower.

OBSERVED
SOLAR FLUX



- GREAT BURSTS OBSERVED AT OTTAWA
- GREAT BURST OBSERVED AT MANILA
- OBSERVED RADIO FLUX ASSOCIATED WITH SOURCES IN McMATH - HULBERT REGION # 11976 & FOLLOWER
- RADIO FLUX OBSERVED FROM ALL OTHER RADIO REGIONS SHOWN IN 1½ MIN ARC SCANS
- REFERENCE QUIET SOLAR LEVEL ABOUT 83 UNITS
- COS θ ASSUMED COSINE CURVE WITH MAXIMUM WHEN REGION # 11976 NEAR SOLAR MERIDIAN
- ? UNCERTAINTY IN E-W SEPARATION DUE TO PILE UP OF REGIONS IN NORTHERN AND SOUTHERN HEMISPHERES

Fig. 7 Plots of observed flux from radio sources associated with plage M #11976 and follower, and from all other radio regions from July 25 to August 10, 1972.

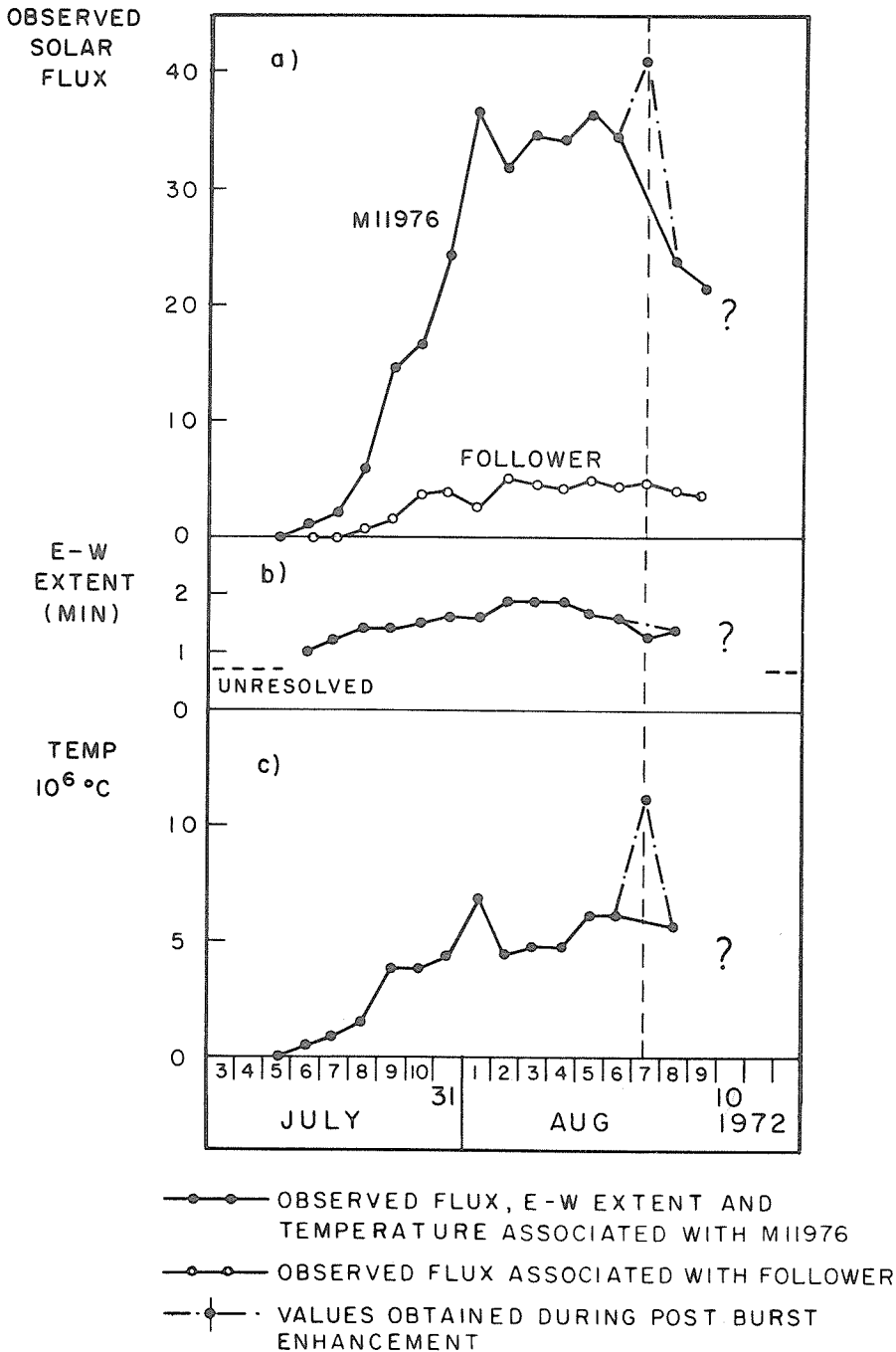
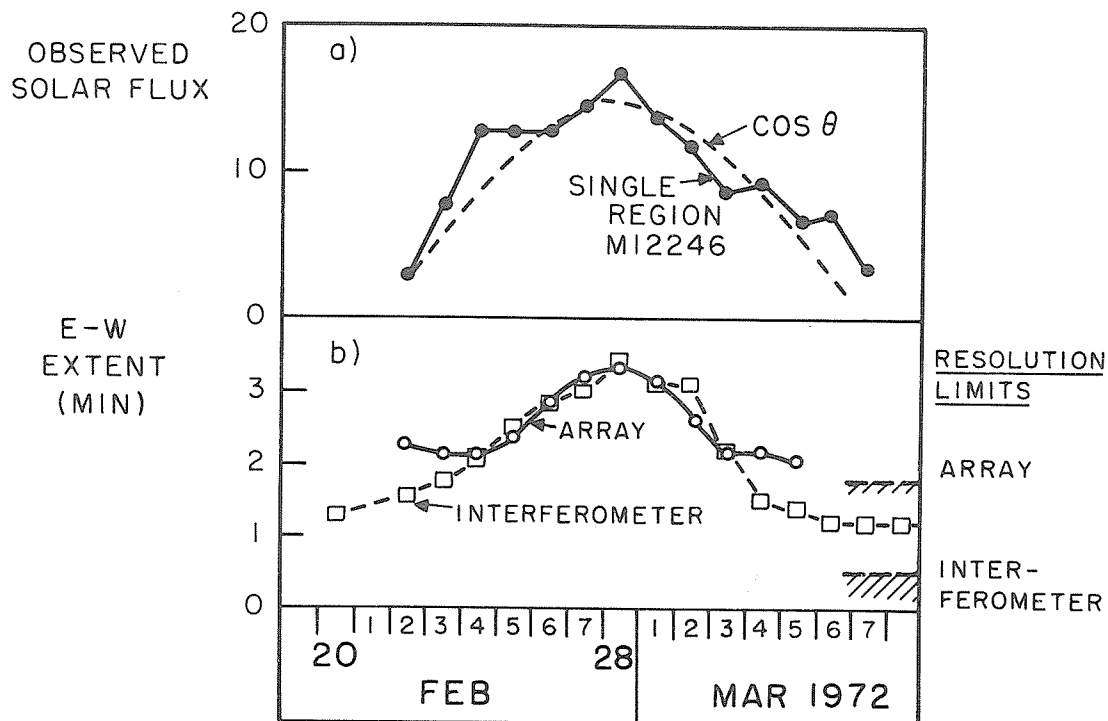


Fig. 8. Plots of observed flux from radio parameters associated with Plage M #11976 alone from July 25 to Aug. 10, 1972.

The possibility that the observed decrease in the total flux is contained in variations which involve all regions not associated with the longitude of the main regions was examined by deriving their fluxes. Values are presented in Table I and plotted in Fig. 7. The curve representing the flux from all other regions appears as a strong out-of-phase component to the flux from the main region with a pronounced decline coinciding with the disappearance of the main region. The two decreases from different regions of the solar surface are compounded in the record of total flux and their simultaneity offers an explanation for the long post-burst depression found in the earlier analysis of the total flux. The single long enduring burst from July 30 to August 3 can also be separated into two components, one in the main region as part of the rapid rise in flux from that region at this time and the other in a different, single region from July 30 to August 1. For convenience this is represented in the total flux designated "other regions" and appears there as a single enhancement observed during a fraction of the day.

Reliability of Analysis

The variations in emission have been evaluated in the presence of various errors of the instrument and methods of reduction. The antenna beam of low resolution provides the basis of the system and has been found to be extremely stable in various operating conditions. The sensitivity of the low resolution drift curves is best determined by reference to the total flux as measured by the solar patrol. Over short periods of time the relative errors are currently of the order of $\pm 1\%$. Flux from individual regions above the quiet sun background can be repeatedly found to within $\pm 2\%$. Since no extensive studies of a statistical kind have been made with the new antenna, another source associated with plage M 12246, has been analysed in a manner similar to the main study and the results plotted in Fig. 9. The fitting of a cosine curve to the flux variations indicate that it is a more stable region than the main one in August. Only part of the scatter in the points in the curve can be explained in terms of the errors previously mentioned. Two curves of the E.-W. half power widths of the scans have been plotted, one for the low resolution and the other for the high resolution curves. Intercomparison of these curves shows that the effect of the increased resolution is noticeable when the regions are on the limbs, while inspection of the profiles when the region is near the center of the disc indicates a flat top several beam widths wide with some structure.



OBSERVED RADIO PARAMETERS WITH
McMATH - HULBERT REGION # 12246

Fig. 9. Plot of observed radio parameters from a radio source associated with McMath-Hulbert plage no. 12246 which shows a cosine visibility curve from Feb. 22 - Mar. 8, 1973.

REFERENCES

- BELL, M.B.,
A.E. COVINGTON and
W.A.G. KENNEDY 1973 Polarization interferometer for 2800 MHz solar noise studies with a 0.5' fan beam, Solar Physics, 28, 123-136.
- COVINGTON, A.E.
Gladys A. HARVEY, and
HELEN W. DODSON 1962 Selected high-resolution strip scans of the 10.7 cm Sun, Astrophys. J., 135, 531.
- COVINGTON, A.E. and
G.A. HARVEY 1961 Coincidence of the explosive phase of solar flares with 10.7 cm solar noise bursts Nature, 192, 152.
- COVINGTON, A.E. and
G.H. HARVEY 1959 Resolving power of 3 antenna patterns Cdn. Jour. of Physics, 37, 1216.
- COVINGTON, A.E. and
HELEN W. DODSON 1953 Absorption of 10.7 cm solar radiation during flare of May 19, 1951, Jour. Roy. Astro. Soc. Can., 47, 207.
- COVINGTON, A.E.
H.P. GAGNON AND
J.D. MOORE 1973 Observations of Solar Flux at Algonquin Radio Observatory on 2800 mhz and at the Dominion Radio Astrophysical Observatory on 2700 MHz. Monthly Reports for 1972. Pub. Astrophysical Branch, No. 3, Ottawa, Canada.
- FLETCHER, J.D. 1964 Solar radio emission as criteria for solar proton event warning, American Institute of Aeronautics & Astronautics, 2, 2193.
- HARVEY, GLADYS A. 1965 2800 mc radiation associated with type II and type IV solar radio bursts and the relation with other phenomena, Jour. Geophysical Research, 70, 2961.
- KAUFMANN, PIERRE 1972 Possible long-period oscillations in solar radio emission at microwaves Solar Physics, 23, 178.
- McKINNON, J.A. 1972 Aug. 1972 solar activity and related geophysical effects, NOAA Technical Memorandum ERL SEL 22, SEL, Boulder, Colo.
- SAITO, K. and
A.E. COVINGTON 1963 Microphotometry of a solar flare region producing 10.7 cm impulsive and gradual rise and fall type bursts, Pub. Astro. Soc. Jap., 15, 177.
- WALDMEIER, M. 1953 Limb darkening of the radiation from the sun at $\lambda = 10.7$ cm, Zeitschrift fur Astrophysik BD 32, S 116-124.
- 1972 Solar-Geophysical Data (Prompt Reports) No. 335, part 1, July, page 16, National Oceanic and Atmospheric Administration, Boulder, Colo.

HIGHLIGHTS OF RADIO ACTIVITY DURING DISK PASSAGE OF McMATH PLAGE NO. 11976

by

John P. Castelli and William R. Barron
Air Force Cambridge Research Laboratories
Bedford, Massachusetts

and

Victor L. Badillo
Manila Observatory
Philippine Islands

Introduction

A number of surveys of the August 1972 period have already been generated which have presented an overview of the period [Lincoln and Leighton, 1972; McKinnon, 1972, etc.]. Several of the present authors prepared a summary of the important radio activity of the period which was circulated as a personal communication to many researchers in September 1972. Later this became a comprehensive AFCRL report [Castelli et al., 1973]. In this latter report, the history of the disk passage of McMath plage 11976 was traced from a radio viewpoint - principally in the dm-cm range. The report draws almost exclusively from the patrols at Sagamore Hill, Hamilton, Massachusetts, and Manila Observatory, Philippine Islands. The latter is operated under contract to the USAF. These two stations in August 1972 furnished 100% time surveillance of the radio sun. Discrete frequency activity in the 200 to 35000 MHz range and sweep frequency responses in the 24 to 48 MHz range were observed. At times, optical, ionospheric, and particle emission activity were related to the radio emission.

Despite the large number of many kinds of observations, it may seem strange to claim that there was a shortage of data. Yet in retrospect, such indeed was the case. Certain of the events, notably that of 7 August near 1520 UT, showed the unique value of centimeter and millimeter patrol burst measurements - especially above 8800 MHz. Sagamore Hill was fine in this respect but the lack of data at Manila above 8800 MHz was a serious limitation. During the 7 August proton flare-burst, hard x-ray data would have been valuable to test the Frost-Dennis [1971] suggestion that hard x-rays >200 keV are reliable for determining the time(s) and occurrence(s) of secondary acceleration(s) of particles to high velocities. During the 7 August event, the white light and millimeter radio data have been indispensable.

During the 4 August event at about 0630 UT, white-light flare data would have been most helpful, in view of the other comparison type data available. Yet, neither positive nor negative white-light information is available. The question of primary and secondary acceleration(s) during flash phase(s) of flares is a problem which has received much attention [Svestka, 1966, 1970, Najita and Orrall, 1970, Syrovatskii, 1972, etc.] and which is still unsolved. Type II dekametric burst data for 2 and 4 August were especially helpful. The resolution of Type II data at the University of Colorado at Boulder [Dodge, 1973] for the 7 August event was especially good. Some observatories "missed" these events. They were possibly masked out by the equipment saturating Type IV concurrent event. Apparently some aspect of the University of Colorado equipment permits seeing of Type II's which other equipments could not resolve. The recent availability of the University of Colorado Type II data for four separate events in the 1515-1535 UT period on 7 August is a fortunate circumstance.

Much has been said elsewhere about the many unusual optical and radio signatures which would alert one to the possibility of important future activity. In relation to the August period, it was observed very early that the region, though comprised of numerous spots was extremely compact [Zirin, 1973]. The delta classification of the region, the intense magnetic fields for many days, the unusual plage intensity, the extremely high radio flux density at the higher frequencies early in the period, etc., all alerted forecasters to the possibility of impending activity.

31 July 1972

In considering the highlights of the radio activity of the period, 31 July was a most important day from a solar physics viewpoint. On that date, McMath Plage No. 11976 was the site of many (16) unusual high frequency solar radio events. Unlike most radio bursts, the spectral cutoff of these events (on the low frequency side of f_{max}) was very sharp and generally above 10,000 MHz. This type of phenomenon was a transitory thing - apparently related to some stage of development of the active region. There were none of these events on 30 July and only a few on 1 August. Because of the high frequency characteristic of the

bursts, Manila with 8800 MHz its highest frequency, and indeed most of the other similarly limited observatories, observed nothing. The one important exception was the patrol at Slough, England, which observed some of the Sagamore Hill events at 19,000 and 35,000 MHz during times of viewing overlap. Also, Pennsylvania State at 10,600 MHz observed a small burst flux density increase for most of the Sagamore Hill events which from the apparent nature of the event(s) were cut off before reaching 8800 MHz and were not observed. Hence, data from these two observatories initially helped to confirm the validity of the events.

Several of the radio bursts were unambiguously related to sources within Plage No. 11976 through the use of flare-burst position timing information. From the similarity of the 16 spectra, it was a safe assumption that this region was the location of all the events. The absence of reported optical (flare) data was distressing at the outset, especially since the events were observed in the 7.5 to 15 and 15 to 30 KeV X-ray ranges of the University of New Hampshire OSO-7 experiments. Later inspection of the Cal Tech Big Bear Observatory H-alpha film records for this period confirmed a short duration flare or brightening for all but one of the events. Paradoxically, the event not confirmed was the burst which was most intense at 35,000 MHz.

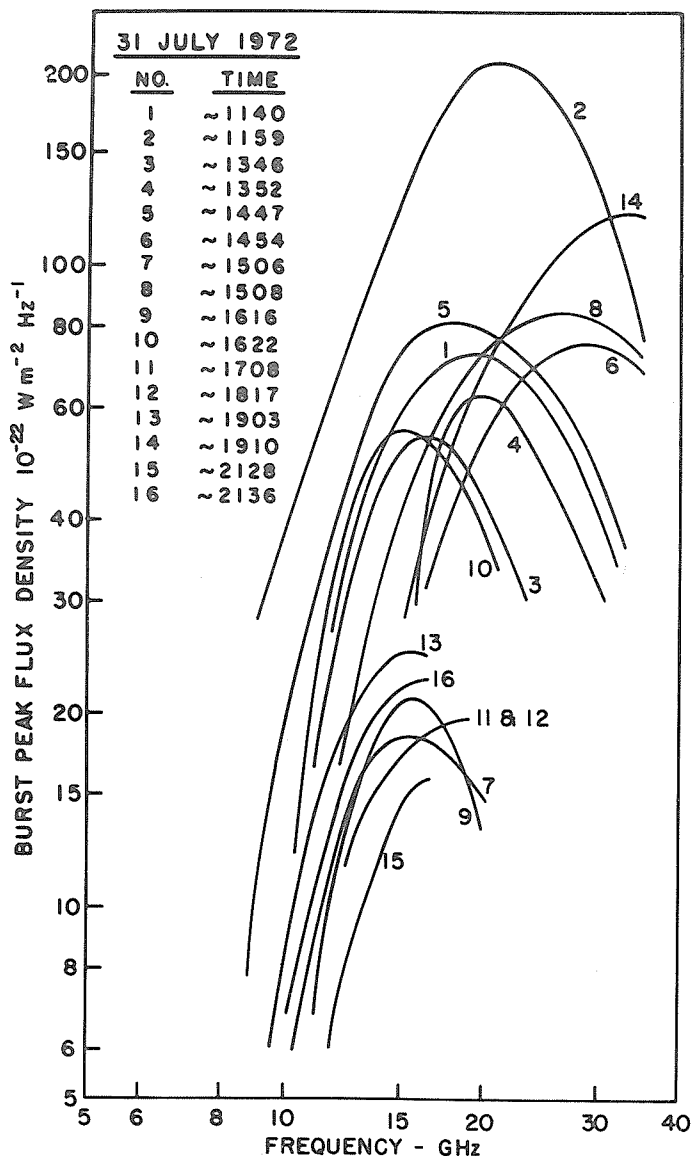


FIG. 1 PEAK FLUX DENSITY SPECTRA OF BURSTS ON JULY 31, 1972. FLUX DENSITY DATA WERE OBTAINED FROM VARIOUS PUBLISHED SOURCES.

Comparing optical, radio, and x-ray data, with only few exceptions, the flare-bursts were characterized by impulsiveness and short duration. Figure 1 shows the peak flux density spectra of the 16 events. Note the following: The spectral maximum when resolved is very high. In contrast, the average f_{\max} for thousands of burst spectra 1968-1971 was only about 6500 MHz. The ratio of f_{\max} to f_{cut} (where f_{cut} is the region of low frequency cut off) is very small (~ 1.5 on average) with f_{cut} occurring generally near or above 10,000 MHz. Average values of f_{\max}/f_{cut} are 3 to 4 [Guidice and Castelli, 1972], though ratios occasionally are as large as 10 for some "great" bursts. It is also evident that slopes on the low frequency side of f_{\max} are very steep (average ≥ 5), which in fact restricts the possibilities of the dominant absorption mechanism. The strong magnetic field in the region is a basic cause of the observed spectra.

In a comprehensive study of the 31 July events, Castelli and Guidice [1973] considered (1) gyrosynchrotron self-absorption, (2) free-free absorption, (3) gyro-resonance absorption, (4) plasma-frequency cut off and (5) ionized medium suppression (Razin effect) to explain the low frequency slope of the burst spectra. (Not too much could be said about the high-frequency side of the spectral maximum, since radiometric sensitivity becomes a problem for small events at 35,000 MHz and above). Whereas for many burst spectra of both large and small events, it is difficult to determine unequivocally the absorption mechanism involved; in the present instance the decision was not difficult. With their unusually high spectral maxima and cutoff frequencies, the spectra of the low-to-moderate intensity bursts (20-200 f.u.) of 31 July 1972 are not statistically typical of those found in a large survey (1968-1971) of burst spectra [Guidice and Castelli, 1972]. It appears that the burst-region parameter that is different (and responsible for the unusual spectra) is the magnetic field in the emitting region which is unusually strong probably because of the relatively low altitude of the bursts in the solar chromosphere. From attenuating mechanism analysis, the most plausible explanation of the observed spectra seems to be gyro-resonance absorption along the lines of analysis of Takakura [1967].

It is not known if a similar development phenomenon takes place for proton-producing regions in general, though a rapid survey fails to disclose periods when spectra similar to those of 31 July 1972 were observed.

Proton Flare Bursts-Early Activity on 2 August 1972

From 2 to 7 August at least 4 proton producing flare-bursts occurred. The first extremely large burst of the sequence was a long duration complex, great burst which took place on 2 August starting at about 0310 U.T. The Manila Observatory recording of this is shown in Figure 2. The burst has the usual characteristics of a proton flare-burst; slow rise to maximum, long duration, values greater than 1000 f.u. at $\lambda = 3$ cm, intense meter wavelength emission, etc. (The 24 to 48 MHz dekanetric activity which coincided with it was a weak continuum event). The associated flare was importance 1B at $N13^\circ$, $E35^\circ-37^\circ$. The start time was before 0316, max 0410 and end after 0506 according to data from Palehua, Hawaii and Teheran, Iran. Statistical radio burst data are given in Table 1.

Table 1

Burst Data From Manila Observatory of Early Event on 2 August 1972

Frequency MHz	Start Time UT	Max Time UT	Duration Minutes	Type Event	Flux Density	
					Peak	Mean
8800	0309.5U	0330.3 0404.0	63.1	47	1750U	760
4995	0309.5U	0331.8 0404.5	62.4	47	1650U 1670U	1020
2695	0311.2U	0331.7 0404.8	60.7	47	2250U 880U	980
1415	0312.4U	0331.5 0406.8	59.0	47	2200U 326U	370
606	0312.4U	0323.0 0340.5	90.0	47	1060U 950U 3000U	680

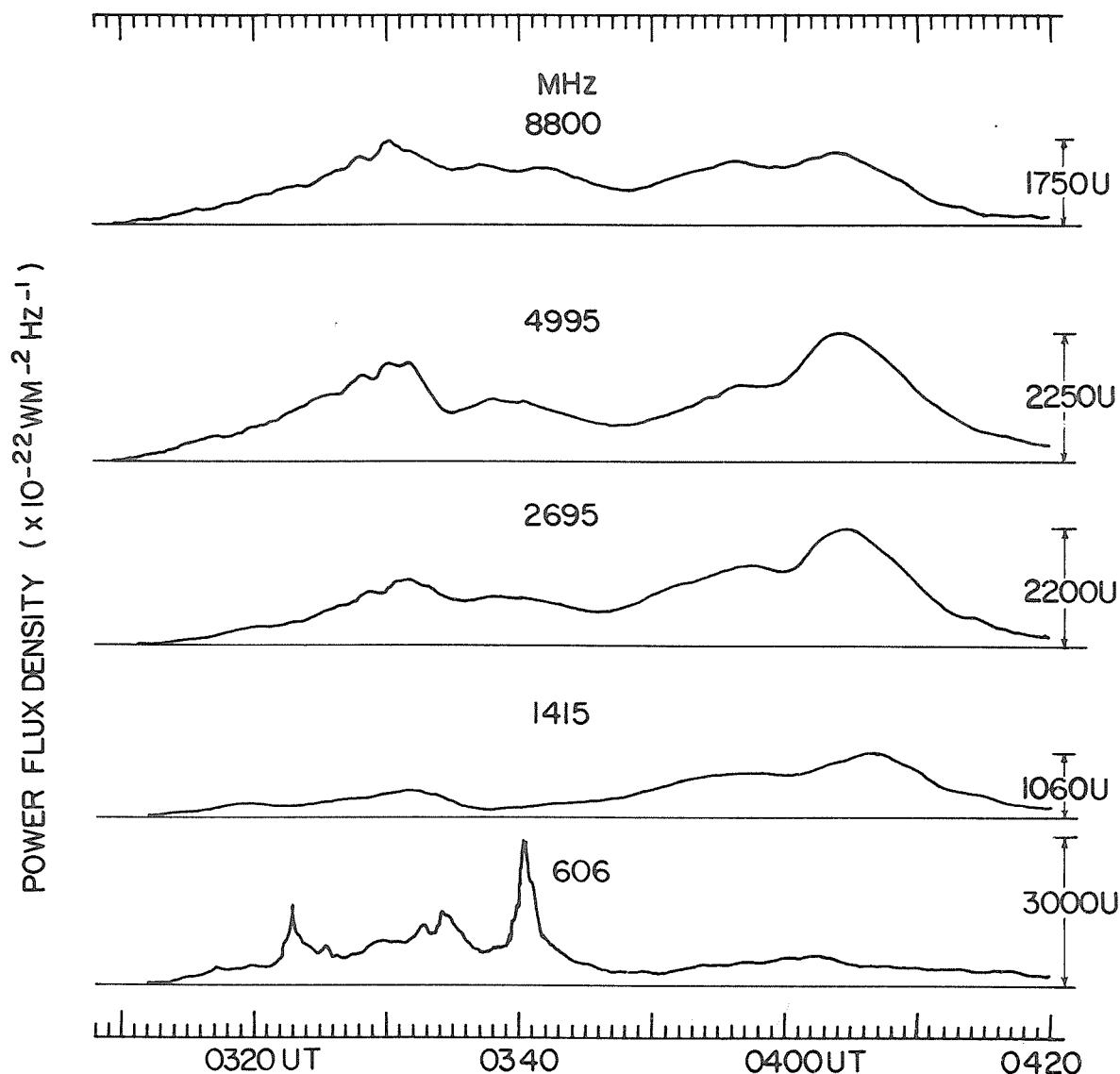


FIG. 2 GREAT RADIO BURST OBSERVED ON 02 AUGUST 1972
 AT MANILA OBSERVATORY , R.P.
 U- DUE TO HEAVY RAIN

By 1800 U.T. on 2 August, the ATS-1 satellite in the 5-21 and 21-70 MeV ranges began to show a slow increase in particle count, apparently from this event.

At 1837 U.T., Sagamore Hill was recording another great burst which was to last for about 12 minutes. The start to max times were generally less than 2 minutes. For completeness these data are shown in Table 2. Note that the event had an extremely hard spectrum. Note also the weakness of the event at the longer wavelengths.

From local sunrise at Sagamore Hill at about 1200 on 2 August until about 2024 U.T. the 24-48 MHz interferometer registered mainly an Intensity 2 continuum event.

2 August 1972-The Principal Event

The largest radio event of 2 August began between 1946 and 1952 with a precursor of 40 to 50 minutes duration having intensities of several hundred flux units. An enhancement persisted into the complex (three maxima) burst which became impulsive near 2020 U.T. It is impossible to accurately describe the period statistically, though a reasonable summary of the burst parameters is presented in Table 3.

Table 2

Burst Data From Sagamore Hill for Event of 2 August 1972 Near 1830 UT

Frequency MHz	Start Time UT	Max Time UT	Duration Minutes	Type Event	Flux Density	
					Peak	Mean
35000	1838.4	1839.6	10.1	47	810	300
*15400	1837.9	1839.6	11.6	46	490	175
*8800	1838.0	1839.6	11.5	47	640	250
*4995	1838.2	1839.6	11.5	47	990	400
*2695	1837.9	1840.3	12.2	47	580	200
*1415	1838.3	1840.2	10.9	4	165	70
*606	1838.8	1843.4	10.9	3	16.6	7.0

*These had post burst increases starting at 1849.5 and lasting generally 50 to 60 minutes with simple 1's and simple 2's superimposed at about 1908.5.

Table 3

Burst Data from Sagamore Hill for Principal Event on 2 August 1972

Frequency MHz	Start Time UT	Max Time UT	Duration Minutes	Type Event	Flux Density	
					Peak	Mean
35000	2036.5	2145.5	139.5U	47	950	250
15400	2039.0	2144.4	140.0U	47	3300	850
8800	2035.3	2144.5	157.7U	47	10720	2500
4995	2035.2	2144.5	169.8U	47	9050	2000
2695	2033.3	2144.0	185.7U	47	9256	1700
1415	2032.7	2121.9	186.3U	47	15000	3800
1415	2032.7	2149.0		47	7500	
606	1959.4	2141.2	221.1U	47	80000	18000
410	1958.8	2141.2	238.2U	49	190000	2900
245	2000.3	2142.2	236.7	49	14800	3700

A clearer impression of the event is gained from the Sagamore Hill burst profiles shown in Figures 3a, b, and c. An intensity 3, type II burst was also observed there at 36 to 48 MHz during the period from 2145.7 to 2149.5.

The dekameter continuum which had persisted much of the day broke into a type IV burst of intensity 2 at 2024 and slowly increased to intensity 3 at 2045. Thereafter, it declined into a continuum of long duration on 2 and 3 August increasing again in strength to a type IV during much of 3 August and 4 August and back again to a continuum. There was a pronounced increase in intensity to type IV on 4 August at about 0635 U.T. This persisted for the next five or six hours. Thereafter a continuum prevailed until 1800 U.T. on 5 August. Comparison of the events at Manila and Sagamore Hill however, suggests that there is a difference in equipment sensitivity.

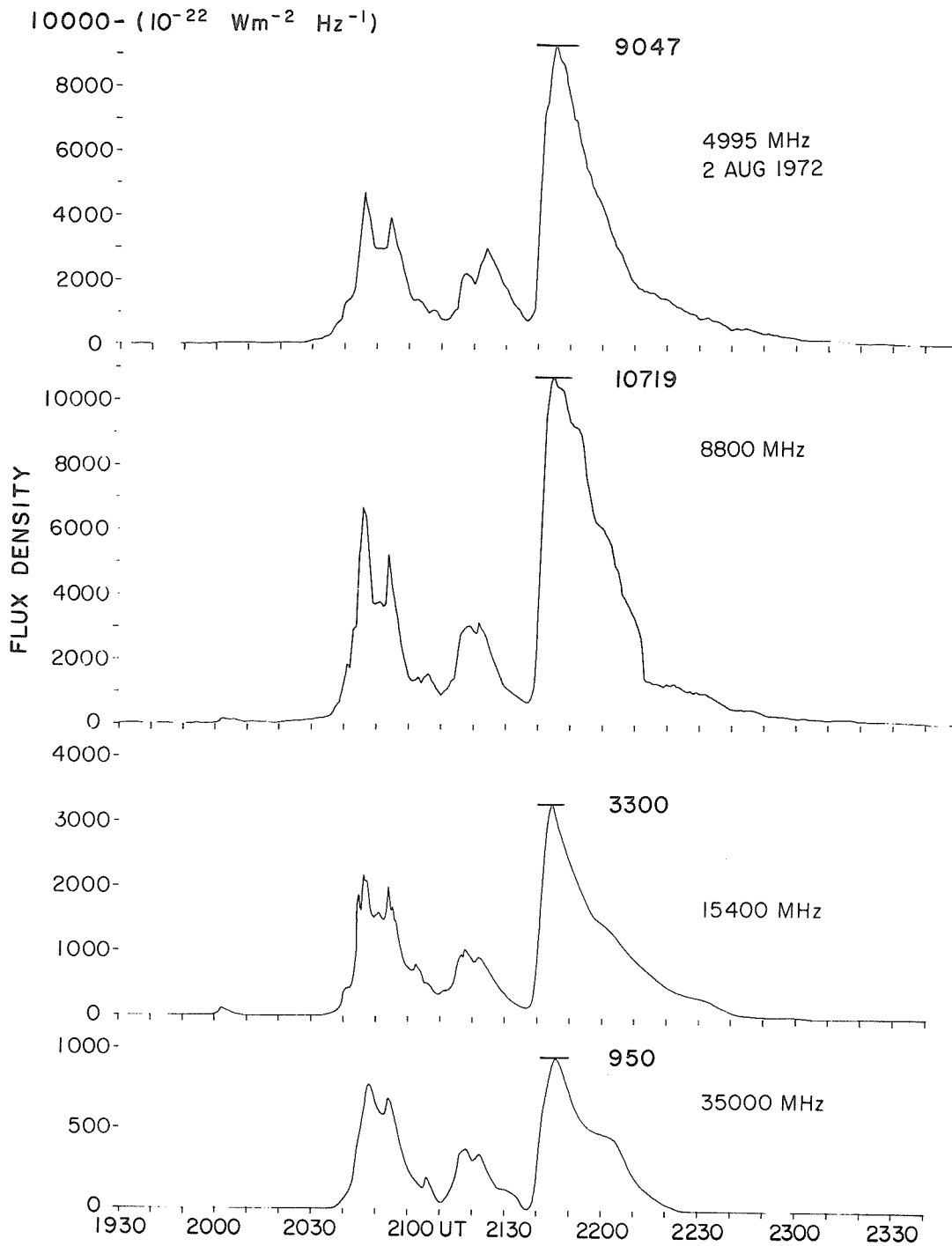


FIG. 3a GREAT BURST OBSERVED 2 AUGUST 1972 AT SAGAMORE HILL RADIO OBSERVATORY, HAMILTON, MASS.

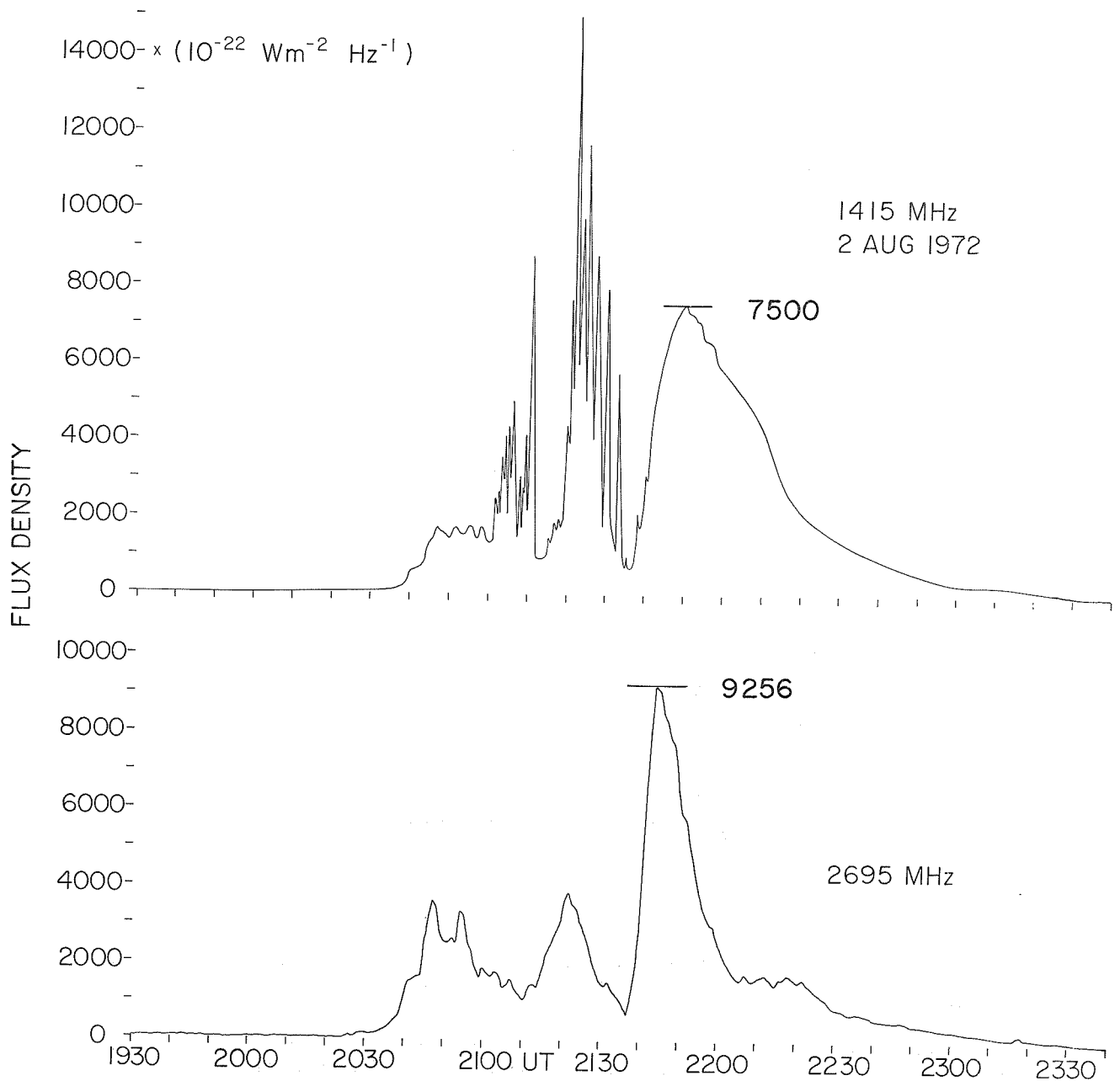


FIG. 3b GREAT BURST OBSERVED 2 AUGUST 1972 AT SAGAMORE HILL RADIO OBSERVATORY, HAMILTON, MASS.

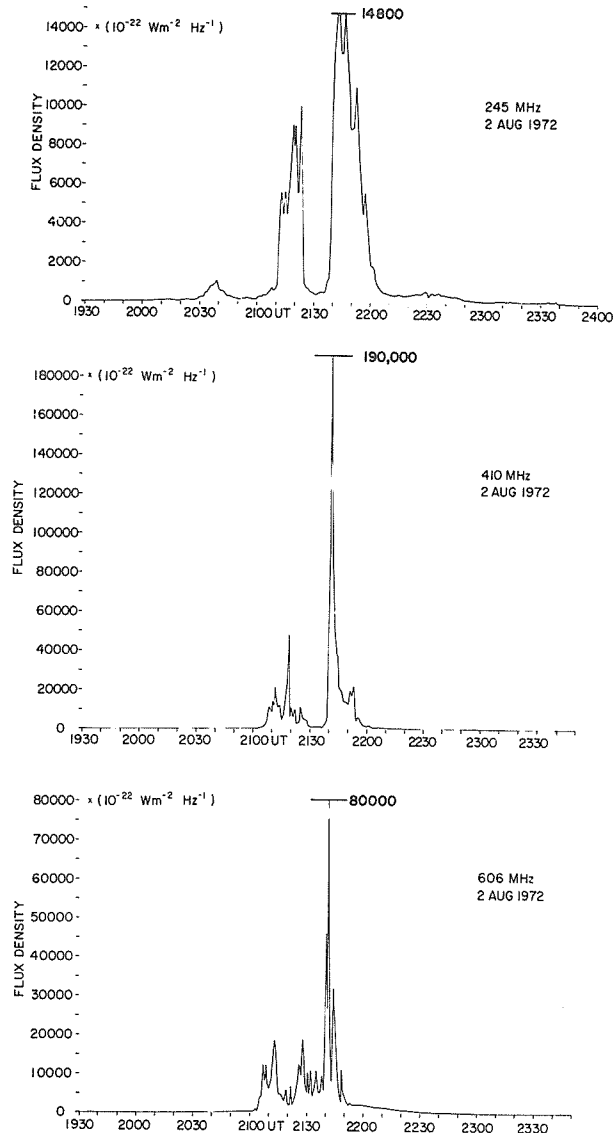


FIG. 3C GREAT BURST OBSERVED 2 AUGUST 1972 AT SAGAMORE HILL RADIO OBSERVATORY HAMILTON, MASS.

The flare associated with the 2000 U.T. event of 2 August is generally classified as a type 3B at N17, E28 (Long 7.1°). Film data from Palehua shows a start time of 2006, max at 2051 and ending at 2336 U.T.

There can be no doubt that the activity of this event added to the particle emission and PCA triggered by the flare-burst at about 0300. This had reached >1.5 dB at 0000 U.T. (Thule) on 4 August.

Though moderate to intense dekameter activity persisted on 3 August, the discrete frequency events were few and small. Nevertheless, the highest frequencies were again favored among the bursts which did occur. Noise storm activity is another question. This persisted at 245 and 410 MHz for 5 days after 2 August.

The 4 August 1972 Event

On 4 August the second in the series of extremely large bursts occurred. The source of this was a 2B or possibly 3B flare (Teheran) located in the same region now at about N15, E09 (Long. 7.5°), according to data from Teheran and Athens. The flare which started at about 0617 U.T. had a max at 0633 and ended at about 0857. The radio burst as recorded at Manila was among the highest ever recorded at 8800 MHz. In view of its intensity at 8800 MHz, we would have expected a very strong millimeter component. Table 4 gives the burst statistics.

Table 4

Burst Data from Manila Observatory for Event on 4 August 1972 Near 0630 UT

Frequency MHz	Start Time UT	Max Time UT	Duration Minutes	Type Event	Flux Density	
					Peak	Mean
8800	0618.8	0634.3	26.4	47	36500	26600
4995	0618.4	0625.5 0635.0	26.8	47	11000 19500	14100
2695	0618.4	0624.7 0635.7	26.3	47	6600 7500	4700
1415	0618.5	0626.7 0633.4	28.7	47	5000 6700	2800
606	0620.0	0643.1U	28.2	47	~60000U	
245	0623.5	0642.3	181.0	47	UNCAL	

Figure 4 gives the Manila burst profiles. At the higher frequencies the burst structure was almost featureless, lacking usually observed complex structure. Millimeter data from other sources [Croom, 1972], confirms both the high values recorded at Manila at 8800 MHz and the hardness of the spectrum. The long duration and large flux density values resulted in an extremely high integrated flux density. An intensity 2 type II burst was also observed at 24 to 48 MHz between 0629.6 and 0633.5. We shall limit our comments on the dekameter sweep frequency activity until later when we shall briefly summarize our impressions.

On 4 August the PCA continued to increase influenced by the proton flare-burst at 0620 U.T. The peak flux density spectrum of this and other events of the period will be discussed later. Actually the magnitude of the proton event was predictable from the centimeter burst integrated flux density. The PCA at Thule, measured with 30 MHz riometers, exceeded 14 dB on 4 August at 1200 U.T.; other stations measured polar cap absorptions as high as 30 dB. There is no doubt that this was the largest particle event of the series, based on Pioneer IX data [Lincoln and Leighton, 1972] and Explorer 41 and 43 data [Bostrum, 1972]. The 8800 MHz integrated flux density was also the highest.

After the great burst near 0620 U.T., the remainder of 4 August, except for a few small bursts was dominated by noise storm activity. The same was true of 5 August which was extremely quiet at cm wavelengths. On 6 August noise storm activity was present, but now there was a reappearance of short cm burst activity.

7 August 1972

On 7 August noise storm activity at 245 and 410 MHz increased and centimeter bursts became more numerous though there was no 24 to 48 MHz dekametric activity. By 1200 U.T. on 7 August the Thule riometer at 30 MHz had declined to 2.0 dB. Then at about 1422 U.T. the third enormous burst of the period began. This ultimately reached a maximum near 1520 UT. The associated flare at N14, W40 (Long. 10°) was importance 3B beginning at about 1455 UT, reaching maxima at 1521 and 1529 and ending after 1930 UT, according to patrols at Ramey and Boulder. The flare was clearly visible in white light at the Sacramento Peak Observatory for seven or eight minutes with a maximum at about 1522 UT, though it probably began before 1519 UT [Rust, 1973].

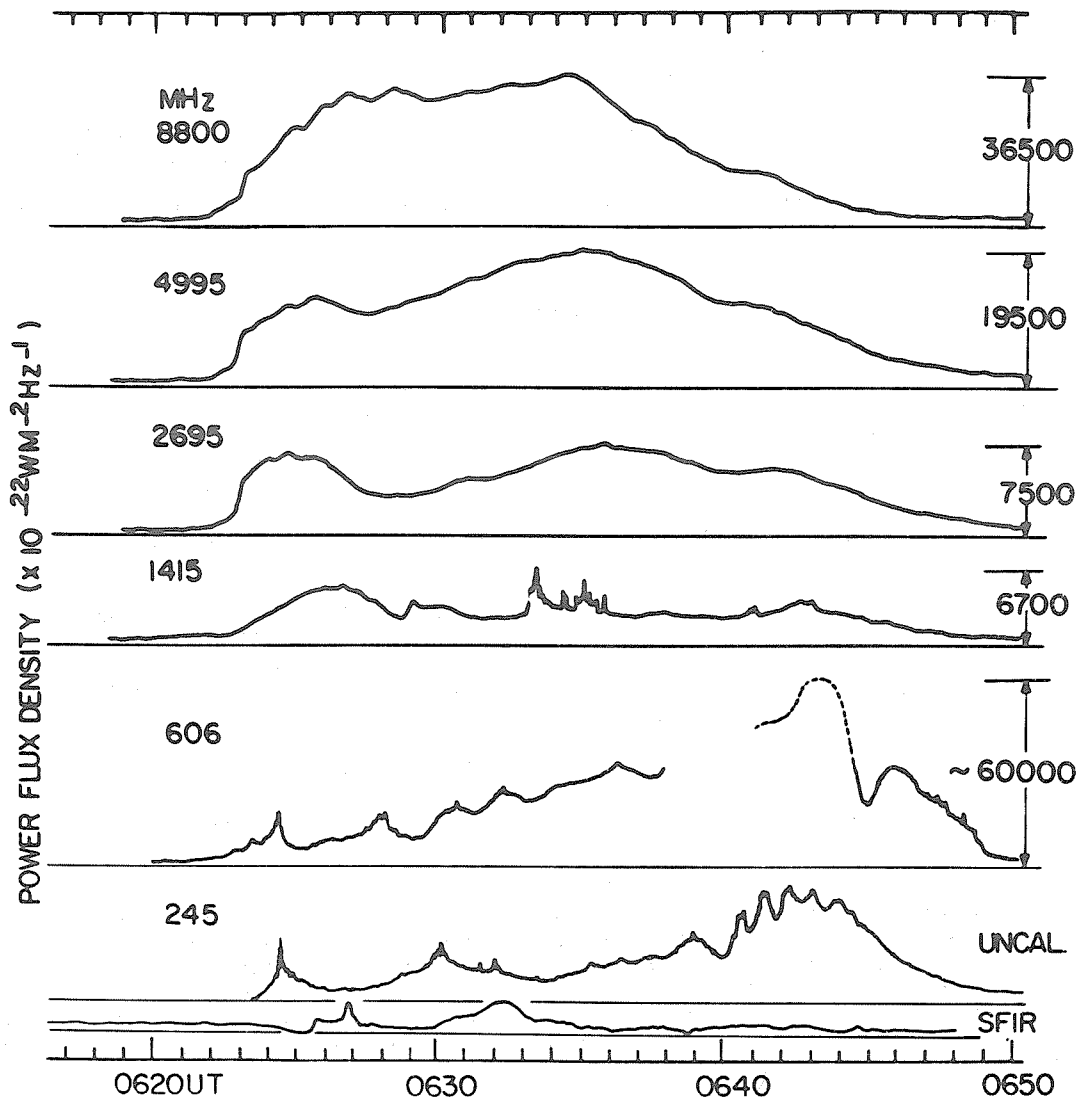


FIG. 4 GREAT RADIO BURST OBSERVED ON 04 AUGUST 1972
AT MANILA OBSERVATORY , R. P.

By 1540 UT a Ground Level Event had begun at the Deep River Neutron Monitor Station. At 1610, this attained a 6.1% increase over the 1540 level. At 2300 UT the level had returned to its original value.

The PCA which early on 7 August had declined to 2.0 dB at Thule, now started to rise again, reaching 10.2 dB at 1800 UT on 8 August and possibly 12.0 dB by 9 August.

The radio event was observed at Sagamore Hill on all systems. Table 5, lists the burst statistics. At mid cm range wavelengths, the burst or at least the preheating started as early as 1422 UT according to information gained from experimental high gain channels. The period between then and the impulsive part of the burst is what Syrovatskii, [1972] would have called the quiet phase of the flare.

Table 5

Burst Data from Sagamore Hill for Event of 7 August 1972 Near 1520 UT

Frequency MHz	Start Time UT	Max Time UT	Duration Minutes	Type Event	Flux Density	
					Peak	Mean
35000	1507.9	1521.8	26.0	47	14700	4800
15400	1443.0	1522.6	23.6	47	18600	4600
8800	1434.0	1521.9	51.4	47	27000	8900
4995	1422.0	1526.6	51.7	47	8400	2100
2695	1435.5	1526.8	63.5	47	3900	980
1415	1458.2	1516.0	31.8	47	4200	1000
606	1451.9	1521.8	38.1	47	6900	1700
410	1451.5	1521.6	39.8	49	9500	1100
245	1436.0	1522.4	58.5	49	1400	340

Figure 5 shows the Sagamore Hill burst profiles of this event. The post-burst increases which are not shown persisted longer than three hours before decaying to pre-burst levels. Note that the complexity of structure is greatest at 15,400 and 35000 MHz. Note also the progressive delay of burst maximum in the 8800 to 2695 MHz range - in contrast to the alignment of various burst components across the entire band. The meter wavelength activity was far from spectacular. It is significant that the 245 and 410 MHz noise storm activity which had continued from 3 to 7 August suddenly ended at about 1752 UT, after the great burst. This quenching of noise storm activity had been noted by Barron, [1972] and many times by Abrami, [1972] at 234 MHz. An intense dekametric type IV event of short duration in the 24 to 48 MHz range began suddenly at 1514.8 and ended at 1555 UT. At somewhat shorter wavelengths the type IV event was in progress earlier. A group of type III's occurred in the dekameter band between 1512 and 1514 UT. Though the occurrence of type III bursts has been documented for proton events, the present authors prefer to relate the times of acceleration(s) of particles to maximum velocities with the short wavelength microwave burst features. They would also relate the evolution of dynamic processes, culminating in dekametric type II bursts; to times when the gradients of short centimeter wavelength burst features were the steepest.

A certain number of qualitative conclusions can be derived from rapid inspection of burst profiles. In figure 5, for example, though burst maxima at the highest frequencies were near 1522 UT, and though the spectrum was quite hard at this time, there were at least two earlier times near 1516 and 1518 UT when burst intensities were very high. While this in itself is qualitatively useful, it is only when we plot the burst flux density spectra for many instants of time that we find quantitative evidence that the burst peak flux density spectrum (above f_{max} near 9000 MHz) was extremely hard at 1516 UT and hardest at 1518 UT. Figure 6 shows the spectra at several different times. We would relate these times to the accelerations and start of mechanisms producing the three type II bursts between ~ 1520 and 1530 reported by Dodge, [1973]. A fourth type II after 1530 UT remains a mystery to us. Our first impulse is to look for features in ~ 200 KeV X-ray ranges late in the event, as described by Frost and Dennis, [1971]. But, without this information, and limited to the microwave data, we can only speculate about a possible significance of the $\lambda \approx 10$ cm. burst "peaking" as late at ~ 1527 , (correlated with meter λ coronal activity) - as a possible indicator of the often invoked but elusive secondary acceleration.

For a short duration impulsive burst, it is logical to invoke a single acceleration of short duration in the flare-burst region. However for a long duration complex burst such as shown in figure 5, it is reasonable to assume that the particle acceleration is not instantaneous, but rather continues over some finite period of time with variations in the acceleration and in the energy distribution of the accelerated electrons. Though there are different theories of how white light flares are produced, most are agreed that the event begins very soon after highly energetic particles are produced. During the 7 August event(s) the white light flare beginning before 1519 UT could not be related to the burst time of maximum near 1522 UT. Rather the time of maximum burst spectral hardness at 1518 UT is the probable time for the beginning of the white light event. The burst power spectral index α at this or any time, relates to the energy spectral index in a known manner only for the ultrarelativistic case. The relation between α and γ in the present case is not precisely known, though progress is being made in this direction, [Ko, 1973].

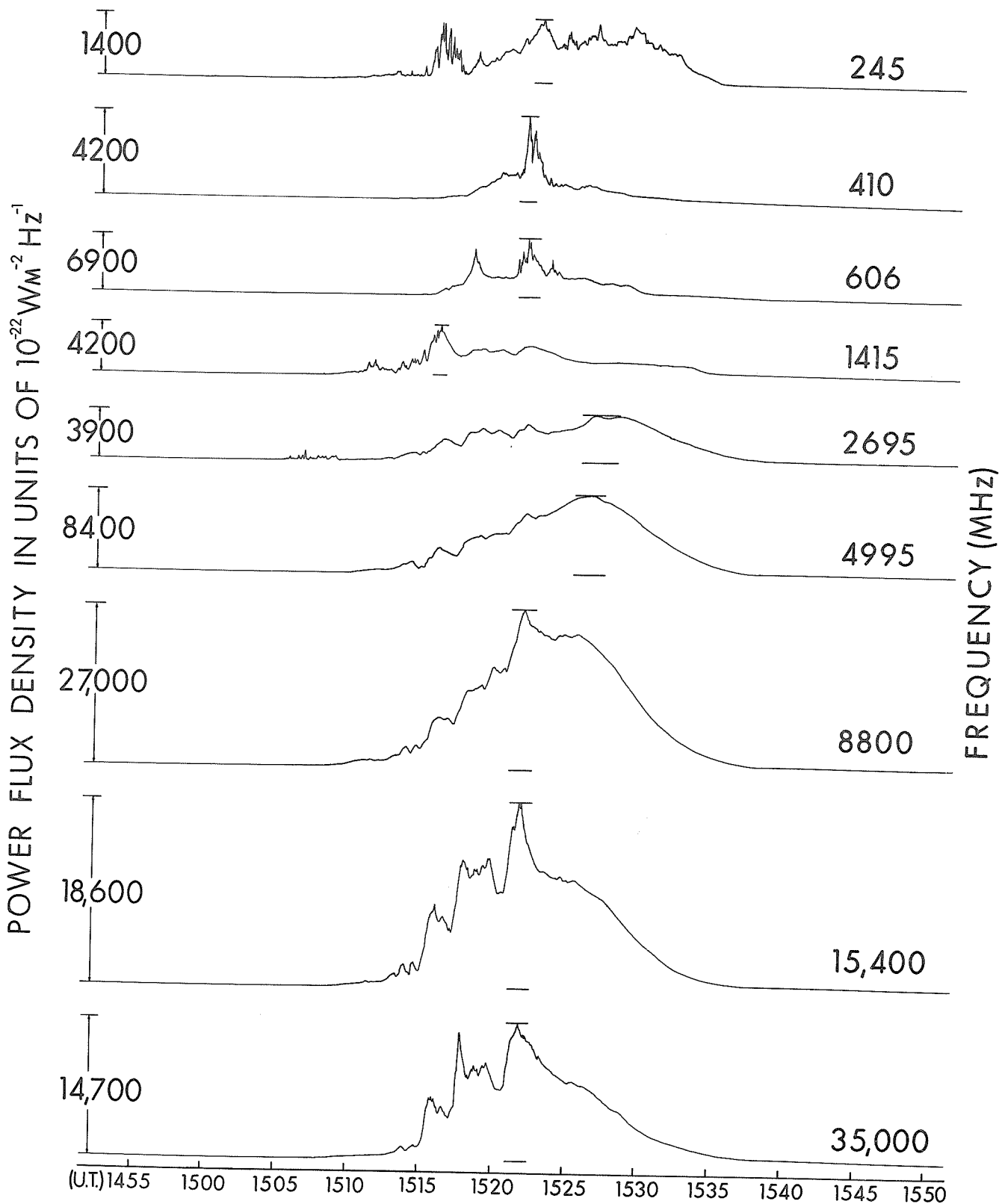


FIG. 5 GREAT BURST OBSERVED 7 AUGUST, 1972
 AT SAGAMORE HILL RADIO OBSERVATORY
 HAMILTON, MASS.

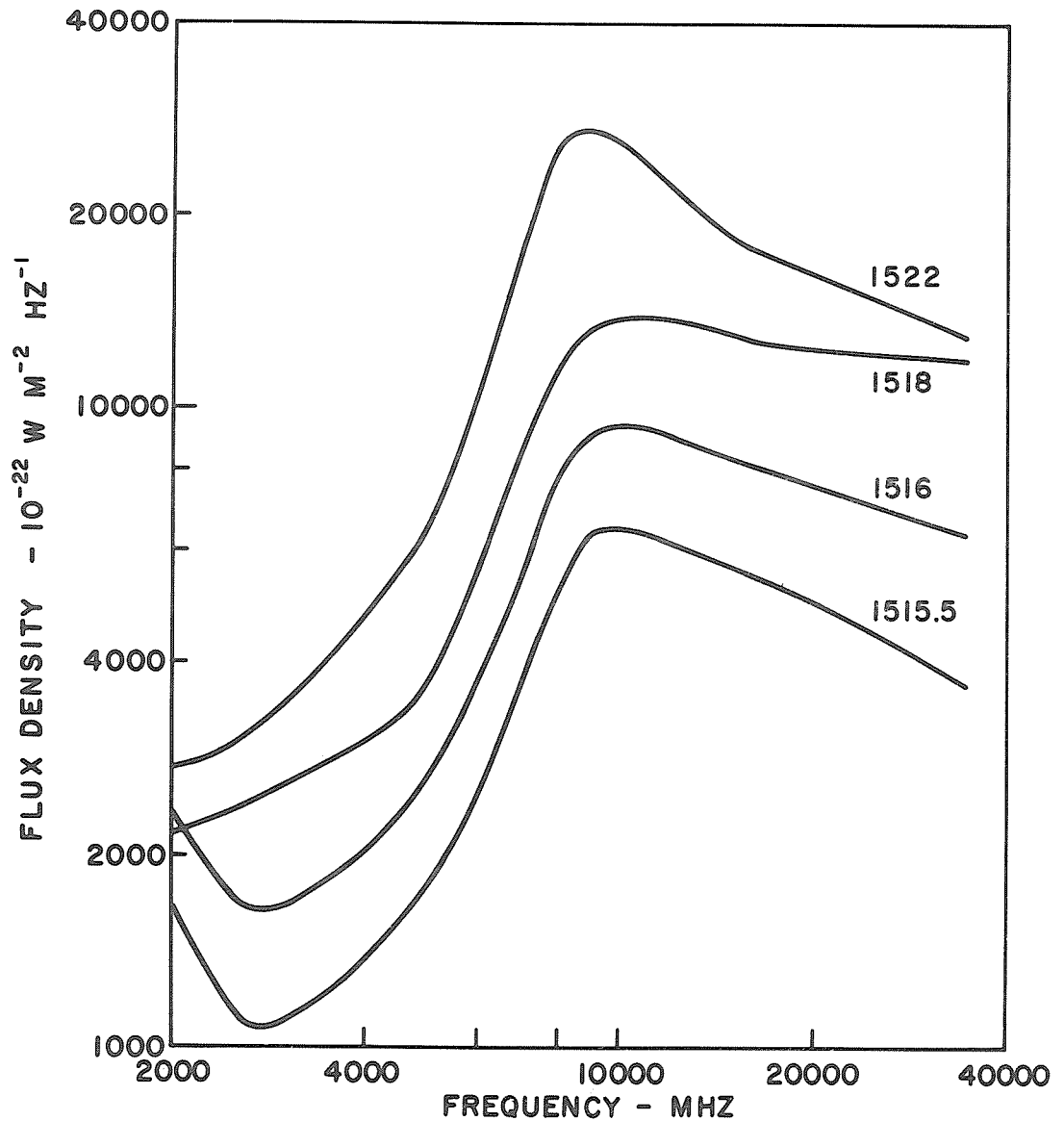


FIG. 6 FLUX DENSITY SPECTRA AT DIFFERENT TIMES DURING EVENT OF 7 AUGUST 1972 (SAGAMORE HILL DATA). NOTE THAT SPECTRUM ABOVE f_{max} IS HARDEST AT 1518 UT.

THE PEAK FLUX DENSITY SPECTRA

During the present sunspot cycle, the peak flux density spectra of bursts have often been considered for their value as signatures of geophysical events [Castelli et al., 1967, and Castelli and Guidice, 1972]. It has been found that great bursts in the 500-10,000 MHz range have a peak flux density spectral signature which has been reliably related to proton events. In the present series, all four of the principal events which exceeded 1000 flux units in the $\lambda = 3$ cm range had the U-shaped spectrum, so called. These are shown in Figure 7. The data unless otherwise noted were recorded at Sagamore Hill or at Manila. The latter had coverage only in the 606-8800 MHz range, while Sagamore Hill monitors the sun additionally at 245, 410, 15,400 and 35,000 MHz. The vertical broken lines in the figure show the range of frequencies where the U-shaped spectral signature is found and for which burst flux density criteria apply. The signature is especially useful for bursts of 1000-10000 f.u. in the $\lambda = 3$ cm range. All four events had a decisive U spectrum.

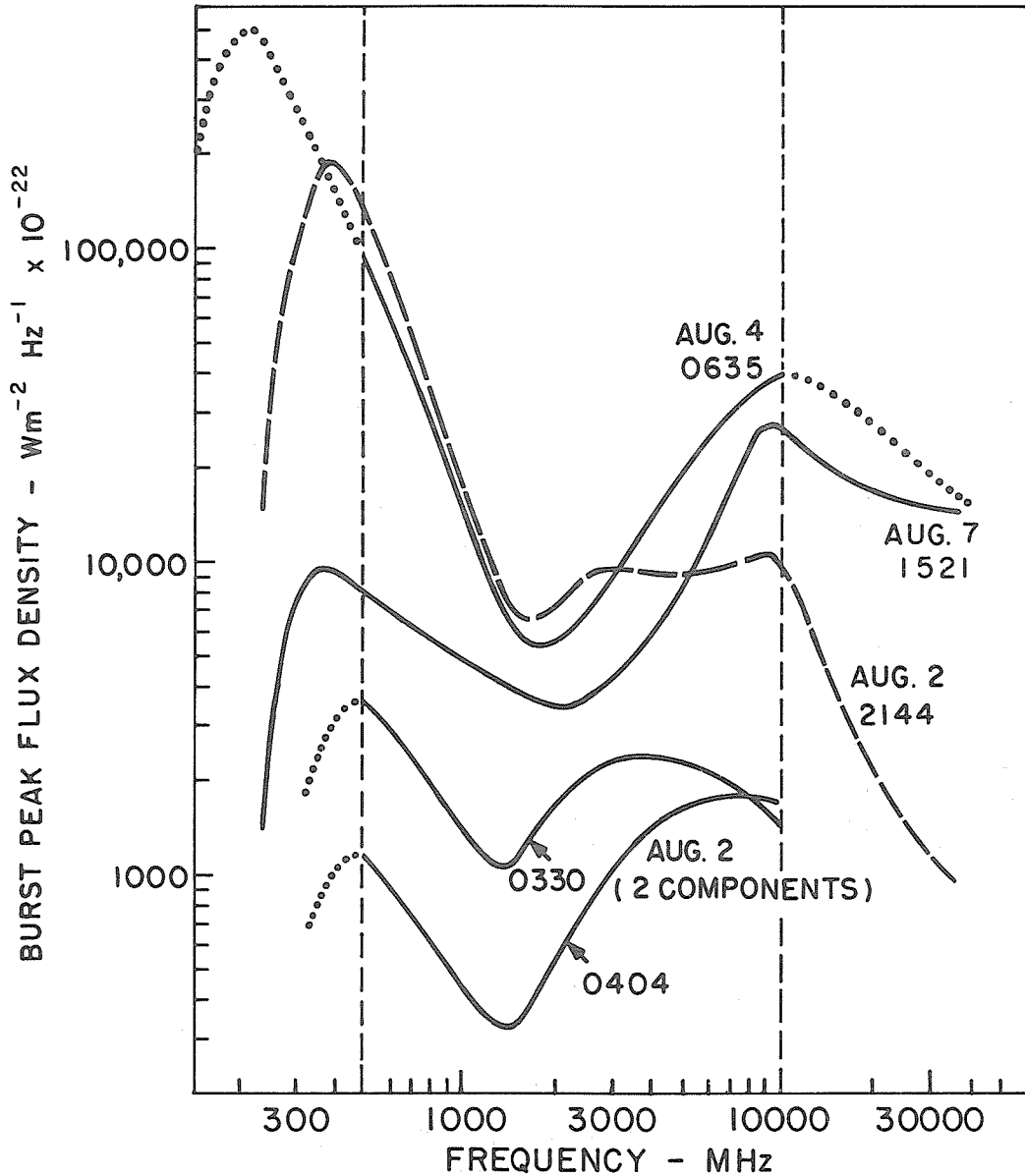


FIG. 7 PEAK FLUX DENSITY SPECTRA OF RADIO EVENTS DURING ACTIVE PERIOD IN AUGUST 1972. NOTE U SHAPED SPECTRA BETWEEN BROKEN LINES USED FOR YES - NO PREDICTION OF PROTON ACTIVITY. NOTE EMISSION PEAKS AND SPECTRAL HARDNESS ON 4 & 7 AUGUST. (SAGAMORE HILL & MANILA DATA)

The data plotted in this figure and the actual bursts from which they were drawn have been seen in earlier tables and figures. The spectrum of the first event of the series is shown in the lower part of the figure. Two spectral components are shown. Because of the far easterly position of the flare-bursts, particle association was weak, with protons slow in arriving. Nevertheless an increased particle count was recorded before the second event of the series followed between 1800 and 2200 UT on 2 August. Data received from other observatories confirms that there was no increase above 10000 MHz or below 500-600 MHz.

The second event of the series was observed some 16-18 hours later. Several things are outstanding about this event. Note the high flux density at 8800 MHz (some 30 times above the quiet sun) but much weaker intensity above 10000 MHz (not a hard spectrum) with less than 1000 f.u. at 35000 MHz. The greatest intensity of this event was in the meter-wavelength range with 100,000 to 200,000 f.u. or about 10,000 times the quiet sun.

The spectrum of the third in the series of events is shown at the top of the figure. This event with a maximum on 4 August at 0635 UT may have been the most intense of the series and appears to have been responsible for the largest increase of >10 MeV particles. Note the extremely high intensities below 500 MHz and above 10,000 MHz. Sections of the curve shown by a dotted line reflect data points from various European observatories. Like the 2 August event, the burst spectrum here was very strong in the meter-wavelength range. Unlike the 2 August event, this event had a hard spectrum at short wavelengths based on millimeter wavelength data reported from Slough at 19,000 and 35,000 MHz.

The fourth event of the series (7 August) had a radio maximum at about 1521 U.T. at Sagamore Hill. The U is present in the figure, but note also the hard spectrum in the short cm and mm-wavelength range. Note also in the meter-wavelength range to the left of the vertical broken line, burst intensities are 1 or 2 orders of magnitude weaker than the events of 2 and 4 August. Yet, this event had both white light flare and ground level cosmic ray association. As discussed earlier, it is believed that the intensity of the burst at short wavelengths and hardness of the spectrum are fairly reliable signatures of more energetic particles for white light flare and GLE association.

From this viewpoint, we might have expected similar associations for the 4 August event. Actually, recently received data collected at the Thule super neutron monitor station [Carrigan, Editor, 1972] shows a GLE starting at about 1325 UT with a maximum at 1433 UT. This event was considerably larger than the GLE of 7 August recorded at the same site. Both the intensity and spectral hardness of the 4 August radio burst in the cm - mm range suggests that the associated GLE might be larger. The long delay between the 4 August GLE onset and the probable source proton-flare-burst at about 0633 is anomalous [Pomerantz and Duggal, 1972] with highly energetic particles arriving so late, possibly after the onset of less energetic protons, e.g., >10 MeV. To the present, no white flare has been associated with the 4 August, 0633 event.

BURST INTEGRATED FLUX DENSITY

While burst peak flux density data as shown in Figure 7 are used as a "yes-no" predictor of PCAs and >10 MeV proton events, the burst integrated flux density (mean flux density times burst duration) can be used as a quantitative predictor of the maximum proton flux with energies >10 MeV [Straka, 1970]. The series of intense bursts in August 1972 provided data to test earlier successful studies on small to moderate size events against very large bursts and proton events.

Burst integrated flux density for the four principal events has been calculated and is given for each available frequency in Joules m⁻²Hz⁻¹ in Table 6.

Table 6

Integrated Flux Density in Units of Joules M⁻² Hz⁻¹

Frequency MHz	2 Aug 0340	2 Aug 2000	4 August	7 August
35000		2 x 10 ⁻¹⁶		0.87 x 10 ⁻¹⁵
15400		7.1 x 10 ⁻¹⁶		1.06 x 10 ⁻¹⁵
8800	4 x 10 ⁻¹⁶	2.4 x 10 ⁻¹⁵	3.5 x 10 ⁻¹⁵	1.84 x 10 ⁻¹⁵
4995	5 x 10 ⁻¹⁶	2.0 x 10 ⁻¹⁵	1.7 x 10 ⁻¹⁵	0.61 x 10 ⁻¹⁵
2695	4 x 10 ⁻¹⁶	1.8 x 10 ⁻¹⁵	0.7 x 10 ⁻¹⁵	0.33 x 10 ⁻¹⁵
1415	2 x 10 ⁻¹⁶	4.2 x 10 ⁻¹⁵	0.7 x 10 ⁻¹⁵	0.25 x 10 ⁻¹⁵
606	3 x 10 ⁻¹⁶	2.34 x 10 ⁻¹⁴	3.7 x 10 ⁻¹⁵	0.22 x 10 ⁻¹⁵
410		4.1 x 10 ⁻¹⁵		0.09 x 10 ⁻¹⁵
245		5.25 x 10 ⁻¹⁵		0.09 x 10 ⁻¹⁵

The integrated flux density spectra are shown in Figure 8. In general, the spectra are similar to the peak flux density spectra of Figure 7. At 8800 MHz, the integrated flux density of 3.5×10^{-15} Joules $m^{-2}Hz^{-1}$, for the 4 August event, was among the highest of the sunspot cycle.

BURST ENERGY (TRANSFORMED INTO RADIATION)

From the data presented in Table 6 and Figure 8, it is possible to determine the energy for the several bursts at the sun for portions of the radio band. These data are presented in Table 7. Beyond this, one can arrive at corresponding estimates of energy in the H-alpha and X-ray bands. During the period, in the radio events, there was a shift (over days) in the outpouring of energy from the lower frequency band to the higher frequency part of the observed spectrum.

Table 7

Burst Energy

Event	Energy - Ergs 600 - 8800 MHz	Energy - Ergs 600 - 35,000 MHz
2 August 1972 0330 UT	4.7×10^{24}	
2 August 1972 2130 UT	39×10^{24}	71×10^{24}
4 August 1972 0630 UT	21×10^{24}	$120 \times 10^{24} *$
7 August 1972 1520 UT	8.9×10^{24}	49×10^{24}

* From use of Manila data with additional input from Slough, England

DEKAMETER SWEEP FREQUENCY ACTIVITY

Dekameter activity played an important role in the period. While Sagamore Hill and Manila complement each other, they both operate with a limited bandwidth (24-48 MHz). Because of the spectral characteristics of coronal events, sometimes radio emission is so weak as to be undetected at heights where 24-48 MHz emission originates. Nevertheless, strong events are observed in this range. Recognizing that there are restrictions of limited bandwidth, one may still gain a picture of the large amount of dekameter activity which occurred by referring to Figure 9. There can be no doubt that some of the longest duration Type IV events ever recorded took place between 2 and 5 August 1972.

CONCLUSIONS

The highlights of radio activity during disk passage of McMath plage No. 11976 have been presented. The events which the authors feel are most important from a solar physics viewpoint have been emphasized. The characteristics of the 31 July events allow for almost unambiguous interpretation of bursts having this type spectrum. The availability of several types of data for correlation with the radio event on 7 August, have been helpful in studies which relate to the particle-acceleration-mechanism and timing. Detailed analysis of burst spectral slope development at frequencies above f_{max} offers an exciting new application of microwave burst data.

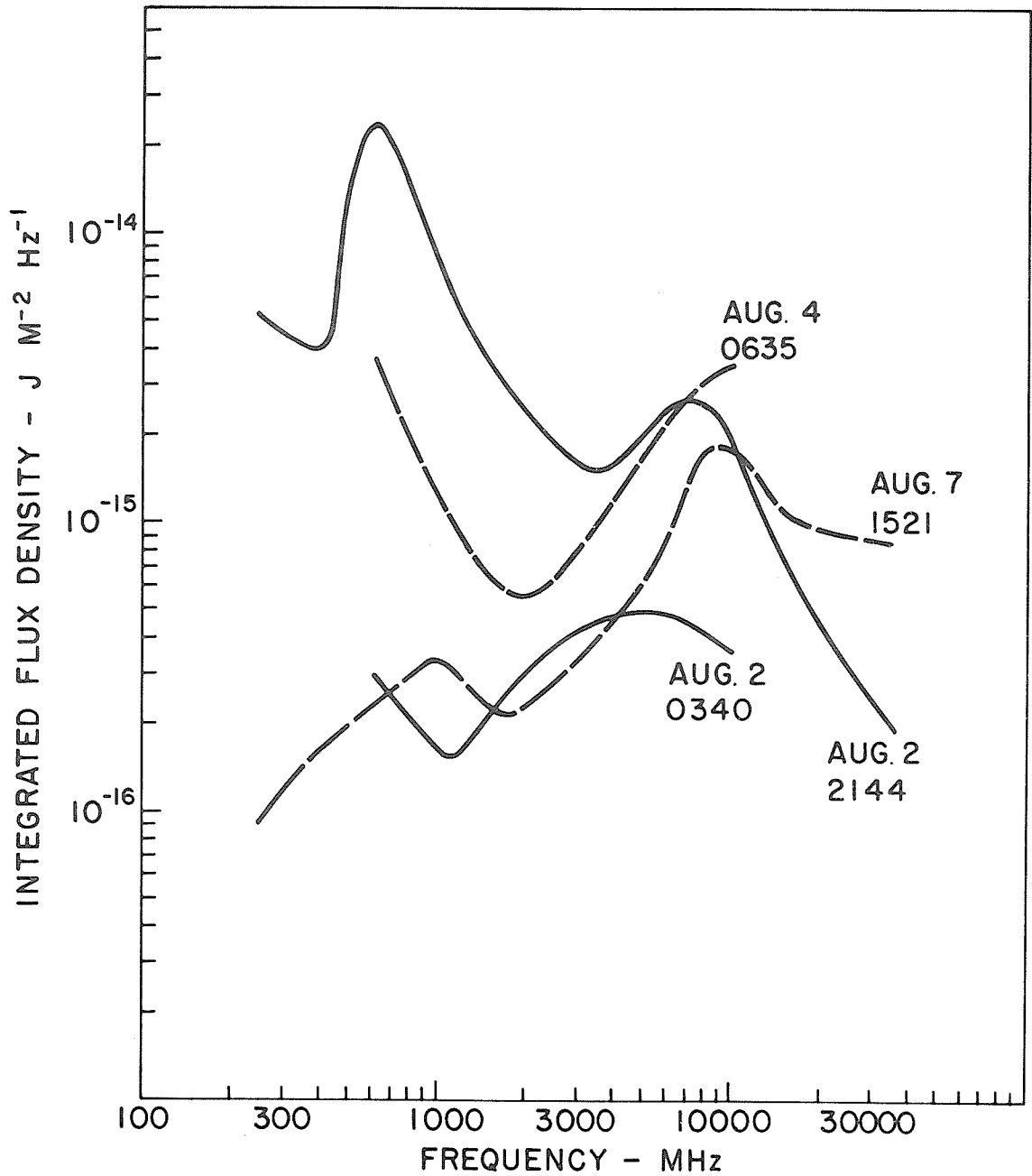


FIG 8 INTEGRATED FLUX DENSITY FOR PROTON ASSOCIATED BURSTS OF AUGUST 1972. CURVES DERIVED FROM SAGAMORE HILL AND MANILA DATA.

Castelli, J.P. W.R. Barron and J. Aarons	1973	Solar activity in August 1972, A.F. Cambridge Research Labs., <u>AFCRL- TR-73- 0086</u>
Castelli, J.P. D.A. Guidice D.J. Forrest and R.A. Babcock	1973	Solar Bursts at $\lambda = 2$ cm on 31 July, 1972 , Submitted to <u>J. Geophys. Res.</u>
Croom, D.	1972	<u>Solar Radio Bulletin, No 34</u> , Radio and Space Research Station, Ditton Park, Slough, England
Dodge, J.C.	1973	Interferometric radio spectrum of the solar corona, 1-11 August 1972. <u>Univ. of Colorado, Dept of Astro-Geophysics, No. SN-1.</u>
Frost, K.J. and B.R. Dennis	1971	Evidence from hard x-rays for two stage particle acceleration in a solar flare, <u>Astrophys. J. 165 655-659</u>
Guidice, D.A. and J.P. Castelli	1972	Spectral characteristics of microwave bursts, <u>Proc of NASA Symposium on High Energy Phenomena on the Sun, Greenbelt, Maryland, September 1972</u>
Ko, H.C.	1973	Private Communication
Lincoln, J.V. and H.I. Leighton	1972	Preliminary compilation of data for retrospective world interval July 26- August 14, 1972. U.S. Dept. of Commerce, <u>World Data Center A, Report # UAG-21</u>
McKinnon, J.A.	1972	August 1972 solar activity and related geophysical effects. <u>NOAA Technical Memorandum TM-ERL SEL-22.</u>
Najita, K. and F.Q. Orrall	1970	White light events as photospheric flares, <u>Solar Phys., 15, 176-194</u>
Pomerantz, M.A.	1972	Private Communication
Svestka, Z .	1966	Optical observations of solar flares, <u>Space Science Reviews, 5, 388-418.</u>
Svestka, Z.	1970	The phase of particle acceleration in flare development, <u>Solar Phys., 13, 471-489.</u>
Syrovatskii, S.I.	1972	Solar flare time development: three phases, <u>Comments in Astrophysics and Space Physics, Vol. 4, No 8, 65-70.</u>
Takakura, T.	1967	Theory of solar bursts, <u>Solar Phys., 1, 304-353.</u>
Zirin, H.	1973	Private Communication

"A Synoptic View of the Slowly Varying Component of
the Solar Radio Emission During 1972, With Special
Emphasis on the Period 26 July Through 14 August"

by

W.J. Decker and F.L. Wefer
Department of Astronomy
The Pennsylvania State University
University Park, Pennsylvania

Introduction

The Pennsylvania State University Radio Astronomy Observatory (PSURAO) conducts a daily solar patrol at 10.7 GHz, 2.70 GHz and 0.960 GHz. The radiometers and their calibration have been discussed in detail by Hagen and Wefer [1971]. The radiometers are operated primarily as a burst patrol. While the output of each of the three radiometers is recorded at two different gains, the extremely high flux densities of the largest microwave events during the period 26 July through 14 August were well off-scale on all recorder channels. Because of this we are here centering our attention on the slowly varying or S-component during 1972, with special emphasis on the Retrospective World Interval 26 July through 14 August 1972. The PSURAO burst data were included in the preliminary compilation of data for this period by Lincoln and Leighton [1972]. Copies of the chart records will be provided upon request.

Source and Description of Data

Measurements of the background solar flux density are made at eight frequencies daily near 17:00 UT at the Sagamore Hill Solar Radio Observatory of the Air Force Cambridge Research Laboratories (AFCLR). These measurements adjusted to 1 AU are published in the prompt reports section of Solar-Geophysical Data. The background solar flux density is also measured daily near 17:00 UT and adjusted to 1 AU, at PSURAO at three frequencies; however, these daily flux values are not presently regularly published. The data presented in this paper are from these two sources. Table 1 shows the ten radio frequencies of the data and the source of each.

Since it is the change with time of the background solar flux density which is of interest, not the value of the flux density directly, the quantity which will be presented is the relative background solar flux density or "% flux" defined by

$$\zeta_{\nu}(t) = \frac{S_{\nu}(t) - \bar{S}_{\nu}}{\bar{S}_{\nu}} \times 100 \%$$

where $\zeta_{\nu}(t)$ = % flux at frequency ν and time t ,

$S_{\nu}(t)$ = background solar flux density at frequency ν and time t , and

\bar{S}_{ν} = average value of $S_{\nu}(t)$ over the time interval of interest.

In this presentation \bar{S}_{ν} is the average of the available noon values during 1972. These averages are given in Table 1.

There are several advantages in using $\zeta_{\nu}(t)$ instead of $S_{\nu}(t)$ directly. The % flux is more indicative of the S-component since it incorporates both the flux density value and the long term average. The time average of $\zeta_{\nu}(t)$ is zero at each frequency, so that when presented as a contour map, the reference level in the frequency-time plane is horizontal. Comparisons of $\zeta_{\nu}(t)$ at different frequencies are more sound since the % flux is immune from multiplicative calibration errors, including errors in the measurement of the antenna effective areas. The importance of this can be seen in Table 1 where the 2.70 GHz average is anomalously high for this reason.

Table 1. The sources of the data, the logarithms of the radio frequencies, the averages of the 1972 daily flux values, and the heights above the photosphere at which the optical depth reaches unity are tabulated for each of the ten radio frequencies at which data are being used.

Frequency (GHz)	Source of Data	Log ν (GHz)	\bar{S}_ν $10^{-22} \text{ W m}^{-2} \text{ Hz}^{-1}$	$h_{\tau=1}$ 10^3 km
15.4	AFCL	1.19	533	7.2
10.7	PSURAO	1.03	419	9.4
8.80	AFCL	0.94	282	9.6
5.00	AFCL	0.70	157	10.5
2.70	PSURAO	0.43	194	11.5
1.42	AFCL	0.15	80.8	12.8
0.960	PSURAO	-0.02	72.8	14.0
0.606	AFCL	-0.22	56.4	16.0
0.410	AFCL	-0.39	29.3	19.2
0.245	AFCL	-0.61	13.2	32.0

Frequency - Time Contour Map

The % flux during 1972 is presented in Figure 1 as a contour map in the log frequency-time plane. The map is in 3 four-month strips, the right-hand strip covering the period 1 January through 2 May, the middle strip covering 2 May through 1 September, and the right-hand strip 1 September through 1 January 1973. The ordinates are labelled in log frequency. The values of the logarithms of the ten frequencies at which data are being used are given in Table 1 above. The abscissae are labelled in days, with the tic marks located at 17:00 UT. The triangles along the abscissae indicate the time at which the Carrington longitude of the central meridian was zero. Approximately 13.5 synodic rotations are shown, starting with rotation number 1583 beginning on 31.4 December 1971.

In producing the map the values of $S_\nu(t)$ were first converted to $\zeta_\nu(t)$ at each of the ten radio frequencies. Missing values were then filled in by linear (in log ν) interpolation and extrapolation in $\zeta_\nu(t)$. Finally the entire grid for a day (226 x 4) was filled in by linear interpolation, first in log frequency, then in time. The integerized values of % flux were used as indices in printing a symbol in each rectangle of the grid. A portion of the symbol table is shown in Figure 2. The contour lines were drawn at 10%, 30%, 50%, 70%, and 90%. The contour lines have not been labelled since there are only four ambiguous areas. These are lows on the left-hand strip and are indicated by "L". Areas where the % flux exceeded 100% have been completely blackened. During 1972 such areas occurred only at radio frequencies less than 0.5 GHz. An enlargement of the portion of the map covering the interval 25 June through 1 September is shown in Figure 3.

Values of the height above the photosphere at which the optical depth reaches unity at the center of the disk are given in Table 1 [Hagen and Barney, 1968]. These values are naturally lower than the altitudes of active regions summarized by Graf and Bracewell [1973]. Because the $\tau = 1$ height is nearly linear in log frequency for $\nu \geq 1$ GHz, the log frequency-time contour map is also, in a sense, a contour map in the altitude-time plane. The high directivity of S-component sources at low frequencies accounts in large measure for the narrow appearance in time of the enhanced areas along the right-hand side of each strip in Figure 1. The emission from active regions at the low frequencies originates much higher in the atmosphere than the high frequency emission, and in Figure 1 they appear in many cases to be independent. At frequencies greater than 1 GHz, there were seven periods in 1972 during which the % flux exceeded 20%. The periodicity of the S-component is apparent in Figure 1, as is the general decline in solar activity evidenced by the predominance of negative % flux values on the right-hand strip.

← TIME (DAYS)

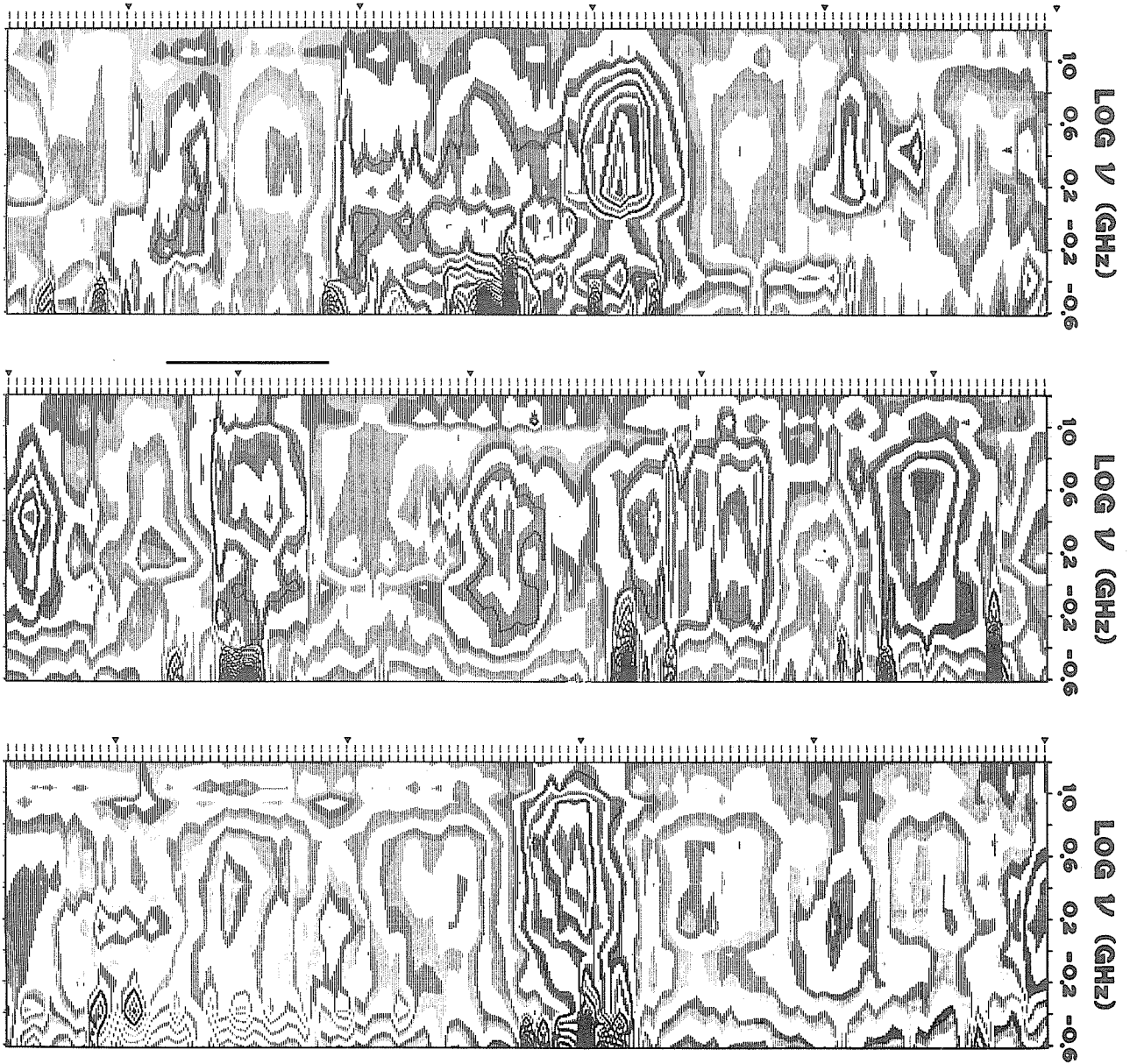


Fig. 1. Contour map of the % flux in the log frequency-time plane for 1972.

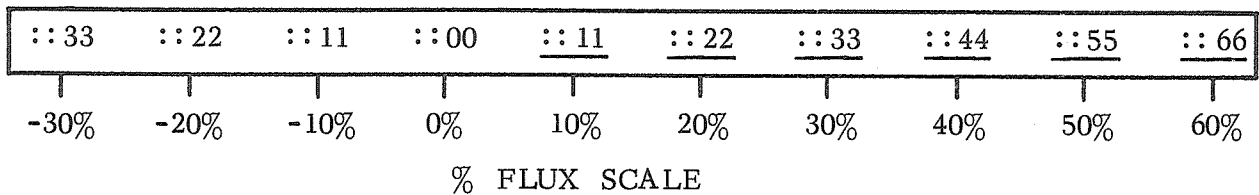


Fig. 2. A portion of the symbol table used in printing the frequency-time contour maps is shown. Eight symbols correspond to a change of 10% in the % flux.

← TIME (DAYS)

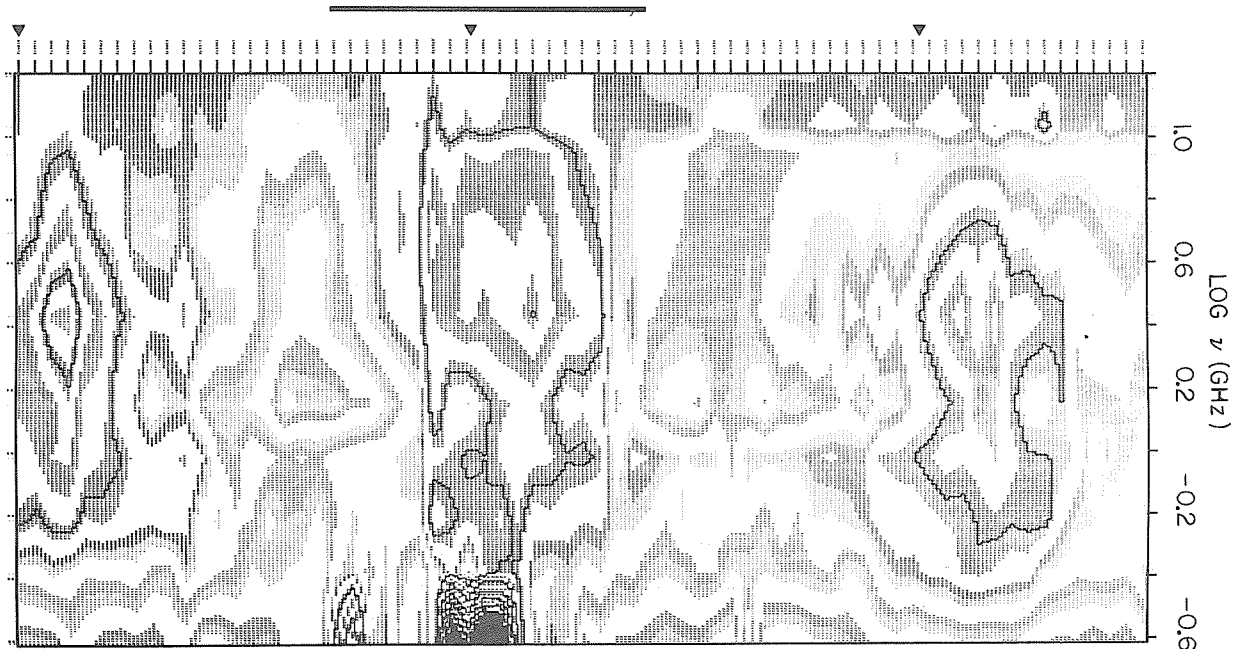


Fig. 3. An enlargement of Figure 1 showing the contour map of % flux for a two month period including the Retrospective World Interval.

The maximum and minimum % flux values for 1972 are shown as a function of radio frequency in Figure 4. The dip in the maximum % curve near 1 GHz was unexpected. The maximum values at 5.00, 2.70, 1.42 and 0.960 GHz all originate in the enhanced area near the center of the left-hand strip of Figure 1. The structure of this single area therefore strongly effects the shape of the maximum curve and causes the dip. It is not unusual for enhanced areas on % flux contour maps to display this structure. Two additional examples are the area near the center of the right-hand strip of Figure 1 and the area associated with the Behind-The-Limb event of 1 September 1971 [Wefer, 1972].

The Retrospective World Interval

The Retrospective World Interval 26 July through 14 August 1972 is indicated in Figures 1 and 3 by the black band along the ordinates. The 9.1 cm. Stanford maps and the 10.7 cm. ARO East-West Scans [Lincoln and Leighton, 1972] indicate that during much of this period McMath Region 11976 was the dominant region on the disk and so was mainly responsible for the enhanced area on the frequency-time % flux contour map. A comparison of the development of the enhanced area with the appearance of region 976 is instructive. Region 976 first appeared on the McMath-Hulbert Calcium Report [Lincoln and Leighton, 1972] on 28 July, although X-Ray and 9.1 cm active regions were apparent on the east limb on 27 July. The % flux first reached 10% on 28 July, and remained high through the central meridian passage of region 976 on 4 August. The % flux decreased to less than 10% on 8 August, the day following the large flares, and several days before region 976 completed west limb passage.

The % flux peaked at 30.2% at 2.70 GHz on 1 August. Note the extensions of the 10% contour line towards higher frequencies on 1 and 7 August. The AFCRL data on 7 August were effected by a burst, and both of these features are probably artificial in the sense that the measurements do not correctly reflect the strength of the S-component alone. The maximum % flux values during the Retrospective World Interval are shown in Figure 4. The enhanced area whose association with region 976 was shown above appeared one rotation before and three rotations after the Retrospective World Interval, although the association of these four enhanced areas with the calcium plage regions is not clearly established because of the presence of other active regions on the disk.

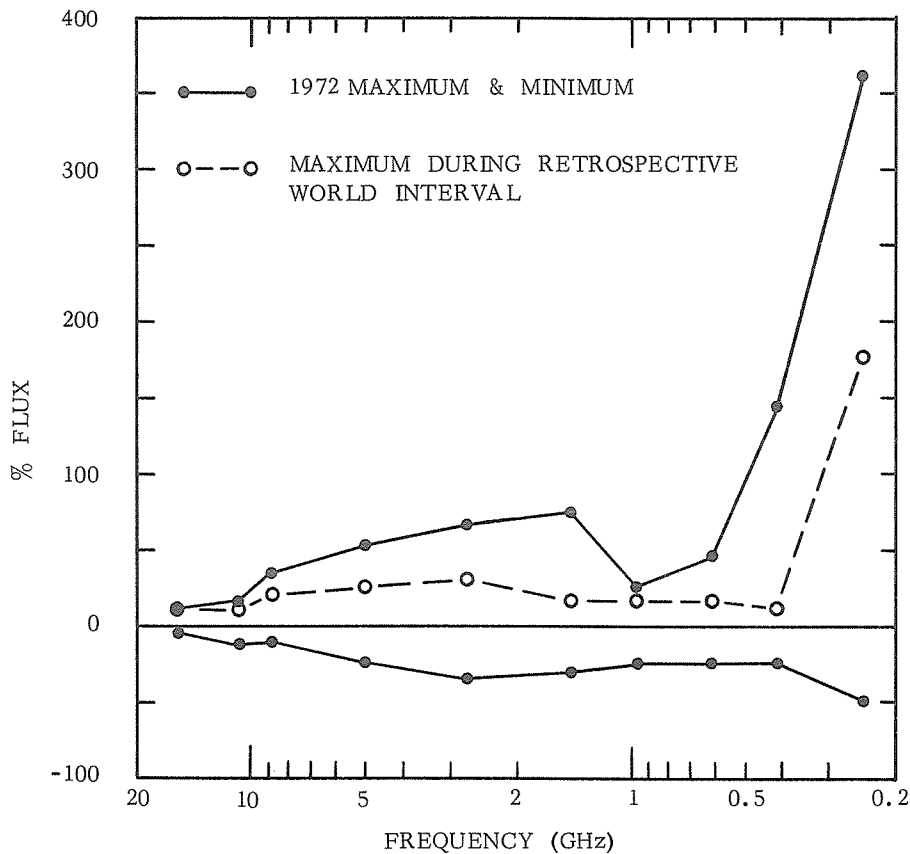


Fig. 4. Maximum and minimum envelopes for the % flux during 1972, as functions of radio frequency.

Single Frequency Synoptic Maps

Single frequency synoptic maps for 1972 are shown in figures 5, 6 and 7. This type of map was devised to show the relation between successive increases in the S-component. These maps were constructed as follows. First, each daily % flux value was assigned an abscissa (X) and an ordinate (Y) where

- X = number of days since the n th. central meridian passage of Carrington longitude zero, and
 Y = n , the synodic rotation number.

While each daily value of % flux has an infinite set of coordinates, only those for which $0 \leq X \leq 54.5$ were placed on the initial grid of the maps. Each value of % flux thus appears twice. Points were then filled in on the initial grid at intervals of 1/4 day in X and 1/18 rotation number in Y by linear interpolation. On days for which data were not available, the data for the previous and following days were extrapolated for 1/2 day. Similarly, data for the previous and following rotations were extrapolated for 1/18 rotation. Finally, the maps were printed for each frequency using the symbol table of Figure 2. Contour lines were drawn at the -20%, -10%, 0%, 10%, and 20% levels, except at 0.245 GHz where the -10% and 10% contours were omitted for clarity. The vertical lines at X = 13.75, 27.25 and 41.00 days indicate 0.5, 1.0 and 1.5 rotations in the X direction, respectively. The gap in the data at 2.70 GHz extending from the start of rotation 1587 to the middle of rotation 1588 was due to damage to the radiometer caused by lightning.

The Retrospective World Interval is bracketed by triangles on each map at 16.7 and 34.7 days after the start of synodic rotation 1590. The brightening associated with the disk passage of region 976 is not as prominent on these maps as, for example, the passage of region 11748 near the end of synodic rotation 1584. Region 976 is, however, seen to be one of a group of regions which contributed to a general brightening of the hemisphere visible when $L_o = 30^\circ$. This general brightening persisted for five rotations starting with synodic rotation 1587.

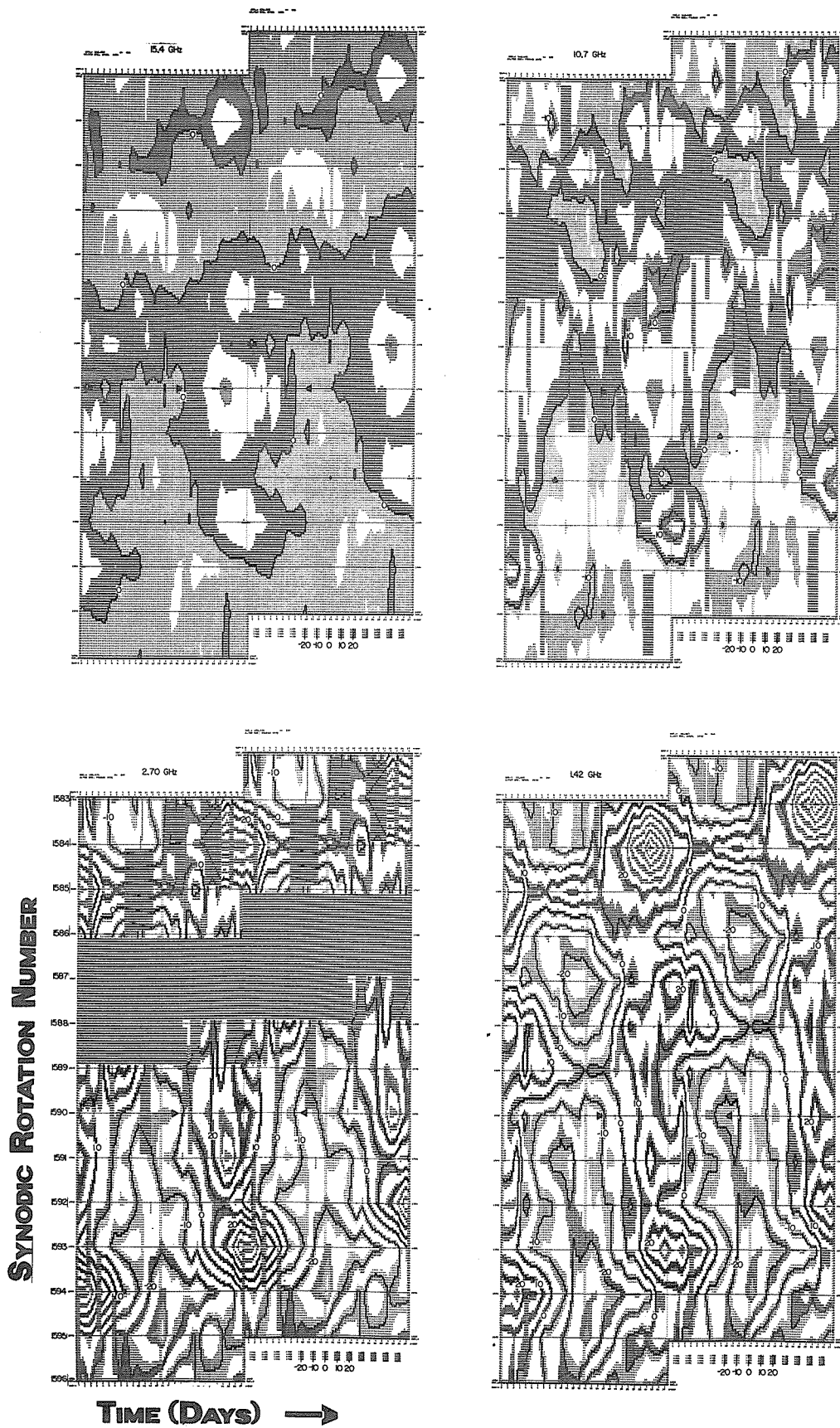


Fig. 5. Single frequency synoptic maps for 1972 at frequencies of 15.4, 10.7, 2.70 and 1.42 GHz.

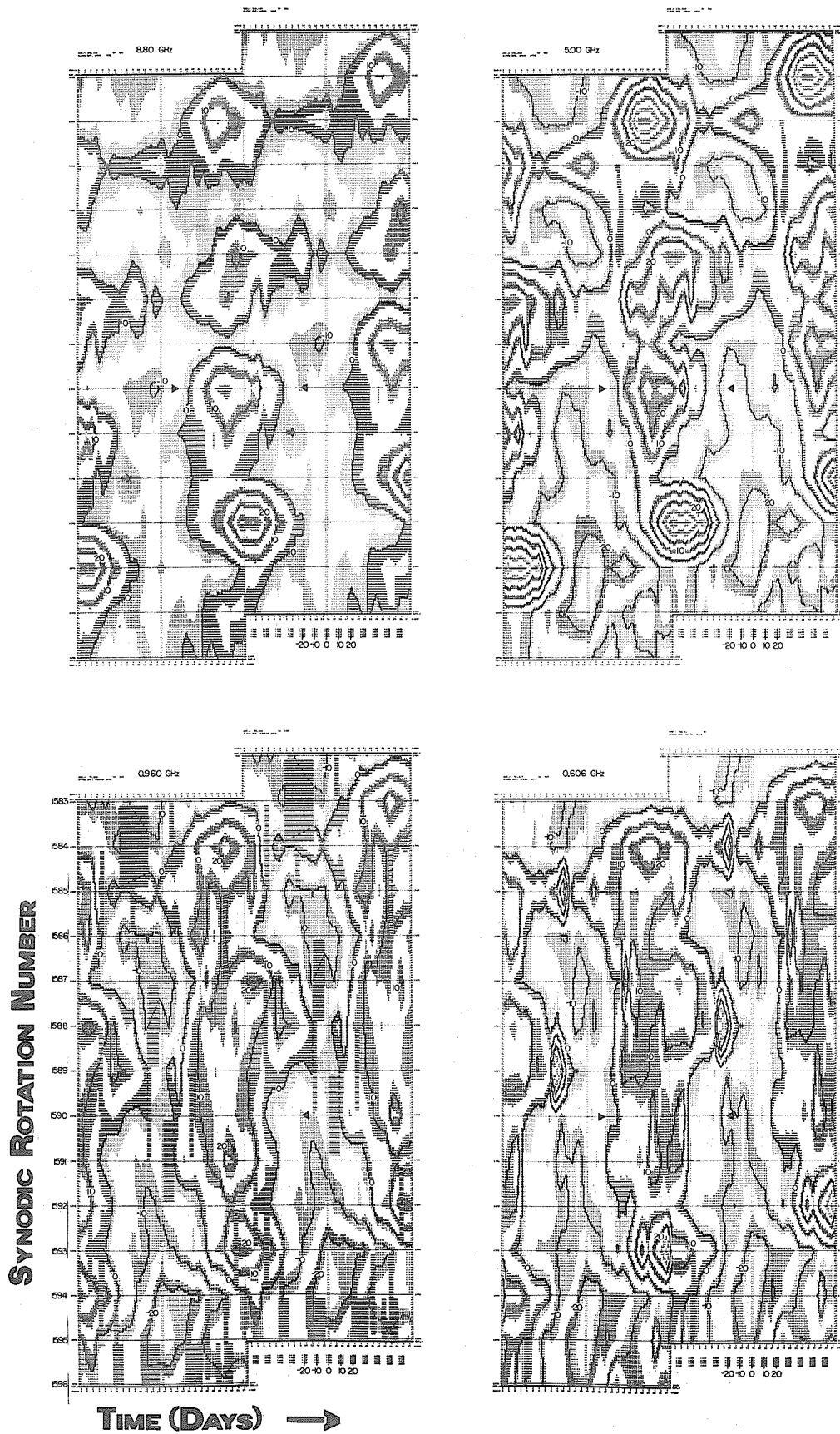


Fig. 6. Single frequency synoptic maps for 1972 at frequencies of 8.80, 5.00, 0.960, and 0.606 G

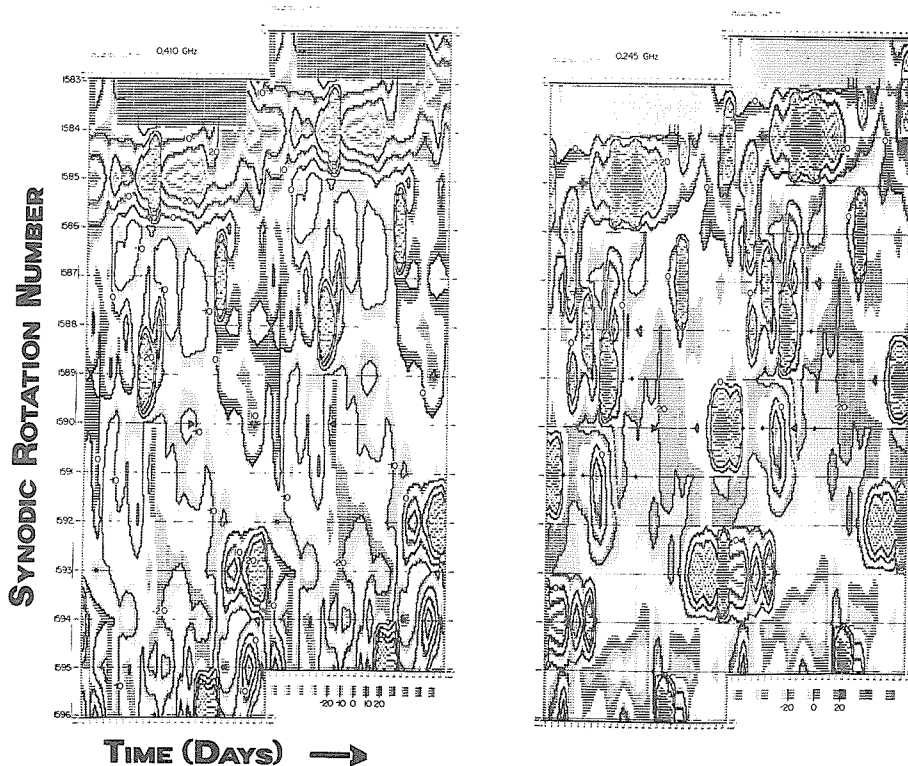


Fig. 7. Single frequency synoptic maps for 1972 at frequencies of 0.410 and 0.245 GHz.

These maps are convenient in the sense that they allow a large amount of data to be displayed in a concise form; however, each daily value of % flux is composed of contributions from all active regions on the visible disk of the sun and each of these can undergo a significant variation in brightness in a period of time less than that required for disk passage. Because of this, caution must be used in attempting to infer that two or more successive peaks in the % flux on two dates separated by a synodic rotation are due to the return of the same active region. A detailed analysis of the single frequency synoptic maps covering a period of approximately one solar cycle is currently in progress at PSURAO.

REFERENCES

- | | | |
|-------------------------------------|------|--|
| Graf, W. and
Bracewell, R.N. | 1973 | The Height of 9.1 cm Solar Emission from Latitude Shift, <u>Solar Physics</u> , <u>28</u> , 425-433. |
| Hagen, J.P. and
Barney, W.M. | 1968 | A Model for the Early Stage of Solar Radio Bursts, <u>Ap. J.</u> , <u>153</u> , 275-283. |
| Hagen, J.P. and
Wefer, F.L. | 1971 | A Catalog of Distinct Solar Radio Events for Fixed Frequency Observations Made at The Pennsylvania State University Radio Astronomy Observatory During the Period 1 July 1964 Through 30 June 1970, <u>The Pennsylvania State University, Dept. of Astronomy Scientific Report No. 023</u> . |
| Lincoln, J.V. and
Leighton, H.I. | 1972 | Preliminary Compilation of Data for Retrospective World Interval July 26 - August 14, 1972, <u>World Data Center A for Solar-Terrestrial Physics, Report UAG - 21</u> . |
| Wefer, F.L. | 1972 | Centimeter Wavelength Observations of the Behind-the-Limb Flare of 1 September 1971, <u>World Data Center A for Solar-Terrestrial Physics, Report UAG - 24, Part II</u> , 327-333. |

Solar Radio Events at 9.4 to 71 GHz in the Period 26 July - 14 August 1972

by

D. L. Croom and L. D. J. Harris
Science Research Council
Radio and Space Research Station
Ditton Park, Slough, Bucks, England

During the period 26 July to 14 August 1972, a total of 31 events were recorded at Slough on one or more frequencies in the range 9.4 to 71 GHz. Six of these resulted in bursts on 37 GHz, including the two major events on 4 and 7 August, and details of these events are listed in Table 1. The bursts themselves are shown in Figures 1 to 5 and their spectra in Figure 6. In compiling, spectra data from the Air Force Cambridge Research Laboratories, Mass., U.S.A. have been included for three events which were observed at both stations.

Table 1

Main Radio Events Recorded at Slough

Date	Freq. (GHz)	Start (UT)	Max. (UT)	Dur. (Min)	Type	Flux Density $10^{-22} \frac{Wm^{-2}}{Hz}$	Remarks	
72 08 01	9.4	0838.5	0841.1	10	3	156	Tropospheric Interference	
	19.0	0839.5	0840.7	4	3	290		
	37.0	0840	0841.1	2	3	100		
	71.0	No Event Greater than 70 Flux Units						
72 08 01	9.4	0915	0925.8	38	45	105		
	19.0	0917.5	0921.7	24	45	453		
			0925.9			238		
	37.0	0920	0921	1.5	3	45		
72 08 02	9.4	1838.5	1840.0	3u	4	505		Events near sunset F.D. increase relative to post-burst increase
		1854	1855.0	2	4	98		
		1907.5	1908.5	2.5	4	134		
		1840.0	1840.0	u	30	109		
	19.0	1838.6	1840.0	2u	4	475		
		1840.6	1840.6	8.5	30	235		
		1854	1855.0	1.2	4	176		
		1908.5	1909.0	1.0	3	162u		
	37.0	1839.0	1840.0	2.0	4	960	Two spikes of comparable magnitude	
	71.0	Sunset						
72 08 04	9.4	0619.0	0626.8	120	47	14,370	± 10%	
	19.0	0620.0	0626.8	70	47	25,000		
	37.0	0621.9	0626.7	38	47	13,780		
	71.0	0622	0628u	15	47	11,500u		± 25%
72 08 07	9.4	1507	1522.5	100	47	13,750	± 10%	
	19.0	1508	1522.2	87	47	27,200		
	37.0	1510.9	1522.3	29	47	11,100		
	71.0	No Record						
72 08 10	9.4	1103.9	1104.5	3	4	150		
	19.0	1104.2	1104.8	2	4	280		
	37.0	1104.4	1104.5	1	4	180		

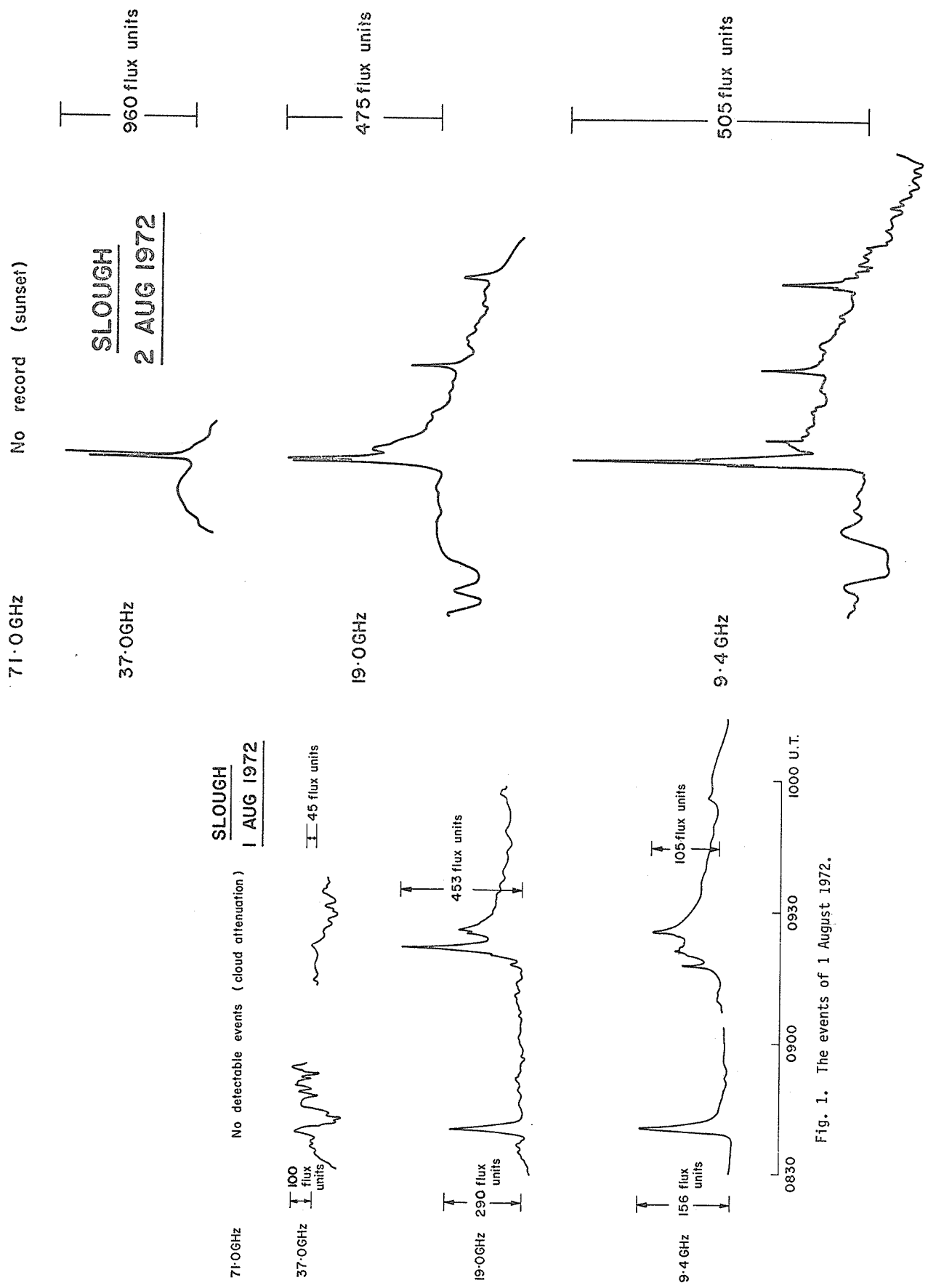


Fig. 1. The events of 1 August 1972.

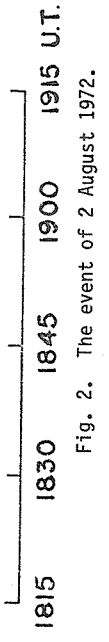


Fig. 2. The event of 2 August 1972.

71.0 GHz

No record

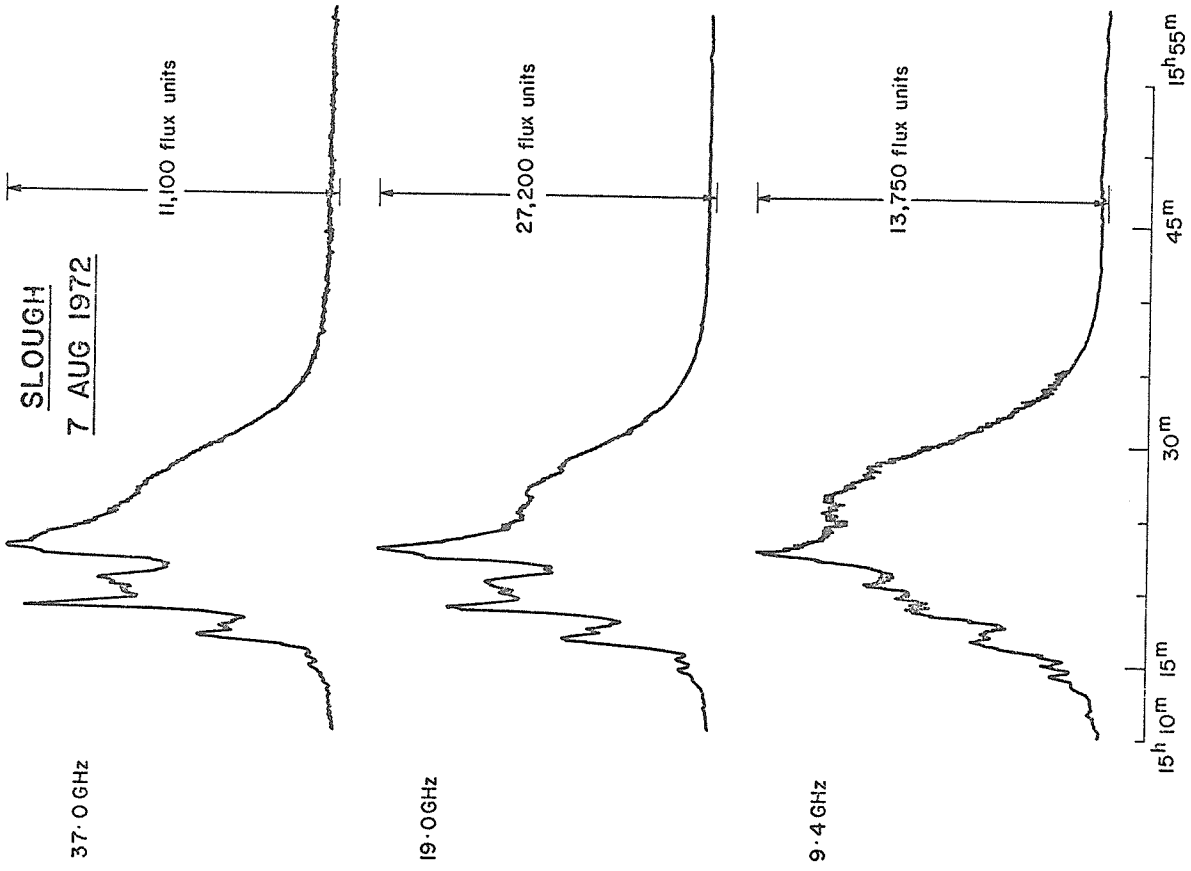


Fig. 4. The event of 7 August 1972.

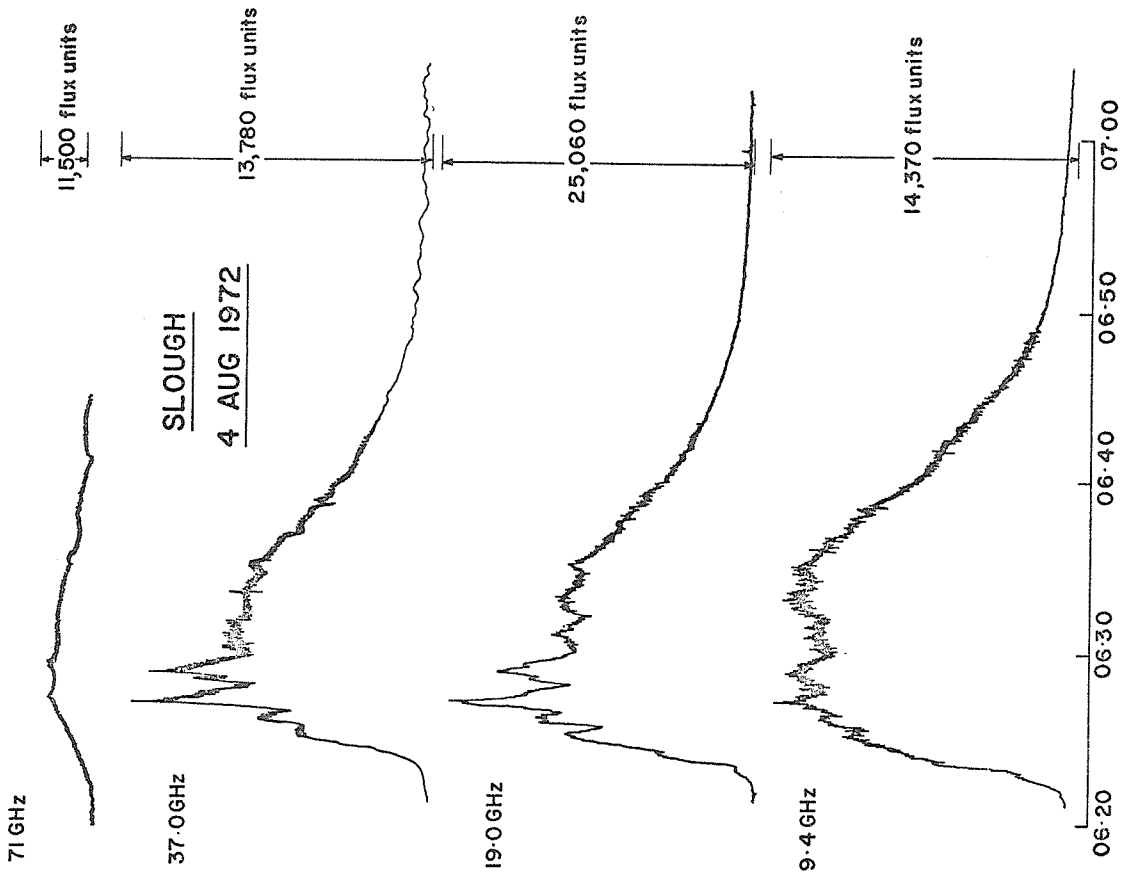


Fig. 3. The event of 4 August 1972.

SLOUGH
10 AUG 1972

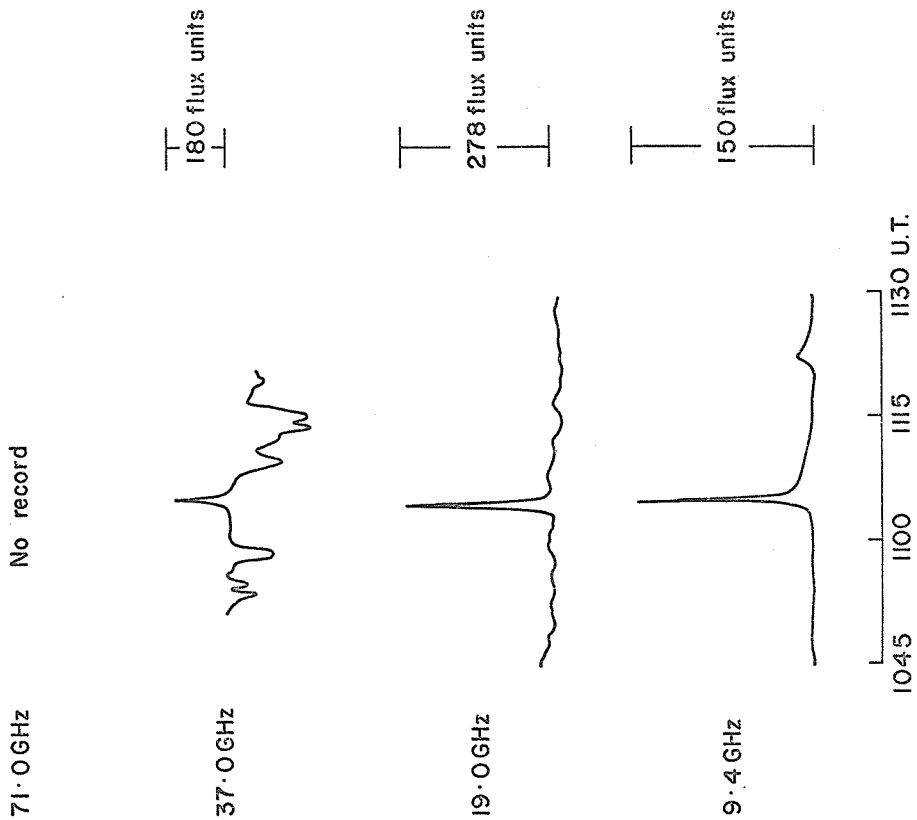


Fig. 5. The event of 10 August 1972.

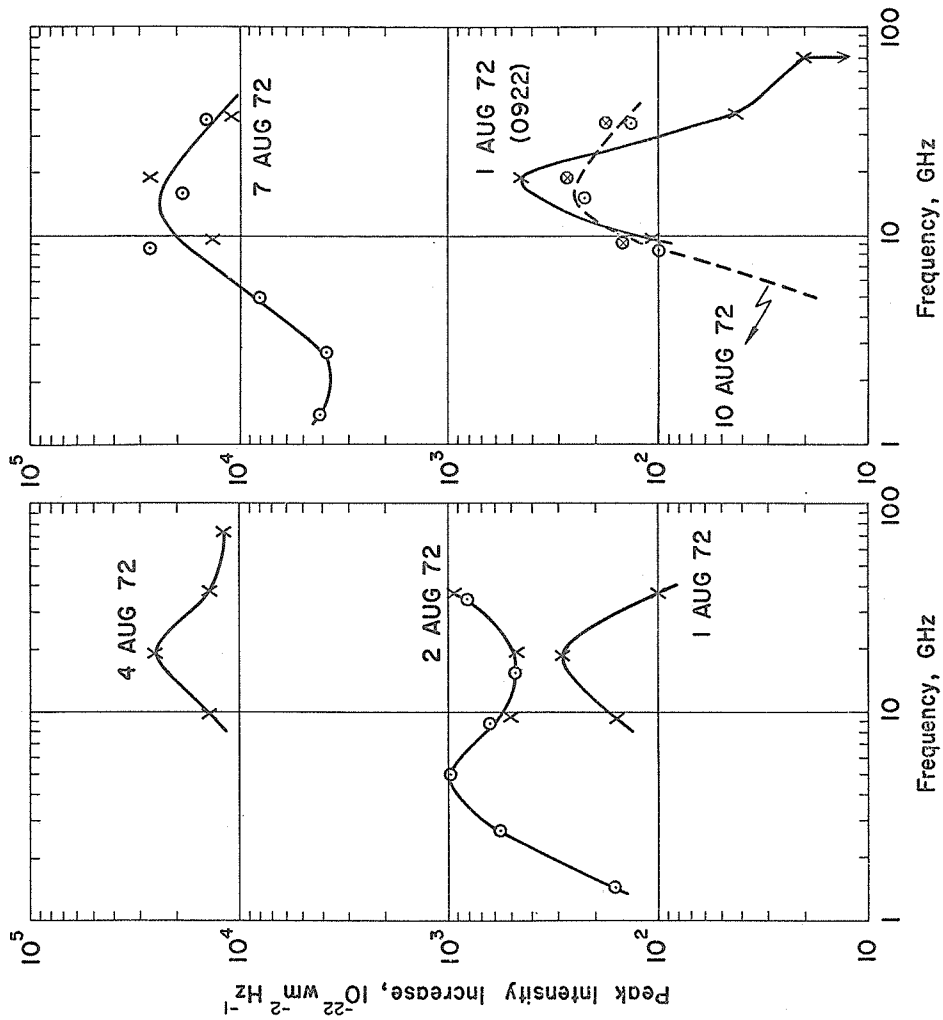


Fig. 6. Peak intensity for some of the August 1972 events.
X or O = Slough, O - AFGL.

There are several interesting features about these events:

- (a) At least one of the events produced a major burst at 71 GHz (approximately $11,500 \times 10^{-22} \text{ Wm}^{-2} \text{ Hz}^{-1}$ on 4 August) and two others almost certainly did, but were not recorded (2 August - sunset for the 71 GHz radiometer, and 7 August - no record available).
- (b) All six events have their spectral peaks above 10 GHz, generally in the 15 - 20 GHz, except for the 2 August event.
- (c) The 2 August event is an example of the rare double peak (centimeter - millimeter) spectrum [Croom, 1973].
- (d) Both of the major events have small, rapid oscillations superimposed on them on 9.4 and 19 GHz, and also on 37 GHz in the case of the 4 August event. These, and the other events, were recorded both on paper chart and on a punched-tape data logger, with a sampling rate at each frequency of $1\frac{1}{2}$ secs and radiometer output time constants of 0.3 and 1 seconds, respectively. From expanded time scale plots of these bursts it can be seen that these oscillations have a very short period of about 4 to 5 secs. The oscillations are more pronounced on the lower frequencies and are damped out earlier on the higher frequencies.
- (e) Table 2 shows the mean durations (T_M of Croom [1971]) together with the peak particle fluxes for $E_p > 10 \text{ Mev}$ as recorded by the Explorer 41 satellite ["Solar-Geophysical Data", 1973]. Both of the major events have the large values of T_M normally associated with major proton events. So also does the 0922 UT event of 2 August. However, although the proton data shows evidence of a weaker proton event preceding the two major ones, this event is more probably attributable to another major radio event which occurred at 0404 UT on 2 August.

Table 2
Mean Durations and Associated Proton Fluxes for the Six Events

Date	T_M (min)	Protons $\text{Ster}^{-1} \text{ cm}^{-2} \text{ sec}^{-1}$
1 Aug (0841 UT)	1.5	-
1 Aug (0922 UT)	7.0	(42)*
2 Aug	2.5	-
4 Aug	12.1	23,000
7 Aug	9.3	3,500
10 Aug	1.0	-

* Probably attributable to event at 0404 UT on 2 August

Acknowledgements

This work was carried out as part of the program of the Science Research Council's Radio and Space Research Station and is published by permission of the Director.

REFERENCES

- | | | |
|-----------------------------|------|---|
| CROOM, D. L. | 1971 | Forecasting the intensity of solar proton events from the time characteristics of solar microwave bursts, <u>Solar Phys.</u> ; <u>19</u> , 171. |
| CROOM, D. L. | 1973 | Solar millimetre bursts, <u>Proc. NASA Symposium on High Energy Phenomenon on the Sun.</u> |
| U.S. DEPARTMENT OF COMMERCE | 1973 | <u>Solar-Geophysical Data</u> , 342 Part II, February 1973 |

by

H. Tanaka and S. Énomé
Toyokawa Observatory, Nagoya University, Japan

The microwave S-component associated with active region McMath 11976 first appeared July 28 on 8 cm and July 29 on 3 cm. It showed very rapid increase in intensity. The history of its evolution is shown in Figure 1 in terms of 3-cm flux and 3-cm to 8-cm flux ratio and in Table 1. Brightness (R + L) and polarization (R - L) distributions of the sun on 3 cm and 8 cm are illustrated in Figures 2 and 3. The gains of the polarization records are about 3.8 and 1.8 times larger than that of the intensity records of 3 cm and 8 cm, respectively.

Table 1

Evolution of Microwave S-Component in Terms of 3 cm and 8 cm Flux

Date 1972	Position Arc min.	Flux	
		3 cm	8 cm
July 28	E15.9	2.7	4.4
29	15.7	13.3	10.0
30	15.0	24.8	19.4
31	13.9	40.3	25.2
Aug 1	12.1	47.1	31.7
2	9.1	59.2	49.4
3	6.3	42.3	40.5
4	2.9	44.3	41.0
5	W 0.9	52.5	44.7
6	4.2	39.6	40.5
7	7.4	40.2	39.1
8	10.1	25.2	22.2
9	12.4	27.7	23.2
10	13.7	27.2	18.8
11	14.4	22.6	22.2

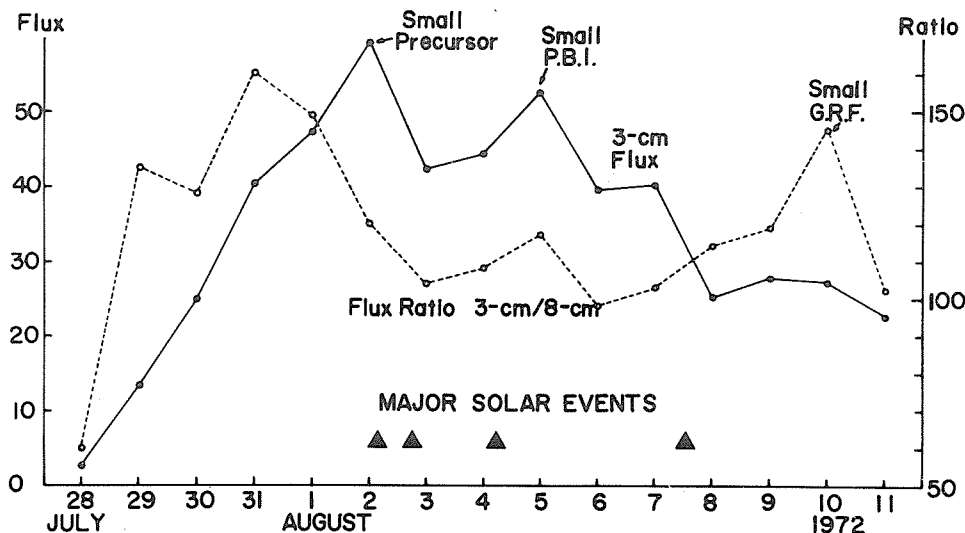


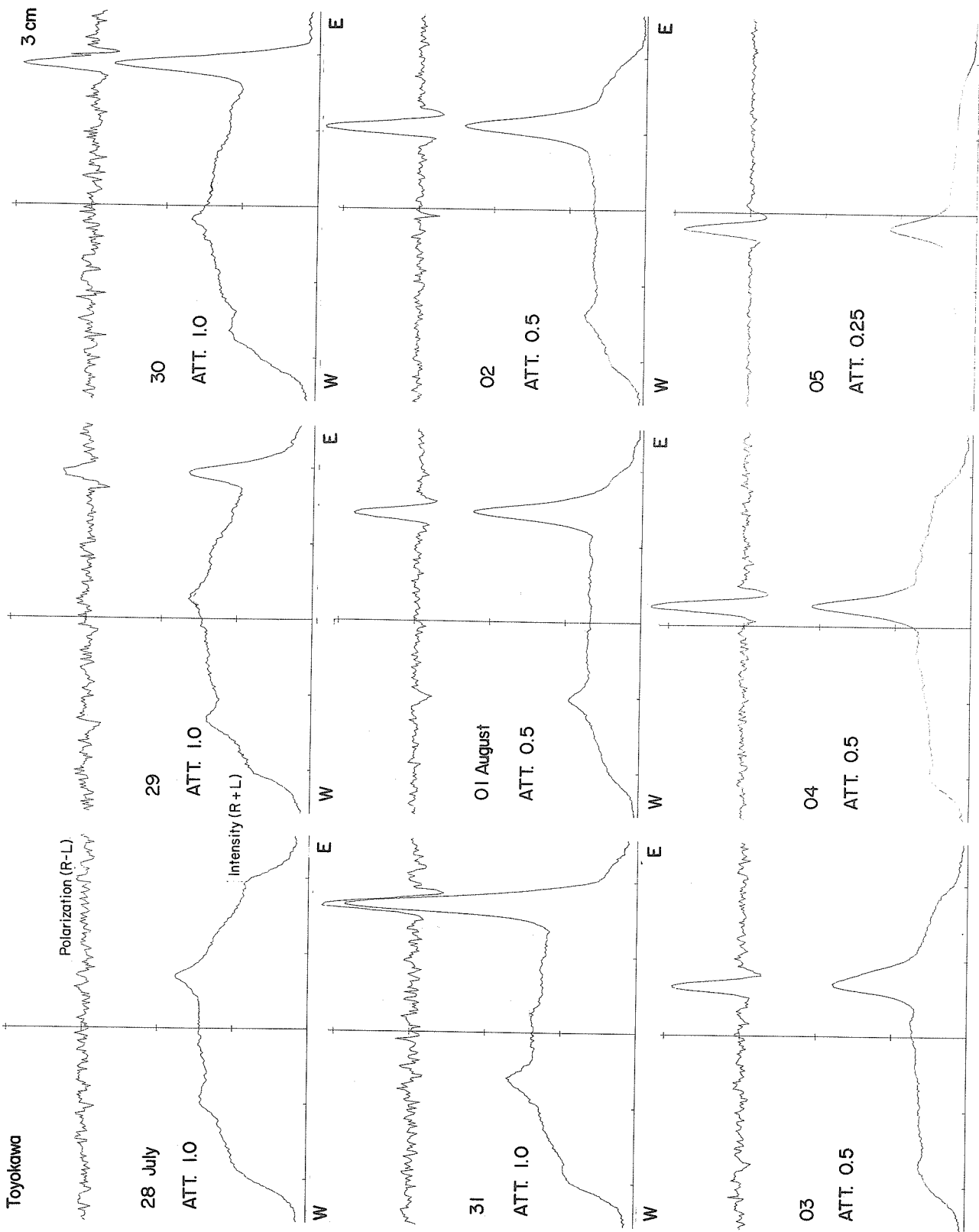
Fig. 1 Time variations of 3-cm flux (filled circle) and 3-cm to 8-cm flux ratio (open circle) for the period July 28 to August 11, 1972

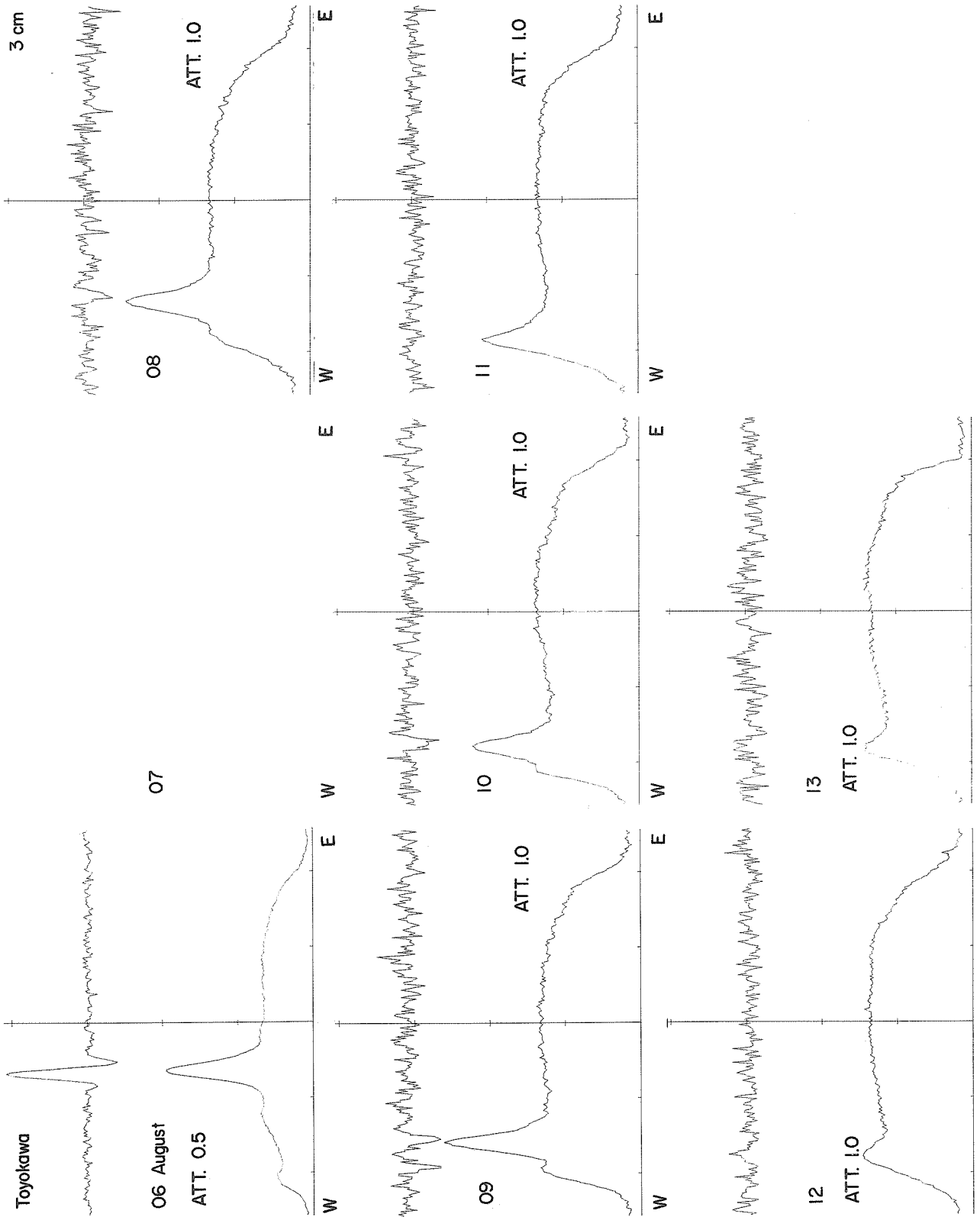
Our messages of forecasting which are communicated through the URSIGRAM network correctly predicted the occurrences of proton flares. The method is due to the fact that high probability of the occurrence is expected for an active region with a large 3-cm flux and a high 3-cm to 8-cm flux ratio of the S-component [Tanaka and Kakinuma, 1964]. The active region possessed a polarization distribution with right-handed polarized central peak and left-handed polarized sub-peaks on either side which we call the P-configuration. An active region with this configuration is very favorable for proton flare occurrence [Tanaka and Énomé, 1973].

During its activity, the region produced four major microwave bursts on August 2, and two bursts on August 4 and on August 7. The first three bursts occurred during daytime in Japan. The time histories of these bursts are shown in Figure 4.

EAST-WEST SOLAR SCANS

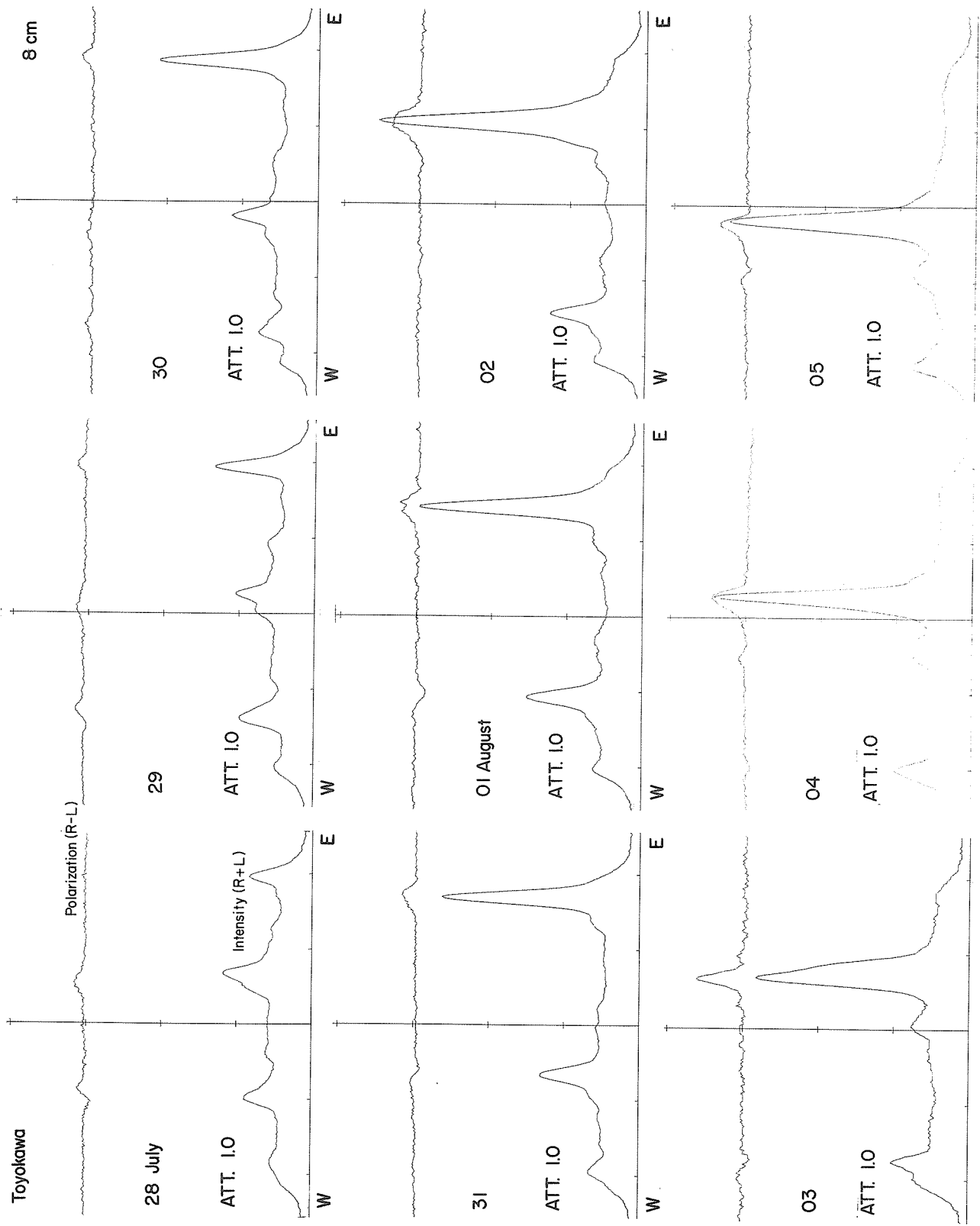
July 28-August 13, 1972



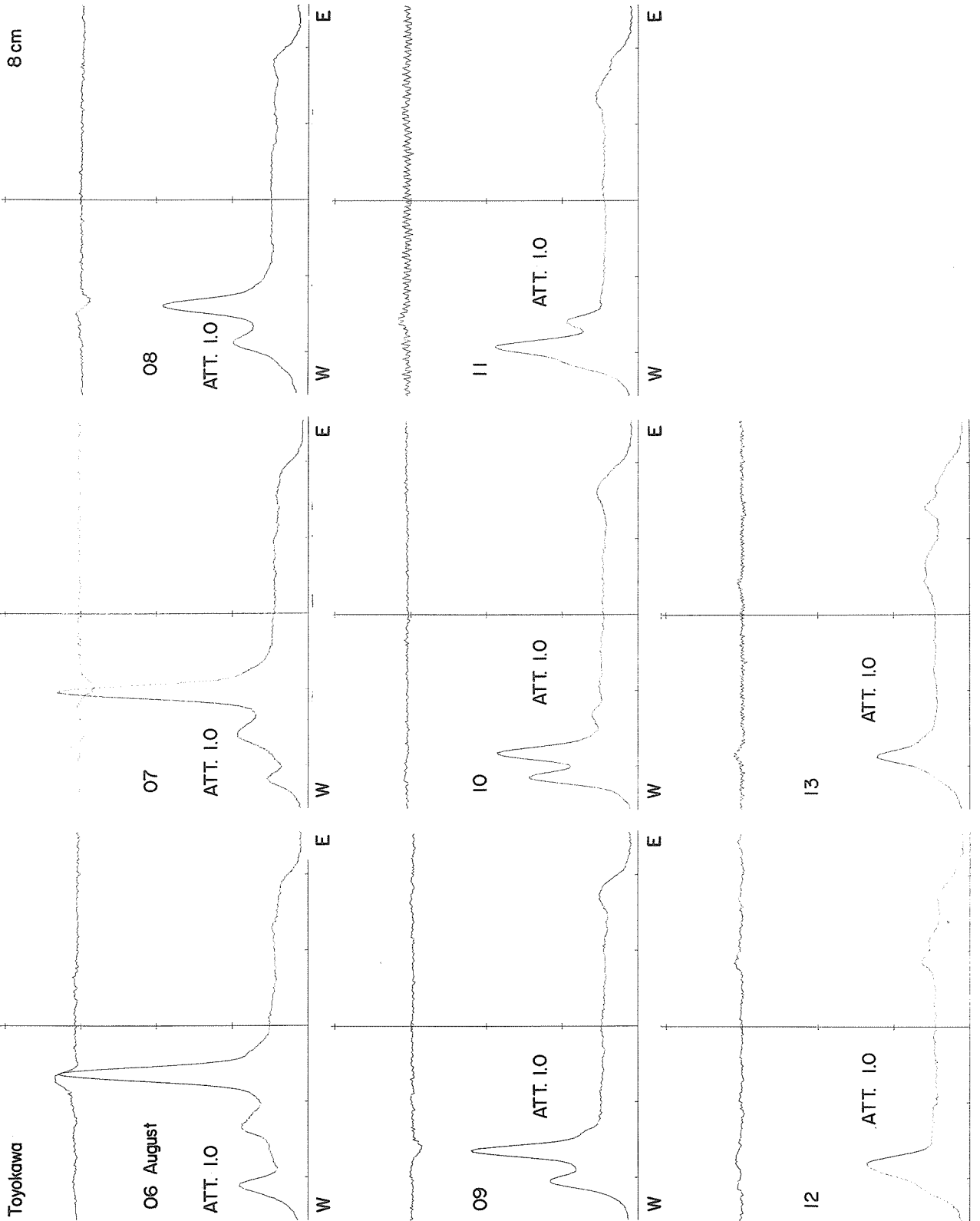


EAST-WEST SOLAR SCANS

July 28 - August 13, 1972



Toyokawa



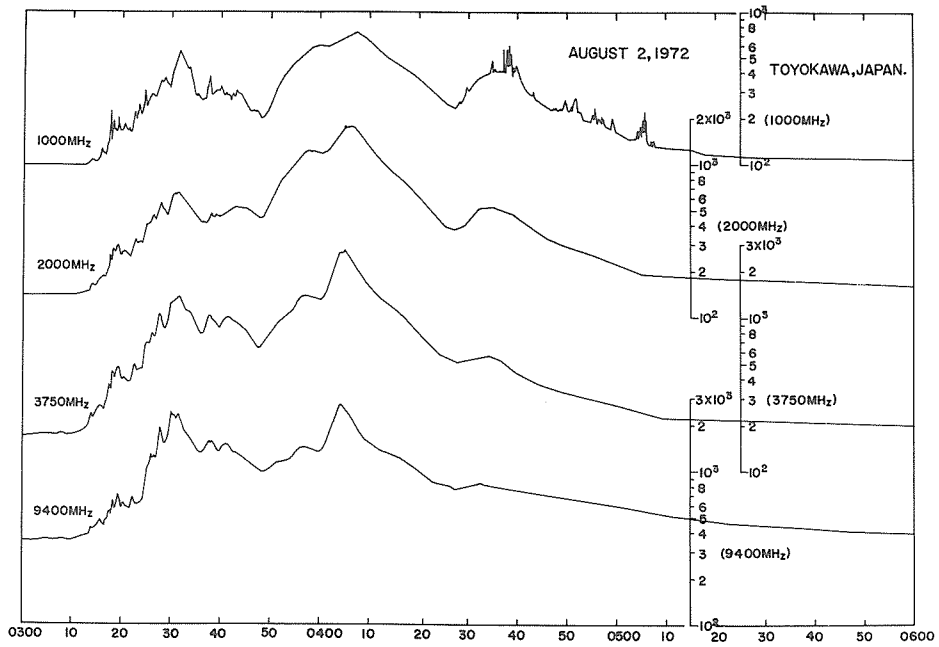


Fig. 4a. Intensity-time histories of the bursts on August 2, 1972 between 0300 - 0600 UT on 9400, 3750, 2000 and 1000 MHz. Units are $10^{-22} \text{ W m}^{-2} \text{ Hz}^{-1}$.

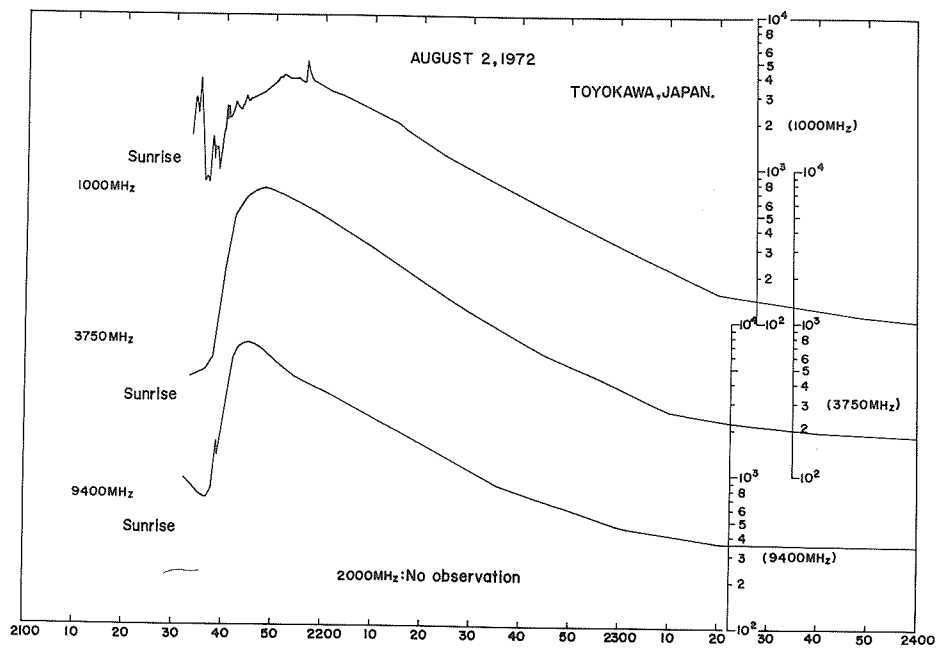


Fig. 4b. Same as Figure 4a for the period 2100 - 2400 UT August 2, 1972.

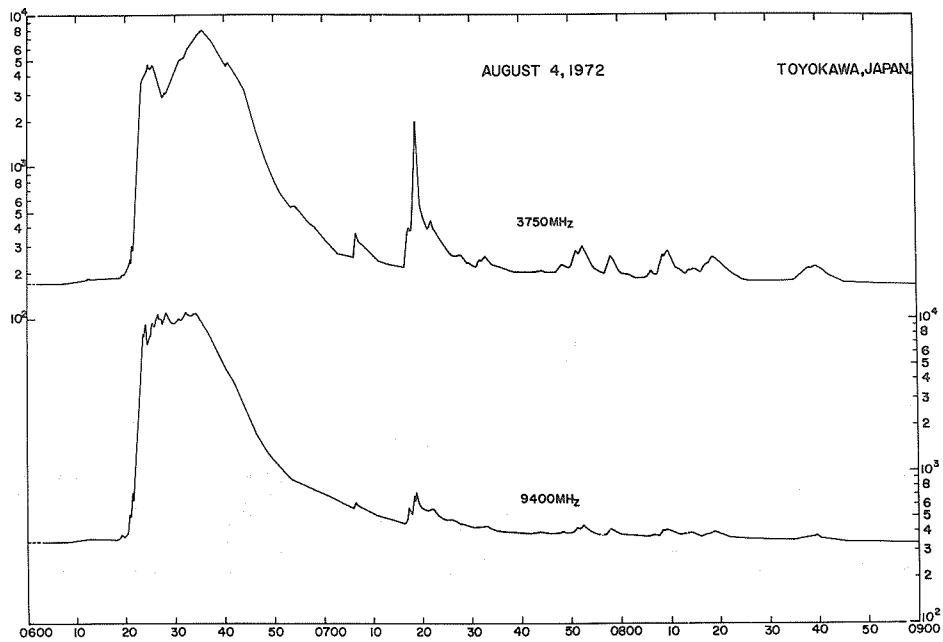
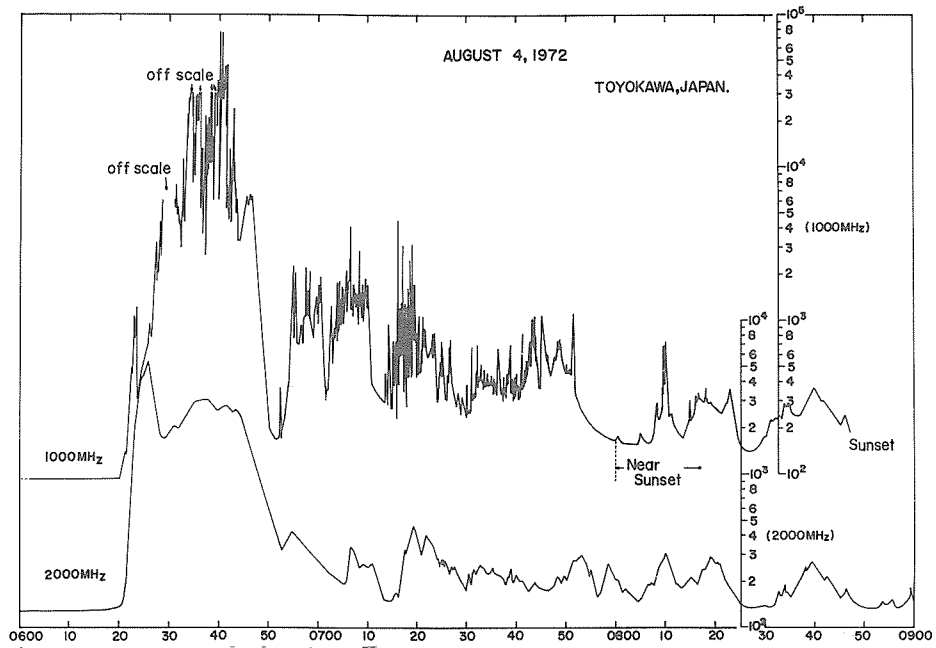


Fig. 4c. Same as Figure 4a for the period 0600 - 0900 UT August 4, 1972.

REFERENCES

TANAKA, H. and T. KAKINUMA 1964

Rep. Ion. Res. Japan, 18, 32.

TANAKA, H. and S. ÉNOMÉ 1973

To be presented at the GOSPAR Symposium, 1973

CULGOORA OBSERVATIONS OF RADIO BURST ACTIVITY FROM
1972 JULY 26 TO AUGUST 14

T.W. Cole
Division of Radiophysics, CSIRO, Sydney, Australia

1. Introduction

This communication summarizes the observations of solar radio bursts made at the Culgoora observatory (150°E., 30°S.) between 1972 July 26 and August 14. There were two major radio instruments in use at Culgoora. Every day during this interval, between the hours of 2038 and 0737 UT, the radiospectrograph [Sheridan 1967] recorded dynamic spectra every one-quarter or one-half second. The radioheliograph [Wild 1967] recorded second-by-second pictures of the 80 MHz and, occasionally, the 160 MHz radio emission from the Sun in both circular polarizations. The hours of observation of the heliograph were from approximately 2300 until 0500 UT on all days during this interval except July 28/29 and July 29/30.

Very little interpretation is contained in this report.

2. Observations

2.1 The period July 26 to August 2

The early part of the interval was dominated by radio burst activity associated with the McMath region 11970. The first activity observed to be related to the major area of interest, McMath region 11976, was a series of type III bursts on July 27 at 0142 and 0338 UT. All burst activity for this early period was type III or III/V, except for a single type II observed on July 27 at 0643.

For the two days July 28/29 and July 29/30 the spectrograph showed a continuous storm of type III bursts. The heliograph was not available to give positional information on this storm, which was distinguished by the bursts being almost exclusively of the IIIb type as defined and discussed by de la Noë and Boischoit [1972]. These bursts, confined almost entirely to the 30 to 50 MHz band and consisting of a chain of fine, reverse drift components, are illustrated in Figure 1. It was observed that for this storm it was only rarely that the IIIb burst was a precursor to a more normal type III burst.

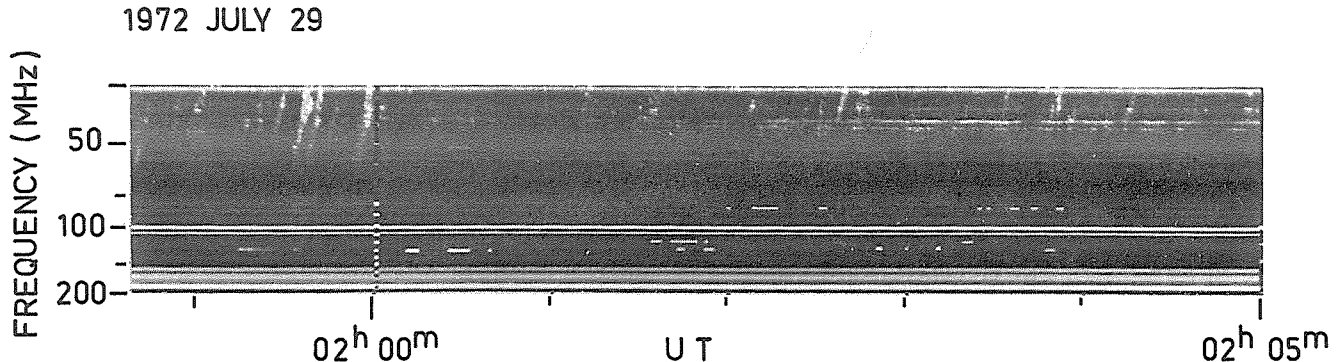


Figure 1 The metric waveband section of dynamic spectrum for the frequencies and times marked to illustrate the type III storm of 1972 July 29.

A series of three homologous inverted-U bursts was observed from region 11976 on July 31 at 0155, 0441 and 0443 UT. They are shown in Figure 2, and indicate a stable, closed magnetic field configuration existing over this region. The (non-harmonic) double structure also indicates that at least two magnetic field loops existed.

The main activity on July 31/August 1 was a number of large type III groups. In particular, the groups at 0125-0133 and 0425-0441 UT consisted of bursts from both of the regions (11970 and 11976) with the major activity occurring at the former region.

The spectrograph showed a type I storm with an associated weak type III storm on August 1/2.

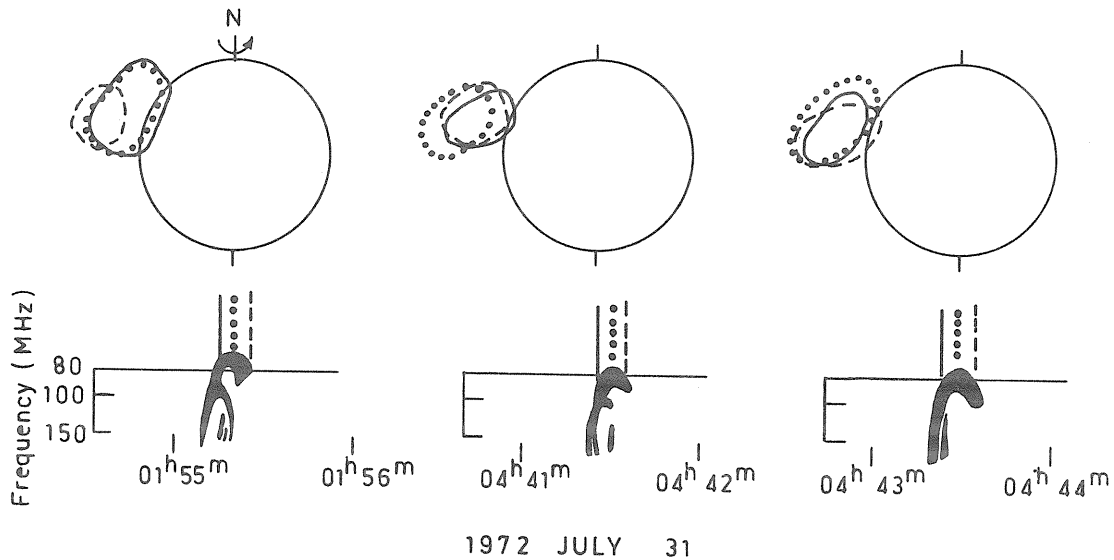


Figure 2 The three homologous type U bursts of 1972 July 31. The half-intensity contours are plotted for the beginning (solid), middle (dashed), and end (dotted) of each event. The source position moves slightly outwards during the events.

2.2 The radio burst of August 2 at 0240 to 0700 UT

A large radio outburst associated with region 11976 began with a large group of type III bursts on August 2 at 0243 UT. This was followed at about 0300 by an increase in the intensity of the continuum emission which had been present, as part of a type I storm, in the metric waveband. At 0312 a continuum emission in the 30 to 100 MHz range (not unlike a type V in appearance) marked the beginning of a short-wave fadeout which continued until around 0500. The spectrograph record is shown in Figure 3.

In the decimetric band the continuum emission reached its peak at around 0340 UT. This continuum was overlaid by absorption and emission pulsations (barely visible in Figure 3). The metric band emission reached its peak at approximately 0400 and then slowly weakened until the observations ceased at 0737.

One interesting feature of the spectrograph record is the changing nature of the emission in the 24 to 74 MHz band. Selected examples are shown in Figure 4. The diffuse, type-III-like emissions of the early period changed to a wisp-like emission which became progressively weaker as reverse drift pairs came to dominate this range.

The radioheliograph record of this event, which was confined to 80 MHz and started at 0400 UT because of instrumental difficulties, reveals a complex source structure. The radio picture at 040202 is shown in Figure 5 for both right-hand and left-hand circular polarization, with successive contours in the ratio of $1/\sqrt{2}$ from the peak intensity in that polarization. The development of the six source components is shown in Figure 6, where half-intensity contours of the sources are shown for a selection of times. The component A (Fig. 5), highly right-hand polarized and at $1.2 R_{\odot}$ from the limb, faded rapidly and was not observed after 040400. Similarly components B, C and D had faded by 040900, when a distinctive development occurred. The component E, a left-hand polarized source at the limb, split into two components, and one of these, together with the slightly displaced right-hand polarized component F, became a moving source. Between 0409 and 0441, when the moving source faded, it had moved $1 R_{\odot}$ to the north-north-east at an average speed of 360 km s^{-1} . It left a bipolar source structure straddling the optical spot group centre (marked by a cross on the diagram). This remained stable for the rest of the observing day.

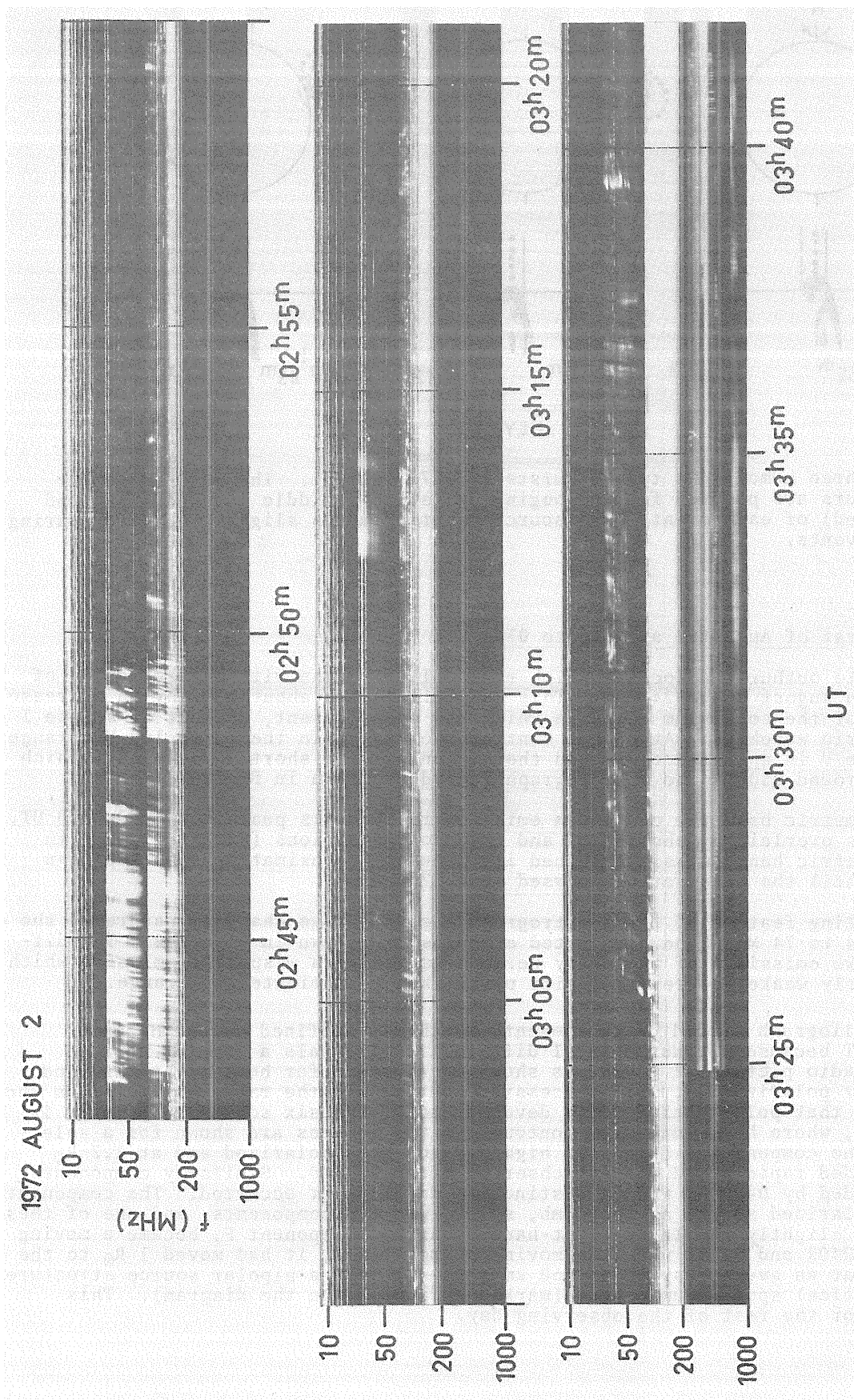


Figure 3 The dynamic spectrum for the beginning of the strong radio event observed on 1972 August 2. The gain change at 0325 UT and frequency banding in the 200 to 1000 MHz band were of instrumental origin.

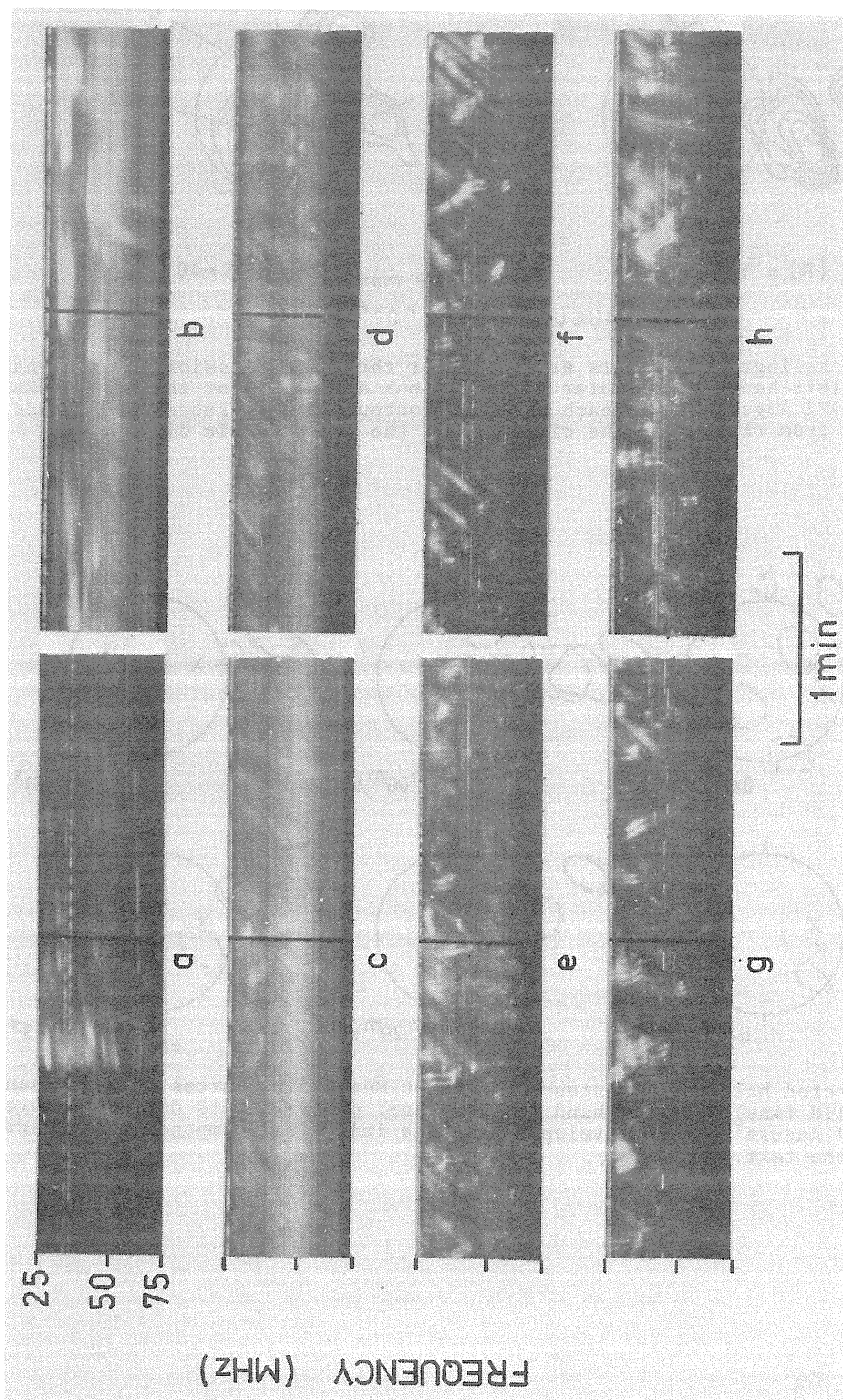


Figure 4 Samples of the dynamic spectrum between 25 and 75 MHz during 1972 August 2 are shown. The samples are at intervals of 20 min: the time mark (dark bar) in sample (a) is at 0330 UT.

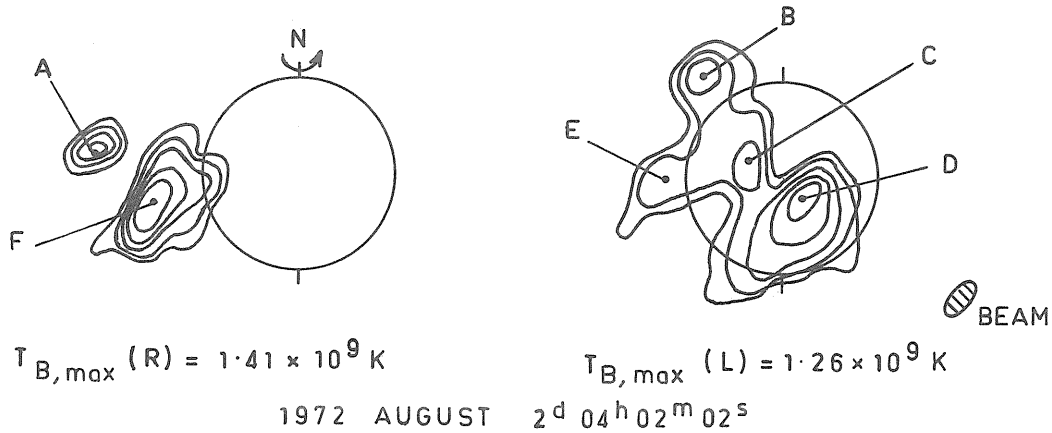


Figure 5 Radioheliograph contours are shown for the radio emission in right-hand (R) and left-hand (L) circular polarizations at 80 MHz for the time 040202 UT on 1972 August 2. In each case the contours are in successive ratios of $1/\sqrt{2}$ from the peak. The circle shows the photospheric disk.

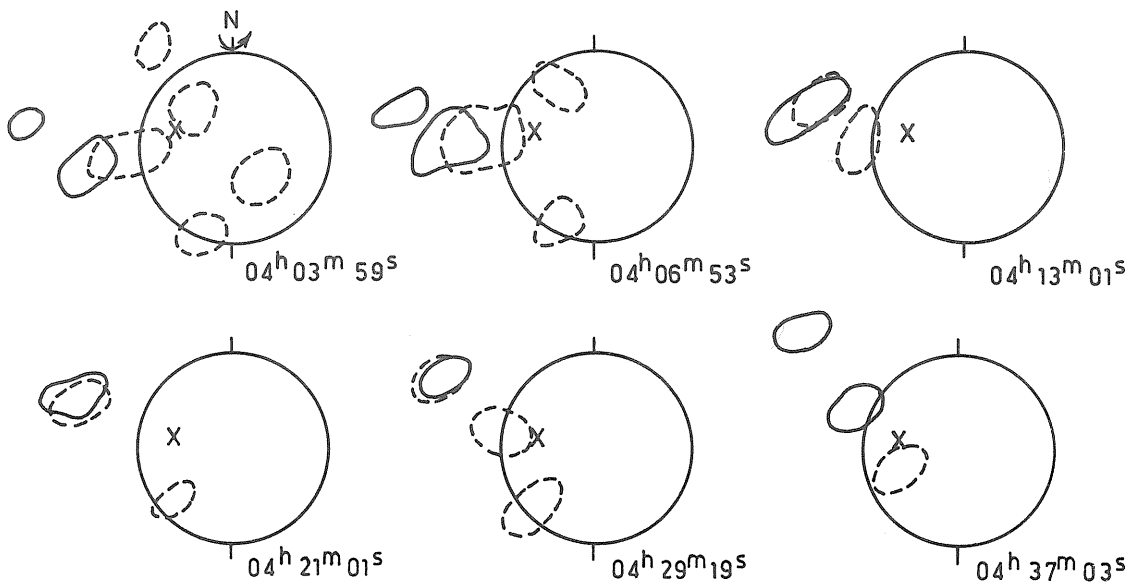


Figure 6 Selected half-power contours of the 80 MHz radio sources in right-hand (solid line) and left-hand (dashed line) polarizations during the event of 1972 August 2. The development of the individual components is described in the text.

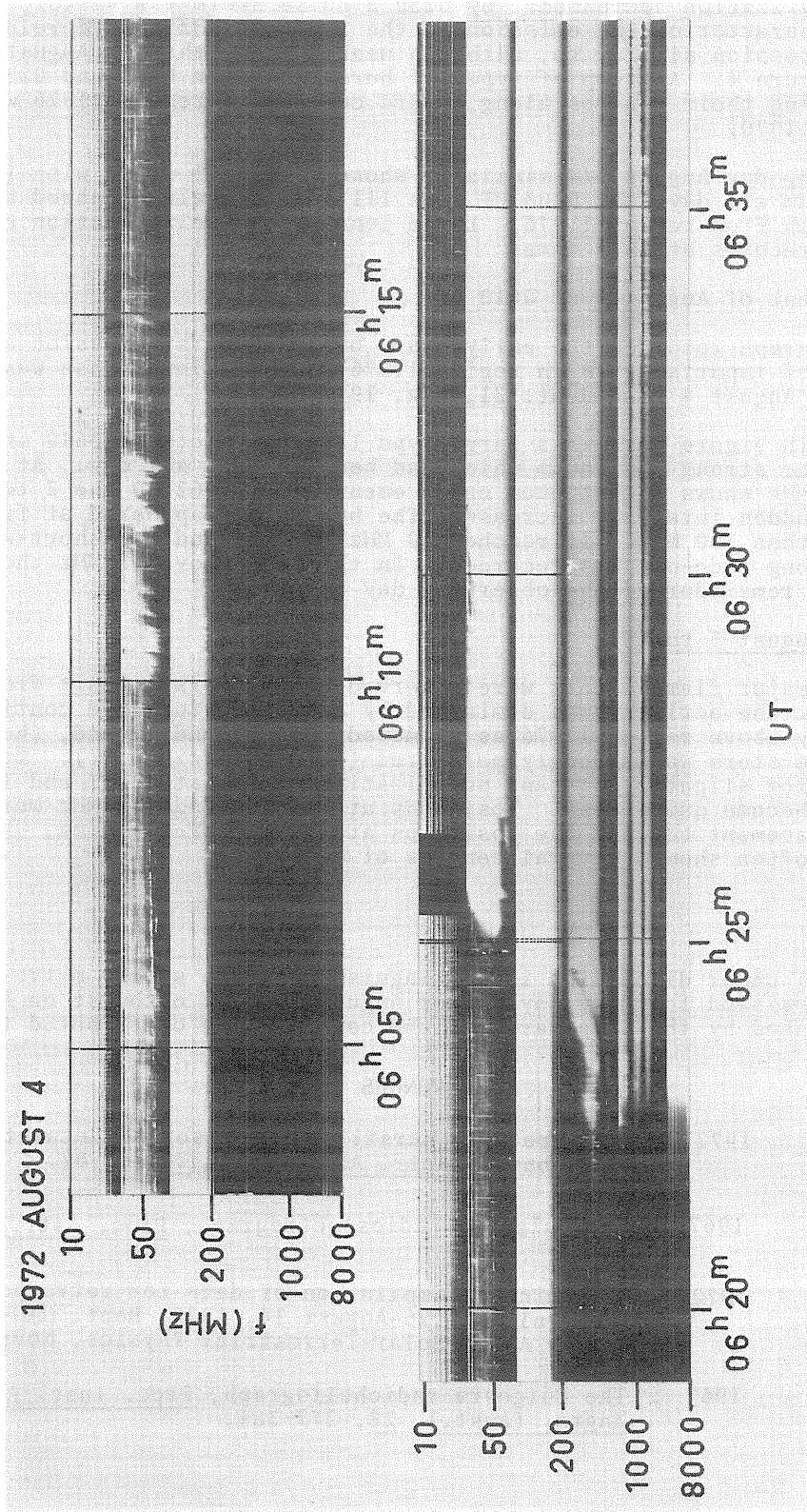


Figure 7 The dynamic spectrum at the start of the very strong radio burst on 1972 August 4 for the times and frequencies marked. The frequency banding in the range 200 to 2000 MHz was an instrumental effect, as was the gap in the low-frequency range between 0626 and 0627 UT.

2.3 The observing periods August 2/3 and August 3/4

From the beginning of observations at 2038 UT the spectrograph showed strong, left-hand polarized continuum with some type III activity. Throughout the day the intensity and polarization decreased: by 0230 a noise storm was visible above the continuum. The character of the emission in the 24 to 74 MHz band developed throughout the day in a progression similar to, although weaker than, that of August 2, which is illustrated in Figure 4. A group of type III bursts between 0232 and 0238 were distinguished by having their centres along an arc connecting region 11976 with the western limb region near 11970.

The observing day August 3/4 similarly showed a type I storm with left-hand polarized continuum all day. At 0403 UT type III bursts again appeared along an arc to the western limb from region 11976. Large ionospheric scintillation effects were also seen on the records at this time.

2.4 The flare event of August 4 at 0610 UT

The spectrograph recorded the early phase of radio burst emission associated with an optical flare of importance 3B in region 11976 whose maximum phase was at approximately 0640 UT on August 4 [UAG Rept. 21, Nov. 1972].

The record in Figure 7 shows a large type III group between 0610 and 0613 UT superimposed on the strong continuum which had been present all day. At 0622 the band from 300 to 8000 MHz shows a continuum enhancement and at 062250 the 2 to 8 GHz band shows a further sudden intensity increase. The burst then appeared at frequencies progressively lower than 300 MHz. It reached 50 MHz at 0625 and the short-wave band at 0626, where a strong fade-out was recorded. In the band above 25 MHz the film remained saturated for the remainder of the observing day (to 0737).

2.5 The period August 5 to 15

No further major flare events were observed at Culgoora. Apart from type III bursts and groups, the activity was dominated by a type I storm and continuum centre observed every day above region 11976 as it moved toward, and around, the western limb. Until August 8 the storm was strongly polarized (left-hand circular). It became unpolarized except for slight right-hand polarization on August 12/13 and 13/14. By August 15 it had become quite weak. Positions at both 80 and 160 MHz were available and there was a displacement between the positions at the two frequencies. At each frequency the storm often showed several centres of activity.

3. Conclusions

The interval under discussion is distinguished by the strong metre-wave continuum emission which persisted for many days after August 2. The outburst on August 2 is further distinguished by the large area of the corona which contributed to this emission.

REFERENCES

- | | | |
|----------------------------------|------|---|
| DE LA NOË, J. and
A. BOISCHOT | 1972 | The type IIIb burst: a precursor of decametre type III radio-burst, <u>Astr. Astrophys.</u> , <u>20</u> , 55-62. |
| SHERIDAN, K.V. | 1967 | The Culgoora radiospectrograph, <u>Proc. Astr. Soc. Aust.</u> , <u>1</u> , 58-9. |
| UAG Report | 1972 | Preliminary compilation of data for retrospective world interval July 26-August 14, 1972, Rept. UAG-21, World Data Center A for Solar-Terrestrial Physics, November 1972. |
| WILD, J.P. (Ed.) | 1967 | The Culgoora radioheliograph, <u>Proc. Inst. Radio Electron. Engrs. (Aust.)</u> , <u>28</u> , 277-384. |

Metric Radio Continuum Activity Associated with the
Active Region McMath No. 11976 in August 1972

by

Kunitomo Sakurai*
Radio Astronomy Branch
Laboratory for Extraterrestrial Physics
NASA/Goddard Space Flight Center
Greenbelt, Maryland 20771

The active region McMath No. 11976 appeared on the east limb on 29 July 1972. During its passage on the solar disk, this region became active in emission of metric radio continuum and produced four proton flares.

As shown in Figure 1, the activity on the radio continuum at metric frequencies was initially very low but increased as the region approached central meridian of the sun. Maximum activity was reached around 3-4 August. This increase may be related to the emission directivity of the metric continuum [Fokker, 1965]. However in this case, this increase in emission could also be connected with the growth of the sunspot group observed since 31 July. Throughout this growth, four proton flares were produced in this sunspot group and were accompanied by type II and type IV radio bursts. As seen in Figure 1, however, these flares were independent of the flux increase of the long-enduring component of type IV burst: the flux increase at 200 MHz was not observed for several hours or more after those flares. This result is quite different from those for the active region McMath No. 9740 [see, Sakuari, 1973]. This difference seems to be related to the configuration of sunspot magnetic field lines above and near the flare regions.

As mentioned above, emissions of both type II and type IV bursts were observed in association with these flares. Type III burst associations were, however, rare for these flares [T. B. Kuiper, private communication, 1973]. This fact may be explained by assuming that the sunspot magnetic field lines above the flare regions were not extended into interplanetary space. This explanation also seems applicable to non-observation on the long-enduring metric continuum. The formation of this type of sunspot magnetic configuration may be related to the fact that the sunspot group under discussion is isolated from other groups.

I would like to thank Mr. Fujio Yamashita of the Hiraiso Branch, Radio Research Laboratories, Tokyo for his supply of radio records.

REFERENCES

- | | | |
|---------------|------|--|
| SAKURAI, K. | 1973 | <u>Planetary Space Sci.</u> , 21, 17. |
| FOKKER, A. D. | 1965 | <u>Solar System Radio Astronomy</u> , 171, ed. by J. Aarons, Plenum Press, New York. |

*NASA Associate with University of Maryland, Astronomy Program

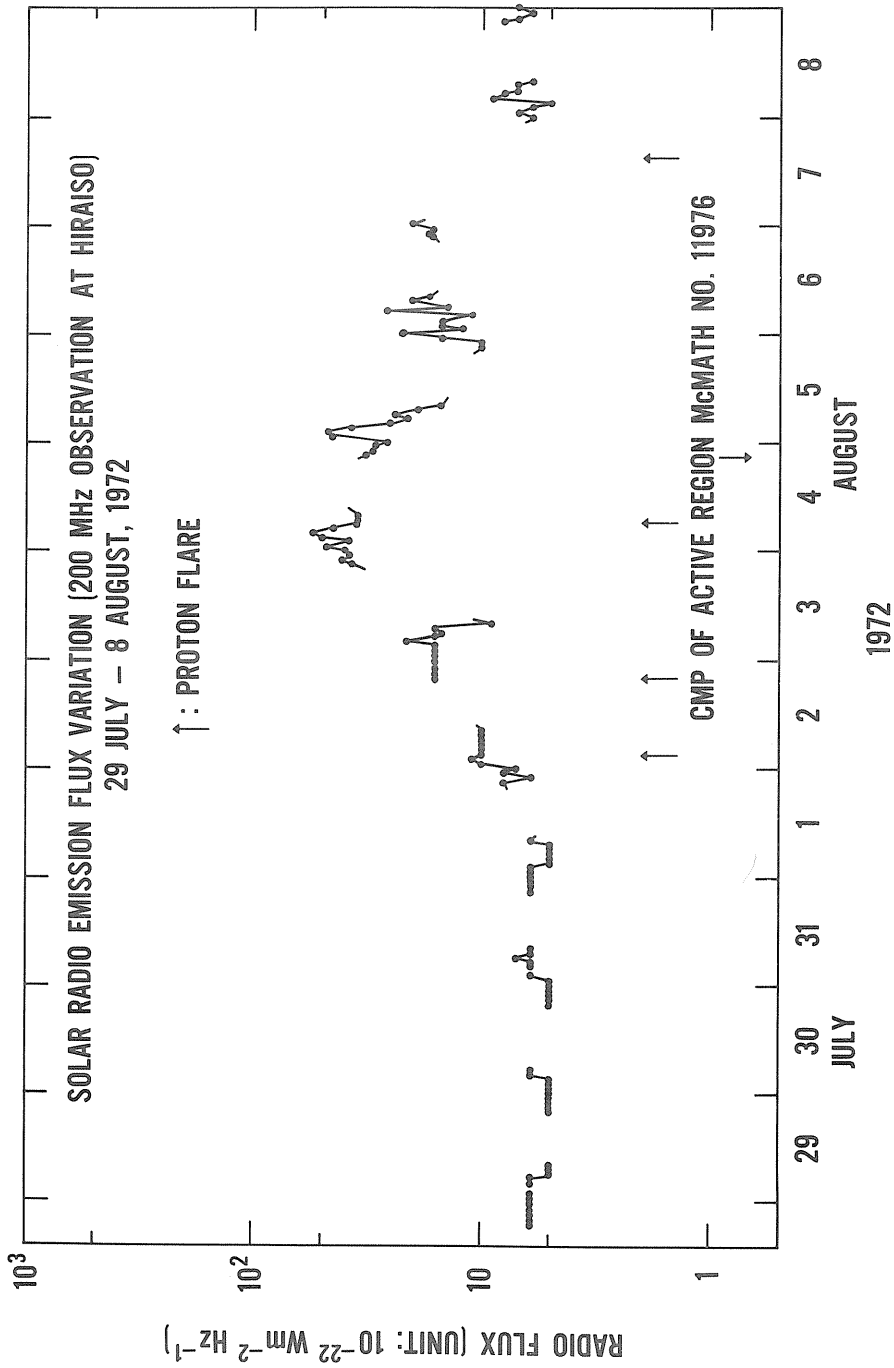


Figure 1 - Metric continuum noise activity during 29 July to 8 August 1972.

Pulses in Radio Bursts of August 1972 Proton Events

by

V. L. Badillo
Manila Observatory
P. O. Box 1231, Manila, Philippines

The extremely intense radio burst of 04 August 1972 starting at about 0620 UT had associated particle events, both a PCA and a probable GLE. It is also interesting because the time structure of the burst may be useful for better understanding the acceleration mechanism of solar cosmic rays.

The burst was recorded over a very wide range, from 71 GHz (in Slough) to the deka-meter wavelengths. In Figure 1 are reconstructed the burst curves recorded at Manila Observatory. The bursts at 8800, 4995 and 2695 MHz have the same general characteristics. However the burst at 1415 MHz is different mainly because of the curious feature starting at about 0632.8 UT. A better appreciation of its character may be had by examining the copy of the actual chart recording exhibited in Figure 2. What can be seen is a cluster of intense spikes closely bunched in time, not unlike the record of the radar pulses of a passing airplane. At least 40 spikes can be counted in the three minute duration of the series of pulses. The structure is not clearly periodic and the intensities of the spikes vary from weak to some having intensities as much as 3,000 flux units above the envelope.

A tentative explanation for a brief regular series of short sharp pulses occurring only in the 100-200 MHz part of a type IV burst was proposed by Wild [1971]. Where a rising shock front intersects the two legs of a magnetic flux loop, the magnetic field is increased. Trapped electrons, Fermi accelerated to relativistic energies, emit synchrotron radiation that increases with time. When the shock front reaches the top of the loop conditions exist such that a series of sharp regular pulses are emitted. Acceleration ceases after the shock front has ascended above the flux loop. Other trapped charged particles, like protons, are similarly accelerated.

The explanation just given may be applied to the event in question. Intensities reach maximum for the bursts at frequencies above 1415 MHz during the pulsation period, while a type II burst in the dekameter curve, manifesting a rising plasma cloud, starts just prior to the pulsation period. The 606 MHz recorder saturated but some manifestation of pulsation may be seen in the copy shown in Figure 2. The estimated duration is indicated in Figure 1. A series of sharp pulses are seen too in the 1000 MHz burst recorded at Toyokawa. In the 245 MHz band, pulsation is rather prolonged, extending from 0624.5 to 0645 UT, and consists of several series of pulses. Another mechanism may be responsible for this.

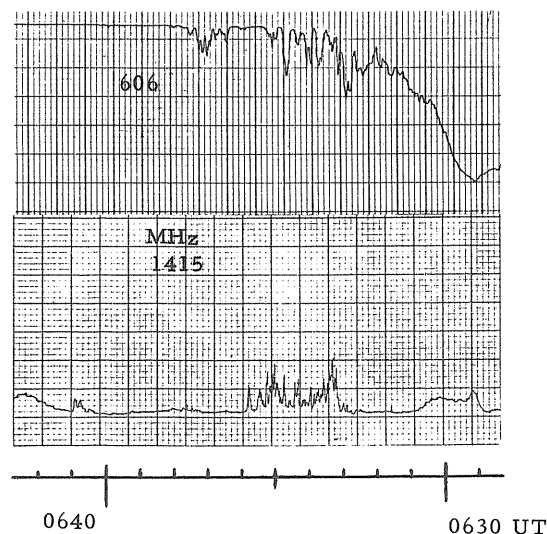


Figure 2. Chart recording of pulsations on 1415 and 606 MHz radiometers. Note that the direction of time is opposite to that of the drawing in Figure 1.

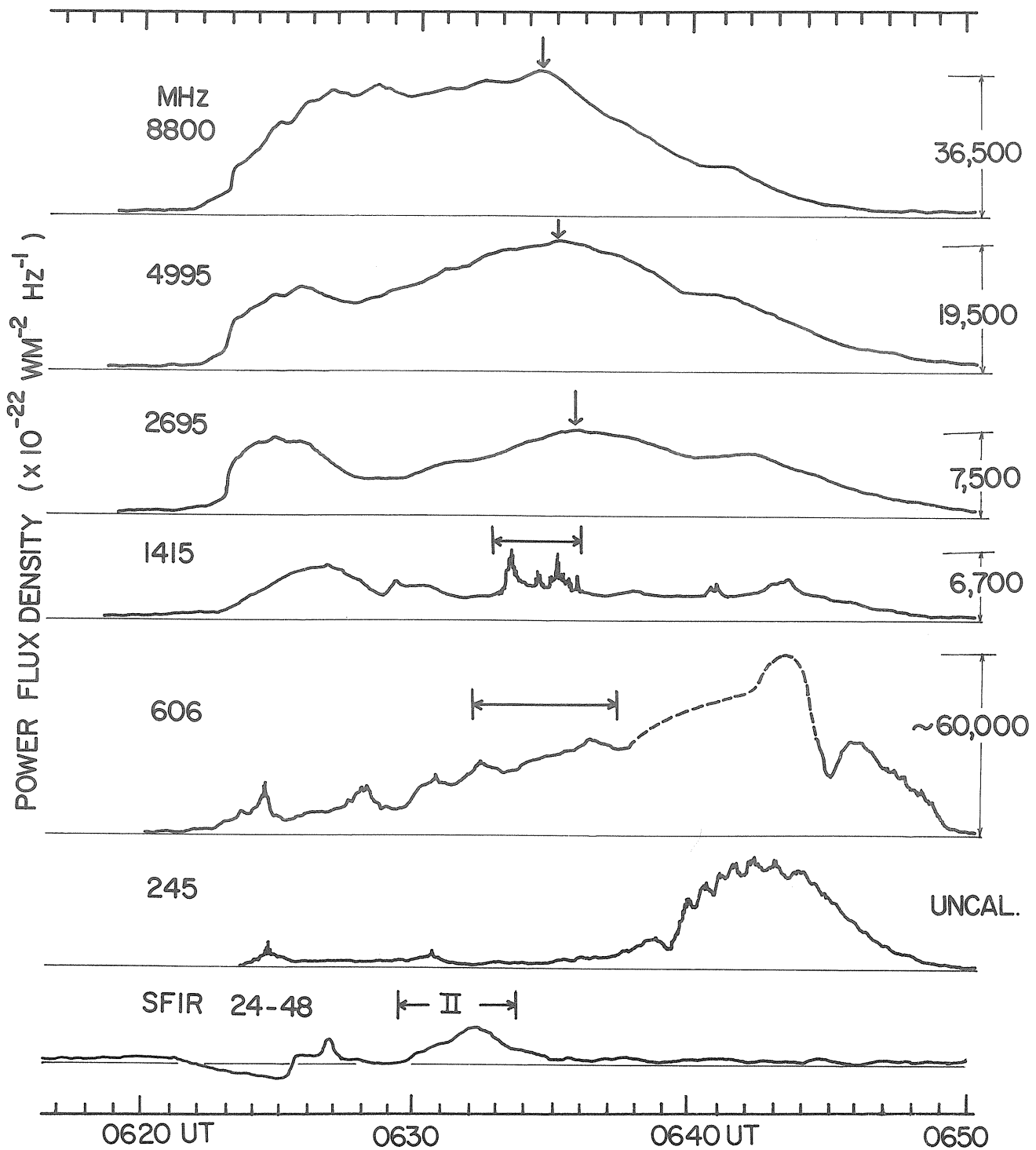


Figure 1. Radio burst observed on 04 August 1972 at Manila Observatory. Dashed lines indicate extrapolated values.

The dekameter burst curve shows heavy absorption starting at about 0621 UT indicating D-region ionization. It is at this time that all the bursts except that at 1415 MHz are markedly impulsive in character. A little later at about 0633 UT the dekameter curve registers a maximum. It is only at this time that SWFs reach maximum, total blackout in fact which lasts for about half an hour.

The radio bursts starting at about 0310 UT on 02 August 1972 and associated with particle emission do not show any series of pulses. In the radio bursts starting at about 2030 UT of the same day and associated with proton emission, a brief period of sharp pulses are recorded in the reconstructed 1415 MHz curve given by Castelli and Barron [1973]. The same paper shows the reconstructed curves for the radio bursts associated with the GLE of 07 August 1972. Brief periods of pulses can be seen in the 1415, 606, 410 and 245 MHz burst curves.

We thank the following: J. P. Castelli and J. J. Hennessey for their encouragement, H. Tanaka for Toyokawa burst curves, J. E. Salcedo and staff for careful measurements, and AFCRL for supporting this work.

REFERENCES

- | | | |
|-------------------------------------|------|---|
| CASTELLI, J. P. and
W. R. BARRON | 1973 | Solar radio activity in August 1972
<u>AFCRL Environmental Research
Papers</u> (in press). |
| WILD, J. P. | 1971 | Solar explosions,
<u>Search</u> , <u>2</u> , 229-233. |

Preliminary Report on the Solar Radio Events
of August 1972 Observed at Ahmedabad (India)

by

R. V. Bhonsle, S. S. Degaonkar, and H. S. Sawant
Physical Research Laboratory
Ahmedabad-9, India

As part of the overall research program in solar-terrestrial physics, the Physical Research Laboratory (PRL) operates a number of instruments for the study of solar radio emissions on different frequencies. Table 1 is a list of different solar radio astronomy instruments being operated at PRL, along with information on the physical quantities measured. We present here observational data of the August 1972 solar events recorded by the instruments listed in Table 1. The data pertain to solar noise storms and SCNA's recorded by riometer on 25 MHz, and the solar flare event of August 4, 1972 as observed by microwave radiometer (2800 MHz), radio polarimeter (35 MHz), and radio spectroscope (40-240 MHz).

Table 1

List of Solar Radio Astronomy Instruments at PRL

Name of the instrument	Frequency	Bandwidth	Antenna	Physical Quantity being measured
1. Solar Radio Spectroscope	40-240 MHz	300 kHz	Log-periodic	Meter wavelength Dynamic Spectrum
2. Solar Radio Polarimeter	35 MHz	6 kHz 12 kHz	Crossed-Yagi	Stokes' polarization parameters
3. Solar Microwave Radiometer	2800 MHz	4 MHz	5'-paraboloidal dish	Solar flux, slowly varying and burst radiation
4. Riometer	25 MHz	10 kHz	Broadside-collinear array of 16 halfwave dipoles	Sudden cosmic noise absorption and solar burst radiation

Figure 1 shows a series of daily riometer records from 0100 to 1200 UT, 1 August to 6 August 1972. The curves show cosmic radio noise intensity and solar bursts on 25 MHz for each of these days, along with the calibration of the system. Our main purpose is to show SCNA's and solar radio noise storm records when the sun was in the antenna beam of the cosmic radio noise receiving equipment. Only two SCNA's are evident on the riometer records of 2 and 4 August, which caused maximum absorption of about 1.6 and 1.3 dB, respectively. The solar flare which occurred at 0621 UT 4 August was not observable as an SCNA as such because of off-scale deflections due to intense solar noise storm. It can be easily seen that the noise storm intensity around local noon increased from 1 August to 4 August. This can be explained if one assumes that the noise storm radiation had an appreciable directivity. This view is further supported by the fact that the center of activity responsible for producing this noise storm was very close to central meridian passage on 4 August when it reached its maximum intensity. Assuming the noise storm had more or less constant intensity throughout the disturbed period, the observed day-to-day changes in intensity can be explained in terms of a rotation of the "directive" beam of solar noise storm radiation at the rate of about $14^\circ/\text{day}$. Thus the cone of emission of solar radiation can be estimated to be between 55 and 60 degrees since the noise storm could be barely observed on 1 August and 6 August and the maximum occurred on 4 August.

Figure 2 is the record of solar radio flux at 2800 MHz made by means of a Dicke-type radiometer on 4 August. On this day, the flux due to the quiet sun and slowly varying component as measured by our instrument was about 140 fu (1 flux unit = 10^{-22} Watts/m²/Hz). It can be seen from Figure 2 that a number of microwave bursts occurred on 4 August. First, a small burst with peak flux of about 40 fu occurred at 0525 UT with 33 minutes duration. This was followed by a strong burst, starting at about 0613 UT. The peak intensity of this burst could not be recorded since the radiometer was saturated due to insufficient dynamic range of the receiver. However, the peak flux recorded during this major radio burst as reported by other observatories is around 5000 fu. It should also be noted that this major event was followed by a series of "fluctuations" in the solar flux on the order of a few hundred

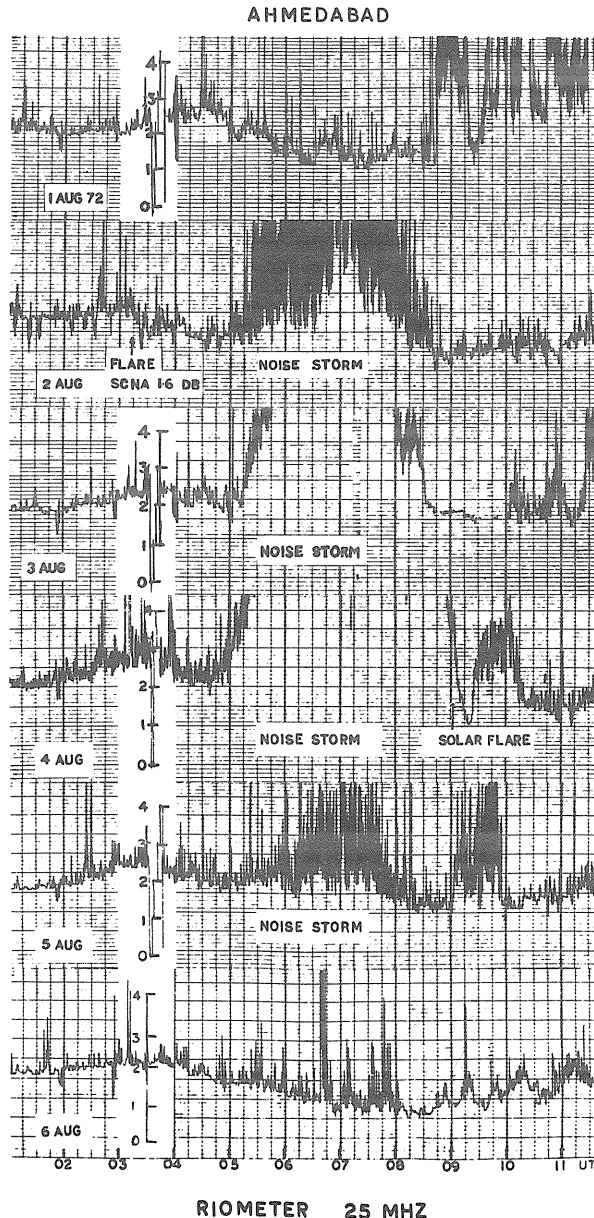


Fig. 1. 25 MHz riometer recordings from 1 August to 6 August 1972

flux units. The H-alpha flares and meter wavelength type III bursts that were reported by various solar observatories are marked at the bottom of the Figure 2. At least five H-alpha flares of importance greater than 2B are identified. Some fluctuations in the burst intensity between 0730 and 0830 UT may be attributed to the small flares.

Figure 3 shows the dynamic spectrum recorded by the solar radio spectroscop (40-240 MHz). A major meter wavelength solar event started at 0625 UT on 4 August 1972 and was superimposed on the background noise storm shown in the riometer record in Figure 1. This background noise storm was just above the sensitivity limit of the radio spectroscop. Therefore, the meter wavelength radiation due to the flare dominated the background noise storm and produced the complex radio spectrum shown in Figure 3. This major event started with Type III group at 0625 UT with their starting frequencies less than 140 MHz showing a lot of fine structure both in time and frequency. A well-defined Type II (slow drift) burst could not be identified as such, but there were some drifting features in the spectrum. However, broad band fluctuations of Type IV can be seen quite clearly. At about 0640 UT the spectrum extended into the higher frequency region implying the injection of higher energy particles into "magnetic bottles," then emitting radio waves by the synchrotron process. A puzzling feature of this spectrum is that there was no well-defined magnetohydrodynamic shockfront like that usually associated with Type II bursts.

SOLAR RADIO BURST AT 2800 MHZ OBSERVED AT AHMEDABAD
4 AUGUST 1972

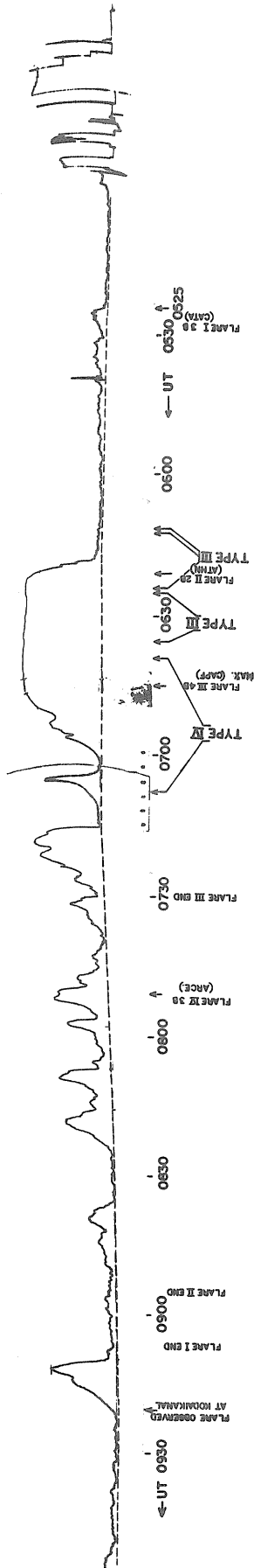


Figure 2. Solar microwave bursts on 4 August 1972.

DYNAMIC SPECTRUM OF SOLAR RADIO BURST AT
METER WAVELENGTHS
ON 4 AUGUST, 1972 AHMEDABAD

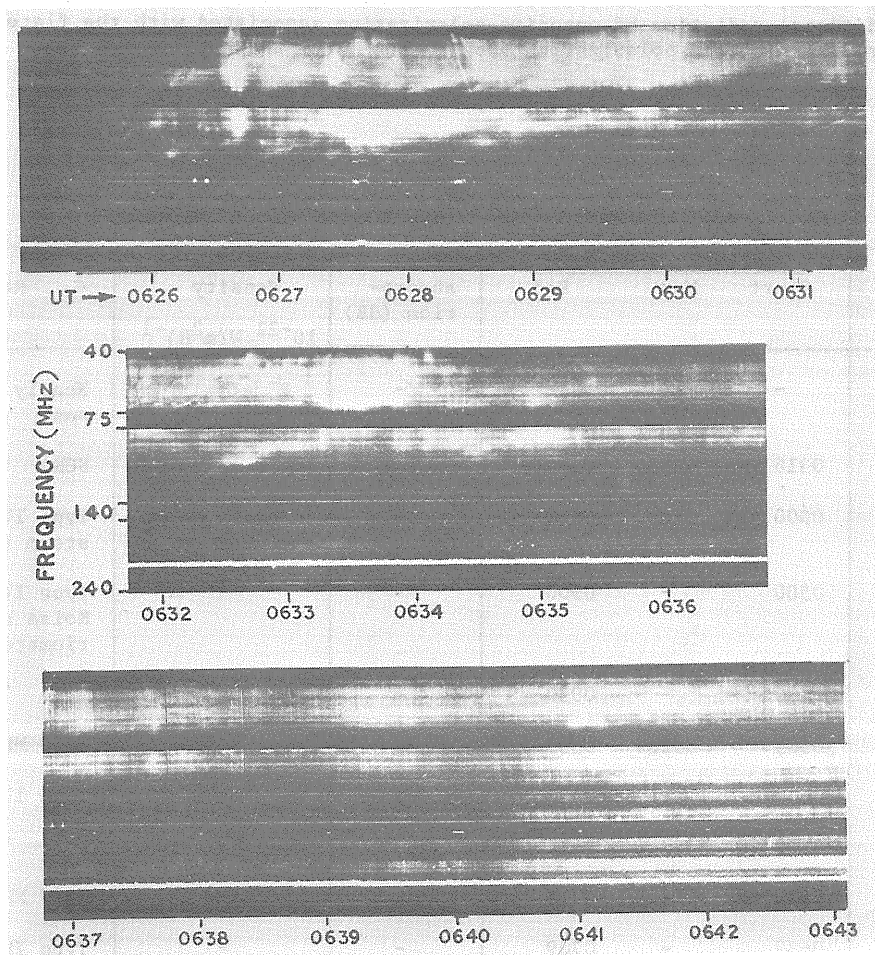


Fig. 3. Dynamic spectrum of meter wavelength solar burst on 4 August 1972.

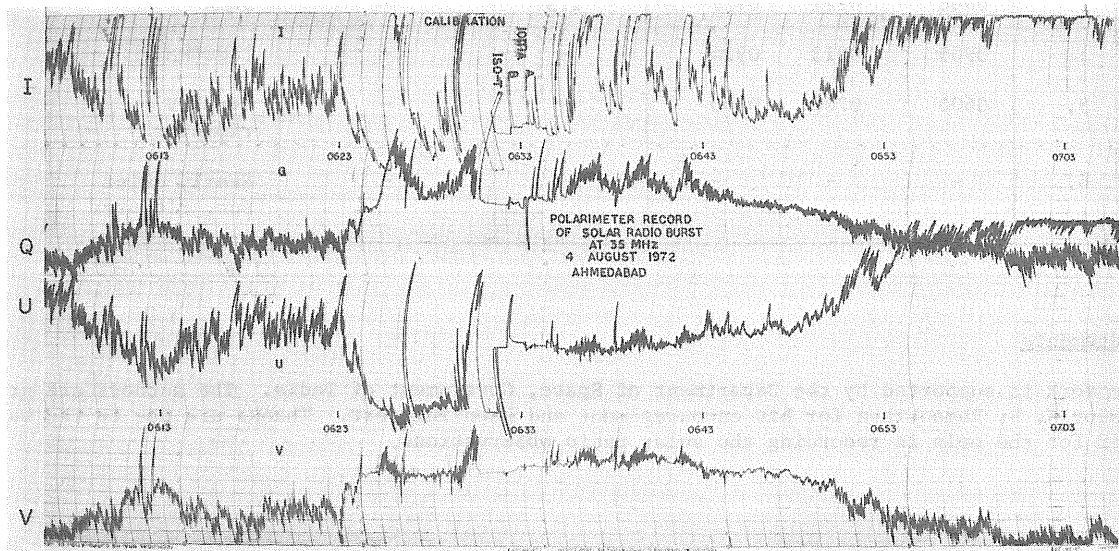


Figure 4. 35 MHz Polarimeter recording on 4 August 1972

Figure 4 shows the record of the time-sharing polarimeter operating on 35 MHz for 4 August from 0607 to 0706 UT. The polarimeter records quantities proportional to Stoke's parameters, I, Q, U, and V, which completely define the state of polarization of the incoming solar radiation. This record shows that the noise storm on 4 August before 0624 UT was left-handed polarized, and at 0625 UT when the major burst began, the sense of polarization became right-handed until 0650 UT. This happened due to a strong additional radiation of opposite polarization associated with the flare. This was further intensified, transforming the polarization back to the left-handed sense.

The chronology of solar events described in this note are summarized in Table 2.

Table 2

List of Outstanding Solar Radio Events at Ahmedabad

Date August 1972	(UT)			Peak absorp- tion (dB)	Peak Flux density $10^{-22} \text{ W(m}^2\text{H)}^{-1}$	Remarks
	Start	Max.	End			
1.	-	-	-	-	-	Nearly quiet sun
2.	0316	0332	0400	1.6	-	SCNA
	0500	0700	0830	-	-	Type IV, Noise storm riometer
3.	0500	-	0900	-	-	Type IV, Strong Noise storm riometer
4.	0430	-	0930	-	-	"
	0525	0528	0558	-	42	2800 MHz
	0612	-	0612.10	-	-	Type III
	0612.40	-	0612.45	-	-	"
	0613	-	0715	-	> 500	2800 MHz
	0639	-	0709	-	-	Type IV
	0716	-	0900	-	490	2800 MHz
	0906	0921	0927	1.3	-	SCNA
	0909	0913	0924	-	-	2800 MHz
5.	0600	0700	0800	-	-	Type IV, riometer
6.	-	-	-	-	-	Nearly quiet sun, riometer

Acknowledgements

This work is supported by the Department of Space, Government of India. The authors are grateful to Professor K. R. Ramanathan for his encouragement and keen interest. Thanks are due to the maintenance staff for the help in recording the solar radio observations.

Solar Radio Emission on 100, 200 and 500 MHz
Observed at Hiraïso

by

F. Yamashita
Hiraïso Branch
Radio Research Laboratories
Japan

Three examples of radio bursts observed at Hiraïso in August 1972 are shown in Figure 1. Also, dynamic spectra using data from Toyokawa, Nobeyama and Kokubunji are presented in Figure 2.

(R+L) and (R-L) of the record on 100 MHz express total flux and intensity of polarization, respectively, where R and L are the right- and left-handed circular component of polarization. (R-L) is scaled linearly and others are logarithmic.

From the records, each burst is seen as a type IV without type II, and on 100 MHz some depressions of polarization were observed. These depressions occurred when their fluxes were increasing, and their periods are some tens of minutes. This may be interpreted as the radiation from a moving source which appears after the start of a type IV burst.

Steady fluxes of 100 and 200 MHz during the period are listed in Table 1.

Table 1

Flux in $10^{-22} \text{W} \cdot \text{m}^{-2} \text{Hz}^{-1}$

Day	UT Hour	00	01	02	03	04	05	06	07	08	09	20	21	22	23	24
(100 MHz)																
1		1	2	2	2	2	2	2	2	2		1	2	2	2	
2		3	12	14	80	102	57	37	30	19		112	153	100	100	
3		98	80	51	52	48	19	18	27	25		107	105	110	120	
4		115	115	117	110	110	100	140	170	130		75	73	78	70	
5		75	74	76	55	45	40	44	43	37		13	12	11	-	
6		17	17	13	11	7	11	8	17	17		7	5	6	5	
(200 MHz)																
1		6	6	6	5	5	5	5	5	6		8	6	8		
2		7	10	11	10	10	10	10	10	10		16	16	16		
3		16	16	16	16	21	16	15	16	9		37	41	38		
4		40	48	38	50	54	45	35	35	35		32	30	29		
5		26	45	46	37	25	21	24	19	15		10	10	15		
6		22	12	15	15	11	26	14	20	17		16	17	16		

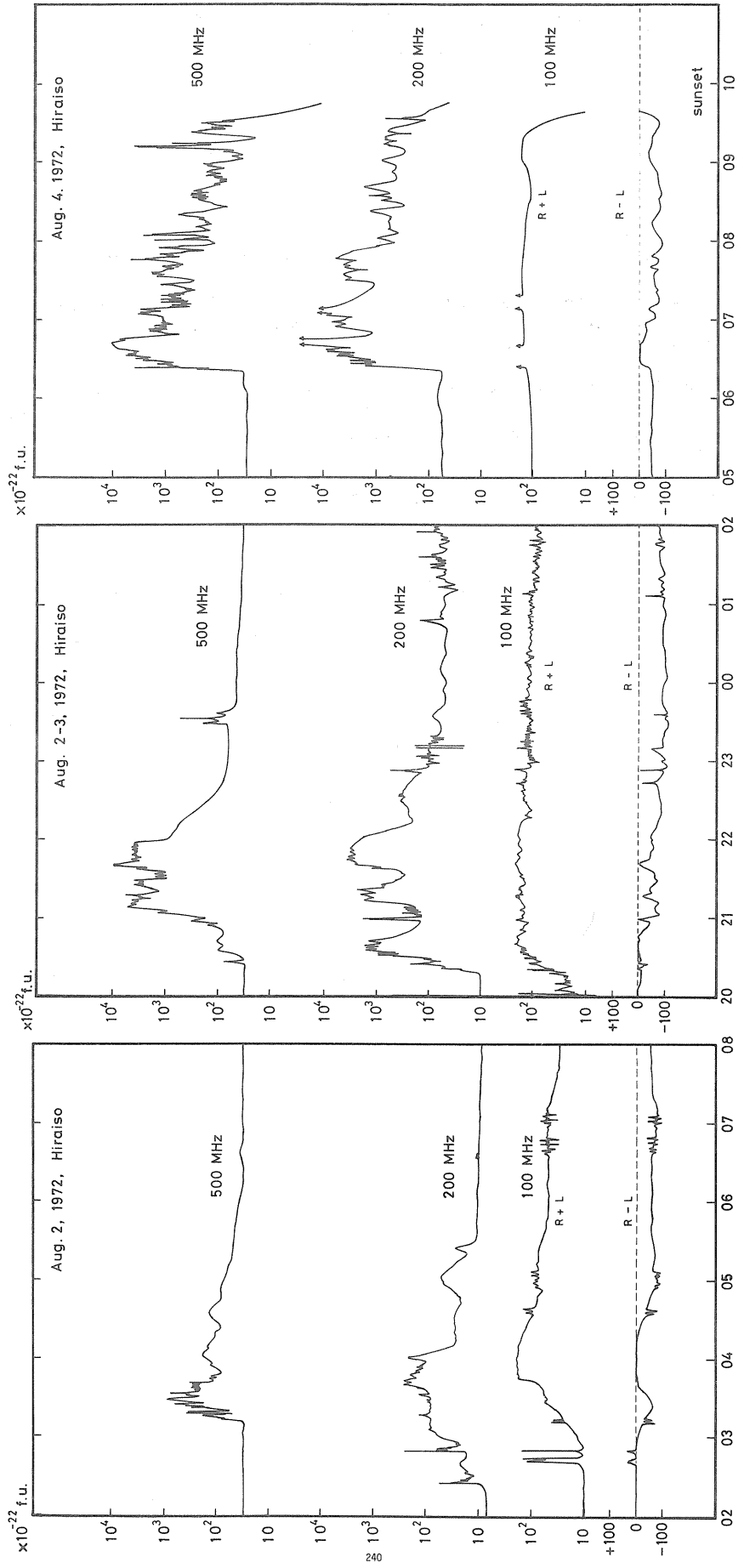


Fig. 1

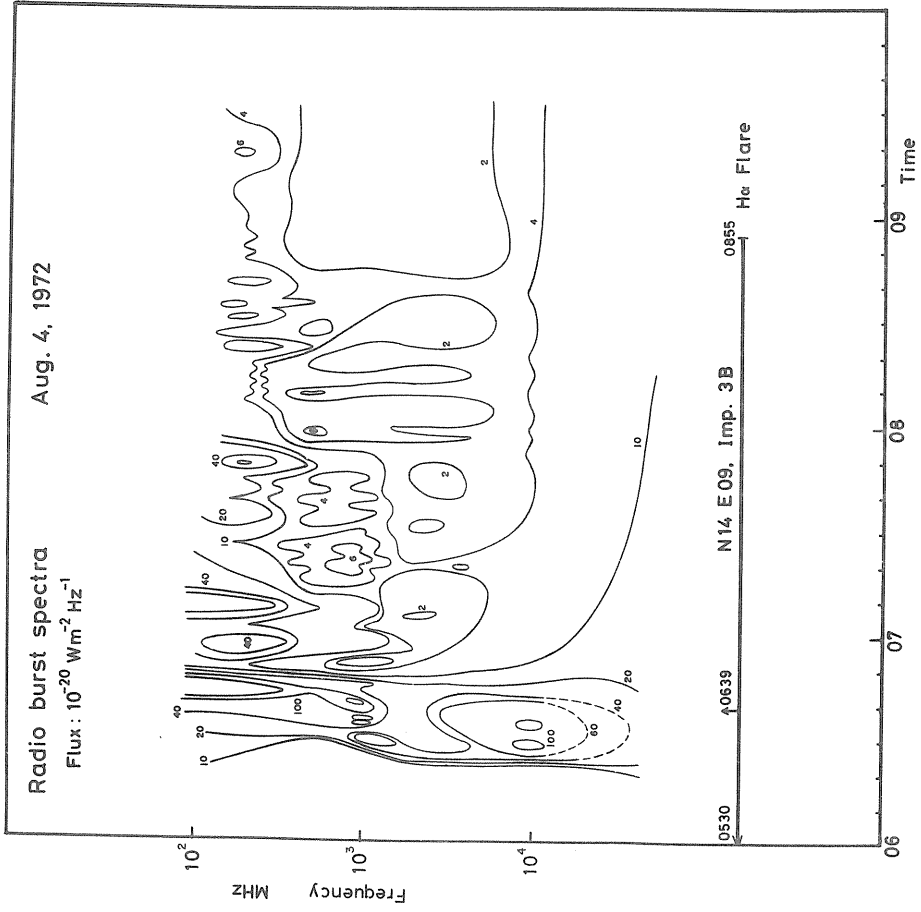
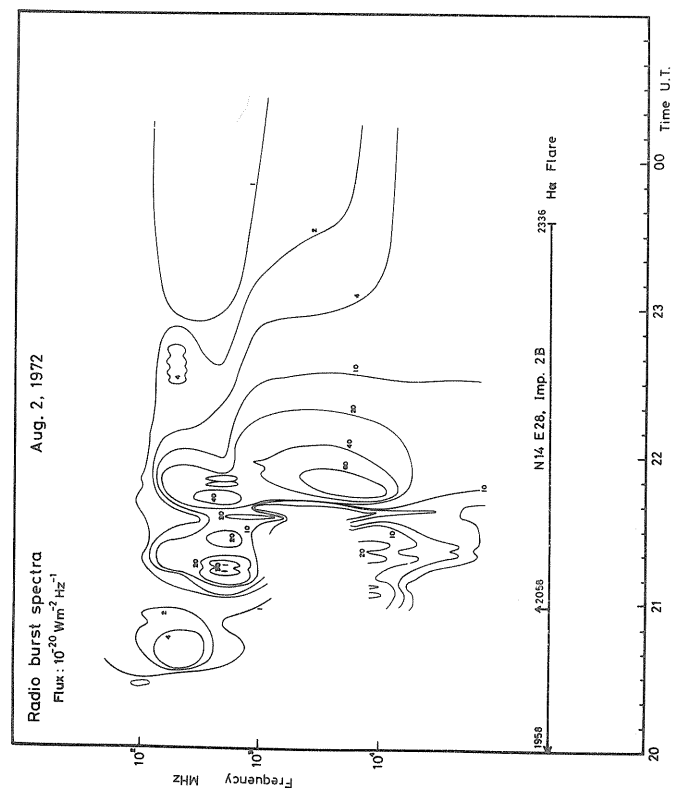
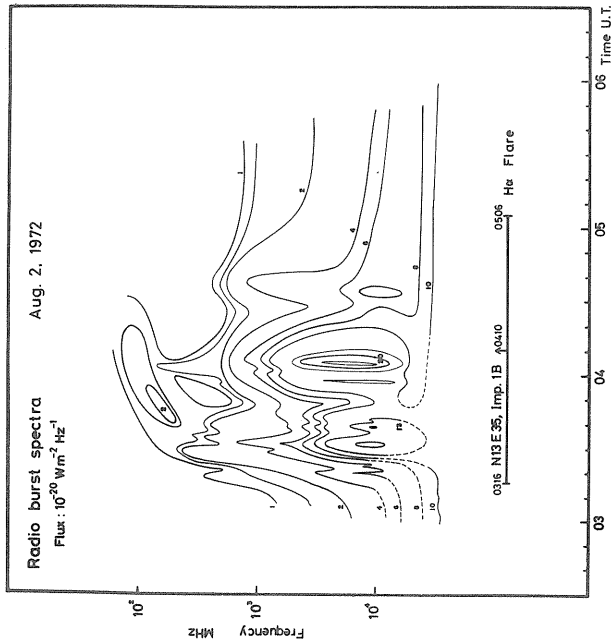


Fig. 2. Dynamic spectra using data from Toyokawa, Nobeyama and Kokubunji for August 2 and 4, 1972.

INTERFEROMETRIC RADIO SPECTRA OF THE SOLAR CORONA
1-11 AUGUST 1972

by

James C. Dodge
Radio Astronomy Observatory
Department of Astro-Geophysics
University of Colorado
Boulder, Colorado 80302

INTRODUCTION

This contribution is a condensation of an observatory publication (Dodge [1973]) which presents dynamic spectra and position maps for the decametric and metric radio burst activity that accompanied the disc passage of McMath Plage Region 11976. That publication is organized to emphasize the development of the radio emission throughout the period of major radio activity. It treats the various types and intensities of observed emission as manifestations of an enduring solar disturbance. In addition, it provides a review of the University of Colorado swept-frequency measurements, details of the interpretation of the data records, and an analysis of the procedure used to obtain position maps from a minicomputer input device which scans calibrated tracings of the interference fringes.

This report concentrates on the burst activity related to the strongest flares of the period. Many of the bursts that were included in the former report to illustrate the general growth, continuity, and decay of the emission surrounding the strong, flare-related events have been eliminated here; however, the growth and decay of the emission is described in the text.

OBSERVING EQUIPMENT

The dynamic spectra in this report were obtained during the daily swept-frequency observations of the sun and Jupiter by the Radio Astronomy Observatory of the University of Colorado. Radio noise is collected with a pair of broadband, directional antennas whose combined collecting area is approximately 1,000 m². The receivers sweep three frequency octaves from 8-80 MHz in a period of 1.5 sec. The spectra are recorded simultaneously on continuously-moving 35 mm film with a light-beam recorder and on facsimile paper. In the format for this report, increases in received noise are recorded as white areas on a dark grey or black background. The narrow dark bands which stripe the emission spectra are interference fringes which permit the determination of the emission's arrival angle.

OBSERVED SOLAR RADIO NOISE

The data period of 1 - 11 August was selected because it includes most of the radio activity which bracketed the four flares of importance 2B or greater (1958 UT 2 August, 0530 UT 4 August, 1455 UT 7 August, and 1227 UT 11 August). The solar observing day during August extended from 1200-0200 UT. Thus, the radio events in close association with the 4 August flare escaped our observation.

Comparisons with other solar observations were obtained principally by reference to Lincoln and Leighton [1972].

24-31 July 1972

Radio activity in the metric and decametric bands began on 24 July 1972, two days earlier than the start of the retrospective world interval (26 July - 14 August 1972). The activity during this period consisted entirely of Type III bursts. The activity showed development in both frequency of burst occurrence and in the ratio of the number of groups of Type III's with high intensity to the number with low intensity (See Table 1).

1-6 August 1972

Radio burst activity on 1 August increased in frequency of occurrence and in variety. In addition to twenty-one Type III events, seven of which were of intensity two or greater, a background emission of weak decametric continuum (Intensity 1- to 1) began at 2030 UT and lasted for three hours.

Date: July	Number of Bursts					
	Intensity < 2			Intensity ≥ 2		
	Isolated Type III's	Groups of III's	Total	Isolated Type III's	Groups of III's	Total
24		1	1		1	1
25	2	2	4		1	1
26	4	2	6	1		1
27	5	5	10		2	2
28	12	5	17	1	9 (3)	10
29	17	6	23	3	7 (5)	10
30	4	5	9	3	4 (1)	7
31	6	3	9	1	2 (1)	3

Table 1. Summary of observed radio bursts 24-31 July 1972. Counts in parentheses represent the number of groups which consisted of ten or more Type III's.

The sequence of burst types from 1-6 August is diagrammed in Figure 1 as a function of burst intensity. There is obvious development in the number and the intensity of the Type III events as well as a progressive increase in the intensity of the decametric continuum prior to the sudden commencement of the strong Type IV burst at 2033 UT on 2 August. There is a gradual decrease in the intensity of the continuum following the Type IV burst. Decametric continuum is distinguished from a Type IV burst by the frequent appearance of Type III bursts from the same location as a weak, irregular continuum background. The frequency of the related Type III bursts seldom exceeds 56 MHz.

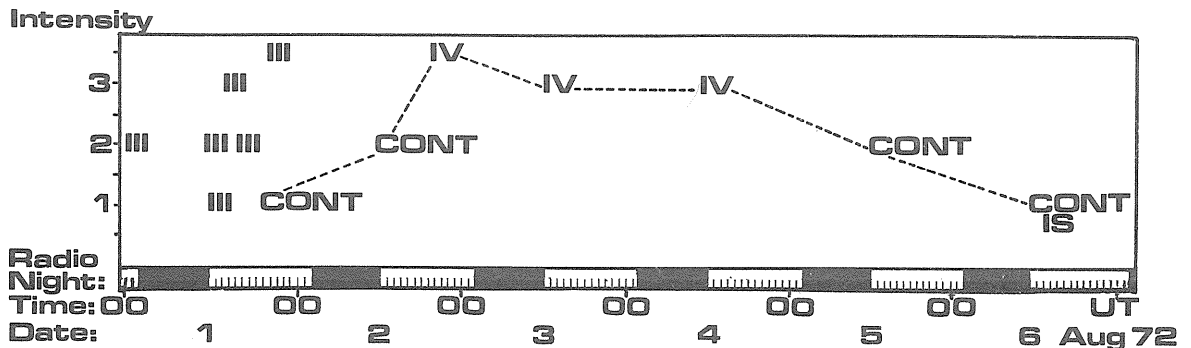
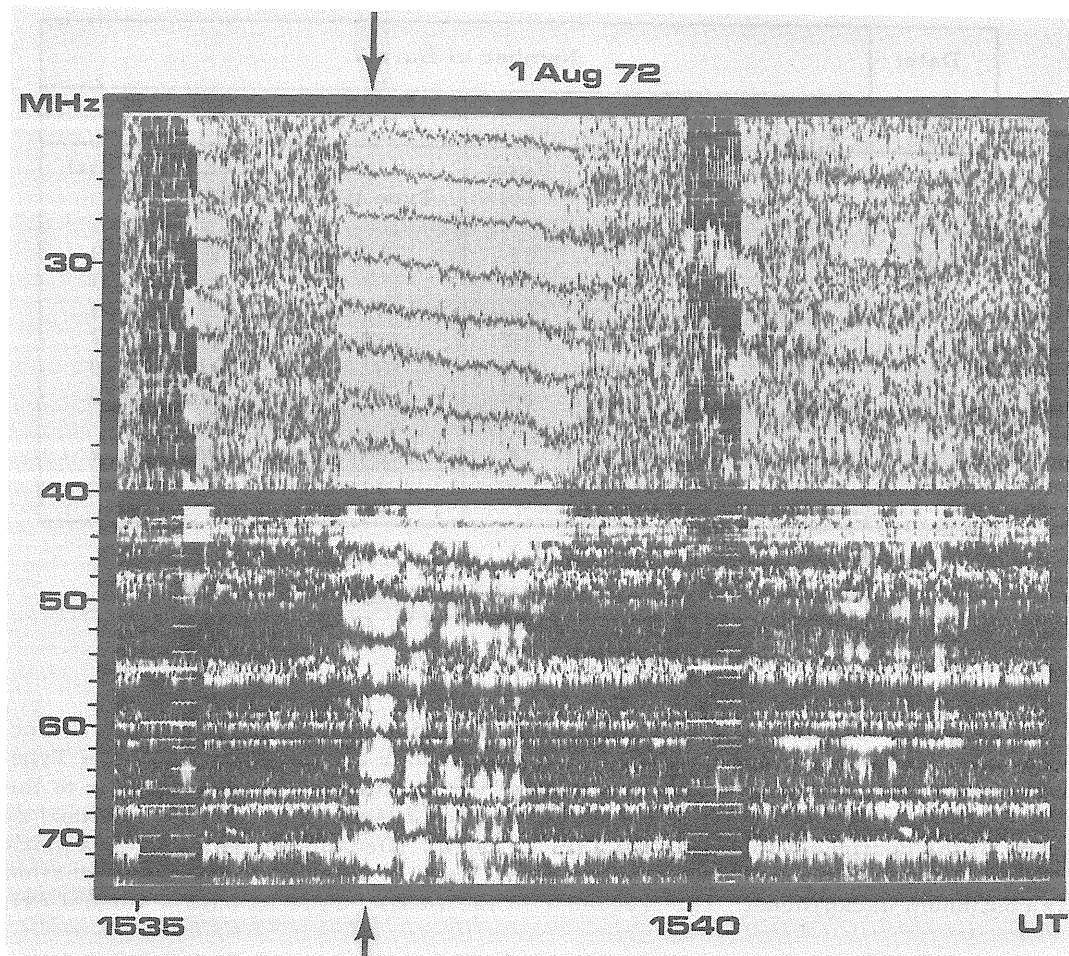


Fig. 1. The development of 20-80 MHz radio emission as a function of both type and intensity (00 UT 1 August 1972 - 0142 UT 7 August 1972).

Figure 2 shows a hierarchy of Type III burst groups. Components of the three principal groups have been classified as Type III, Int. 1; Type IIIG, Int. 2; and Type IIIG, Int. 1 respectively. The central group in the 40-80 MHz range shows further subdivision into six, nearly-periodic subgroups. On a still smaller scale, each of the six subgroups has a cluster of about three intensity peaks.



Type: IIIG
 Intensity: 3
 Occurrence: Isolated
 Associations: Subflare
 1537-1555 UT, several
 eruptive centers, N14 E44

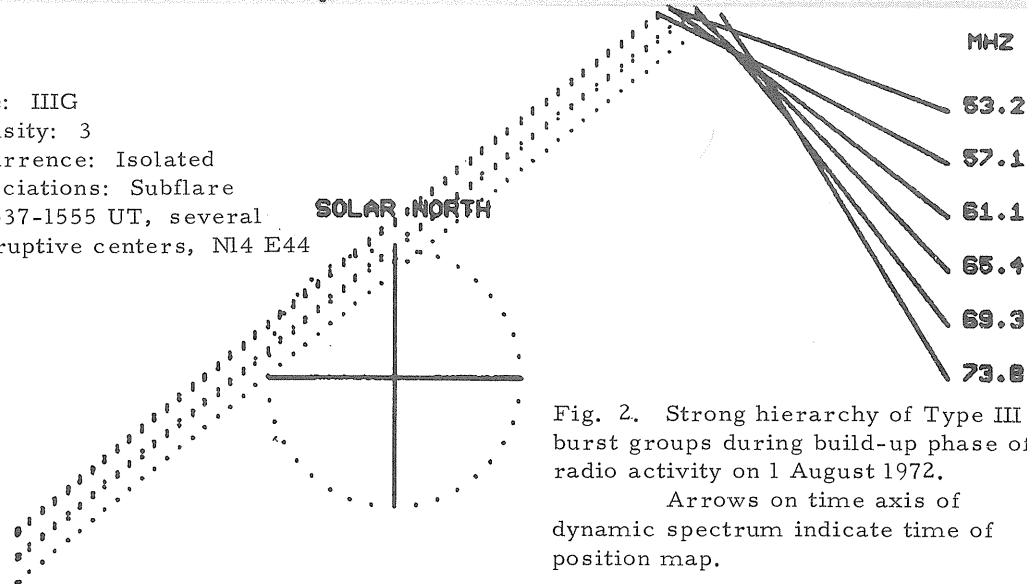


Fig. 2. Strong hierarchy of Type III burst groups during build-up phase of radio activity on 1 August 1972.

Arrows on time axis of dynamic spectrum indicate time of position map.

Figure 2 illustrates the spectrum and the implied position loci for one of the seven strong Type III bursts on 1 August. Estimated fringe frequency scanning errors (± 32 kHz) imply maximum relative position locus errors of $0.02 R_{\odot}$. However, geophysical factors such as ionospheric scintillation, refraction, and position wobble due to multiple sources contribute more to position uncertainty than the process of measuring and converting fringe frequencies to angular positions. For this event, adjacent sets of interferometer lobe nulls are separated from the illustrated group by $1.7 R_{\odot}$.

On 2 August, the sun emitted radio noise continuously across at least 12-80 MHz throughout our periods of radio observability. The initial decametric continuum was typical of that category of emission. For example, in the period 1300-1500 UT only 11 Type III's extended to >70 MHz from more than 70 such bursts (usually < 0.1 min in duration). Most of these short-lived bursts were not observed above 56 MHz. Those bursts which did not extend above 56 MHz seldom produced any noticeable shifts in the interference fringes, thus it can be assumed that they were produced in the same source region as the continuum background. The continuum showed periods of uniform intensification and fading through most of 2 August.

The character of the emission changed suddenly and dramatically at 2033 UT when a period of intensity 2 decametric continuum ended and an intensity 3+ Type IV burst began. The most probable source of the particles responsible for the Type IV emission was a region at N13 E28 which had flared with importance 2B at 1958 UT and with importance 1B at 2006 UT.

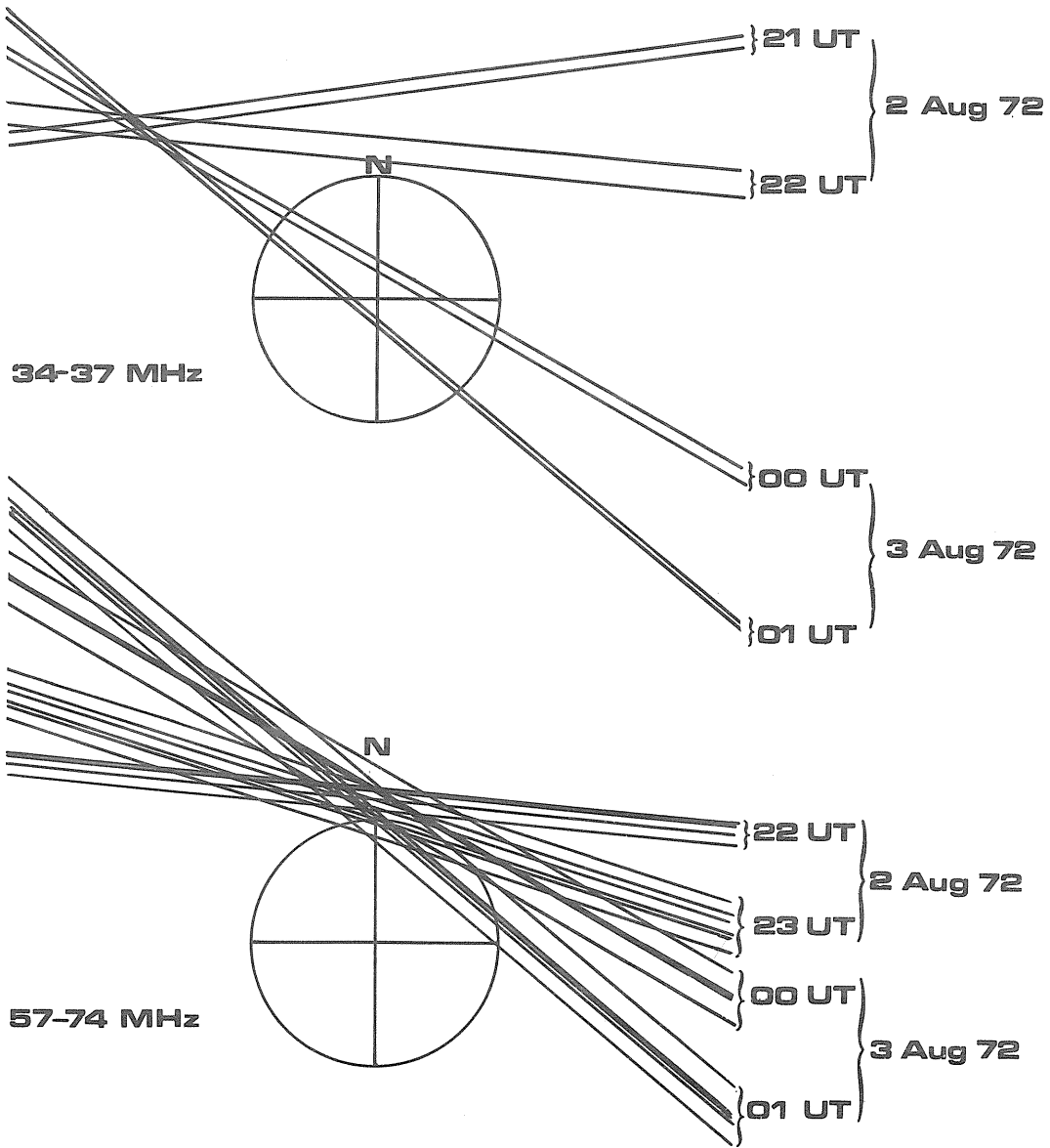
Continuous, strong Type IV emission was observed for the remainder of the observing day on 2 August and again throughout 3 and 4 August. The emission saturated the records from 20-80 MHz until the latter part of 4 August. Many Type III's were observed during the weaker periods of the Type IV burst. The positions of these differed slightly from that of the Type IV because obvious fringe frequency changes occurred during the Type III's.

One advantage of the saturated records during the strong Type IV burst was that the interference fringes that were produced were exceptionally narrow and distinct. This characteristic allowed the determination of high-confidence position loci over long segments of the Type IV burst. The rotation of the Earth changes the angle of position loci with respect to the solar coordinate system. Thus, if the emission originates from the same location for long enough, an estimate of the average two-dimensional position of the emission may be found at the intersections of the Earth-rotated position loci.

Figure 3 shows the results of using this technique for a five hour period during the early part of the Type IV burst. Figure 4 is a fringe intersection diagram for a six hour period which began 18 hrs after the end of the period represented by Figure 3. The intersection in Figure 4 is distinctly southwestward of the intersections in Figure 3. The apparent positions agree rather well with reasonable decametric extrapolations of the positions determined by the 169 MHz interferometer at Nançay (Lincoln and Leighton [1972]). Similarly, the fringe intersections can be compared with the extrapolated E - W motion of the principle peak of 10.7 cm radiation as measured by the Algonquin Radio Observatory of Canada (ibid.). The E - W scans at 21 and 43 cm made at Fleurs, Australia also show this peak (ibid.).

By 1225 UT on 5 August, the emission had changed its character to that of decametric continuum (Intensity 2) once again. The number of observed Type III's at that time was enormous. More than 80 clearly definable Type III intensity maxima were observed in one hour between 1400 and 1500 UT on 5 August.

The continuum emission weakened to intensity 1- by 1800 UT on 6 August and the number of Type III intensity maxima had decreased to only 5-6 hr^{-1} . The emission continued to diminish in intensity until it dropped below the threshold of detection at 0142 UT on 7 August.



Type IV Positions (2101 UT 2 Aug 72 - 0106 UT 3 Aug 72)

Fig. 3. This diagram illustrates the relative absence of source motion for the Type IV burst which began at 2033 UT on 2 August 1972. The upper plot shows the intersection of two adjacent lines (34-37 MHz) from each of four sets of position loci over a four hour span. The remaining lines did not show this tight intersection. The lower plot shows all lines (57-74 MHz) from four consecutive sets of fringe frequency measurements one hour apart.

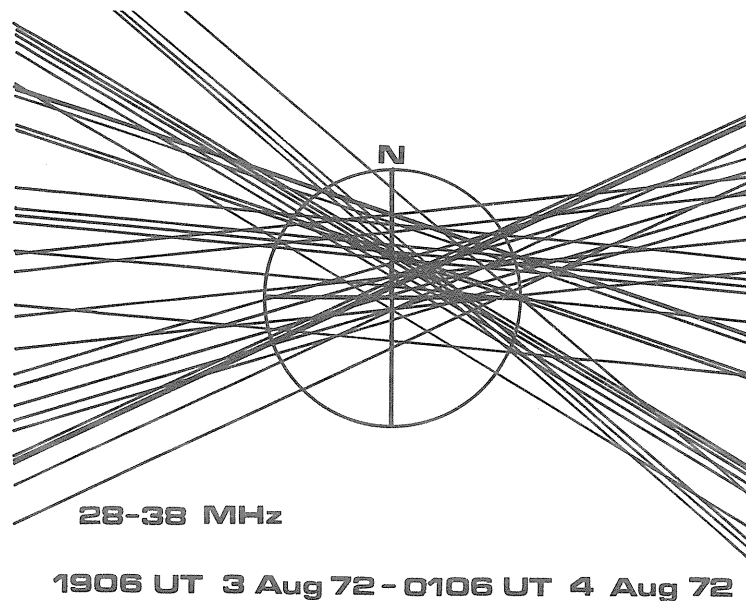


Fig. 4. The intersection of six fringe position lines per hour from 28-38 MHz during the period 1906 UT on 3 August to 0106 UT on 4 August. This is a nonselective plot which presents all analyzed fringe lines during that six hour period. Thus, the indicated region of maximum fringe intersection can be taken to represent a time and frequency average of the location of the Type IV burst for six hours of continuous decametric emission.

7 August 1972

The principal radio activity on this date was that associated with the great solar flares which began at approximately 1445 UT. During the following half hour, many flares were reported from the region at N12-16 W32-40. The several flares varied in importance from 1B through 4B.

Figure 5 demonstrates the sequence of radio activity which followed the flares. Activity began with a few minutes of moderate intensity Type IV (>60 MHz) and one each Type III and Type IIIG burst. Suddenly, at 1514.6 UT, an intensity 3 Type IV burst began at 20-80 MHz. The Type IV burst covered the whole frequency span until 1552 UT and then showed a frequency-dependent fade-out with a cutoff which sloped linearly from 80 MHz at 1552 UT to 20 MHz at 1635 UT. Thereafter, an intensity 1+ continuum appeared from 20-80 MHz and faded progressively to a 1- continuum at 1900 UT on 7 August. The continuum remained at the threshold of detection until 1710 UT on 8 August.

Beneath the activity diagram in Fig. 5 are shown the related times of flare maxima and the displaced times of reported flare starts (Lincoln and Leighton [1972]). Both types of data are plotted as a function of the importance of the bursts. Notice that three reports of an intensity 3-4B flare reaching its maximum occurred within the minute before the strong Type III burst (~1531 UT). Also notice that if the flare starting times are shifted in time 25 minutes relative to the complicated activity during the first 25 minutes of the Type IV, there is a match between the spans of both measures of the activity. The flare starting times are plotted with this 25 minute displacement.

The slopes of the leading edges of the traced Type II bursts were evaluated for their implied radial components of velocity. The time difference between the starting times of the emission at 40 MHz and 28 MHz was used in each case with the distance ($0.255 R_{\odot}$) between those two frequencies determined from the 10 x van de Hulst model of solar electron density variation with height.

The four Type II bursts in the order of their occurrence had radial components of velocity of 3.9, 4.9, 1.4, and 0.9×10^3 km sec⁻¹.

When the component of radial velocity in the first Type II burst is computed from the slope of the axis of the burst spectrum rather than the leading edge, the four Type II's show a progressive decrease in radial velocity (i. e. 9.55, 4.9, 1.4, and 0.9×10^3 km sec⁻¹). This higher velocity estimate for the first Type II applies to that portion of the coronal disturbance which produced the maximum intensity core of the emission.

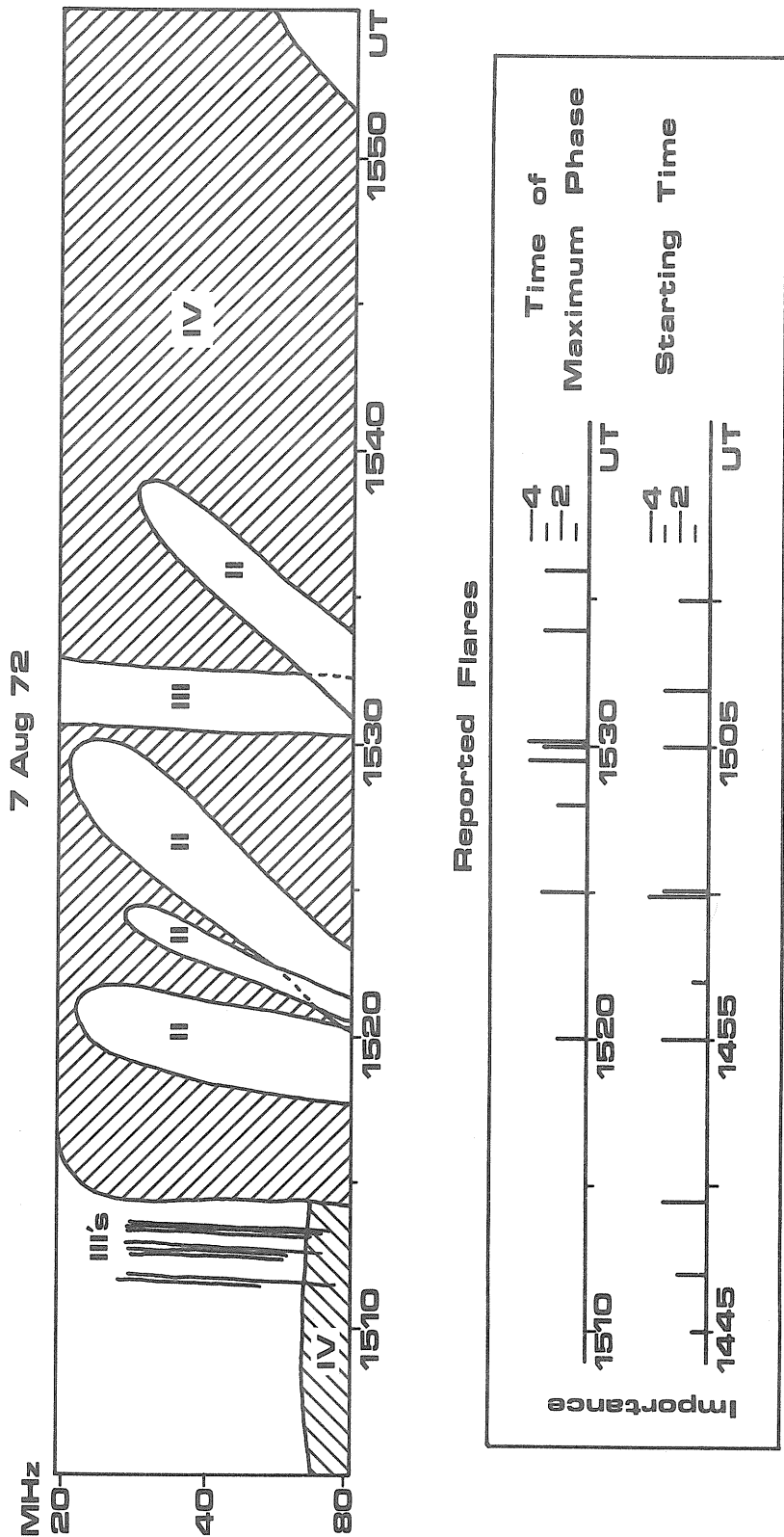


Fig. 5. Diagram of the initial, simultaneous emission portion of the 20-80 MHz radio burst emission associated with the great flares of 7 Aug 72.

The post-IV continuum endured for 26 hrs with uneven background emission and irregular groups of Type III's. Again, these Type III's seldom exceeded 56 MHz.

Figure 6 indicates the position of the continuum as estimated by the intersection of position loci separated in time by ~6.5 hrs.

The positions were actually made in the Type III's rather than the continuum background. This is because the fringes showed no frequency shifts between the background and the bursts and because the stronger Type III emission produced narrower fringes. Narrow fringes allow more precise measurement of the instantaneous fringe frequencies.

The plot of position loci for 0036 UT on 8 August shows alternating positions with increasing frequency. This is the effect of a drift in the reference level at which the negative fringes are inverted. The correct position locus is midway between the alternate sets.

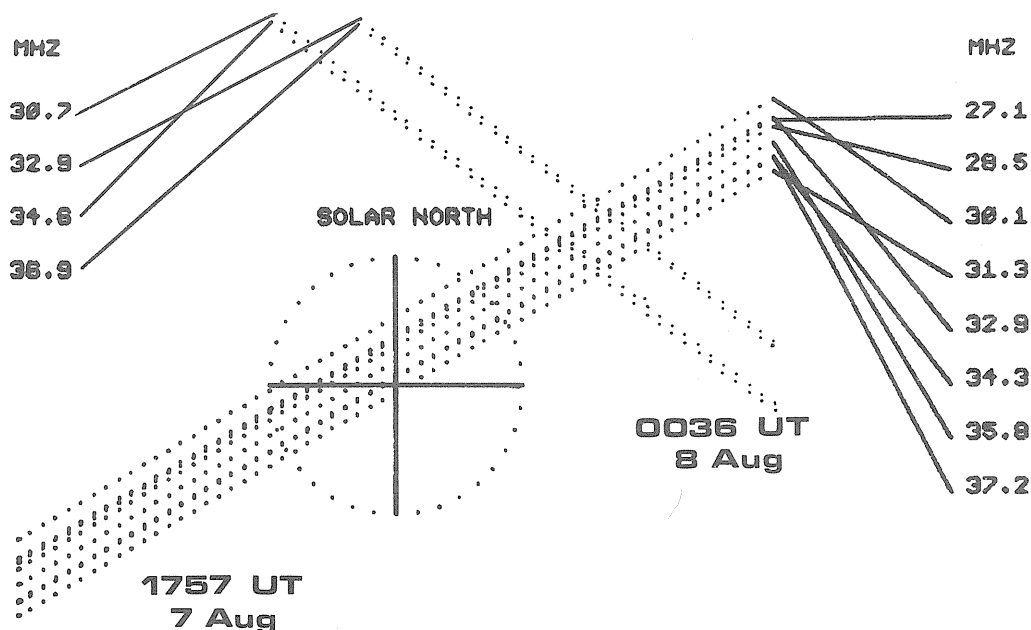


Fig. 6. Location of the continuum following the major Type IV burst on 7 August 1972.

8-10 August 1972

The faint, residual, background continuum following the major Type IV on 7 August remained until 1710 UT on 8 August. The continuum was just above the threshold of detection and was classified as intensity 1--.

The radio burst activity during 8-10 August consisted primarily of isolated Type III bursts.

Figure 7 provides an illustration of the smooth, moderately-intense period of decametric continuum from which one Type III component was selected for the 0036 UT position evaluation.

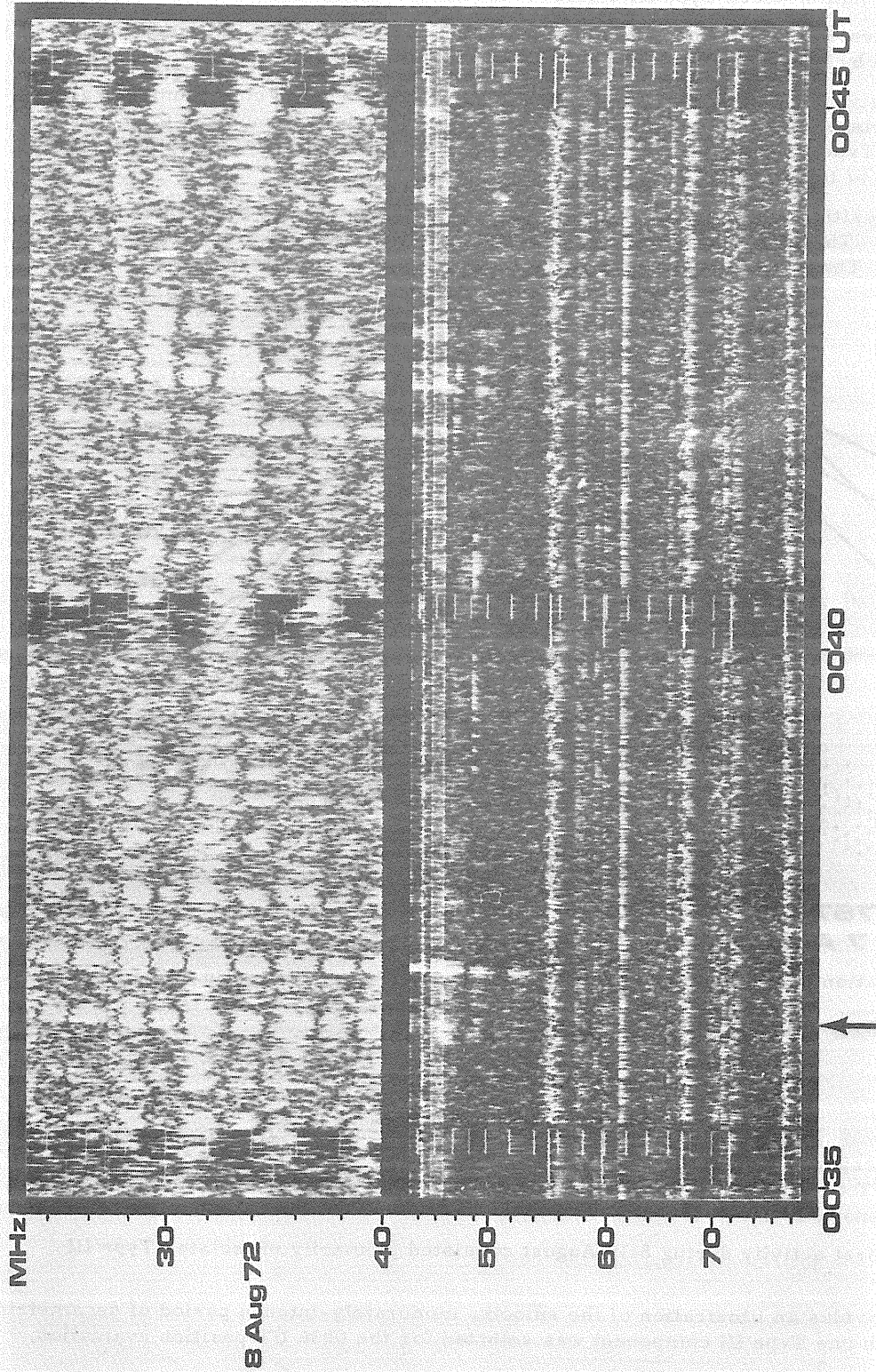


Fig. 7. This spectrum illustrates a smooth, moderately-intense period of continuum from 0035-0045 UT on 8 August. The arrow indicates the time of the fringe frequency scan that was used to evaluate the location of the continuum. Constant-frequency marks from 55-80 MHz are interference from radio and television transmissions.

11 August 1972

As McMath Region 11976 rotated past the west limb of the sun on 11 August, the region flared once again and produced a variety of decametric and metric radio burst activity. Figure 8 shows that the sequence of bursts following the great flare of 11 August is similar to that which occurred on 7 August.

Figures 9 and 10 show the detailed dynamic spectra of the 11 August series of events. The top spectrum in Figure 9 illustrates a frequent characteristic of the stronger Type II events, i. e. a precursor group of continuous, decametric Type III bursts of intensity comparable to that of the Type II bursts. Figure 10 gives detailed spectra, intensities, radial velocities, and position loci for the period at the onset of the Type IV burst.

Although the 11 August event was an early morning observation at Nederland, Colorado, the interference fringes do not show the potentially ruinous effects of irregular ionospheric refraction. This fact does not preclude the possibility that all of the fringes are shifted by a certain amount, but it does allow us to perform relative position analyses. The two sets of position loci in Figure 10 represent the Type III at 1241 UT and the II-IV combined emission at 1251 UT. The loci confirm what one would suspect from sighting along the fringes from burst to burst. All of the various types of emission must have been received from nearly the same direction.

The Type IV portion of the radio event shows progressive cutoff at lower and lower frequencies with increasing time. This characteristic also was observed in the 7 August event. The similarity ends there, however. No enduring continuum followed the Type IV cutoff as it did for the 7 August event.

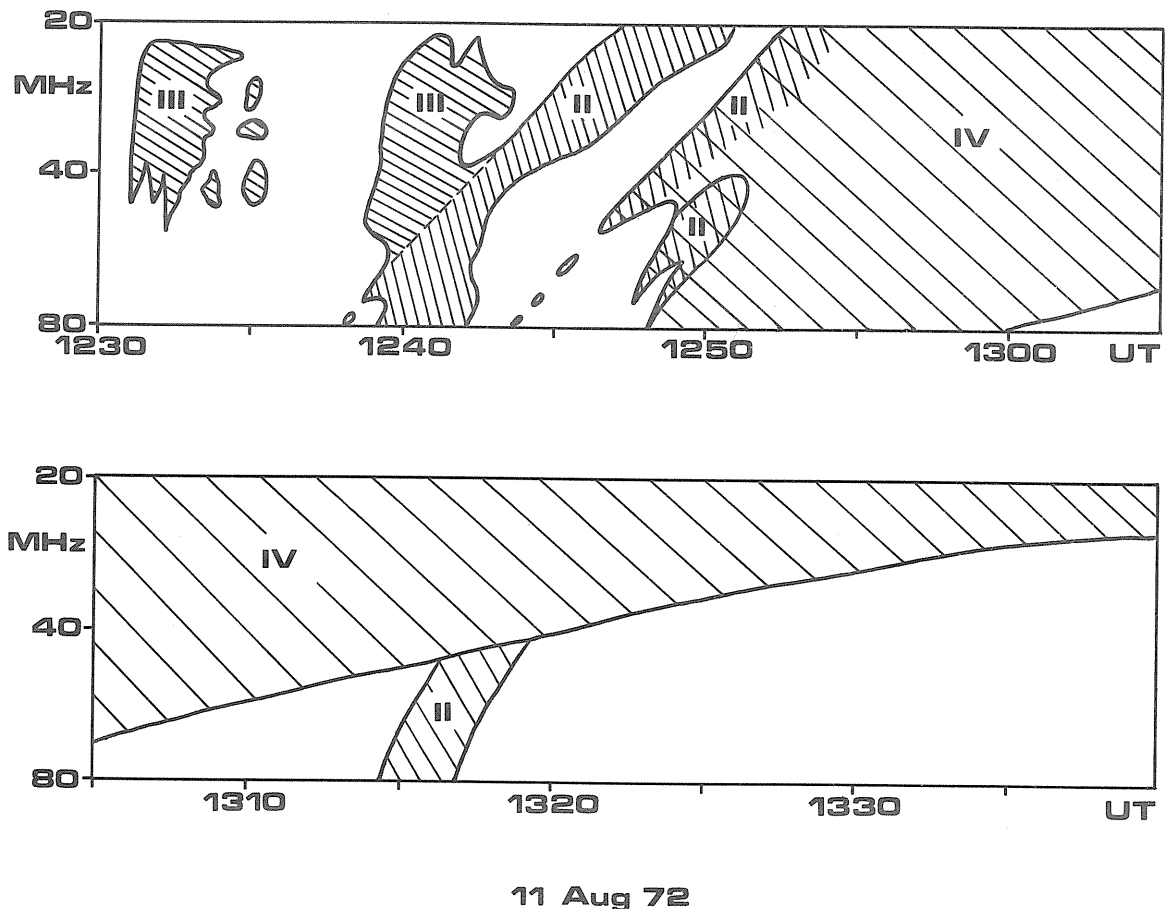


Fig. 8. Sequence of radio spectra following the 2B flare at 1230E UT on 11 August 1972.

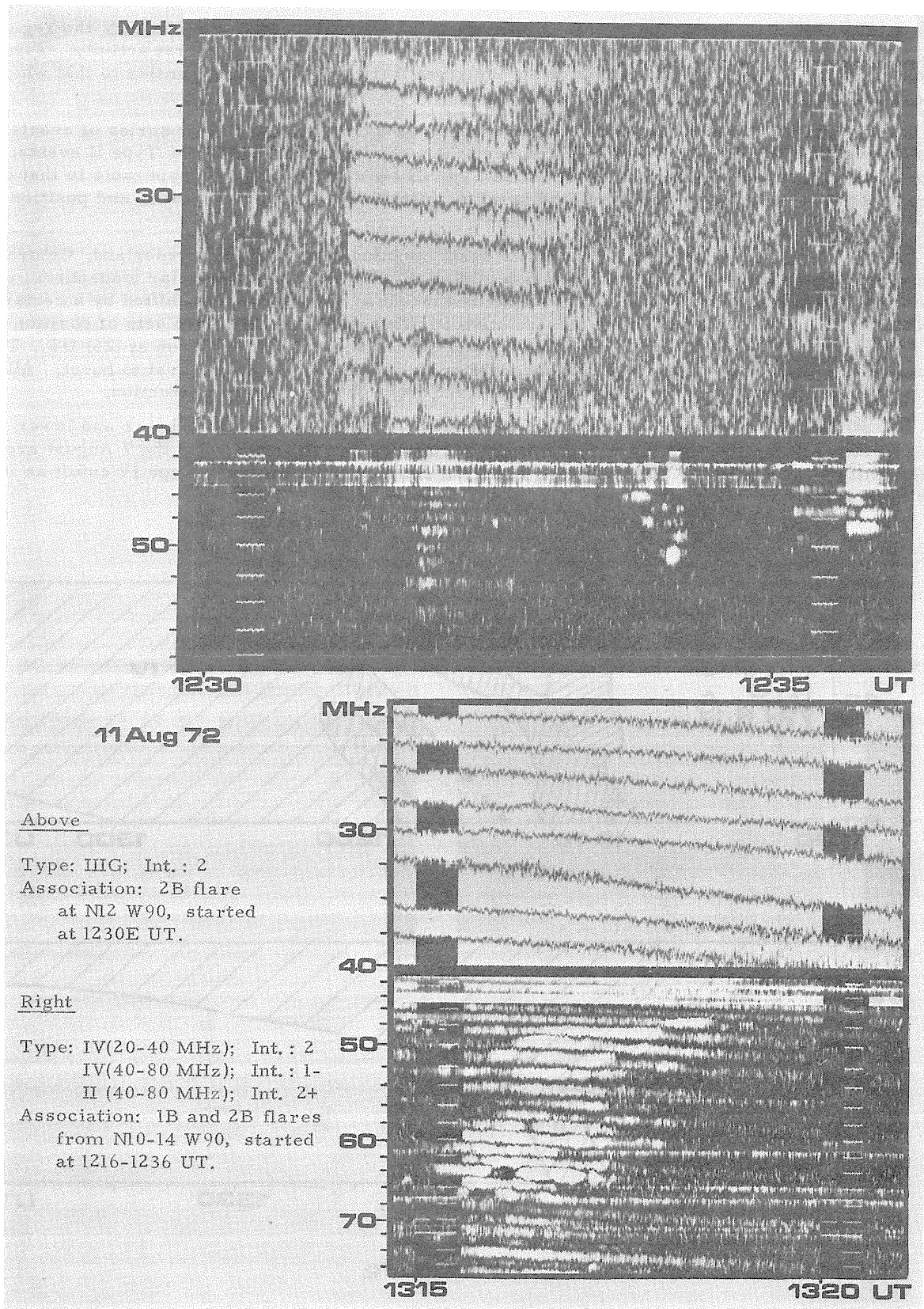
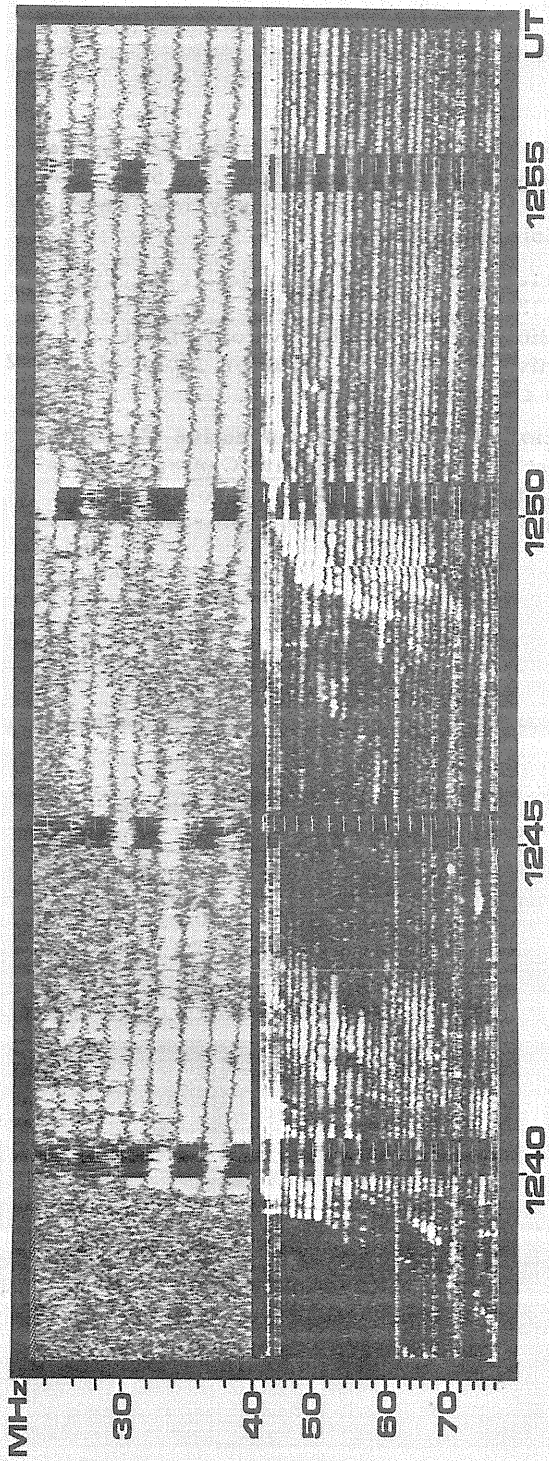


Fig. 9. Top: Spectrum of the decametric Type III G precursor to the Type II-IV onset;
 Bottom right: Spectrum of the metric band Type II burst at ~ 35 min after the Type II-IV onset.



11 Aug 72

Type:	Intensity:
III (1239.2-1242.5)	2
II(1) (1239.0-1251.0)	1+
II(2) (1243.6-1252.8)	1-
II(3) (1248.0-1251.0)	3

Radial Component of Velocity:	(10^3 km sec^{-1})
Burst	
II(1)	0.97
II(2)	0.90
II(3)	2.00

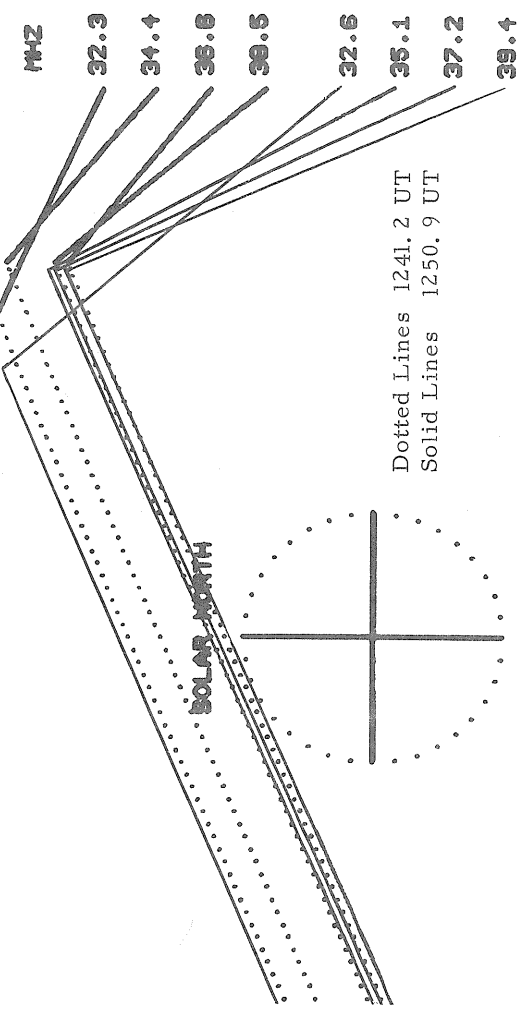


Fig. 10. Spectra, intensities, radial velocities, and position loci for the Type II-IV burst onset following the 2B flare at 1230E UT on 11 August 1972.

Dynamic Spectra of Four Solar Radio Bursts
During the Period 1972 August 2-7

by

Alan Maxwell

Harvard Radio Astronomy Station, Fort Davis, Texas 79734

This report describes the dynamic spectral characteristics of four solar radio bursts that occurred during the period of intense solar activity associated with the passage of McMath plage region No. 11976 across the solar disk, during the first half of August, 1972. At this time, the sweep-frequency equipment at Fort Davis covered the frequency range 10-2000 MHz [details of the antennas and receivers have been given elsewhere: Maxwell, 1971] and it was in operation daily from sunrise (approx. 1250 UT) to sunset (approx. 0135).

1972 August 2, 1839-1843 UT.

This radio burst was associated with a class 2B flare at N14 E26 that covered the period 1839-1844(max.)-1857. Figure 1 shows that, at Fort Davis, type IV continuum emission was recorded in the band 750-2000 MHz from approximately 1839-1843, and that faint type III bursts occurred at approximately the same time in the meter band. The interest in this radio burst lies in its association with an intense impulsive burst of hard X-rays [Datlowe *et al.*, 1973] and with point-like optical flashes, of size ≤ 1 arc sec and durations ≤ 10 sec, that were observed in the optical band at λ 3835 A [Tanaka and Zirin, 1973].

1972 August 2, 1959-2310 UT.

The radio bursts over this period were associated with a class 2B flare at N14 E28 that covered the period 1958-2058(?max.)-2336. There was a burst of hard X-rays that began at about 1958 and reached a maximum at about 2044. Figure 2 shows that, at Fort Davis a group of type III bursts was recorded over the period 1959-2003. The major radio outburst began, however, at approximately 2021, with a storm of type III bursts in the meter band that continued until 2100. Type IV emission began in the meter and decimeter bands at approximately 2021, became intense at 2031, gradually spread to cover the dekameter band, and continued until about 2310. Note that from 2040-2044 there was a burst in the meter band (from 100-30 MHz) with the characteristics of a type II burst, possibly indicating the passage of a shock wave with the velocity of the order of 1000 km/sec through the outer corona. From 2023 until sunset, there was radio emission in the meter and dekameter bands in the form of type I noise storm bursts.

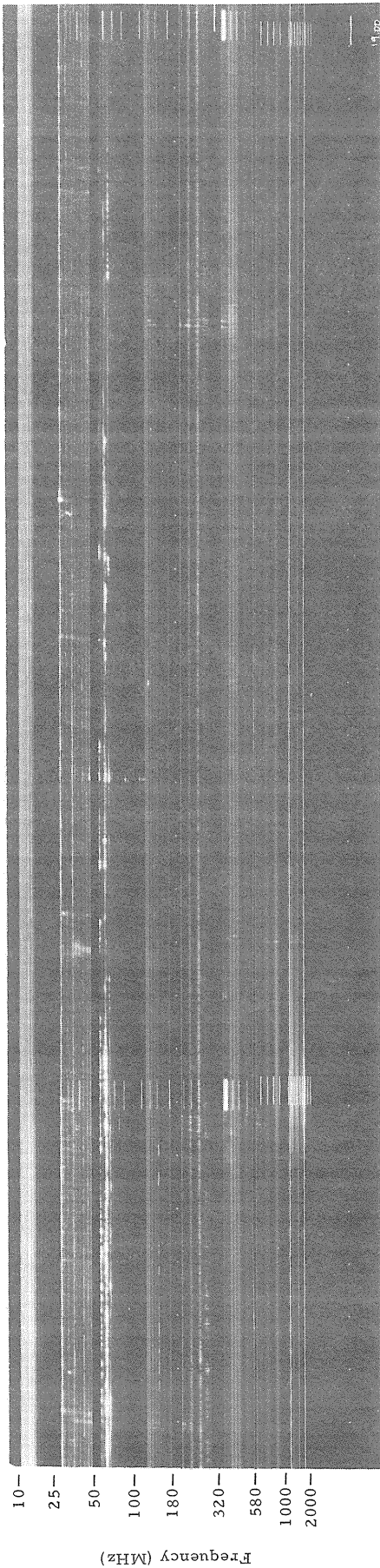


Figure 1. Dynamic spectrum of the solar radio burst of 1972 August 2, 1839-1843 UT. Note the short-lived type IV burst in the frequency range 750-2000 MHz and the associated faint type III bursts at lower frequencies.

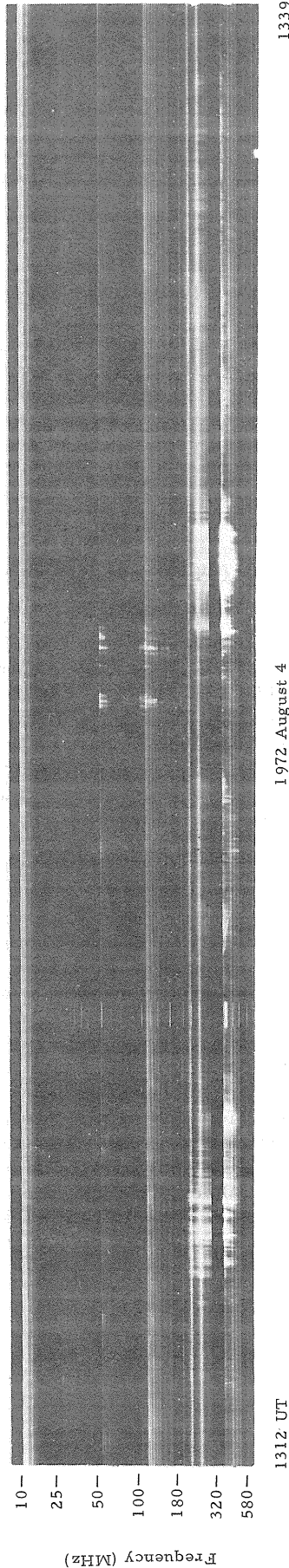


Figure 3. Dynamic spectrum of the solar radio burst of 1972 August 4, 1315-1338 UT. Note that the receivers in the band 550-2000 MHz were not operating; at that time, the sun was below the horizon limits of the 85-ft antenna used with these receivers.

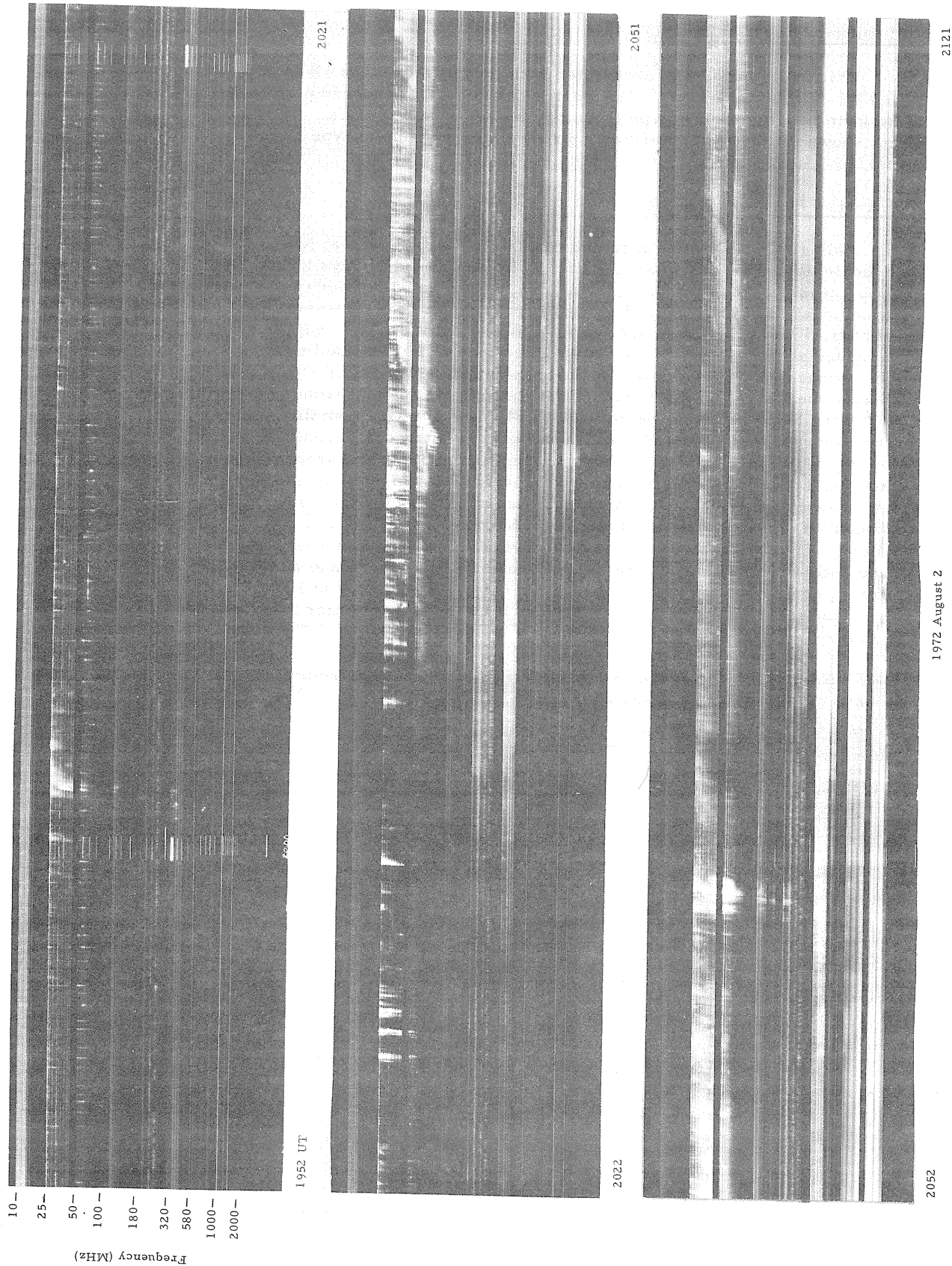


Figure 2. Dynamic spectrum of the solar radio burst of 1972 August 2, commencing 1959 UT. There was a group of type III bursts from approximately 1959-2003 but the main radio outburst did not begin until approximately 2021. Note that there is considerable instrumental "hash" on the band 180-320 MHz.

1972 August 4, 1315-1338 UT.

This radio burst was associated with the flare of class -B at N13 W01 from 1308-1310(max.)-1342. The Fort Davis record shows radio emission in the form of a mixture of type III and pulsating type IV bursts. The radio bursts shown in the figure were also preceded by a group of type III bursts from 1304-1305.

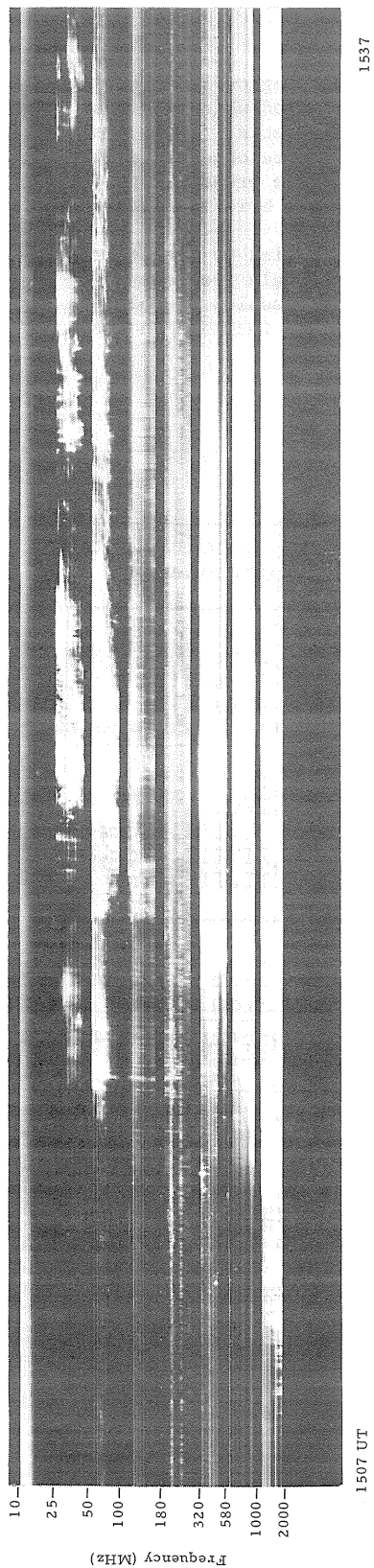
1972 August 7, 1508-1950 UT.

This radio burst was associated with a class 3B flare at N16 W35 over the period 1505-1536(max.)-1930. A burst of hard X-rays began about 1436 and reached a maximum at about 1535. A ground-level solar particle event began at 1515 and reached a maximum at about 1530 [Mathews and Lanzerotti, 1973]. Figure 4 shows the commencement of the radio burst, as recorded at Fort Davis. The onset of the burst was heralded by a group of type III bursts in the microwave band, the upper envelope of which possibly delineates the progress of a type II burst through the lower corona (Figure 5). In the meter band, over the period 1519-1540, there was a complex series of type II bursts that revealed components of at least two different velocities: the one with the greater slope corresponding to a shock wave propagating outward with a radial velocity of approximately 3000 km/sec and the burst with the lesser slope corresponding to a shock moving outward with a radial component of approximately 1000 km/sec [Maxwell and Rinehart, in preparation]. The progress of the slower moving of the type II bursts was subsequently tracked through the outer corona and the interplanetary medium with radio equipment carried on the IMP-6 satellite [Malitson and Stone, 1973]. Type IV emission was observed from 1508-1950 and, in the microwave band, it contained pulsations.

This work was carried out with the financial support from NSF Grant GA-36266 and from USAF Contract F19628-73-C-0231.

REFERENCES

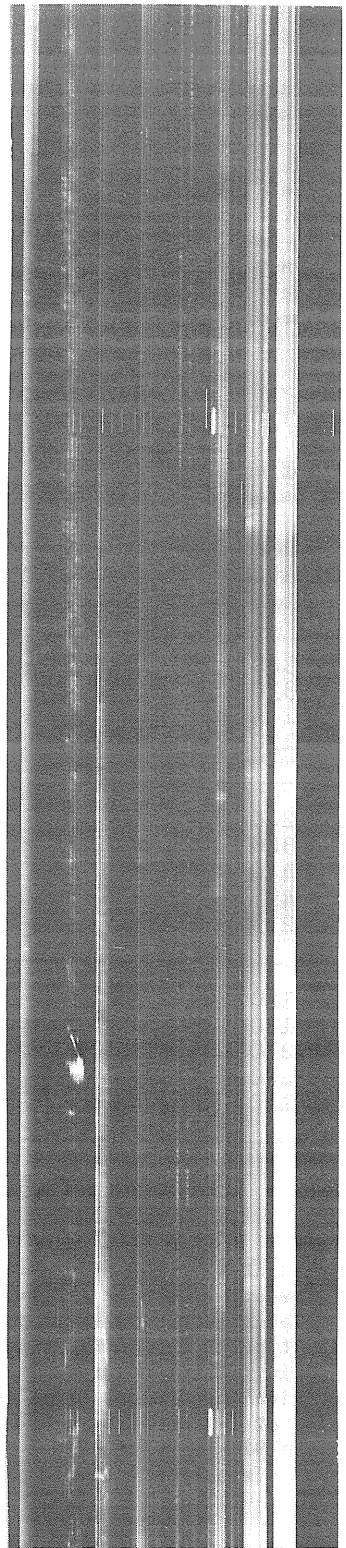
- DATLOWE, D. , PETERSON, L. E. , TANAKA, K. , and ZIRIN, H. 1973 Bull. Amer. Astron. Soc. , in press
(AAS Sol. Phys. Div. Meeting, Jan. 1973)
- MALITSON, H. H. , and STONE, R. G. 1973 Bull. Amer. Astron. Soc. , in press
(AAS Sol. Phys. Div. Meeting, Jan. 1973)
- MATHEWS, T. , and LANZEROTTI, L. J. 1973 Nature, 241, 335.
- MAXWELL, A. 1971 Solar Phys. , 16, 224.
- TANAKA, K. , and ZIRIN, H. 1973 Bull. Amer. Astron. Soc. , in press
(AAS Sol. Phys. Div. Meeting, Jan. 1973)



1608

1972 August 7

Figure 4. Dynamic spectrum of the solar radio burst of 1972 August 7, commencing 1508 UT. Note the pulsations in the band 100-180 MHz during the period 1527-1531. Note also that there is considerable instrumental "hash" on the band 180-320 MHz.



1515

1972 August 7

Figure 5. Enlargement of the microwave band for the first 8 minutes of the burst shown in Figure 4. Note the clearly defined type III bursts in the microwave band. The envelope of the top side of these bursts has the characteristic slope of a type II burst and may therefore delineate the progress of a type II shock wave through the solar atmosphere.

On the Type IV Bursts of August 2, 4, and 7, 1972

by

A. Böhme and A. Krüger
Zentralinstitut für Solar-terrestrische Physik der
Akademie der Wissenschaften der DDR (HHI) Bereich C 1
15 Potsdam / Telegrafenberg, G.D.R.

Connected with the transit of the strong active region related to McMath plage region 11976 during the first ten days of August 1972, a series of remarkable flare-burst events occurred which were associated with violent disturbances in interplanetary space and with terrestrial effects. Among these, type IV bursts of August 2 (0303 UT), August 4 (0540 UT), and August 7 (1422 UT) were observed at the Solar Radio Observatory Trensorf near Potsdam of the Heinrich-Hertz-Institute. The present report gives a phenomenological description of these events. Some remarkable features are briefly discussed.

An extract of the observations at selected frequencies is given in Table 1. Copies of single frequency flux records are shown in Figures 1 - 3. Spectral diagrams derived from single frequency observations of the bursts of August 4 and 7, 1972 are given in Figures 4 and 5. Results of polarization measurements at special frequencies (denoted by "P" in Figures 4 and 5) are included in the discussion.

Table 1

Compilation of the Data of the Type IV Bursts
of August 2, 4 and 7 at Selected Frequencies.

Date	Frequency MHz	Starting Time UT	Time of Maximum UT	Duration Min.	Maximum Intensity	Frequency Range MHz	Spectral Components
Aug. 2	9500	< 0400	0404	> 360	2120:	9500- 30	IV μ IVdm IVdm IVmB
	1500	< 0400	0404:	> 330	> 1260		
	234	< 0330	0351	> 114	200		
	113	0341	0410	> 120	700		
Aug. 4	9500	0607:	0630:	> 240	> 5300	9500- 23	IV μ IVdm II?III, IVdm, B II?III, IVdm, B II, III, IVmB
	1500	0540:	0624:	> 360	> 1400		
	234	0621:	0642:	440	500000		
	113	0624:	0646:	492	9000		
	23	0625:	0632:	> 275	90000		
Aug. 7	9500	1300	1525:	> 180	> 5300	9500- 23	IV μ IVdm IVdm II, IVA?B? II, IVA?B?
	1500	1320	1524.5	> 180	> 1400		
	234	1429:	1522:	> 230	1600		
	113	1438:	1521:	> 220	20000		
	23	> 1512	1522	> 120	10000		

0304 UT August 2

The initial phase of this event is not well-represented by the HHI-measurements because the burst started some minutes before sunrise at Trensorf. Nevertheless, it can be stated with certainty, that no type II burst was present on meter waves. Spectral observations from other stations [Lincoln et al., 1972] support this conclusion. The missing type II component is rather surprising since an extremely strong shock front observed by Pioneer 10 in interplanetary space was assumed to be related to this event [McKinnon, 1972]. Obviously, the physical conditions (complex magnetic structure) in the active region were not favorable for an emission of a type II burst in that stage of development. Apparently also the next strong flare-burst event at 1928 UT August 2 had no associated type II burst [Lincoln et al., 1972]. The event of 0617 UT August 4 was related to only a weak and short duration type II burst.

At the frequencies ≤ 113 MHz the radio event is proposed to be classified mainly as a IVmB burst in spite of its left-handed sense of circular polarization. Also, the polarization on 9500, 1500, and 775 MHz, presumably indicating a dominating influence of northern magnetic polarity, showed that the leading spot hypothesis did not apply to this event. In spite of the relatively strong intensity of the type IV μ burst the type IVmB component remained comparatively weak, especially at low frequencies. So far as can be concluded from spectral and polarization characteristics, no moving type IV phase is expected for this event.

0540 UT August 4

The type IV μ component reached extraordinarily strong intensities at both centimeter and millimeter wavelengths (cf. also Lincoln et al., [1972]). The sense of circular polarization on 3000, 1500 and 775 MHz changed repeatedly during the main phase of the event indicating a complex development in space and time (again the leading spot polarity seemed to be suppressed most of the time). Between 1500 and 775 MHz a reversal of the sense of polarization (from right to left) was well-expressed in the post-maximum stage of the event.

A very strong emission band was centered on about 234 MHz which is proposed to be regarded as type IV μ component, though in contrast to the normal case this emission extended up to 113 MHz. At lower frequencies the event should be classified as a type IV μ B burst, though being polarized in the left-handed sense.

An interesting known feature of the meter wave continuum is the pulsating structure which sometimes modulates the intensity in a quasi-periodic manner during strong flare-burst events. Usually these pulsations are restricted to the frequency range of about 200 - 100 MHz and have periods on the order of one second with a modulation of intensity sometimes lasting for one minute or more [Abrami, 1970; Rosenberg, 1970; McLean et al., 1971]. In the present case of the August 4 event, however, we observed exceptionally strong pulsations at decameter waves (maximum between 40 and 23 MHz) with periods on the order of five minutes (cf. Figure 2a). The same modulations have also been found in records of the degree of polarization.

Another surprising feature is the following: Though the type IV burst was related to the strongest proton event of the present solar cycle, the mA₁-component, if at all present, was very poorly developed. Normally, besides the type IV μ burst, a quasi-stationary broadband gyro-synchrotron emission component in the meter region (called type IVmA₁ burst) appears to be typical for association with an enhanced outflow of high energy protons from the sun [Böhme, 1972; Akinyan et al., 1971; Böhme, 1971]. An interpretation of a missing strong type IVmA₁ component may be proposed in the form of the following alternative variants:

Type IVmA₁ components occur preferably in active regions of not very 'complex' structure [Böhme, 1971]. Indicated by the high intensity of the microwave emission, the main part of the particle acceleration evidently took place in deeper levels of the solar atmosphere. A second stage acceleration at greater coronal heights seems not necessary here. Concerning the unexpected low intensities of special radio components, principally the influence of absorption should be taken into account.

Applying an acceleration mechanism of the type suggested by McLean et al. [1971], the production of high energy particles should be closely connected with the existence of pulsations on the meter wave continuum occurring in the post-maximum phase of the radio emission which have nothing to do with a type IVmA₁ component.

1422 UT August 7

The initial phase of this event was characterized by a relatively slow multi-step-like increase of intensity leading to a remarkable scattering of the maxima at different frequencies. In spite of its shorter duration the polarization behavior was even more complicated than in the preceding type IV bursts of this series.

Spectrum and morphology of the type IV μ component somewhat resembled those of the previous August 4 event. However, in comparison with the former event the sense of polarization appeared reversed, and the intensities remained somewhat weaker.

The type IV μ component exhibited only a narrow-band peak on 775 MHz (polarization: right handed).

On meter waves the structure was rather complex including the polarization characteristics. A strong type II burst started at about 1513 UT, extending up to 23 MHz. Type IVmA components seem to be indicated.

In contrast to the foregoing event the type IV μ B component appeared only weakly developed, leading to the much shorter duration of the event on meter waves.

From this event a rather complicated magnetic field structure, in particular at heights greater than 0.5 R₀ above the photosphere, may be deduced. The behavior is very similar to that of the type IV burst of May 28, 1967 which also was the last of a series of strong type IV bursts [Böhme, 1971].

REFERENCES

- ABRAMI, A. 1970 Solar Phys., 11, 104
- AKINYAN, S. T., 1971 Solar Phys., 20, 112
 E. I. MOGILEVSKY,
 A. BÖHME and
 A. KRÜGER
- BÖHME, A., 1969 Suppl. Serie of Solar Data, Vol. 1, No. 7, 125
 A. KRÜGER, and
 H. KUNZEL
- BÖHME, A. 1971 Doctoral Thesis, Berlin
- BÖHME, A. 1972 Solar Phys., 25, 478
- LINCOLN, J. V. and 1972 Preliminary Compilation of Data for Retrospective
 HOPE I. LEIGHTON World Interval July 26 - August 14, 1972, World Data
 Center A, Report UAG-21, Upper Atmosphere Geophysics,
 November 1972
- MCKINNON, J. A. 1972 August 1972 Solar Activity and Related Geophysical
 Effects, NOAA Technical Memorandum TM-ERL, SEL-22,
 December 1972
- MCLEAN, D. J. , 1971 Nature, 234, No. 5325, 140
 K. V. SHERIDAN,
 R. T. STEWART and
 J. P. WILD 1971 Nature, 234, No. 5325, 140
- ROSENBERG, H. 1970 Astron. Astrophys., 9, 159

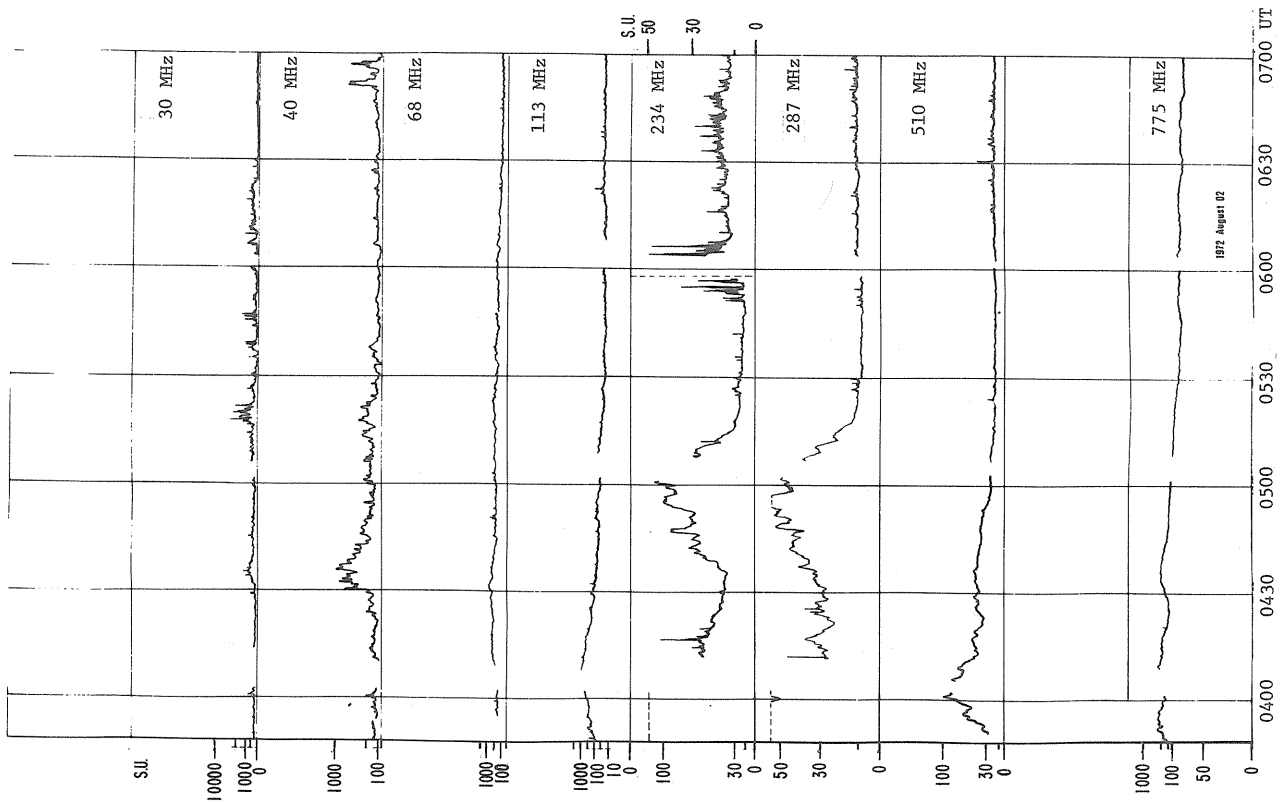


Fig. 1a.

Fig. 1a, b. Single frequency flux records of burst of August 2, 1972.

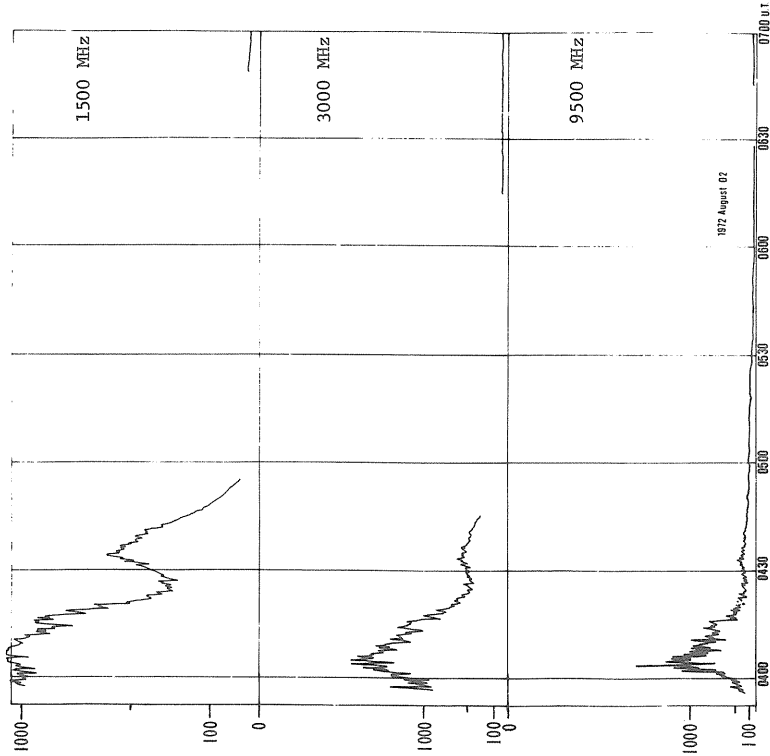


Fig. 1b.

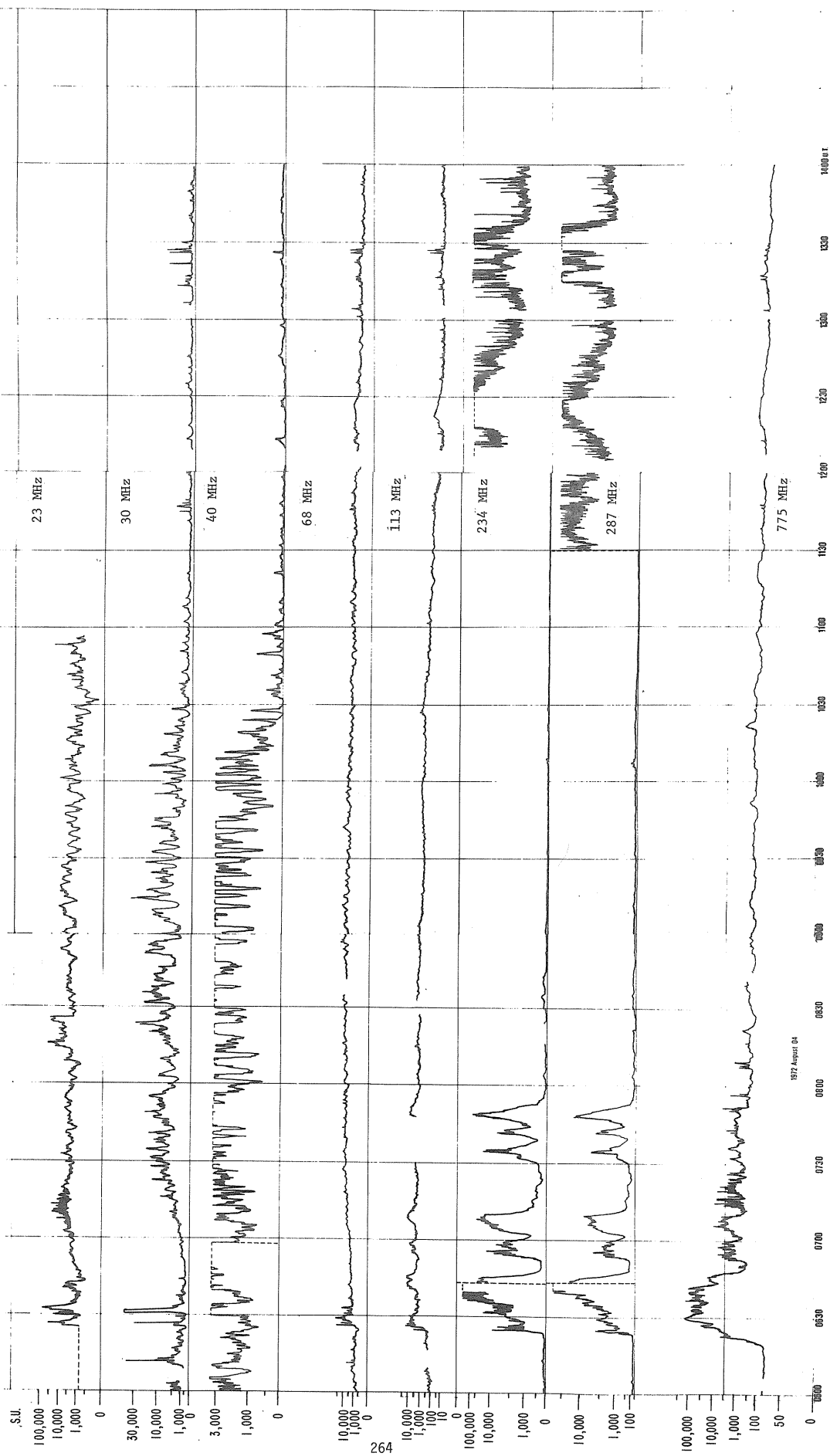


Fig. 2a. Single frequency flux records of burst of August 4, 1972.

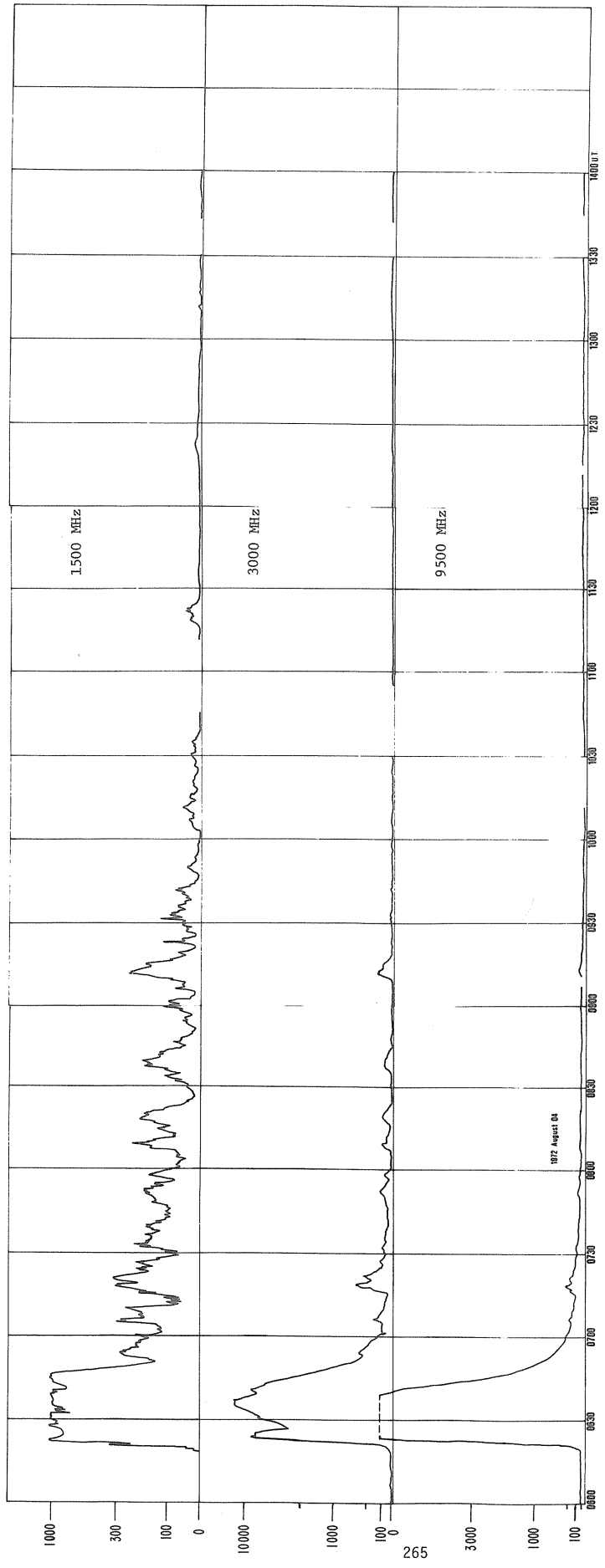


Fig. 2b. Single frequency flux records of burst of August 4, 1972.

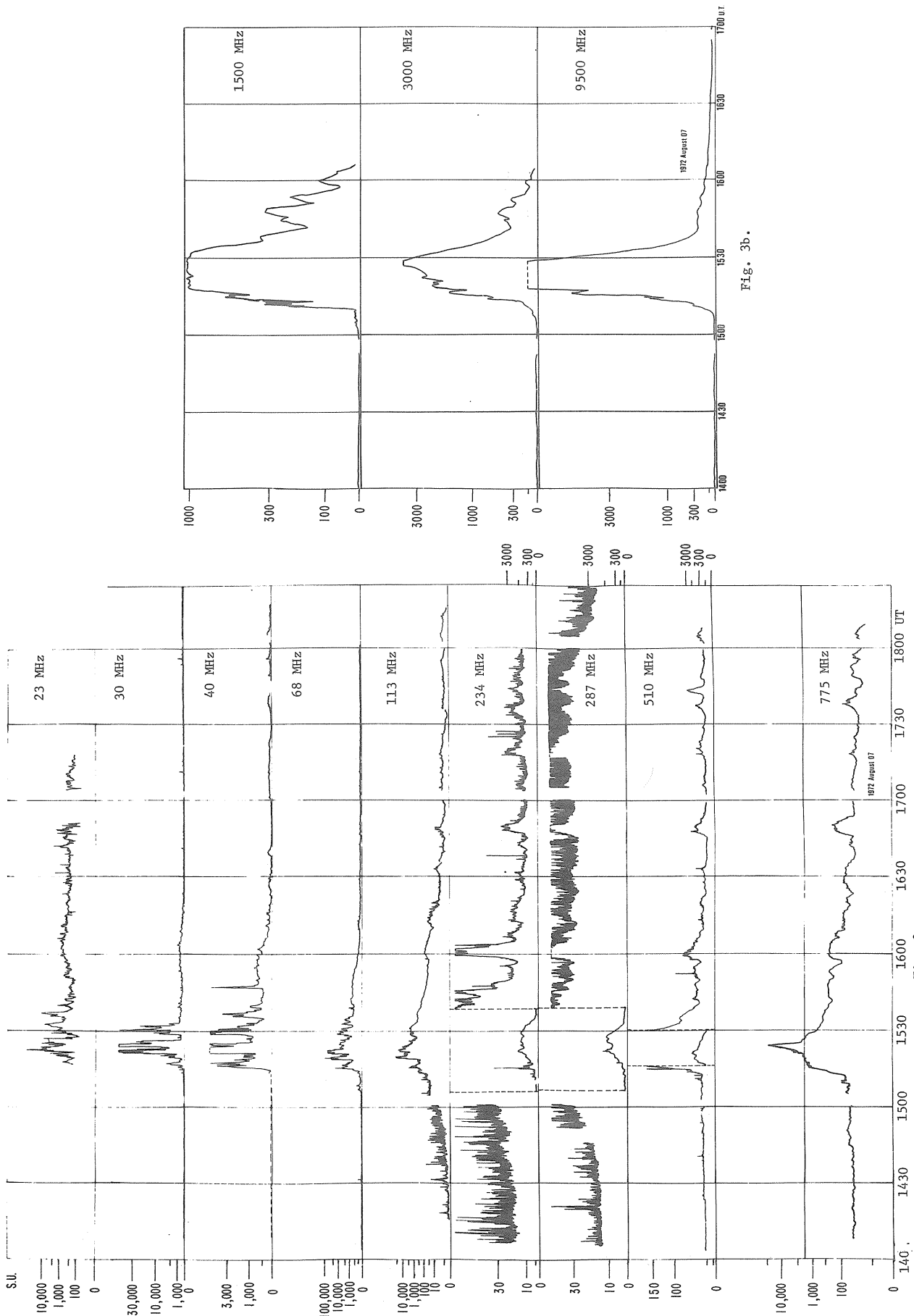


Fig. 3a.

Fig. 3b.

Fig. 3a, b. Single frequency flux records for burst of August 7, 1972.

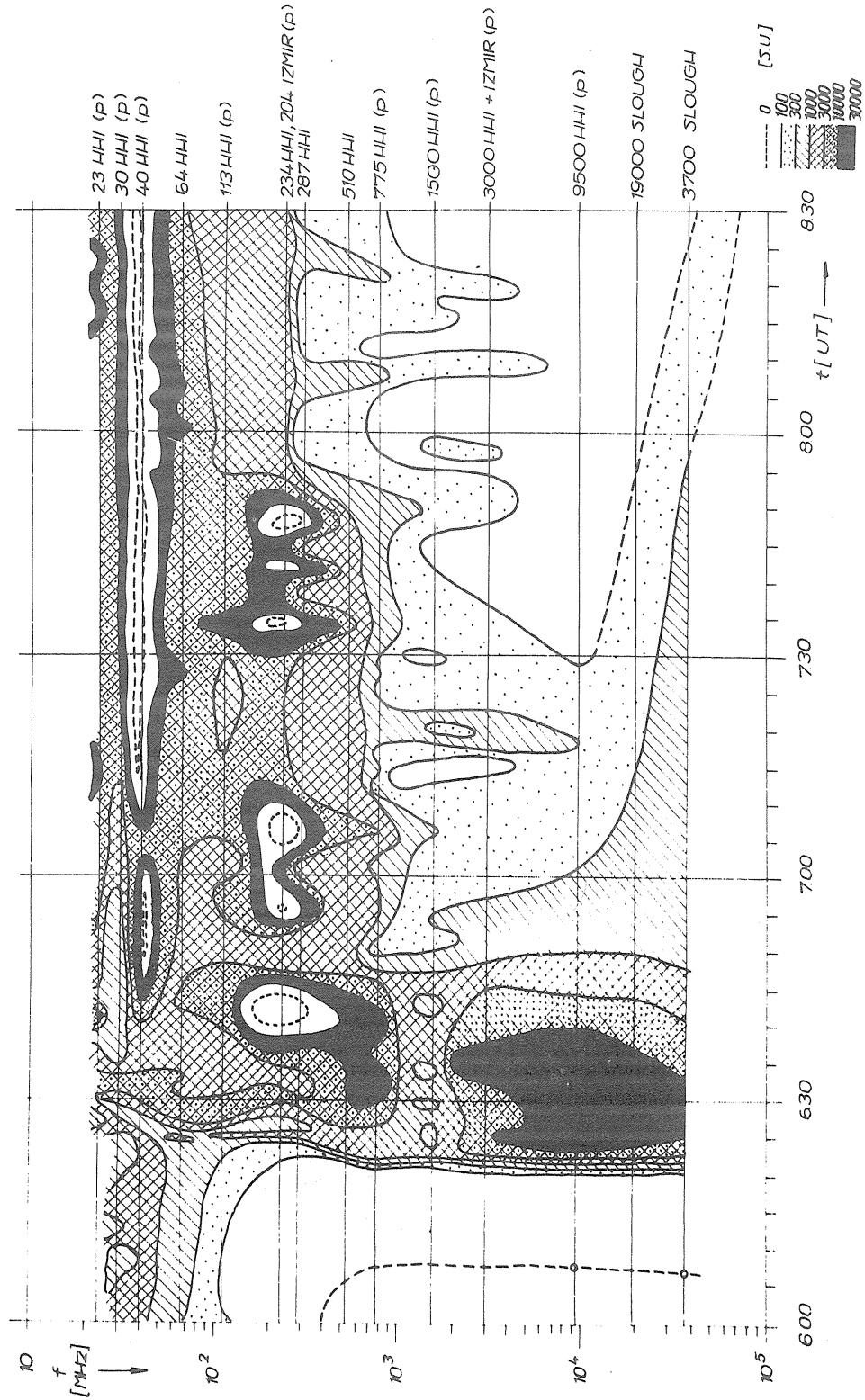


Fig. 4. Spectral diagram of burst of August 4, 1972.

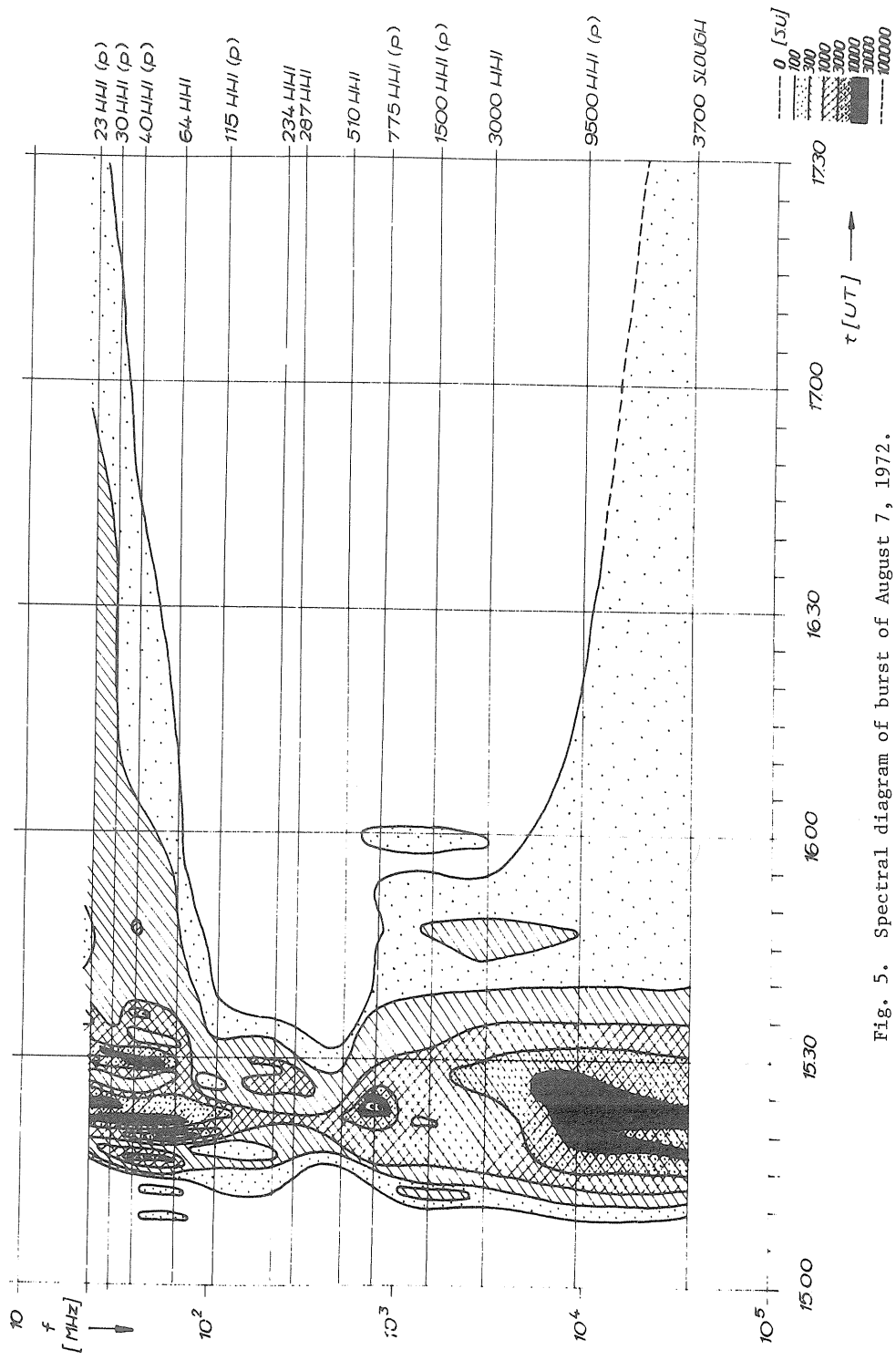


Fig. 5. Spectral diagram of burst of August 7, 1972.

The Type IV Bursts of August 4 and 7, 1972 Associated with p-Flares

by

H. Urbarz
Astronomical Institute of Tübingen University
Weissenau Station

The active McMath region 11976 crossed the east limb of the sun on July 29, 1972, evidently with a complex magnetic structure of one spot group. During the East-West transit of region 976 seven low importance flares (1N to 1B) occurred. Table 1 shows data of three large flares, the associated bursts were recorded by the Weissenau broadband radiospectrograph. The flare of November 25 is included for comparison of the associated events, the preliminary data show scattering between the given values.

day 72	start UT	end UT	max UT	position	dura- tion	imp	McMath No.
Aug. 04	0530	0855	0639	N 14 E 09	205	3B	11976
Aug. 07	1455	1722	1636	N 14 W 37	150	3B	
Aug. 11	1227	1307	1235	N 13 W 90	40	2B	
Nov. 25	0805	0926	0828	S 05 W 44	8	1F	12115

The large flares in regions 976 and 115 were associated with Type IV-bursts. Figures 1a to 1d show the dynamic spectra of the associated radio bursts. The events of August 4 and 7 are broadband Type IV bursts, probably with type II emission superposed, while on August 11 a weak Type II burst is found on the record. The Type IV burst of November is confined to dm-waves. Only the beginning of the spectrum of the August 4 burst is shown in Figure 1a, having a total duration of five hours. In Figures 2a, 2b, and 2c the maximum absolute fluxes are plotted versus frequency of consecutive maxima showing V-type spectra except on November 25 where the m-wave component is lacking.

Table 2 gives magnetic classification and area of the sunspot groups of region 976 and 115.

day 72	McMath No.	Mt. Wilson No.	Magnetic class	area	sunspot class
25 Nov	12115	19044	βf	270	Eso
04 Aug	11976	18937	βf		
		18935	δ	1140	Fkc
07 Aug	11976	18935	δ	910	Ekc
		18942	αp		
10 Aug	11976	18935	δ	840	Dkc

For symbols see "Solar-Geophysical Data," Descriptive Text [1973].

Table 3 is a survey of particle emission and maximum intensities of radio and x-ray bursts associated with the flares.

Table 3										
McMath region 11976										
day 72	Mt. Wilson group No.	p-events	burst type	burst durat. Min.	max. radio burst flux. F.U.			max x-ray burst int. erg/cm ² s		
					cm/mm	dm	m/dkm	0,5-3 Å (x10 ⁻⁵)	1-8 Å (x10 ⁻⁴)	8-20 Å (x10 ⁻³)
04 Aug	18935	Explor.37 Riom PCA	IV/II V-spect	4h45m	2x10 ⁴	3x10 ³	1x10 ⁵	7500	4600	430
07 Aug	18935	Explor.37	IV/II V-spect	50m	2x10 ⁴	3x10 ³	2x10 ⁴	9000	4500	440
11 Aug	18935	/	/	8m	/	/	/	370	810	400
McMath region 12115										
25 Nov	19044	/	IV V-spect.	1st event 36m 2nd event 11m	1x10 ²	1x10 ³	1x10 ²	170	490	300

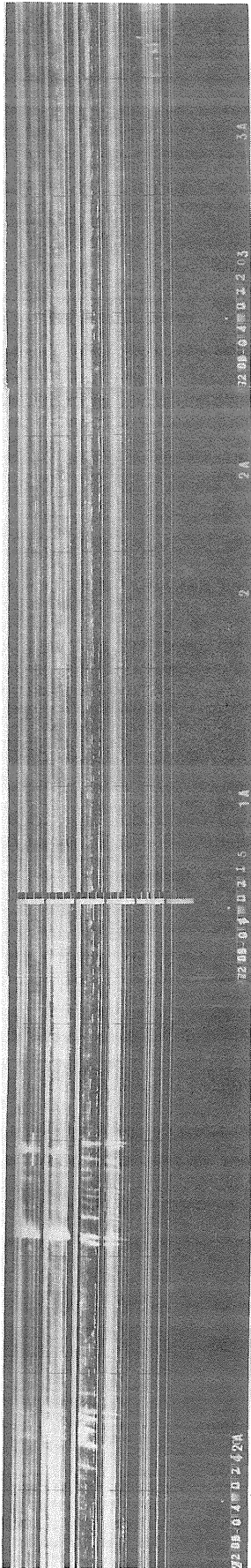
In Region 976 showing a complex magnetic δ - configuration in one of the spot groups, five large flares occurred within a few days. The flares of August 4 and 7 occurred together with the emission of energetic protons directly measured by satellite monitors. The data considered confirm the association of V-spectra-Type IV-bursts with the emission of energetic protons during large flares. However, on August 11 a Type II burst occurred during a 2B flare on the West limb. The spot area had declined since August 4, but the magnetic δ -configuration was still present on August 10, as observations showed. On November 25 an isolated dm/cm Type IV burst occurred during a 2B flare in spotgroup 044, which showed a magnetic $\beta\gamma$ -configuration. The m/dkm-wave component was lacking and the maximum fluxes were smaller by a factor of 100 than the fluxes of the V-spectra. No emission of energetic particles was found at the events of August 11 and November 25. These groups of associated events give an example of the typical features observed in p-events and non-p-events, respectively. The statistics comprising many events show that the correlation of simultaneous dkm/m- and of cm/mm-wave bursts with the emission of energetic protons during large flares is very high. This indicates a possible relation of a post-acceleration process of particles to the forming of the source of the dkm/m-wave burst in the coronal trapping region during the burst start. The burst source of the cm/mm-wave Type IV burst is assumed to be located in the lower corona emitting the high frequency part of the V-spectrum. Thus V-spectra may be explained by the emission of two synchrotron burst sources in different coronal heights [Urbarz, 1970].

When the flare position was W37° on August 7, GLE-effects were observed indicating relativistic protons. Duration of the Type IV burst was 50 minutes. On August 4, however, the flare-burst position was near central meridian and the burst duration was five hours, a very rare phenomenon, but there was no evidence of GLE-effects. The satellite monitors gave only information of protons of higher energies than 60 Mev in both cases. The first phenomenon in question may be due to a directivity in emission of protons of peak energies. A change of directivity in the postmaximum phase of the Type IV emission may yield the second phenomenon mentioned [Urbarz, 1973].

From Table 3 one finds an increasing X-ray flux in the continuum towards smaller wavelengths in the case of the p-events. The non-p-events show maximum intensity in the center of the measured x-ray spectrum. During the large flares of August 4 and 7, the 0.5 Mev and 2.2 Mev gamma ray emission lines were detected directly the first time by satellite monitors indicating nuclear processes in the flare region [Chubb, 1972].

REFERENCES

- URBARZ, H. 1970 Solar Phys., 13, 458
- URBARZ, H. 1973 Kleinheubacher Berichte, FTZ Darmstadt 1973, Bd.16,491
- CHUBB, E. L. 1972 Lecture given at the Astronomical Institute of Tübingen University
- MCKINNON, J. A. 1972 August 1972 Solar Activity and Related Geophysical Effects, NOAA Tech. Mem. ERL SEL-22, Dec. 1972, Boulder
- LINCOLN, J. V. and H. I. LEIGHTON 1972 Preliminary Compilation of Data For Retrospective World Interval July 26 - August 14, 1972, WDCA-STP. Report UAG-21, November 1972
- 1972, 1973 Solar Geophysical Data, reporting on August 1972 and November 1972 events, U.S. Department of Commerce, (Boulder, Colorado, U.S.A. 80302)



0613 UT August, 04, 72

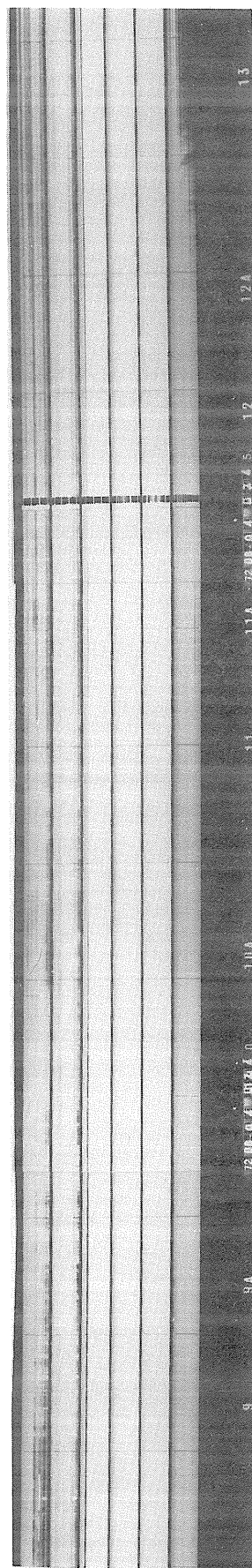
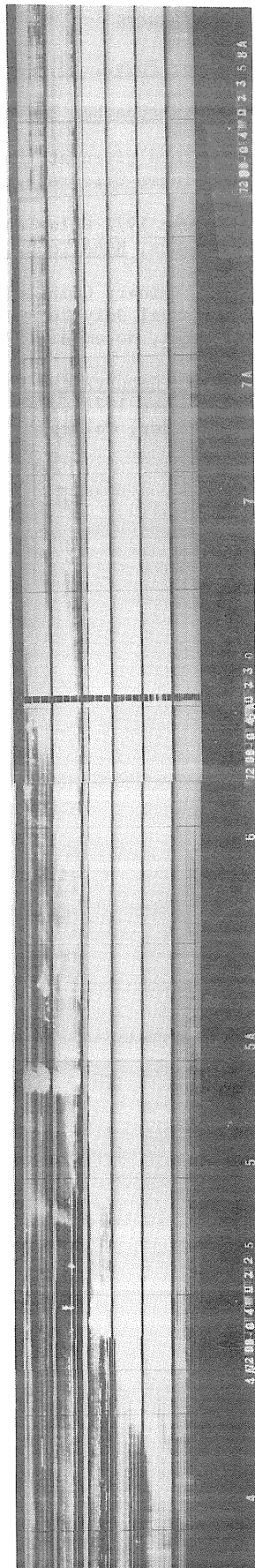
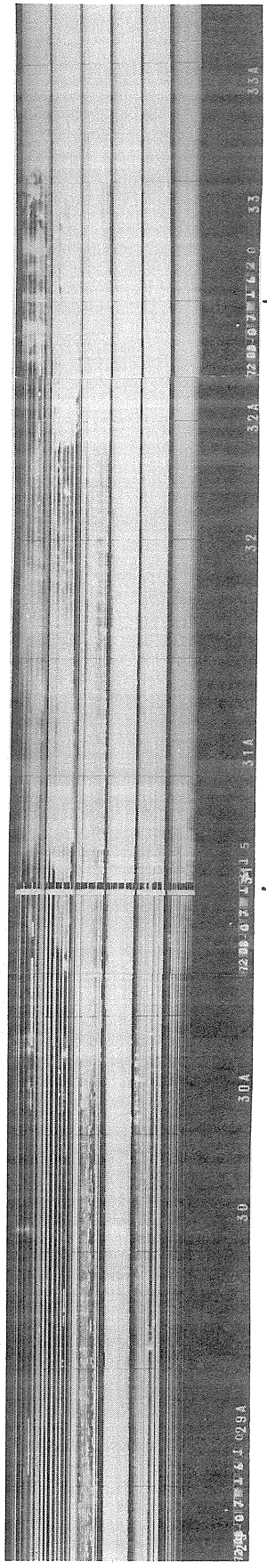


Fig. 1a.



1 520 UT

1 51 5 UT

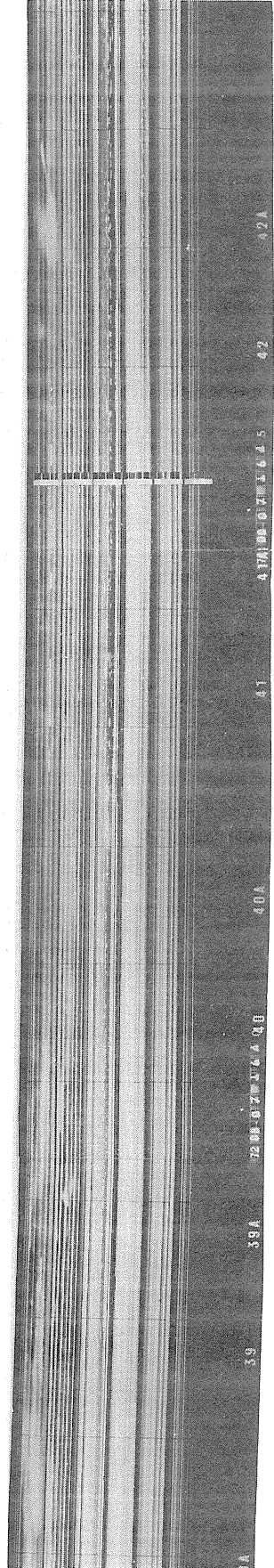
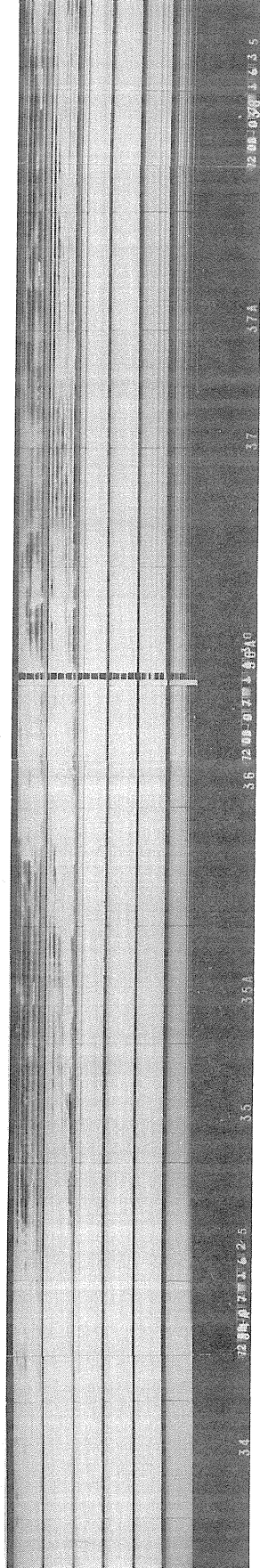
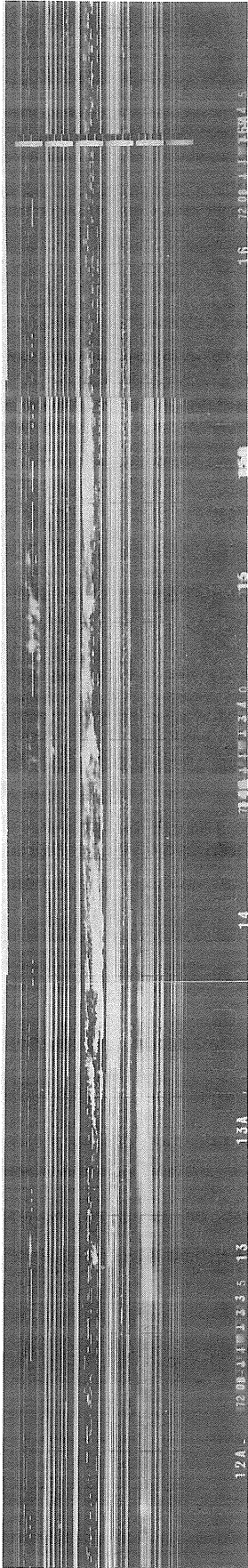


Fig. 1b.



1240 UT

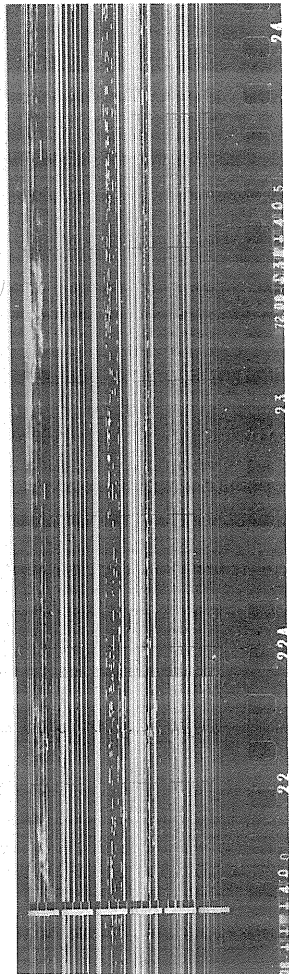
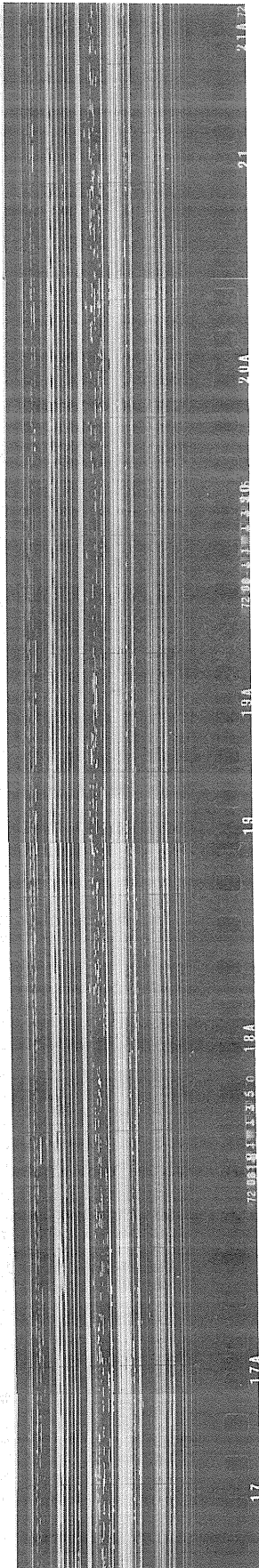
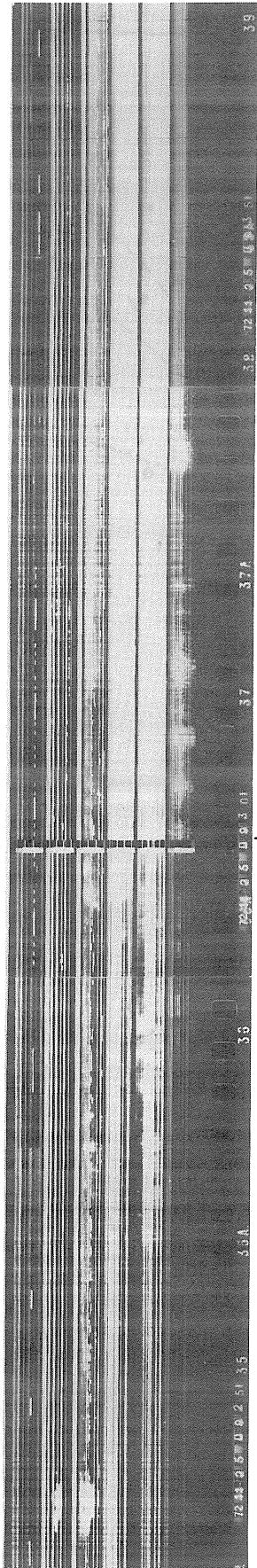
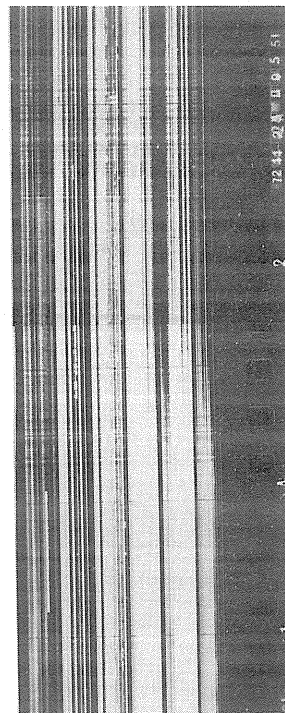
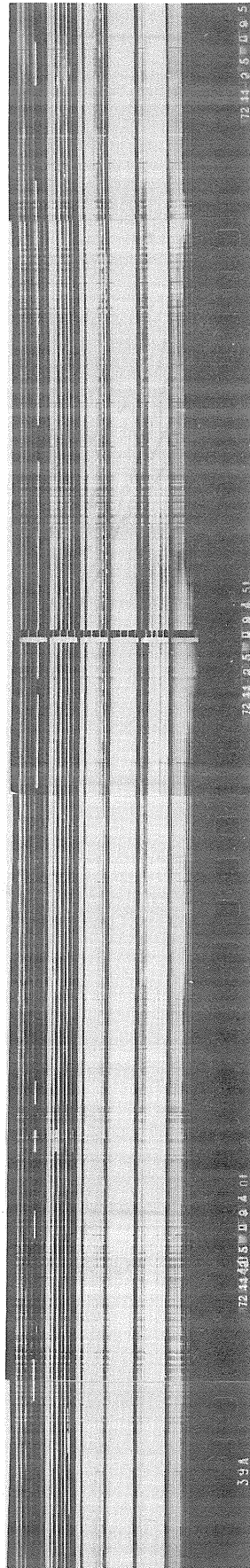


Fig. 1C.



November, 25, 72 0730UT

0735 UT



0755UT

0925 UT

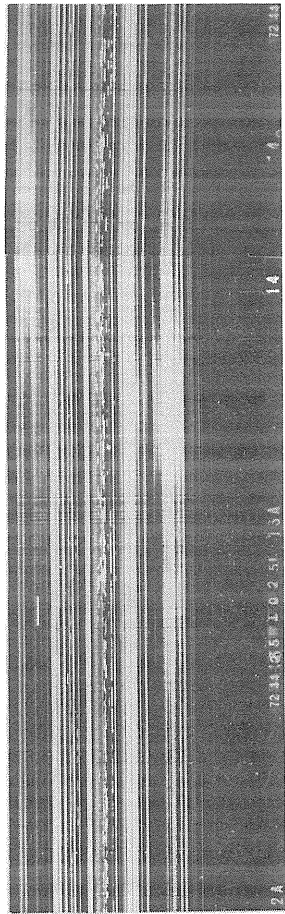


Fig. 1d.

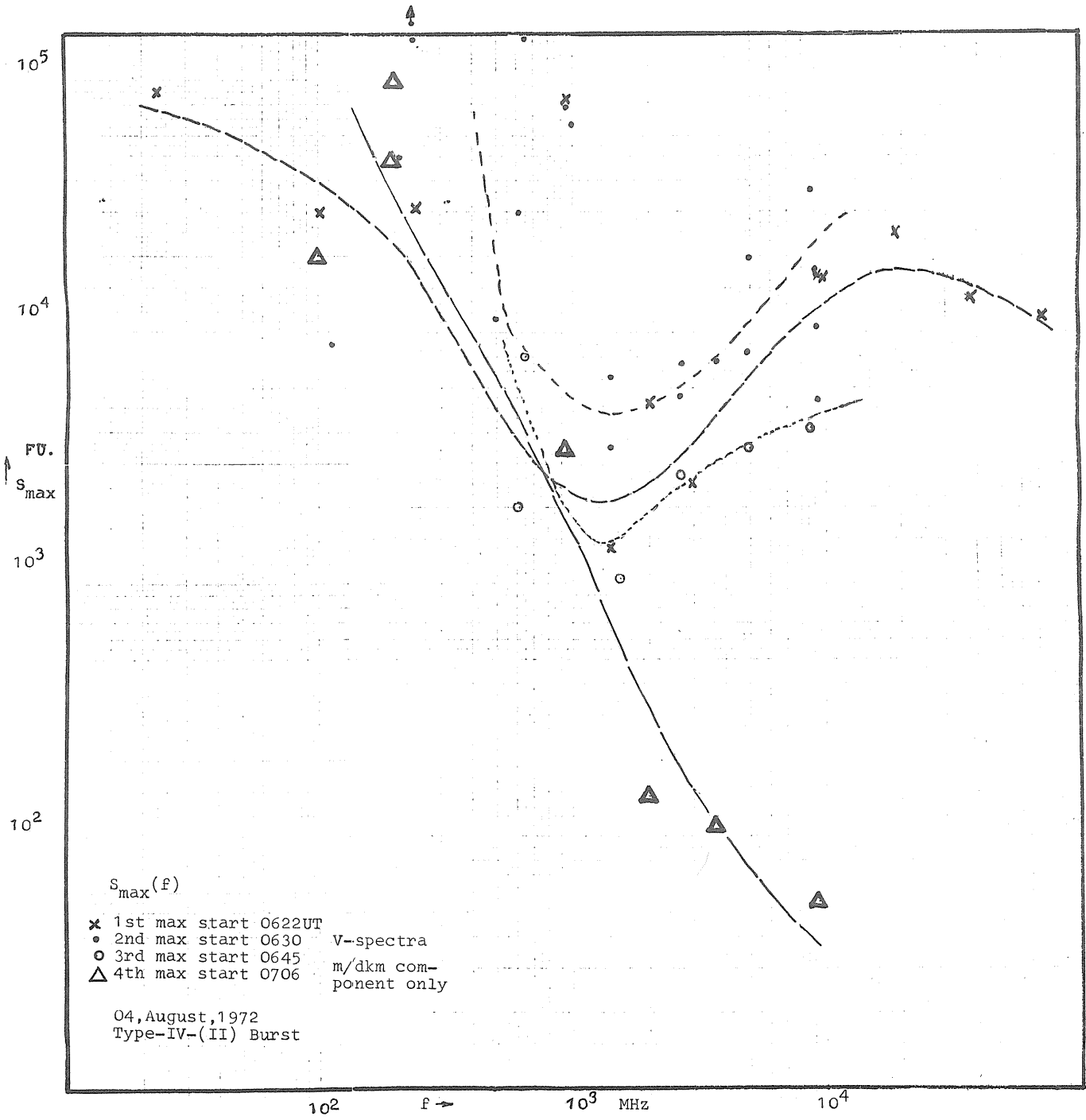


Fig. 2a.

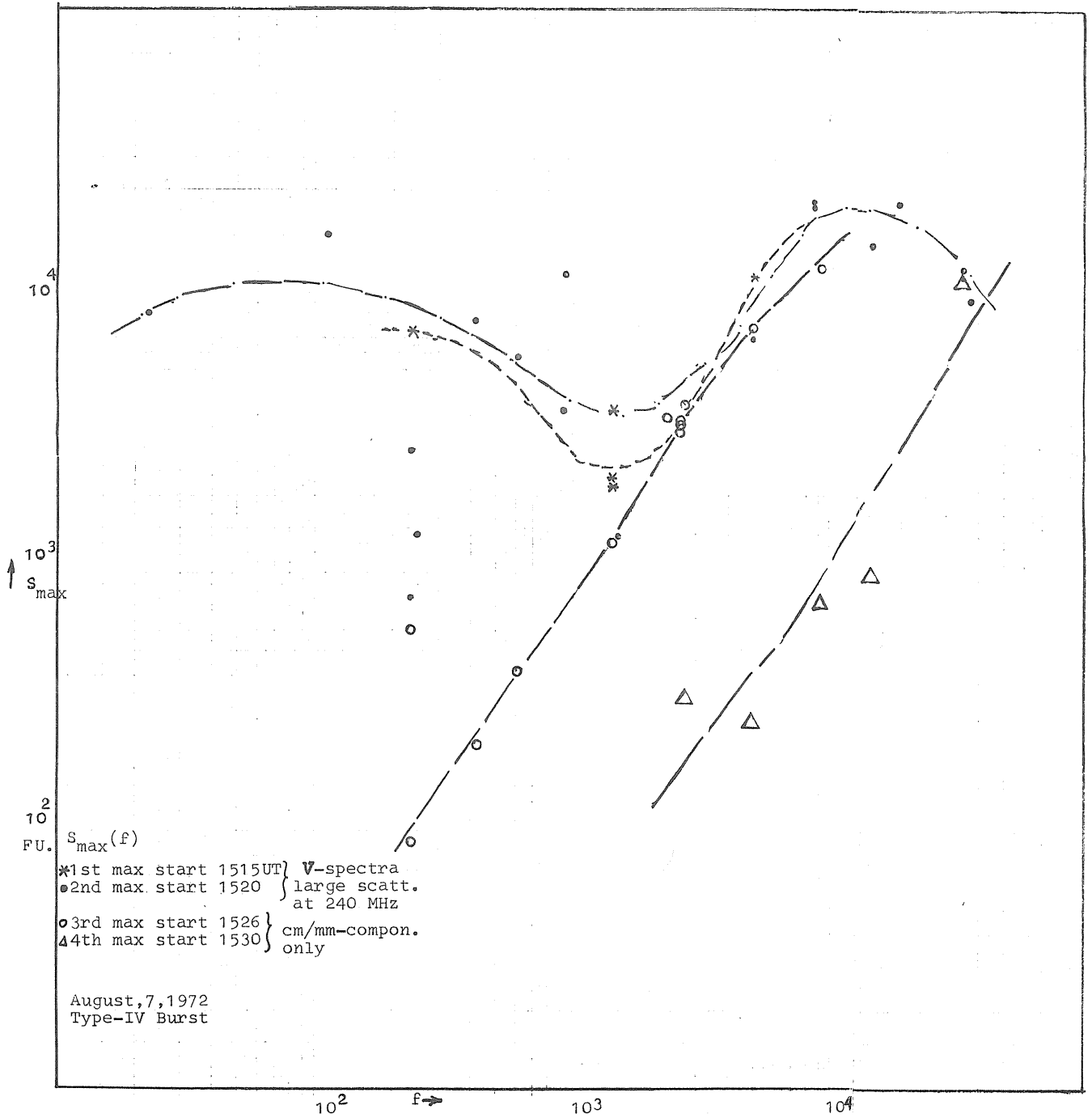


Fig. 2b.

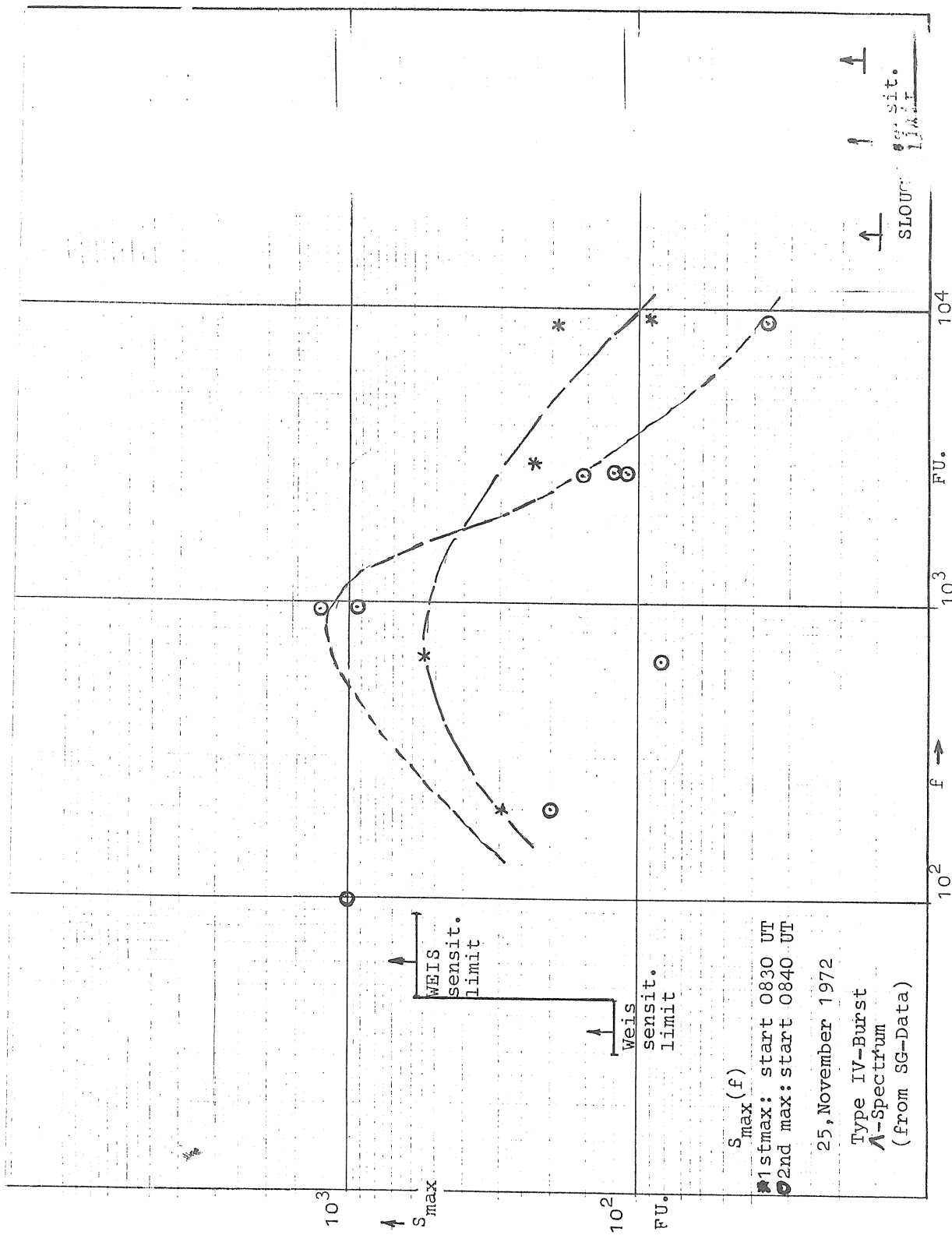


Fig. 2c

About Two Type IV Events on August 4 and 7, 1972
Polarimetric Measurements at 237 MHz

by

Paolo Santin and Paolo Zlobec
Astronomical Observatory
Trieste, Italy

The magnetically complex McMath region 11976 (N14, L=9) produced some major flares and related activity in the first days of August 1972. In this time interval, the most interesting data recorded by our polarimeter on 237 MHz were on August 4 (0620 UT ~ sunset) and August 7 (1500 UT ~ sunset); sunset was at about 1730 UT. These two type IV events were connected with the long enduring and exceptionally strong flares of August 4 (start 0617, max. 0640, end 0853 UT; importance 3B) and August 7 (start 1449, max. 1534, end 1721 UT; importance 3B); this information was published in "Solar-Geophysical Data" [1973].

In this paper the solar radio emission is analyzed with particular emphasis on the circular polarization of the recorded radiation. It was possible to do this, even using an instrument with low resolving power, due to the much higher values of flux density coming from the active region than from the remaining solar surface. Figures 1, 2 and 3 show the behavior of the total flux density and its polarization; the contribution of the quiet Sun on 237 MHz is about 10 solar flux units ($1 \text{ sfu} = 10^{-22} \text{ Wm}^{-2} \text{ Hz}^{-1}$).

Our radio polarimeter, fed by a ten meter parabolic antenna, has a bandwidth of 0.5 MHz [Sedmak, 1970]. Its output gives: 1) the sum and the difference of the two circularly polarized components L+R and L-R with a low time resolution (paper speed = 20 cm/h, time constant = 0.5 sec), and 2) the two separate components L and R with high time resolution (paper speed = 2 mm/sec or more, time constant lower than 12 msec). Figures 1 and 3 were plotted on the basis of calculations made with the data given by output (1), and Figure 2 is an example of output (2). We thus have the total flux density and the degree of circular polarization ($=100(L-R)/(L+R)$), whose accuracy can generally be considered to be better than 10%.

Figure 1 shows the behavior of the first type IV event from 0620 to 1250 UT. In the previous interval beginning with our recording time (0538) the flux density was about 40 sfu and the degree of circular polarization was about 65% L. After the event, similarly low mean values were recorded no sooner than about 1500 UT. The time interval later than 1250 UT is not reported since interesting phenomenon is decreasing.

The rapid flux increase begins at about 0623 UT, but growing continues in some intervals with flux varying rapidly until 0642 UT with a peak of about 280,000 sfu. During this period the polarization degree is much lower (for almost 10 minutes the polarization is about zero) than before and after. For one hour and a half some flux density peaks follow each other and almost reach the previously reported value; however, the flux density is practically above 2,000 sfu. Concurrently, the polarization degree is generally higher than 80% L and the slight decreases are in agreement with the diminishing of the flux density. After 0800 UT the trend of the flux density is generally decreasing, and it is possible to see long enduring time intervals where the slope is practically linear in the logarithmic scale of the drawing (that is, an exponential type decrease) surmounted by groups of stronger bursts. The corresponding polarization degree is slightly decreasing while the mentioned groups of stronger bursts are practically totally L-handed polarized (see Figure 2). Only the strengthening of the flux after 1200 UT is exceptional with the polarization degree shifting towards zero, especially in phases when the flux increases; however the active region is always the same.

For August 4 we also have radio interferometric measurements at 408 MHz. The recorded interval is 0900 - 1300 UT, and all this time the position of the source on the Sun is constant and near to the optical center. The radiometric behavior of the flux density in the quoted period is very similar to the 237 MHz one (for example, we see at about 1040 UT both on 237 and 408 MHz a considerable flux decrease). The constant position and the common development show that the event is at our wavelengths probably a "stationary type IV burst", at least for the period after 0900 UT.

The type IV event of August 7 begins just after 1500 UT. Before this time it was a partially L-handed polarized noise storm of near constant intensity (30 sfu). The polarization degree of the entire phenomenon is low. There are only sporadic groups of bursts having strong polarization which may also come from other active radio regions. We must further say that the polarization of the continuum after 1600 UT is probably faintly influenced by a man-made interference; therefore, we suppose that the polarization of the continuum is closer to zero than it appears in Figure 3.

For this type IV event we do not have interferometric and radiometric data at 408 MHz.

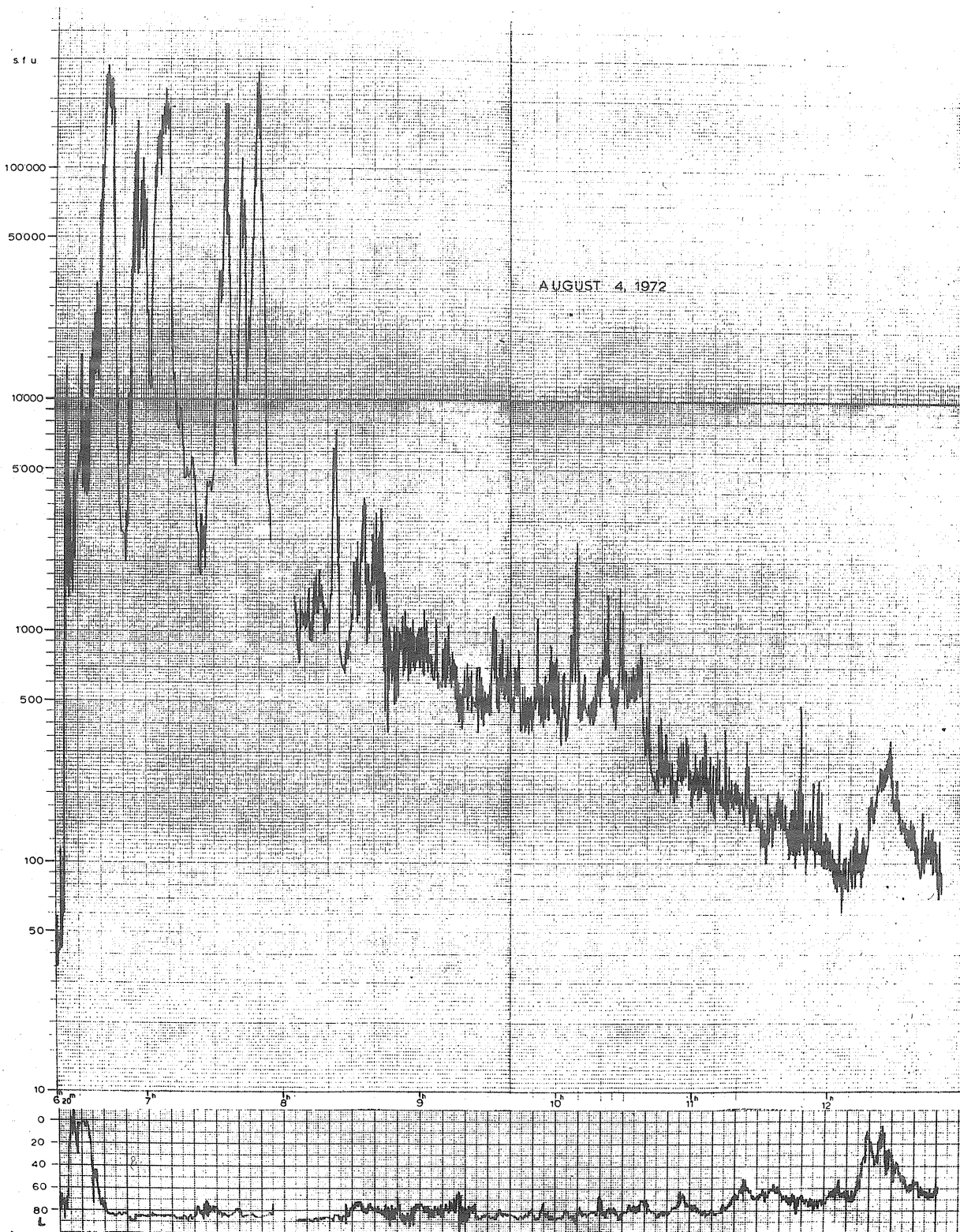


Fig. 1. Flux density and degree of circular polarization for August 4, 1972.

REFERENCES

SEDMAK, G.	1970	Trieste Astronomical Observatory, <u>Osservazioni Solari</u> , 18 suppl.
	1973	Solar-Geophysical Data, 342 Part II, February 1973, U.S. Department of Commerce, (Boulder, Colorado U.S.A. 80302).

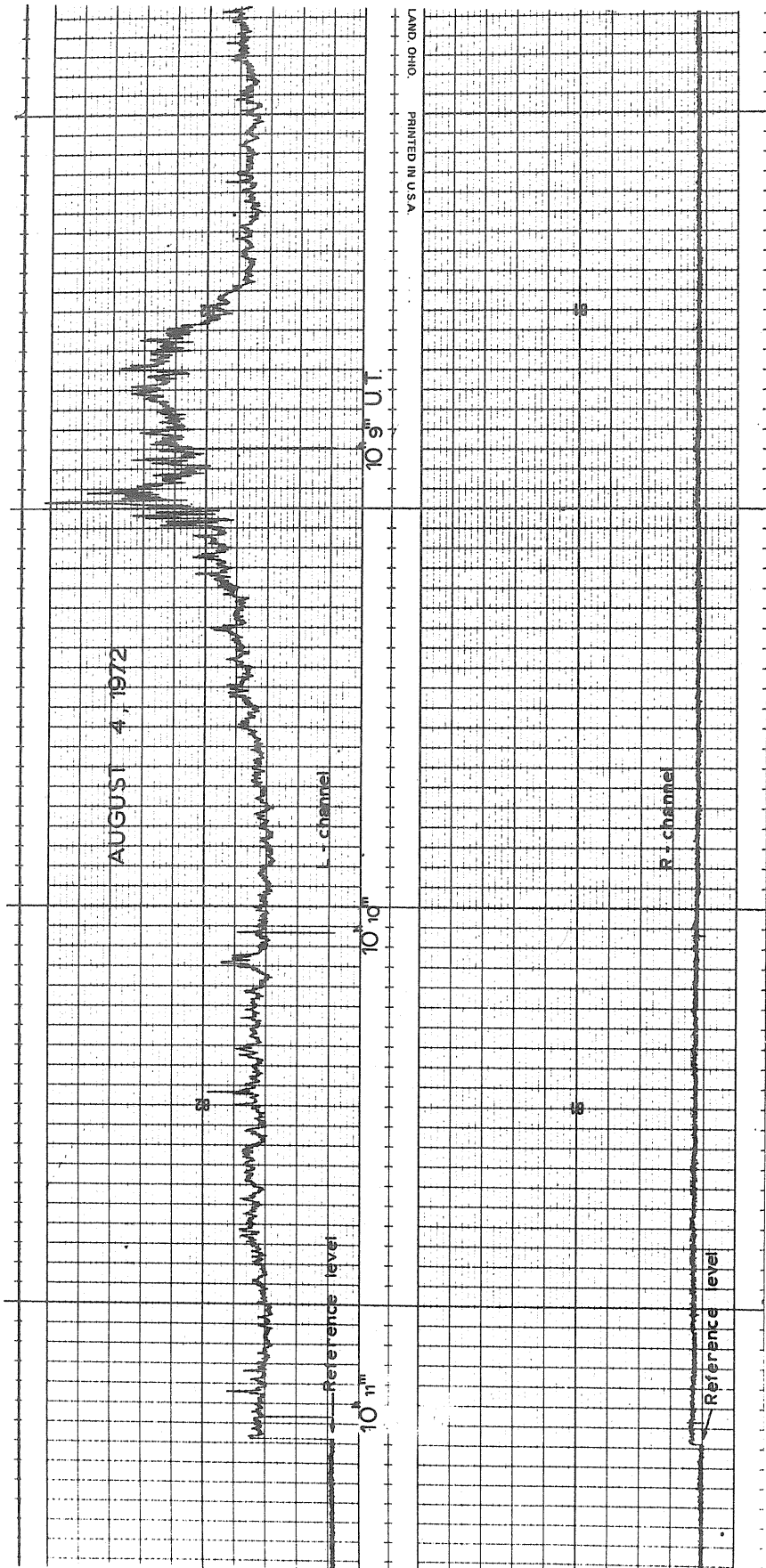


Fig. 2. Example of the high speed (2mm/sec) recording. The two polarized signals are separately recorded (the scales are the same).

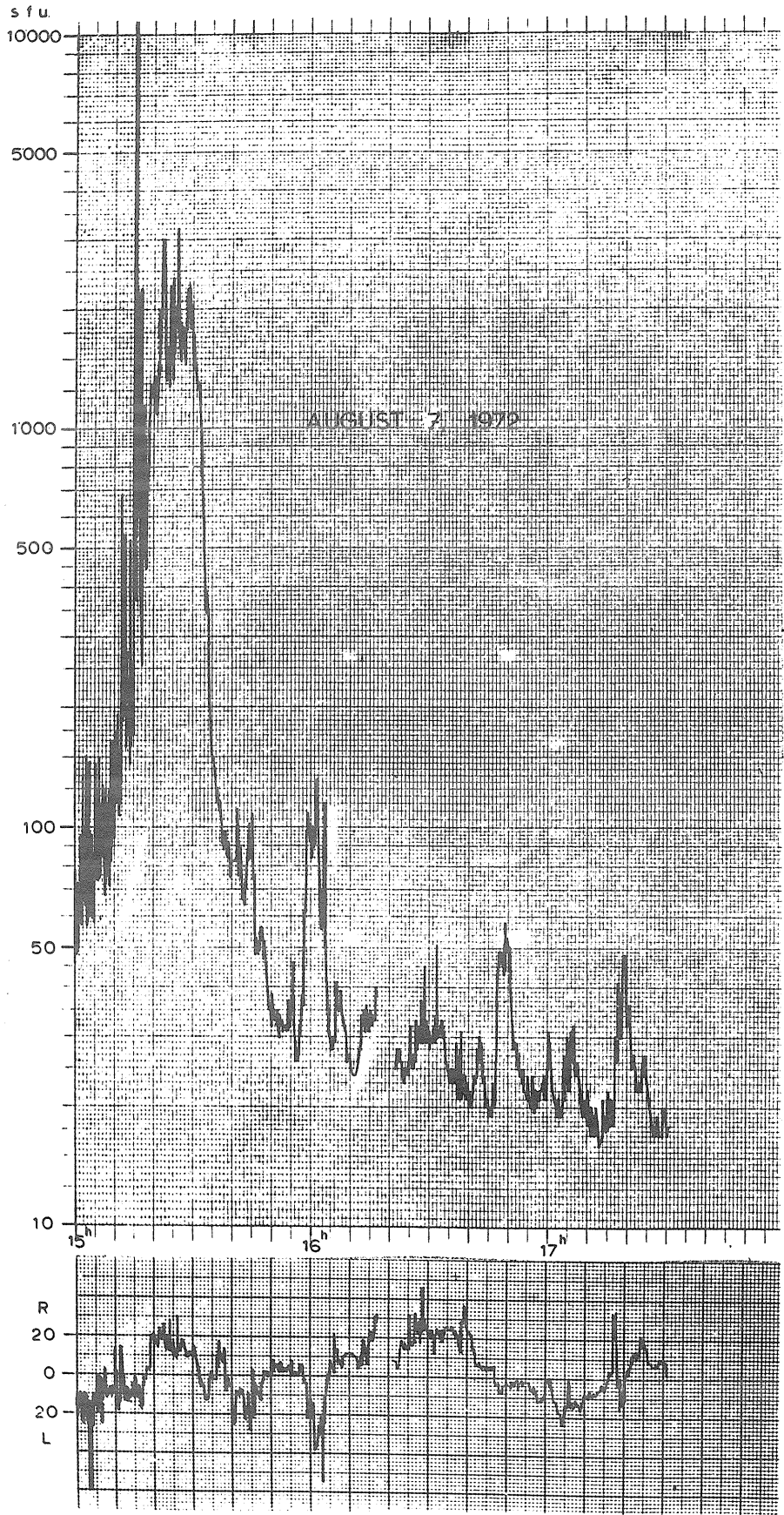


Fig. 3. Flux density and degree of circular polarization for August 7, 1972.

Swept Frequency Interferometer Data Analysis
for the Type IV Event of 1972, August 12

by

Anthony C. Riddle
Department of Astro-Geophysics
University of Colorado
Boulder, Colorado 80302

A moving Type IV event was observed with the University of Colorado swept-frequency interferometer on 1972 August 12 commenced at 2052 UT. Optical observations prior to and during the Type IV event showed no flare activity on the disk. A limb surge was observed on the west limb (latitude N25) commencing at 2022 UT [Lincoln and Leighton, 1972]. Later coronal observations taken in Hawaii (courtesy of R. Hansen, HAO) show an H α spray extending to $\sim 1R_{\odot}$ above the surface by 2100 UT. The footpoint of this spray was at a position angle 315° Geocentric (a latitude of N29 if on the limb). It is assumed that all this activity is associated with region McMath 11976 which, at the time of the activity, was 17° beyond the west limb.

The radio data in the frequency range 8-80 MHz first showed activity with a weak Type III burst at 2038 UT. Two other weak Type III bursts preceded the Type IV which commenced, at frequencies near the top of the range, at 2052 UT. The intensity of the activity built up towards a peak at 2115 UT and decayed slowly until 2240 UT after which no further trace could be seen. There was a tendency for the frequency of maximum emission to decrease as time progressed. The stronger activity is shown in Figure 1 which covers the time period 2055-2225 UT and the frequency bands 18-40 MHz and 40-80 MHz. A detailed description of the record format has recently been given by Dodge [1973].

Determination of fringe positions from the radio observations was made at 5 minute intervals from 2100 to 2220 for fringes in the 18-40 MHz band. The data in the 40-80 MHz band was not suitable for primary analysis as, in general, the fringes were too weak (partially due to lower sensitivity in this band). However a few fringe position determinations were made and they confirmed the positions derived from the lower frequency band. At any instant of time there was a tendency for the high frequency fringes to appear to be further from the center of the sun, however the dispersion was well within the individual measurement errors. Consequently an average position was determined from the mean of the positions of all fringes observed at any one time. The accuracy of each mean is estimated to be about $R_{\odot}/4$.

A second coordinate was determined by making the assumption that the source moved along a radial line at position angle 315° Geocentric. This assumption is consistent with the H α surge and flare spray observations and also is consistent with two dimensional radio observations made later (2324 UT to 0130 UT) at Culgoora (private communication K. V. Sheridan) which showed two stationary 160 MHz sources to be at position angle 315° Geocentric and at radii 1.4 R_{\odot} and 1.7 R_{\odot} . The intersection of this radial line and the fringe lines gave radial positions for the Type IV source which are shown in Figure 2.

A straight line has been fitted to the radio data in Figure 2. The deviations of the data points from the line are consistent with the accuracy of the fringe position determinations.

Positions derived from the optical data are also shown in Figure 2 [Hansen, 1972]. The close fit of the optical data to the line indicate that the association of radio and optical data was justified. The slope of the line indicates a velocity of ~ 340 km/sec for the disturbance causing the Type IV burst. It would appear that this disturbance left the limb at about the same time that the surge developed and that it travelled with a similar velocity to, but ahead of, the material seen in H α by the Mauna Loa coronagraph.

The observation of H α brightening out to 2 R_{\odot} and a Type IV burst out to 5 R_{\odot} indicates major solar activity. It might be expected then that strong Type III bursts and a Type II burst would precede the moving Type IV burst. However the position of McMath region 11976, 17° behind the limb, would make it difficult for plasma frequency radiation (involved in Type II and Type III bursts) to reach the observer. The Type IV radiation at 40 MHz was first observed at $\sim 2\frac{1}{2} R_{\odot}$ which is consistent with the expected minimum radius for a 40 MHz source situated above a point beyond the limb.

Acknowledgement

This research was supported by the National Science Foundation under Grant No. GP-28038.

1972 Aug 12

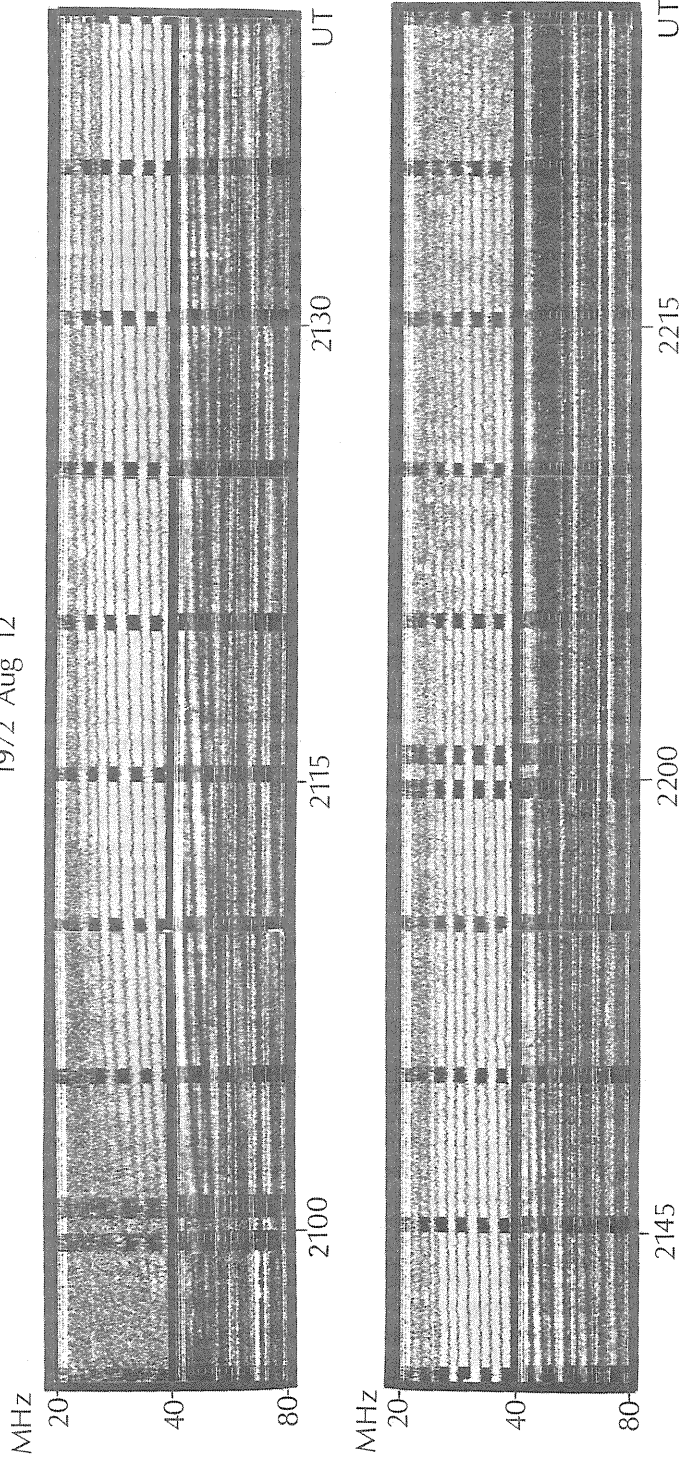


Figure 1

University of Colorado's Swept-frequency Interferometer record for the Type IV burst of 1972, Aug 12.

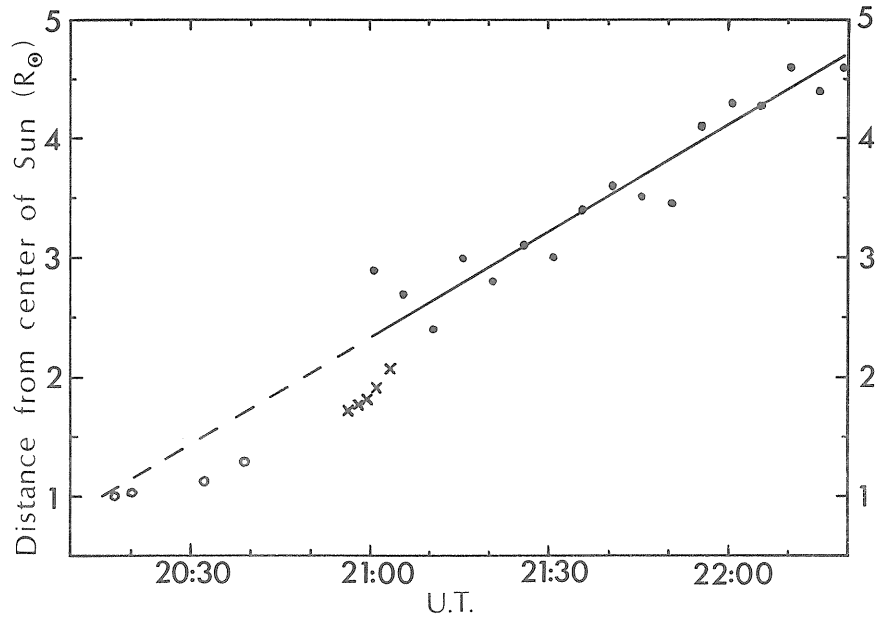
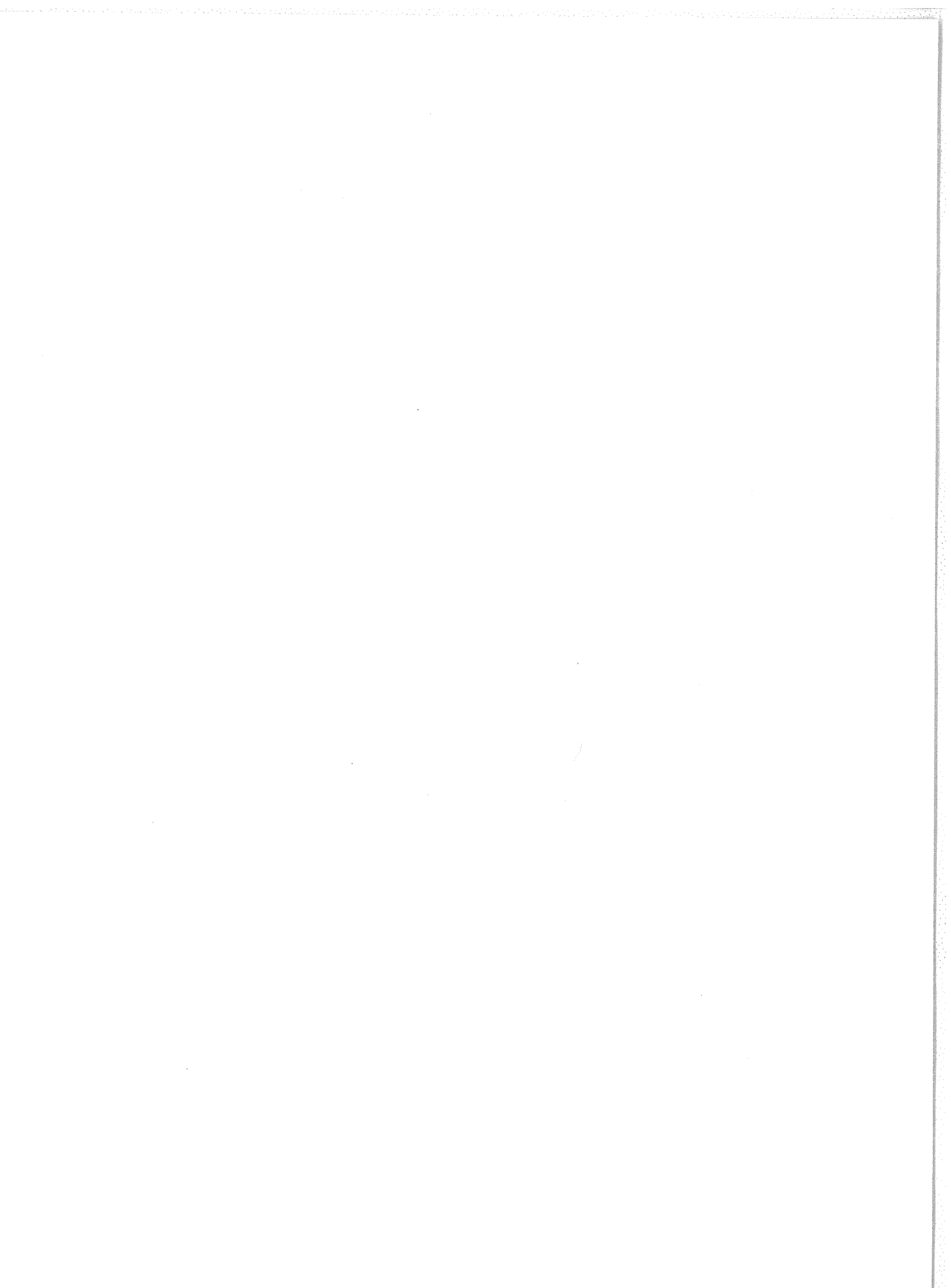


Figure 2 Radial distance of the Type IV event of 1972, August 12 as derived from the University of Colorado swept-frequency interferometer (dots). Also shown are the positions derived by Hansen (1972) for the furthest material seen in H α by the Boulder flare patrol (open circles) and the Mauna Loa coronagraph (crosses).

References

- | | | |
|---|------|--|
| DODGE, J. | 1973 | Solar Activity 1-11 August 1972, University of Colorado, Radio Astronomy Observatory Report SN-1. |
| LINCOLN, J. VIRGINIA and LEIGHTON, HOPE I. (Editors) | 1972 | Preliminary Computation of Data for Retrospective World Interval July 26 - August 14, World Data Center A, Upper Atmosphere Geophysics Report UAG-21, 61 |
| HANSEN, R., GARCIA, C., LEE, R., RUSH J., TANDBERG-HANSEN, E., and YASUKAWA, E. | 1972 | The Flare Spray of 12 August 1972. Presented at A. G. U. Fall Meeting, San Francisco, 1972 |



Publication Notice

WORLD DATA CENTER A for SOLAR-TERRESTRIAL PHYSICS REPORT UAG
(Prepared by World Data Center A for Solar-Terrestrial Physics, NOAA, Boulder, Colorado)

These reports are for sale through the National Climatic Center, Federal Building, Asheville, NC 28801, Attn: Publications. Subscription price: \$9.00 a year; \$2.50 additional for foreign mailing; single copy price varies. These reports are issued on an irregular basis with 6 to 12 reports being issued each year. Therefore, in some years the single copy rate will be less than the subscription price, and in some years the single copy rate will be more than the subscription price. Make checks and money orders payable to: Department of Commerce, NOAA.

Upper Atmosphere Geophysics Report UAG-1, "IQSY Night Airglow Data" by L. L. Smith, F. E. Roach and J. M. McKennan of Aeronomy Laboratory, ESSA Research Laboratories, July 1968, single copy price \$1.75.

Upper Atmosphere Geophysics Report UAG-2, "A Reevaluation of Solar Flares, 1964-1966" by Helen W. Dodson and E. Ruth Hedeman of McMath-Hulbert Observatory, The University of Michigan, August 1968, single copy price 30 cents.

Upper Atmosphere Geophysics Report UAG-3, "Observations of Jupiter's Sporadic Radio Emission in the Range 7.6-41 MHz, 6 July 1966 through 8 September 1968" by James W. Warwick and George A. Dulk, Department of Astro-Geophysics, University of Colorado, October 1968, single copy price 30 cents.

Upper Atmosphere Geophysics Report UAG-4, "Abbreviated Calendar Record 1966-1967" by J. Virginia Lincoln, Hope I. Leighton and Dorothy K. Kropp, Aeronomy and Space Data Center, Space Disturbances Laboratory, ESSA Research Laboratories, January 1969, single copy price \$1.25.

Upper Atmosphere Geophysics Report UAG-5, "Data on Solar Event of May 23, 1967 and its Geophysical Effects" compiled by J. Virginia Lincoln, World Data Center A, Upper Atmosphere Geophysics, ESSA, February 1969, single copy price 65 cents.

Upper Atmosphere Geophysics Report UAG-6, "International Geophysical Calendars 1957-1969" by A. H. Shapley and J. Virginia Lincoln, ESSA Research Laboratories, March 1969, single copy price 30 cents.

Upper Atmosphere Geophysics Report UAG-7, "Observations of the Solar Electron Corona: February 1964-January 1968" by Richard T. Hansen, High Altitude Observatory, Boulder, Colorado and Kamuela, Hawaii, October 1969, single copy price 15 cents.

Upper Atmosphere Geophysics Report UAG-8, "Data on Solar Geophysical Activity October 24-November 6, 1968", Parts 1 and 2, compiled by J. Virginia Lincoln, World Data Center A, Upper Atmosphere Geophysics, ESSA, March 1970, single copy price (includes Parts 1 and 2) \$1.75.

Upper Atmosphere Geophysics Report UAG-9, "Data on Cosmic Ray Event of November 18, 1968 and Associated Phenomena" compiled by J. Virginia Lincoln, World Data Center A, Upper Atmosphere Geophysics, ESSA, April 1970, single copy price 55 cents.

Upper Atmosphere Geophysics Report UAG-10, "Atlas of Ionograms" edited by A. H. Shapley, ESSA Research Laboratories, May 1970, single copy price \$1.50.

Upper Atmosphere Geophysics Report UAG-11, "Catalogue of Data on Solar-Terrestrial Physics" compiled by J. Virginia Lincoln and H. Patricia Smith, World Data Center A, Upper Atmosphere Geophysics, ESSA, June 1970, single copy price \$1.50.

Upper Atmosphere Geophysics Report UAG-12, "Solar-Geophysical Activity Associated with the Major Geomagnetic Storm of March 8, 1970", Parts 1, 2 and 3, compiled by J. Virginia Lincoln and Dale B. Bucknam, World Data Center A, Upper Atmosphere Geophysics, NOAA, April 1971, single copy price (includes Parts 1-3) \$3.00.

Upper Atmosphere Geophysics Report UAG-13, "Data on the Solar Proton Event of November 2, 1969 through the Geomagnetic Storm of November 8-10, 1969" compiled by Dale B. Bucknam and J. Virginia Lincoln, World Data Center A, Upper Atmosphere Geophysics, NOAA, May 1971, single copy price 50 cents.

Upper Atmosphere Geophysics Report UAG-14, "An Experimental Comprehensive Flare Index and its Derivation for 'Major' Flares 1955-1969" by Helen W. Dodson and E. Ruth Hedeman, McMath-Hulbert Observatory, University of Michigan, July 1971, single copy price 30 cents.

Upper Atmosphere Geophysics Report UAG-15, "Catalogue of Data on Solar-Terrestrial Physics" prepared by Research Laboratories, NOAA, Boulder, Colorado, July 1971, single copy price \$1.50. (Supersedes Report UAG-11, June 1970.)

Upper Atmosphere Geophysics Report UAG-16, "Temporal Development of the Geographical Distribution of Auroral Absorption for 30 Substorm Events in each of IQSY (1964-65) and IASY (1969)" by F. T. Berkey, V. M. Driatskiy, K. Henriksen, D. H. Jelly, T. I. Shchuka, A. Theander and J. Yliniemi, September 1971, single copy price 70 cents.

Upper Atmosphere Geophysics Report UAG-17, "Ionospheric Drift Velocity Measurements at Jicamarca, Peru (July 1967 - March 1970)" by Ben B. Balsley, Aeronomy Laboratory, National Oceanic and Atmospheric Administration, Boulder, Colorado, and Ronald F. Woodman, Jicamarca Radar Observatory, Instituto Geofisico del Perú, Lima, Peru, October 1971, single copy price 35 cents.

Upper Atmosphere Geophysics Report UAG-18, "A Study of Polar Cap and Auroral Zone Magnetic Variations" by K. Kawasaki and S. I. Akasofu, Geophysical Institute, University of Alaska, June 1972, single copy price 20 cents.

Upper Atmosphere Geophysics Report UAG-19, "Reevaluation of Solar Flares 1967" by Helen W. Dodson and E. Ruth Hedeman of McMath-Hulbert Observatory, The University of Michigan, and Marta Rovira de Miceli, San Miguel Observatory, Argentina, June 1972, single copy price 15 cents.

Report UAG-20, "Catalogue of Data on Solar-Terrestrial Physics", prepared by Environmental Data Service, NOAA, Boulder, Colorado, October 1972, single copy price \$1.50. (Supersedes Report UAG-15, July 1971.)

Report UAG-21, "Preliminary Compilation of Data for Retrospective World Interval July 26 - August 14, 1972" compiled by J. Virginia Lincoln and Hope I. Leighton, World Data Center A for Solar-Terrestrial Physics, November 1972, single copy price 70 cents.

Report UAG-22, "Auroral Electrojet Magnetic Activity Indices (AE) for 1970" by Joe Haskell Allen, National Geophysical and Solar-Terrestrial Data Center, Environmental Data Service, November 1972, single copy price 75 cents.

Report UAG-23, "U.R.S.I. Handbook of Ionogram Interpretation and Reduction", Second Edition, November 1972, edited by W. R. Piggott, Radio and Space Research Station, Slough U.K., and K. Rawer, Arbeitsgruppe für Physikalische Weltraumforschung, Freiburg, G.F.R., November 1972, single copy price \$1.75.

Report UAG-24, "Data on Solar-Geophysical Activity Associated with the Major Ground Level Cosmic Ray Events of 24 January and 1 September 1971", Parts 1 and 2, compiled by Helen E. Coffey and J. Virginia Lincoln, World Data Center A for Solar-Terrestrial Physics, December 1972, single copy price (includes Parts 1 and 2) \$2.00.

Report UAG-25, "Observations of Jupiter's Sporadic Radio Emission in the Range 7.6-41 MHz, 9 September 1968 through 9 December 1971", by James W. Warwick, George A. Dulk and David G. Swann, Department of Astro-Geophysics, University of Colorado, February 1973, single copy price 35¢.

Report UAG-26, "Data Compilation for the Magnetospherically Quiet Periods February 19-23 and November 29 - December 3, 1970", compiled by Helen E. Coffey and J. Virginia Lincoln, World Data Center A for Solar-Terrestrial Physics, May 1973, single copy price 70 cents.